

1-1-1993

Synthesis of specifically functionalized polymers and their adsorption at the solid-solution interface/

Brant U. Kolb
University of Massachusetts Amherst

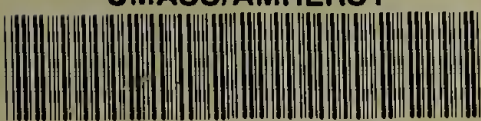
Follow this and additional works at: https://scholarworks.umass.edu/dissertations_1

Recommended Citation

Kolb, Brant U., "Synthesis of specifically functionalized polymers and their adsorption at the solid-solution interface/" (1993). *Doctoral Dissertations 1896 - February 2014*. 809.
<https://doi.org/10.7275/y9qr-yc83> https://scholarworks.umass.edu/dissertations_1/809

This Open Access Dissertation is brought to you for free and open access by ScholarWorks@UMass Amherst. It has been accepted for inclusion in Doctoral Dissertations 1896 - February 2014 by an authorized administrator of ScholarWorks@UMass Amherst. For more information, please contact scholarworks@library.umass.edu.

UMASS/AMHERST



312066008195008

SYNTHESIS OF SPECIFICALLY FUNCTIONALIZED
POLYMERS AND THEIR ADSORPTION AT THE
SOLID-SOLUTION INTERFACE

A Dissertation Presented

by

BRANT U. KOLB

Submitted to the Graduate School of the
University of Massachusetts in partial fulfillment
of the degree requirements for the degree of

DOCTOR OF PHILOSOPHY

February 1993

Polymer Science and Engineering

© Copyright by Brant U. Kolb 1993
All Rights Reserved

SYNTHESIS OF SPECIFICALLY FUNCTIONALIZED
POLYMERS AND THEIR ADSORPTION AT THE
SOLID-SOLUTION INTERFACE

A Dissertation Presented

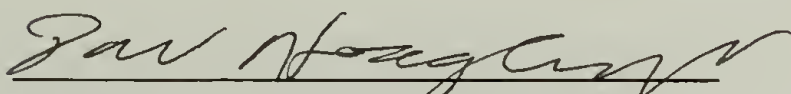
by

BRANT U. KOLB

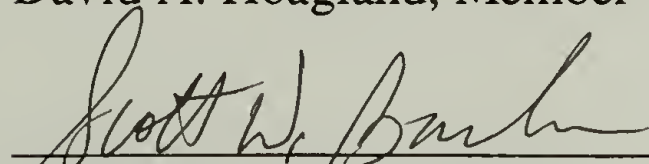
Approved as to style and content by:



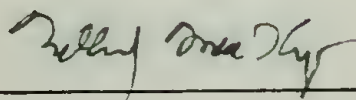
Thomas J. McCarthy, Chair



David A. Hoagland, Member



Scott W. Barton, Member



William J. MacKnight, Department Head
Polymer Science and Engineering

ACKNOWLEDGMENTS

I would like to thank my advisor Tom McCarthy for help, advice, and support through my many years at UMASS. He teaches much about science and life through both his words and actions and is thus an invaluable asset in anyones graduate career. I would also like to thank my other commitee members Dr. Dave Hoagland and Dr. Scott Barton for their time and insightful comments.

Thanks to all McCarthy group members, past and present, for stimulating discussions and scientific collaboration. Thanks for the friendship and good times both in and out of Lab. They have been a great group of people to work with. Damo thanks for all our technical arguements (they were great fun even if I'm the worst debater). I would also like to thank all the other members of the department and freinds that I've encountered in these past years, who have made this time both more productive and more enjoyable. Thanks to Dave Soderstrom who helped develop the column adsorption technique described in chapter 3.

Special thanks goes to my wife Dr. Nicole Franchina who has managed to illuminate every facet of my life and helped me to see all our possibilities. She has been an irreplaceable force in the drive to complete this work. She provided scientific insight and emotional support as well as the more easily measured assistance with typing, formatting, proof-reading and figure making. There is no doubt that without her this document would not be complete and my future would not be as bright.

Thanks to my mother and father (Sally and Bob) for everything (who could deliniate it?). Special thanks for giving me a love of learning which has made endeavors such as this thesis possible. My sister, Amy, and brothers, Blake and Rob, also deserve thanks I can't put into words.

ABSTRACT

SYNTHESIS OF SPECIFICALLY FUNCTIONALIZED POLYMERS AND THEIR ADSORPTION AT THE SOLID-SOLUTION INTERFACE

FEBRUARY 1993

BRANT U. KOLB, B.S.Ch.E., UNIVERSITY OF MINNESOTA
Ph.D., UNIVERSITY OF MASSACHUSETTS

Directed by: Professor Thomas J. McCarthy

The synthesis and adsorption characteristics of specifically functionalized block copolymers have been investigated. Specifically functionalized polymers are block copolymers of controlled MW, MWD, block size and block placement, and meet the requirement that one of the blocks interact strongly with a given surface whereas the other one does not. Synthetic procedures involved living anionic polymerization of various monomers, allowing preparation of narrow-dispersity block copolymers of specific molecular weight, overall composition, block lengths and (in one system used) block placement. The location (along the chain) of the surface attachment could be controlled through appropriate block sequences.

The grafting of polystyrene chains to the surface of poly(chlorotri-fluoroethylene) film was accomplished by reaction of the surface with three living polymer anions: polystyryl lithium, butadiene endcapped

polystyryl lithium and ethylenesulfide endcapped polystyryl lithium. The effects of solvent, reaction temperature, reaction time and anion concentration on the grafted layer were studied by XPS, ATR-IR, gravimetrics and contact angle. The synthesis of styrene/propylenesulfide block copolymers was studied in some detail and was found to result in polymeric dimers caused by disulfide formation. These disulfide linkages were cleaved by reaction with dithiothreitol (DTT). Endcapping with ethyl bromide stabilized the polymers against disulfide formation and degradation of the polypropylenesulfide block. These polymers were adsorbed onto gold surfaces (from THF and cyclohexane) and analyzed by XPS, contact angle, and photomodulated external reflectance IR spectroscopy. The amount adsorbed was found to decrease with increasing size of the polypropylenesulfide (sticky) block. The largest body of work presented discusses the synthesis of SF polymers with controlled placement of SF blocks at desired locations along the chain. This work focussed on the specific functionalization of the styrene blocks in styrene/*tert*-butyl styrene block copolymers. The various sulfonation reactions investigated gave poor results. Reaction with DEOM/SnCl₄ was found to be very selective, controllable and allowed introduction of hydroxydiethyl malonate SF at various positions along the chain. The adsorption of these (diblock and triblock) polymers to various silica surfaces was investigated. The data are qualitatively compared with theoretical predictions by both Marques and Evers.

TABLE OF CONTENTS

	page
ACKNOWLEDGMENTS	iv
ABSTRACT	vi
LIST OF TABLES	xiii
LIST OF FIGURES	xv
LIST OF SCHEMES	xxiii

CHAPTER

I. INTRODUCTION: SYNTHESIS OF SPECIFICALLY FUNCTIONALIZED POLYMERS AND THEIR ADSORPTION AT THE SOLID-SOLUTION INTERFACE	1
Polymer Surface Modification	2
Sticky Foot Polymer Adsorption: Concepts and Objectives	4
Homopolymer Adsorption: Background and Discussion	7
Copolymer Adsorption: Background and Discussion	19
Synthetic Aspects	44
Surface Analysis Techniques	49
X-Ray Photoelectron Spectroscopy	49
Contact Angle	52
Attenuated Total Reflectance IR (ATR IR) Spectroscopy	53
References	55
II. SYNTHESIS OF SPECIFICALLY FUNCTIONALIZED POLY(4- <i>TERT</i> -BUTYLSTYRENE) COPOLYMERS AND THEIR ADSORPTION AT THE SILICA-SOLUTION INTERFACE: EXPERIMENTAL	68
Materials Handling	68
Materials	69

Precursor Polymer Synthesis: Materials	71
Solvent Systems	71
Cyclohexane	73
Cyclohexane/Benzene Azeotrope	73
Cyclohexane/THF Spike	73
THF	73
Styrene	73
<i>para-tert</i> -Butylstyrene	74
Precursor Polymer Synthesis: Methods	75
Polymerization Vessel	75
Polymerization	76
Termination	76
Sulfonations: Exxon Method	77
Procedure 1	77
Procedure 2	78
Sulfonations: Vink Method	79
Sulfonations: TEP complexed ClSO_3H	79
Sulfonamide Formation: Via uncomplexed ClSO_3H	80
Sulfonamide Formation: Via Sulfamyl Chlorides	81
Preparation of PipSO_2Cl	81
$\text{PipSO}_2\text{Cl}/\text{AlCl}_3$ Modifications	82
$\text{PipSO}_2\text{Cl}/\text{SnCl}_4$ Modifications	82
Diethyloxomalonate Modification Reactions	82
DEOM/ SnCl_4 : Small Molecule Reactions	83
DEOM/ SnCl_4 : Polymer Modifications	83
Hydrolysis of the Diethylhydroxymalonate Sticky Foot	85
Procedure 1	85
Procedure 2	86
Reduction of the Diethylhydroxymalonate Sticky Foot	87
Determination of the Critical Displacer Concentration	87
UV-Vis Calibrations	89
Adsorptions to Aerosil 120	89
Method 1	89
Method 2	90

Method 3	90
Method 4	91
Adsorptions to Glass Beads	92
Adsorptions to Glass Microscope Slides	94
Adsorptions: Measurement via Column Method	95
References	97
III. SYNTHESIS OF SPECIFICALLY FUNCTIONALIZED POLY(4- TERT-BUTYLSTYRENE) COPOLYMERS AND THEIR ADSORPTION AT THE SILICA-SOLUTION INTERFACE: RESULTS AND DISCUSSION	98
Objective	98
Introduction	99
Synthesis: General Aspects	102
Precursor Polymer.Synthesis	104
Modifications Reactions: General Aspects	113
Sulfonation Reactions	116
Sulfonamide Formation	130
Discussion: Sulfonation and Sulfonamidation Reactions	143
Modification Via Diethyloxomalonate	154
Transformations of the Hydroxy Diethylmalonate Moiety	186
Adsorption Results: Introduction	198
Measurement of the Adsorption	199
Thin Layer Chromatography Results	201
Polymer Adsorptions: Solvents and Surfaces	217
Adsorptions on Glass Microscope Slides	218
Adsorptions on Aerosil 120	233
Batch Adsorptions on Glass Beads	250
Column Adsorption: Measurements and Results	253
Conclusions	296
References	304
IV. SYNTHESIS OF STYRENE-PROPYLENE SULFIDE BLOCK COPOLYMERS AND THEIR ADSORPTION TO THE GOLD-SOLUTION INTERFACE.....	310
Introduction	310
Synthesis of Poly(styrene-co-propylene sulfide) Block Copolymers	311
Background	311

Experimental: Synthetic Aspects	315
Polymer Synthesis	316
Triphenyl Phosphine Reductions	318
Reductions with Zinc/Acetic Acid	319
Reductions with Cl ₂	319
Dithiothreitol Reductions	319
Results and Discussion: Synthetic Aspects	321
Methods for Synthesis	328
Purification of Materials for Synthesis	330
Polymerizations	336
Poly(propylene sulfide) Chain Degradation	337
Oxidative Coupling	340
Reduction of Disulfides	343
Effect of Na/Benzophenone Drying on THF	351
Reduction of PTFE Stir Bar with PSLi	353
Conclusions: Synthetic Aspects	354
Adsorption of Poly(styrene- <i>co</i> -propylene sulfide) Block Copolymers	356
Experimental	356
Materials for Adsorption Experiments	356
Materials Handling	356
Methods of Analysis	357
Adsorption Experiments	357
Polarization Modulation External Reflection Spectroscopy (PMGRS)	358
Results and Discussion	358
References	367

V. REACTIONS OF POLYSTYRYL ANIONS WITH POLY(CHLOROTRIFLUOROETHYLENE) AT THE FILM-SOLUTION INTERFACE	370
Introduction	370
Experimental	374
Materials	374
Materials Handling	374
Methods	374
Reactions with PCTFE Films	376

Reactions of PSLi with PCTFE	376
Reactions of PSBLi with PCTFE	377
Reactions of PSSLi with PCTFE	379
Solvent Swelling of PCTFE Film	384
Results	384
Reactions of PCTFE with PSLi	387
Reactions of PCTFE with PSBLi	397
Reactions of PCTFE with PSSLi	406
Discussion and Conclusions	410
References	417
BIBLIOGRAPHY	420

LIST OF TABLES

TABLE	page
1.1 MJ Block Copolymer Scaling Regimes.....	24
1.2 List of Symbols for Adsorption Discussion.....	42
3.1 Precursor Polymers: Molecular Weight, Polydispersity and Percent Sticky Foot Information.....	107
3.2 Precursor Polymers II: Molecular Weight, Polydispersity and Percent Sticky Foot Information.....	108
3.3 PS/PtBS Copolymer Composition Data: ¹ HNMR.....	112
3.4 Sulfonation Reactions: Exxon Method.....	121
3.5 Aliphatic:Aromatic ¹ H NMR Data for Sulfonated Copolymers.....	125
3.6 Elemental Analysis Results for Sulfonated Copolymers.....	126
3.7 Sulfonation Reactions: ClSO ₃ H with Complexing Agents.....	129
3.8 Synthesis of Sulfonamide: Thionyl Chloride Path.....	132
3.9 Sulfonamides: Reactions with Uncomplexed ClSO ₃ H.....	134
3.10 Sulfonamide Formation via Reaction with Sulfamyl Chlorides.....	136
3.11 Sulfonamide Reactions Catalyzed with SnCl ₄	141
3.12 DEOM Reactions on Small Molecules.....	156
3.13 DEOM Reactions: Initial Polymer Modifications.....	157
3.14 DEOM Modified Polymers: Molecular Weight, Sticky Foot Content, Percent Conversion and Reaction Conditions.....	158

3.15	DEOM Modified Polymers: Molecular Weight, Polydispersity and Percent Sticky Foot Information.....	172
3.16	Precursor, Modified Polymer and Model Compound: R _f Values on Silica.....	203
3.17	Critical Displacer Concentrations (ϕ_{cr}): Solvent (DCE).....	214
3.18	Adsorbed Layer Thickness as Determined by XPS.....	228
3.19	Comparison of Determination of the Amount Adsorbed: V _{sat} versus Integral Method.....	259
4.1	Various Disulfide Reduction Attempts.....	320
4.2	Disulfide Reductions of Block Copolymers with DTT in THF.....	322
4.3	Disulfide Reductions of Block Copolymers with DTT in DMF.....	324
4.4	PS/PPrS Block Copolymers Synthesized Using the Developed Methods.....	355
4.5	PS/PPrS Polymers Prepared for Adsorption Studies.....	359
4.6	Contact Angle Data for PS/PPrS Polymers Adsorbed on Gold (Water is the Probe Fluid).....	360
4.7	Adsorbance and Graft Density of PS-PPrS Copolymers.....	364
5.1	Reactions of PSLi with PCTFE.film.....	378
5.2	Reactions of PSBLi with PCTFE.film.....	380
5.3	Reactions of PSSLi with PCTFE.....	382
5.4	XPS Atomic Composition Data for PSLi Reacted with PCTFE in Benzene at Room Temperature.....	396
5.5	XPS Atomic Composition Data for the Reaction of PSBLi with PCTFE in Benzene at 80 °C.....	406

LIST OF FIGURES

FIGURE	page
1.1 Pictorial representation of the adsorption of "sticky foot" polymers.....	6
1.2 A) Experimental adsorption isotherms for polystyrene/chrome/cyclohexane (308K); $M_w=7.6 \times 10^6$ (m), $M_w=1.1 \times 10^5$ (l), (reprinted from reference 61).....	15
1.3 The adsorbed amount, Γ (full curves), as a function of chain length, n , for three values of bulk concentration ϕ_s^b and values of χ : $\chi = 0$ (athermal solvent) and $\chi = 0.5$ (theta solvent).....	17
1.4 Graft density (A) and amount adsorbed vs. mole fraction sticky block for diblock copolymers calculated using MJ diblock theory (reprinted from reference 126).....	26
1.5 The adsorbed amount, θ^a , in equivalents of monolayers (a), the ratio θ_A^a/θ_{hA}^a between the amount of A-segments θ_A^a in adsorbed AB-copolymer and the adsorbed amount θ_{hA}^a of A-homopolymer (b), the hydrodynamic layer thickness, δ_h , in lattice layers (c), and the degree of stretching δ_h/r_b (d), as a function of the fraction, v_a , of A-segments in the AB-copolymer.....	29
1.6 The effect of surface affinity of the A-segments on the adsorbed amount.....	32
1.7 The adsorbed amount, θ^a , as a function of the number, r_b , of B-segments per chain at various values of r_a	34
1.8 Experimental data of Wu et. al. for the adsorption of MMA/DMAEM copolymers onto silica from 2-propanol.....	37
1.9 Comparison of measured values of the adsorbed amount, as a function of the PEO fraction, with the predicted behavior by the MJ model for the adsorbed amount at a total chain length of $N_T=1500$ (reprinted from reference 126).....	38

3.1	Illustration of the structural control that has been attained through the synthetic procedures reported in this chapter.....	100
3.2	Hydroxydiethylmalonate sticky foot polymer.....	101
3.3	IR spectrum of a 50/50 random copolymer (R50/114k-p) sulfonated with SO ₃ /TEP (See Table 3.4, ExxSulf-3).....	123
3.4	¹ H NMR spectrum (in D ₂ O) of a 90/10 random copolymer (R90/75k-p) sulfonated with SO ₃ /TEP (See Table 3.4, ExxSulf-2).....	124
3.5	¹ H NMR spectrum of polystyrene homopolymer modified by reaction with PipSO ₂ Cl/AlCl ₃ to 76% conversion (See Table 3.10, PipPS2).....	138
3.6	¹ H NMR spectrum of <i>iso</i> -butylbenzene derivative of DEOM/SnCl ₄ reaction (See Table 3.12, B19-5).....	163
3.7	¹ H NMR spectrum of a 23% styrene precursor polymer (T23/12k p).....	173
3.8	¹ H NMR spectrum of a 23% SF polymer (T23/12k TM4).....	174
3.9	¹ H NMR spectrum of DEOM modified homopolymer polystyrene (PSM2, 95% conversion).....	176
3.10	¹ H NMR spectrum of DEOM modified copolymer (Mn = 33 K) containing 95% styrene units (D95/33K).....	177
3.11	IR spectra of T23/12K and the precursor copolymer.....	178
3.12	IR spectrum of D23/33K p modified by reaction with DEOM and SnCl ₄	179
3.13	¹ H NMR spectrum of DEOM modification control reaction on PtBS (PtBS88M2).....	182
3.14	Size exclusion chromatograms of three different polymers after reaction with the DEOM system.....	184

3.15	Subsequent transformations of the hydroxy diethylmalonate sticky foot.....	187
3.16	^1H NMR spectrum of hydrolyzed PSM2 in D_2O	191
3.17	IR spectrum of a 95% SF hydrolyzed copolymer (D95/33K).....	193
3.18	IR spectrum of 23% SF copolymer (D23/13K DM4) after reduction to the triol with LiAlH_4	196
3.19	TLC displacer data for modified and precursor polymers on silica (eluent CCl_4 , displacer ethyl acetate).....	207
3.20	TLC displacer data for modified polymers on silica (eluent DCE, displacer ethyl acetate).....	210
3.21	TLC displacer data for modified polymers on silica (eluent DCE, displacer THF).....	211
3.22	TLC displacer data for modified polymers on silica (eluent DCE, displacer IsoOH).....	212
3.23	Critical displacer concentrations.....	215
3.24	XPS spectra (15° takeoff angle) of a 23% SF diblock, 23% triblock, unmodified precursor and solvent control for the adsorption onto glass microscope slides from DCE (25°C , 24 h, approximately 1.0 mg/mL).....	220
3.25	XPS atomic composition data (% carbon, 15° takeoff angle) for polymers adsorbed onto glass microscope slides from DCE (22°C , 24 h).....	221
3.26	XPS atomic composition data (% silicon, 15° takeoff angle) for polymers adsorbed onto glass microscope slides from DCE (22°C , 24 h).....	222
3.27	XPS atomic composition data (% oxygen, 15° takeoff angle) for polymers adsorbed onto glass microscope slides from DCE (22°C , 24 h).....	223
3.28	XPS atomic composition data (% carbon, 75° takeoff angle) for polymers adsorbed onto glass microscope slides from DCE (22°C , 24 h).....	224

3.29	XPS atomic composition data (% silicon, 75° takeoff angle) for polymers adsorbed onto glass microscope slides from DCE (22 °C, 24 h).....	225
3.30	XPS atomic composition data (% oxygen, 75° takeoff angle) for polymers adsorbed onto glass microscope slides from DCE (22 °C, 24 h).....	226
3.31	Advancing contact angle data (water is probe liquid) for polymers adsorbed onto glass microscope slides from DCE (22 °C, 24 h).....	229
3.32	Receding contact angle data (water is probe liquid) for polymers adsorbed onto glass microscope slides from DCE (22 °C, 24 h).....	230
3.33	Adsorption kinetics of triblock copolymer (23% SF, 12K) modified (TM1) and unmodified (T) on Aerosil 120 (Solvent DCE, 22 °C).....	240
3.34	Adsorption isotherm of 23% triblock copolymer ($M_n=12K$, T23/12K TM1) on Aerosil 120 from DCE at 22 °C.....	241
3.35	Adsorption isotherm of 23% diblock copolymer ($M_n=13K$, D23/13K DM2) on Aerosil 120 from DCE at 22 °C.....	242
3.36	Adsorption isotherm of 23% triblock copolymer modified to 60% conversion ($M_n=12K$, T23/12K TM2) on Aerosil 120 from DCE at 22 °C.....	243
3.37	Adsorption isotherm of 23% diblock copolymer modified to 56% conversion ($M_n=12K$, T23/12K TM2) on Aerosil 120 from DCE at 22 °C.....	244
3.38	Combined adsorption isotherms for D23/13K DM2, D23/13K DM3, T23/12K TM1 and T23/12K TM2.....	245
3.39	Adsorption (triangles) and desorption (squares) isotherms for 23% triblock copolymer ($M_n=12K$, T23/12K TM1) on Aerosil 120 from DCE at 22 °C.....	247
3.40	Effect of temperature on adsorbance of 23% triblock ($M_n=12K$, T23/12K TM1).....	249

3.41	Adsorption data for 23% SF diblock and triblock copolymers from DCE onto 3-10 μm glass beads.....	252
3.42	Column adsorption apparatus.....	254
3.43	Column adsorption method explanation.....	256
3.44	Column adsorption manipulation.....	258
3.45	Column dead volume determination for V_{sat} method using silica gel (5 x 0.46 cm column, 0.93 g silica gel).....	261
3.46	V_{sat} data for 5.8% SF diblock copolymer, $M_n = 51\text{K}$ (D5/50K).....	265
3.47	V_{sat} data for 13.0% SF diblock copolymer, $M_n = 49\text{K}$ (D12/50K).....	266
3.48	V_{sat} data for 23.5% SF diblock copolymer, $M_n = 46.5\text{K}$ (D23/50K).....	267
3.49	V_{sat} data for 38.2% SF diblock copolymer, $M_n = 52.2\text{ K}$ (D40/50K).....	268
3.50	V_{sat} data for 6.2% SF triblock copolymer, $M_n = 46\text{ K}$ (T5/50K).....	269
3.51	V_{sat} data for 13.8% SF triblock copolymer, $M_n = 50.2\text{ K}$ (T12/50K).....	270
3.52	V_{sat} data for 24% SF triblock copolymer, $M_n = 46\text{ K}$ (T23/50K).....	271
3.53	V_{sat} data for 41.2% SF triblock copolymer, $M_n = 58.5\text{ K}$ (T40/50K).....	272
3.54	V_{sat} response and derivative data for D12/50K (0.5 mg/mL).....	276
3.55	V_{sat} response and derivative data for D23/50K (0.98 mg/mL).....	277
3.56	V_{sat} response and derivative data for D23/50K (0.98 mg/mL).....	278
3.57	V_{sat} response and derivative data for D40/50K (1.02 mg/mL).....	279

3.58	Vsat response and derivative data for T5/50K (1.00 mg/mL).....	280
3.59	Vsat response and derivative data for T12/50K (1.00 mg/mL).....	281
3.60	Vsat response and derivative data for T40/50K (0.29 mg/mL).....	282
3.61	Adsorption isotherm 5.8% SF diblock copolymer, $M_n = 51$ K, (D5/50K) on silica gel determined using the Vsat method.....	283
3.62	Adsorption isotherm 13.2 % SF diblock copolymer, $M_n = 49$ K, (D12/50K) on silica gel determined using Vsat method (DCE, 22°C).....	284
3.63	Adsorption isotherm 41.7 % SF diblock copolymer, $M_n = 58.5$ K, (T40/50K) on silica gel determined using Vsat method (DCE, 22°C).....	285
3.64	Combined adsorption isotherms for D5/50K (5.8% SF, 51K), D12/50K (13.2% SF, 49 K) and T40/50K (42% SF, 58.5K) copolymers on silica gel using Vsat method (DCE, 22 °C).....	286
3.65	Adsorbance (@ 1.0 mg/mL, in the plateau region) vs. Sticky Foot content for diblock and triblock copolymers ($M_n \sim 50$ K).....	288
3.66	Vsat data for 6.2% SF triblock copolymer, $M_n = 46$ K (T5/50K).....	293
3.67	Vsat data for 38.2% SF triblock copolymer, $M_n = 52$ K (D40/50K).....	294
3.68	Effect of temperature on adsorbance of T5/50K and D40/50K copolymers to silica gel via Vsat method (DCE, 22 °C).....	295
4.1	Reaction scheme for synthesis of poly(styrene- <i>co</i> -propylene sulfide) block copolymers.....	312
4.2	Typical GPC trace of PS/PPrS block copolymer that was synthesized at the start of this research (MeOH/H ⁺ terminated; CaH ₂ drying agent).....	329

4.3	Upper GPC trace shows the presence of a “dead PS” fraction due to inefficient drying of PrS with CaH_2	333
4.4	PPrS block degradation is acid catalyzed (H^+ , Et_3OBF_4); it will lead to increased polydispersity and eventually PS homopolymer.....	338
4.5	PS- <i>co</i> -PPrS block copolymers show increased stability toward degradation due to endcapping with ethyl bromide.....	341
4.6	Oxidative coupling of sulfur terminated polymers results in disulfide formation (a).....	342
4.7	Thiol-ended polymers are unstable to disulfide formation and result in coupling to form the corresponding triblock copolymer.....	344
4.8	Dithiothreitol reduction of disulfide linkages in PS- <i>co</i> -PPrS block copolymers.....	346
4.9	GPC traces of PS- <i>co</i> -PPrS block copolymers before (left) and after (right) reaction with DTT for PS ₉₅ -PPrS ₅ (top), PS ₉₀ -PPrS ₁₀ (middle) and PS ₇₅ -PPrS ₂₅ (bottom).....	347
4.10	The IR spectrum of the adsorbed copolymer (PS ₉₅ -PPrS ₅) in the C-H stretching region obtained via PMGR IR (solid line).....	361
4.11	XPS survey spectra (15° takeoff) of the PS ₇₅ - PPrS ₂₅ and PS ₉₅ -PPrS ₅ copolymers adsorbed to gold.....	363
5.1	Illustration of the range of interface structures possible for reaction of polystyrene chains with the surface of PCTFE film.....	373
5.2	Plot of absorbance (310 nm) vs. reaction time for the reaction of PCTFE film with PSLi ($n = 50$; 0.004 M) in THF at room temperature.....	389
5.3	ATR IR spectra of (a) virgin PCTFE film and (b) PCTE film which had been reacted with PSLi ($n = 50$; 0.035 M) in THF at room temperature for 17 h.....	390

5.4	Plots of absorbance (310 nm and 230 nm) vs. reaction time for the reaction of PSLi ($n = 39$; 0.027 M) in benzene at room temperature.....	393
5.5	ATR IR spectrum of PCTFE film that had been reacted with PSLi ($n = 39$; 0.027) in benzene at room temperature for 1 h.....	394
5.6	XPS spectrum of (a) PCTFE film and (b) PCTFE film which had been reacted with PSLi ($n = 39$; 0.027 M) in benzene at room temperature.....	395
5.7	Plot of absorbance (310 nm) vs, reaction time for the reaction of PCTFE film with PSBLi ($n = 50$; 0.004 M) in THF at room temperature.....	398
5.8	Changes in mass vs. reaction time for PCTFE film samples reacted with PSBLi ($n = 50$; 0.004 M) in THF at room temperature.....	399
5.9	Change in mass vs. reaction time for PCTFE film samples reacted with PSBLi ($n = 50$; 0.004 M) at room temperature in hexane/THF (67:33) (S), THF/ benzene (75:25) (I), THF/benzene (50:50) (O), benzene (G), and benzene/hexane (35:65) (n).....	402
5.10	ATR IR spectrum of PCTFE film that had been reacted with PSBLi ($n = 50$; 0.024 M) in refluxing benzene for 3 h.....	404
5.11	XPS spectrum of PCTFE film that had been reacted with PSBLi ($n = 50$; 0.024 M) in refluxing benzene for 14 h.....	405
5.12	XPS and ATR IR spectra of PCTFE film samples that had been reacted with PSBLi (0.024 M) in refluxing benzene for 2 h: (a) PSBLi, $n = 5$; (b) PSBLi, $n = 50$	407
5.13	ATR IR spectra of PCTFE film samples that had been reacted with PSSLi ($n \sim 50$) in THF with the following conditions: (a) room temperature, 0.04 M, 37 min; (b) refluxing THF, 0.02 M, 3 h.....	409

LIST OF SCHEMES

SCHEME	page
1.1 Sample/Detector Geometry for Variable Angle XPS.....	51
3.1 Precursor Polymer Synthesis.....	106
3.2 Electrophilic Aromatic Substitution.....	113
3.3 Aromatic Sulfone Formation.....	115
3.4 Jacobsen Reaction.....	115
3.5 Sulfur Trioxide Complexes: Relative Reactivities.....	117
3.6 Sulfonamide Formation: Thionyl Chloride.....	130
3.7 Sulfonamide Formation: Chlorosulfonic Acid.....	131
3.8 Sulfonamide Formation: Sulfamyl Chloride/ AlCl_3	135
3.9 Possible Acid and Hydroxyl Functionality via Sulfonamides.....	147
3.10 Water Solubility Facilitated at High pH.....	148
3.11 Friedel Crafts Alkylation Reactions.....	151
3.12 Friedel Crafts Acylations.....	153
3.13 Diethyloxomalonate Modification Reaction.....	154
3.14 Polymer Modification with DEOM/ SnCl_4	169
3.15 Hydroxy Diethylmalonate Hydrolysis.....	189
3.16 Reduction of the Sticky Foot to the Triol.....	195
4.1 Reaction of <i>sec</i> -Butyllithium with THF.....	335
4.2 Disulfide Formation.....	340

CHAPTER I

INTRODUCTION: SYNTHESIS OF SPECIFICALLY FUNCTIONALIZED POLYMERS AND THEIR ADSORPTION AT THE SOLID-SOLUTION INTERFACE

Surface properties of solid materials are important in many areas of technology.^{1, 2} These areas include wettability,^{3,4} adhesion/dehesion, biocompatibility,⁵ friction and drag modification among others.^{1, 2} The correlation of macroscopic surface properties such as wettability, adhesion and friction with microscopic chemical structure should lead to a more fundamental understanding of surface properties.¹ This, in turn, should result in better and rational methods for obtaining desired surface characteristics. In this thesis it is premised that these macroscopic properties are, at least in some way, related to the functional group chemistry of the surface, to the scale and extent of surface roughness, to the “surface modulus”, and to the morphology. It is also premised that the above mentioned parameters are interrelated and not exclusive. The McCarthy group uses chemistry to modify the properties of a given surface in a controlled, characterizable manner to try to better understand surface phenomena. To this end two major approaches have been developed: 1) chemical modification of known polymer surfaces and 2) adsorption of specifically functionalized polymers to surfaces. Neither surface modification nor polymer adsorption are novel ideas in themselves⁶ but we apply an original twist to each case. The research presented in this thesis involves some aspects of both of these strategies although polymer

adsorption is the major focus. A short review of the chemical surface modification route will be given and then attention will be turned to specifically functionalized (SF) polymer adsorption.

Polymer Surface Modification

Surface treatments have been carried out on polymers with the objective of increasing wettability and adhesion properties of the polymers.^{3,4} For the most part, the methods are harsh, non-selective conversions that result in a wide range of functional groups including hydroxyl, carboxylic acid, ketone, aldehyde and carbon-carbon double and triple bonds. Among these approaches to polymer surface modification are plasma and corona discharge techniques, surface graft polymerizations using ultra-violet (UV) radiation, and chemical modification. Less commonly used methods include entrapment-functionalization,^{7,8} surface reconstruction,⁹⁻¹¹ flame treatment³ and UV-induced crosslinking.¹² Gas plasma treatments can induce changes in the morphology, roughness, chemical composition, and molecular weight of a polymer surface.¹³ Some plasma treatments have been used to implant fluorine-containing moieties on surfaces¹⁴⁻¹⁷ as a means of reducing wettability. Experiments using oxygen-containing plasmas for surface treatments indicate that short exposure times effect changes in the chemical composition of the surface whereas longer times tend to cause more physical changes, namely etching of the surface.¹⁸ Surface graft polymerizations using acrylic monomers have been carried out on polyethylene^{12,19} and poly(ethylene terephthalate) (PET)²⁰ films by photoinitiation methods (sometimes using benzophenone as a photosensitizer¹²) to increase the wettability of these surfaces. In some cases, grafted polymer chains could be functionalized¹⁹ for further surface

property control. Chemical polymer surface modifications encompass a wide variety of reaction types. In general these reactions (can) cause less physical damage than other surface treatments. These modifications include oxidations^{21,22} and reductions,²³ halogenations^{24,25} and dehydrohalogenations,²⁶ sulfonations,^{27,28} ozonations,²⁹ and aromatic electrophilic substitutions.³⁰ Chemical derivatizations^{31,32} of surface-confined functional groups are sometimes carried out for XPS identification purposes (labelling reactions).

The modifications performed in the McCarthy group involve specific chemical reactions that incorporate only one type of functional group on a surface (surface modifications do not allow the luxury of purification after the reaction is carried out). The modifications, in general, result in controlled functionality with well characterized modification depth and functional group spacing. In this way, the effect of an acid versus an alcohol group on the surface properties can be examined. The effects of functionality on the wettability (using various solvents), adhesion and friction properties are studied. The effect of surface confinement on the reactivities of various functional groups is also studied. It is found that the chemistry has a direct impact on surface properties via incorporation of different functionalities but also an indirect impact through modification of other surface properties such as modulus.

The polymer films chosen for surface modification are by necessity chemically inert substrates. Chemical inertness of the bulk material allows the use of a range of reaction conditions to introduce new properties to the surface (prepare a reactive exterior) without affecting the underlying

material (maintain an inert interior). Substrates that have been used by the McCarthy group for modification include several fluoropolymer films which are known for high chemical resistance, low wettability and poor adhesion characteristics. Among them are poly(vinylidene fluoride) (PVF₂),³³⁻³⁶ poly(tetrafluoroethylene) (PTFE),^{37,38} poly(tetrafluoroethylene-co-hexafluoropropylene) (FEP)^{36,39} and poly(chlorotrifluoroethylene) (PCTFE).^{36,40-46} Nonfluorinated chemically resistant polymers, including polyethylene (PE),⁴⁷ polypropylene (PP)^{48,49} and poly(ether ether ketone) (PEEK)⁵⁰⁻⁵² which also have poor wetting properties, have been used for surface modification, as well. Initial modification of all of these polymer films entails reactions (many with protected functionality) to introduce functional groups (reactive handles) to the surface; these reactive handles provide a means of further functionalizing the surface. The wetting properties of these substrates can be changed dramatically with chemical surface modification by the introduction of various polar functional groups,³³⁻⁴⁹ and the adhesion properties can be manipulated as well.⁴⁴

Sticky Foot Polymer Adsorption: Concepts and Objectives⁵³

Adsorption is the phenomenon whereby molecules in solution spontaneously form a concentrated layer at the interface. The properties of an interface can be changed dramatically as a result of adsorption. A familiar example of this is the dramatic decrease in surface tension (and thus ease of bubble formation) observed when a small amount of soap is added to water. Here the soap molecules adsorb to the air/water interface and cover it with low surface energy hydrocarbon tails. The adsorption of a polymer chain results in a rather diffuse interface with polymer segments distributed over many molecular layers perpendicular to the interface.

This adsorption is induced by a net favorable interaction of the polymer chain segments with the surface. Thus the actual chemical structure of a given polymer repeat unit will determine whether a polymer is attracted to or repelled by the surface. We are studying polymer adsorption with the objectives of controlling the amount and conformation of adsorbed polymer chains and ultimately, through this control, regulating interfacial properties. Our strategy is to prepare polymers containing specific functional groups ("sticky feet" = SF) in well-defined densities and locations and to allow these polymers to adsorb to a surface from a solvent (or solvent mixture) from which the polymer would not adsorb, were it not functionalized. Figure 1.1 describes this strategy with several topologies that could be used. The SF groups located at various points along the chain interact more strongly with the surface than do the regular polymer segments. It is thus our intention to control the structure of the adsorbed polymer layer by use of these much stronger interactions: we induce only particular parts of the polymer chain to adsorb (stick to the surface). Figure 1.1 illustrates various sticky foot architectures and the adsorbed structures which might be obtained. In route a, a polymer with no sticky foot does not adsorb under the experimental conditions. Attachment of SF blocks (big and small) to one end of the chain (routes b and e) results in an adsorbed layer made up of polymer tails, whereas route c shows loop formation when sticky feet are attached to both ends. For various other architectures other adsorbed structures can be obtained. The structures obtained will also depend on the overall sticky/non-sticky composition of the chain.

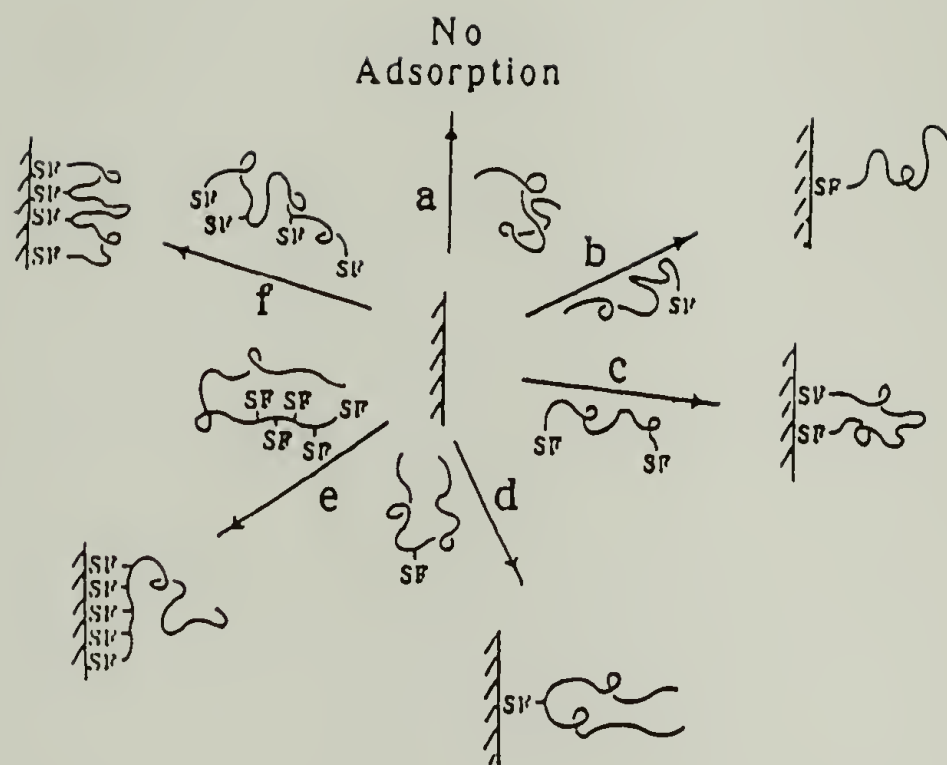


Figure 1.1 Pictorial representation of the adsorption of "sticky foot" polymers. Route a shows the nonadsorption of the unfunctionalized polymer. Routes b through f represent a few of the sticky foot sequences possible (SF = sticky foot).

Polymers adsorbed to a surface can modify the solvent-swelled properties of a device, such as drag characteristics, and the overall density of small particles suspended in solution. They can also change the functionality of the surface by concentrating functional groups in the surface region. The functionality and wettability of subsequently dried surfaces can be changed.

This thesis is divided into three parts, each of which corresponds to some route shown in Figure 1.1: 1) grafting of polystyrene chains to PCTFE films (Figure 1.1, route b); 2) adsorption of polystyrene-polypropylene sulfide block copolymers and thiol terminated polystyrenes to gold surfaces (Figure 1.1, routes b & e); 3) adsorption of poly(*tert*-butylstyrene) specifically functionalized with 2-hydroxydiethylmalonate groups to silica surfaces (Figure 1.1, all routes possible). The work in part 1 was done in collaboration with P. A. Patton^{45,46,47} and that in the second was a dual effort with D. A. Waldman.⁵⁵⁻⁵⁷ Each part will be discussed in detail in its respective chapter. Each of these projects involves an integration of different aspects of science, some of which are not the most common of venues; these include anionic living polymer synthesis, surface analysis and polymer adsorption. To facilitate a better understanding of the contributions presented here and the experiments carried out, a general background to these areas will be given in the remainder of this chapter. See end of this section for list of symbols used in the discussion below.

Homopolymer Adsorption: Background and Discussion

The goal of the research proposed here is the synthesis and characterization of specifically functionalized polymers (sticky foot, SF)

and the subsequent evaluation of their adsorption characteristics. The motivation behind this is twofold: First, we feel that incorporation of various functional group sequences on the polymer chain will enable a control over the structure of the adsorbed layer that is currently not possible (Figure 1.1). Thus different SF sequences will be used and their effect on the amount of polymer adsorbed (and eventually on the layer thickness) will be evaluated. These different adsorbed structures may lead to different or more efficient uses of polymers in surface applications. For instance it is known that diblock copolymers can be used to stabilize colloidal systems while triblocks will flocculate them.⁵⁸ The second motivation behind this research is the use of these well characterized and, in some senses, simpler polymers (they are simpler in the structure they will form on the surface, i.e. we know where the attachments will be) to better study various fundamentals of the physics of polymer adsorption. The remainder of this discussion is broken into the following parts: First the basic physical picture of homopolymer and copolymer adsorption will be given, drawing on both current theory and experimental data as well as my own interpretation of the phenomena. These concepts will then be extended to the case of sticky foot adsorption (SF adsorption can be thought of as adsorption of block copolymers with various architectures). Particular attention will be paid to any effects of chain architecture and composition.

Polymer adsorption has been the subject of much research from both purely scientific and practical vantages. This is true because of its importance in technologies including adhesion,⁶³ colloid stabilization and destabilization,⁵⁸ corrosion inhibition,⁶⁴ biocompatibility,⁶⁵ and

lubrication.⁶⁶ Homopolymer⁶²⁻⁹⁴ as well as block⁹⁵⁻¹³³ and random¹³⁴⁻¹⁴⁶ copolymer physisorption to solid surfaces has been studied quite extensively and much literature has been published on this subject. Recently there has been an interest in terminally attached chemisorbed (grafted) chains because of the polymer brush structures they form.¹⁴⁷⁻¹⁶² Polymer adsorption combines the complex nature of polymer chains in solution with the complexity of surface phenomena, thus polymer adsorption is only starting to be understood on a general theoretical basis. In the succeeding paragraphs, I will give an overview of the present state of understanding (in polymer adsorption) and also try to paint a qualitative picture of the major aspects we are concerned with in this project.

When a polymer molecule is brought in the vicinity of a surface it will either be attracted to the surface (if the surface-segment interaction is strong enough) and form an adsorption layer, or the coil will be repelled from the surface forming a depletion layer. The work presented in this thesis deals only with the former phenomenon. We are concerned not only with the amount of polymer adsorbed but also with the structure of the chains in the vicinity of the surface. Segments of adsorbed polymer molecules exist as trains (segments directly bound to the surface), loops (segments which have train segments on either side) and tails which are only attached to the surface by one end. Experimentally the adsorbed amount per surface site, Γ ,¹⁶³ fractional surface coverage, θ ,¹⁶⁴ the bound fraction, p ,¹⁶⁵ and various layer thicknesses, L ¹⁶⁶ can be measured. (See the end of this section for a list of the symbols used.) The thickness measured depends on the method of measurement (i.e. the segment density has some distribution and different methods are sensitive to different

moments of the distribution).⁶² There has been extensive theoretical work in the area of polymer adsorption for more than 40 years. The early work concentrated on the conformations of single chains on a surface.⁶⁷⁻⁷² These were not very practical since by their very nature, surfaces tend to congregate material. All (early) experimental adsorption resulted in polymer layers of many molecules overlapping themselves and the results could not be compared with theory. Eventually theories took into account the segment-segment interactions in the adsorbed layer.⁷³⁻⁷⁵ The newest methods of theoretical investigation include Monte Carlo calculations,⁷⁶ scaling concepts,⁷⁷ and a number of mean-field theories⁷⁸⁻⁸⁰ of which that of Scheutjens and Fleer (S&F)⁸⁰ is the most comprehensive.

There are three main energetic contributions to consider in polymer adsorption, including solvent and segment interactions with the surface, conformational entropy losses of the polymer chain and osmotic (crowding) forces in the adsorbed layer (adsorption results in a much higher segment concentration than in the bulk solution). The first of these is described in terms of a surface interaction parameter χ_s .^{73,80} This is the free energy difference per segment when a solvent molecule is displaced from a surface site by a chain segment, the reference states being each component in its pure state (positive χ_s means that the polymer segment wants to adsorb). It should be stressed that χ_s is an energy difference between having a polymer segment or a solvent molecule at the surface. This has a number of consequences. The adsorption can be driven by high interaction energies (exothermic) between the polymer segment and the surface. In a different scenario both interactions (solvent, polymer segment) with the surface can be endothermic (as is the case with many low

energy solids) but the polymer adsorbs because it is the “lesser of two evils”. In this case the polymer chain is acting like a soap molecule to help decrease a highly unfavorable interaction between the surface and the solvent. The choice of solvent has an impact on the adsorption characteristics of a polymer because a solvent with a higher interaction energy (than a given polymer segment) will preclude adsorption of the chain.

The second and third factors controlling polymer adsorption concern the loss of conformational entropy (of the chain upon adsorption) and osmotic (crowding) forces in the adsorbed layer. When chain segments are attached to a surface the total number of possible conformations decreases with respect to a coil in solution, and this in turn decreases the conformational entropy of the chain with respect to that in free solution. The entropy loss is considered to be constant for each successive bound segment¹⁶⁷ and is described theoretically in terms of a critical surface interaction parameter χ_{sc} .^{75,80} This has been determined theoretically^{75,80} to be positive and of the order of a few tenths of a kT .¹⁶⁸ The osmotic term could actually be considered a "crowding term" which is determined by how much segment density can be forced to the surface. For a given adsorbed polymer layer there will be an osmotic force that wants to dilute the polymer segments as much as possible, the most dilute case is as a free random coil. This force tends to work against and limit the adsorption. Due to the long chain nature of polymer coils in solution, how they pack (i.e. what is crowded for them) is related to segment-segment and segment-solvent interactions, thus the Flory/Huggins solution interaction parameter, χ , is the appropriate energy parameter to

consider.⁸⁰ It should also be mentioned that the surface interaction parameter may become important because the crowding that can be tolerated has to be "paid for" by the surface interaction.

Polymer adsorption is governed by a competition between the three forces defined above. A net surface interaction is, in general, needed to drive the adsorption; the decrease in conformational entropy and the osmotic crowding effects tend to work against and limit the adsorption. It is generally accepted that a polymer molecule will not adsorb unless its surface interaction parameter, χ_s , is greater than the critical surface interaction parameter, χ_{sc} .⁸⁰ Recently thin layer chromatography has been used to measure the χ_s and χ_{sc} for a number of polymer/solvent/surface systems.^{84,85,89} Homopolymer physisorption occurs with surface interaction parameters, χ_s , of approximately 0.5 to 4.0 kT. The major term limiting the amount of polymer adsorbed and the diffuseness of the layer¹⁶⁹ seems to be the osmotic crowding forces. The basic picture is the surface-segment interaction energy, χ_s , gained upon adsorption drives more and more polymer to adsorb. As more polymer adsorbs the bound fraction, p , per molecule decreases (and thus so does the interaction energy). Eventually the segment density becomes too high for the surface interactions to "pay for" and the adsorption stops.¹⁷⁰ The goal of this work is to increase the surface interaction energy with respect to the conformational entropy and osmotic effects such that it becomes the dominant energy term. This allows us to do three important things. One, the increase in χ_s by means of specific functionality can overcome the χ_{sc} and solvation forces to induce adsorption in otherwise non-adsorbing systems. Two, the placement of specific functionality can also be used to

increase surface interaction energy which in turn will pay for higher crowding and thus increase the amount of polymer adsorbed. Three, the placement of these groups at specific places along the chain should also allow us to tailor the actual structure of the chains on the surface, for instance using SF on both ends of a chain to suppress all tail formation.

The behavior of polymers and small molecules in solution and, in particular, at surfaces differs as a result of the connectivity of the polymer chain. This is manifest in the fact that the dissolved chain allows a large volume fraction of solvent within its coil boundaries and thus facilitates rather easy deformations. Adsorbed polymer layers are not simple monolayer coverages; the polyfunctional nature of the chain, where each individual segment has the capacity to be attracted to (or repelled by) the surface has a major effect on its adsorption behavior. We see cooperativity effects for polymers where large swings in behavior are seen for relatively small changes in the environment. The transition from nonadsorbing to adsorbing is very rapid and one finds that for:

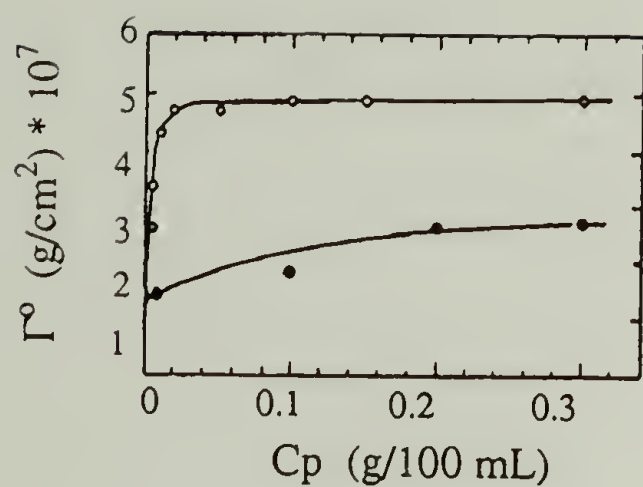
$\chi_s < \chi_{sc}$	Depletion layer	1.1
----------------------	-----------------	-----

$\chi_s > \chi_{sc}$	Adsorption layer	1.2
----------------------	------------------	-----

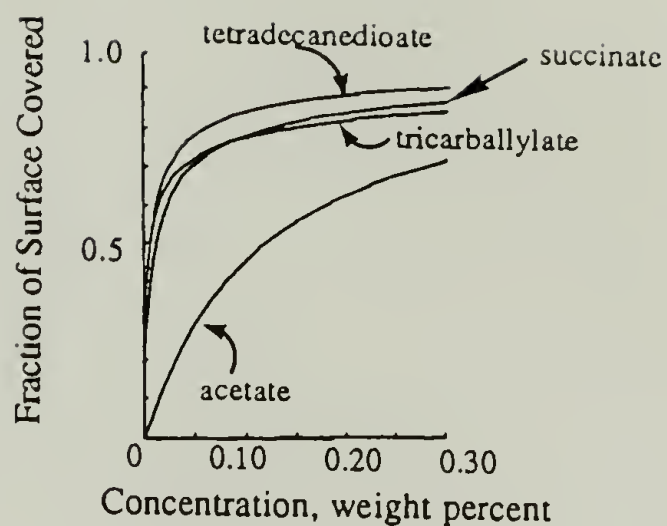
The adsorption layer is usually found to be rather dense at all values of χ_s greater than χ_{sc} . This "all or nothing" critical behavior is typical of polymers and results from chain connectivity. The analogy can be drawn that a small molecule has one "adsorbing foot" per molecule whereas a polymer chain has many. This effect can most easily be seen in the difference in the adsorption isotherms (amount of material adsorbed versus

equilibrium concentration) of polymer chains and small molecules.

Typical polymer isotherm shapes are shown in Figure 1.2(A). These isotherms have the characteristic high affinity shape: a steep rise in amount adsorbed with concentration and then a plateau region at relatively low solute concentrations. The lower molecular weight sample shows the effect of polydispersity in decreasing the affinity of the isotherm. The effect of polyfunctionality is illustrated in Figure 1.2(B): Here the adsorption isotherms of *n*-dodecyl esters with one SF (acetate), two SF (succinate) and three SF (tricarballate) are shown. There is a rapid move to the high affinity type with increase in functionality. The polyfunctionality changes both the rate of adsorption and the rate of desorption. The adsorption rate is increased just by virtue of the fact that once one segment has attached to the surface it has brought a whole bunch of others with it raising the effective concentration of adsorbing species in the vicinity of the surface. On the other hand the rate of desorption is lowered; all the segments must desorb at once in order for a polymer chain to totally desorb and diffuse away from the surface. In essence putting a bunch of adsorbing species on a chain effectively increases the equilibrium constant of the chain relative to the single sticky foot. Another reason for high affinity isotherms of polymers is the size of the molecule vs. the size of the sticking part, i.e. the smaller the bound fraction, p , the more that can be adsorbed: as this ratio gets higher a larger portion of the molecule will not be adsorbed leaving more room for others. This is illustrated in the case of the tetradecanedioate ester which is approximately the same size as the tricarballate but has only two SF. The polyfunctional nature of the chain becomes more important as the sticking energy of the SF decreases.



A



B

Figure 1.2 A) Experimental adsorption isotherms for polystyrene/chrome/cyclohexane (308K); $M_w=7.6 \times 10^6$ (○), $M_w=1.1 \times 10^5$ (●), (reprinted from reference 61). B) Effect of polyfunctionality on adsorption. Smoothed isotherms for n-dodecyl esters on silica from n-decane at 25 °C (reprinted from reference 60).

The scenario discussed so far is that of homopolymer adsorption via segment/surface interactions which are more or less reversible (segment/surface and segment/solvent interactions have low activation energies) and thus leading to a polymer layer that is in dynamic equilibrium. This is not in the same sense as with small molecules though, where different molecules are adsorbed/desorbed (replaced) and diffuse away from the surface. In the case of polymers the segments in the adsorbed layer are in dynamic equilibrium with each other but because of the polyfunctional nature discussed above, the polymer chains themselves rarely diffuse away from the surface. Thus if we stand back and look at the adsorbed layer from a distance we see no real change with time, but if we look closer the coils are exchanging interaction segments and thus their conformations are always changing. This may not be true for all cases: a chain may have sticky feet that are very tightly bound individually leading to kinetic trapping of non-equilibrium conformations and amounts adsorbed on the surface.

The theory of Scheutjens and Fleer (S&F) for homopolymers has been found to be in relatively good agreement with experimental data.⁶² Scheutjens and Fleer found that chains, of 100 or more segments, adsorb with high affinity type isotherms that are commonly found for monodisperse polymers.³⁵ This high affinity has been born out by numerous experiments and, as was discussed, is caused by the connectivity and high molecular weight of the chain. Figure 1.3 shows some of the major conclusions of S&F theory for homopolymer adsorption. They found the amount adsorbed, Γ , to increase with surface-segment interaction, χ_s , as was expected. This can be seen in Figure 1.3 by

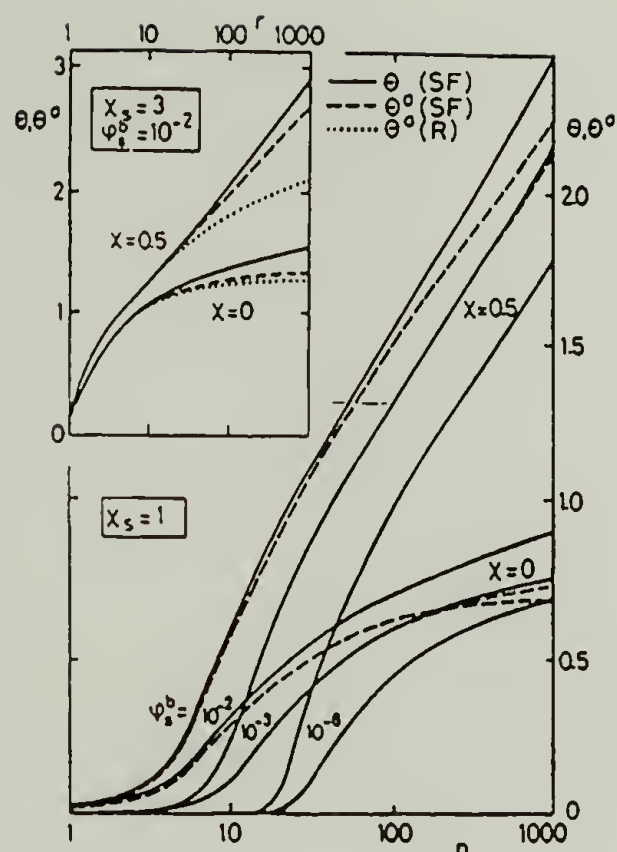


Figure 1.3 The adsorbed amount, Γ (full curves), as a function of chain length, n , for three values of bulk concentration ϕ_s^b and values of χ : $\chi = 0$ (athermal solvent) and $\chi = 0.5$ (theta solvent). The inset shows the effect of increasing the interaction energy, χ_s (reprinted from reference 62).

comparing the amount adsorbed in the figure ($\chi_s=1$) and in the inset ($\chi_s=3$). The plateau amount adsorbed was found to increase with increasing χ_s up to a plateau level at χ_s values above 2. The surfaces were fully saturated ($\theta=1$) when χ_s reached 4. The theory also predicts Γ to increase with decreasing solvent power. This is shown in Figure 1.3 where the amount adsorbed is plotted for athermal and theta solvents. This has also been borne out by the experiments of Kawaguchi et. al.⁸⁶ The molecular weight dependence was also found to depend on solvent quality; the theory predicts an increase in Γ with MW until a plateau region is reached for a good solvent. The theory predicts no plateau region for the adsorption from a theta solvent (see Figure 1.3). These results have been somewhat substantiated experimentally for polystyrene on chrome⁸⁶ and poly(ethylene oxide) on PS latex.⁸⁷ The main idea here is that both the amount adsorbed and its molecular weight dependence increase as the solvent power decreases (as solvent power increases crowding effects become more prominent). Good solvents expand the polymer coil more than theta solvents do. Adsorbing under theta conditions is akin to adsorbing with a smaller buoy (see below) because more polymer chains can fit. The segment density profile was found to decrease monotonically away from the surface.^{80,88} deGennes predicts a "self-similar" segment density profile where the mesh size in the adsorbed layer grows as the distance away from the surface is increased. Recently it has been shown that this agrees rather well with the calculations of Scheutjens and Fleer.⁸² In general, the relatively small surface/segment interactions are trying to stretch (distort) the chain parallel to plane of the surface. In other words, the interactions tend to flatten the chain to the surface at the expense of higher segment concentration.

Scheutjens and Fleer found that the tails extend much further from the surface than the loops. The tail layer tapers away from the thinner loop layer. These tails make up a very small fraction of the total adsorbed segments but are thought to be very important in hydrodynamics effects and in interactions between surfaces with adsorbed polymer. This suggests that from the practical point of view of using adsorbed polymers for colloidal stabilization, etc., one would want these long tails. It also suggests that from an experimental point of view, if one wants to see different characteristics between say sticky feet on the ends vs. in the middle, hydrodynamic measurements might show the most sensitivity.

Surface coverage, θ , and bound fraction, p , were found to correlate best with the amount adsorbed. The percentage of segments in trains decreases and the percentage in loops increase with increasing with N . (This makes rather intuitive sense.) As the surface gets effectively filled up, the segments have to be in either loops or tails and because there can at most be only two tails no matter how long the chain is, and most of the extra segments have to go into loops. S&F also show that the amount adsorbed is a linear function of $\log N$ in a theta solvent, whereas in good solvents it levels off at high N .

Copolymer Adsorption: Background and Discussion

A direct extension of homopolymer adsorption is copolymer adsorption. As in other areas of polymer applications the use of a copolymer allows much more control over the properties of a polymer system. As a case in point, we can look at the area of colloidal stabilization and destabilization.⁵⁸ Colloidal dispersions are small (1-100 nm) particles

dispersed in a medium (for our applications a liquid). The surface to volume ratio is such that if the particles get close enough together, van der Waals interactions are strong enough to stick them together (van der Waals forces drop off rapidly with distance). This aggregation or flocculation is often detrimental to the properties of the system. It has been found that polymers can stabilize these systems from this aggregation by adsorbing to the surface and forming a repulsive corona of polymer segments around the particle. The repulsion comes from an increase in osmotic crowding as two particles are brought close enough together that their adsorbed layers touch. This keeps the particles far enough apart to keep the van der Waals attractions at bay. There is a major dilemma with homopolymers in this regard. One needs a large amount of rather tightly held polymer adsorbed to form a dense layer (poor solvent conditions) but the layer thickness should be large to keep the van der Waals attraction as low as possible (good solvent conditions). It is found, however, that repulsion of the two layers in theta conditions is not strong enough and the particles flocculate. Under good solvent conditions the adsorbed layers repel each other, but the amount of polymer adsorbed is often low and easily desorbed. Some polymers have been found to fulfill stabilization requirements at high surface coverages but it has been seen that at low surface coverages (all adsorption must go through this point at least once) the polymer chains can bridge between particles and cause flocculation. Homopolymers are also relatively weakly held (as opposed to block copolymers) and can be desorbed by increasing the osmotic crowding in a surface forces apparatus. Klein et. al. have reported both the pressure induced desorption and the bridging effect in polystyrene adsorption to mica.^{93,94} Copolymers are the obvious solution to the above problems. It has been shown numerous times

that the incorporation of comonomers or end-functionality to a polymer chain can greatly enhance the amount of polymer adsorbed.

^{115,117,120,130,137} Thus block copolymers can be made to have one block (the anchor block) to anchor the chain strongly to the surface while the other block (buoy) is extended out into (solution in good solvent) to form a dense, repulsive polymer brush.

The applications of these polymer brush concepts to understanding things like this colloidal stabilization and polymer micelles has led to a large amount of experimental¹⁵⁵⁻¹⁶² and theoretical work.^{76,78,79,147-154} These are systems in which the polymer is tethered to the surface by one end; in most cases it is assumed that the brush-forming polymer chain does not interact with the surface. Experimentally polymer brushes can be obtained by grafting the chain end covalently (or some other strong bond type) to the surface or adsorbing block copolymers to the surface where one of the blocks is used to anchor the chain to the surface and the other end is stretched out into the solution forming the brush. Recent predictions of the structure of these grafted layers include the scaling approach of Alexander¹⁴⁷ and deGennes,¹⁴⁸ mean field theories of Scheutjens and Fleer,⁷⁶ Ploehn and Russel,⁷⁸ and Milner, Witten and Cates,⁷⁹ Monte Carlo calculations of Cosgrove⁷⁶ et. al., Chakrabarti¹⁴⁹ and molecular dynamics simulations of Murat and Grest.¹⁵⁰ In each of the above treatments the main parameters that determine the layer thickness are the length of the chain, N , and the graft density, σ .¹⁷² These theories concentrate on predicting the layer thickness, segment density profile and repulsion characteristics (surface forces apparatus and colloidal stabilization). They all, to first approximation, determine that the thickness of the adsorbed

layer, L , is proportional to N and to the cube root of the graft density as shown in Equation 1.3 where a is the monomer length (this is deGennes' original prediction).

$$L = N \sigma^{1/3} a \quad 1.3$$

The theories of Alexander¹⁴⁷ and deGennes¹⁴⁸ determine a step function for the segment density profile, $\rho(z)$. More recently Milner et. al.⁷⁹ have determined that the density profile should be parabolic in shape. S&F theory and Monte Carlo calculations predict a maximum in $\rho(z)$ at a distance close to the surface followed by a decrease which is approximately parabolic.⁷⁶ The agreement of these different theories has been discussed recently by Milner¹⁵¹ and Wijmans.¹⁵⁴ The experimental verification has been slower in coming and has basically been studied by neutron scattering and reflectivity experiments or by measurements using the surface forces apparatus. Experimental verification has been hampered by the fact that the theories have treated the graft density as an adjustable parameter rather than the dependent variable that it is in real systems. This is somewhat a result of one of the main physical characteristics (and thus main assumptions): that the chains are in the "strong stretching" regime. This requires a high graft density to force the over-crowded chains to stretch out normal to the surface. Experimentally this is neither easily achieved nor easily verified. By its nature the "strong stretching" regime is a relatively high energy state requiring the chains to be distorted from their usual dimensions. (These factors have been discussed in the block copolymer adsorption theories of Marques,^{103,104} Munch¹⁰⁵ and Evers^{95,96,97}). Many experimental verifications of the main scaling

character (Equation 1.3) have been reported^{110,126,129} and density profiles resembling those predicted have been seen by neutron reflectivity.^{108,111}

Block and random copolymers have been studied from the more practical viewpoint of how much polymer is adsorbed and the kinetics of this adsorption process has been discussed. Both of these aspects have been addressed experimentally.

Block copolymer adsorption theories have been proposed by Munch et. al.¹⁰⁵ and Marques et. al.¹⁰⁴ for selective solvents, and Marques et. al.¹⁰³ and Evers et. al.^{95,96,97} for non-selective solvents. The salient feature of each of these theories is that the amount of polymer adsorbed is a function of the length of both blocks. In the theory of Marques and Joanny (MJ), the polymer is anchored by the A block (N_A segments) which adsorbs pretty much as a homopolymer in a good solvent so it has a "fluffy" self-similar structure at the solid surface, and the buoy block (B, N_B segments) is stretched out into solution. They consider the surface interaction energy (χ_s) to be large and define the asymmetry factor β , as the ratio of the Flory radii of the two blocks.

$$\beta = (N_A/N_B)^{3/5} = R_{Bf}/R_{Af} \text{ asymmetry factor} \quad 1.4$$

They regard the layer thickness to vary as predicted by brush theories, as in Equation 1.3 ($L = N_B \sigma^{1/3} a$). The graft density is determined by the relative sizes of the two blocks and they predict three scaling regimes based on the value of N_A and N_B with respect to β (Table 1.1).

Table 1.1 MJ Block Copolymer Scaling Regimes.

<u>Regime</u>	<u>Graft Density</u>	<u>Layer Thickness^a</u>
MJ-3D $1 < \beta < N_A^{1/2}$	$N_A^{-1/2}$	$N_B N_A^{1/3} a$
MJ-2D (semi-dilute) $N_A^{1/2} < \beta < N_A^{3/4}$	β^{-2}	$N_B^{3/5} N_A^{2/5} a$
MJ-2D (dilute) $\beta > N_A^{3/4}$	β^{-2}	$N_B^{3/5} N_A^{2/5} a$

^a a is the linear dimension of a monomer unit.

Guzonas et. al.¹²⁶ refined the MJ theory and defined three regimes of their own which are denoted as highly asymmetric (regime I), moderately asymmetric (regime II), and symmetric (regime III). The highly asymmetric regime corresponds to both MJ-2D regimes while the moderately asymmetric case corresponds to the MJ-3D case. The symmetric regime ($\beta > 1$) has no MJ counterpart and corresponds to the regime where the anchor block is larger than the buoy. In this case there is no interaction and no stretch in the buoy block. Chains in this regime are not stretched and the polymer follows homopolymer adsorption behavior and the amount adsorbed is only a function of the sticky block. The layer thickness does not scale as in the stretched regimes. At smaller anchor block sizes (with respect to the buoy block) the polymer is in regime II. Here the buoys overlap and are stretched, but the graft density is only a function of the sticky block size ($\sigma = N_A^{-1}$). This is just a result of the space filling constraint and mass balance. The amount adsorbed is then in given in Equation 1.5.

$$\Gamma = (N_A + N_B) \sigma \quad 1.5$$

For chains of constant length, Γ is equal to $1/v_A$ (v_A =mole fraction of SF, $\Gamma=N/v_A N=1/v_A$). In these first two regimes, the graft density and amount adsorbed depend only on the size of the anchor block and are thus anchor dominated. At (relatively) smaller sticky block sizes, the buoy block is large enough to affect the energy balance significantly and the graft density is a function of both blocks ($\sigma=\beta^{-2}$) (anchor/buoy regime). A drop in the graft density and the amount adsorbed is observed. The cross-over, from anchor dominated to the anchor buoy regime occurs at $\beta=N_A^{1/2}$. Figure 1.4(A) plots the graft density and Figure 1.4(B) the amount adsorbed in these two regions as a function of mole fraction SF (PEO fraction in this case) for a number of different chain lengths. The amount of polymer adsorbed at all molecular weights follows the $1/v_A$ curve in the anchor dominated regime ($\beta < N_A^{1/2}$) until the cross over to the anchor/buoy regime at $\beta=N_A^{1/2}$. Note that the maximum occurs at lower values of v_A as the chain length is increased and this also results in more polymer adsorbed for the longer polymers. This, we propose is due primarily to the geometry imposed when the sticky block lies on the surface; the surface area required for the anchor is considered a linear function of N_A . Layer thickness can be calculated from Equation 1.3 for the anchor dominated regime ($L=N_B N_A^{-1/3}$). This gives a segment density in the brush as:

$$\rho(x)_{\text{average}} = N_B / (N_B N_A^{2/3}) \quad 1.6$$

which simplifies to

$$\rho(x)_{\text{average}} = N^{-2/3} v_A^{-2/3} \quad 1.7$$

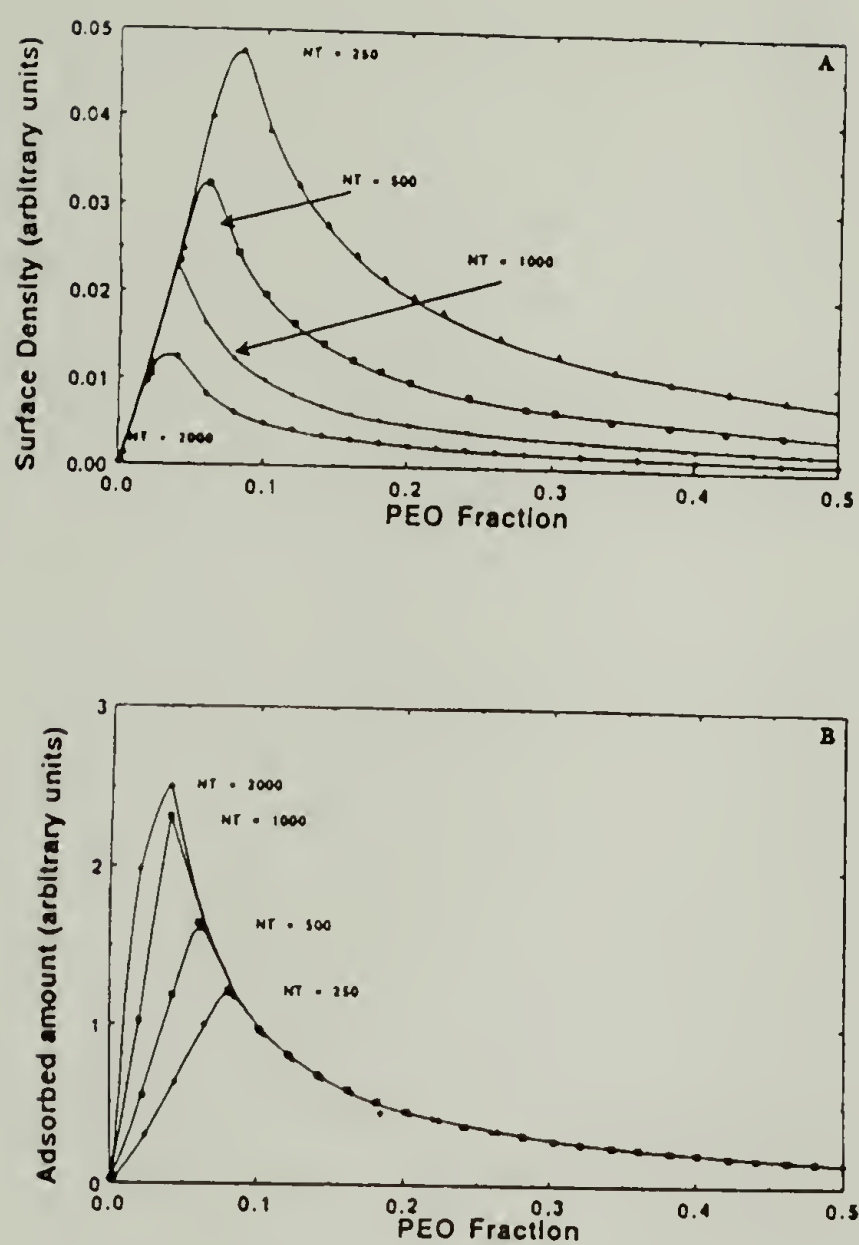


Figure 1.4 Graft density (A) and amount adsorbed vs. mole fraction sticky block for diblock copolymers calculated using MJ diblock theory (reprinted from reference 126).

Thus if there is some threshold segment density, ρ_{\max} , that cannot be tolerated, then the composition at which this occurs, v_A^{\max} , can be calculated as

$$v_A^{\max} = \rho_{\max}^{-3/2} N^{-1} \quad 1.8$$

From Equation 1.7 we see that the segment density is a decreasing function of N ; this explains the N dependence that is seen in Figure 1.4. All molecular weights follow the same curve ($\Gamma=1/v_A$) in the anchor dominated regime and the Γ drops when the segment density becomes a factor. This can be estimated as v_A^{\max} and as Equation 1.8 shows, this gets smaller as the chain gets larger.

Evers et. al. have applied S&F mean field lattice theory to the case of block copolymer adsorption.^{95, 96, 97} They look at the effects of solvent quality, surface affinity, molecular weight and copolymer composition on such properties as the amount adsorbed, hydrodynamic thickness and the the segment density distribution in the vicinity of the surface. Diblock (AB) and triblock (ABA) type copolymers are considered (the A block is sticky). All bulk χ parameters are assumed to be less than or equal to 0.5 ($\chi_{AB}, \chi_{AO}, \chi_{BO} \leq 0.5$) and micelle formation is not considered (experimentally for the case of selective solvents micelle formation has been found to be a factor in the adsorption).^{117,115} They find that the A block adsorbs almost flat on the surface with the B block forming almost entirely tails for the AB copolymer and almost entirely loops for the triblock $A_{100}B_{200}A_{100}$ ($\chi_{AS}=-10$, is the surface interaction parameter for the A block; in this theory strong adsorption means negative χ_s

parameters). There is also some evidence for a small amount of sticky ended tails in the case of the triblock adsorption. It is also seen (for the symmetric diblock case) that increasing χ_{BS} to a strong surface interaction (but not as strong as χ_{AS}) does not have much effect on the adsorbed layer structure; the A block still competes effectively and covers the surface so the B block cannot adsorb. This is different than what is seen for the case of grafted polymers where a surface interaction of the buoy block will result in a segment density that decreases monotonically away from the surface in much the same way a homopolymer does.⁸⁸ $A_{100}B_{400}$ shows the A block highly flattened and concentrated on the surface (a few atomic layers) whereas the B block is a tail that dangles 80 layers into the solution. They find, as with homopolymers, a weak dependence of amount adsorbed on the solution concentration; it increases with increasing concentration. The effect of chain composition (at constant chain length) on the amount adsorbed (Evers uses θ^a for the amount adsorbed) is shown in Figure 1.5(a). Note the qualitative resemblance of these curves to the curves predicted by Marques/Joanny (MJ) theory (Figure 1.4 (B)). We see that for a strongly adsorbing A block and total chain segments greater than about 10, Evers et. al. observe a maximum in the amount adsorbed vs. composition plot (they define the v_A where this maximum occurs as v_A^{opt} , the optimum composition). The amount adsorbed increases and the v_A^{opt} shifts to lower SF content as the chain length increases (Evers uses r as the number of segments in the chain, subscripts refer to the blocks). This trend was also seen in the MJ predictions and an explanation was given above (see Equations 1.6, 1.7 and 1.8). Figure 1.5(c) shows that the hydrodynamic layer thickness (Evers calls this δ_h) shows the same general trend as the amount adsorbed: It increases with chain length and shows a

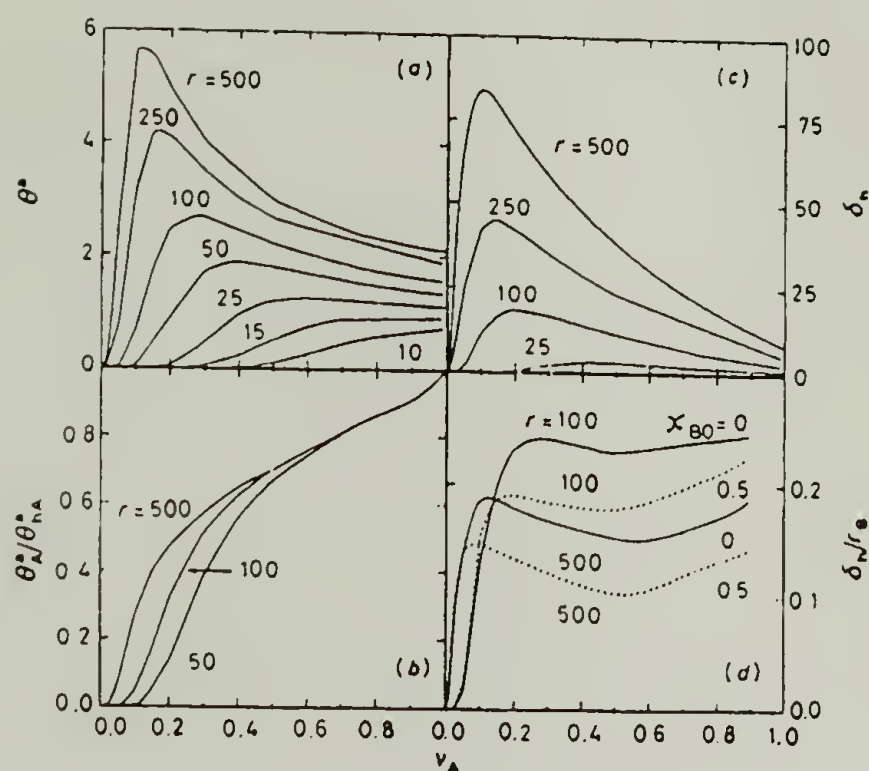


Figure 1.5 The adsorbed amount, θ^a , in equivalents of monolayers (a), the ratio θ_A^a/θ_{hA}^a between the amount of A-segments θ_A^a in adsorbed AB-copolymer and the adsorbed amount θ_{hA}^a of A-homopolymer (b), the hydrodynamic layer thickness, δ_h , in lattice layers (c), and the degree of stretching δ_h/r_b (d), as a function of the fraction, v_a , of A-segments in the AB-copolymer. The total chain length r is indicated. The A-segments are strongly adsorbing ($\chi_{as}=-8$), the B-segments are non-adsorbing ($\chi_{bs}=\chi_{os}=0$). Other parameters: $\chi_{ao}=\chi_{ab}=0.5$, bulk volume fraction $\phi_b=10^{-4}$. In (a)-(c), $\chi_{bo}=0$ and in (d) $\chi_{bo}=0$ or 0.5 (reprinted from reference 96).

maximum at v_A^{opt} . Thus the composition where the copolymer will have its highest adsorbed amount and its largest hydrodynamic thickness is at v_A^{opt} . Figure 1.5(d) plots the δ_h/r_B ratio (\sim hydrodynamic thickness to contour length) as a function of composition. Here we see a measure of how much a chain is stretched (take this as a measure of the incipient crowding) and we see that lower molecular weight chains are stretched more than high molecular weight ones (this is the result derived in Equations 1.6 - 1.8). We also see the expected result with the good and theta solvents: The good solvents give a more expanded layer. Figure 1.5(b) shows a plot of the ratio θ_A^a/θ_{hA}^a versus v_A . The amount of A segments adsorbed for the copolymer is given by θ_A^a and θ_{hA}^a is the corresponding value when homopolymer A of the same chain length is adsorbed. If the same total amount of polymer was adsorbed independent of composition then, $\theta_A^a/\theta_{hA}^a = v_A$. We see this approximated at the high v_A end of the plot. If the amount of A units adsorbed is independent of composition (i.e. $\sigma = 1/N_A$; MJ-3D regime) then $\theta_A^a/\theta_{hA}^a = 1$ at all compositions. As can be seen the actual predictions fall somewhere in between. The following explanation was given: As the fraction of sticky feet in the copolymer decreases, the competition for the surface sites also decreases (there are fewer A segments). This results in an increase in the bound fraction of the A blocks (they find approximately 85% bound at v_A^{opt}). This increase in percentage bound segments expands the area taken by the anchor block on the surface and this results in a slower rise in graft density (and thus amount adsorbed) than the $1/v_A$ that is predicted by just packing constraints (MJ theory). Evers et. al. derive a simple equation that fits the high v_A side of the curves in Figure 1.5(a) fairly well for the higher molecular weights.

$$\theta_A^a = \theta_{hA}^a (1 + \alpha(r_B/r_A)) \quad 1.9$$

Where α is a parameter determined mainly by $\chi_{BS}-\chi_{AS}$: The difference in the surface affinity of the two blocks (for nonadsorbing B blocks this turns into the A block surface affinity, χ_{AS}). The data shown in Figure 1.5 have $\alpha=0.4$, here the B block has no affinity for the surface and the A block's affinity is quite large ($\chi_{AS}=-8$). Equation 1.9 can be rewritten in terms of v_A as shown in Equation 1.10.

$$\theta_A^a = \theta_{hA}^a (\alpha/v_A - \alpha + 1) \quad 1.10$$

This should be compared with the predictions of MJ where the amount adsorbed goes as $1/v_A$. We see that for values of $\alpha < 1$ Evers predicts lower (normalized) amounts adsorbed than the MJ theory but as the value of α approaches 1 the two predictions agree more and are equal at $\alpha=1$. This is to say that Evers predicts a lower amount adsorbed that approaches the MJ predictions at very high SF strength. Figure 1.6 shows Evers data for this effect of the surface affinity of the A block on the amount adsorbed. One can see that as the surface affinity is decreased, the amount of polymer adsorbed decreases and the v_A^{opt} is shifted to higher values. The effect observed here is that the increasing surface affinity of the A block causes more polymer to be adsorbed and the v_A^{opt} occurs at a smaller fraction. Below some critical value the maximum disappears and the amount of copolymer adsorbed is never higher than the sticky homopolymer A. Note the similarity between this plot and Figure 1.5(a) where the chain length was varied. This similarity lends credence to the idea that the buoy repulsions have a larger effect at lower v_A . The v_A^{opt} and the high v_A

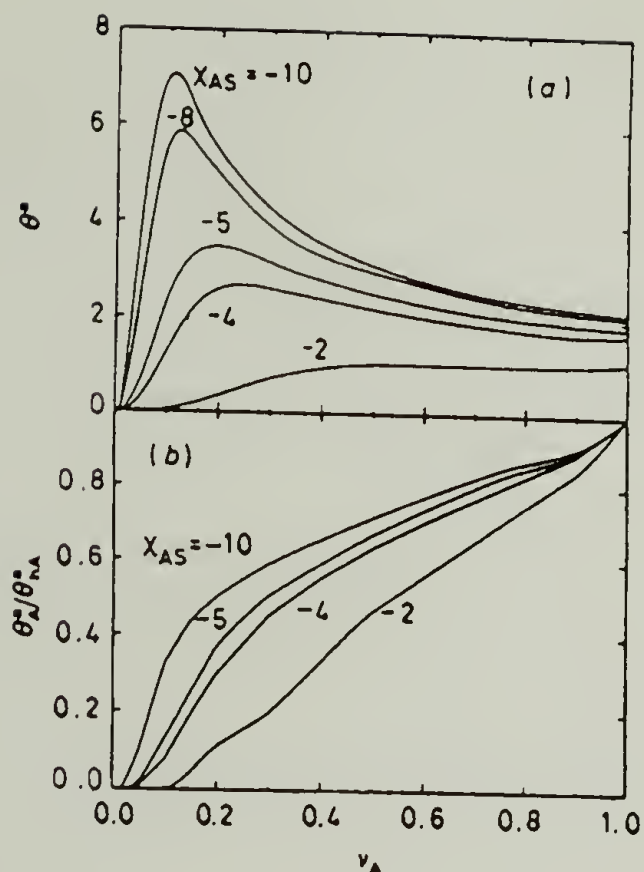


Figure 1.6 The effect of surface affinity of the A-segments on the adsorbed amount. The adsorbed amount θ^a (a) and the ratio θ_A^a/θ_{hA}^a (b) are plotted as a function of the fraction of A-segments per chain, for $r=500$ and for different adsorption affinities of the A-segments. All other parameters are the same as in Figure 1.5 (reprinted from reference 96).

curve shape are functions of this competition; the sticky foot strength is a factor in this competition, although it was ignored by Marques. Evers et. al. also find that, as the sticking strength of the B block increases, a competition (for the surface sites) develops between the two blocks and the maximums are not as pronounced. It should be noted that Evers gives no descriptions of how α is calculated and an asymptote at 1 is not mentioned. Equation 1.10 gives even higher amounts adsorbed at values of $\alpha > 1$. It should be noted though, that we do not expect α to go too high because: We see that for a fairly high surface interaction ($\chi_{AS} = -8$), $\alpha = 0.4$.

Plots of the amount adsorbed where the A block size is held constant and the buoy size is increased are shown in Figure 1.7. What we see is another substantiation of the line of reasoning developed above. What Evers et. al. find is (what we expect intuitively) that initially the amount adsorbed increases until a maximum at some value of r_B , and then the amount adsorbed starts decreasing again. The r_B value at which the maximum occurs increases with increasing r_A . Thus we see the anchor dominated, anchor/buoy and buoy dominated regimes.

Their results also indicate that the layer thickness is larger with increased solvent quality for the B block. The effect of solvent quality on the amount adsorbed is a function of the length of the A block and its surface affinity. In other words, in the anchor dominated regime, a better solvent for the B block will expand the adsorbed layer but will not affect how much polymer is adsorbed. This has been seen by Webster in the adsorption of PS-PVP block copolymers onto mica.¹¹⁶ The hydrodynamic layer thickness was calculated from the measured pressure drop through a

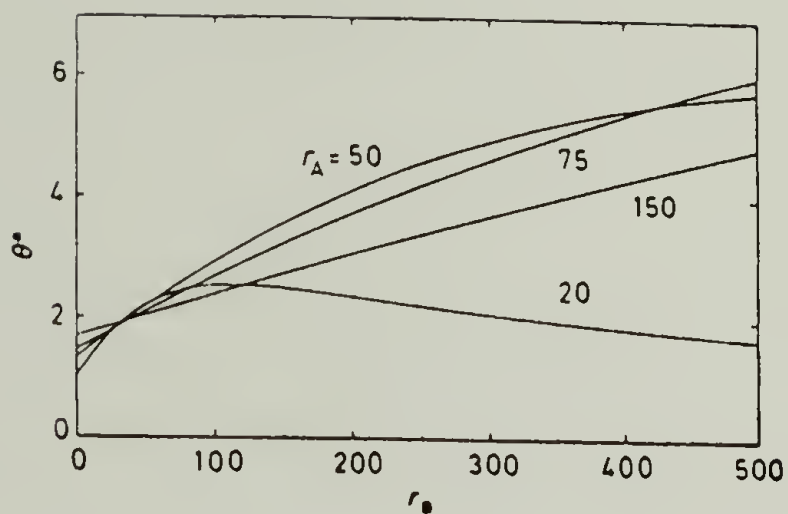


Figure 1.7 The adsorbed amount, θ^a , as a function of the number, r_b , of B-segments per chain at various values of r_a . In this case $\chi_{bo}=0$ and all other parameters are the same as Figure 1.5 (reprinted from reference 96).

porous mica wafer. They found that toluene gave a larger thickness than heptane in this case (toluene is a good solvent for PS whereas heptane is a poor one).

Another result that Evers obtained (that is important to this work) is that for given AB (diblock) and BAB (triblock) copolymers of the same overall composition, the diblock adsorbs more. It looks like the difference increases as the polymer moves further into the anchor/buoy regime. The corresponding layer thicknesses act accordingly.

Marques et. al.¹⁰⁴ have discussed these effects for the case of a selective solvent. They assume the anchor block is in bad solvent conditions: The A block is thought to precipitate out on the surface and form a very concentrated wetting layer. The results are similar to those described above for a nonselective solvent. At relatively high SF content the amount adsorbed is mostly a function of the molecular weight of the anchor block and is basically just a space filling type constraint. Then as the relative sizes become more disproportionate the buoy block begins to have an effect. This eventually results in a maximum in the amount adsorbed as a function of SF content.

Experimentally these general trends of of an anchor dominated regime, anchor/buoy regime and buoy dominated regime (i.e. no adsorption) have been seen. Most recently Wu et.al.¹³⁰ reported a maximum in the amount adsorbed versus %SF curve for the case of methyl methacrylate/(dimethylamino)ethyl methacrylate copolymers adsorbed onto colloidal silica from 2-propanol. In this case the MMA segments are

non-adsorbing under the experimental conditions whereas the DMAEM units are strongly adsorbing. In this data they observe that the amount adsorbed and v_A^{\max} both increase with MW. Their data was replotted and discussed by Guzonas et. al.¹²⁷ the data can be seen in Figure 1.8. The data fit well qualitatively with predictions of both Marques and Evers. Guzonas et. al.¹²⁶ also report their data for the adsorption of styrene/ethylene oxide copolymers to mica from toluene. These data are shown in Figure 1.9; no maximum was confirmed but one can see that the data fit pretty well to that predicted by MJ.

Kawaguchi et al.¹³⁷ have reported a maximum in a plot of the amount adsorbed vs. composition for MMA/Styrene random copolymers adsorbed onto silica (aerosil) from carbon tetrachloride. In this case both homopolymers adsorb (PMMA (1.0 mg/m²; PS 0.5 mg/m²). They found the maximum occurred at approximately 25% MMA with an adsorbance of about 1.4 mg/m². They also did similar experiments using styrene/butadiene random copolymers onto silica (aerosil) from cyclohexane.¹⁴⁰ Here the interaction energy is presumably not as strong; they see (as predicted by Evers for low sticking energies) no maximum in the amount adsorbed versus composition data. Cosgrove et. al.¹³⁶ found that random incorporation of either 1% or 5% (dimethylamino)ethyl methacrylate in PMMA resulted in large increases in the amount adsorbed to silica as measured by SANS. They also did Monte Carlo simulations which predicted the behavior. Parsonage et al.¹²⁹ have made an extensive study of the function of chain composition on the amount adsorbed for PS/PVP block copolymers onto mica from toluene (selective solvent); their data indicate the same trends as above. Stouffer et al.¹²⁰ have adsorbed

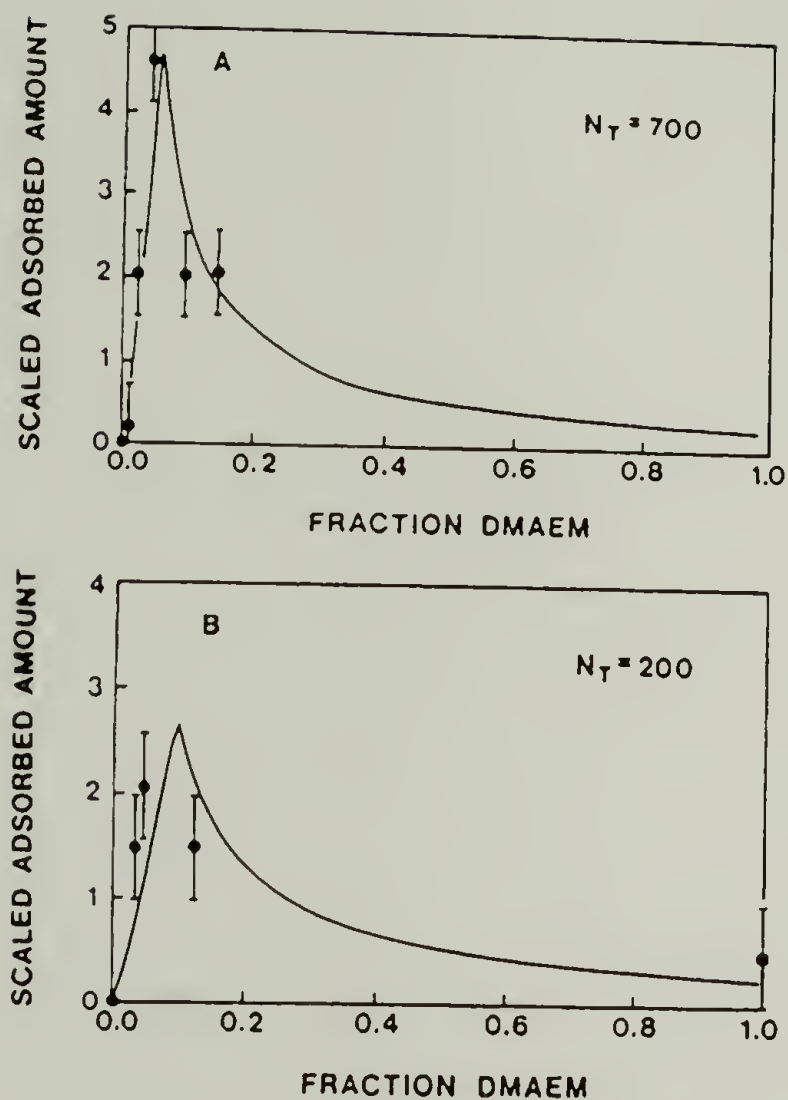


Figure 1.8 Experimental data of Wu et. al. for the adsorption of MMA/DMAEM copolymers onto silica from 2-propanol. The solid lines are the calculated predictions from MJ theory (reprinted from reference 127).

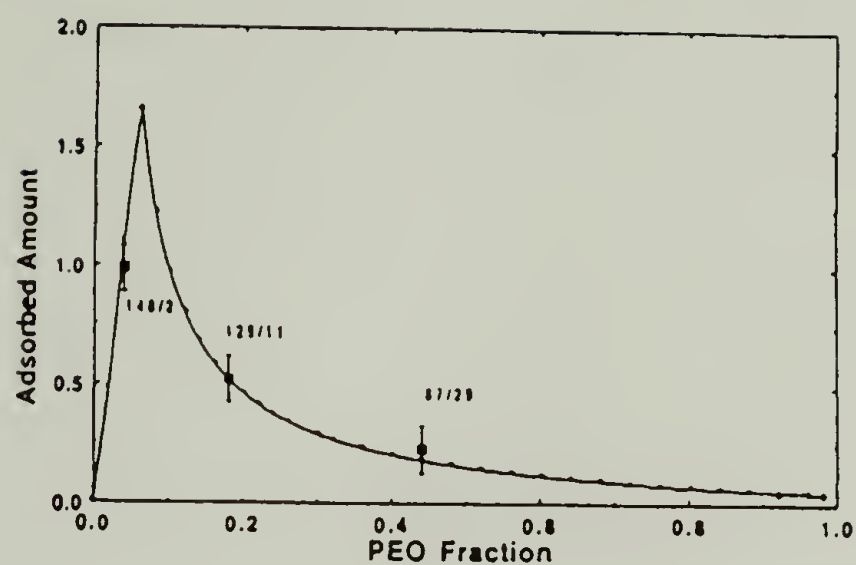


Figure 1.9 Comparison of measured values of the adsorbed amount, as a function of the PEO fraction, with the predicted behavior by the MJ model for the adsorbed amount at a total chain length of $N_T=1500$ (reprinted from reference 126).

styrene/propylene sulfide block copolymers on gold from THF. They report an increasing amount adsorbed as the %SF is decreased; a maximum is not observed but the curve is seen to level out at low %SF. This behavior can be anticipated due to the very large gold/sulfide interaction energy. Munch and Gast ¹¹⁵ and Tassin et al.¹¹⁷ have also reported that the amount adsorbed is dependent on both blocks. These results serve to confirm the theories of Marques and Evers in at least a qualitative sense and also show the range of behavior that can be exhibited due to different SF strengths, etc. An additional proof of the competition between the surface interaction energy and the osmotic crowding can be seen in the recently reported data of Klein et. al.¹⁶⁰ They adsorb PS-X ($X = N^+(CH_3)_2(CH_2)_3SO_3^-$) onto mica in a surface forces apparatus. They find that PS-X ($M_n=26.5K$) can easily displace the PS-X ($M_n=375K$). But the displacement does not work in the other direction. The adsorbed shorter chain is more favorable because the crowding forces are not as strong (but the interaction energy for both chains is the same because these chains are just end-functionalized, i.e. one SF per chain). These types of trends (tradeoffs between strength of SF and osmotic crowding) can also be seen in the work of Iyengar et. al.¹⁵⁵ with carboxyl and hydroxyl terminated polystyrenes.

The kinetics of block copolymer adsorption has also been studied in theory⁹⁹ and experiments.^{109,112,113,115,117} It is reported that adsorption is generally much faster than that of homopolymers (usually using a much stronger sticky foot). It is generally found that the adsorption proceeds in at least two stages. The first stage is extremely fast (the surface is usually saturated in less than 5 min); the surface is just completely covered by

adsorbing polymer. The second stage (time on the order of hours) begins when the chains have to diffuse through this initial adsorbed layer. It has also been reported¹⁰⁹ that another extremely long time process exists where the adsorbed polymer relaxes and rearranges.

We propose the following interpretation of block copolymer adsorption. The polymers are anchored to the surface via the sticky block. The driving force for the adsorption is either strong surface-segment interactions between the sticky block and the surface or poor solvent quality for the sticky block. The total chain interaction energy is raised by increasing the number of sticky feet (block size), increasing the sticking energy per foot, increasing the bound fraction of the sticky block or decreasing the solvent quality for the sticky block. The forces opposing the adsorption are osmotic crowding and chain stretching in the buoy polymer, caused by the high segment density. Increases in the buoy block length (other variables held constant) and solvent power (for the buoy block) oppose the adsorption. The amount of chains adsorbed (graft density) is the result of equilibrium between these opposing forces. The thickness of the adsorbed layer ($L=N_B\sigma^{1/3}$) is directly related to the amount adsorbed (grafting density) and thus it is dependent on this equilibrium also. For the case where the surface interaction is the dominant force, the amount adsorbed is determined by the surface area available and the size of the sticky block, i.e. a small block take up less room on the surface and allows more chains to be adsorbed ($\sigma=N_A^{-1}$). For large sticky blocks (relative to the buoy) the surface interaction energy is large and the buoy stretching (crowding) is small. Thus the surface interaction dominates and the grafting density depends mostly on the sticky block. As the buoy size

increases relative to the sticky block, crowding and stretching energies become important and the resulting graft density is dependent on both blocks (anchor/buoy regime). Where this cross-over, from one regime to another, takes place depends on the sticky foot strength and the goodness of the solvent. MJ theory predicts this at $\beta=N_A^{1/2}$ whereas Evers results show that it depends on sticky foot strength. We propose that MJ theory is the limit of Evers theory at very high χ_s . The Evers theory gives a more gradual transition from anchor dominated to anchor/buoy regime that begins at higher v_A and is a function of the sticky foot strength. An additional complication in the above scenario is that the bound fraction of the sticky block may also change with changing conditions. This may in fact be the mechanism for the transition between the two regimes. For example the bound fraction of a sticky block may increase (thus increase the chain interaction energy) to compensate for the additional segment density that a decrease in v_A effects: This change in the bound fraction may well affect the surface packing density of the sticky block and thus bring about changes in this regard also. Thus buoy crowding opposes the adsorption and SF interaction energy drives it. The buoy repulsions are increased with decreasing molecular weight and the interaction energy is decreased with a decrease in the χ_{AS} . We see the similarity in these two parameters by comparing their effect on the amount adsorbed as seen in Figures 1.5 and 1.6. This competition is manifest first as a change in the shape the of the Γ versus v_A curve and ultimately in the location of the maximum; factors opposing adsorption cause a shift to lower values of v_A^{opt} . Deconvolution of these different effects warrants further investigation and some of those aspects will be addressed in subsequent pages of this thesis. We view sticky foot polymer adsorption in much the

same way as discussed for block copolymers above but with the added variable of sticky foot architecture along the chain. The chain architecture is seen to affect the adsorbed layer thickness and thus the segment density. It is postulated that a triblock copolymer ABA will adsorb as a loop structure (Evers predicts this to be true) and thus have a smaller layer thickness (and thus a higher segment density) than a diblock copolymer with the same molecular weight and composition. This higher density will in turn affect the energy balance and cause the transition from anchor dominated to anchor/buoy regime to occur at higher v_A . The data presented in chapter III show that this results in lower amount adsorbed. As has already been presented Evers predicts a smaller adsorbed amount for BAB triblocks (these triblocks should also have enhanced segment density over the triblocks as well). In this thesis we investigate the relation between the adsorbed polymer layer and the polymer composition, architecture and molecular weight.

Table 1.2 List of Symbols for Adsorption Discussion.

<u>Symbol</u>	<u>Description</u>
Γ	Amount of polymer Adsorbed (also called the adsorbance). Has units of weight or equivalent monolayers per area. Also has the θ symbol in discussions of Evers theory.
θ	Fractional Surface Coverage
p	Bound fraction
L	Layer thickness (solvent swelled)

continued next page

Table 1.2 continued

χ_{sc}	Critical surface interaction parameter.
χ_s	Surface interaction parameter. The energy gained when a polymer segment replaces a solvent molecule adsorbed to the surface (positive means adsorption favored).
χ_{AS}	Surface interaction parameter of block A in copolymer adsorption. (negative means that the block is strongly adsorbed).
χ_{BS}	Surface interaction parameter of block B in copolymer adsorption. (negative means that the block is strongly adsorbed).
χ	Flory/Huggins interaction parameter (Polymer/solvent).
χ_{AB}	Flory/Huggins interaction parameter (A block/B block).
χ_{A0}	Flory/Huggins interaction parameter (A block/solvent).
χ_{B0}	Flory/Huggins interaction parameter (B block/solvent).
N	Chain length (number of Segments).
N_A	Chain length of A block (number of A Segments).
N_B	Chain length of B block (number of B Segments).
$\rho(z)$	Segment density distribution away from the surface.
ρ_{max}	Segment density maximum.
σ	Chain graft density.
a	Linear dimension of a monomer unit.
β	Asymmetry factor.
v_A	Mole fraction of A segments in the copolymer.
v_A^{max}	Mole fraction of A segments in the copolymer when the maximum segment density is reached.
v_A^{opt}	Mole fraction of A segments in the copolymer when the maximum in the amount adsorbed is reached (in Evers theory).

Synthetic Aspects

An essential prerequisite to the study of the adsorption of specifically functionalized polymers is the synthesis of these types of polymers with these types of structures (Figure 1.1). This synthesis is not a trivial matter and a large portion of the work presented here concerns the synthetic aspects of the project. The synthesis must allow control over the size and placement of the sticky blocks along the chain (i.e. block architecture) and over the overall chain size and composition; low polydispersities are required for all structural distributions of the chains. Ideally, this synthesis would be versatile enough to allow chemical manipulation to change the chemical structure of the sticky feet. For the block copolymers that we desire to use for adsorption, the chemical composition of the two portions of the chain must be dissimilar enough (in terms of polarity) that one type of copolymer segment will act as a sticky foot and adsorb preferentially; this requires incorporation of polar functionality into the chain. As will be discussed, this polar functionality adds a new dimension of complexity to the synthesis of these block structures. It will be shown that the synthetic route developed in this thesis work accomplishes the goals for the structural control elements that were enumerated above. Such control over the structure of polar block copolymers has rarely been reported in the literature previously.

Living polymerization is the means of choice for the preparation of polymers with block structures and narrow distributions. The basic requirements, regardless of the means of propagation (anionic, cationic, ROMP etc.) are fast initiation and lack of unintentional termination reactions of the propagating chain end. In these systems each initiator

molecule yields one polymer chain. All chains are initiated and grow simultaneously until the monomer is gone; this results in chains that are very close to the same length. The degree of polymerization is determined by ratio of monomer to initiator (Equation 1.11).

$$DP_N = [M]/[I] \quad 1.11$$

Because of simultaneous initiation and the absence of transfer and termination reactions the polymerization is found to follow Poisson statistics; this enables preparation of chains and blocks with narrow molecular weight distributions. In a "living" system the reactive chain end remains active until deliberately terminated (killed). Because of this living nature, diblock copolymers can be prepared by the addition of a second monomer, M_2 , after consumption of M_1 . If M_2 will also initiate polymerization of M_1 (this is not always the case), then a triblock copolymer can be formed via addition of M_1 following consumption of M_2 . In principle, additional blocks can be made in a similar fashion. This synthetic strategy can be used to prepare polymers of essentially any block structure (or sequence). The feasibility of this scheme hinges on the lack of extraneous side reactions of the chain end (i.e. chain transfer to monomer, polymer, solvent etc., or reactions with impurities) which result in dead polymer chain, unable to incorporate more monomer. In general exclusion of these extraneous reactions can be obtained with only specific monomer systems under rigorously clean conditions.¹⁷³⁻¹⁷⁷ From Equation 1.11 it is seen that the amount of initiator used for the polymerization decreases as the desired molecular weight is increased (some manipulation of $[M]$ can be done but ultimately the initiator

concentration must be decreased). The preparation of higher molecular weight polymers requires more stringent adherence to the non-reactivity and purity requirements than the lower molecular weights; thus we will see that high molecular weight living systems are very rare.

In practice, very few systems actually meet all of the requirements assumed in the discussion above. Living anionic techniques ¹⁷²⁻¹⁷⁷ have been the most experimentally profitable although other living systems¹⁷⁸⁻¹⁸¹ have been developed. The "livingness" and hence structural control inherent in these other systems is not as great as in the classic anionic synthesis of vinyl hydrocarbon monomer systems (these monomers such as styrene, butadiene, isoprene and *tert*-butylstyrene have the most "living" qualities ^{173,175}). The remainder of the discussion here will focus specifically on anionic living polymerization and the inherent architectural control possible for the incorporation of polar functionality. Direct polymerization of polar monomers in these living anionic systems is not feasible.¹⁷³ The carbanion can react with the electrophilic and/or acidic moieties on the monomer and the polymer, thus the polymerization is terminated prematurely. Some relatively polar monomers, including propylene oxide, ethylene oxide, propylene sulfide, 2-vinylpyridine and *tert*-butylacrylate are found to be stable under living anionic conditions. Diblock copolymers containing these monomers (and a nonpolar hydrocarbon monomer) can be prepared by initial polymerization of the hydrocarbon monomer followed by addition of the polar monomer. This is the procedure used to prepare most of the block copolymers that have been reported for adsorption studies (including the styrene-propylene sulfide polymers discussed in Chapter IV of this thesis). A major

drawback of these preparations is that only the diblock copolymers can be easily prepared. The higher relative stability of the polar monomer propagating anion precludes its initiation of the first monomer and thus triblock and multi-block structures cannot be prepared by addition of the first monomer again. Triblock copolymers (ABA) can be prepared using double initiation systems such as Na/napthalene, but this requires a new initiation system and allows the preparation of only symmetric block structures. The inverted triblock copolymer (BAB) can be prepared by using new chemistry to couple the living ends. This synthesis requires that the coupling reaction be 100% efficient and again only symmetric block structures can be obtained. No architectures higher than triblocks are possible. End-functionalization has also been researched; procedures for the attachment of a single carboxylic acid or alcohol group have been reported.^{175,182} This method yields only one SF per chain. Double ended and center functionalization have also been achieved through procedures similar to those described above for the block copolymers. The same disadvantages apply as well. A solution to the problem discussed above has been pioneered by Nakahama and associates and involves the polymerization of protected polar monomers followed by deprotection to yield the desired copolymer structure.¹⁸³ This strategy is also used in our group to produce styrene/4-vinylphenol polymers.¹⁸⁴ The phenol is protected as a *tert*-butyldimethylsilyl ether. Some of these polymerizations are reported to reinitiate both monomers and thus a range of block structures can be prepared. Deprotection of the polymerized monomer unit yields the desired block structure. The recent work of Teyssie with tempered (LiCl) anionic polymerizations of methacrylates and methyl methacrylates also have potential for the synthesis of these types of

polymers.¹⁸⁵ The inherent livingness of these systems is less than the straight hydrocarbon monomer systems.

The "most living" anionic systems involve polymerization of vinyl hydrocarbon monomers; these types of monomers are the best example of the general living system discussed above. The drawback with these systems for our studies is the nonpolar (nonsticky) nature of the monomer units. The strategy used in this work was to polymerize precursor polymers of known architecture from these living nonpolar monomer systems and then add polar functionality to one of the copolymer segments via selective modification. This strategy has been used by Kendall et. al. (the McCarthy group) in the preparation of SF polymers via selective modification of the alkene functionality in styrene/butadiene (or isoprene) copolymers.¹⁸⁶ Hydroboration-oxidation was used to obtain alcohols¹⁸⁷ and hydrosilylation was used to incorporate $-\text{Si}(\text{OR})_3$ functionality on the chain. Valint and Bock have reported selective sulfonation of the styrene segments of styrene/*tert*-butyl styrene copolymers to obtain hydrophobically associating diblock and triblock copolymers.^{188,189} The work reported in this thesis utilized the styrene/*tert*-butyl styrene monomer pair as well. The crux of this method is the selective chemical modification of one of the monomers over the other. The first half of Chapter III is devoted to this discussion. Anionic syntheses involve a major amount preparation and purification¹⁷⁴ and these aspects are addressed in Chapter IV.

Surface Analysis Techniques

Analysis of polymer surfaces requires special analytical techniques which probe at very shallow depths. The surface of a material is loosely defined as the region which can be influenced by its environment and, relative to the bulk, this region contains little material, thus bulk analysis yields little information about the surface. Various surface analytical techniques probe the surface at varied depths and reveal different types of information. The major surface analysis techniques used in this work are XPS, ATR-IR, and contact angle measurement. A brief discussion of these three techniques follows.

X-Ray Photoelectron Spectroscopy. X-ray photoelectron spectroscopy (XPS) utilizes the photoelectric effect to reveal the atomic composition of the outer surface region of a material, ranging from depths of 10 - 100 or 200 Å.¹⁹⁰⁻¹⁹² In this technique, the sample is exposed to (nearly) monoenergetic soft x-rays under ultra high vacuum. The x-rays excite the atoms and due to the photoelectric effect electrons are ejected. The detector analyzes the kinetic energy of the core electrons (E_k) and determines the binding energy of an electron in an atomic orbital of the source element (E_b) with

$$E_k = h\nu - E_b - \phi \quad 1.12$$

where $h\nu$ is the energy of the x-ray photons and ϕ is the work function of the spectrometer. Each atomic orbital of every element has a distinct binding energy, and XPS reveals the number of emitted electrons per element present. Other factors are important in quantitative determination of surface atomic composition including sensitivity factor corrections. The

photoelectric cross-sections of the atoms comprising the surface vary and this means that peak sizes between elements cannot be compared directly. Atomic sensitivity factors compensate for differences in electron mean free paths and efficiencies of photoelectron generation and detection between elements.¹⁹²

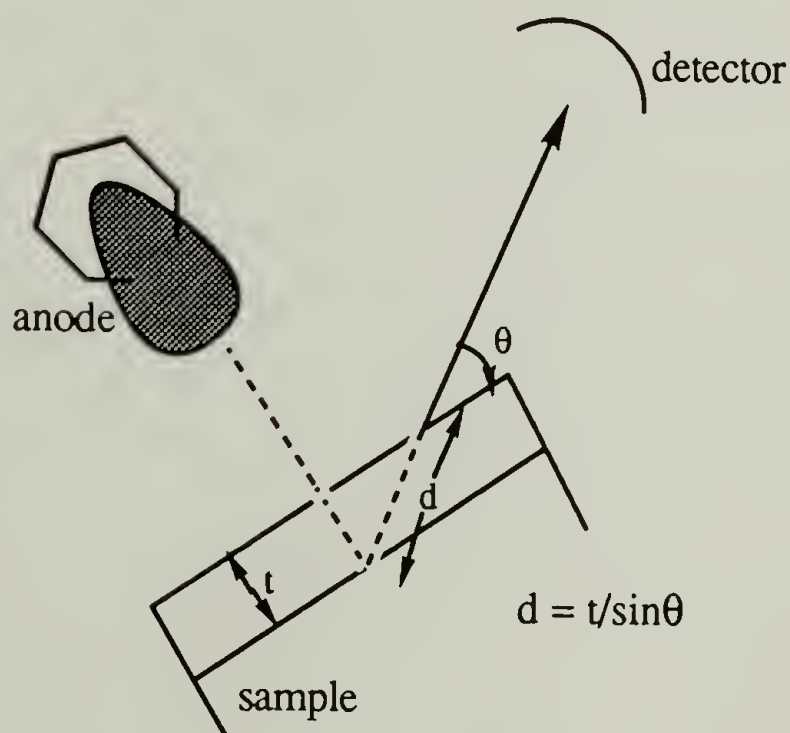
The surface sensitivity of XPS can be ascribed to the finite escape depth of the ejected photoelectrons. Electrons travel only short distances through matter due to inelastic scattering, and as a result XPS sensitivity decreases exponentially with depth. The the number of electrons (N) detected relates to the number ejected (N_0) as

$$N = N_0 e^{-\left(\frac{z}{\lambda \sin \theta}\right)} \quad 1.13$$

where z is the thickness of the material traversed (in the z direction), λ is the mean free path of an electron in a given material and θ is the angle to the detector (from the plane of the sample surface).¹⁹⁰ This exponential decrease in sensitivity indicates that XPS data can be biased high by functionality concentrated in the outermost surface layers. The mean free path of an electron in a material depends on its kinetic energy,¹⁹⁰ and using Mg K_α excitation, the mean free path for C_{1s} electrons has been determined to be 14 Å.¹⁹¹ For XPS analysis of all film samples carried out for this dissertation, both the Mg K_α and Al K_α anodes were used and 14 Å was used as a mean free path length for depth determinations.

Variable angle XPS analysis utilizes the dependence of the escape depth of ejected electrons on the angle between sample and detector, and

this allows assessment of the vertical homogeneity of the sample. At shallow angles, electrons have to travel through more of the solid sample to reach the detector so only those emitted from the outermost layers are analyzed. At steeper angles, electrons ejected from deeper within the sample still reach the detector and this allows analysis of material at greater depths. All samples in this work were analyzed at 15° and 75° takeoff angles (between the plane of the sample surface and detector). The scheme below describes the sample/detector geometry. From integration of



Scheme 1.1 Sample/Detector Geometry in Variable Angle XPS.

equation 1.13 within the limits of 0 to thickness t , we can determine the intensity (or number (N) of electrons detected) as

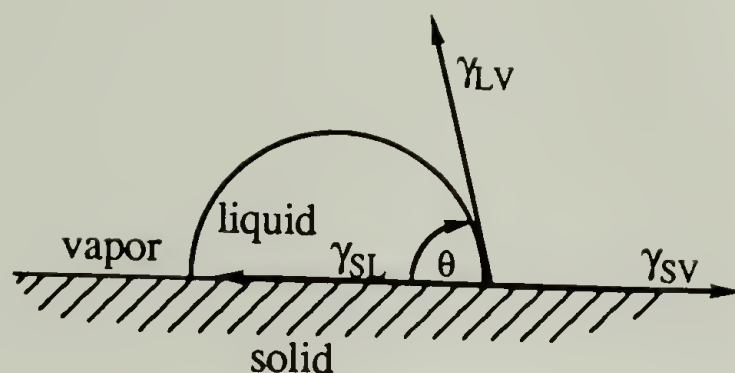
$$N = k\lambda \sin\theta (1 - e^{-\left(\frac{t}{\lambda \sin\theta}\right)}) \quad 1.14$$

where k is a constant. Data from the 15° takeoff angle represent the atomic concentration of the top 11 Å of the film sample and equation 1.14 indicates that 94% of the electrons detected originate from this region. Spectra recorded at the 75° takeoff angle represent the composition of the outer 40 Å of the surface and 95% of the electrons detected are emitted from this region. Roughly 54% of the photoelectrons measured at 75° actually originate in the top 11 Å of the material. For this reason, large discrepancies between data recorded at 15° and 75° can reveal information about the distribution of functionality in a sample.

Contact Angle. Contact angle measurements provide the most surface-selective analysis of all the surface analytical techniques employed because only the outermost layers of the surface are sampled. Contact angle measurements are used to describe the surface tension of a material as well as give an indication of surface wettability. Young's equation¹⁹²

$$\gamma_{sv} - \gamma_{sl} = \gamma_{lv} \cos \theta \quad 1.15$$

treats the angle (θ) formed by a liquid resting on a solid plane as the result of the mechanical equilibrium established as the balance of the three surface tensions involved, namely γ_{sl} from the solid-liquid interface, γ_{lv} from the liquid-vapor interface and γ_{sv} of the solid-vapor interface. For the dynamic measurements made on these surfaces, water was used as the probe fluid, and advancing (θ_A) and receding (θ_R) angles were recorded as



water was added to and withdrawn from the drop. In this technique, it is assumed that the surface is completely smooth, immobile, nondeforming, chemically homogeneous and does not interact with the probe fluid.¹⁹⁴ Within these requirements, a surface should have equal advancing and receding contact angles, but in reality surfaces do not meet all of these requirements and the advancing and receding angles differ; this is termed contact angle hysteresis. Hysteresis can stem from a variety (or combination) of causes, namely chemical heterogeneity,¹⁹⁵ surface roughness,¹⁹⁶ and low mechanical properties of the surface.¹⁹⁴ Swelling of the surface layers with the probe fluid also can cause hysteresis.¹⁹⁴

Attenuated Total Reflectance IR (ATR IR) Spectroscopy.¹⁹⁷ ATR IR spectroscopy enables one to obtain an IR spectrum of the top $\sim 0.1\text{-}1\ \mu\text{m}$ of the sample (note it looks at a much deeper region than either XPS and contact angle). ATR IR is based on the principle of total internal reflection: When a light wave traveling in a more dense medium hits an interface of a less dense medium the light beam is totally reflected (no refraction) if the angle of incidence is lower than Brewster's angle (zero energy loss). This total internal reflection sets up an evanescent wave (in

the rarer medium) with an exponential amplitude decay in the z direction away from the surface. This is given in equation 1.16.

$$E = E_0 \exp(-2\pi/\lambda_1(\sin^2\theta - \eta_2/\eta_1)^2)^{0.5z} \quad 1.16$$

E_0 is the amplitude of the electric field at the interface and η_1 and η_2 are the refractive indices of the denser and rarer media respectively, and λ_1 is the wavelength of radiation in the denser medium (λ/η_1). If an absorbing medium (i.e. the sample) is brought close enough to interact with the evanescent wave, some of the radiation will be absorbed and less than 100% reflection will be obtained. The analytical method involves placing the sample against the side of an internal reflection element (IRE) and then directing IR radiation through the crystal. The sample interacts with the evanescent wave similar to a transmitted light beam and one obtains a IR spectrum of the top layer of the surface.

References

1. For a review, see Ward, W.J.; McCarthy, T.J. In *Encyclopedia of Polymer Science and Engineering*, 2nd ed.; Mark, H.F.; Bikales, N.M.; Overberger, C.G.; Menges, G.; Kroschwitz, J.I., eds.; John Wiley and Sons: New York, 1989; suppl. vol., p. 674.
2. Clark, D. T.; Feast, W. J. *Polymer Surfaces*, Wiley-Interscience: New York, 1978. and references therein.
3. Brewis, D.M.; Briggs, D. *Polymer* **1981**, 22, 7 and references therein.
4. Hsieh, Y.-L.; Timm, D.A.; Wu, M. *J. Appl. Polym. Sci.* **1989**, 38, 1719.
5. Triolo, P.M.; Andrade, J.D. *J. Biomed. Mater. Res.* **1983**, 17, 129.
6. Examples and references will be given subsequently.
7. Bergbreiter, D.E.; Hu, H.-P.; Hein, M.D. *Macromolecules* **1989**, 22, 654.
8. Bergbreiter, D.E.; Chen, Z.; Hu, H.-P.; *Macromolecules* **1984**, 17, 2111.
9. Gagnon, D.R.; McCarthy, T.J. *J. Appl. Polym. Sci.* **1984**, 29, 4335.
10. Cross, E.M.; McCarthy, T.J. *Macromolecules* **1990**, 23, 3921.
11. Ruckenstein, E.; Gourisankar, S.V. *J. Coll. and Interf. Sci.* **1985**, 107, 488.
12. Oster G.; Oster, G.K.; Moroson, H. *J. Polm. Sci.* **1959**, 34, 671.
13. Coopes, I.H.; Gifkins, K.J. *J. Macromol. Sci.-Chem.* **1982**, A17, 217.
14. Yasuda, T.; Okuno, T.; Yoshida, K.; Yasuda, H. *J. Polm. Sci., Polym. Phys.* **1988**, 26, 1781.
15. Corbin, G.A.; Cohen, R.E.; Baddour, R.F. *Macromolecules* **1985**, 18, 98.
16. Clark, D.T.; Feast, E.J.; Musgrave, W.K.R.; Ritchie, I. *J. Polm. Sci. Polym. Chem.* **1975**, 13, 857.
17. Kogoma, M.; Kasai, H.; Takahashi, K.; Moriwaki, T.; Okazaki, S. *J. Phys. D: Appl. Phys.* **1987**, 20, 147.

18. Morra, M.; Occhiello, E.; Garbassi, F. *Langmuir*, **1989**, *5*, 872.
19. Allmér, K.; Hult, A.; Rånby, B. *J. Polym. Sci. Polym. Chem.* **1989**, *27*, 1641.
20. Uchida, E.; Uyama, Y.; Ikada, Y. *J. Polym. Sci. Polym. Chem.* **1989**, *27*, 527.
21. Rasmussen, J.R.; Stredonsky, E.R.; Whitesides, G.M. *J. Am. Chem. Soc.* **1977**, *99*, 4736.
22. Rasmussen, J.R.; Bergbreiter, D.E.; Whitesides, G.M. *J. Am. Chem. Soc.* **1977**, *99*, 4746.
23. Barker, D.J.; Brewis, D.M.; Dahm, R.H. *Polymer* **1978**, *19*, 856.
24. Nambu, K. *J. Appl. Polym. Sci.* **1960**, *4*, 69.
25. Campbell, T.W.; Lyman, D.J. *J. Polym. Sci.* **1961**, *55*, 169.
26. Urban, M.W.; Salazar-Rojas, E.M. *Macromolecules* **1988**, *21*, 372.
27. Gibson, H.W.; Bailey, F.C. *Macromolecules* **1980**, *13*, 34.
28. Matsuda, T.; Litt, M.H. *J. Polym. Sci. Polym. Chem.* **1974**, *12*, 489.
29. Peeling, J.; Clark, D.T. *J. Polym. Sci. Polym. Chem.* **1983**, *21*, 2047.
30. Trott, G.F. *J. Appl. Polym. Sci.* **1974**, *18*, 1411.
31. Batich, C.D.; Wendt, R.C. In *Photon, Electron, and Ion Probes of Polymer Structure and Properties*, Dwight, D.W.; Fabishi, T.J.; Thomas, H.R., eds. ACS Symp. Ser., 1981, *162*, Ch. 15.
32. Everhart, D.S.; Reilley, C.N. *Anal. Chem.* **1981**, *53*, 665.
33. Dias, A.J.; McCarthy, T.J. *Macromolecules* **1984**, *17*, 2529.
34. Brennan, J.V.; McCarthy, T.J. *Polym. Prepr. (Am. Chem. Soc., Div. Polym. Chem.)* **1988**, *29*(2), 338.
35. Brennan, J.V.; McCarthy, T.J. *Polym. Prepr. (Am. Chem. Soc., Div. Polym. Chem.)* **1989**, *30*(2), 152.
36. Shoichet, M.S.; McCarthy, T.J. *Macromolecules* **1991**, *24*, 982.
37. Costello, C.A.; McCarthy, T.J. *Macromolecules* **1987**, *20*, 2819.
38. Costello, C.A.; McCarthy, T.J. *Macromolecules* **1984**, *17*, 2940.
39. Bening, R.C.; McCarthy, T.J. *Macromolecules* **1990**, *23*, 2648.

40. Bee, T.G.; McCarthy, T.J. *Macromolecules* **1992**, *25*, 2093.
41. Lee, K.-W.; McCarthy, T.J. *Macromolecules* **1988**, *21*, 2318.
42. Dias, A.J.; McCarthy, T.J. *Macromolecules* **1987**, *20*, 2068.
43. Dias, A.J.; McCarthy, T.J. *Macromolecules* **1985**, *18*, 1826.
44. Lee, K.-W.; McCarthy, T.J. *Macromolecules* **1988**, *21*, 3353.
45. Kolb, B. U.; Patton, P. A.; McCarthy, T. J. *Macromolecules* **1990**, *23*, 366.
46. Kolb, B. U.; Patton, P. A.; McCarthy, T. J. *Polym. Prepr. (Am. Chem. Soc., Div. Polym. Chem.)*, **1987**, *28*(2), 248.
47. Cross, E.M.; McCarthy, T.J. *Polym. Prepr. (Am. Chem. Soc., Div. Polym. Chem.)* **1989**, *30*(1), 422.
48. Lee, K.-W.; McCarthy, T.J. *Polym. Prepr. (Am. Chem. Soc., Div. Polym. Chem.)* **1987**, *28*, 250.
49. Lee, K.-W.; McCarthy, T.J. *Macromolecules* **1988**, *21*, 309.
50. Franchina, N.L.; McCarthy, T.J. *Macromolecules* **1991**, *24*, 3045.
51. Franchina, N.L.; McCarthy, T.J. In *Chemically Modified Surfaces*; Mottola, H.A.; Steinmetz, J.R. eds., Elsevier Science Publishers: New York, 1991, 173.
52. Franchina, unpublished work on PEEK-alcohol surfaces.
53. A rigorous treatment will be given subsequently.
54. Patton, P. A. Ph.D. Dissertation, Polymer Science and Engineering Department, Univ.of Mass., 1987.
55. Waldman, D. A.; Kolb, B. U.; McCarthy, T. J.; Hsu, S. L. *Langmuir* **1991**, in press.
56. Waldman, D. A.; Kolb, B. U.; McCarthy, T. J.; Hsu, S. L. *Proc. of A.C.S. Div. of Polym. Mat.* **1988**, *59*, 326.
57. Waldman D. A. Ph.D. Dissertation, Polymer Science and Engineering Department, Univ. of Mass., 1990.
58. Napper, D. *Polymeric Stabilization of Colloidal Dispersions*; Academic: London, 1983.

59. For good general reviews see Fontana,⁶⁰ Kawaguchi⁶¹ and Cohen Stuart.⁶²
60. Fontana, J. B. In *The Chemistry of Biological Surfaces* ed. Hair, M. Marcel Dekker: New York 1971.
61. Takahashi, A.; Kawaguchi, M. *Advances in Polymer Science* Vol.46, Springer-Verlag: Berlin Heidelberg, 1982.
62. Cohen Stuart, M. A.; Cosgrove, T.; Vincent, B. *Advances in Coll. & Int. Sci.* **1986**, 24, 143-239.
63. Mittal, K. L. Ed. *Adhesion Aspects of Polymer Coatings*; Plenum: New York, 1983.
64. Leidheiser, H., Jr. In *Corrosion Mechanisms*; Mansfield, F., Ed.; Marcel Dekker: New York, 1987.
65. Hair, M. Ed., *The Chemistry of Biosurfaces*, Vol 1 & 2, Marcel Dekker, New York, 1971.
66. Dorinson, A.; Ludema, K. C. *Mechanisms and Chemistry in Lubrication*; Elsevier: Amsterdam, 1985.
67. Simha, R.; Frish, H. L.; Frish F. R. *J Phys. Chem.* **1953**, 57, 584; Frish, H. L.; Simha, R. *J. Chem. Phys.* **1956**, 24, 652; **1957**, 27, 702.
68. Silberberg, A. *J. Phys. Chem.* **1962**, 66, 1872, 1884; *J. Chem. Phys.* **1967**, 46, 1105.
69. DiMarzio, E. A. *J. Chem. Phys.* **1965**, 42, 2101; DiMarzio, E. A.; McCrackin, F. L. *ibid.*, **1965**, 43, 539; Hoeve, C. A. J.; DiMarzio, E. A.; Peyser, P. *ibid.*, **1965**, 42, 2558.
70. Rubin, R. J.; *J. Chem. Phys.* **1965**, 43, 2392; *J. Res. Natl. Bur. Stand., Sect. B*, **1966**, 70, 237.
71. Roe, R. J. *J. Chem Phys.* **1965**, 43, 1591; **1966**, 44, 4264.
72. Motomura, K.; Matuura, R. *J. Chem. Phys.* **1969**, 50, 1281; Motomura, K.; Sekita, K.; Matuura, R. *Bull. Chem. Soc. Jpn.*, **1971**, 44, 1243; Motomura, K.; Morol, Y.; Matuura, R. *ibid.*, **1971**, 44, 1248.
73. Silberberg, A. *J. Chem. Phys.* **1968**, 48, 2835.
74. Hoeve, C. A. J. *J. Polym. Sci. C*. **1970**, 30, 361; *ibid.*, **1971**, 34, 1.

75. Roe, R. J. *J. Chem. Phys.* **1974**, *60*, 4192.
76. Cosgrove, T.; Heath, T. G.; van Lent, B.; Scheutjens, J. M. H. M. *Macromolecules* **1987**, *20*, 1692-1696; Cosgrove, T. *J. Chem. Soc. Faraday Trans.* **1990**, *86*(9), 1323-1332.
77. deGennes, P. G. *Macromolecules* **1982**, *15*, 492; *Adv. Coll. & Int. Sci.* **1987**, *27*, 189-209.
78. Ploehn, H. J.; Russel, W. B. *Macromolecules* **1988**, *21*, 1075; **1989**, *22*, 266.
79. Milner, S. T.; Witten, T. A.; Cates, M. E. *Macromolecules* **1988**, *21*, 2610-2619.
80. Scheutjens, J. M. H. M.; Fleer, G. J. *J. Phys. Chem.* **1979**, *83*(12), 1619-1635; **1980**, *84*(2), 178-190.
81. Bohmer, M. R.; Evers, O. A.; Scheutjens, J. M. H. M. *Macromolecules*, **1990**, *23*, 2288-2301; Blaakmeer, J.; Bohmer, M. R.; Cohen Stuart, M. A.; Fleer, G. J. *Macromolecules* **1990**, *23*, 2301-2309.
82. van der Linden, C. C.; Leermakers, F. *Macromolecules* **1992**, *25*(13), 3449.
83. Kawaguchi, M.; Funayama, A.; Yamauchi, S.; Takahashi, A.; Kato, T. *J. Coll. & Interface Sci.* **1988**, *121*(1), 130-135.
84. Cohen Stuart, M. A.; Fleer, G. J.; Scheutjens, J. M. H. M. *J. Coll. & Interface Sci.* **1984**, *97*(2), 515-525; **1984**, *97*(2), 526-535.
85. van der Beek, G. P.; Cohen Stuart, M. A.; Fleer, G. J.; Hofman, J. E. *Langmuir* **1989**, *5*, 1180-1186.
86. Kawaguchi, M.; Takahashi, A. *Macromolecules* **1983**, *16*, 1465-1469.
87. Cohen Stuart, M. A.; Waajen, F. H. W. H.; Cosgrove, T.; Vincent, B.; Crowley, T. L. *Macromolecules* **1984**, *17*, 1825-1830.
88. Cosgrove, T. *J. Chem. Soc.; Faraday Trans* **1990**, *86*(9), 1323-1332.
89. van der Beek, G. P.; Cohen Stuart, M. A.; Fleer, G. J.; Hofman J. E. *Macromolecules* **1991**, *24*(25), 6600.

90. van der Beek, G. P.; Cohen Stuart, M. A. *Macromolecules* **1991**, 24(12), 3553.
91. Johnson, H.; Granick, S. *Macromolecules* **1991**, 24(10), 3023.
92. Ingersent, K.; Klein, J.; Pincus, P. *Macromolecules* **1990**, 23(2), 548-560.
93. Almog, Y.; Klein, J. *Macromolecules* **1985**, 106(1), 33.
94. Klein, J.; Luckham, P. F. *Macromolecules* **1984**, 17(5), 1041.
95. Evers, O. A.; Scheutjens, J. M. H. M.; Fleer, G. J. *Macromolecules* **1990**, 23(25), 5221.
96. Evers, O. A.; Scheutjens, J. M. H. M.; Fleer, G. J. *Chem. Soc. Faraday Trans.* **1990**, 86(9), 1333.
97. Evers, O. A.; Scheutjens, J. M. H. M.; Fleer, G. J. *Macromolecules* **1991**, 24(20), 5558.
98. Balazs, A. C.; Gempe, M.; Lantman, C. W.; *Macromolecules* **1991**, 24(1), 168.
99. Johner, A.; Joanny, J. F. *Macromolecules* **1990**, 23(26), 5299.
100. Balazs, A. C.; Huang K.; Lantman, C. W. *Macromolecules* **1990**, 23(21), 4641.
101. Balazs, A. C.; Lewandowski, S. *Macromolecules* **1990**, 23(3), 839.
102. van Lent, B.; Scheutjens, J. M. H. J. *Macromolecules* **1989**, 22(4), 1931.
103. Marques, C.; Joanny, J. F. *Macromolecules* **1989**, 22(4), 1454.
104. Marques, C.; Joanny, J. F.; Leibler, L. *Macromolecules* **1988**, 21(4), 1051-1059.
105. Munch, M. R.; Gast, A. P. *Macromolecules* **1988**, 21(5), 1360-1366, 1366.
106. ten Brinke, G.; Hadziioannou G. *Macromolecules* **1987**, 20(3), 489.
107. Shim, D.; Marques, C.; Cates, M. *Macromolecules* **1991**, 24(19), 5309.

108. Field, J. B.; Toprakcioglu, C.; Ball, R. C.; Stanley, H. B.; Dai, L.; Barford, W.; Penfold, J.; Smith, G.; and Hamilton, W. *Macromolecules* **1992**, 25(1), 434.
109. Leermakers, F. M. A.; Gast, A. P. *Macromolecules* **1991**, 24(3), 718.
110. Hair, M. L.; Guzonas, D.; Boils, D. *Macromolecules* **1991**, 24(1), 341.
111. Cosgrove, T.; Heath, T. G.; Phipps, J. S.; Richardson, R. M. *Macromolecules* **1991**, 24(1), 94.
112. Munch, M. R.; Gast, A. P. *J. Chem. Soc. Faraday Trans.* **1990**, 86(9), 1341.
113. Killmann, E.; Fulka, C.; Reiner, M. *J. Chem. Soc. Faraday Trans.* **1990**, 86(9), 1389.
114. Satija, S. K.; Majkrzak, C. F.; Russel, T. P.; Sinha, S. K.; Sirota, E. B.; Hughes, G. J. *Macromolecules* **1990**, 23(16), 3860.
115. Munch, M. R.; Gast, A. P. *Macromolecules* **1990**, 23(8), 2313.
116. Webber, R. M.; Anderson, J. L.; Jhon, M. S. *Macromolecules* **1990**, 23(4), 1026.
117. Tassin, J. F.; Siemens, R. L.; Wing, T. T.; Hadziioannou, G.; Swalen, J. D.; Smith, B. A. *J. Phys. Chem.* **1989**, 93(5), 2106-2111.
118. Marra, J.; Hair, M. L. *Colloids and Surfaces* **1988/89**, 34, 215.
119. Taunton, H. J.; Toprakcioglu, C.; Klein, J. *Macromolecules* **1988**, 21(11), 3336.
120. Stouffer, J. M.; McCarthy, T. J. *Macromolecules* **1988**, 21(5), 1204-1208.
121. Baker, J. A.; Berg, J. C. *Langmuir* **1988**, 4(4), 1055.
122. Ansarifard, A.; Luckham, P. F. *Polymer* **1988**, 29, 329.
123. Luckham, P. F.; Klein, J. *J. Colloid and Interface Sci.* **1987**, 117, 149.
124. Hadziioannou, G.; Patel, S.; Granick, S.; Tirrell, M. *J. Am. Chem. Soc.* **1986**, 108(11), 2869.

125. Blum, F. D.; Sihna, B. R.; Schwab, F. C. *Macromolecules* **1990**, 23(15), 3592.
126. Guzonas, D. A.; Boils, D.; Tripp, C. P.; Hair, M. L. *Macromolecules* **1992**, 25(9), 2434.
127. Guzonas, D.; Hair, M. L.; Cosgrove, T. *Macromolecules* **1992**, 25(10), 2777.
128. Guzonas, D.; Boils, D.; Hair, M. *Macromolecules* **1991**, 24(11), 3383.
129. Parsonage, E.; Tirrell, M.; Watanabe, H.; Nuzzo, R. *Macromolecules* **1991**, 24(8), 1987.
130. Wu, D. T.; Yokayama, A.; Setterquist, R. *Polymer Journal* **1991**, 23(5), 709.
131. Malmsten, M.; Linse, P.; Cosgrove, T. *Macromolecules* **1992**, 25(9), 2474.
132. Motschmann, H.; Stamm, M.; Toprakcioglu *Macromolecules* **1991**, 24(12), 3681
133. Huguenard, C.; Varoqui, R.; Pefferkorn, E. *Macromolecules* **1991**, 24(9), 2226
134. Marques, C. M.; Joanny, J. F. *Macromolecules* **1990**, 23(1), 268.
135. Kim, M. W.; Peiffer, D. G.; Hsiung, H.; Rasing, Th.; Shen, Y. R. *Macromolecules* **1991**, 24(1), 319.
136. Cosgrove, T.; Finch, N. A.; Webster, J. R. P. *Macromolecules* **1990**, 23(13), 3353.
137. Yamagiwa, S.; Kawaguchi, M.; K, Kato, Takahashi, A. *Macromolecules* **1989**, 22(5), 2199.
138. Kawaguchi, M.; Itoh, K.; Yamagiwa, S.; Takahaski, A. *Macromolecules* **1989**, 22(5), 2204.
139. Kawaguchi, M.; Funayama, A.; Yamauchi, S.; Takahashi, A.; Kato, T. *J. Colloid and Interface Sci.* **1988**, 121(1), 130.
140. Kawaguchi, M.; Aoki, M.; Takahashi, A. *Macromolecules* **1983**, 16(4), 635.

141. Kawaguchi, M.; Inoue, A.; Takahashi, A. *Polymer Journal* **1983**, *15*(7), 537.
142. Howard, G. J.; McGrath, M. J. *J. Polymer Sci.* **1977**, *15*, 1721.
143. Howard, G. J.; McGrath, M. J. *J. Polymer Sci.: Part A-2*, **1977**, *15*, 1705.
144. Barron, M. J.; Howard, G. J. *J. Polymer Sci.: Chem. Ed.* **1974**, *12*, 1269.
145. Hopkins, A.; Howard, G. J.; *J. Polymer Sci.: Part A-2*, **1971**, *9*, 841.
146. Herd, J. M.; Hopkins, A. J.; Howard, G. J. *J. Polymer Sci.: Part C*, **1971**, *34*, 211.
147. Alexander, S. *J. Phys. (Paris)* **1977**, *38*, 983.
148. deGennes, P. G. *Macromolecules* **1980**, *13*, 1069.
149. Chakrabarti, A.; Toral, R. *Macromolecules* **1990**, *23*(7), 2016.
150. Murat, M.; Grest, G. S. *Macromolecules* **1989**, *22*(10), 4054.
151. Milner, S. T. *J. Chem. Soc.; Faraday Trans.* **1990**, *86*(9), 1349
152. Whitmore, M. D.; Noolandi, J. *Macromolecules* **1990**, *23*(13), 3321.
153. Dan, N.; Tirrell, M. *Macromolecules* **1992**, *25*(11), 2890.
154. Wijmans, C. M.; Scheutjens, J. M. H. M., Zhulina, E. B. *Macromolecules* **1992**, *25*(10), 2657.
155. Iyengar, D. R.; McCarthy, T. J. *Macromolecules* **1990**, *23*(20), 4344.
156. Brown, H. R.; Char K.; Deline, V. R. *Macromolecules* **1990**, *23*(13), 3383-3385.
157. Taunton, H. J.; Toprakcioglu, C.; Fetters, L. J.; Klein, J. *Macromolecules* **1990**, *23*(2), 571-580.
158. Char K.; Frank, C. W.; Gast A. P. *Langmuir* **1989**, *5*(6), 1335-1340.

159. Kawaguchi, M.; Kowarabayashi, M.; Nagata, N.; Kato, T.; Yoshioka, A.; Takahashi, A. *Macromolecules* **1988**, 21(4), 1059.
160. Klein, J.; Kamiyama, Y.; Yoshizawa, H.; Israelachvili, J.; Fetters, L. J.; Pincus, P. *Macromolecules* **1992**, 25(7), 2062.
161. Auroy, P.; Auvray, L.; Leger, L. *Macromolecules* **1991**, 24(18), 5158.
162. Kim, M. W.; Fetters, L. J.; Chen, W.; Shen, Y. *Macromolecules* **1991**, 24(14), 4216.
163. This is also called the adsorbance; it is basically the dry weight (after solvent removal) of polymer adsorbed per surface site. Typically, we measure the weight adsorbed per weight of powder (of known surface area/weight). Theories tend to talk about monolayer equivalents of the dry film per surface site. In all respects it just a measure of the actual weight of polymer adsorbed to the surface.
164. This describes the layer in direct contact with the surface and is defined such that for $\theta=1.0$ the surface is saturated; $\theta=0.0$ there are no adsorbed segments.
165. Not all the segments of an adsorbed chain are directly attached to the surface (trains); many dangle into the solution. The bound fraction, p , is a measure of what percentage of chain units are bound to the surface. A value of $p=1.0$ means every segment of the chain is attached to the surface, thus the chain is in a perfectly flat conformation.
166. The adsorbed layer in solution is not a uniform layer; there exists a segment density distribution, $\rho(z)$, perpendicular to the surface. This layer is made up of trains in contact with the surface, a rather dense layer of loops and finally a very extended, diffuse layer of tails. The thickness of the layer then must be an average defined in much the same way average molecular weights are defined from their distributions. Different methods of measurement see different thickness averages, thus ellipsometry measures a thickness close to that of the loop layer while methods that measure dynamic thicknesses (photocorrelation spectroscopy and sedimentation) measure the long tails' thickness.

167. The validity of this assumption is not obvious but a number of things suggest that it is valid. 1) All isolated chain theories have predicted a very flattened (p close to 1) chain conformation on the surface.⁶⁷⁻⁷² This has also been found experimentally that adsorptions from dilute solutions have very high bound fractions.⁸³ Both these suggest that the conformational entropy decrease upon adsorption is over-powered by the surface-segment interactions.
168. The critical surface interaction parameter, χ_{sc} , has been found to be negative for cases where specific surface-solvent interactions.⁸⁴
169. The diffuseness of the layer can be described in terms of the amount adsorbed, Γ , and the layer thickness, t , as Γ/t .
170. There are also kinetic factors which control how much polymer is adsorbed. This is especially true for adsorption from very dilute solution where the chains have time to flatten out and cover up the surface sites before others can adsorb.
171. High affinity isotherms refer to rapid increase of amount adsorbed with concentration then a plateau after which no further increase is seen.
172. The graft density is the number of chains per area of surface normalized to the area of a monomer unit.
173. Odian, G. G. *Principles of Polymerization 2nd Ed.*, Plenum Press: New York, 1970, Chapter 5.
174. Morton, M.; Fetters, L. J. *Rubber Chem. & Tech.* **1975**, 8(3), 359.
175. Young, R. N.; Quirk, R. P.; Fetters, L. J. *Advances in Polymer Science* Vol. 56, Springer-Verlag: Berlin Heidelberg, 1984.
176. Rempp, P.; Franta, E.; Herz, J. E. *Adv. in Polymer Science* Vol. 86, Springer-Verlag: Berlin Heidelberg, 1984, 145.
177. Morton, M. *Anionic Polymerization: Principles and Practice*, Academic Press: New York, 1983.
178. This reference is for the living cationic polymerizations of vinyl ethers with the HI/I_2 catalyst system. Sawamoto, M.; Kanaoka, S.; Omura, T.; Higashimura, T. *Polym. Prepr. (Am. Chem. Soc., Div. Polym. Chem.)* **1992**, 32(1), 148.

179. These references are for living ring opening metathesis polymerizations (ROMP). Risse, W.; Grubbs, R. H. *Polym. Prepr. (Am. Chem. Soc., Div. Polym. Chem.)* **1983**, 30(1), 193; Cannizzo, L. F.; Grubbs, R. H. *Macromolecules* **1988**, 21, 1961; Cannizzo, L. F.; Grubbs, R. H. *Macromolecules* **1987**, 20, 1488.
180. These references are for the living polymerizations of epoxides and lactones with aluminum porphorin systems. Aida, T.; Maekawa, Y.; Asano, S.; Inoue, S. *Macromolecules* **1988**, 21, 1195; Kuroki, M.; Nashimoto, S.; Aida, T.; Inoue, S. *Macromolecules* **1988**, 3115; Shimasaki, K.; Aida, T.; Inoue, S. *Macromolecules* **1987**, 20, 3076; Endo, M.; Aida, T.; Inoue, S. *Macromolecules* **1987**, 20, 2982.
181. These references are for Group Transfer Polymerizations. Webster, O. W.; Hertler, W. R.; Sogah, D. Y.; Fornham W. B.; RajanBabu, T. V. *J. Am. Chem. Soc.* **1983**, 105, 5706; Webster, O. W.; Hertler, W. R.; Sogah, D. Y.; Fornham W. B.; RajanBabu, T. V. *Polym. Prepr. (Am. Chem. Soc., Div. Polym. Chem.)* **1983**, 24(2), 52, 54; Yu, H. S.; Choi, W. J.; Lim, K. T.; Choi, S. K. *Macromolecules* **1988**, 21, 2893.
182. End-functionalization has also been used in this group to prepare the carboxylic acid, alcohol and also a perfluorinated ester end group. Iyengar, D. Ph.D. Dissertation, Polymer Science and Engineering Department, Univ. of Mass., 1992; Franchina, N. L. Ph.D. Dissertation, Polymer Science and Engineering Department, Univ. of Mass., 1992.
183. Ishizone, T.; Kato, R.; Ishino, Y.; Hirao, A.; Nakahama, S. *Macromolecules* **1991**, 24, 1449; Taki, T.; Hirao, A.; Nakahama, S. *Macromolecules* **1991**, 24, 1455; Hirao, A.; Ishino, Y.; Nakahama, S. *Macromolecules* **1988**, 21, 561; Hirao, A.; Nakahama, S. *Macromolecules* **1987**, 20, 2968.
184. Viviano, K. R. dissertation research, descriptions in progress reports.

185. Varshney, S. K.; Jacobs, C.; Hautekeer, J.; Bayard, P.; Jerome, R.; Fayt, R.; Teyssie, Ph. *Macromolecules* **1991**, 24, 4997; Varshney, S. K.; Hautekeer, J.; Fayt, R.; Jerome, R.; Teyssie, Ph. *Macromolecules* **1990**, 23, 2618; Hautekeer, J.; Varshney, S. K.; Fayt, R.; Jacobs, C.; Jerome, R.; Teyssie, Ph. *Macromolecules* **1990**, 23, 3893; Jacobs, C.; Varshney, S. K.; Hautekeer, J.; Fayt, R.; Jerome, R.; Teyssie, Ph. *Macromolecules* **1990**, 23, 4024; Varshney, S. K.; Jacobs, C.; Hautekeer, J.; Bayard, P.; Jerome, R.; Fayt, R.; Teyssie, Ph. *Macromolecules* **1991**, 24, 4997; Fayt, R.; Forte, R.; Jacobs, C.; Jerome, R.; Ouhadi, T.; Teyssie, Ph.; Varshney, S. K. *Macromolecules* **1987**, 20, 4997.
186. Kendall, E. W.; McCarthy, T. J. *Polym. Prepr. (Am. Chem. Soc., Div. Polym. Chem.)* **1992**, 33(2), 158.
187. Chung, T. C. *Macromolecules* **1988**, 21(7), 1902.
188. Valint Jr., P. L.; Boch, J. *Macromolecules*, **1988**, 21, 175.
189. Valint Jr., P. L.; Boch, J. U.S. Patent 4,492,785 1985.
190. Andrade, J.D.; Gregonis, D.E.; Smith, L.M. In *Surface and Interfacial Aspects of Biomedical Polymers* Andrade, J.D. ed. Plenum: New York, 1986, Vol. 1, Ch. 5.
191. Clark, D.T.; Thomas, H.R. *J. Polym. Sci., Polym. Chem. Ed.* **1977**, 15, 2843.
192. Muilenberg, G.E. *Handbook of X-Ray Photoelectron Spectroscopy*, Perkin-Elmer Corp., 1979.
193. Zisman, W.A. *Adv. Chem. Ser.* **1964**, 43, 1, and references therein.
194. Reference 190, Ch. 7.
195. Johnson, R.E.; Dettre, R.H. *J. Phys. Chem.* **1964**, 68, 1744.
196. Huh, C.; Mason, S.G. *J. Coll. and Interf. Sci.* **1977**, 60, 11.
197. Harrick, N. J. *Internal Reflection Spectroscopy*, Harrick Scientific Corporation: Ossining, New York, 1979.

CHAPTER II

SYNTHESIS OF SPECIFICALLY FUNCTIONALIZED POLY(4-*TERT*-BUTYLSTYRENE) POLYMERS AND THEIR ADSORPTION AT THE SILICA-SOLUTION INTERFACE: EXPERIMENTAL

Materials Handling

Chemical manipulations were carried out using cannula and gas tight syringes under an inert N₂ atmosphere, unless stated otherwise. The transfers of the concentrated strong acids are one exception to this rule. The N₂ (Merriam Graves, prepurified) was further dried and deoxygenated by passage through a column filled with drierite and P₂O₅ and then a column filled with activated BTS catalyst. Schlenk type glassware was used for most reactions and distillations; this glassware was equipped with side arms (Schlenk arms) containing a teflon stopcock and a 14/20 female joint. The joint was fitted with a rubber septum (Aldrich) to create an antechamber easily purged with N₂ to facilitate transfers via cannula or syringe. The stopcock was used to close off the antechamber to the vessel, thus giving two lines of defense against the outside atmosphere. Teflon-covered magnetic stir bars were used to agitate the reactions unless stated otherwise. Solvents and reagents were distilled and stored in Schlenk storage flasks consisting of a sealed round bottom (RB) flask with an attached Schlenk arm. Most reactions and distillations were carried out in Schlenk flasks and Schlenk tubes. The Schlenk flasks had a regular ground glass (GG) joint (usually 24/40, either male or female) at the normal spot to facilitate introduction of stir bars and solids, and also to connect other

needed glassware. Schlenk tubes were similar but were much smaller (and taller), usually giving an opening via a #20 or #25 O-ring joint (24/40 GG joints were also used). The trap-to-trap distillations were performed in a one piece all glass apparatus that consisted of a trap and a side arm for the connection of the required distillation pot (many times this was just a Schlenk tube). The procedures described here involve two rather incompatible chemistries namely, anionic polymerization (which requires total elimination of all proton sources) and Friedel Crafts and sulfonation chemistry which uses strong acids. The two types of chemistry were carried out on separate sides of the lab to decrease the chance of contamination.

Materials

Aluminum trichloride (Solid, Fisher and Aldrich) was used as received.

Aluminum trichloride (1.0 M solution in nitrobenzene, Aldrich) was used as received.

sec-Butyllithium (1.3 M solution in hexanes, Aldrich) was diluted or used as received. The concentration was determined by titration of biphenyl methanol or via an anionic polymerization and determination of the molecular weight of the resultant polystyrene.

Carbon tetrachloride (Aldrich or Fisher, HPLC) was used as received.

Chlorosulfonic acid (Aldrich) was used as received.

Dichloroethane (Aldrich) was distilled from CaH_2 .

Diethyloxomalonate (Aldrich) was used as received.

Isopropanol (Fisher, HPLC) was used as received.

Ethyl acetate (Fisher, HPLC) was used as received.

Lithium aluminum hydride (Aldrich) was used as received.

Methanol (Fisher, HPLC or Tech grade) was used as received.

Methylene chloride (Fisher, HPLC) was distilled from CaH_2 or used as received.

Piperidine (Aldrich) used as received.

Sodium hydroxide (Fisher) was used as received.

Styrene (Aldrich) was distilled from CaH_2 and then dibutylmagnesium.

Sulfuric acid (30 % SO_3) (Aldrich) was used as received.

Sulfuryl chloride (Aldrich) was used as received.

Sulfur trioxide (Aldrich) was used as received.

Tetrahydrofuran (Fisher or Aldrich, HPLC or Specgrade) was distilled from either CaH_2 or Na/benzophenone dianion, or used as received.

Tin tetrachloride (neat and as a 1 M solution in hexane and MeCl_2) (Aldrich) was used as received.

para-tert-Butylstyrene (Aldrich or homemade) was distilled from CaH_2 and then dibutylmagnesium.

Triethylphosphate (Aldrich) was used as received.

Precursor Polymer Synthesis: Materials

Solvent Systems. The solvents used for anionic living polymerizations have a large effect on both the rate of initiation (and thus the polydispersity) and rate of propagation. The experimental procedures required for different solvents also vary widely; the advantages and disadvantages of four different systems have been evaluated. The precursor copolymers, styrene-*co-tert*-butylstyrene, were prepared in four different solvent systems: THF (100%) [B9-16,36,43,57,58,], cyclohexane (100%) [B9-102;B18-14,23], cyclohexane/benzene azeotrope (45:55) [B21-13,22,30], cyclohexane spiked with THF (~10 X initiator concentration) [B21-51]. The 100% THF system yields very narrow MW distributions and the polymerization times are short (this becomes important when

multi-block polymers are prepared). The disadvantage of using THF is that it is very hygroscopic. Procedures have been developed to obtain reproducible results when THF is used (these can be found in Chapter IV). It is recommended that THF be used only when solvency requires it. Polymerizations carried out in cyclohexane are much simpler because cyclohexane is much easier to dry and the polymerization does not require lower temperatures. This works especially well for PtBS because, unlike polystyrene, cyclohexane is a good solvent for PtBS at room temperature. Cyclohexane was used to prepare a number of block copolymers in this work but it has two minor disadvantages: 1) the initiation rate is slow (relative to THF) and therefore the molecular weight distributions of the resultant polymer are not as narrow (as THF), and 2) the polymerization rate is slow; this requires each block to be polymerized for hours (> 6 h, monomer consumption was monitored by GC) and this becomes a prohibitively long synthesis when multiblock structures are to be prepared. The increase in time can result in more than just inconvenience because as the polymerization time gets longer any slow rate of contamination from outside sources becomes more significant. Benzene has initiation and propagation rate properties between those of THF and cyclohexane. A benzene/cyclohexane azeotrope was used to take advantage of these faster rates and to use as little benzene as possible (for disposal considerations, etc.). The azeotrope facilitated one pot drying of the solvent system (from PSLi) before polymerization. This azeotrope works well and a number of polymers were made in this fashion. The THF spiking method was the last system that we tried and it looks promising, yielding short polymerization times and narrow MWDs. Because such a small amount of THF is used, the rigorous drying procedures outlined in Chapter IV need not be used.

Cyclohexane. Cyclohexane was initially distilled from CaH_2 and stored in a storage flask under N_2 . The day before the polymerizations were to be carried out it was added to a 500 mL RB Schlenk flask that was assembled with a stillhead and a 250 mL storage flask. The system was kept under positive nitrogen pressure and teflon tape was used to seal the joints. The flask was charged with cyclohexane (~300 mL), styrene (~1 mL) and enough *sec*-BuLi (or *n*-BuLi) to obtain a dark orange/red anion color. This was polymerized at room temperature overnight and distilled directly before use the next day.

Cyclohexane/Benzene Azeotrope. The same general procedure was used as described for the cyclohexane above, except that the flask was charged with an approximately 55:45 mixture of benzene/cyclohexane (bpt 78 °C).

Cyclohexane/THF Spike. Cyclohexane was dried as described above and the polymerization started as described below. The THF was added via a 100 mL syringe after the first block (or the initiator) was added.

THF. THF was dried and used following the procedures outlined in Chapter IV.

Styrene. Approximately 300 mL of styrene was distilled from CaH_2 at 30 mm Hg and stored under N_2 in a storage flask in the freezer. It was further dried with dibutylmagnesium (Bu_2Mg) just prior to use following a procedure developed from Morton.¹ Approximately 1 - 4 mL of 0.5 M Bu_2Mg (Alfa) in hexane was transferred via cannula into a purged Schlenk

tube (with a grease joint) and then the solvent was pulled off, leaving a white solid. Styrene (10 - 20 mL) was added (via cannula) and stirred at room temperature for 1 - 4 h, after which time the solution became bright yellow. This color indicates living polymerization of styrene and the absence of water and other impurities. This polymerization is extremely slow (occurring over days), so the dry styrene can be used at much later points in time. The tube containing the yellow solution was attached to a trap-to-trap distillation apparatus and the solution was degassed with three freeze-pump-thaw cycles and then transferred. The dry monomer was used within an hour or so.

para-tert-Butylstyrene. The polymers were prepared from commercial *para-tert*-butylstyrene monomer (containing up to 5% ortho and meta isomers) and from homemade *para-tert*-butylstyrene monomer which was essentially free of the contaminating isomers. The monomer was first dried by vacuum distillation from CaH_2 (this monomer polymerizes much more easily than styrene and therefore it was not stored for more than a few days). The monomer was exposed to dibutylmagnesium in the same fashion as described above for styrene and the same yellow color appears to indicate dryness. The trap-to-trap (t-t-t) distillation was carried out using a very short arm t-t-t apparatus and a one piece tube; this allowed the whole tube to be submerged in a water bath ($\sim 50\text{-}70^\circ\text{C}$). Warming the tube and wrapping foil around the arm, etc., facilitates this transfer because the monomer barely comes over at room temperature.

Precursor Polymer Synthesis: Methods

All polymerizations were carried out in base bath-cleaned glassware that was stored in a drying oven at approximately 80-100°C for at least 12 h. All glassware was assembled hot and under N₂ purge. Teflon stopcocks were preferred to grease stopcocks, but vacuum grease was used and found preferable to teflon sleeves on ground glass joints. All transfers were done via cannula or gas-tight luer-tip syringe. All needles and cannula were cleaned with hexane, 1.0 M HCl, 1.0 M NaOH, H₂O, and acetone, and then purged dry and kept in the oven until right before use. Transfers were also facilitated by a portable antechamber made from 75 x 9 mm piece of glass tubing fitted on both ends with the appropriate septa and then purged with N₂. During the assembly and transfers, clean latex gloves were worn at all times to minimize contamination by perspiration and oils from hands. All assembled glassware (reaction vessels, distillation apparatus, trap-to-trap and storage apparatus) were further dried by purging 10 min with N₂ and then a repeated pump/flame/backfill cycle. All solvents and monomers were distilled directly before use. *sec*-Butyllithium (*s*BuLi) was diluted with dry hexane or heptane and stored in 15 ml Schlenk tubes. The best results are obtained when the initiator is diluted directly before polymerization (i.e. the diluted *s*BuLi is not as stable with time).

Polymerization Vessel. The polymerizations were carried out in 250 mL round bottom (RB) Schlenk flasks fitted with a glass plug and a glass-covered stir bar. The preferred flask has the male ground glass (GG) joint, although both kinds were used. The joint was sealed by judicious use of grease (Apiezon M or N) followed by a wrapping of teflon tape. Care was taken not to use an excessive amount of grease because this can

contaminate the flask, especially because the flasks are dried by flaming under vacuum. Two other flasks were designed to allow even cleaner systems. The two disadvantages of the flask described above are the greased opening and the teflon stopcock. These were eliminated by sealing the stir bar inside the flask. The normal stopcocks were replaced by a special one (from Ace Glass), the "flic-it", which is a vacuum plug designed to allow insertion of a cannula or needle. These worked fairly well, but the seal depended on an O-ring and this sometimes caused problems. Another design used small rotflow valves with the opening modified so that a small gauge cannula or needle could be pushed through and into the reaction flask. These worked very well.

Polymerization. The purifications described above were performed and the reaction vessel was charged with solvent (~50 mL) and then the correct amount of initiator was added via syringe. The monomer was then added via syringe and the solution turned yellow, orange or red, depending on how much initiator was added. The reactions in cyclohexane were allowed to polymerize overnight (except the small blocks). When the first monomer was consumed the second was added etc., and when the last block was finished the reaction was terminated.

Termination. Another consideration is the matter of termination. It is well known that the living polymer chain will react with adventitious CO_2 to first obtain the carboxylate; this can react again to form the ketone and even a third time to form the alcohol. These reactions produce polymers with the correct molecular weight, the dimer and the trimer, respectively.¹ Because of such reactions, the proton source added to terminate the

polymerization must be thoroughly degassed. After this requirement is met, the method of termination is a personal preference although most methods are not 100% fool proof. The degassing (actually removing CO₂ and oxygen) procedure can be accomplished via bubbling N₂ through the solvent (which is not recommended) or a series of freeze-pump-thaw cycles (recommended). The use of MeOH (100%) can cause the storage tube to break during these cycles (the MeOH can be mixed with another solvent such as benzene or THF to alleviate this problem). Isopropanol can be used neat (but it freezes as a glass, probably not as amenable to degassing) or mixed with cyclohexane. The ~10% isopropanol in cyclohexane is the termination mixture of choice for this work. The degassing procedure consists of 4-6 freeze-pump-thaw cycles followed by at least a 15 min purge of the tube antechamber via cannula through the reaction vessel antechamber.

Sulfonations: Exxon Method²

Table 3.4 in the results and discussion section (Chapter III) contains data from these reactions.

Procedure 1. [B9-22] The polymer (5.0 g, 28.9 mmols of styrene units, R70/155K-p) was dissolved in DCE (100 mL) in a N₂-purged Schlenk tube (solution 1). Sulfur trioxide (3.5 g, 43 mmol, Aldrich Sulfan brand) was added to a large Schlenk tube in a glove bag and DCE (100 mL) was added; the solid dissolved (solution 2). Sulfur trioxide is a very corrosive solid and even in the glove bag it fumed profusely and turned the inside walls of the glove bag green in <30 sec (needless to say we do not recommended transferring SO₃ in a good glove box). Triethylphosphate

(TEP) (8.36 mmol) and DCE (~ 50 mL) were placed in a 250 mL RB flask with a teflon stir bar and purged with N₂ (solution 3). The three solutions were cooled to 0 °C and small amounts of solution 1 and then solution 2 were added alternately to solution 3 with stirring. The polymer precipitated from the solution and was filtered and washed with pentane. The resultant polymer dissolved to slight haziness in water and was neutralized (with NaOH) and dialyzed.

Procedure 2. [B9-72,74,76,78, 79] This procedure is similar to that reported above but the SO₃ was obtained by trap-to-trap distillation from 30% fuming H₂SO₄. The fuming H₂SO₄ is much easier to handle than the solid sulfan that was obtained from Aldrich (the solid nature precludes normal inert atmosphere transfers via cannula). A typical trap-to-trap setup was used but two additional cold traps were placed between the distillation and the vacuum manifold (i.e. there were four traps between the H₂SO₄ and the vacuum pump). The distillation was carried out at 0 mm Hg with ~40 °C tap water used as the heat source. A white needle-like solid (10.68 mmol, weight before and after were used to determine this) was isolated (it was solid at room temperature); DCE (~25 mL) and TEP (1.77 mole) were added to dissolve the solid. A 16% complexed SO₃ solution (solution 2) was prepared in this manner.

The polymer (0.3 g, 2.7 mmol, R90/174k-p) was placed in a N₂-purged Schlenk tube and DCE (6 mL) was added to dissolve the polymer (solution 1). DCE (6 mL) and TEP (0.8 mL, 0.46 mmol) were added to a 40 mL N₂-purged test tube (solution 3). Solution 3 was cooled to 0 °C and solution 1 (1 mL) was added followed by solution 2 (0.5 mL) with stirring.

These additions were continued over a period of ~20 min (a total of 4.8 mmole of SO_3 were added). The polymer precipitated after approximately 5 min resulting in a light pink solid. The reaction was continued for ~15 min after additions were complete. Dry pentane (20 mL) was added to form a better (less gooey, precipitate) which was filtered to obtain a brownish grey product. The product was dissolved in MeOH (~20 mL), dialyzed to neutrality against water, and lyophilized to obtain a slightly sticky light yellow product.

Sulfonations: Vink Method³

The procedure of Vink et. al. was followed to sulfonate a polymer sample [B9-27]. Concentrated sulfuric acid (25 mL, 95-98%, 469 mmol) was placed in a 250 mL RB flask equipped with a teflon stir bar and cooled to 0 °C and P_2O_5 (5.5 g, 38.7 mmol) was added slowly. Polymer (0.79 g, 6.5 mmol, R70/155k-p) was dissolved in cyclohexane (40 mL) and the solution was heated to 40 °C to completely dissolve the polymer. The acid solution was also heated to 40 °C and the polymer solution was slowly added with stirring. A brownish viscous solution resulted which was allowed to react for 1.25 h and then stopped by addition of crushed ice (15 g). The solution was transferred to a separatory funnel where it formed three layers (36 h). The aqueous layers were dialyzed against H_2O and lyophilized. Some solid polymer particles remained that would not dissolve in water.

Sulfonations: TEP complexed ClSO_3H .

Table 3.7 in the results and discussion section (Chapter III) contains data about these reactions.

A small N₂-purged Schlenk tube [B11-39] was charged with ClSO₃H (0.5 mL, 7.5 mmol) and DCE (10 mL) and TEP (0.8 mL; 4.6 mmol) was added to obtain a clear solution with slight yellow tint. The solution was divided in half for use in two different modification reactions (solution 2). PS homopolymer (0.25 g, in ~5 mL DCE) was added to one half of solution 2 and allowed to react for 50 min at RT. The polymer precipitated as a gooey glob on the bottom of the flask and was isolated by decanting the solution. The polymer dissolved in MeOH but was immediately precipitated by the addition of NaOH/H₂O. PtBS homopolymer (0.25 g in ~5 mL DCE) was added to the second portion of solution 2. The polymer precipitated initially but redissolved giving a clear solution after an hour of reaction. IR showed that very little sulfonation had occurred.

Sulfonamide Formation: Via uncomplexed ClSO₃H

Table 3.9 in the results and discussion section (Chapter III) contains data about these reactions.

A N₂-purged test tube was charged with ClSO₃H (1 mL) and DCE (5 mL), and another N₂ purged test tube was charged with polymer (0.36 g, T14/12k-p) and DCE (5 mL) (B11-14). The acid solution was cooled to 0 °C and the polymer solution was added with stirring over a period of 5 min, after which time the polymer precipitated. The reaction was allowed to proceed for 2.5 h, the stirring was stopped and two layers formed. The top layer was removed via cannula and reacted with dibutylamine, but no polymer was isolated (i.e. the top layer contained no polymer). The lower

portion, which was allowed to react at RT an additional 24 h, was very dark in color and contained some solids. Dibutylamine was added slowly (~2 mL) and eventually all the solids disappeared. This reaction was carried out for 10 h after which time the contents were poured into MeOH. No precipitation occurred so the solvent was allowed to evaporate and a gooey polymer was obtained. The polymer was dissolved in THF and precipitated in H₂O, and then extracted with water in a Soxhlet extractor for 20 h and dried at RT under reduced pressure.

Sulfonamide Formation: Via Sulfamyl Chlorides

These reactions have been reported in the literature for small molecule chemistry.⁴

Preparation of PipSO₂Cl. [B11-60,80; B13-31] The procedure of Gupta was followed for the reaction of piperidine (Pip) with sulfuryl chloride (Cl₂SO₂).⁴ A 2 L RB Schlenk flask was charged with Cl₂SO₂ (24 mL), CHCl₃ (300 mL) and a teflon-covered stir bar. The flask was purged with N₂ and attached to a NaOH trap to catch the HCl produced. A 100 mL graduated cylinder was charged with piperidine (25 mL) and triethylamine (30 mL) and purged with N₂. Both solutions were cooled to 0 °C and the amine solution was slowly added to the stirred Cl₂SO₂ solution (HCl evolved). The addition was accomplished over a 1.5 h period and then allowed to react for an additional 1 h. The solution was washed with water and 10% HCl and then the CHCl₃ was removed via rotary evaporation to obtain a light yellow oil. The oil was then fractionally distilled at 0 mm Hg and the product came over at 74-76 °C as a clear oil.

PipSO₂Cl/AlCl₃ Modifications. Table 3.10 in the results and discussion section (Chapter III) contains data about these reactions. The polymer (0.42 g, PS homopolymer) was placed in a Schlenk tube (fitted with a water jacket to facilitate reflux) and a nitrobenzene solution of AlCl₃ (15 mL, 1.0 M) was added to the tube at RT (B11-84). The polymer dissolved and formed a dark orange/red solution. The sulfamyl chloride, PipSO₂Cl (2.8 mL), was added via syringe and no visible changes were observed. The reaction was run for 18 h at 60-65 °C. At this time the solution was a darker, more greenish color. The solution was allowed to cool and was poured into 10% HCl/H₂O (~30 mL), and then CHCl₃ (30 mL) was added. The mixture was put into a separatory funnel and, after shaking, the black organic layer became tan colored. The organic layer was washed twice with HCl/H₂O, hexane was added to the solution and a light brown glumpy polymer precipitate was obtained. The polymer was redissolved in THF (60-70 mL) and precipitated by addition of hexane (~100 mL). A light brown solid was obtained.

PipSO₂Cl/SnCl₄ Modifications. Table 3.11 in the results and discussion section (Chapter III) contains data about these reactions. The modifications were carried out similar to the AlCl₃-catalyzed reactions but MeCl₂ was used as reaction solvent.

Diethyloxomalonate Modification Reactions

These reactions have been reported in the literature for small molecule chemistry.⁵

DEOM/SnCl₄: Small Molecule Reactions. Table 3.12 in the results and discussion section (Chapter III) contains data about these reactions. A 35 mL RB flask was charged with *iso*-butylbenzene (1.47 g, 12.8 mmol), DEOM (2.2 mL, 14.3 mmol), DCE (7 mL) and a teflon-covered stir bar [B19-5]. The flask was purged with N₂, cooled to 0 °C and neat SnCl₄ (2.2 mL, 18.7 mmol) was added via syringe with stirring. The solution was allowed to react at 0 °C for 15 min, was then warmed to room temperature and maintained in the dark. After 1.5 h the flask was full of white crystals (stir bar would not spin). The flask was charged with MeCl₂ (5 mL) but not many of the crystals dissolved. The contents were poured into 1.0 M HCl and all solids dissolved. The organic layer was separated and washed with H₂O, dried with MgSO₄ and evaporated at RT to obtain a viscous oil. The oil was dissolved a minimum of pentane and the product was recrystallized at 0 °C.

DEOM/SnCl₄: Polymer Modifications. Table 3.14 in the results and discussion section (Chapter III) contains data about these reactions. A 25 mL RB flask was charged with polymer (0.60 g), DEOM (1 mL, 6.5 mmol), DCE (5 mL) and a teflon covered stir bar [B21-76#3]. The flask was purged with N₂, cooled to 0 °C and neat SnCl₄ (1 mL, 8.5 mmol) was added via syringe with stirring. The solution was maintained at 0 °C for 15 min and then allowed to warm to and react at RT in the dark (the solution is a light yellow color at this time). The reaction was carried out for ~16 h after which time the solution was a dark orange color and very viscous. The solution was poured into 1.0 M HCl/MeOH mixture (15 mL/45 mL) and a gooey polymer glob was obtained which was redissolved in THF (20-

30 mL) and precipitated in H₂O/MeOH (25 mL/55 mL). The general purification procedures outlined below were then carried out.

The typical modification procedure involved dissolving the precursor polymer (~500 mg) in 5 mL of solvent (DCE or CH₂Cl₂) and adding 1 mL of DEOM (under dry N₂). The solution was cooled to 0 °C and 1 mL of neat SnCl₄ was added via syringe over a period of a few minutes, and then the reaction solution was allowed to warm to room temperature. The reaction was carried out in the dark for the appropriate length of time (usually about 15-24 h). As the reaction proceeded, an orange color developed and the solution became noticeably more viscous (especially for polymers with high styrene content). Polymers with larger SF content sometimes exhibited polymer precipitation or a "pearliness" in the solution. The resulting sticky foot polymers are somewhat soluble in methanol (PS homopolymer modified by this reaction is soluble in methanol), and therefore direct precipitation into methanol does not work. Instead, polymer solutions were poured into a mixture of HCl (1.0 M)/methanol (15 mL/45 mL), and the polymers precipitated out as gooey blobs. Each polymer was separated from the liquid via filtration and/or decanting. The polymer was redissolved in THF and precipitated in water/methanol mixtures (the ratio changes depending on the SF content of the polymer for instance, 25 mL/55 mL for a 23% SF copolymer). Most often, a nice white, easily filtered polymer was obtained. On occasion, the particles were too small and the polymer was difficult to filter. (This happens when the water/methanol ratio is not correct). Small insoluble particulates have been found in the polymer even after numerous precipitations. These are presumed to be various tin salts formed during

the workup. They have been removed by filtration (micro filter with 2 μm pores) but this is difficult because the filters fill up so fast. The best way to separate the solids is via centrifugation. As a final step, the polymers are freeze-dried from benzene and washed with a non-solvent organic compound (usually methanol). This is a good general procedure for washing difficult-to-remove small molecule impurities from the polymer. The freeze-drying creates a large surface area and washing with a non-solvent will usually take away any organic impurity (small molecules are usually miscible with a much wider range of solvents). The reason that this step is required with these polymers is because the precipitation in water/methanol solution causes the small molecules to precipitate with the polymer, and therefore repeated precipitations are not an efficient purification procedure.

Hydrolysis of the Diethylhydroxymalonate Sticky Foot

Procedure 1. This procedure was used to hydrolyze DEOM-modified PS homopolymer (the hydrolysis proceeds differently when copolymers are used, see procedure 2). A 100 mL beaker was charged with polymer (0.22 g, PSM2) and a teflon-covered stir bar [B20-80 also see B19-67]. A 5% NaOH solution (~20 mL) was added, with stirring, and a white slurry resulted. This was stirred for ~5 min without much visual change in the solution and then solid NaOH (3 pellets) was added and the mixture was stirred without significant change. The beaker was placed in a temperature bath (~45 °C) and almost immediately the slurry became a slightly hazy solution; this was allowed to react for an additional 20 min.

The reaction mixture was dialyzed to neutral conditions against distilled water and lyophilized to obtain a nice white powder.

Procedure 2. This procedure was used to hydrolyze DEOM modified PS/PtBS copolymers. Modified block copolymers with 5% *tert*-butyl units (D95/33k, Table 3.15 entry 25) and 10% *tert*-butyl units (D90/13k, Table 3.15 entry 24) were also hydrolyzed. The D95 contains 91% SF and the D90 contains 88% SF [B22-132]. The same general hydrolysis procedure was applied to these as was used for PSM2 above. The polymer powders (~350 mg) were added to a 10% aqueous NaOH solution (11 mL) in a test tube and heated to 50 °C with stirring. It was expected that they would dissolve quickly as did the PSM2, but this did not happen. The polymer solid changed form somewhat and looked like it was partially dissolving, but total dissolution of the PSM2 was not realized immediately. After 2 hours (at 60 °C) the solutions were not clear (a significant amount of solids was present). The solutions were allowed to cool and more solids formed, and the liquid was decanted off and dialyzed. Water was added to the solid precipitate and upon stirring it dissolved, and this was dialyzed as well. There were minor differences between the D95 and the D90 (with the D95 acting more like the PSM2) but both pretty much acted the same. After dialysis and lyophilization, polymer was obtained from both the decanted and the precipitated fractions. More D95 was obtained from the decanted part (i.e. more D95 was in solution during the hydrolysis). The polymers were isolated as nice white solids that dissolved in water to give clear to very slightly hazy solutions ("blue haze"). The solutions were extremely viscous and formed transient gels upon sitting.

Reduction of the Diethylhydroxymalonate Sticky Foot

A N₂-purged Schlenk tube was charged with LiAlH₄ (~100 mg), THF (5 mL) and a teflon covered stir bar. A solution of polymer (100 mg, D23/13k DM3) and THF (5 mL) was added to the Schlenk tube via syringe over a period of 5 min. The reaction was carried out at 18 °C for ~12 h. The reaction was stopped by slowly adding (via pipet) a 10% aqueous NaOH solution until the hydride was used up (the fizzing stops); solids form in light brown, granular chunks. The mixture was separated by filtration and only a very small amount of polymer was found in the liquid phase. The brown solid was placed in THF (it did not dissolve) and 1 M HCl was added, at which time some of the solid may have dissolved. The liquid was isolated, concentrated and the polymer was precipitated in H₂O.

Determination of the Critical Displacer Concentration

Thin Layer Chromatography was performed on silica plates cut and stored in an oven for >24 h (~200 - 250 °C). Most of the plates were cut to a length of 10 cm with 6 cm used as the actual run. For the DCE/EA systems, the plates were not activated, but were used right from the box. The plates were spotted using a ~10 mg/mL solution in methylene chloride (more polar solvents such as THF cause a broader hollow spot that results in an ω shaped spot after elution, i.e. mini-TLC). The spots were made by applying ~0.5 µl solution via a 1.0 µl syringe with a flat tipped needle. The spots were then allowed to dry ~10-15 min at RT. The spots were visualized via black light (fluorescence plates were used).

This method was used to measure the critical displacer concentrations [B18-59]. A 500 mL reaction kettle was used as the development chamber with a teflon stir bar and a large filter paper to assist in the vapor equilibrium (no grease was used on the joints). This large chamber was used so that large plates could be used; this allowed 11 spots to be run on one plate. A 125 mL addition funnel was attached at one side port of the reaction kettle and fishing string with a small clamp at the end was threaded through the center hole via an adapter to decrease the opening size. The remaining holes were plugged with polypropylene stoppers. This setup allowed the TLC plate to be suspended above the solvent/displacer mixture for equilibration, as suggested by van der Beek⁶ et. al., and then be lowered into the solvent to start the elution. Each plate was equilibrated for ~20 min and then lowered into the mixture for development. After the run was completed, more displacer (ethyl acetate) was added and the process was started again. This setup works well but is cumbersome (with the reaction kettle) so a 1 Qt ball jar was used as the development chamber for some of the DCE/displacer experiments [B22-144,;B23-7,19]; a small hole was drilled in the lid to allow the fishing line to pass through. The same procedure as above was used with the exception that the displacer was added via syringe or graduated cylinder (depending on what was appropriate). A few notes are in order here: The ball jar lids have a rubber type seal that is dissolved by certain solvents, including THF. The solvent vapor can condense on these and cause impurities to fall back into the solution. This is detrimental to the experiment because the impurities can act as displacers. The solution to the problem is to use the lids upside down. Also, the equilibrations described here were not for the 45 min that van der Beek recommends; using longer equilibration times

would probably be better. There was some evidence that the chamber may not have been saturated with vapor, thus a better means of insuring this is recommended. Single composition TLC determinations were done in 6 oz. jars with a filter paper wick and no initial equilibration [B18-50].

UV-Vis Calibrations

A 50 mL volumetric flask was charged with polymer (57.8 mg of T23/12k TM1) and filled to the line with DCE [B18-72]. Four other calibration solutions were prepared via successive dilution (25 mL pipet, 50 mL volumetric flask). All procedures were done under ambient conditions in Goessmann 142. The UV calibration curve was obtained by scanning from 400 nm to 250 nm: The computer picked the maximum peak (within these limits) and determined the absorbance. The baseline was taken at 380 nm. The other calibrations followed similar procedures.

Adsorptions to Aerosil 120

Method 1. [B18-77] Aerosil was cleaned at $>300\text{ }^{\circ}\text{C}$ in dry air for 48 h. This procedure dries the silica but also burns all the organics off the surface.^{7,8} The aerosil cannot be cleaned by washing with solvents and then drying because the particles become much more aggregated if this is done (the whole physical appearance of the solid changes drastically). A 250 mL jacketed RB flask (with teflon stir bar) was charged with silica (0.59 g) and dry DCE (70 mL). The silica/DCE was allowed to equilibrate at $25\text{ }^{\circ}\text{C}$ (a circulator was used to obtain the correct temperature) for 45 min. A polymer solution (1.067 mg/mL; 50 mL; of T23/12k TM1) was prepared and added to the stirred solution. A 5 mL aliquot was taken after

2 min and placed in a centrifuge tube and spun down for 40 min (setting #6). UV spectroscopy was used to measure the concentration and determine the adsorption. This procedure was repeated at various times to obtain other data points. The circulator was used to both raise and lower the adsorption temperature and the amounts adsorbed at these temperatures were measured similarly (to the above procedure), but a foam rubber tube was used to insulate the solution while it was being separated in the centrifuge.

Method 2. [B18-92, 115] This method involves isotherm construction via measurement of single data points. We used 15 mL centrifuge tubes with polypropylene tops sealed with teflon tape (neither septa nor glue were used because displacer molecules and UV contaminants can be extracted from them). All quantitation was done by weight, the measurements being performed with an analytical balance (accuracy of ± 0.05 mg). We weighed the silica (~ 15 mg) into each tube and added the polymer solution with shaking. The tubes were spun down (with a centrifuge) and the adsorbance measured within 30 min. Another measurement was taken after ~ 24 h.

Method 3. [B18-129] This method was used for isotherm construction via successive additions. The adsorptions were carried out in a ~ 20 mL centrifuge tube and all additions were quantified by weight (analytical balance). The tube, with a small teflon stir bar, was weighed and the silica added (0.10250 g) then DCE was added (12.683 g) and the suspension was allowed to equilibrate. A solution (9.44 mg/mL, 5 mL) of T23/12k TM1 was prepared and aliquots of it were added (and weighed) to

the centrifuge tube. The adsorption was carried out for the desired length of time. The tube was spun down (in the centrifuge) and the concentration was measured via UV; the solution was then added back to the tube and reweighed to determine the amount of solution lost. Mass balance was used to determine the amount adsorbed and then another aliquot of polymer solution was added to yield a higher concentration and the whole measurement process was repeated. In this way the entire isotherm was constructed. The dilution experiments were carried out by spinning the tube down, taking a known amount solution out and replacing it with solvent, and then measuring the concentration.

Method 4. [B19-54] A stock suspension of Aerosil in DCE was prepared (203.3mg /22.13mL). The suspension was weighed into (~10mL) each of two centrifuge tubes and the diblock and triblock copolymer solutions (~1.2 mg/mL, exact measures were determined) were added to the tubes. Both tubes immediately changed from an almost perfectly clear appearance to a very hazy appearance. The aerosil and DCE must have similar refractive indices whereas the refractive index of the adsorbed layer (high polymer concentration) does not match as well, therefore the solution gets hazy. This is good evidence for the extremely fast adsorption behavior (when unmodified, nonadsorbing polymer was added to a similar suspension this haziness was not observed). Each solution was stirred for a few minutes and then allowed to settle; both settled, within minutes, to a hazy blue underlayer and a clear overlayer. Then two aliquots were taken from each top layer; for one set the concentration was measured by UV spectroscopy without filtering or centrifuging. The diblock (D23/13k DM3) measured an adsorbance of 0.9163 mg/m² (@ c=0.6014mg/ml) and

the triblock (T23/12k TM2) measured an adsorbance of 0.6882 mg/m^2 (@ $c=0.6841 \text{ mg/ml}$). The other two aliquots were spun down for 70 min in the centrifuge (at this point the tubes are fairly warm). The solutions were allowed to cool and the adsorbance was determined: The diblock had 0.9163 mg/m^2 (@ 0.6010 mg/mL) and triblock 0.689 mg/m^2 (@ 0.680 mg/mL). This is pretty much the same as the unspun samples; at this point we believe that the diblock has not yet dispersed the aerosil. IR spectroscopy was used to check for aerosil in both solutions; none was found in the triblock and very little in the diblock. The original solutions were stirred for 2 hours and then allowed to settle. The triblock settled into a clear layer on top and a hazy layer on the bottom. But the diblock copolymer resulted in a top layer which had a "bluish tinge", suggesting that some of the aerosil had not settled out. More polymer was added to the mixtures and it was found that the diblock solution became hazier. Large differences were observed visually for the behavior of the two architectures.

Adsorptions to Glass Beads

The modified polymer was adsorbed onto glass beads (Polysciences, 30-50 μm in diameter) [B19-91]. The beads were a somewhat coarse off-white solid (~fine sand); they were easy to manipulate because they would settle out easily. The beads (5 g) were placed in a Schlenk tube and washed with 2X10 mL of THF; 1X10 mL of MeOH and pumped down at $\sim 220^\circ\text{C}$ for 15 h. A solution of polymer (5.3 mg, D23/13k DM1) in dry DCE (5 mL) was prepared (1.06 mg/mL). The solution (4.7 mL) was injected onto the glass beads with stirring and a greyish looking suspension was obtained. The suspension was stirred for 100 min and then stopped. Most

of the solids settled quickly and 1.5 mL of solution was pipeted into a 15 mL centrifuge tube and spun down on #7 for 30 min. At this time a small amount of particulates could be seen in the solution. The concentration was measured by UV spectroscopy ($A=1.7372$; $c=0.9557$). The solution was filtered through a 0.2 μm filter (this removed all the particulates) and the concentration was measured again ($A=1.7285$; $c=0.9506$). The initial solution was $A=1.9774$; $c=1.0963$. Thus we observed a significant drop in the concentration which gives an adsorbance value of 0.1370 mg/g.

Polymer was adsorbed onto smaller glass beads (Polysciences, 3-10 μm in diameter) [B19-96]. The glass beads (1.0128 g) were weighed into a #20 Schlenk tube and THF (20 mL) was added for washing. The suspension was stirred (it stirred easily) for 5 min and allowed to settle (after 40 min there were still particles floating around). The top portion of the solvent was removed and MeOH (20 mL) was added; the suspension was stirred and allowed to settle 40 min after which time the solvent was removed and the beads were pumped down over night at 230 $^{\circ}\text{C}$. A polymer solution (1.6 mg/mL, D23/13K DM1) was prepared in dry DCE and added (3 mL) to the glass beads with stirring (1.5 h). An aliquot was taken and spun down and the concentration determined by UV ($A=1.588$; $c=0.8526$ mg/mL). The initial polymer solution was measured also ($A=2.2357$ and $c=1.3046$ mg/mL). This gives an adsorbance of 1.33 mg/g of small glass beads.

The adsorptions reported in the results and discussion section (Chapter III) were carried with the glass beads (3-10 μm) and the procedure described above [B19-98, 118, 125]. It was found that there was

a contaminant that was displaced from the beads during the adsorption. This contaminant had absorbed in the UV region starting from about 280 nm (the amount of absorbance was small at 280 nm and increased as the wavelength went down) and this interfered with the normal concentration determination method (see UV calibration above). This problem was circumvented by measuring the absorbance maximum located approximately at 271 nm and determining the baseline at 280 nm. Therefore any change in the absorbance caused by the contaminant was also measured in the baseline and thus its effect on the measurement was greatly diminished.

Adsorptions to Glass Microscope Slides

The polymers were adsorbed on Fisher glass microscope slides cut to dimensions of 1X2 cm [B18-88, B19-121]. The slides were cleaned in Nochromix for ~45 min on each side. They were taken out of the acid with tweezers and placed in a 250 mL beaker and rinsed with ~1 l of doubly distilled water (Gilmont still) in 50 mL portions. The slides were then sonicated in distilled water for approximately 2 h with the water changed periodically. They were then sonicated in MeOH (HPLC grade, no additional purification) for ~1 h. The adsorptions were started by taking the slide out of the MeOH with a tweezers and placing it in 20 mL of DCE where it was swirled around and then placed in another DCE container (this was done three times); the slide was then placed in a small glass vial with polypropylene top containing the polymer solution (the slides were never allowed to become dry during this whole process so the solvents were protecting the surface). The adsorptions were run in the dark in a circulator at 25 °C for 3.5 days. They were stopped by using a

tweezers to transfer the slide from the adsorption solution to a beaker for a CCl_4 rinse and subsequently a cyclohexane rinse. The slides were then pumped down at room temperature.

The XPS spectra for these films were carried out as normal with two exceptions: 1) the slides were dipped in hexane and blown off directly before mounting for XPS (this procedure of N. Franchina greatly diminished the ambient silicon on the surface) and 2) the dugout XPS sample holder was used. This was filled just high enough so that top edge of the sample was flush with the sample holder. In this way the edges of the glass are not detected by XPS.

Adsorptions: Measurement via Column Method

The general schematic of the column method, experimental procedure and explanation of the data are given in Chapter III. The solvents (THF and DCE) were dried by distillation from CaH_2 in a continuous still and plumbed directly into the column setup using stainless steel and FEP tubing. The polymer solutions were prepared using DCE from this source and were kept under a dry N_2 atmosphere before and during use. The clean, dry columns (5 x 0.46 cm) were filled with (unactivated) silica gel (~0.93 g) under ambient conditions and packed by tapping the column on the counter and or by using an engraver to cause the column to vibrate as the silica was added. The silica gel used was an old bottle of EM Scientific (SX0143K-1 Grade 950, 60-200 mesh). This product has been discontinued and the replacement that EM Scientific sells now is SX0143L Grade 923, 100-200 mesh. The properties of this material are reported to be pore volume=0.4 cm^3/g , specific area 700 m^2/g

and bulk density of 46 lbs/ft³. The columns were filled before each run, the upstream end was attached to the apparatus and ~5 mL of solvent was pumped through at a rate of 1 mL/min to push the air out. The other end was then attached to the apparatus and the column was conditioned at 0.5 mL/min for approximately 20 min. The adsorptions that we have reported were carried out at a flowrate of 0.25 mL/min. Other flowrates were tested but we found that the pump was not as reliable at the slower rates. A syringe pump was also used but we found that the pressure drops became too large when the small 3-10 μ m beads were used. We discovered an interesting effect with our earlier work. The column was washed (previous polymer desorbed) with THF and then rinsed with DCE. The adsorption was run using a syringe pump to push the polymer solution through the column. The pump could not maintain the correct flowrate during with initial adsorption run because the pressure drop was too high. We found though that we could rinse the solution (but not desorb the polymer) out of the column with DCE and then use the syringe pump to push the polymer solution through again. The pressure drop was not nearly as great this second time and the pump could easily pump at the desired rate. We interpreted this change as evidence that the polymer had adsorbed and caused a large decrease in the surface energy of the solid which resulted in a much lower pressure drop.

References

1. Morton, M.; Fetters L. J. *Rubber Chem. & Tech.*, **1975**, 8(3), 359.
2. Valint Jr., P. L.; Bock, J. *Macromolecules* **1988**, 21, 175.
3. Vink, H. *Makromol. Chem.* **1981**, 182, 279.
4. Gupta, S. K. *Synthesis* **1977**, 39.
5. Ghosh, S.; Pardo, S. N.; Solomon, R. G. *J. Org. Chem.* **1982**, 47, 4692.
6. van der Beek, G. P.; Cohen Stuart, M. A. , Fleer, G. J.; Hofman, J. E. *Langmuir* **1989**, 5, 1180.
7. Personal communication, C. Tripp, Xerox, Canada.
8. Tripp, C. P.; Hair, M. L. *Langmuir*, **1991**, 7, 923.

CHAPTER III

SYNTHESIS OF SPECIFICALLY FUNCTIONALIZED POLY(4-*TERT*-BUTYLSTYRENE) COPOLYMERS AND THEIR ADSORPTION AT THE SILICA-SOLUTION INTERFACE: RESULTS AND DISCUSSION

Objective

The overall objective of this work is to tailor-make polymer chains of controlled structure and investigate how the structure of the chain affects the way in which the polymer adsorbs to the surface. We can then use what we learn to design chains to render specific interfacial structures for particular uses. This is a rather broad goal and by necessity must be broken up into a number of pieces. The work presented in this thesis chapter is some preliminary work toward this overall goal. The first requirement for this work is a polymer system where we have control over the MW, MWD, composition and block sequence through synthetic procedures. Since no such systems are available we developed the one described here and a large fraction of this work was devoted to the synthesis of these types of polymers.

Our other two objectives pertain to the adsorption characteristics of these polymers. We want to evaluate the effect of sticky foot content and sequence distribution on the amount adsorbed, Γ , for the copolymer molecules, and to evaluate the effect of the sticky foot content and sequence distribution on the effective surface interaction parameter, $\chi_{s,eff}$, of the copolymer molecules.

Introduction

Due to the complexity inherent in most real phenomena, gaining a physical understanding can be greatly facilitated by the study of model systems. The simplicity of model systems (in this case polymer molecules) with respect to the actual molecules can help to elucidate the different contributions (and magnitudes) of the various factors involved. In this sense, model compounds can be designed to have a negligible effect on a given variable; this can be used to isolate the effect of each of the variables on the function and structure of the given system. In the same sense, many times model compounds will have enhanced or new applications because they can be “designed for a given application”. The work reported in this thesis chapter involves the development of a synthetic method enabling us to make a wide range of polymer structures; such magnitude of structural control has not been often reported in the literature. The polymers prepared will be used specifically as model compounds in the study of polymer adsorption but should have uses in many other areas of polymer study and application. Figure 3.1 illustrates the types of polymers that can be synthesized and the specific control that we have over the structure. It will be shown that the polymer system developed allows control over the molecular weight, block size and the placement of functional groups, with all distributions having low degrees of polydispersity. The type of functional group and its spacing within a block can be somewhat controlled as well.

The synthesis of these types of polymers is not a trivial matter and much work was devoted to this before a suitable system was found. The first part of the chapter will detail this procedure and the synthetic aspects



Figure 3.1 Illustration of the structural control that has been attained through the synthetic procedures reported in this chapter. Chains of predicted molecular weight and narrow MWD can be obtained. The two blocks (differentiated above by line thickness) can be placed at the desired locations along the chain. The size of all blocks can be controlled independently.

of the work. The polymer system that was finally developed and used is a modified copolymer of styrene and para-*tert*-butylstyrene which results in the copolymer structure depicted below in Figure 3.2. The sticky foot is a

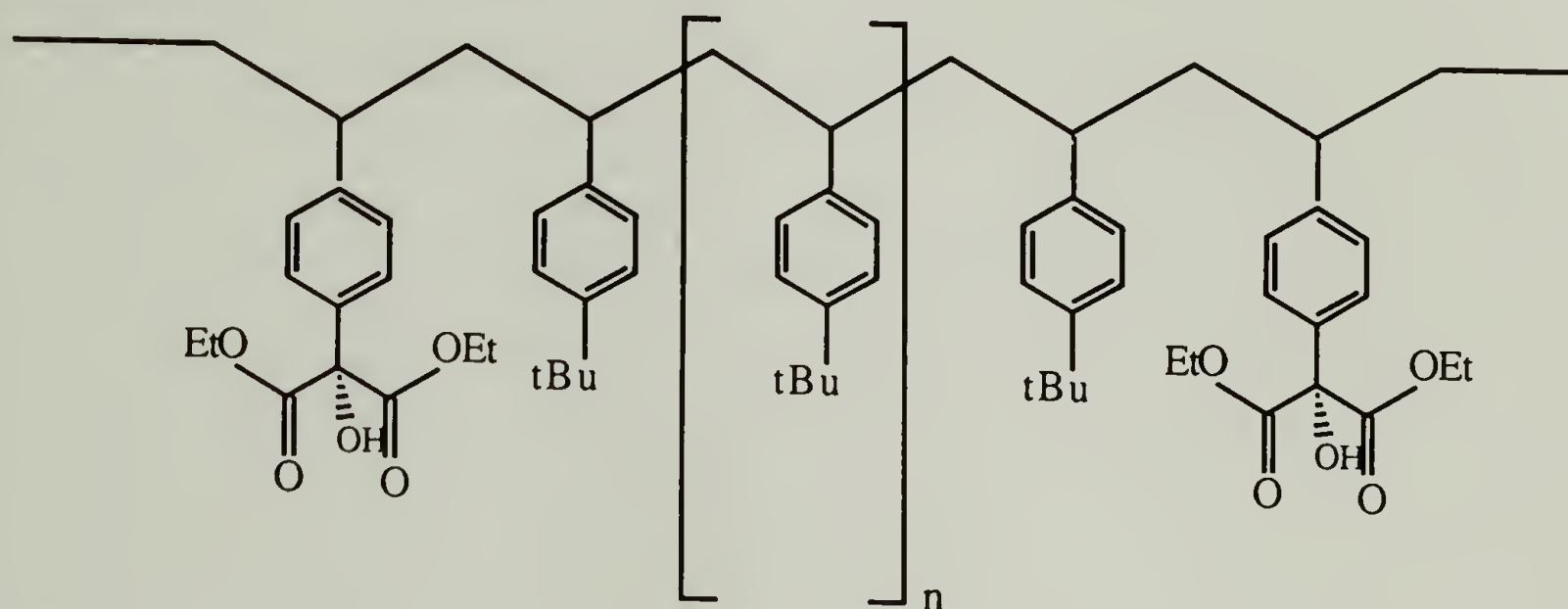


Figure 3.2 Hydroxydiethylmalonate sticky foot polymer.

diethyl hydroxymalonate moiety attached at the para position of the phenyl rings in polystyrene monomer units of the precursor polymer. The *tert*-butylstyrene (tBS) units are the spacer segments between the sticky feet.

The second half of this chapter deals with the study of the adsorption of these types of polymers. This requires a reliable method for measuring the amount adsorbed, and to this end, a number of possible methods were surveyed and developed. The advantages and disadvantages of these different methods will be described in the adsorption section, and the adsorption data obtained will be discussed.

Polymer adsorption is a subject of great current interest with many applications, the main aspects of which were discussed in Chapter 1. It will be shown that definite differences are observed between the adsorption characteristics of two polymers of different architectures (AB diblocks and ABA triblocks). The diblock copolymers have been found to have a higher adsorbance than the triblock copolymers of the same composition. The diblock copolymers have also been observed to stabilize colloidal dispersions whereas the triblock copolymer flocculate the same suspensions. We have observed that the polymer architecture has little effect on the adsorption/desorption equilibrium as was indicated by measurement of critical displacer concentrations by thin layer chromatography (TLC).

Synthesis: General Aspects

The strategy used for the synthesis was to prepare a precursor polymer of the appropriate structure (anionically) and then selectively modify one of the monomer pairs to obtain the sticky moiety. A discussion of this strategy and other possibilities has been given in Chapter 1. The main requirement for this is the ability to selectively functionalize one of the monomer units while the other remains completely inert. Failure to meet this requirement results in the placement of rogue sticky feet on the nonsticky block. Relatively few monomers pairs exist which allow the synthesis of the desired precursor block structures; these are basically limited to the vinyl hydrocarbon monomers such as styrene, *para-tert*-butylstyrene, butadiene and isoprene (see Chapter I Synthetic Aspects for a more detailed discussion). The pair chosen determines the type of modification chemistry that will be applicable and also the difficulty with

which total selectivity can be achieved. The monomer pair used here, styrene and *p-tert*-butylstyrene, requires the selective modification of one aromatic ring. This is achieved by taking advantage of the bulkiness of tertiary butyl group and the polymer backbone that sterically hinder addition to the *tert*-butylstyrene ring. This requires the use of a large electrophile and relatively mild conditions. A different system, such as copolymers of styrene and hydrogenated butadiene would inherently decrease the selectivity needed because only one ring is present.

The synthesis of these "sticky foot" (SF) polymers involves anionic copolymerization of styrene and *p-tert*-butylstyrene monomers to obtain the appropriate precursor block copolymer. This monomer pair is rare, in that each monomer can initiate the polymerization of the other. This allows the synthesis of any copolymer sequence desired. Thus blocks of potential sticky feet can be placed at any desired location along the chain. The second step involves the selective functionalization of the polystyrene units. This reaction must be quantitative for the PS units and completely unreactive towards the PtBS units. The chemistry that was adopted for this purpose complies with the goals stated above; it involves the Friedel Crafts reaction of diethyl oxomalonate (DEOM) at the para position of the styrene phenyl ring to form the *para*-2-hydroxy diethylmalonate sticky foot. The data shows that we can make these types of polymers, that the modification is selective to the styrene units, that one can obtain full or partial functionalization through manipulation of reaction conditions and that the modification does not effect the MWD. In addition it will be shown that this sticky foot is a reactive handle that can be used to quantitatively convert the hydroxy diethylmalonate unit to other functional groups. In

particular the diester can be reduced to the triol, or hydrolyzed to the acid salt. The hydrolyzed blocks are water-soluble and this enables us to prepare hydrophobically associating water-soluble block copolymers of many different architectures. We have also developed a new synthesis that yields 100% *para-tert*-butylstyrene because of the infeasibility of purifying the commercially available monomer (contains 5% other isomers). The ortho and meta isomers have the potential of being functionalized by DEOM and thus are a source of rogue sticky feet in the *tert*-butylstyrene block.

Precursor polymer Synthesis

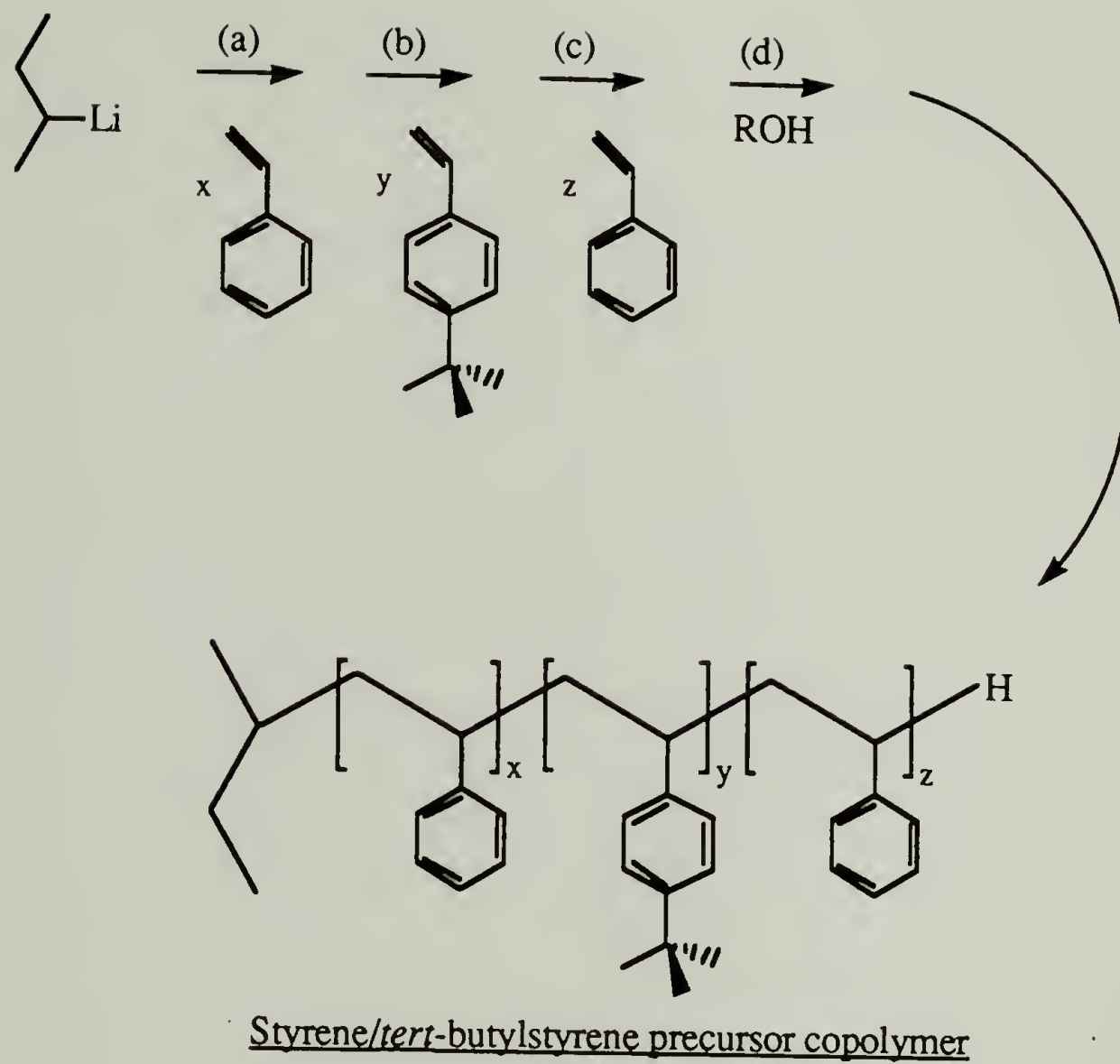
The precursor polymer system chosen should be one which allows control over monomer placement along the chain, as well as control over the composition and molecular weight. For this reason each of the monomers in the pair must be capable of initiating polymerization of the other. These requirements are fulfilled by the monomer pair of styrene and *p-tert*-butylstyrene which has been reported to undergo living polymerization to obtain both block and random structures.¹⁻⁴ Chen & Fetters⁴ determined reactivity ratios for the styrene/*tert*-butylstyrene system at 20 °C in benzene with lithium counterion, and these are 1.3 (± 0.12) and .86 (± 0.10) respectively. They also added THF to the system to break up the known chain-end aggregation, and this had little effect on the reactivity ratios. THF, cyclohexane and benzene were all used as solvents in this work.

A number of precursor copolymers of styrene and *para-tert*-butylstyrene were prepared with various compositions, molecular weights and chain architectures. A list of the polymers, their composition,

molecular weight, polydispersity and architecture can be found in Table 3.1 (polymers made with 100% tBS) and Table 3.2 (polymers made with commercial monomer). Only three architectures were synthesized: random, diblock and triblock (sticky blocks occupy the ends of the chain). The precursor polymers are named in the following fashion: D23/13k-p or T40/50k-p. This nomenclature yields the following information: D, T or R represents diblock, triblock or random copolymer, respectively. The number following the letter indicates the mole % styrene in the polymer. The number after the slash indicates polymer molecular weight (in units of 1000 daltons), and p denotes precursor.

The synthesis is described in Scheme 3.1; the polymerization was initiated by *sec*-butyllithium and various block structures were obtained by the sequential addition of the appropriate amount of monomer. Scheme 3.1 shows the synthesis of a styrene_x-*tert*-butylstyrene_y-styrene_z triblock copolymer. The termination is accomplished by addition of a proton source such as methanol or isopropanol (see Chapter II for details). Anionic synthesis requires extremely rigorous purification procedures and techniques.⁵ A discussion of the general aspects of the synthetic procedure can be found in Chapters II and IV.

The polymers in Table 3.1 were, for the most part prepared using either cyclohexane (entries 7, 8, 13 and 14) or a cyclohexane/benzene (all other entries except 18 and 22) azeotropic mixture (45:55) at room temperature. The initiation rate and propagation rate were rather slow in cyclohexane (polymerization time was on the order of hours). The use of benzene increases both rates and thus preparation of the multi-block



Scheme 3.1 Precursor Polymer Synthesis

Table 3.1 Precursor Polymers: Molecular Weight, Polydispersity and Percent Sticky Foot Information.

<u>Sample</u>	<u>% Styrene</u>	<u>M_n</u>	<u>PDI</u>	<u>Architecture</u>
1. D5/50k-p	5	50,637	1.054	diblock
2. ^a D5/179k-p	5	179,028	1.083	diblock
3. T5/50k-p	5	44,946	1.04	triblock
4. D12/50k-p	12	46,972	1.041	diblock
5. T12/50k-p	12	48,328	1.051	triblock
6. ^a T12/156-p	12	155,715	1.058	triblock
7. D23/13k-p	23	12,394	1.090	diblock
8. T23/12k-p	23	11,596	1.070	triblock
9. D23/50k-p	23	43,273	1.036	diblock
10. ^a D23/43k-p	23	43,186	1.039	diblock
11. T23/50k-p	23	43,451	1.039	triblock
12. ^b AT23/50k-p	23	49,711	1.044	triblock
13. D23/76k-p	23	75,917	1.069	diblock
14. T23/81k-p	23	81,350	1.098	triblock
15. D28/73k-p	28	73,128	1.070	diblock
16. T28/69k-p	28	69,505	1.050	triblock
17. D28/110k-p	28	110,934	1.021	diblock
18. ^b AT37/71k-p	37	71,490	1.021	triblock
19. D40/50k-p	40	41,307	1.107	diblock
20. T40/50k-p	40	48,392	1.047	triblock
21. D77/58k-p	77	58,663	1.045	diblock
22. ^c R80/184k-p	80	184,382	1.136	random
23. D86/87k-p	86	87,531	1.02	diblock
24. D90/16k-p	90	16,423	1.025	diblock
25. D94/110k-p	94	110,109	1.025	diblock
26. D95/33k-p	95	33,551	1.023	diblock
27. T95/33k-p	95	32,604	1.019	triblock
28. D98/110k-p	98	110,472	1.027	diblock
29. D99/657k-p	99.2	657,162	1.151	diblock

^a These polymers end-capped with ethylene oxide.

^b Asymmetric triblock copolymers.

^c Made with commercial monomer in THF.

Table 3.2 Precursor Polymers II: Molecular Weight, Polydispersity and Percent Sticky Foot Information.^a

<u>Sample</u>	<u>% Styrene</u>	<u>M_n</u>	<u>PDI</u>	<u>Architecture</u>
1. D02/5.9k-p	2.3	5,896 ^d	1.1	diblock
2. T04/4.2k-p	4.1	4,234 ^d	1.1	triblock
3. T14/12k-p	21.6	11,987 ^d	1.1	triblock
4. b, ^c R50/256k-p	50	255,781	1.07	random
5. ^c R50/684k-p	50	684,475	1.06	random
6. ^c R50/114k-p	50	114,022	1.07	random
7. ^c R60/73k-p	60	73,257	1.06	random
8. ^c R60/241k-p	60	220,945	1.04	random
9. ^c R70/155k-p	70	155,626	1.06	random
10. ^c R80/247k-p	80	247,435	1.06	random
11. ^c R90/175k-p	90	174,514	1.05	random
12. ^c PTBS/116k-p	0	116,169	1.03	homopolymer

a These polymers made with commercial *tert*-butylstyrene in THF

b Has substantial dimer.

c Polymer made in THF with commercial monomer

d Data determined with RI detector, calibration not correct: real mw T14/12k-p is 25,256.
Also note that the polydispersity indices are higher with this detector.

structures was more convenient (the time between monomer additions was less). It seems that the cyclohexane/benzene mixture results in slightly narrower MWDs because of the faster initiation as compared with neat cyclohexane. It should also be noted that styrene seems to give slightly more narrow MWDs than the tBS: this can be seen by comparing the PDIs of the polymers with high styrene content (entries 23 through 28 Table 3.1) with the copolymers with a higher percentage of PtBS. Both cyclohexane and benzene are good solvents for the PtBS chains at room temperature and therefore polymer precipitation was not a concern for the copolymer synthesis. Polymerizations that are carried out in THF require much shorter times; the polymerization is complete within minutes as compared with the many hours required in cyclohexane. They result in much narrower molecular weight distributions (because of the faster rates of initiation). The slower initiation rate (in cyclohexane vs. THF) can be seen easily upon addition of monomer to initiator: in THF an orange color develops instantaneously, due to the formation of the polystyryl anion, whereas in cyclohexane, the final (orange) color is not obtained until a few minutes have passed. The polymerization itself is much more difficult to run in THF than in cyclohexane or benzene because of the hygroscopic nature of the solvent (THF). Thus most polymerizations were not carried out in THF (see Chapters II and IV for a more detailed discussion). We found that addition of a very small amount of THF (roughly 10 times the initiator concentration) to a polymerization in cyclohexane results in much faster rates of initiation and much narrower molecular weight distributions. Entries 16 and 18 are copolymers of essentially equal molecular weights but entry 16 was polymerized in cyclohexane (PDI=1.05) and entry 18 was polymerized using THF-spiked cyclohexane

(PDI=1.02). The difference in the molecular weight distributions of these two polymers is seen more clearly by comparison of the actual GPC traces where the THF-assisted polymerization chromatogram easily fits within the curve of the other. Three polymers (Table 3.1 entries 6, 10 and 12) were endcapped with ethylene oxide (to obtain a hydroxyl group); this can be used to place a perfluoro ester at the end of the chain. Table 3.1 also contains two asymmetric triblock copolymers that can be used for surface loop to trail transition studies. It was found that oxidative coupling (not CO₂ coupling) caused the formation of a small amount of coupled polymer in a number of samples; attempts were made to isolate the cause but these proved unsuccessful. The bulk of the polymers reported in Table 3.2 (all entries except 1, 2 and 3) were of random architecture and were prepared using commercial monomer and THF as the polymerization solvent. The polymerizations were carried out in THF at -78 °C following procedures outlined in Chapter I. It was found that all these polymers had a small low molecular weight tail. It was not ascertained whether this was caused by the random polymerization or whether it was an effect of the commercial monomer. The tail was not obtained when styrene homopolymers or styrene/propylene sulfide block copolymers were prepared (Chapter IV).

The precursor polymers were characterized with IR, NMR, gel permeation chromatography (GPC) and TLC. Infrared spectra of the precursor polymers show the emergence of the methyl C-H stretches (2965 cm⁻¹, 2866 cm⁻¹), an added ring mode (1502 cm⁻¹), the *tert*-butyl doublet (1392 cm⁻¹ and 1362 cm⁻¹) and the aromatic out-of-plane *tert*-butyl vibration at 828 cm⁻¹ as the percentage of *tert*-butylstyrene is increased. Proton NMR spectra of the precursor polymers show the emergence of the

tert-butyl resonance at 1.25 ppm with increasing *tert*-butyl content. GPC shows that narrow molecular weight distributions were obtained with predictable molecular weights.

The polymers were prepared by sequential addition of the monomers. Gas chromatography (GC) was used to follow the extent of reaction to determine when the next monomer could be added. Gravimetric determinations of the yield of the resultant polymers indicate greater than 95% yield in most cases (this can be taken as quantitative conversion because one would expect to lose some of the product in precipitation, isolation and so forth). These two methods of analysis prove that all of the monomer was polymerized and thus the block structures are confirmed and the polymer compositions are indicated by the amount of each monomer used to make a particular polymer. The compositions determined by amounts of the monomers used agree well with those determined by proton NMR. The aromatic to aliphatic ratio, \emptyset , from these spectra was used to determine the actual copolymer composition, $x(\emptyset)$. The following equation was used [B9-119]:

$$x(\emptyset) = (12\emptyset - 4) / (1 + 9\emptyset) \quad 3.1$$

One can see from Table 3.3 that there is good agreement between NMR and the expected composition, especially for the random copolymers. The compositions (of the precursor polymers) used in this thesis are determined from the ratio of the monomers added, and not the NMR data.

Table 3.3 PS/PtBS Copolymer Composition Data:
 ^1H NMR.

<u>Sample</u>	<u>Styrene %^a</u>	<u>\bar{Q}^b</u>	<u>$x(\bar{Q})$^c</u>
PtBS B9-57	0.0	0.327	-0.019
PS50R 50/50 B9-57	50.0	0.599	0.499
PS70R 70/30 B9-16	70.0	0.853	0.719
PS90R 90/10 B9-43	90.0	0.129	0.910

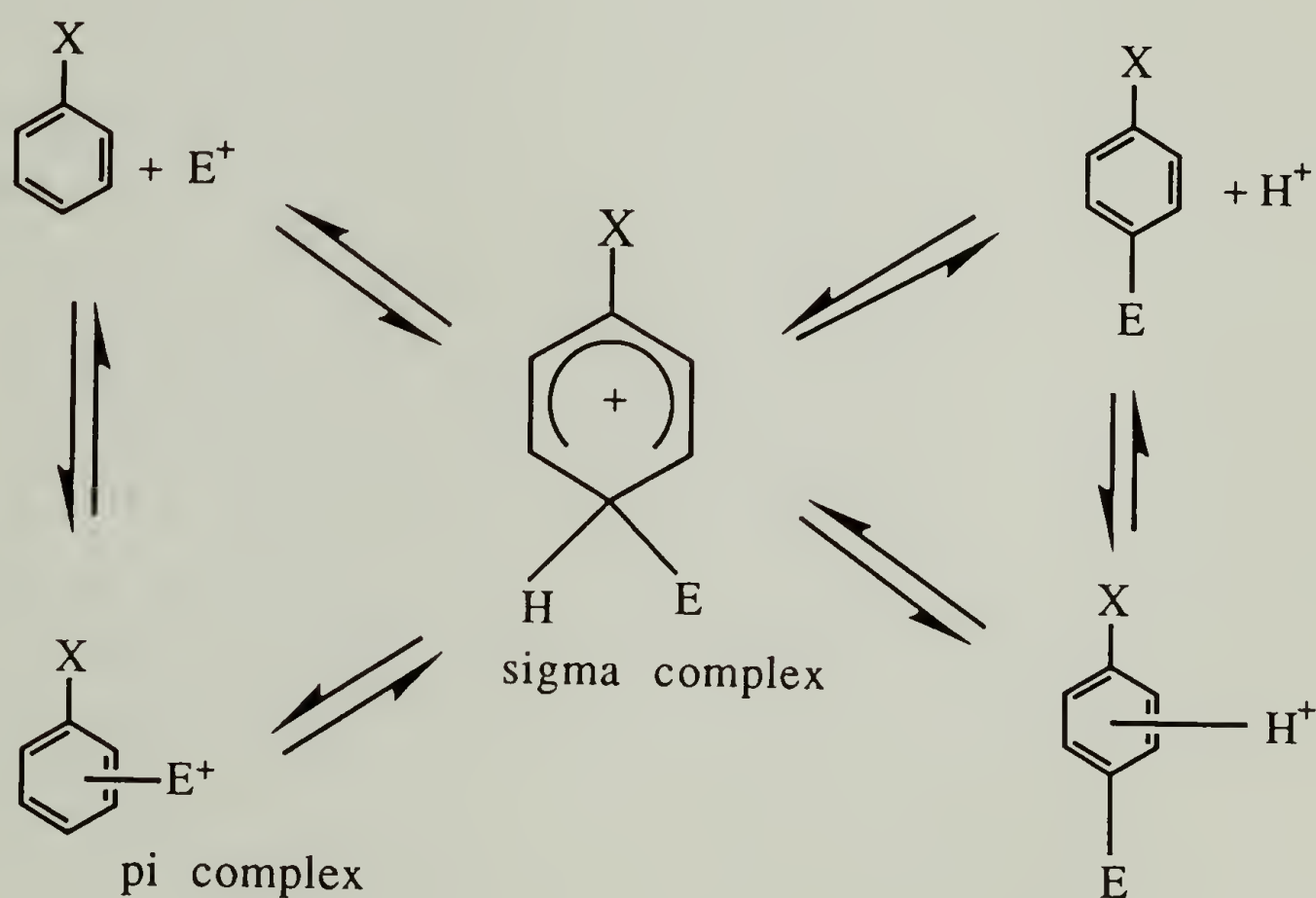
^a Expected styrene content calculated from ratio of monomers reacted

^b Ratio of aromatic to aliphatic protons

^c Mole fraction of styrene units as calculated by equation 3.1

Modification Reactions: General Aspects

A suitable modification reaction requires that the styrene monomer units react relatively easily while the PtBS units remain inert. The type of reaction that has been carried out on these copolymers is electrophilic aromatic substitution (EAS)⁶⁻¹⁰ which occurs selectively at the para position of the styrene monomer unit. The general reaction mechanism for EAS reactions is shown below in Scheme 3.2.6



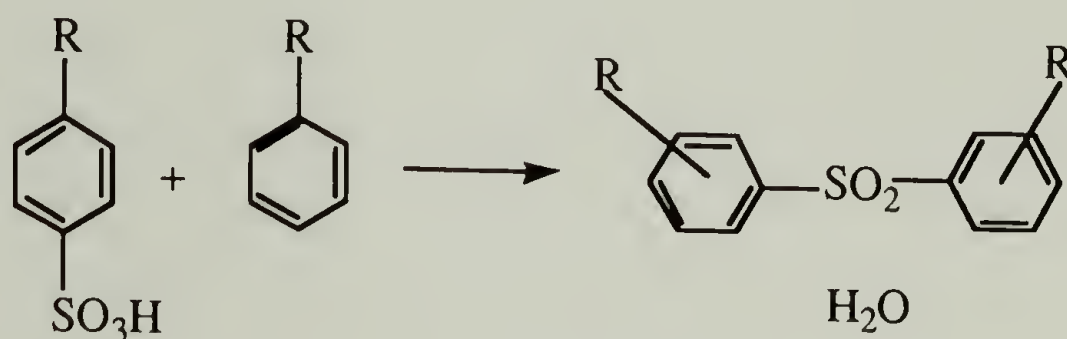
Scheme 3.2 Electrophilic Aromatic Substitution.

Here the electrophile, E^+ , adds to the ring forming a sigma complex. The pathway may or may not include the pi complex. In most cases the formation of the sigma complex is the rate determining step, although in a number of instances, formation of the electrophile (for example, some

nitration) or subsequent deprotonation have been found to at least partially contribute.⁶ The identity of substituent X is known to affect the overall reactivity of the ring and also the placement of the substituent on the ring (ortho, meta, para). These effects, called the selectivity, have been extensively studied.^{6,8,12} Inductive electronics, pi electron interactions, and sterics all contribute to the selectivity. For most reactions of this type the highest activation energy state is close in structure to the sigma complex and thus substituents that lower the energy of the sigma complex increase the reaction rate. Because of the electron-deficient character of the sigma complex, substituents that donate electron density (either inductively or by resonance) lower the energy of the sigma complex and increase the rate; these are said to activate the ring. Electron withdrawing groups destabilize the transition state and deactivate the ring. The important point here is that the ability of X to influence the reaction (and the selectivity) depends on where, along the reaction coordinate, the highest energy state is. Therefore, less reactive electrophiles show more selectivity between different rings and different positions (ortho vs. para) on the same ring. The bottom line is that if selectivity is important (as it is here), one wants to use less reactive electrophiles and rings. Most electrophilic aromatic substitution reactions are irreversible under normal conditions, resulting in kinetic products. Thus the selectivity and rate differences discussed above are very important in determining the product one will obtain. Sulfonation and Friedel Crafts alkylation are exceptions to the rule with the reverse reaction favored at elevated temperatures and catalyzed by strong protonic or Lewis acids. In many instances of electrophilic substitutions, the electrophile is not reactive enough alone but complexation with protonic or Lewis acids increases the electrophilicity and ring addition is accomplished.

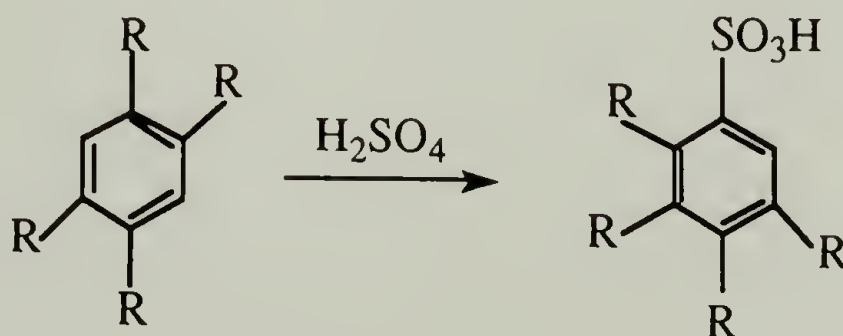
These Lewis acids range in reactivity (strength); for example, AlCl_3 is very reactive whereas SnCl_4 is considerably less so.¹³

There are a few potential side reactions that could complicate this synthesis. The first is reaction of the original product with an additional ring, as is illustrated in the sulfone formation below.¹⁴ The Jacobsen



Scheme 3.3 Aromatic Sulfone Formation.

reaction (shown in Scheme 3.4) is a result of the reversibility of Friedel Crafts alkylations and results in alkyl group migration under highly acidic conditions (i.e. strong Lewis acids).¹⁵



Scheme 3.4 Jacobsen Reaction.

Because of the relative stability of the *tert*-butyl carbenium ion, tertiary butyl groups are especially susceptible to this migration. It has been reported that when *tert*-butyl or isopropyl groups are present, ipso substitution (addition at the substituted carbon) can occur, which in turn causes the butyl group to migrate to another ring or be split off as the corresponding alkene.¹⁵ As will be mentioned in the discussion, this may indeed be happening to the polymer in some of the reactions reported here.

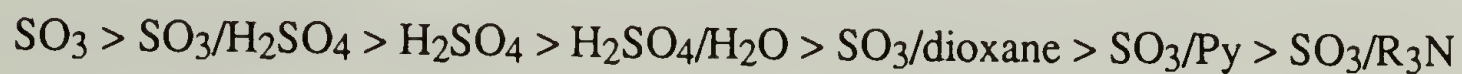
The modification reactions had two main goals: 1) The synthesis of SF type polymers for adsorption studies and 2) The synthesis of sulfonated water-soluble polymers for gel electrophoresis studies. These goals were attempted concurrently, and thus many of the reactions were run in an effort to sulfonate the ring. However, these sulfonations were determined to be inadequate and polymer modification with diethyloxomalonate was developed. These two sets of reactions (sulfonations and DEOM/SnCl₄) will be discussed separately.

Sulfonation Reactions

Selective sulfonation was the first modification investigated for these PS/PtBS copolymers. The reaction of sulfur trioxide complexed with triethylphosphate was reported to be selective to the styrene unit by Bock and Valint.^{1,2} Presumably the sulfonating electrophile is too sterically hindered to react at positions ortho to either the *tert*-butyl group or the polymer backbone. Sulfonated random copolymers were to be used for electrophoresis experiments to test the counter-ion condensation theories of Manning.¹⁶ It was also thought that small amounts of the sulfonate groups on the polymer chain would be good sticky feet for polymer adsorption

and would lead to interesting adsorption characteristics on charged surfaces. Kawaguchi et. al. had reported the adsorption of sulfonated polystyrene to platinum electrodes.¹⁷ It was found that conditions resulting in selective sulfonation were difficult to achieve and the resulting products were not the best for the electrophoresis studies.

Sulfonation of aromatic rings is an old reaction and has been carried out many different ways.^{18,19} Much work has been done in elucidating the structure of the acting electrophile in sulfonation reactions, the identity of which depends on reaction conditions. Suffice it to say, the reactive species can be viewed as sulfur trioxide, SO_3 , or some complex thereof.²⁰ Uncomplexed sulfur trioxide is extremely reactive and very difficult to work with.²¹ It is usually complexed with a Lewis base to tame its reactivity. The greater the basicity of the complexing agent the more stable the complex and the less reactive. Thus we have the following order of reactivities:



Scheme 3.5 Sulfur Trioxide Complexes: Relative Reactivities.

H_2SO_4 forms a complex with water ($\text{pK}_a = -1.7$, H_3O^+) which is more reactive than a complex with Me_3N ($\text{pK}_a = 9.79$, Me_3NH^+). The complexes at the low end of the reactivity scale are used to make sulfates from alcohols, but they will not react with aromatic rings.

Trialkylphosphates are also used to tame reactivity and in these complexes the reactivity depends on the ratio of SO_3 to phosphate. These complexes with trialkylphosphates will be discussed subsequently. Because of the side reactions, principally sulfone formation, sulfonating PS has not been a trivial thing. A survey of the literature shows three main ways of doing this, in addition to the method reported by Exxon to make ionomers. These four methods will be summarized below.

The first method developed specifically for sulfonation of polystyrene was that of Turbek.²² In this paper, he describes a method for sulfonating PS without an increase in molecular weight, i.e. no sulfone formation. This is the method subsequently used by Valint and Bock at Exxon. The activity of SO_3 is controlled by complexing with trialkylphosphates at different molar ratios. One can see that each phosphate molecule has four Lewis base sites to complex with SO_3 , the phosphoryl oxygen ($(\text{EtO})_3\text{P}\underline{\text{O}}$) being the most basic followed by the three ester oxygens ($(\text{Et}\underline{\text{O}})_3\text{PO}$). The phosphoryl oxygen bond is too basic: 1:1 mixtures of triethylphosphate in dichloroethane at reflux temperatures do not react with aromatic rings, but they will sulfonate alcohols. Increasing the ratio of SO_3 to the phosphate to 2:1, 3:1, or 4:1 allows the ester oxygens to be used and these facilitate sulfonation of polystyrene without crosslinking. Typical conditions used by Turbek were: $\text{SO}_3:(\text{EtO})_3\text{PO}$ (3:1); 25 °C; 10 min; 2% polymer solution in dichloroethane with a ratio of SO_3 to polymer repeat unit of 2:1. These conditions resulted in water-soluble polymer with no evidence of cross-linking (i.e. sulfone formation) as evidenced by viscometry (although this method of analysis may not allow detection of only a few percent). It should also be mentioned that

poly(vinyltoluene) sulfonates to a comparable extent as polystyrene under the same conditions, which indicates that at least the methyl group does not hinder the reaction. It was also found that anywhere from 20-40% of the sulfonation product was the ethyl ester and not the acid. Turbek postulated this might be why sulfone formation is not a problem with this reaction. The paper also mentions that preformation of the complex leads to more reproducible results. The Exxon group followed this general procedure with a few changes. The overall ratio of $\text{SO}_3:(\text{EtO})_3\text{PO}$ was 5.5:1 (which is quite high) but the SO_3 was added to the polymer phosphate solution a little at a time. The copolymers they used had 5-11% *tert*-butylstyrene content and all were water-soluble after sulfonation. Elemental analysis was used to determine the sulfonate content and this agreed with what was expected from the copolymer composition.

The second method for sulfonation was reported by Carrol and Eisenberg,²³ in 1966. This is a heterogeneous reaction where finely divided (large surface area) polymer powder (200 mg, 1.92 mmole) is added to 100% H_2SO_4 (40 mL) to which has been added 400 mg (1.96 mmole) of AgSO_4 as a catalyst (note the catalyst is used in stoichiometric proportion to the polymer). The reaction was run at room temperature for approximately 15 min, at which time all the polymer had been transformed and was dissolved. They reported that titration and elemental analysis data indicate almost 100% reaction and light scattering and sedimentation showed no crosslinking or degradation. After the polymer was dialyzed, neutralized and lyophilized, they obtained a nice white powder. They also found that reactions run under these conditions for 24 hours showed no change in products.

The next sulfonation procedure, developed specifically for polystyrene, was reported by Vink.²⁴ This procedure is rather similar to the Eisenberg method, the difference being how one creates the surface area for the two phase system. In this procedure, polystyrene (1.5 g, 15 mmol) is dissolved in 75 mL cyclohexane. This is added, with stirring, to a solution of 50 mL H₂SO₄ (97%) and 0.11 g (0.77 mmole) P₂O₅ (or AgSO₄) as an accelerator (catalyst). The reaction is run at 40 °C for 1.5 hours and then worked up by dialysis, etc. As one can see this method is actually quite similar to that of Eisenberg and is said to give 98-100% sulfonation by titration.

The fourth procedure I would like to mention is that of Exxon for making ionomers.²⁵ In this case, the end product is a lightly sulfonated PS (1-5 mole %). The active electrophile is acetyl sulfate produced in situ by reaction of acetic anhydride and H₂SO₄. The general procedure is to dissolve 200 g (1923 mmole) PS in 500 mL DCE and then add the appropriate amount of anhydride (40.6 mmole). H₂SO₄ (26 mmole) is added slowly at 50 °C, and the reaction is run for 1hr. One can see from this that one adds only as much H₂SO₄ as desired. The procedure did not mention the upper limit of sulfonation obtainable by this method.

The Turbek method ((EtO)₃PO, Exxon modified) and the Vink method were the only two of the four above mentioned procedures that were used to sulfonate polymers. Table 3.4 gives the notebook references and conditions for these sulfonations using the Exxon method ((EtO)₃PO). All polymers, except the control, were soluble in water, methanol or a

Table 3.4 Sulfonation Reactions: Exxon Method.

<u>Sample</u>	<u>Reaction Conditions</u>
ExxSulf-1 B9-22 R70/155k-p (precursor)	<p>S1: 5.0g (28.9mmole) polymer; 100ml DCE S2: 3.5g (43.3mmole) SO₃ ; 100ml DCE S2: ~8.36 mmole EtO₃PO in DCE</p> <p>Alternated addition at 0 °C; polymer ppt. washed w/ pentane; obtained polymer that would dissolve to slight haziness in water small amount of MeOH cleared solution.</p>
ExxSulf-2 B9-74 R90/174k-p (precursor)	<p>S1: 0.3g (2.7mmole) polymer; 6ml DCE S2: (4.8mmole) SO₃, (0.77mmole) TEP, 10ml DCE S3: 0.08ml (.46mmole); 6ml DCE</p> <p>Cooled to 0°C, alternated S2 1ml then S1 0.5ml over 20min; 15min additional polymer ppt.; washed with pentane; redissolved in 20ml MeOH; dialized to neutrality, then 0.2M NaCL, lyophilized. Obtained 0.63g of slightly yellow product.</p>
ExxSulf-3 B9-76 R50/114k-p (precursor)	<p>S1: 0.31g (1.16 mmole) polymer; 6ml DCE S2: (2.3 mmole) SO₃; (0.37mmole)TEP 6ml DCE S3: DCE forgot TEP</p> <p>Did rxn same as above; obtained 0.8g of slightly yellow powder</p>
ExxSulf-4 B9-78 R70/155k-p (precursor)	<p>S1: 0.29g (1.7mmole) polymer; 6ml DCE S2: (2.0mmole) SO₃; (0.32 mmole)TEP 5ml DCE S3: 0.01ml (0.06mmole) TEP; DCE</p> <p>Ran rxn same as above two; dialysis bag broke no polymer recovered</p>
ExxSulf-5 B9-79 PtBS/116k-p (precursor)	<p>S1: 0.12g(.75mmole) polymer; 4ml DCE S2: (1.6mmole) SO₃; (0.26mmole) TEP 4ml DCE S3: TEP (not sure how much); DCE</p> <p>Did rxn same as 3 above, but the polymer didn't ppt. even after 12hr rxn. Assumed no sulfonation occurred so didn't work up.</p>

S1 = solution 1, S2 = solution 2, S3 = solution 3: S1 and S2 are always added alternately, with stirring, to S3.

TEP = (EtO)₃PO

mixture of both. This result was contrary to that reported in the Valint/Bock Patent ² which stated "polymers down to 80% sulfonation were water-soluble". We found that polymers with 50% *tert*-butylstyrene groups became water/methanol soluble (dissolved easily in methanol and were dialyzed against water and did not fall out of solution). Gel electrophoresis data showed what appeared to be sulfone formation, as evidenced by the presence of polymeric dimers and trimers. Figure 3.3 shows the infrared spectrum of a 50% PtBS (ExxSulf-3) copolymer. One can see the absorbances expected for the sodium salt of the acid. The -SO₂- and -CSO- stretches are located at 1183 cm⁻¹, 1129 cm⁻¹ and 1042 cm⁻¹, 1029 cm⁻¹ respectively. These correspond quite well those of *p*-toluene sodium sulfonate (1198, 1132, 1050 and 1008 cm⁻¹). The absorbances at 3441 cm⁻¹ and 1640 cm⁻¹ are due to water of hydration. The ratio of the CH₃ aliphatic stretch (2963 cm⁻¹) to the -CH₂- methylene stretch (2924 cm⁻¹) in the two polymers shows that there is still a greater number of *tert*-butyl groups in the 50% copolymer than in the 90% copolymer. Figure 3.4 shows the ¹H NMR spectra of the 90% styrene sulfonated copolymer (in D₂O); note the high ratio of the aromatic versus the aliphatic peak areas, ω . Table 3.5 contains data obtained from NMR for the ratio calculated for 100% sulfonation of the styrene units in the copolymer and the value calculated for a 100% sulfonated polystyrene homopolymer. One can see there are large discrepancies in the measured versus the calculated ratios.

Extensive sulfonation alone cannot account for these high omega values. One explanation for this is that the *tert*-butyl groups are being

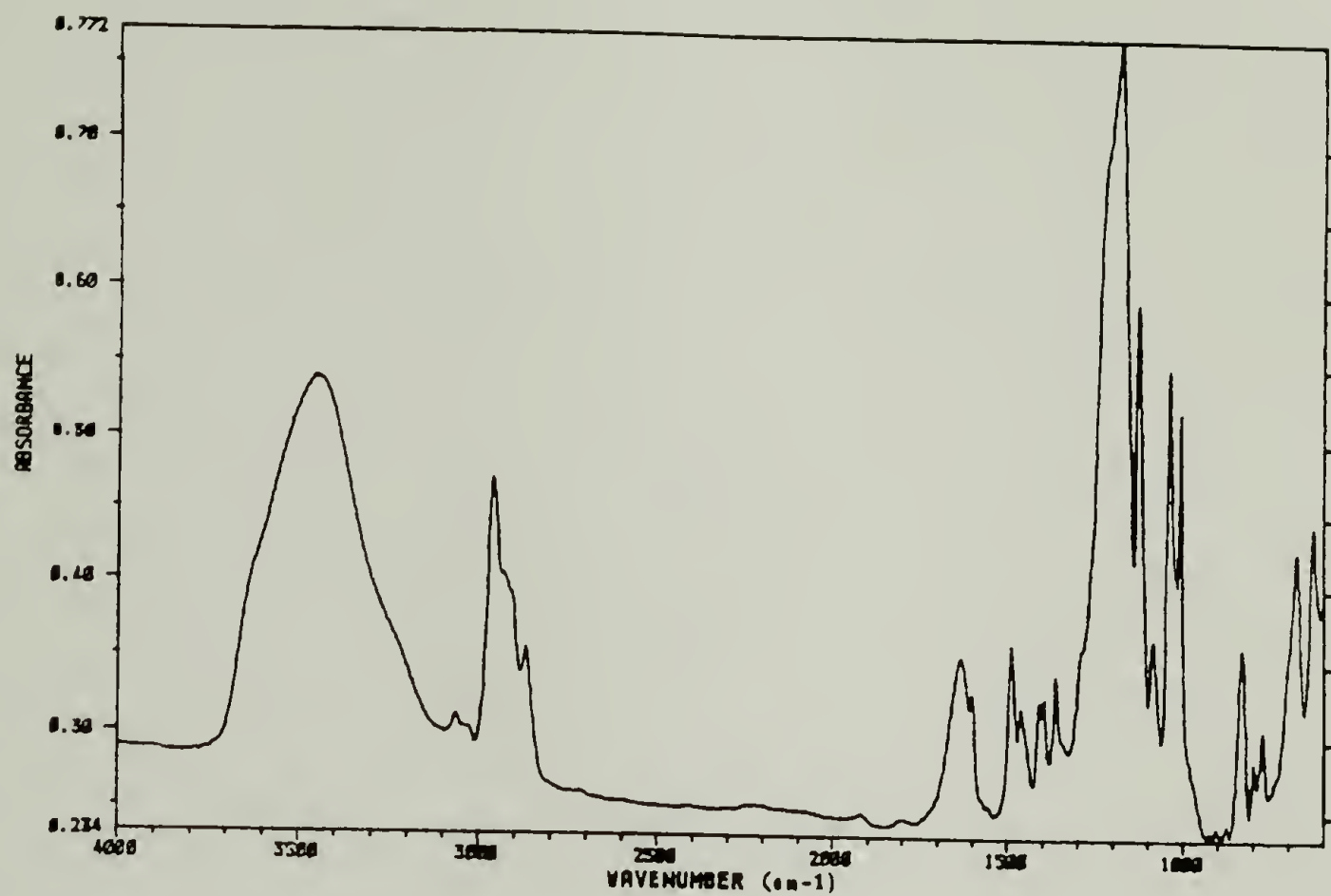


Figure 3.3 IR spectrum of a 50/50 random copolymer (R50/114k-p) sulfonated with SO₃/TEP (See Table 3.4, ExxSulf-3).

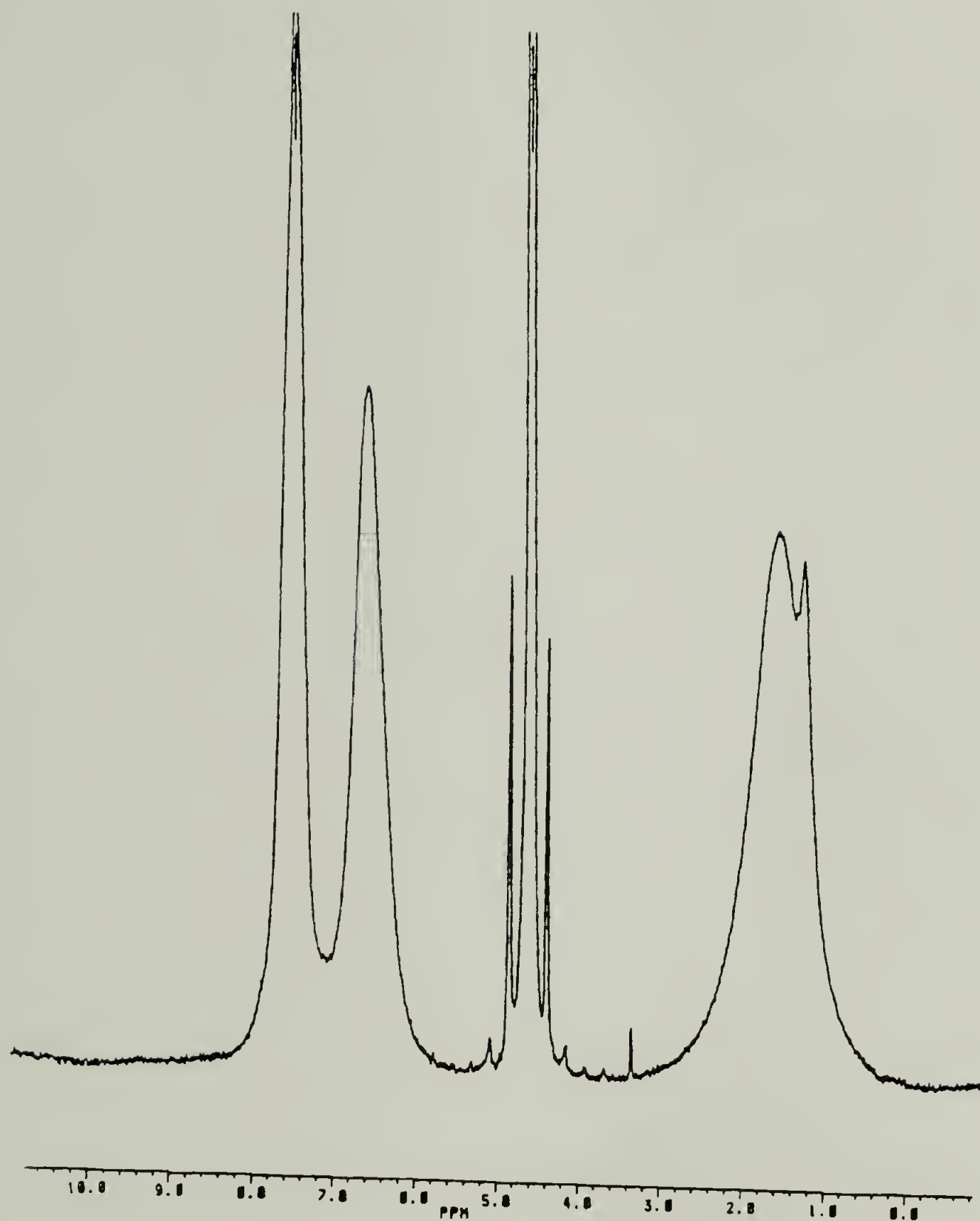


Figure 3.4 ^1H NMR spectrum (in D_2O) of a 90/10 random copolymer (R90/75k-p) sulfonated with SO_3/TEP (See Table 3.4, ExxSulf-2).

Table 3.5 Aromatic:Aliphatic ^1H NMR Data for Sulfonated Copolymers.

	<u>$\omega(\text{NMR})$</u>	<u>$\omega(\text{calc})$</u>	<u>$\omega(\text{fully sulfonated PS})$</u>
50/50	1.05	0.53	1.33
90/10	1.29	1.04	1.33

cleaved from the ring (retro Friedel Crafts reaction). Another explanation is that the hydrophobic parts of the polymer aggregate and are not sampled by the spectrometer. This solvency effect has been observed before: the hydroxyl resonance of the 1,2,3-triol (the triol polymer obtained from a reduced DEOM modified polymer) is not seen in a straight $d\text{-CHCl}_3$ solution, whereas upon addition of a small amount $d\text{-MeOH}$, the peak is detected (the peak due to CD_3OH is also seen). Elemental analysis was performed on these two polymers and *para*-styrene sodium sulfonate as a control (Table 3.6). The initial analysis indicated the presence of a fair amount of NaCl (the polymers were dialyzed against a NaCl solution), so they were dialyzed in running tap water for over a week to obtain the second set of numbers. Note that the sulfur content of both copolymers is much higher than the expected amount, suggesting either over-sulfonation or cleavage of the tertiary butyl groups. The high hydrogen content can be explained as due to the amount of water that must be in the samples as indicated by the great amount of oxygen (sulfur:oxygen should be 3:1).

The control reaction, PtBS (ExxSulf-5, Table 3.4), did not react to the extent that the copolymers did. After 12 h one finds that no

Table 3.6 Elemental Analysis Results for Sulfonated Copolymers.

<u>Styrenesodium sulfonate</u>	Expected	$C_8H_7O_3S_1Na_1$
	Obtained	$C_8H_{7.5}O_{3.6}S_{0.9}Na_{1.1}Cl_{0.1}$
<u>90/10</u>	Expected	$C_8H_{7.5}O_{2.6}S_{0.9}Na_{0.9}$
	1st	$C_8H_{9.7}O_{8.0}S_{1.2}Na_{5.5}Cl_{5.1}$
	2nd	$C_8H_{22}O_{18.6}S_{1.8}Na_{0.1}Cl_{0.1}$
<u>50/50</u>	Expected	$C_8H_{9.2}O_{1.2}S_{0.4}Na_{0.4}$
	1st	$C_8H_{10.6}O_{4.3}S_{0.8}Na_{4.1}Cl_{3.8}$
	2nd	$C_8H_{13.6}O_{5.8}S_{0.8}Na_{0.1}Cl_{0.1}$
<u>PSS100</u>	Calculated	$C_8H_7O_3S_1Na_1$

precipitation occurs in the reaction mixture (the copolymers precipitate almost immediately). This suggests that the PtBS is unreactive under these conditions. The data reported for these sulfonations is inconclusive as to what is really happening. NMR and elemental analysis data and solubility behavior suggest that the tertiary butyl groups may be cleaved and that over-sulfonation may occur, although the IR data and the control reaction suggest that this is not the case.

The method of Vink [B9-27-31] was used to sulfonate a 70% styrene random copolymer (R70/155k-p). The reaction was run exactly like that reported by Vink (scaled by half) using the following conditions: 25 mL conc. H_2SO_4 (469 mmol), 5.5 g P_2O_5 (38.7 mmol), 0.79 g polymer (6.5 mmol) dissolved in 40 mL cyclohexane. The polymer solution was added to the acid with stirring at 40 °C (1.25 h) and a brownish viscous solution was obtained. The reaction was terminated by addition of ice and separation (the solution was allowed to separate for 36 h). Infrared spectroscopy confirmed the presence of sulfonic acid groups in the polymer. The polymer was dialyzed with water but a substantial amount of material was insoluble. This was probably caused by sulfone formation which would crosslink the polymer.

Chlorosulfonic acid was also used as a source of SO_3 in these experiments because sulfur trioxide is extremely difficult to work with. Sulfur trioxide can be purchased as a low melting solid which polymerizes to a low ceiling temperature polymer, but this solid is very difficult to handle. Chlorosulfonic acid, ClSO_3H , can be regarded as a complex of SO_3 with HCl . The chloride ion is not a good base, so this reagent is quite

reactive. Stronger bases (amines or phosphates, for example) will displace the chloride ion and form complexes with the SO_3 . A number of reactions were run using ClSO_3H and various complexing agents (Table 3.7). As would be expected the complexes with triethylamine (Et_3N) were not reactive enough to cause sulfonation, as evidenced by IR. Other reactions with complexes of pyridine did not result in sulfonation either. As one would expect, a 1:1 complex with triethylphosphate ($(\text{EtO})_3\text{PO}$) showed no reaction by either IR or GPC (the polymers eluted at their original times). Some interesting results were obtained when the ratio of SO_3 :TEP was increased to 1.63:1.0; substantial sulfonation of polystyrene occurs with very little reaction on the PtBS homopolymer as evidenced by IR. Small absorbances, at 1304 cm^{-1} and 1184 cm^{-1} , present in the spectrum of the control polymer suggest that a small amount of sulfonation occurred on PtBS. On the other hand, the PS spectra shows large peaks due to sulfonation at 1364 , 1177 , 1100 , 1048 and 909 cm^{-1} . This peak pattern matches (fairly well) that of ethyl *p*-toluene sulfonate which shows peaks at 1355 , 1180 , 1100 , 1000 , 920 , 820 , and 780 cm^{-1} . It appears that the ester was formed in this case. The peaks could be due to residual $(\text{EtO})_3\text{PO}$, but this is unlikely because the ester was hydrolyzed by dissolving in water with a small amount of ethanol to make everything dissolve. NaOH was added and the mixture was refluxed for 4 h. After dialysis and lyophilysis, a slightly discolored powder was obtained. The IR shows the expected peaks for the sodium salt (1192 , 1130 , 1041 , 1011 cm^{-1}). The results above suggest that there probably is some way to vary reaction time, temperature and/or SO_3 /phosphate ratio to obtain selective sulfonation of PS/PtBS copolymers. However, no further reactions were completed in this area. We thought that a proton NMR tag that would be

Table 3.7 Sulfonation Reactions: ClSO₃H with Complexing Agents.

<u>Sample</u>	<u>Reaction Conditions</u>
ClSA-1 (B11-33) PtBS/116k-p (precursor)	S1: 0.25g (1.6mmoles) polymer; 8mL DCE S2: 0.5mL (7.5mmole) ClSO ₃ H, 2.0mL (15.0mmol) TEA, 2.5 mL DCE S2 added to S1 at 0 °C; polymer ppt immediately; React 0.5hr; ppt in MeOH. No Sulfonation as evidenced by IR
ClSA-2 (B11-33) T04/4.2k-p (precursor)	S1: 0.25g (1.6mmol) polymer; 8mL DCE S2: 0.5mL(7.5mmol) ClSO ₃ H; 2.0mL (15mmol) TEA 2.5 mL DCE Reaction run same as ClSulf-1; No sulfonation as evidenced by IR
ClSA-3 B11-34 D21/12k-p (precursor)	S1: 0.25g polymer; 8mL DCE S2: 0.5mL (7.5mmol) ClSO ₃ H; 1.5mL (11.2mmol) TEA 2.5mL DCE Added S2 to S1 slowly at 45 °C; polymer ppt.; React 1hr; No sulfonation as evidenced by IR
ClSA-4 B11-34 R50/50k-p (precursor)	S1: 0.25g polymer; 8mL DCE S2: 0.5mL (7.5mmol) ClSO ₃ H; 1.5mL (11.2mmol) TEA 2.5mL DCE Reaction conditions same as ClSA-3 but let react at RT for 4 days. No sulfonation as evidenced by IR
ClSA-5 B11-38 PS/36k-p (precursor)	S1: 0.25g polymer; DCE S2: 0.25mL (3.75mmol) ClSO ₃ H; 0.9mL (5.3mmol) TEP 5mL DCE Added S1 to S2 at 0 °C; no ppt formed; reacted RT 18hr; ppt in MeOH fine white powder; No sulfonation by IR also GPC traces of before and after are almost identical
ClSA-6 B11-39 PtBS/116k-p (precursor)	S1: 0.25g polymer; DCE S2: 0.25mL(3.75mmol) ClSO ₃ H; 0.9mL (5.3mmol)TEP 5mL DCE Added S1 to S2 at 0 °C; got immediate ppt; React at RT 18hr; ppt in MeOH. No sulfonation by IR also GPCs match well.
ClSA-7 B11-39 PS/36k-p (precursor)	S1: 0.25g polymer; DCE S2: 0.25mL (3.75mmol) ClSO ₃ H; 0.4mL(2.3mmol)TEP 5mL DCE Added S1 to S2 at 0 °C; ppt formed after 50min. isolated ppt. Polymer ppt soluble in MeOH but not water, IR shows reaction occurred, most likely the ester was formed.

continued next page

Table 3.7 continued

CISA-8
B11-39
PtBS/116k-p
(precursor)

S1: 0.25g polymer; DCE
S2: 0.25mL(3.75mmol) ClSO₃H;
0.4mL(2.3mmol)TEP 5mL DCE

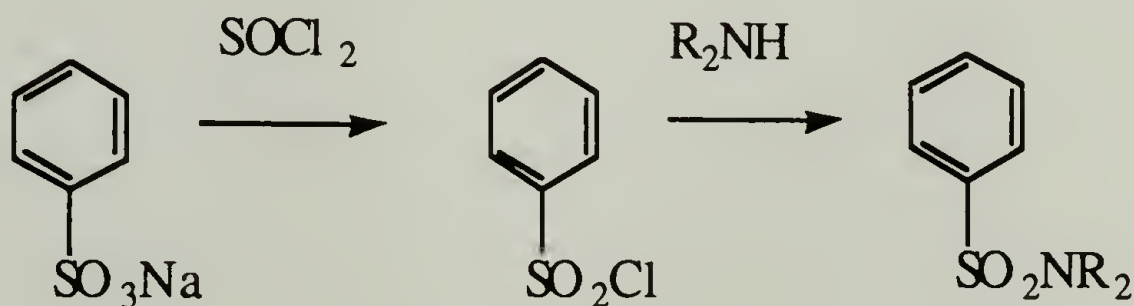
Added S1 to S2 at 0 °C; immediate ppt redissolved within minutes;
React 1hr; ppt in MeOH. IR shows small amount of sulfonation,
also the polymer would not elute from the GPC

TEA = Triethylamine, TPE = (EtO)₃PO

organically soluble and subsequently hydrolyzable would be a good analysis tool. The sulfonate ester is rather hydrolytically unstable and was presumed not to be a good choice, but the sulfonamide is more stable and seemed like the perfect choice.

Sulfonamide Formation

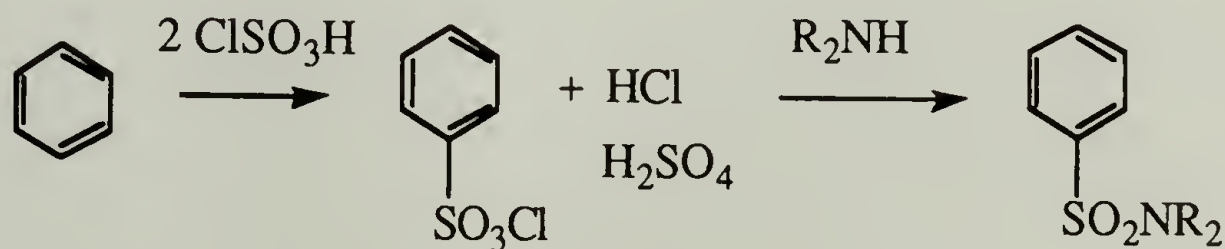
There are basically three methods for introducing this functionality to polystyrene. One method is conversion of the acid (or its salt) to the acid chloride (via reaction with thionyl chloride, for example) followed by reaction with an amine as illustrated below in Scheme 3.6. A similar reaction scheme has been reported on crosslinked polystyrene gel.^{26,27} This reaction was performed on both sulfonated polystyrene and the small



Scheme 3.6 Sulfonamide Formation: Thionyl Chloride.

molecule analog, *p*-toluenesulfonate sodium salt, using dibutylamine in the amidation step (Table 3.8). The model reaction was run twice. In the first reaction, an oil was isolated that was almost equal parts sulfonyl chloride and sulfonamide as evidenced by IR data that contain peaks at 1377 cm^{-1} and 1175 cm^{-1} which correspond to the chloride, and at 1139 cm^{-1} and 1157 cm^{-1} corresponding to the sulfonamide. Addition of more amine resulted in loss of the acid chloride as evidenced by IR. The product, a dark oil, could be separated on a silica column with dichlorethane (DCE). The sulfonamide elutes with DCE, but the byproduct requires a stronger solvent (such as THF) for elution to occur, suggesting a more polar moiety, such as the sulfonic acid. TLC data indicate that reducing the reaction time decreased the amount of byproduct (second entry in Table 3.8). Proton NMR spectra show peaks other than those from the sulfonamide itself. The reaction carried out with polystyrene (homopolymer) resulted in insoluble products assumed to be due to sulfone formation. This crosslinking could probably be controlled through use of shorter reaction times.

A second method for sulfonamide formation is via reaction with ClSO_3H (Scheme 3.7) to make the sulfonyl chloride²⁸ followed by addition of the appropriate amine.



Scheme 3.7 Sulfonamide Formation: Chlorosulfonic Acid.

Table 3.8 Synthesis of Sulfonamide:
Thionyl Chloride Path.

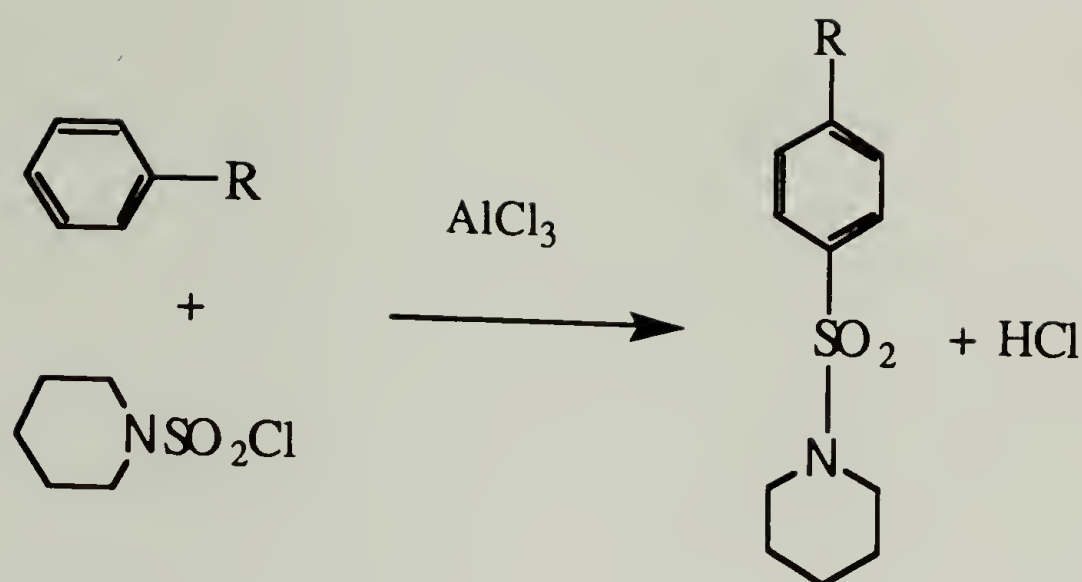
<u>Sample</u>	<u>Reaction Conditions</u>
TosylNBu ₂ (B11-50)	<p>S1: 1.06g (5.58mmol) TosylNa; 8mL DMF (slurry) S2: 1mL (13.7mmol) SOCl₂; 8mL DCE S3: 1mL (13.7mmol) SOCl₂ S4: Bu₂NH</p> <p>Added S2 to S1 at RT; got milky white added S3; React 12hr RT; Added S4 let react 1hr; washed 10% HCl ran IR got sulfonyl chloride and sulfonamide; added more amine washed with 10% HCl isolated dark oil from organic phase. IR shows that sulfonamide is at least one of major products. TLC showed two spots on SiO₂ with DCE.</p>
TosylNBu ₂ (B11-58)	<p>S1: 0.7g (3.9mmol); 10mL DMF S2: 1ml (13.7mmol); 10mL DCE S3: Bu₂NH</p> <p>Added S2 to S1 at RT; React 45min.; added enough amine to turn basic. Washed 10% HCl , and water. Isolated fairly dark oil from organic layer. TLC (DCE, SiO₂) showed one spot, probably not the sulfone.</p>
Polystyrene (B11-57)	<p>Ran in DMF/DCE at RT 36hr; ended up with insoluble mess.</p>

This reaction was run a number of times (Table 3.9) and the poly(sulfonamide) was recovered in good yield. PS, PtBS and their copolymers were used as substrates along with the model reaction starting with toluene (Table 3.9). The model reactions worked well, sulfone formation is not a problem. IR spectroscopy was used to confirm the formation of tosyl chloride when the reaction was run on toluene (bands at 1377 cm^{-1} and 1175 cm^{-1}). Upon reaction with dibutylamine, the corresponding sulfonamide is obtained (IR bands at 1341 and 1157 cm^{-1}). The reaction was run on T14/12k-p copolymer, and the IR data indicate formation of the dibutyl sulfonamide which matches well with model compound synthesized. So it seems this method can be used to form the sulfonamide on the polymer without extensive sulfone formation. NMR data were not obtained. The problem with this reaction sequence is that ClSO_3H reacts with PtBS also. The control reaction resulted in polymer that was soluble in MeOH; this was taken as proof that reaction had occurred on the PtBS homopolymer (no other analyses were performed on these). It seems that these conditions cause ipso addition and subsequent loss of the *t*-butyl group, or ClSO_3H may be reactive enough to add to the ortho positions on the polymer. At any rate its utility for making sticky footed polymers with the PS/PtBS system is rather low. As will be discussed later, there are other uses for this reaction.

Sulfonamides can also be obtained via Friedel Crafts catalyzed reaction of sulfamylchlorides with aromatic rings as illustrated in Scheme 3.8. This reaction was reported by Gupta²⁹ to work with benzene, toluene and chlorobenzene. The sulfamylchlorides were prepared from dialkyamines (diethylamine and piperidine) and sulfuryl chloride, Cl_2SO_2 ,

Table 3.9 Sulfonamides:
Reactions with Uncomplexed ClSO₃H.

<u>Sample</u>	<u>Reaction Conditions</u>
TosylCl (B11-8)	<p>S1: 1mL(9.4mmol) toluene S2: 2mL (30.3mmol) ClSO₃H; 5mL DCE</p> <p>Added S1 to S2 at 0 °C over 15min; warmup RT; React 1.5hr total; Poured into crushed ice; separated organic layer; pulled solvent off. Obtained white crystals IR matches commercial TsCl.</p>
TosylNBu ₂ (B11-11)	<p>S1: 1ml (9.4mmol) toluene S2: 2ml (30.3mmol) ClSO₃H; 5ml DCE S3: Bu₂NH (pH basic)</p> <p>Added S1 to S2 at 0 °C 15min; Reacted at RT 1.5hr; formed two phases; cooled to 0°C added S3 slowly let react overnight; Worked up in 10% HCl to get rid of excess amine. Organic layer contained sulfonamide.</p>
T14/12k-p (B11-14)	<p>S1: 0.36g polymer; 5mL DCE S2: 1mL (15mmol) ClSO₃H; 5mL DCE S3: Bu₂NH</p> <p>Added S1 to S2 at 0 °C; got a ppt; react 2.5hr seems to have somewhat redissolved; settled into layers separated and added amine to both. Obtained the sulfonamide from the bottom layer after washing with acid etc. This was determined by IR.</p>
PtBS (B11-28)	<p>S1: 0.25g polymer; 5mL DCE S2: 0.3mL (9.0mmol); 6mL DCE S3: Bu₂NH (4ml)</p> <p>Added S1 to S2 at 0 °C; ppt immediately; react 25min.; added S3; react 20min. The resultant polymer dissolves in MeOH, this was taken to mean the polymer reacted. No spectra were obtained.</p>



Scheme 3.8 Sulfonamide Formation: Sulfamyl Chloride/ AlCl_3 .

these were then used in a 1:1 ratio with AlCl_3 to react with the aromatic ring. High yields and almost exclusive para selectivity were reported. The reactions were carried out neat with an excess of the aromatic compound. Because of the high conversion and para selectivity it was thought that this might be a good reaction to use for these polymers. The procedure had to be modified to include a solvent (for obvious reasons) and nitrobenzene was found to both dissolve the polymer and not interfere with the reaction. Piperidine was the amine used in this synthesis and it was reacted with sulfuryl chloride using the procedure of Gupta. The reaction in nitrobenzene of PS homopolymer works quite well; as can be seen in Table 3.10, five reactions were carried out with PS homopolymer under varied conditions in an attempt to get 100% conversion of the rings. Conversions of 54% to 100% were obtained as determined by NMR (the ratio of the aromatic to aliphatic protons was used)[B11-74]. Figure 3.5 shows the proton NMR spectrum of a PS homopolymer modified to 76% conversion; one can see the piperidine protons at 2.92 and 1.55 ppm. One can see the

Table 3.10 Sulfonamide Formation via Reaction with Sulfamyl Chlorides.

<u>Sample</u>	<u>Reaction Conditions</u>
PipPS1 B11-68 PS homopolymer	0.223g (2.14 mmole) polymer 5mL (5 mmole) AlCl ₃ in nitrobenzene 0.9 mL (6.73 mmole) PipSO ₂ Cl; 2.5 mL nitrobenzene. 50°C, 2 h 54% conversion, almost white polymer, MWD not affected, elution time lower
PipPS2 B11-75 PS homopolymer	0.26 g (2.5 mmole) polymer 10mL (10 mmole) AlCl ₃ in nitrobenzene 1.8 mL (14 mmole) PipSO ₂ Cl 60°C, 3.25 h 76% conversion, almost white polymer, MWD not affected, elution time lower
PipPS3 B11-84 PS homopolymer	0.42 g (4.04 mmole) polymer 15mL (15 mmole) AlCl ₃ in nitrobenzene 2.8 mL (20.9 mmole) PipSO ₂ Cl 60-65°C, 18 h 100% conversion, almost white polymer, MWD not affected, elution time lower
PiPPS4 B11-113 PS homopolymer	0.42 g (4.04 mmole) polymer 6.3 mL (6.3 mmole) AlCl ₃ in nitrobenzene 1 mL (20.9 mmole) PipSO ₂ Cl; 6.3 nitrobenzene 70°C, 12 h 89% conversion, almost white polymer, MWD not affected, elution time lower
PipPS5 B13-10 PS homopolymer	0.135 g (1.3 mmole) polymer 2 mL (2 mmole) AlCl ₃ in nitrobenzene 1.5 mL (11.2 mmole) PipSO ₂ Cl; 8 mL nitrobenzene 55°C, 5 h 67% conversion, almost white polymer, MWD not affected, elution time lower
PipPtBS1 B11-77 PtBS/116k-p	0.15 g (0.94 mmole) polymer 5mL (5 mmole) AlCl ₃ in nitrobenzene 0.9 mL (6.73 mmole) PipSO ₂ Cl; 8 mL nitrobenzene 45°C, 3 h 0% conversion, almost white polymer, MWD not affected, elution time stays same

continued next page

Table 3.10 continued

PipPtBS2 B13-10 PtBS/116k-p	0.098 g (0.61 mmole) polymer 2 mL (2 mmole) AlCl ₃ in nitrobenzene 0.7 mL (5.23 mmole) PipSO ₂ Cl; 14 mL nitrobenzene 55°C, 5 h ~5% conversion, slightly brown polymer, slight low molecular weight tail
PipPS/PtBS1 B11-115 R60/241k-p	0.41 g (3.25 mmole) polymer 6.5 mL (6.5 mmole) AlCl ₃ in nitrobenzene 1 mL (7.5 mmole) PipSO ₂ Cl; 6.5 mL nitrobenzene 70°C, 12 h 49% conversion, very dark polymer, MWD very broad and weird shaped
PipPS/PtBS2 B11-122 R60/241k-p	0.37 g (2.95 mmole) polymer 12 mL (12 mmole) AlCl ₃ in nitrobenzene 3 mL (22.5 mmole) PipSO ₂ Cl 60°C, 3.25 h 89% conversion, very dark polymer, MWD very broad and weird shaped
PipPS/PtBS2 B11-126 R60/241k-p	0.24 g (1.87 mmole) polymer 12 mL (12 mmole) AlCl ₃ in nitrobenzene 3 mL (22.5 mmole) PipSO ₂ Cl; 6.5 mL nitrobenzene 60°C, 4.25 h 100% conversion, very dark polymer, MWD very broad and weird shaped
PipPS/PtBSB1 B11-126 T14/12k-p	0.247 g (2.14 mmole) polymer 12 mL (12 mmole) AlCl ₃ in nitrobenzene 3 mL (3 mmole) PipSO ₂ Cl 60°C, 4.25 h NMR showed functionalization, very dark polymer, MWD very broad and weird shaped (not as much as the 60% copolymers)
PipPS/PtBSB2 B11-126 T04/4.2k-p	0.217 g (1.36 mmole) polymer 12 mL (12 mmole) AlCl ₃ in nitrobenzene 3 mL (22.5 mmole) PipSO ₂ Cl 60°C, 4.25 h very dark polymer, MWD very broad and weird shaped (not as much as the others)

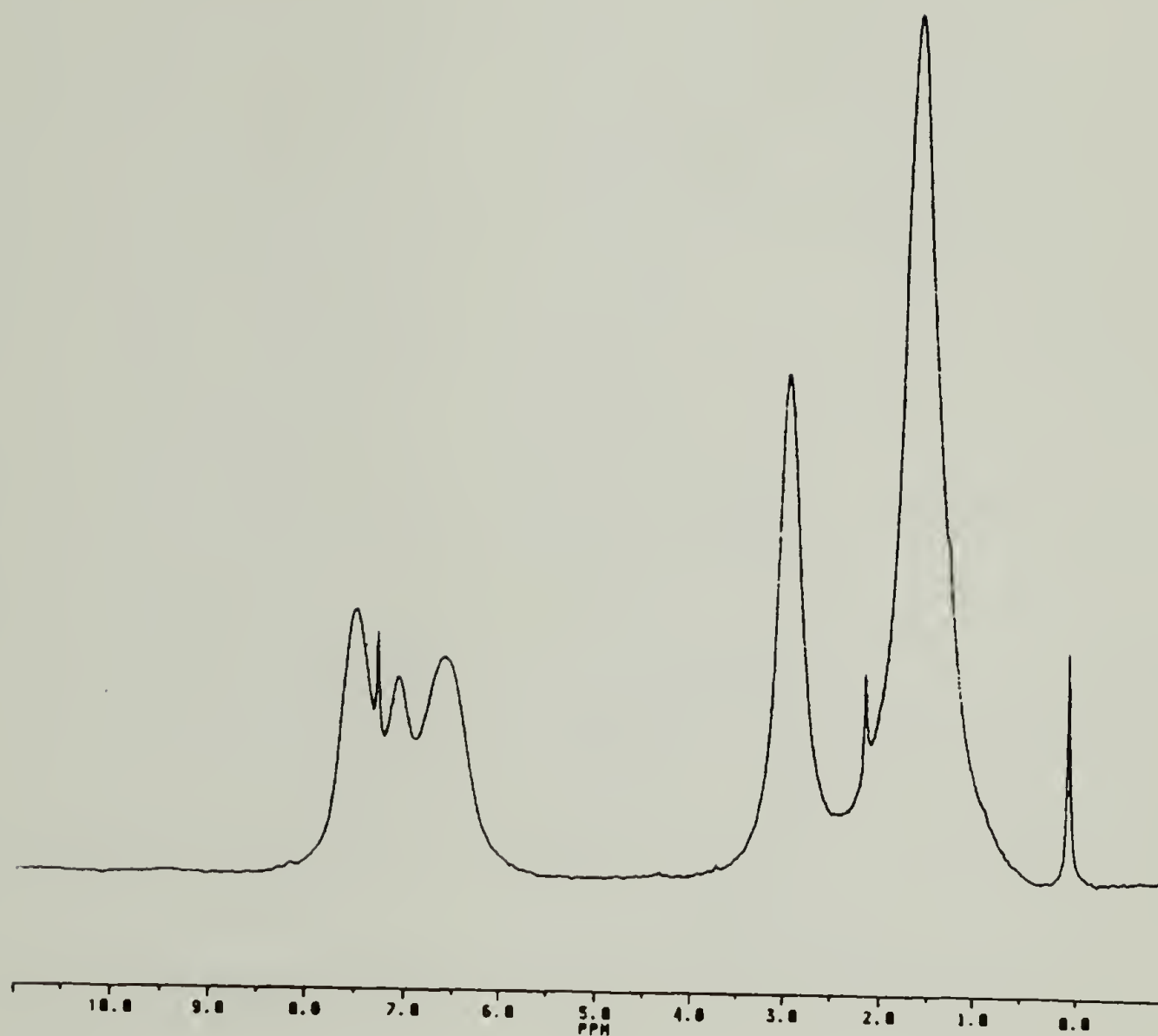


Figure 3.5 ^1H NMR spectrum of polystyrene homopolymer modified by reaction with $\text{PipSO}_2\text{Cl}/\text{AlCl}_3$ to 76% conversion (See Table 3.10, PipPS2).

peak shift in the aromatic region from 7.0 ppm (PS) to 7.4 ppm for the sulfonamide. The sample with 100% conversion has no 7.0 ppm resonance at all. The main factors in determining conversion are reaction time and reactant ratio, repeat unit:sulfamyl chloride:aluminum (XRP: SC: Al). The products obtained when PS homopolymer was used as the substrate were a little discolored but it was found that they could be made almost white by treatment with acid. The modification does not effect the MWD as was evidenced by GPC. The elution time changes but the distribution stays narrow. The control reactions (PtBS homopolymer) worked well as can be seen from Table 3.10; the reactions yielded 0% and 5% reaction as determined by NMR. Neither the molecular weight nor its distribution were adversely affected by the reaction. PipPtBS1 shows no effects at all (the decrease in elution time of one second is within experimental error). On the other hand, the second control shows a significant decrease in elution time (1131 sec to 1126 sec) it also shows a low molecular weight tail. This corresponds to the small amount of reaction seen for this case. Possible explanations for this will be discussed later. These polymers were only very slightly discolored.

The subsequent modification of the copolymers was not as straight forward as the above results would suggest. It was found that under essentially the same conditions (as above) one obtained very brown polymers from which little of the color could be washed out. The NMR spectra for these polymers look normal (i.e. no extraneous peaks, the differences could be attributed to different conversions). The percent conversion, of the styrene units, for the R60/73k-p copolymers was 49%, 89%, 100% (Table 3.10). These are based on the ratio of aromatic to

aliphatic areas. GPC showed very significant broadening (of both the front and back) of the peak. The precursor polymer was 73K with a polydispersity of 1.06. After the reaction the main peak shifted to higher molecular weight reminiscent of the polystyrene homopolymer modification, but a huge high molecular weight tail and large low molecular tail also are also seen (all in all, the MWD was significantly affected by the modification). The reaction was carried out with T14/12k-p and T04/4k-p and similar results were obtained for all of the polymers. The resulting polymers were very brown and had broad molecular weight distributions. The main peak for the 14% styrene polymer was shifted to higher molecular weight and had smaller tails on both sides. The polymer containing 4% styrene showed the least bizarre behavior: its elution time was shifted, but only a high molecular weight tail (that was not as large as the others) was observed.

The main reason for the problems observed for the copolymers was that AlCl_3 is too strong a catalyst, causing cleavage, rearrangement and ispo addition of tertiary butyl-substituted phenyl rings (see discussion section). The obvious answer was to use a milder catalyst that would allow reaction without causing these detrimental side effects. Tin tetrachloride is a much milder catalyst than AlCl_3 and reactions were run using this (Table 3.11). The reaction of the sulfamyl chloride with the polymer was run a number of times using SnCl_4 as the catalyst but no reaction was observed.

The utility of this reaction would be greatly enhanced if the resultant sulfonamide could be used as a reactive handle for the formation of other functional groups. One of the most obvious possibilities is the sulfonate

Table 3.11 Sulfonamide Reactions Catalyzed with SnCl₄.

<u>Sample</u>	<u>Reaction Conditions</u>
B13-43 R50/114k-p	0.155 g (0.58 mmole) polymer 4 mL (4 mmole) SnCl ₄ in MeCl ₂ 0.5 mL (3.74 mmole) PipSO ₂ Cl Room Temperature, 24 h No reaction as evidenced by IR
B13-44 PS homopolymer	0.25 g (2.45 mmole) polymer 8 mL (8 mmole) SnCl ₄ in Hexane 1 mL (7.48 mmole) PipSO ₂ Cl, 15 mL DCE 70°C, ~9 h + 5h + 12 h (@ RT) No reaction as evidenced by IR at all three check points.

group. A number of attempts were made to hydrolyze the piperidine sulfonamide,³⁰ none of which resulted in any significant amount of reaction. The reaction attempts included the following hydrolysis conditions: refluxing THF/water/tosic acid, refluxing THF/water/HCl and refluxing DMF/water/HCl. These reactions were run for approximately 36 h with no hydrolysis observed. Transamidation is also a possible route to other functional groups. The tosyl sulfonamide was refluxed in aniline with HCl for 15 h, but no evidence of reaction was observed.³⁰

The utility of the piperidine sulfonamide as a sticky foot was demonstrated via Thin Layer Chromatography (TLC) where it was found that PipPS1, PipPS2 and PipPS3 would not elute on silica, alumina, or polyamide TLC plates with methanol, DCE, benzene, toluene, chloroform or even THF (unmodified polystyrene elutes with an $R_f = 1$ under all these conditions). This shows that we can effect selective adsorption via incorporation of this sulfonamide sticky foot.

From the results obtained, we concluded that the sulfamyl chloride is not reactive enough (to add to the phenyl rings) using the tin catalyst and that the sulfonamide, when prepared with $AlCl_3$ catalysis, is very stable to hydrolysis. Thus, using this reaction as a means for PS sulfonation is not a viable alternative, unless a more reactive molecule (i.e. catalyzed by a weak lewis acid) that would yield a hydrolyzable group (but not so easy as to form the sulfone) can be found. To this end, sulfuryl chloride was reacted with 2-propanol and added to PS in DCE (reaction was catalyzed with $SnCl_4$). We obtained a water-soluble sulfonated polymer sample. The analogous reaction was run using octanol, but no sulfonation occurred.

One explanation of these results is that the propanol is a secondary alcohol and does not readily react with the sulfuryl chloride, allowing the sulfuryl chloride to react with the polymer as such, instead of as the mono-ester. Not enough experiments were completed to fully understand this, but we do think that it is a worthwhile endeavor to use sulfuryl chloride in combination with a (relatively) easily cleavable group that can be used to protect the reaction from sulfone formation.

Discussion: Sulfonation and Sulfonamidation Reactions

The sulfonations were carried out mostly following the Exxon-modified Turbek method using triethylphosphate to tame the reactivity of the sulfur trioxide. This method yielded sulfonated polymers that were essentially water-soluble, even when the precursor used was only 50% polystyrene. The NMR data for these polymers indicate a fairly large decrease in the aliphatic proton resonances; in particular it appears that the *tert*-butyl peak at 1.25 ppm decreases with respect to the polymer backbone resonance at 1.5 ppm. Elemental analysis data show a greater sulfur to carbon ratio than would be expected for sulfonation of only the styrene units of the copolymer, although the IR shows evidence for retention of a fair amount of the tertiary butyl groups on the copolymer. The control reaction was carried out with the PtBS homopolymer which did not precipitate out of solution as do polymers with a substantial number of styrene units. The elemental analysis data and increased solubility could result from over-sulfonation (of the copolymer chains) without any carbon-carbon bond breaking. The NMR data can be explained only in terms of tertiary butyl group cleavage or the inability of the NMR to

sample the *tert*-butyl groups in D₂O (this type of behavior has been observed in other systems). It is known that *tert*-butyl groups can be displaced fairly easily in these types of reactions because of the stability of the *tert*-butyl cation. March³¹ reports that treatment of rings containing *tert*-butyl and, to some extent, isopropyl groups with sulfuric acid leads to ipso substitution and subsequent bond cleavage. Carey and Sundberg³² state that one of the most frequently encountered examples of ipso substitution is with highly branched aliphatic substituents. They mention specific examples for nitration and halogenation reactions but do not specifically mention sulfonation. They also say, as one would expect, that the amount of this ipso substitution increases as substitution on the ring increases. It has also been reported that the presence of an alkyl-accepting ring can greatly enhance the reaction of sterically congested alkyl-substituted rings under certain conditions (see sulfonamide discussion next section). Ipso substitution at the *tert*-butyl group would lead to a decrease in the aliphatic:aromatic ratio measured by NMR, increase in water solubility and also a higher sulfur to carbon ratio. Thus, cleavage of the *tert*-butyl groups agrees with most of the data and is substantiated by the literature. It should be noted that calculations based on the NMR data (Table 3.5) suggest that the 90/10 (PS/PtBS) copolymer was essentially 100% sulfonated and the 50/50 one was approximately 90% sulfonated; this corresponds to cleavage of all the *tert*-butyl groups in the 90/10 copolymer and 80% of those initially present in the 50/50 copolymer. It is known that the reactivity of sulfur trioxide depends on the ratio with TEP and this reaction has been reported by Boch and Valint to be selective. The explanation may be somewhere in between, where one really needs to control the ratio very well. The reaction procedure involved addition of

uncomplexed SO_3 (in solution) to a solution of polymer and phosphate, so local concentrations of SO_3 would depend on the stirring efficiency and the rate of addition. In retrospect, formation of the complex before exposure to the polymer may have been the best way to alleviate problems with mixing or variations in concentrations.

The other set of reactions that closely resembles the Turbek method are those using the $\text{ClSO}_3\text{H}/(\text{EtO})_3\text{PO}$ system. These reactions are the type just discussed as a solution to the problem in the preceding paragraph, i.e. the complex was made prior to addition to the polymer solution. The reaction entries (7) and (8) in Table 3.7 show a large selectivity for polystyrene over poly(*tert*-butylstyrene). No NMR spectra were obtained, but comparison of IR spectra of the polymer before and after reaction suggests that total dealkylation did not occur. Dealkylation and sulfonation of PtBS homopolymer were not observed by IR and the solubility of the polymer was not changed. Thus, if the appropriate precautions are taken, selective sulfonations may be achieved. It should also be noted that chlorosulfonic acid is much easier to use than SO_3 ; the differences in the sulfonations (if any) are not known but none are expected.

A word about the other three types of sulfonations is in order because the Vink and the Eisenburg methods are probably fairly good means of making 100% sulfonated polystyrene. Some concern exists about sulfone formation and dealkylation (of *tert*-butyl groups) when copolymers are used. These methods are not conducive to random sulfonations of less than 100%. Both methods employ a heterogenous reaction mixture with a large excess of sulfonating agent and one has to control the extent of

sulfonation with reaction time (which is usually very fast). On the other hand, both the Turbek method and the ionomer method are carried out in solution with the amount of SO_3 added equal to the number of rings one wants to sulfonate, so controlling the percent sulfonation with these two methods should be relatively straightforward (this control has been exhibited with the ionomer method). This point is addressed because the best way to make randomly sulfonated polystyrene for electrophoresis studies may be to use polystyrene homopolymer and just react it to different extents of sulfonation. This has a number of advantages and should be feasible with either the Turbek or the ionomer method. The synthesis would be greatly simplified because one could use one polystyrene homopolymer to make many different electrophoresis samples, effectively removing the problem of variability in DP among the different precursor polymers required for the copolymer method. Another advantage is that the polymers would probably be water-soluble down to lower sulfonate content (i.e. large, bulky hydrophobic *tert*-butyl groups would not be present). Yet another advantage is elimination of the possibility of cleaving the *tert*-butyl groups, which we have seen is a nontrivial problem. Or we could turn this around a little, and start out with PtBS and run the reaction to cleave as many *t*-butyl groups as we desired to obtain a different water-soluble copolymer. One last point to be made here is that acetyl sulfate may prove to be selective and work well for the PS/PtBS copolymers.

We thought that the sulfonations could be followed better analytically if the sulfonate groups could be tagged with an organic-soluble NMR tag. We figured that sulfone formation was not a good choice because of the

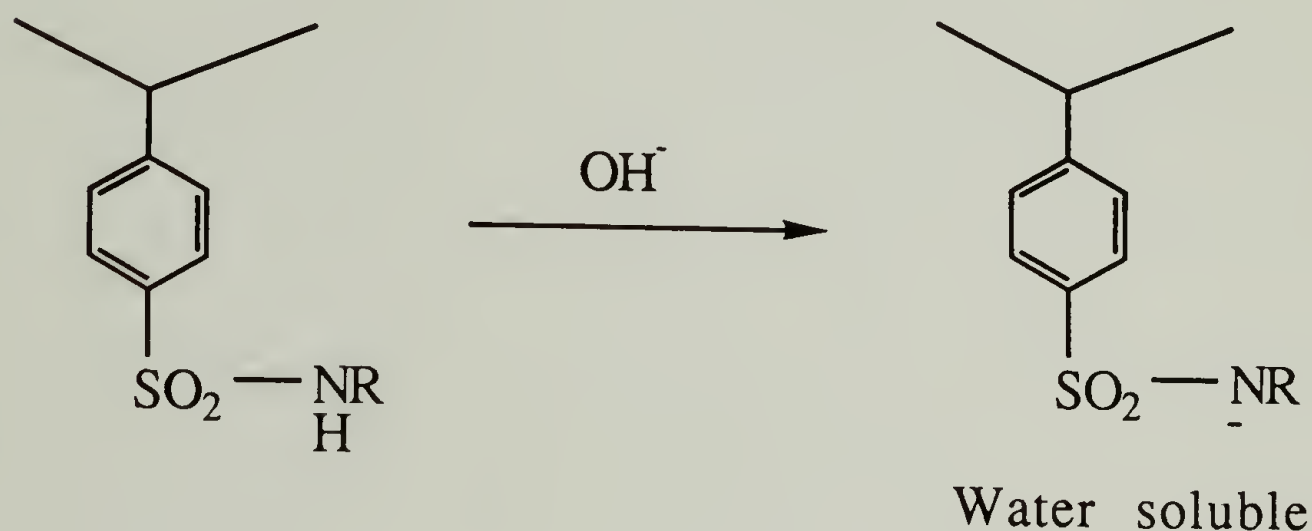
possibility of extraneous crosslinking. The ester could have been formed, but it is fairly hydrolytically unstable and so was not used. Formation of the sulfonamide seemed like the perfect choice for many reasons.

The synthesis of the polysulfonamide brought a whole new set of possibilities to bear on this research. First of all, sulfonamides are stable species: hydrolysis and reductive cleavage are possible, but not very easy. The synthetic aspect seemed very straightforward (initially) because one could use amines, such as Bu_2NH , to tag each sulfonate with 18 protons which could be detected easily by NMR. The sulfonamides formed would be organic-soluble which would help in the analysis and would also open the door for adsorption experiments with sticky foot polymers in organic (not aqueous) media. Aside from all this was the fact that some sulfonamides are 'sulfa-drugs' and the possibility of making some kind of poly(drug) was appealing. On a more practical level, the possibility exists for putting different sticky feet on the polymer by reaction with various amines. Scheme 3.9 shows two amines which would introduce carboxylic acid and/or hydroxyl functionality.



Scheme 3.9 Possible Acid and Hydroxyl Functionality via Sulfonamides.

Thus, this reaction would yield great versatility. One interesting possibility is the synthesis of polymers that are organic-soluble under neutral conditions but water-soluble at high pH (this transition is shown in Scheme 3.10). The two possible routes that would lead to sulfonamides with this



Scheme 3.10 Water Solubility Facilitated at High pH.

versatility are those using SOCl_2 or ClSO_3H (the Friedel Crafts reaction of PipSO_2Cl does not lend itself as easily to all of the above mentioned products).

Reactions with chlorosulfonic acid worked well to form the polysulfonamide and the polymers remained soluble, so little or no crosslinking occurred. (GPC data were not obtained, so the actual amount of dimer formation is not known.) The problem with this reaction is that the ClSO_3H also reacts with PtBS thus removing the possibility of selective functionalization of the PS/PtBS system. One may be able to use this

reaction to make polymers with different amounts of sulfonamide from polystyrene homopolymer; these would be random sticky foot polymers.

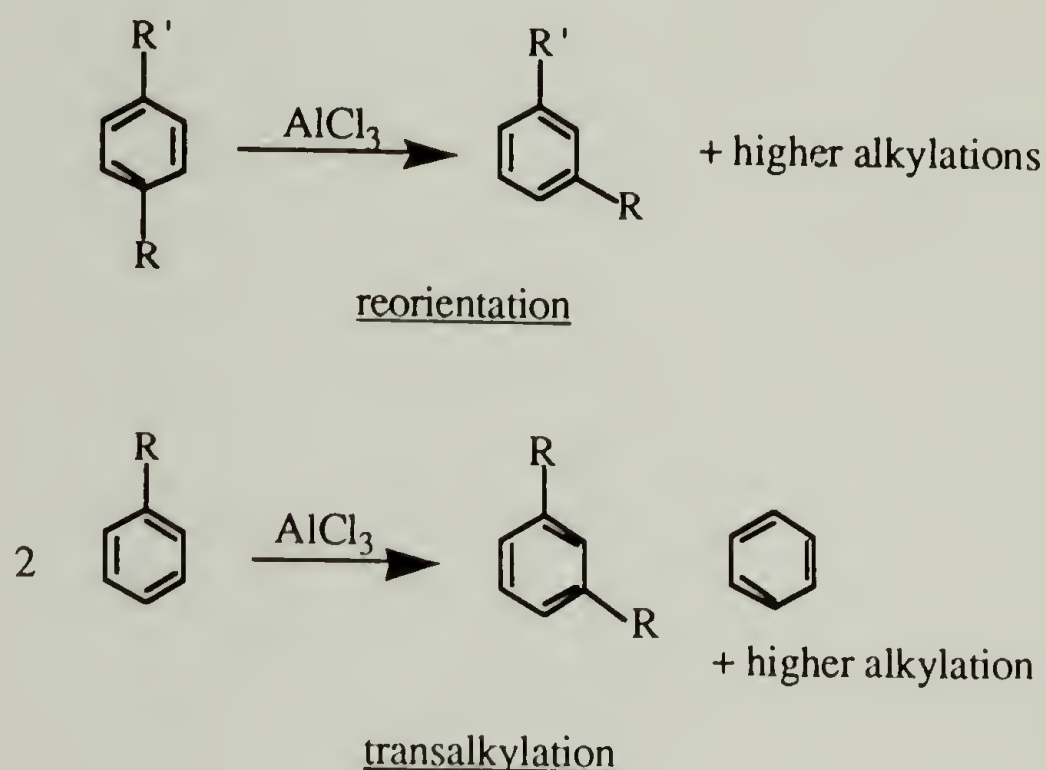
The other method requires the reaction of the polyacid salt (water-soluble) with SOCl_2 to form the sulfonyl chloride (organic-soluble, water-sensitive). The solubility difference creates somewhat of a problem in getting the two reagents to react. The other problem one encounters is sulfone formation, which leads to crosslinks. It was found in the model reactions that this problem could be diminished by decreasing the time of reaction. This may indeed work for the polymer samples, but it should be pointed out that these systems cannot tolerate even minute amounts of sulfone formation. Another point that should be made with regard to using this reaction scheme to make the above-mentioned polymers is that it requires that one be able to selectively sulfonate the PS/PtBS system. To summarize this general area, the development of this type of reaction would lead to many synthetic possibilities.

The third method of sulfonamide formation is via the use of sulfamyl chlorides in Friedel Crafts-type acylation of aromatic rings. It should be pointed out that this reaction does not, in general, have as many of the advantages as making the sulfonamides by the other two methods. In general, only dialkylsulfonamides can be used and these have proved extremely stable to any kind of hydrolysis or transamidation reaction. If one wants to make the dialkylsulfonamide as a sticky foot itself then this reaction scheme is as good as any. The reaction was reported by Gupta²⁹ to go in high yields with almost exclusive para substitution, which is why it was selected as a possible sticky foot reaction. The reaction worked

extremely well on polystyrene homopolymer yielding (depending on the conditions) 54% to 100% sulfonamidation with no change in the MWD. One interesting fact is that the GPC elution time is not very sensitive to the amount of sulfonamidation in this range of conversion. The polymers at 67 and 89% conversion eluted at essentially the same time (the coils being dissolved but in a very collapsed state). We observed slight discoloration of the polymer. Subsequent reactions with the *tert*-butylstyrene homopolymer gave good results, yielding 0% and 5% reaction by NMR and very little change by GPC (for MWD and molecular weight). These control polymers were also very slightly discolored. One would think it quite trivial to run this reaction on the copolymers of these monomers, but this was not the case. The copolymers turned rather dark brown during the reaction and this color could not be washed out. The GPC data indicate very unusual peak shapes with broad MWDs, although the NMRs of these polymers did not show anything unusual. The question is why do the copolymers behave so much differently than the respective homopolymers.

Friedel Crafts alkylations are, in general, reversible and one will obtain a range of products upon mixing alkylbenzenes with FC catalysts under strong enough conditions. Roberts and Khalaf have written an extensive review of this chemistry.³³ Two general types of reactions that can occur are reorientation and transalkylation, shown in Scheme 3.11. The extent to which these phenomena occur depends on the activity of the catalyst, the reaction time and the temperature. In all cases one obtains a mixture of products, the identity of which depends on the substituents. Determination of the mechanism has been the subject of extensive research. Some alkyl groups migrate on the same ring whereas others use an

intermolecular process. This also depends on the strength of the catalyst. Data in the literature reveal that the reaction of *para-tert*-butyltoluene with $\text{AlCl}_3/\text{MeNO}_2$ is very slow.



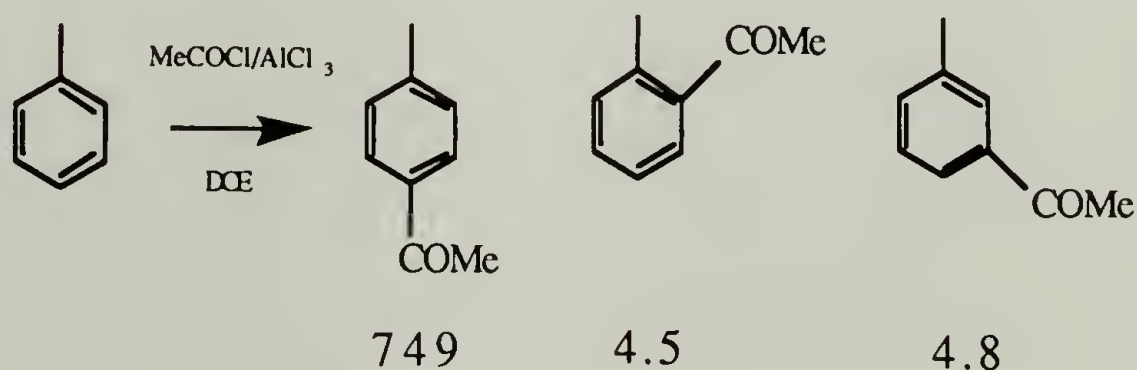
Scheme 3.11 Friedel Crafts Alkylation Reactions.

The work of Allen³⁴ et. al shows this clearly: They determined the mechanism by which a series of alkyl toluenes (methyl, ethyl, isopropyl and *tert*-butyl) rearrange when catalyzed by $\text{AlCl}_3\text{-HCl}$. It was concluded that the methyl group isomerizes entirely by the intramolecular mechanism, the ethyl mostly intramolecularly, the isopropyl mostly intermolecularly and the tertiary butyl entirely by an intermolecular mechanism. They proved this by showing that *para-tert*-butyltoluene, when treated with the catalyst did not produce any reorientation, but upon addition of toluene or *ortho* xylene to the reaction mixture, rearrangement

occurred. Presumably the reasons for this are that: 1) the *tert*-butyl group must move via an intermolecular mechanism and 2) the *para-tert*-butyltoluene is too sterically hindered allow a third alkyl group to attach. Therefore pure *para-tert*-butyltoluene has no way of reorienting. On the other hand, an alkyl acceptor ring such as toluene will easily catalyze the reaction. One can see the similarity between this and the copolymer reactions with $\text{PIPSO}_2\text{Cl}/\text{AlCl}_3$. The PtBS homopolymer is like the *para-tert*-butyltoluene case where the reaction proceeds very slowly. The presence of the styrene units of the copolymer has an effect similar to addition of the xylene to the (small molecule) reaction mixture; the reactions become much faster. This seems all well and good but there are a few things to be wary of. First, isopropyl groups (similar to the polymer backbone) are also known to do these kinds of reactions, but in this case they would require stronger conditions. It is known that secondary carbocations are not as stable as tertiary ones, and long alkyl chains are known to slow the reaction. This helps to explain some aspects of the reaction (with the polymers). The fact that the *tert*-butyl groups transfer in one instance and not another does not inherently explain the unusual MWDs. One possible explanation is that the reaction forms highly substituted, highly reactive aromatic rings which may eventually lead to crosslinking and/or backbone cleavage. Carbocations may do hydride transfers with the backbone or the piperidine units. Once free carbocations are present, the possibilities for many reactions arise. Another explanation is that aluminum may complex very well with highly substituted rings. The solution to this problem is rather simple; the reaction should work fine if a less active catalyst is used. To this end, the reaction was run with

SnCl_4 as the catalyst, but the reaction did not work, indicating that this catalyst is too weak. A catalyst of intermediate strength is required.

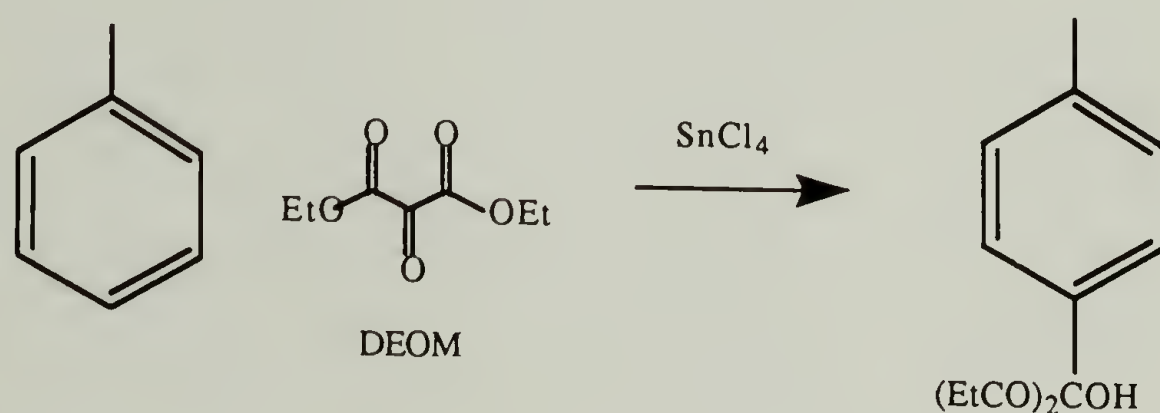
It was determined that most of the reaction conditions (involving the sulfur as the electrophile) described above were fairly harsh and that one must be extremely careful with the conditions to achieve selectivity. Finally efforts to introduce sulfur functionality were abandoned and new chemistry involving carbon-carbon bond formation on the ring was investigated. Normal Friedel Crafts acylation using acetyl chloride (shown in Scheme 3.12) to form the methyl ketone is quite selective and may proceed with a catalyst less active than aluminum chloride.³⁵ Higher selectivity may even be achieved with a milder catalyst (if the reaction still works). This acylation reaction can introduce ketones to the chain, which are a versatile functional group, but not very sticky in their own right. Another reaction that allows very good selectivity and the introduction of a stickier moiety is the Friedel Crafts reaction with diethyloxomalonate which is the subject of the next section.



Scheme 3.12 Friedel Crafts Acylations.

Modification Via Diethyloxomalonate

Diethyloxomalonate (DEOM) reacts with mildly activated aromatic rings to yield a hydroxy diethylmalonate moiety³⁶ (Scheme 3.13). The reaction is catalyzed by a rather weak Lewis acid, SnCl_4 , and thus it is innocuous to the tertiary butyl groups on the precursor polymer.



Scheme 3.13 Diethyloxomalonate Modification Reaction.

The DEOM molecule is rather large and is reported to react almost exclusively at the para position. The reaction has been reported for many alkyl benzenes.³⁷⁻⁴⁰ The different R groups which have been used are Me, Et, *i*-Pr, *tert*-Bt, *tert*-Am, and *n*-Pr with yields of 40% to 95%. Ghosh³⁶ has reported that *iso*-butylbenzene (12 mmole), DEOM (10 mmole) and SnCl_4 (12.5 mmole) react at room temperature for 3 h in methylene chloride to give 94% yield of the hydroxy diethylmalonate moiety. It has also been reported that if the para position is occupied, the DEOM will add to the ortho carbon.⁴¹ DEOM was reacted with reacted *para*-xylene under conditions similar to those above, and the hydroxy diethylmalonate compound was obtained in 57% yield. The work presented here uses the

much bulkier *tert*-butyl groups and the polymer backbone to hinder the reaction at the ortho carbons. This increase in bulkiness was found to have a substantial impact: full conversion of the styrene monomer units was obtained with very little or no addition of the DEOM to *tert*-butylstyrene units.

The reaction was carried out on both homopolymers and many copolymers as well as small molecule model compounds. The small molecule data can be found in Table 3.12 and the polymer modification data are recorded in Tables 3.13 and 3.14. The modifications were carried out in methylene chloride (CH_2Cl_2) or dichloroethane (DCE). Chlorinated hydrocarbon solvents can be used because SnCl_4 is a much milder catalyst and will not facilitate alkylation as AlCl_3 will do with these solvents (this is a major advantage over the sulfamyl chloride reaction because these are much nicer solvents to use than nitrobenzene). DCE seems to work a little better than CH_2Cl_2 (modified polymer seems more soluble), and it allows latitude for higher temperature reactions (although it was found that room temperature reaction was adequate).

The DEOM/ SnCl_4 reaction has been found to be quite satisfactory for small molecules as well as polymers. Reactions were carried out on small molecules to help us understand the chemistry better and to make single sticky foot model compounds for physical studies. Model compounds were synthesized from toluene, *n*-propylbenzene, and *iso*-butylbenzene (Table 3.12). The toluene and *iso*-butyl benzene derivatives both crystallized out of the reaction mixture while the *n*-propyl did not (subsequent attempts to crystallize this compound under various conditions

Table 3.12 DEOM Reactions on Small Molecules.

<u>Sample</u>	<u>Conditions</u>
<u>1.</u> B13-27	0.223 g (1.19 mmol) p-di-tert-butylbenzene 0.28 mL (1.43 mmol) DEOM 1.4 mL (1.4 mmol) SnCl ₄ /hexane 5-10 mL CH ₂ Cl ₂ Room temperature, 5 hr No precipitate formed, starting material isolated (Mpt 76-79 °C)
<u>2.</u> B13-29	2 mL (23.8 mmol) toluene 2 mL (13.1 mmol) DEOM 11 mL (11 mmol) SnCl ₄ /hexane CH ₂ Cl ₂ Room Temperature, 4 hr White precipitate formed, product confirmed by NMR
<u>3.</u> B18-28	1 mL (7.0 mmol) n-propylbenzene (0.41 M) 1 mL (6.5 mmol) DEOM (0.38 M) 10 mL (10 mmol) SnCl ₄ /hexane (0.59 M) 5 mL CH ₂ Cl ₂ Room Temperature Reaction followed by GC about 83% conversion of the n-propylbenzene was obtained in 21.5 h
<u>4.</u> B18-40	2 mL (14 mmol) n-propylbenzene (0.98 M) 3.2 mL (21 mmol) DEOM (1.48 M) 4 mL (~20 mmol) SnCl ₄ /hexane (1.41 M) 5 mL CH ₂ Cl ₂ Room Temperature Reaction followed by GC about 98% conversion of the n-propylbenzene was obtained in 3 h. Product was confirmed by NMR.
<u>5.</u> B19-5	1.47 g (12.8 mmol) iso-butylbenzene (0.99 M) 2.2 mL (14.3 mmol) DEOM (1.11 M) 2.2 mL (18.7 mmol) SnCl ₄ (1.45 M) 7 mL CH ₂ Cl ₂ Room Temperature Product crystalizes out, recrystallized from pentane (Mpt 34-36 °C). Structure confirmed by NMR.

Table 3.13 DEOM Reactions: Initial Polymer Modifications.

<u>Sample/M_n^a</u>	<u>% SF</u>	<u>Convzn^b</u>	<u>Conditions</u>
<u>1.</u> T02/4.2k 7,980 ^c B13-64	~2	~1.6	0.25 g T02/12k-p (14.3 mg/mL) 0.3 mL DEOM (1.96 mmol)(0.20 M) 2.25 mL (2.2 mmol) SnCl ₄ /hexane (0.21M) ~15 mL dichloroethane RT, 2 h; 68 °C, 3 h; RT, 15 h
<u>2.</u> T14/12k TM1 25,610 ^c B13-25	~2.0	~0.14	0.27 g T14/12k-p (24.5 mg/mL) 0.33 mL DEOM (2.16 mmol)(0.20 M) 2.3 mL (2.3 mmol) SnCl ₄ /hexane (0.21M) 7-10 mL CH ₂ Cl ₂ RT, 4 h
<u>3.</u> T14/12k TM2 26,728 ^c B13-52	9.3	0.66	0.24 g T14/12k-p (13.7 mg/mL) 0.30 mL DEOM (1.96 mmol)(0.11 M) 2.25 mL (2.25 mmol) SnCl ₄ /hexane (0.13M) ~15 mL dichloroethane RT, 1 h; 70 °C, 2 h; RT, 16 h
<u>4.</u> T14/12k TM3 26,571 ^c B13-58	3.3	0.23	0.17 g T14/12k-p (11.3 mg/mL) 0.30 mL DEOM (1.96 mmol)(0.13 M) 2.25 mL (2.25 mmol) SnCl ₄ /hexane (0.15M) 10-15 mL dichloroethane RT, 2 h; 68°C, 3 h; RT, 15 h
<u>5.</u> R50/256k 335,980 ^c B13-48	14	0.28	0.23 g R50/114k-p (11.5 mg/mL) 0.6 mL DEOM (3.9 mmol)(0.20 M) 4.5 mL (4.5 mmol) SnCl ₄ /hexane (0.23 M) ~15 mL CH ₂ Cl ₂ RT 19 h, 0 °C 1 h
<u>6.</u> R90/175k ----- B13-60	> 50	> 0.5	0.25 g R90/175k-p (10.8 mg/mL) 1.0 mL DEOM (6.5 mmol)(0.28 M) 7.5 mL (7.5 mmol) SnCl ₄ /hexane (0.32M) ~15 mL dichloroethane RT, 2 h; 68 °C, 3 h; RT, 16 h
<u>7.</u> PtBS 225,782 ^c B13-40	~0	N/A	0.10 g PtBS/116k-p (10 mg/mL) 0.20 mL DEOM (1.31 mmol) (0.13 M) 1.5 mL (1.5 mmol) SnCl ₄ /hexane (0.15M) 5-10 mL CH ₂ Cl ₂ ; RT, 4 h

^a Mn of modified polymer versus polystyrene standards

^b Conversion calculated from ratio of aromatic to ester methylene peak areas in ¹H NMR, using the expected composition as the styrene content.

^c Molecular weights of precursor determined using RI detector therefore they do not coincide with the others. Corresponding molecular weight precursor determined on UV detector is 25,256 for 2, 3, 4; 331,143 for 5.

Table 3.14 DEOM Modified Polymers: Molecular Weight, Sticky Foot Content, Percent Conversion and Reaction Conditions.

<u>Sample /M_n^a</u>	<u>%SF</u>	<u>convzn^b</u>	<u>Conditions</u>
<u>1.</u> D5/50k 51,002 B21p76#1	5.80	1.16	0.61 g B21p23#2 (87.3 mg/ml) 1.0 ml DEOM (6.5 mmol) (0.93 M) 1.0 mL SnCl ₄ (8.5 mmol) (1.21 M) 5 mL DCE RT, 16.5 h
<u>2.</u> T5/50k 45,744 B21p76#5	6.18	1.24	0.61 g B21p30#1 (87.0 mg/mL) 1.0 ml DEOM (6.5 mmol) (0.93 M) 1.0 mL SnCl ₄ (8.5 mmol) (1.21 M) 5 mL DCE RT, 19 h
<u>3.</u> D12/50k 48,998 B21p76#2	13.16	1.09	0.61 g B21p23#3 (86.7 mg/mL) 1.0 ml DEOM (6.5 mmol) (0.93 M) 1.0 mL SnCl ₄ (8.5 mmol) (1.21 M) 5 mL DCE RT, 17 h
<u>4.</u> T12/50K 50,189 B21p76#6	13.84	1.15	0.62 g B21p30#2 (88.2 mg/mL) 1.0 ml DEOM (6.5 mmol) (0.93 M) 1.0 mL SnCl ₄ (8.5 mmol) (1.21 M) 5 mL DCE RT, 19.5 h
<u>5.</u> D23/76k 80,753 B20p129#1	16.37	0.71	0.65 g B20p105d (71.9 mg/mL) 1.0 mL DEOM (6.5 mmol) (0.72 M) 1.0 mL SnCl ₄ (8.5 mmol) (0.94 M) 7 mL DCE RT, 5 h
<u>6.</u> T23/81k 89,996 B20p129#2	16.59	0.72	0.64 g B20p105t (71 mg/mL) 1.0 ml DEOM (6.5 mmol) (0.72 M) 1.0 ml SnCl ₄ (8.5 mmol) (0.94 M) 7 mL DCE RT, 6 h
<u>7.</u> D23/13k DM1 14,485 ^c B18p46	18.68	0.81	0.53 g B18p24 (75.3 mg/mL) 1.0 mL DEOM (6.5 mmol) (0.93 M) 1.0 mL SnCl ₄ (8.5 mmol) (1.21 M) 5 mL CH ₂ Cl ₂ RT, 5.5 h

continued next page

Table 3.14 continued

<u>8.</u> D23/13k DM2 14,595 ^c B18p54a	24.41	1.06	0.50 g B18p24 (71.1 mg/mL) 1.0 mL DEOM (6.5 mmol) (.93 M) 1.0 mL SnCl ₄ (8.5 mmol) (1.21 M) 5 mL CH ₂ Cl ₂ RT, 40 h
<u>9.</u> T23/12k TM1 14,267 ^c B18p54b	24.69	1.07	0.49 g B18p25 (70.5 mg/mL) 1.0 mL DEOM (6.5 mmol) (.93 M) 1.0 mL SnCl ₄ (8.5 mmol) (1.21 M) 5 mL CH ₂ Cl ₂ RT, 40 h
<u>10.</u> D23/13k DM3 11,818 B19p5	12.82	0.56	0.5131 g B18p24 (62.3 mg/mL) 0.6 mL DEOM (3.9 mmol) (0.47M) 0.6 mL SnCl ₄ (5.1 mmol) (0.62M) 7 mL CH ₂ Cl ₂ RT, 7.25 h
<u>11.</u> T23/12K TM2 10,721 B19p5	13.71	0.60	0.51 g B18p25 (61.9 mg/mL) 0.6 mL DEOM (3.9 mmol) (0.47 M) 0.6 mL SnCl ₄ (5.1 mmol) (0.62 M) 7 mL CH ₂ Cl ₂ RT, 6.5 h
<u>12.</u> D23/13k DM4 11,544 B19p70	19.95	0.87	0.62 g B18p24 (88.5 mg/mL) 1.0 mL DEOM (6.5 mmol) (0.91 M) 1.0 mL SnCl ₄ (8.5 mmol) (1.21 M) 5 mL CH ₂ Cl ₂ RT, 26 h work-up problems/ poor polymer
<u>13.</u> T23/12k TM3 10,524 B19p68	24.32	1.06	0.64 g B18p25 (90.7 mg/mL) 1.0 mL DEOM (6.5 mmol) (0.91 M) 1.0 mL SnCl ₄ (8.5 mmol) (1.21 M) 5 mL CH ₂ Cl ₂ RT, 24 h work-up problems/ poor polymer
<u>14.</u> D23/13k DM5 10,381 B19p105d	22.43	0.96	0.59 g B18p24 (83.6 mg/mL) 1.0 mL DEOM (6.5 mmol) (0.91M) 1.0 mL SnCl ₄ (8.5 mmol) (1.21 M) 5 mL CH ₂ Cl ₂ , RT, 26 h
<u>15.</u> T23/12k TM4 10,524 B19p105t	23.09	1.00	0.56 g B18p25 (80.6 mg/mL) 1.0 mL DEOM (6.5 mmol) (0.91 M) 1.0 mL SnCl ₄ (8.5 mmol) (1.21 M) 5 mL CH ₂ Cl ₂ , RT, 26 h

continued next page

Table 3.14 continued

<u>16.</u> D23/13k DM6 10,253 B20p84d	23.94	1.04	0.53g B18p24 (75 mg/mL) 1.0 mL DEOM (6.5 mmol) (0.91 M) 1.0 mL SnCl ₄ (8.5 mmol) (1.21 M) 5 mL DCE RT, 15 h
<u>17.</u> T23/12K TM5 10,249 B20p84t	24.69	1.07	0.51 g B18p25 (72.8 mg/mL) 1.0 mL DEOM (6.5 mmol) (0.91 M) 1.0 mL SnCl ₄ (8.5 mmol) (1.21 M) 5 mL DCE RT, 14 h
<u>18.</u> D23/50k 46,575 B21p76#3	23.47	1.02	0.60 g B21p23#5 (85.8 mg/mL) 1.0 ml DEOM (6.5 mmol) (0.93 M) 1.0 mL SnCl ₄ (8.5 mmol) (1.21 M) 5 mL DCE, RT, 18 h
<u>19.</u> T23/50k 45,921 B21p76#7	24.04	1.04	0.60 g B21p30#4 (85.7 mg/mL) 1.0 ml DEOM (6.5 mmol) (0.93 M) 1.0 mL SnCl ₄ (8.5 mmol) (1.21 M) 5 mL DCE, RT, 20 h
<u>20.</u> D40/50k 52,240 B21p76#4	38.17	0.95	0.60 g B21p23#6 (85.8 mg/mL) 1.0 ml DEOM (6.5 mmol) (0.93 M) 1.0 mL SnCl ₄ (8.5 mmol) (1.21 M) 5 mL DCE, RT, 18.5 h
<u>21.</u> T40/50k 58,500 B21p76#8	41.72	1.04	0.59 g B21p30#5 (85.3 mg/mL) 1.0 ml DEOM (6.5 mmol) (0.93 M) 1.0 mL SnCl ₄ (8.5 mmol) (1.21 M) 5 mL DCE; RT, 20.5 h
<u>22.</u> D77/59k 78,721 B20p130	48.33	0.63	0.74 g B20p105#1 (74.2 mg/mL) 1.0 ml DEOM (6.5 mmol) (0.93 M) 1.0 mL SnCl ₄ (8.5 mmol) (1.21 M) 8 mL DCE; RT, 3.25 h
<u>23.</u> R80/184k 235,738 B20p84	51.24	0.64	0.52 g B9p43 (49.4 mg/mL) 1.5 mL DEOM (9.75 mmol) (0.93M) 1.5 mL SnCl ₄ (12.7 mmol) (1.21 M) 7.5 mL DCE; RT, 2 h
<u>24.</u> D90/16k 24,919 B21p76#9	87.62	0.97	0.60 g B21p15#1 (85.2 mg/mL) 1.0 ml DEOM (6.5 mmol) (0.93 M) 1.0 mL SnCl ₄ (8.5 mmol) (1.21 M) 5 mL DCE; RT, 21 h

continued next page

Table 3.14 continued

<u>25.</u> D95/33k 50,609 B21p76#10	90.92	0.96	0.61 g B21p15#2 (87.7 mg/mL) 1.0 mL DEOM (6.5 mmol) (0.93 M) 1.0 mL SnCl ₄ (8.5 mmol) (1.21 M) 5 mL DCE RT, 21.5 h
<u>26.</u> PSM1 14,625 B19p5	67.10	0.67	0.49 g N127A (60.4 mg/mL) 0.6 mL DEOM (3.9 mmol) (0.47 M) 0.6 mL SnCl ₄ (5.1 mmol) (0.62 M) 7 mL CH ₂ Cl ₂ RT, 24 h
<u>27.</u> PSM2 ----- B19p72	94.73	0.95	0.51 g B13p73#2 (71.7 mg/mL) 1.0 mL DEOM (6.5 mmol) (0.91 M) 1.0 mL SnCl ₄ (8.5 mmol) (1.21 M) 5 mL CH ₂ Cl ₂ RT, 48 h
<u>28.</u> PSOFM ^d 5,517 B20p129#4	55.26	0.55	0.32 g NF8P83 (54.9 mg/mL) 0.3 mL DEOM (1.95 mmol) (0.34 M) 0.5 mL SnCl ₄ (4.25 mmol) (0.73M) 5 mL DCE RT, 7 h (original polymer run before software change so can't compare MWs)
<u>29.</u> PtBS88M1 12,669 ^c B18p54c	2.9 ^e	N/A	0.24 g B18p16 (67.1 mg/mL) 0.5 mL DEOM (3.25 mmol) (0.93 M) 0.5 mL SnCl ₄ (4.25 mmol) (1.21 M) 2.5 mL CH ₂ Cl ₂ RT, >24 h
<u>30.</u> PtBS88M2 8978 B19p5	0.0	N/A	0.27g B18p16 (33.1 mg/mL) 0.6 mL DEOM (3.9 mmol) (0.47 M) 0.6 mL SnCl ₄ (5.1 mmol) (0.62 M) 7 mL CH ₂ Cl ₂ RT, 8 h
<u>31.</u> PtBS88M3 8978 B19p71	1.4 ^e	N/A	0.21 g B18p16 (30.6 mg/mL) 0.5 mL DEOM (3.25 mmol) (0.45 M) 0.5 mL SnCl ₄ (4.25 mmol) (0.6 M) 5 mL CH ₂ Cl ₂ RT, 48 h

^a Mn of modified polymer versus polystyrene standards

^b Conversion calculated from ratio of aromatic to ester methylene peak areas in ¹H NMR, using the expected composition as the styrene content.

^c Molecular weights determined before software switch on the GPC therefore they do not coincide with the others (i.e. after the switch, the new did not match the old).

^d Polystyrene homopolymer end-capped with perfluorodecanoate (N. Franchina).

^e Number is deceptively large for what is seen in actual spectrum. Also some contributions could be from starting product.

were also fruitless). The *n*-propylbenzene derivative was found to crystallize over long periods time when the solvent was allowed to evaporate into the air. The NMR spectra obtained for these three model compounds confirmed their structure. Figure 3.6 is the proton NMR spectrum of the *iso*-butylbenzene derivative; note the doublet of doublets (7.48, 7.58, 7.18 and 7.10 ppm) which is characteristic of para-substituted rings with substituents of substantially different shielding character. The quartet (4.42, 4.34, 4.25 and 4.16 ppm) centered at approximately 4.3 ppm is due to the methylene protons α to the oxygen in the ester functionality ($-\text{CO}_2\text{CH}_2\text{CH}_3$), these are present for all derivatives and are well resolved from the other resonances. The ratio of this peak area to that of the aromatic protons was used to determine the styrene conversion obtained for the polymer samples. The doublet located at 2.52 and 2.43 ppm is due to benzylic methylenes of the *iso*-butyl group while the broad multiplet at 1.8 ppm is a combination of the methine proton and the hydroxyl proton (the hydroxyl proton is variable in the NMR spectra of these compounds). Finally, the triplet at 1.37, 1.28, 1.20 ppm and doublet at 0.94, 0.86 ppm are due to the ester and the isobutyl methyl groups, respectively. Spectra of the toluene and *n*-propylbenzene derivatives agree well (toluene - doublet of doublets 7.57, 7.47, 7.21, 7.10; quartet 4.41, 4.32, 4.24, 4.15; singlet 2.34; broad peak 1.65; triplet 1.37, 1.28, 1.20; *n*-propyl benzene doublet of doublets 7.59, 7.49, 7.21, 7.11; quartet 4.42, 4.34, 4.25, 4.16; triplet 2.68, 2.60, 2.50; broad multiplet 1.60; triplet 1.38, 1.29, 1.20; triplet 1.02, 0.94, 0.84 ppm). These spectra agree well with those reported by Ghosh. The effect of concentration on the reaction kinetics can be seen in the two modifications of *n*-propylbenzene (Table 3.12). In entry 3, all

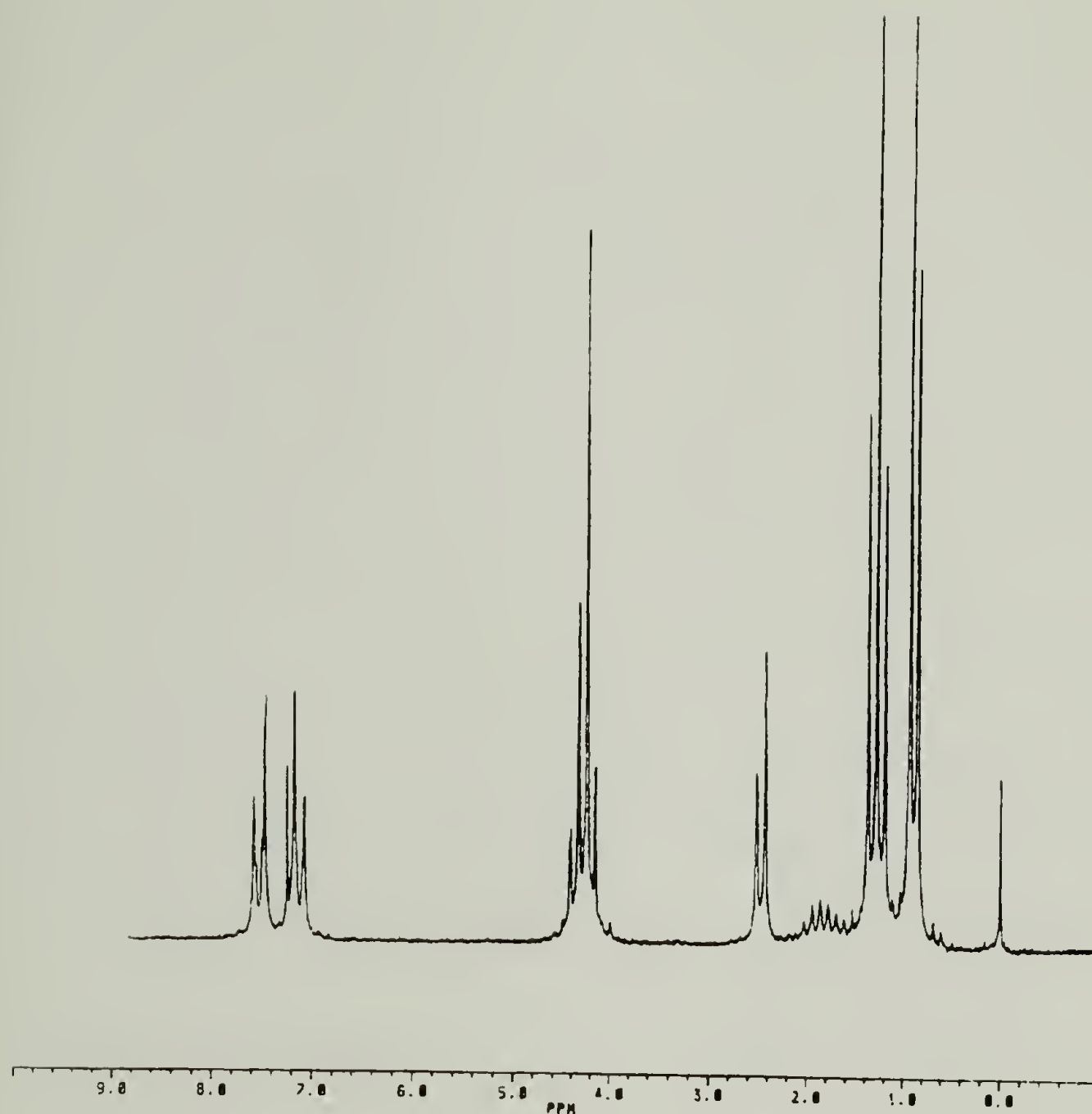


Figure 3.6 ^1H NMR spectrum of *iso*-butylbenzene derivative of DEOM/ SnCl_4 reaction (See Table 3.12, B19-5).

of the concentrations were less than 0.4 M and GC analysis shows that there was only about 86% conversion after 21.5 hours. In entry 4, the concentration was increased to approximately 1.4 M, and in this case 98% conversion was obtained within 3 hours. In the control reaction run on *para-di-tert*-butylbenzene (Table 3.12, entry 1), no crystallization was observed in the reaction pot and the starting material was isolated in the end. This indicates that carbons ortho to tertiary butyl groups are much less susceptible to addition by DEOM than unhindered carbons at the para position.

The isobutyl derivative was recrystallized from pentane at 0 °C to obtain a crystalline solid with a melting point of 34-36 °C. This is in disagreement with that reported by Ghosh of 116-117 °C. The melting range (34-36 °C) is fairly narrow, thus the discrepancy should not be attributed to impurities. The *n*-propyl derivative does not crystallize out of solution. It is miscible with methanol and diethyl ether at 25 and -60 °C and with pentane at 25 °C but phase separates between 25 °C and -20 °C. This suggests that the pentane/hydroxy diethylmalonate solution interactions are fairly unfavorable and that the entropy of mixing is just barely getting the small molecule into solution at room temperature (there are no complications from crystallization energies), and thus we would expect pentane and other hydrocarbons to be poor solvents for the modified block. On the other hand, the energetics with ether and methanol are much less unfavorable and we expect them to be better solvents for the sticky block.

The initial reactions carried out with DEOM used stock solutions of SnCl_4 (1.0 M) as the source of the catalyst (see Table 3.13 and first four entries of Table 3.12). DEOM was added to the polymers in these cases but the conversions were low (even for polymers with relatively low styrene content). The average conditions for these initial modifications were a DEOM and SnCl_4 concentration of 0.1 to 0.2 M ($[\text{SnCl}_4]$ is a little higher in most cases). Entries 2 and 5 in Table 3.13 show conversions of 0.14 and 0.28 for two polymers run in CH_2Cl_2 at room temperature for up to 19 hours. The reaction solvent was changed to DCE to be able to run the reaction at higher temperatures (Table 3.13 entries 1,3,4, and 6). The reactant concentrations were kept fairly constant, but the reaction time and temperature were varied quite extensively in an attempt to achieve higher conversions. Reactions ranging from 4 h to 19 h at room temperature and reactions heated almost to reflux (68 °C) for up to 3 h with subsequent long time room temperature reactions did not result in full conversion of the styrene units. One exception was the full conversion of the 2% styrene copolymer. This problem was solved by using neat SnCl_4 . Reactions carried out using neat SnCl_4 (Table 3.14) resulted in full conversion for many polymers. The neat SnCl_4 allowed use of much higher reactant concentrations while employing equimolar amounts of DEOM and SnCl_4 . This can be seen by comparing the concentrations in the two tables (3.13 and 3.14). The initial reactions were carried out with concentrations in the 0.1 to 0.2 M range and those using neat SnCl_4 were mostly around 0.9 M, a 5 to 10 fold increase in concentration. Table 3.14 shows that full conversions were obtained for numerous polymers and that, even for polymers containing large amounts of styrene, conversions close to one have been obtained. The polymers in entries 8, 9, 14, 15, 16, and 17 were

all prepared from the same 23% styrene diblock and triblock copolymer pair. All six modifications were run under nearly identical concentration conditions with reaction times of 15 h, 26 h and 40 h. In all cases the conversions are close to one. This tells us that the higher concentrations of reagents allow full conversion of the styrene units and this is substantiated by the reproducibility of the data. We know that we have reached the conversion limit which shows that the reaction stops and that we are converting all the styrene units and leaving the others alone. Closer inspection of the table shows that the conversion can be controlled by reaction time and reactant concentration. The effect of reaction time is seen in the entries 7, 8 and 9 in which a 23% styrene copolymer was reacted under identical concentration conditions but for 5.5 h in 7 and 40 h in the other two. One can see that the shorter time resulted in a conversion of only 0.81 while the longer times gave full conversion. Comparison with entries 16 and 17 shows that the reaction is complete after 15 h. Thus we can say that the reaction reaches complete conversion between 5.5 and 15 hours. Other entries in the table, although not for the same polymers, also suggest that the reaction is complete within 15 hours. A survey of the rest of the table finds that all polymers (irrespective of the styrene composition) that have been reacted in solutions with concentrations of ~ 0.9 M and for times longer than 15 h all have conversions greater than 0.95 (i.e. entries 1, 2, 3, 4, 8, 9, 14, 15, 16, 17, 18, 19, 20, 21, 24, 25 and 27). Reactions run at lower concentrations or for shorter times resulted in only partial modification. For example, entries 7, 22, and 23 were all run using concentrations of about 0.9 M but short reaction times, and all resulted in only partial conversion of the styrene groups. As has already been mentioned, the reactant concentration is a very important factor in

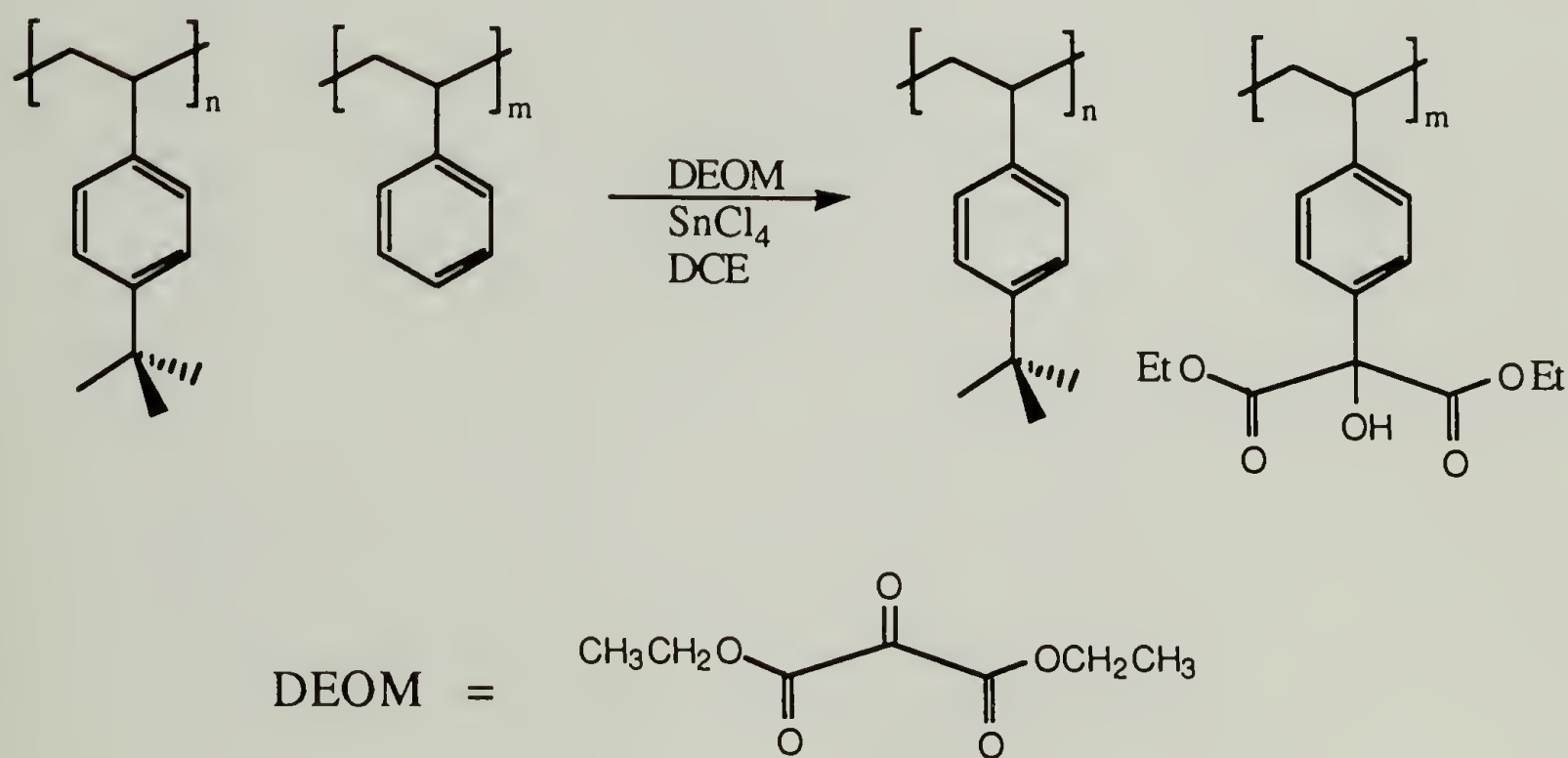
determining the conversion obtained for a given polymer modification. Low concentrations resulted in less than full conversions, even for extended reaction times at elevated temperatures (Table 3.14). Within the high reaction concentration regime discussed here, one can see that the concentration has an effect. Entry 26 shows that PS homopolymer reacted at 0.47 M concentration for 24 h results in only a 67% conversion, whereas it has already been seen that the reaction is complete within 15 hours with a concentration of 0.91 M. There are numerous examples in the table where both short times and lower concentrations together have resulted in lower conversions (5, 6, 10, 11 and 28). The reaction conditions reported in entries 10 and 11 were used deliberately to obtain only partial conversion of the sticky block. These types of polymers can be used to probe the physical phenomena of adsorption, such as the surface packing versus surface interaction energy cross-over (this will be discussed in more detail in the adsorption section). It is surprising that there seems to be a concentration threshold below which full conversion is not attainable for these reactions (i.e. one might expect a decrease in reaction rate, but not a lower equilibrium conversion). One could postulate that the higher concentrations are required to force the DEOM/SnCl₄ complex to partition from the solvent into the polymer coil where it can react. Evidence of this phenomenon has also been observed for the DTT modification reactions of the styrene-propylene sulfide copolymers that are discussed in Chapter IV. This is an interesting effect in itself and warrants further investigation. It may be found that the polymer coil will not partition the reactants in at the lower concentrations and thus only the outside of the coil would be modified. The higher reagent concentrations shift the equilibrium and allow a substantial amount of the reactant into the coil where it can react.

An increase in the polymer concentration should have a similar effect (as increasing the DEOM/ SnCl_4 concentration) and one can imagine a large increase in rate above the chain overlap concentration (i.e. homogeneous solution again).

One should note that the conversions reported for entries 12 and 13 are tainted because of trouble encountered in the work-up. Evidence of alcoholysis with methanol was observed by NMR in these samples. Also note that conversions of some of the low SF content polymers are rather high. This can be explained by problems that were encountered with the precursor polymer synthesis (which resulted in the % styrene used in the calculation being incorrect) and by the fact that the calculated conversions will, in general, be more sensitive to small differences in the peak areas at these low SF contents. An interesting result was obtained with the polymer in entry 28. The precursor polymer used was a perfluorodecanoate end-capped PS homopolymer (supplied by N. Franchina). This was synthesized by reacting hydroxyethyl end-capped PS with perfluorodecanoyl chloride. The modification was carried out to determine the stability of the fluorinated ester under the DEOM modification conditions. Infrared data indicate the presence of the perfluoroester after modification. The carbonyl peak at 1785 cm^{-1} is indicative of the perfluorodecanoate and small C-O and C-F absorbances were seen as shoulders on the larger ester (C-O) absorbances introduced by the DEOM reaction in the 1300 to 1000 cm^{-1} wavenumber range (these shoulders corresponded well with positions of the peaks in the precursor spectrum). The XPS spectra of samples of adsorbed polymer and spun cast polymer films indicate the presence of fluorine, as well. These data reveal that the perfluorodecanoate endgroup is (at least partially) stable to the DEOM modification conditions. (A good

control reaction would have been reaction of perfluoro-endcapped PtBS, or use of a small molecule model compound.) The feasibility of synthesizing a three-component polymer system of controlled architecture thus has been demonstrated. These types of polymers may find many uses, as will be discussed in the adsorption section.

The polymer modifications with DEOM were carried out in either dichloroethane or methylene chloride. The reaction proceeds as shown in Scheme 3.14.



Scheme 3.14 Polymer Modification with DEOM/SnCl₄.

The typical modification procedure involved dissolving the precursor polymer (~500 mg) in 5 mL of solvent (DCE or CH₂Cl₂) and adding 1 mL of DEOM (under dry N₂). The solution was cooled to 0 °C and 1 mL of

neat SnCl_4 was added via syringe over a period of a few minutes, and then the reaction solution was allowed to warm to room temperature. The reaction was carried out in the dark for the appropriate length of time (usually about 15-24 h). As the reaction proceeded, an orange color developed and the solution became noticeably more viscous (especially for polymers with high styrene content). The larger SF contents sometimes resulted in polymer precipitation or a "pearliness" in the solution. The resulting sticky foot polymers are somewhat soluble in methanol (PS homopolymer modified by this reaction is soluble in methanol), and therefore direct precipitation into methanol does not work well. Instead, polymer solutions were poured into a mixture of aqueous HCl (1.0 M)/methanol (15 mL/45 mL), and the polymers precipitated out as gooey blobs. Each polymer was separated from the liquid via filtration and/or decanting. The polymer was redissolved in THF and precipitated in water/methanol mixtures (the ratio changes depending on the SF content of the polymer for instance 25 mL/55 mL for a 23% SF copolymer). Most often, a nice white easily filtered polymer was obtained. On occasion, the particles were too small and the polymer was difficult to filter. (This happens when the water/methanol ratio is not correct). Small insoluble particulates have been found in the polymer even after numerous precipitations. These are presumed to be various tin salts formed during the workup. They have been removed by filtration (micro filter with 2 μm pores) but this is difficult because the filters fill up so fast. The best way to separate the solids is via centrifugation. As a final step, the polymers are freeze-dried from benzene and washed with a non-solvent organic compound (usually methanol). This is a good general procedure for washing difficult-to-remove small molecule impurities from the polymer.

The freeze-drying creates a large surface area and washing with a non-solvent will usually take away any organic impurity (small molecules are usually miscible with a much wider range of solvents). The reason that this step is required with these polymers is because the precipitation in water/methanol solution causes the small molecules to precipitate with the polymer, and therefore repeated precipitations are not an efficient purification procedure.

Table 3.15 contains a list of the modified polymers (and their MW, PDI and %SF) used in subsequent physical experiments. The modified polymer names are derived from the corresponding precursor name (see Table 3.1) with the p suffix eliminated. An additional suffix is used to differentiate between samples when more than one modification of a given precursor was carried out.

Figure 3.7 shows the ^1H NMR spectrum of a 23% styrene precursor polymer (T23/12k-p). One can see the two peaks due to the aromatic ring protons at 7.06 and 6.55 ppm. Each of those peaks is actually a composite peak that is not well resolved. Peaks due to the aliphatic protons of the polymer backbone and the tertiary butyl group are also noted. The main peak at 1.28 ppm matches up well with that of the *tert*-butyl group in the model compound (Figure 3.6). Note the lack of any other resonances present in the precursor polymer spectrum. Figure 3.8 is the proton NMR spectrum of the same precursor polymer after modification with DEOM. Note the quartet located around 4.31 and 4.22 ppm which is due to the methylene protons ($-\text{CO}_2\text{CH}_2\text{CH}_3$) in the ester of the hydroxy diethylmalonate sticky foot. These data agree well with the model

Table 3.15 DEOM Modified Polymers: Molecular Weight, Polydispersity and Percent Sticky Foot Information.

<u>Sample</u>	<u>M_n</u>	<u>PDI</u>	<u>Percent Sticky Foot</u>
1. D5/50k	51,002	1.06	5.80
2. T5/50k	45,744	1.05	6.18
3. D12/50k	48,998	1.05	13.16
4. T12/50K	50,189	1.08	13.84
5. D23/76k	80,753	1.06	16.37
6. T23/81k	89,996	1.08	16.59
7. D23/13k DM1	14,485 ^a	1.07	18.68
8. D23/13k DM2	14,595 ^a	1.07	24.41
9. T23/12k TM1	14,267 ^a	1.06	24.69
10. D23/13k DM3	11,818	1.06	12.82
11. T23/12K TM2	10,721	1.05	13.71
12. D23/13k DM4	11,544	1.07	19.95
13. T23/12k TM3	10,524		24.32
14. D23/13k DM5	10,381	1.06	22.43
15. T23/12k TM4	10,524	1.05	23.09
16. D23/13k DM6	10,253	1.05	23.94
17. T23/12K TM5	10,249	1.05	24.69
18. D23/50k	46,575	1.05	23.47
19. T23/50k	45,921	1.08	24.04
20. D40/50k	52,240	1.05	38.17
21. T40/50k	58,500	1.06	41.72
22. D77/59k	78,721	1.026	48.33
23. R80/184k	235,738	1.16	51.24
24. D90/16k	24,919	1.03	87.62
25. D95/33k	50,609	1.028	90.92
26. PSM1	14,625	1.04	67.10
27. PSM2			94.73
28. PSOFMb	5,517	1.046	55.26
29. PtBS88M1	12,669 ^a	1.10	
30. PtBS88M2	8978	1.102	
31. PtBS88M3			

^a These data were recorded with the old version of the GPC software.

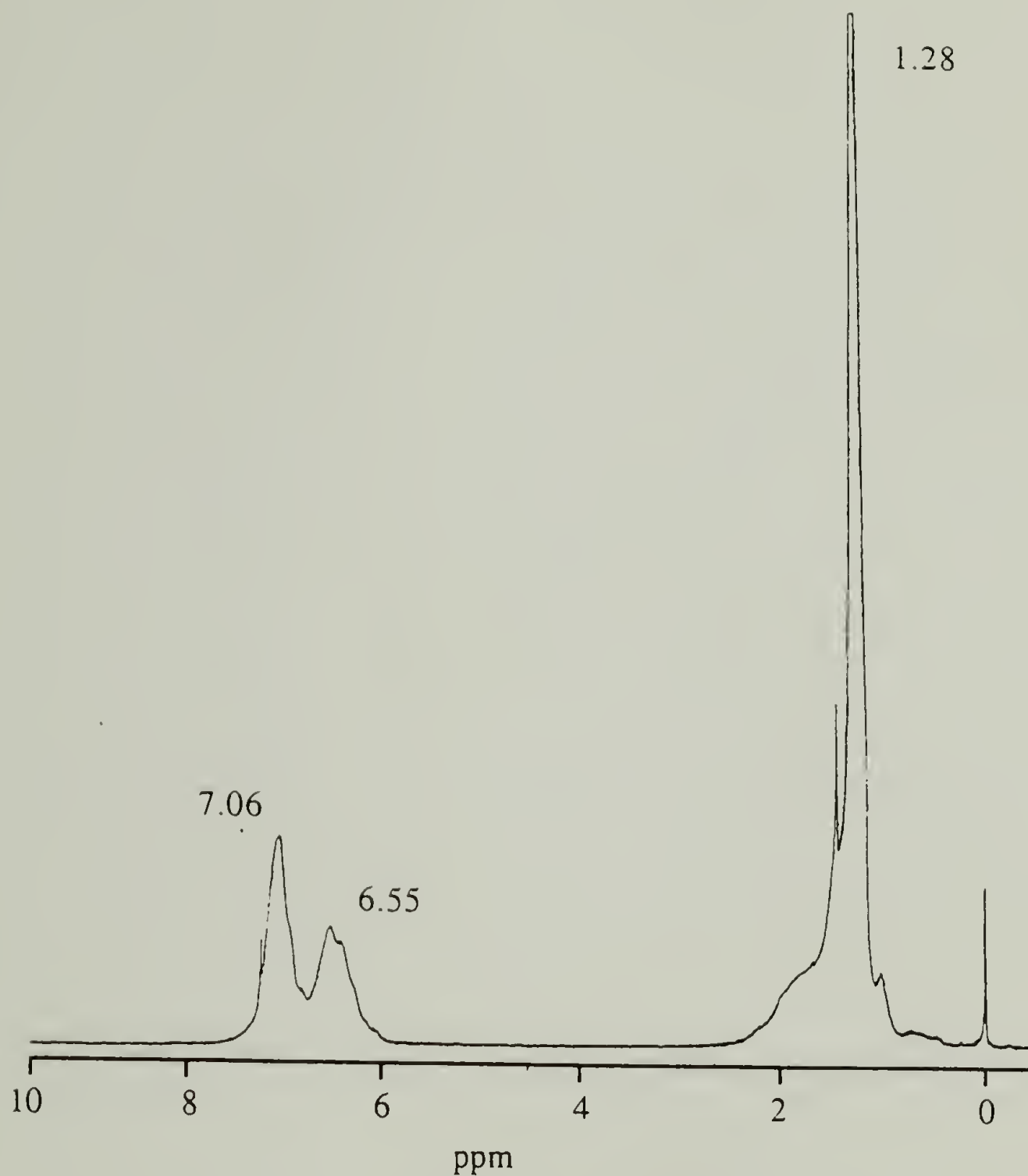


Figure 3.7 ^1H NMR spectrum of a 23% styrene precursor polymer (T23/12k p). This is the precursor for the modified polymer T23/12k TM1. (Solvent CDCl_3)

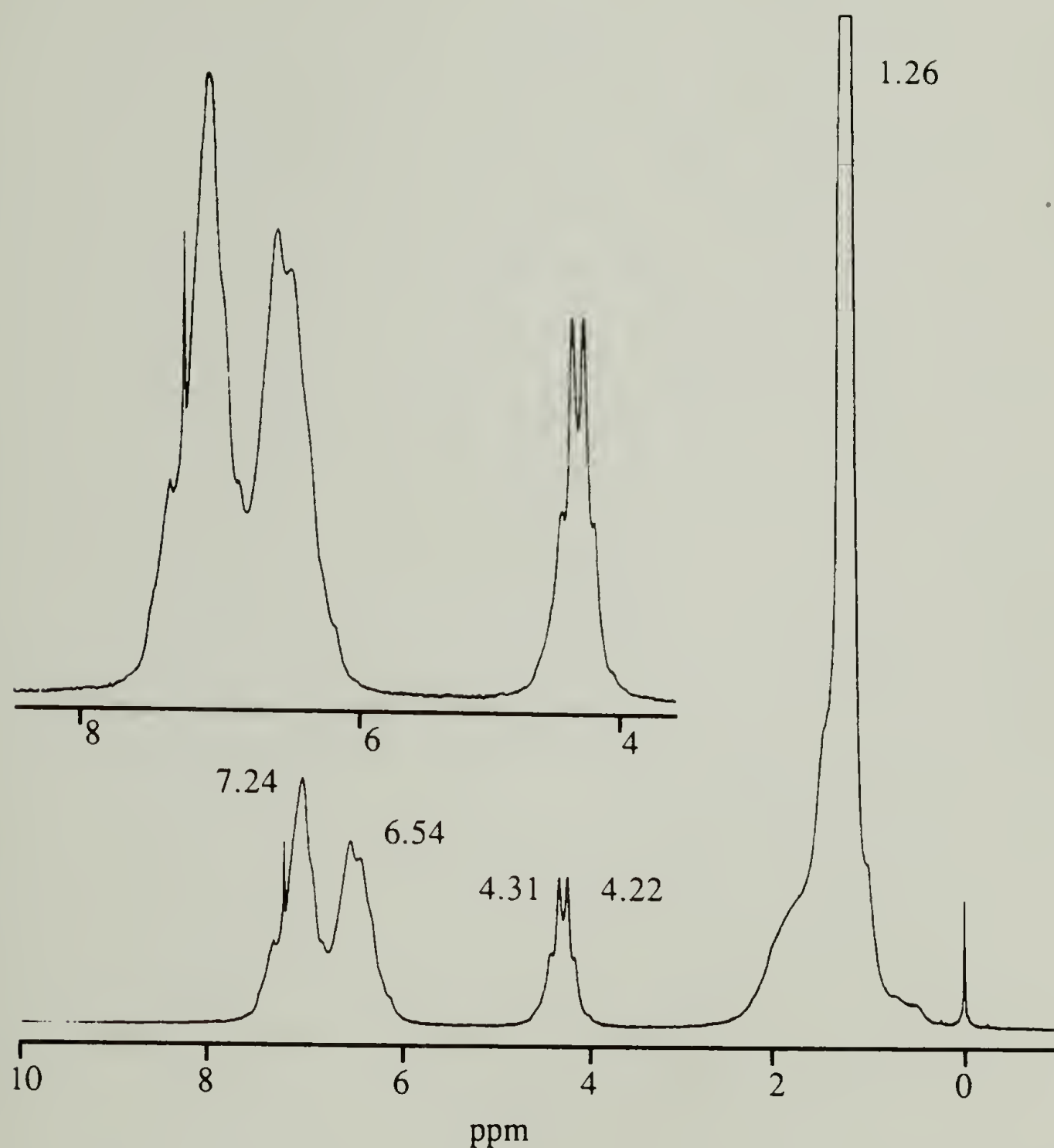


Figure 3.8 ^1H NMR spectrum of a 23% SF polymer (T23/12k TM4). A ratio of the aromatic protons (7.24, 6.54 ppm) to the ester methylene protons, $\text{CO}_2\text{CH}_2\text{CH}_3$ (4.31, 2.22 ppm) gives a DEOM modification conversion of 1.0. (Solvent CDCl_3)

compound resonances. This methylene peak is well resolved from the other peaks and the ratio of its area to that of the aromatic protons was used to determine the percent sticky feet for the polymer modifications. As expected, the ester methylene resonance is larger for higher sticky foot content polymers. Figures 3.9 and 3.10 show the spectra of a 95% styrene copolymer modified to a conversion of 0.95 and that of a polystyrene homopolymer brought to a conversion of 0.96, respectively. Note the much larger peak areas (in Figure 3.10), but identical peak positions. It should be noted that calculation of the conversion using the aliphatic versus aromatic area ratio gave inconsistent results which were both too high and too low as compared to the conversions calculated using the Ester:Aromatic ratio. This can be attributed a smaller overall range (of values) expected for the aliphatic ratio and the much larger peak size discrepancies. Also the spectra were baseline corrected with attention paid to the aromatic and ester peak and thus the baseline below the aliphatics was off a little.

Further proof of modification and sticky foot structure is observed with infrared spectroscopy. Figure 3.11 shows the IR spectra of the precursor and the modified polymers (the same 23% styrene polymer as shown above). The ester carbonyl stretch can be seen, as expected, at 1738 cm^{-1} . Also present are the C-O-C absorbances for the ester at 1269 and 1181 cm^{-1} . The resultant tertiary alcohol has absorbances at 3485 cm^{-1} and about 1110 and 1017 cm^{-1} . Figure 3.12 shows the IR spectrum of the modified 95% styrene copolymer (conversion of 0.95); one can see the peaks corresponding to the ester alcohol functionality are present but are much more intense than the 23% modified polymer (as one would expect). The C-H stretching region is also different (from the 23% copolymer) due

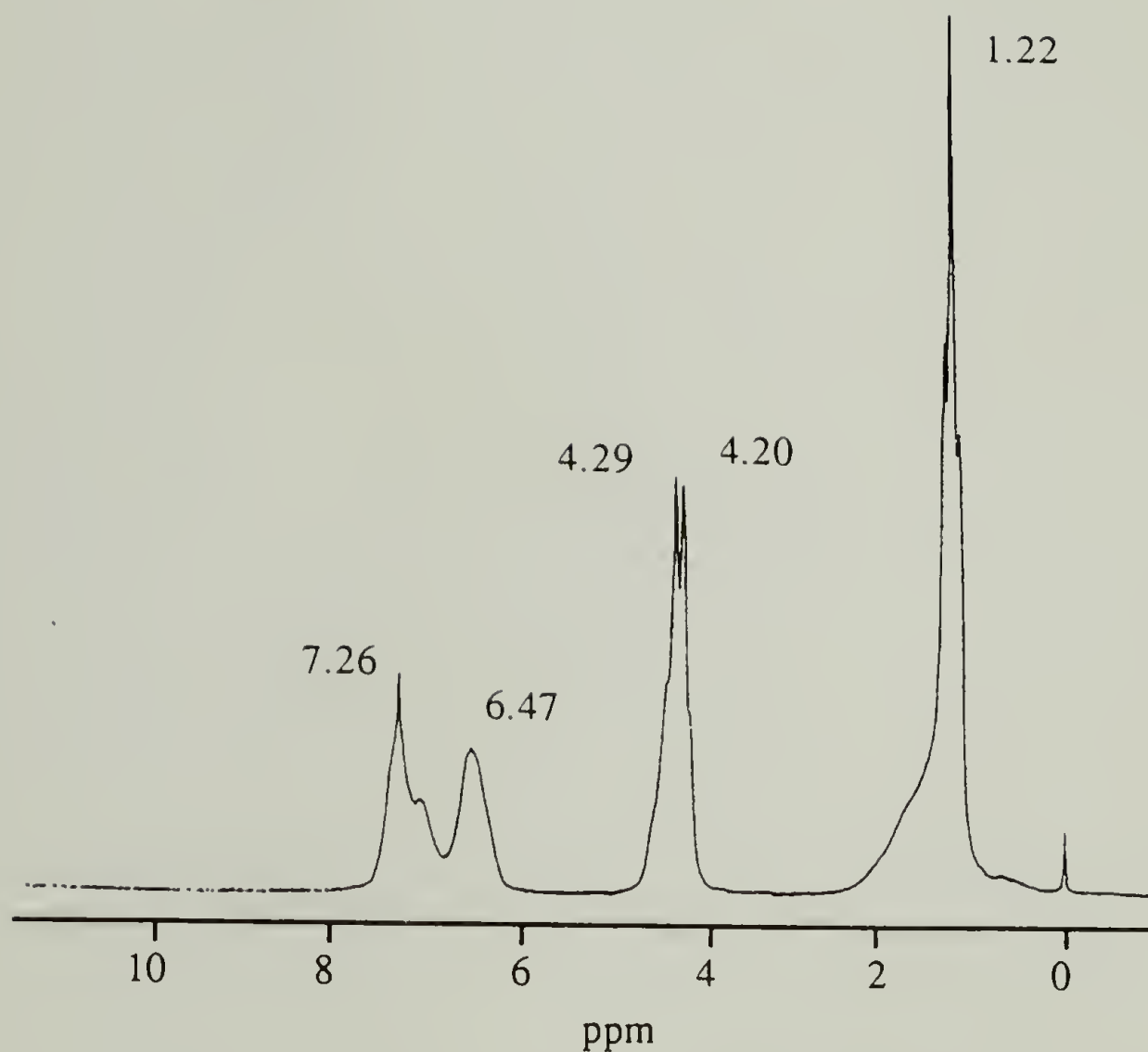


Figure 3.9 ^1H NMR spectrum of DEOM modified homopolymer polystyrene (PSM2, 95% conversion). The resonances at 4.29 ppm and 4.20 ppm are due to the methylenes of the ethyl ester ($\text{CO}_2\text{CH}_2\text{CH}_3$). (Solvent CDCl_3)

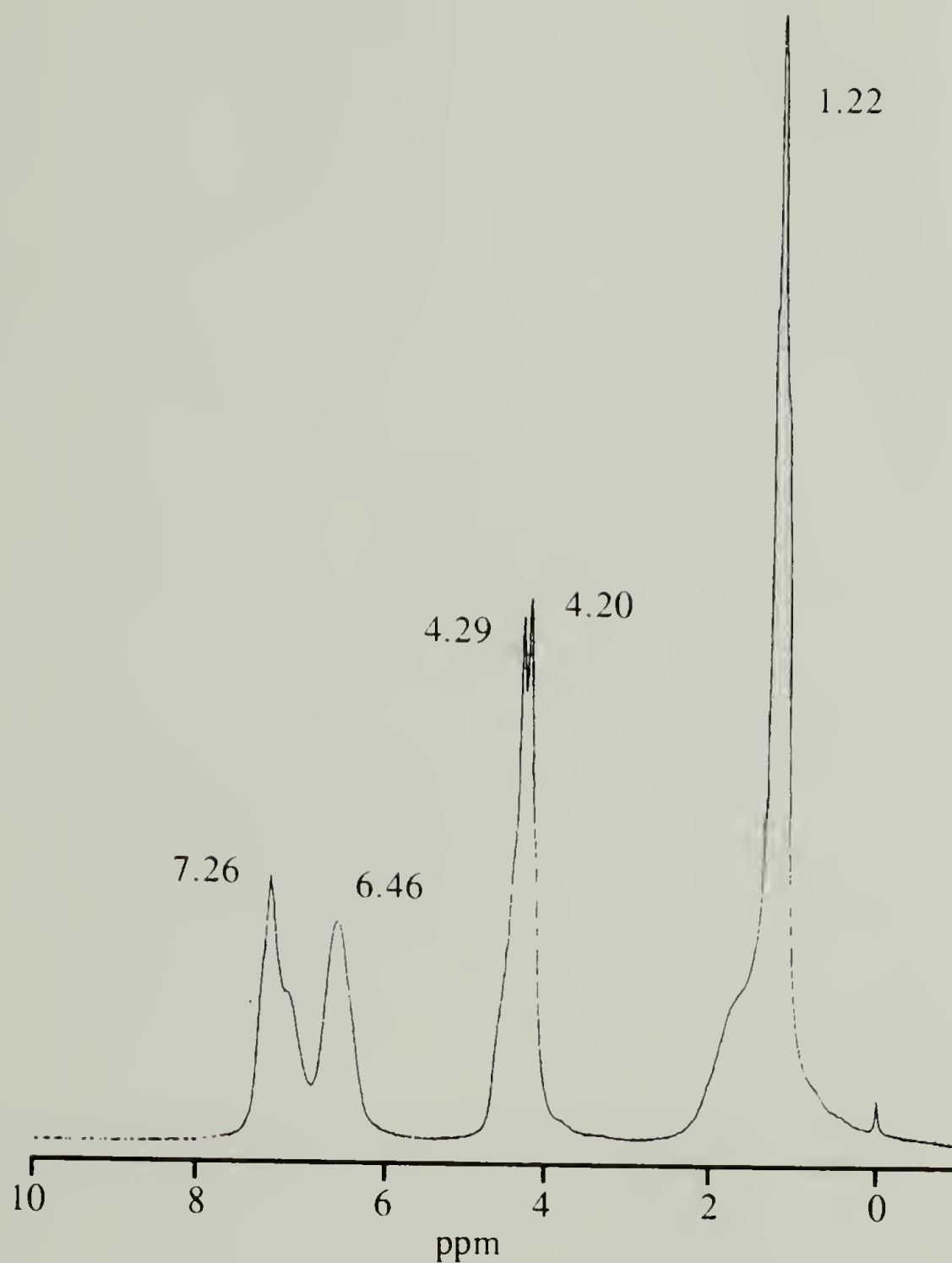


Figure 3.10 ^1H NMR spectrum of DEOM modified copolymer (Mn=33K) containing 95% styrene units (D95/33K). A conversion of 96% is calculated from the ratio of the aromatic protons (7.26, 6.46 ppm) and the ester methylene protons, $\text{CO}_2\text{CH}_2\text{CH}_3$ (4.29, 4.20 ppm). (Solvent CDCl_3)

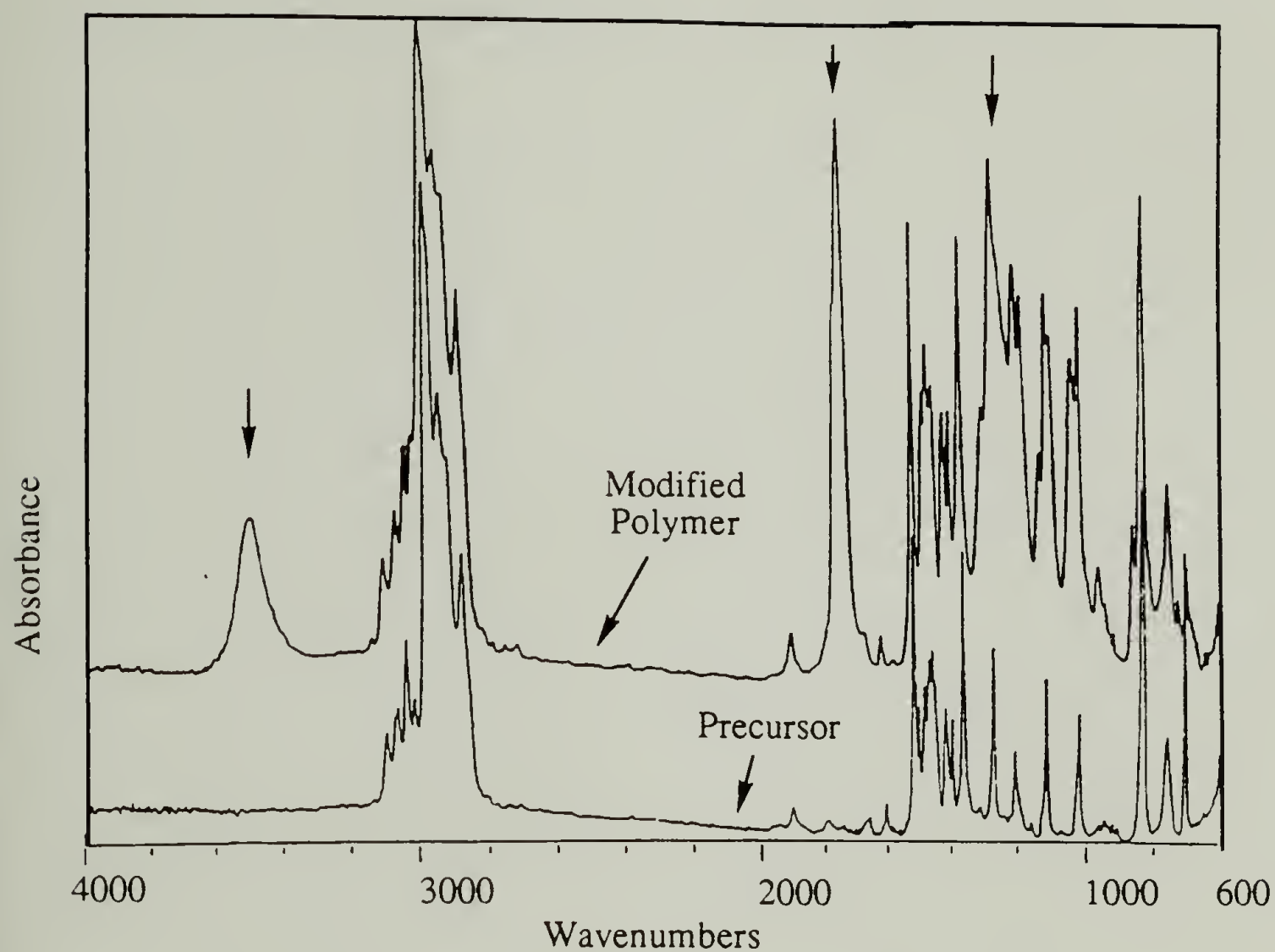


Figure 3.11 IR spectra of T23/12K and the precursor copolymer. Note the additional absorbances due to the ester and hydroxyl functionality incorporated in the polymer.

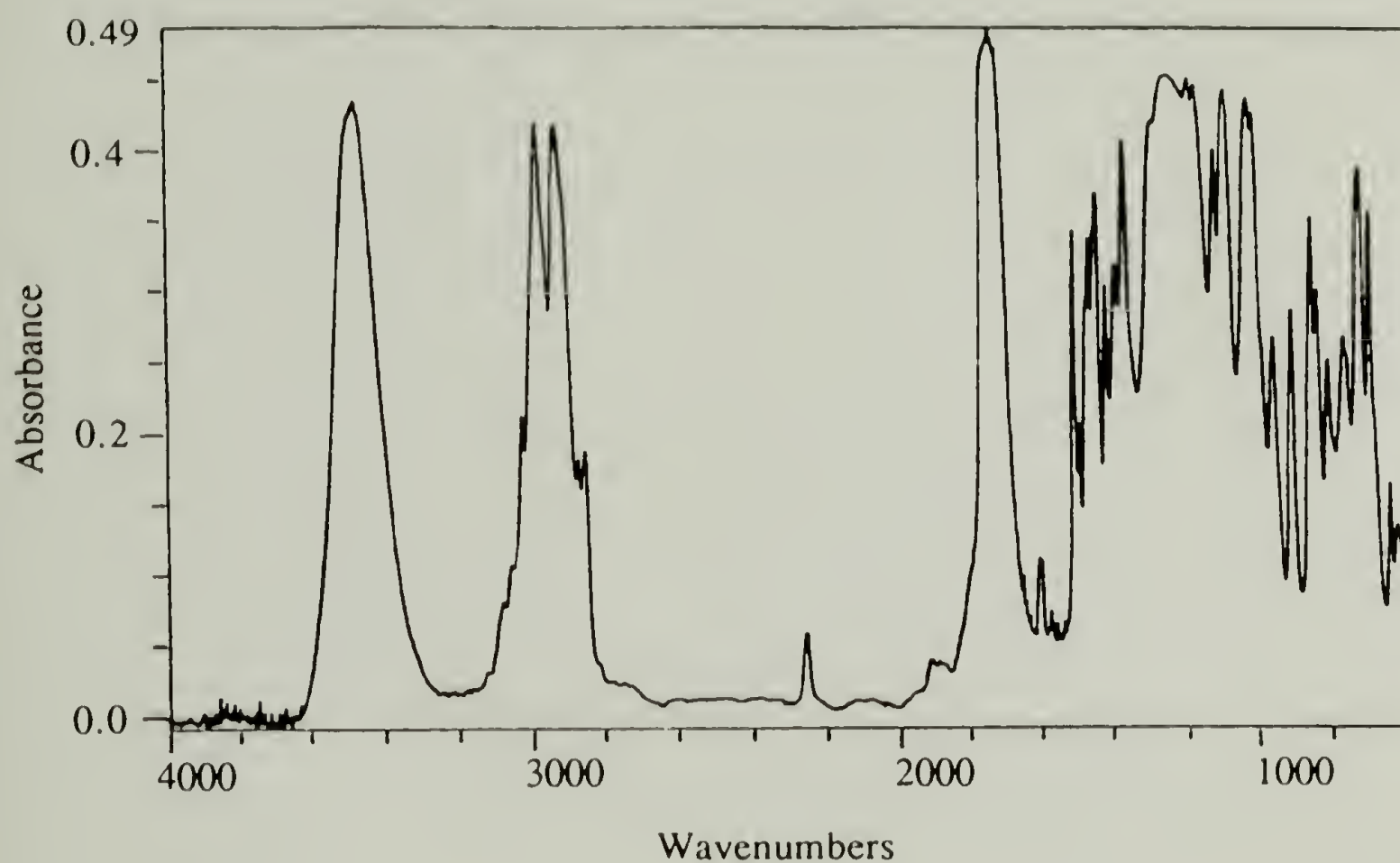


Figure 3.12 IR spectrum of D95/33K p modified by reaction with DEOM and SnCl_4 . Note the additional absorbances due to the ester and hydroxyl functionality incorporated into the polymer.

to the relative increase in the number of methylene carbons (2926 cm^{-1}) versus methyl carbons (2964 cm^{-1}), resulting from the decrease in the *tert*-butyl content and the increase in the ethyl content of the polymer.

The NMR and IR data give very good proof of DEOM modification of the copolymer and, in particular, the ester and hydroxyl functionality present. A few possible side reactions can be ruled out by examination of the spectra. The possibility of alcoholysis of the ester does exist, but that would result in a substantially different NMR spectrum than was obtained for these polymers. The most notable change in the NMR spectrum (that would occur upon alcoholysis) would be a shift in the resonance frequency of the protons on the carbon α to the ester oxygen and a change in the multiplicity of that peak. For example, the methyl ester (which would be the one we expect) would be a singlet with an absorbance at approximately 3.6 to 3.8 ppm.⁴² It should be mentioned that this was observed once when there was trouble with the workup (Table 3.14, entry 13).

The spectroscopic data indicate that no hydrolysis of the esters occurs. If hydrolysis had occurred, one would expect to see the acid proton at low field by NMR, but no peaks are observed there for these polymers. IR spectroscopy, gives the best proof because the acid would be evidenced by a shift in the carbonyl peak to lower wavenumbers ($1700\text{--}1720\text{ cm}^{-1}$ range), and this would most certainly be seen as a shoulder on the main ester peak. The O-H stretch of the acid would be seen as broad band ranging from $3100\text{ to }2500\text{ cm}^{-1}$. The presence of the acid salt could also be easily detected because the carbonyl stretch would be shifted to approximately 1622 cm^{-1} . The hydrolysis reaction has been carried out

intentionally and the acid salt obtained (see next section); indeed the expected shift in the carbonyl peak was observed. With no evidence for ester hydrolysis one would not expect any decarboxylation, and the NMR spectra substantiate this claim. If decarboxylation were to occur, the resulting polymer would have a benzylic methine proton located α to an acid (or an ester) and on the same carbon as the alcohol. This proton would resonate at 5.0 to 5.2 ppm.⁴³ Thus, none of the spectral data suggest that alcoholysis, hydrolysis or decarboxylation occur. One other point to be mentioned here is that the alcohol proton in the modified polymers exhibits rather erratic behavior by NMR. Much of the time the absorbance is not seen, either because it is not being sampled (by the NMR) or because it is buried in the aliphatic protons. At times it has been observed as a shoulder on either side of the ester resonance (at 4.3 ppm). When deuterated benzene is used as the NMR solvent, polymers with high SF concentrations have the absorbance at 5 to 5.5 ppm. We are convinced that this is not the methine from the decarboxylation (mentioned above) because the peak is not present when CDCl_3 is used as the solvent. A survey of the appropriate NMR spectra in the Aldrich catalog reveals that other alcohol protons show the same erratic behavior.

A very important aspect of this modification is its inertness towards the *tert*-butylstyrene monomer units. This is most easily demonstrated in the NMR spectrum (Figure 3.13) of the DEOM control reaction with PtBS homopolymer. One can see that the absorbance at 4.3 ppm (attributed to the ester methylene protons of the modified polymers) is (almost) totally absent. The control reaction was run under a variety of conditions (Table 3.14 entries 29, 30 and 31; Table 3.15 entry 7) and in all cases, the

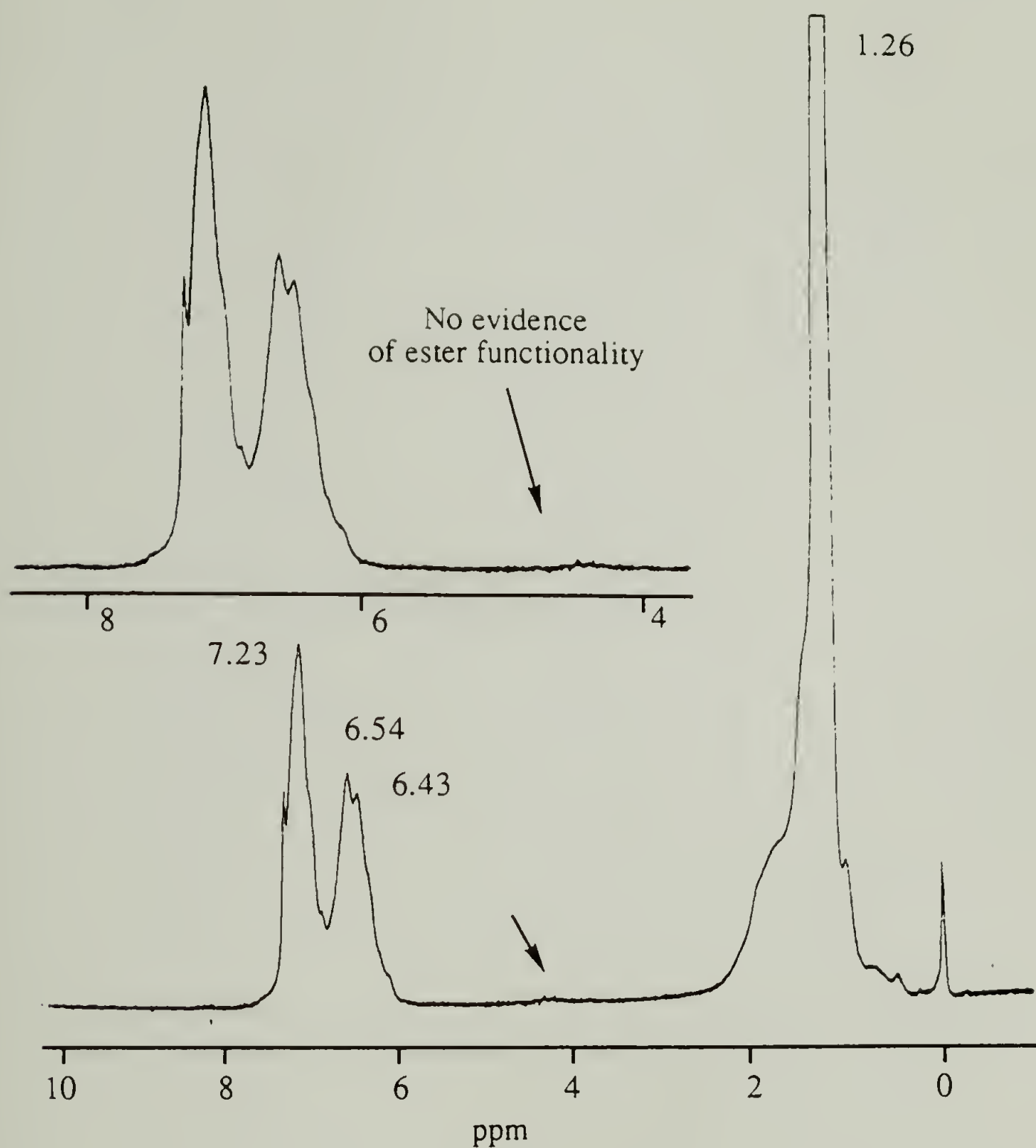


Figure 3.13 ^1H NMR spectrum of DEOM modification control reaction on PtBS (PtBS88M2). Shows negligible evidence of ester functionality at 4.25 ppm. (Solvent CDCl_3)

corresponding resonance was almost nonexistent, thus establishing that DEOM/SnCl₄ does not add to *tert*-butylstyrene units. In some cases, very small peaks that could be attributed to functionalization were detected, but it was not determined whether these were small amounts of modification or contamination from the starting material. Thin Layer Chromatography (TLC) is much more sensitive to slight modification than is NMR. TLC was performed on silica gel for PtBS before and after modification (PtBS88M1 entry 30 Table 3.15) using carbon tetrachloride as the eluent. The original polymer has $R_f = 0.75$ under these conditions, and the data for PtBS88M1 indicate that approximately half of the spot moved (with an $R_f = 0.75$) although the other half did not elute. Upon addition of 3.8 % (by volume) ethyl acetate as a displacer, the modified polymer eluted with an $R_f = 0.75$. We postulate that about one half of the polymer chains were functionalized by one DEOM molecule while the other half were not affected at all. We also postulate that this modification occurs on the chain end where termination by protonation of the benzylic carbanion leads to a relatively less hindered site for DEOM addition when compared to the rest of the PtBS chain. This suggestion is reasonable in light of the fact that the PtBS chain (used in this control) was relatively short (DP~ 60) therefore the chain-end modification would be noticeable. Thus we conclude that, for all extents and purposes, the *tert*-butyl styrene units are inert to the DEOM modification.

Another important quality of this modification system is the lack of detrimental effect it has on the molecular weight distribution of the polymer. Figure 3.14 shows the GPC data for three different polymers before and after exposure to DEOM modification conditions (note that the

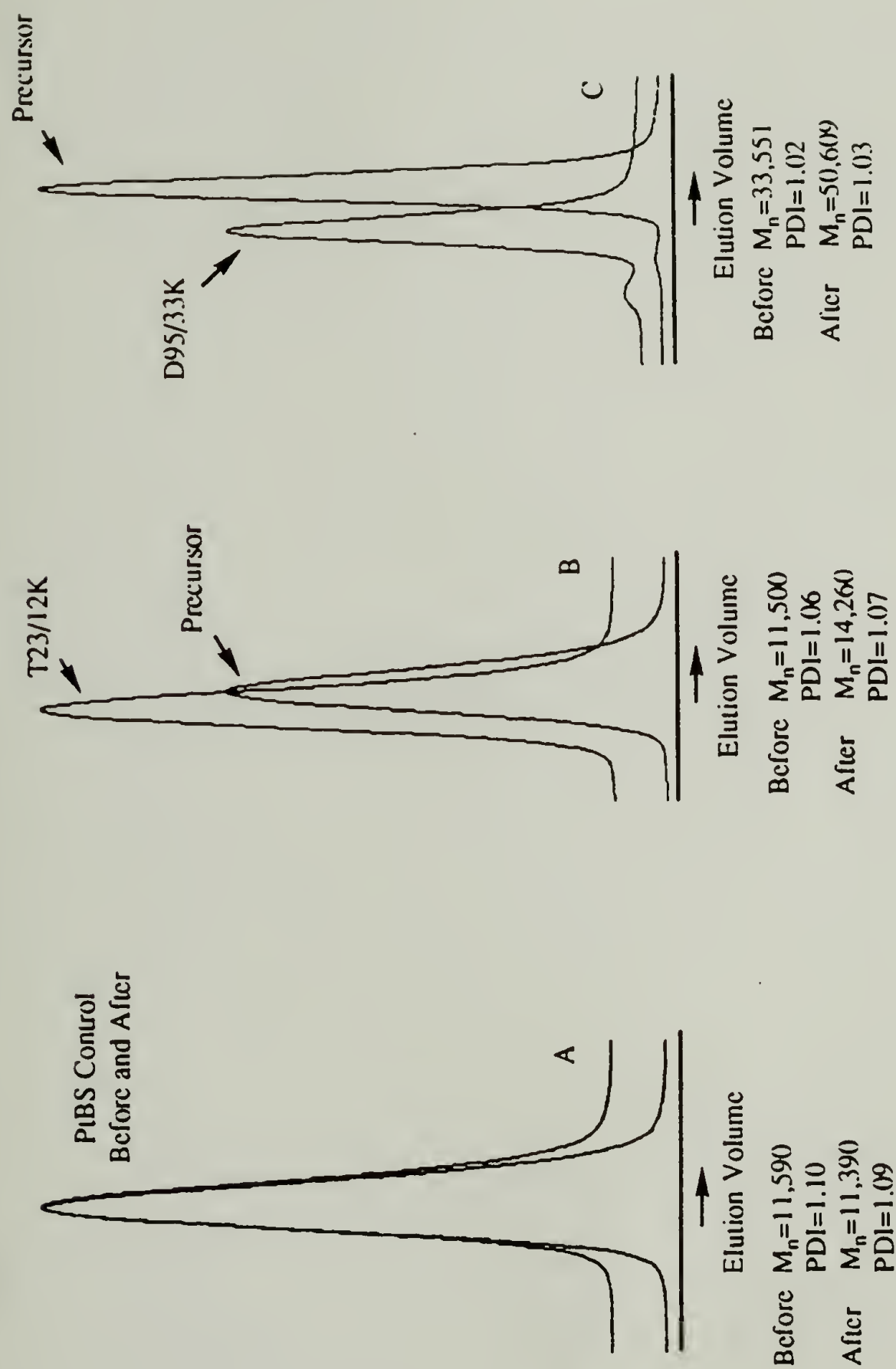


Figure 3.14 Size exclusion chromatograms of three different polymers after reaction with the DEOM system.

PtBS homopolymer control reaction shows no changes (A). A 23% styrene precursor reacts and the molecular weight increases but the MWD stays narrow (B). A 95% styrene copolymer increases more in molecular weight and the distribution stays narrow although a small amount of chain coupling is observed. (All molecular weights are measured against polystyrene standards.)

recorded molecular weights are versus PS standards). Figure 3.14(A) shows that the control reaction has no effect on the elution time of the PtBS homopolymer (i.e. both peaks coincide). This is yet another piece of evidence indicating the inertness of the PtBS blocks toward these reaction conditions. Figure 3.14(B) shows the chromatograms of a triblock copolymer with 23% styrene units (the same polymer as the preceding spectra were shown for). Here we see that the modification has resulted in a decreased elution time, suggesting a larger hydrodynamic coil size. This is reasonable considering that the molecular mass of the polymer chain has been increased by approximately 27%. Also note the narrow distributions (the polydispersity indices are 1.06 and 1.07) both before and after modification. The third chromatogram is for a highly modified precursor (modified polymer contains about 95% SF units). Again we observe narrow distributions indicating that even high SF content does not adversely affect the distribution. The elution time is shifted to lower values, and as expected, it has shifted more than that for the 23% copolymer. In this case, the molecular mass has been increased by approximately 144%. The GPC molecular weights (those tabulated in the figure) are lower than the calculated values, and this suggests that the modified polymer exists in a more collapsed state (i.e. a more dense coil), compared to the precursor molecule in THF. Close inspection of 3.14(C) reveals a small polymeric dimer (i.e. coupled polymer) in both chromatograms. The dimer present in the precursor is a result of either reductive coupling or coupling through reaction with carbon dioxide as has already been discussed in Chapter II and IV. The polymeric dimer in the modified polymer is somewhat larger, and so it must be attributed to something more than the precursor. The most probable explanation is

alcoholysis between the alcohol functionality and an ester group, which may happen slowly with aging of these polymers. This chromatogram was obtained more than one month after the polymers were synthesized. As will be seen, upon hydrolysis those linkages should be cleaved.

In conclusion we have shown that this modification reaction is selective towards styrene monomer units over *tert*-butylstyrene monomer units and also that the polymers prepared have narrow distributions both before and after modification. We can also control the amount of functionality randomly placed on a given styrene block by manipulation of reaction conditions. Thus we have good control over many aspects of polymer structure. Another very useful aspect of this modification is the ability to use subsequent chemical transformations to change the specific functionality of the polymer. The next section will be devoted to this aspect of the synthesis.

Transformations of the Hydroxy Diethylmalonate Moiety

The hydroxy diethylmalonate sticky foot is a versatile group from which a number of chemical transformations are possible; this results in new SF on the polymer chain. Figure 3.15 illustrates a number of possibilities along this vein. The main possibilities include hydrolysis of the esters to obtain the diacid or diacid salt.⁴¹ The base-catalyzed hydrolysis to obtain the diacid salt is illustrated in Figure 3.15(A). This reaction has been carried out and it results in water-soluble ionic blocks. The decarboxylation reaction (Figure 3.15(A₁)) should occur under acidic conditions at elevated temperatures to give the α -hydroxy monoacid functionality,⁴¹ but this has not been carried out at this point in time.

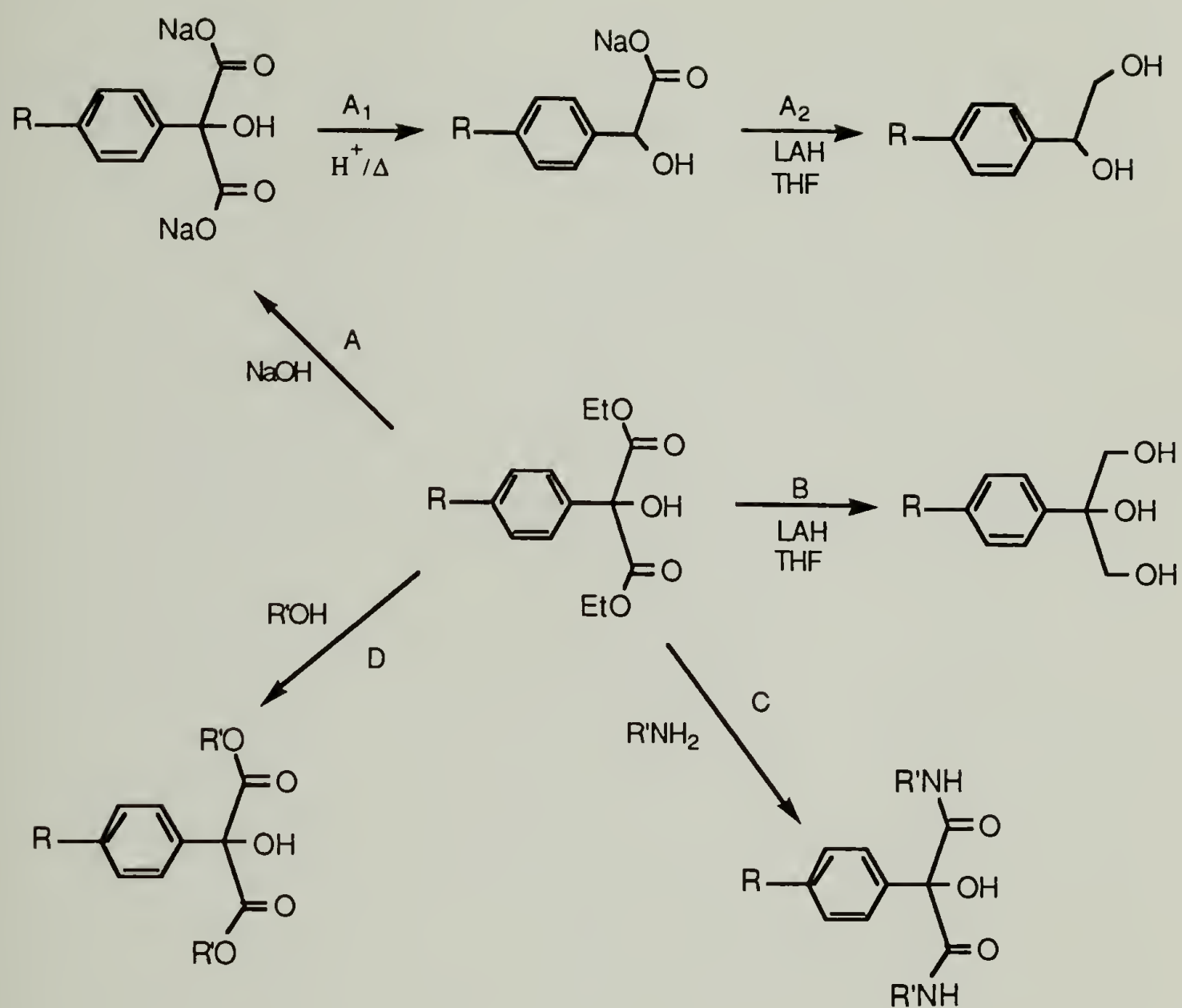
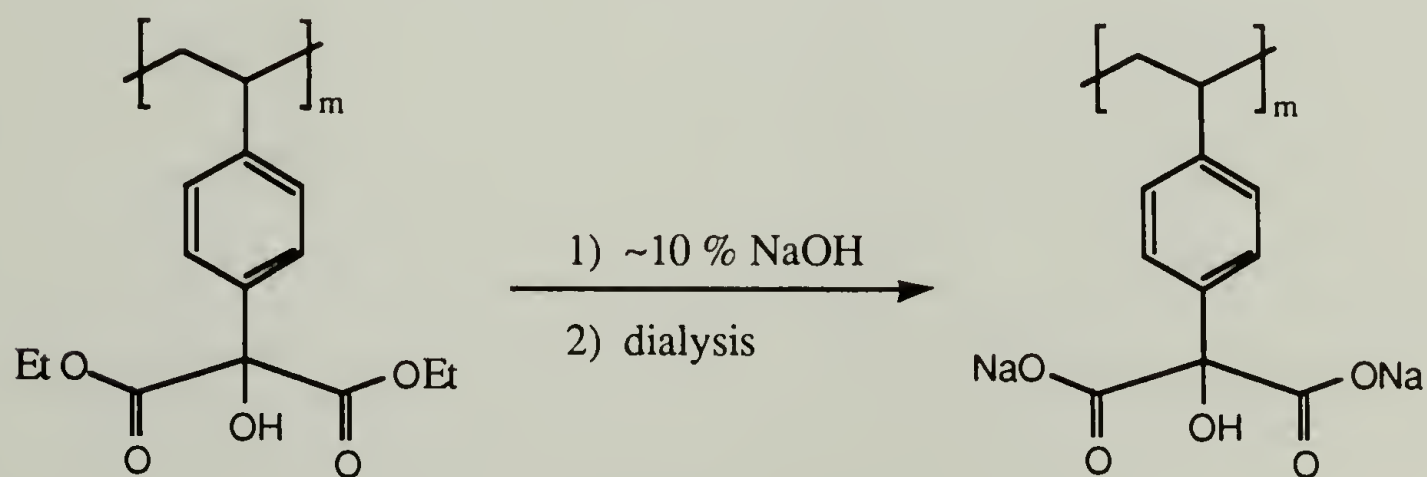


Figure 3.15 Subsequent transformations of the hydroxy diethylmalonate sticky foot.

Alcohol groups can be obtained by the reduction of the ester (for instance using LiAlH_4 or $\text{LiB}(\text{Et})_3\text{H}$)⁴⁴ or the acid (for instance using LiAlH_4 or B_2H_6)⁴⁴. Reduction of the hydroxy diethylmalonate group will lead to formation of the 1,2,3-triol structure illustrated in Figure 3.15(B). This reaction has been carried out with LiAlH_4 and the triol polymer isolated. If the reduction is carried out on the decarboxylated product the 1,2-diol structure will be obtained (Figure 3.15(A₂)). Conversion to a single alcohol group would lead to an interesting series of polymers with sticky feet of increasing strength (i.e. SF containing 1, 2 and 3 alcohol groups); this may be possible through hydrogenolysis of the benzylic alcohol. Replacement of the hydroxyl group in the hydroxy diethylmalonate can be accomplished by direct hydrogenolysis⁴⁵ or via conversion of the alcohol to halide or sulfonate with subsequent reduction of these groups.⁴⁶ The direct replacement of the hydroxyl can be accomplished by a number of reagents most notably Pd/H_2 (1-4 atm, RT)⁴⁷ these mild conditions will not effect the other functionality. This facile cleavage of the benzyl group is used in protection group chemistry, in particular of protection of amines via the carbobenzyloxy ($\text{PhCH}_2\text{O}(\text{CO})\text{NHR}$) group in polypeptide synthesis. Tertiary alcohols have also been reduced by treatment with $\text{TFA}/\text{Ph}_3\text{SiH}$, in this case the carbonium ion is formed by the acid and the hydride is transferred to it.⁴⁸ Tertiary alcohols have been reported to be reduced by hydrogenolysis when the catalyst is platinum bis(triphenylphosphine) dichloride.⁴⁹ Alumino- and borohydrides can be used to reduce both alkyl halides and tosylates, thus conversion of the alcohol to one of these could facilitate the reduction.⁴⁶ The hydrides are most often thought to react by an $\text{S}_\text{n}2$ mechanism. This work requires this displacement at a tertiary carbon, but this is quite activated due to the

electron withdrawing capacity of the ring and both esters. The following one pot procedure has been reported to convert a -OH to a -H: The substrate is treated with pyridine/SO₃ complex to form the sulfate followed by reduction with LiAlH₄. The greatest versatility exists in the possibility of reacting the esters with different alcohols or amines (Figure 3.15(C) &(D)). This would allow incorporation of numerous functional groups via reaction of difunctional molecules. The danger of forming crosslinks (via reaction with the tertiary alcohol on the chain) under these conditions is rather slim due the hindered nature of the alcohol. Any complications could be circumvented by hydrogenolysis of the alcohol before modification, protection via sulfate formation, or through use of amines which are the thermodynamic winner in a war with alcohols. These last types of transformations, alcoholysis and aminolysis, were not studied in this thesis.

The hydroxymalonate esters were easily hydrolyzed using 10% aqueous NaOH to yield the corresponding diacid salt (see Scheme 3.15).



Scheme 3.15 Hydroxy Diethylmalonate Hydrolysis.

The hydrolysis was carried out on four different polymer samples. Hydrolysis of modified polystyrene homopolymer (PSM2, Table 3.15, entry 27) with a SF content of 95% was carried out on two separate occasions, with similar results both times. The polymer powder was put in a 10% aqueous NaOH solution and stirred for approximately 5 to 10 minutes without much visual change. The solution was then heated in warm tap water (about 45 °C) and almost immediately it changed from a white slurry to a hazy solution with almost no solids remaining. This was stirred for an additional 20 minutes and then dialyzed and lyophilized. A nice white powder was isolated which dissolved easily in water to form a perfectly clear solution. Figure 3.16 shows the proton NMR spectrum of the modified, hydrolyzed polystyrene sample in D₂O (the large peak at 4.6 ppm corresponds to protonated D₂O). One can see that the methylene resonance at 4.3 ppm, indicative of the ester, is absent from this spectrum, suggesting that total hydrolysis of the esters was accomplished. The absence of the methine proton ($-\text{CH}\text{CO}_2\text{Na}$) at about 5.1 ppm is used as evidence that the material has not decarboxylated.⁴¹ The IR spectrum of this polymer also confirms the structure (the peaks at 1622, 1411, 1327 and 1095 cm⁻¹ correspond to the acid salt). Modified block copolymers with 5% *tert*-butyl units (D95/33k, Table 3.15 entry 25) and 10% *tert*-butyl units (D90/13k, Table 3.15 entry 24) were also hydrolyzed. The D95 contains 91% SF and the D90 contains 88% SF. The same general hydrolysis procedure was applied to these as was used for PSM2 above. The polymer powders were added to a 10% aqueous NaOH solution and heated to 50 °C with stirring. It was expected that they would soon dissolve as did the PSM2, but this did not happen. The polymer solid changed form somewhat and looked like it was partially dissolving, but

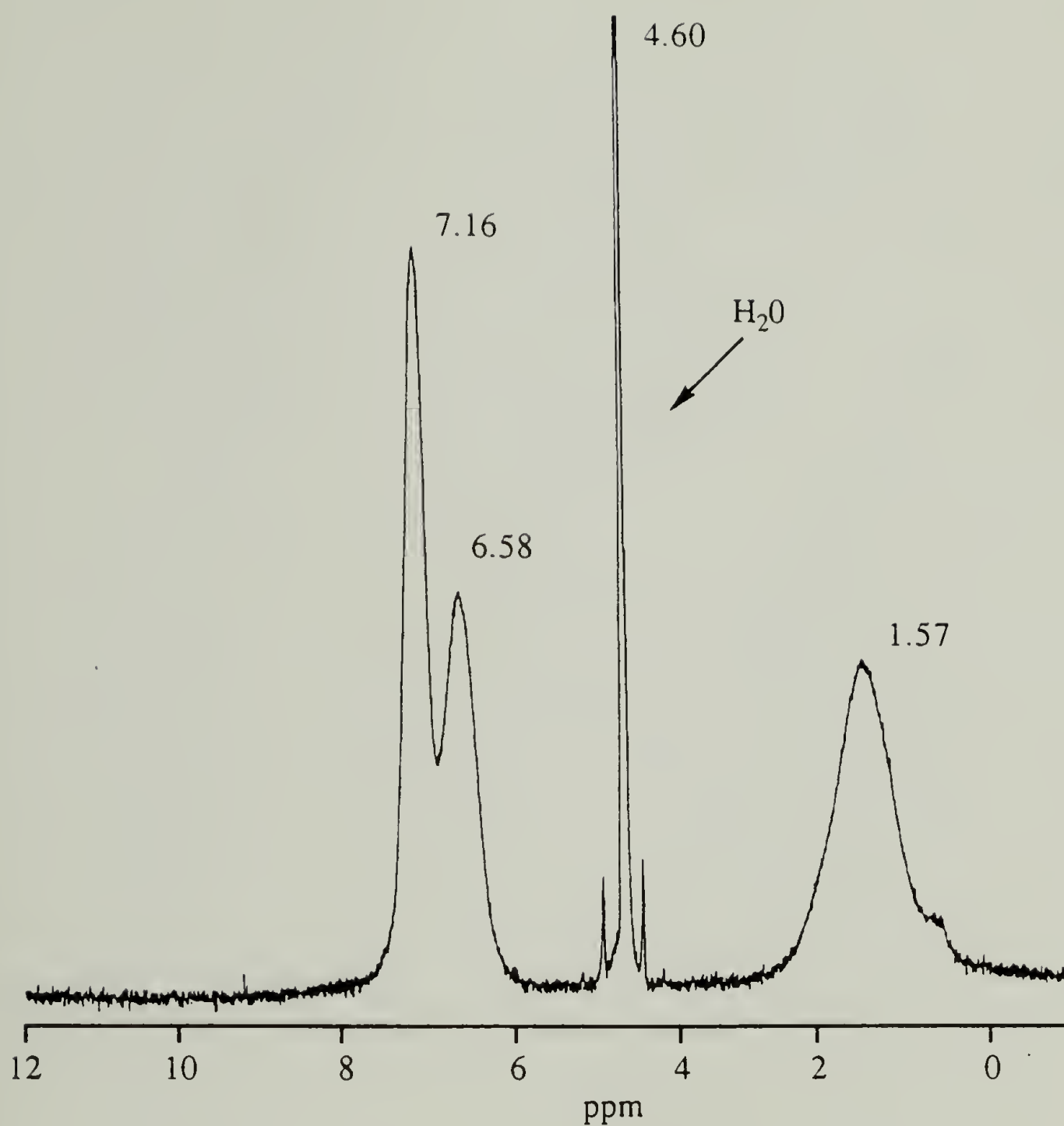


Figure 3.16 ^1H NMR spectrum of hydrolyzed PSM2 in D_2O . The ester peaks centered at 4.25 ppm have disappeared and one sees only the aromatic (7.16 and 6.58 ppm) and aliphatic resonances (1.57 ppm) (the peak at 4.60 ppm is due to protonated D_2O).

total dissolution of the copolymers was not realized immediately. After 2 hours (at 60 °C) the solutions were not clear (lots of solids present). The solutions were allowed to cool and more solids formed, and the liquid was decanted off and dialyzed. Water was added to the solid precipitate and upon stirring it dissolved, and this was dialyzed as well. There were minor differences between the D95 and the D90 (with the D95 acting more like the PSM2) but both pretty much acted the same. After dialysis and lyophilization, the polymer was obtained from both the decanted and the precipitated fractions. More D95 was obtained from the decanted part (i.e. more D95 was in solution during the hydrolysis). The polymers were isolated as nice white solids that dissolved in water to give clear to very slightly hazy solutions ("blue haze"). The solutions were extremely viscous and formed transient gels upon sitting. This high viscosity for such small polymers (DPs of around 150 and 300) is interesting and is probably due to hydrophobic association of the hydrophobic blocks, creating a much larger structure than that of a single chain. Proton NMR was run on these copolymers in D₂O and spectra similar to the one in Figure 3.16 were obtained. There was no evidence of ester functionality. The spectra were not as nice (in terms of the baseline, etc.), due to the viscosity of the solutions, and thus the PSM2 data are shown here. Figure 3.17 shows the IR spectrum of D95, and one can see the absorbances due to the acid salt at 1622, 1411, 1327 and 1095 cm⁻¹; note the absence of those peaks associated with the ester. The hydrolysis was also carried out with an 80% random copolymer (R80/184, Table 3.15, entry 23) (note that in this case the initial modification was incomplete, resulting in only a 51% SF). The reaction was carried out in a manner similar to the ones described above. Its behavior was similar to the other copolymers in that the solids would not

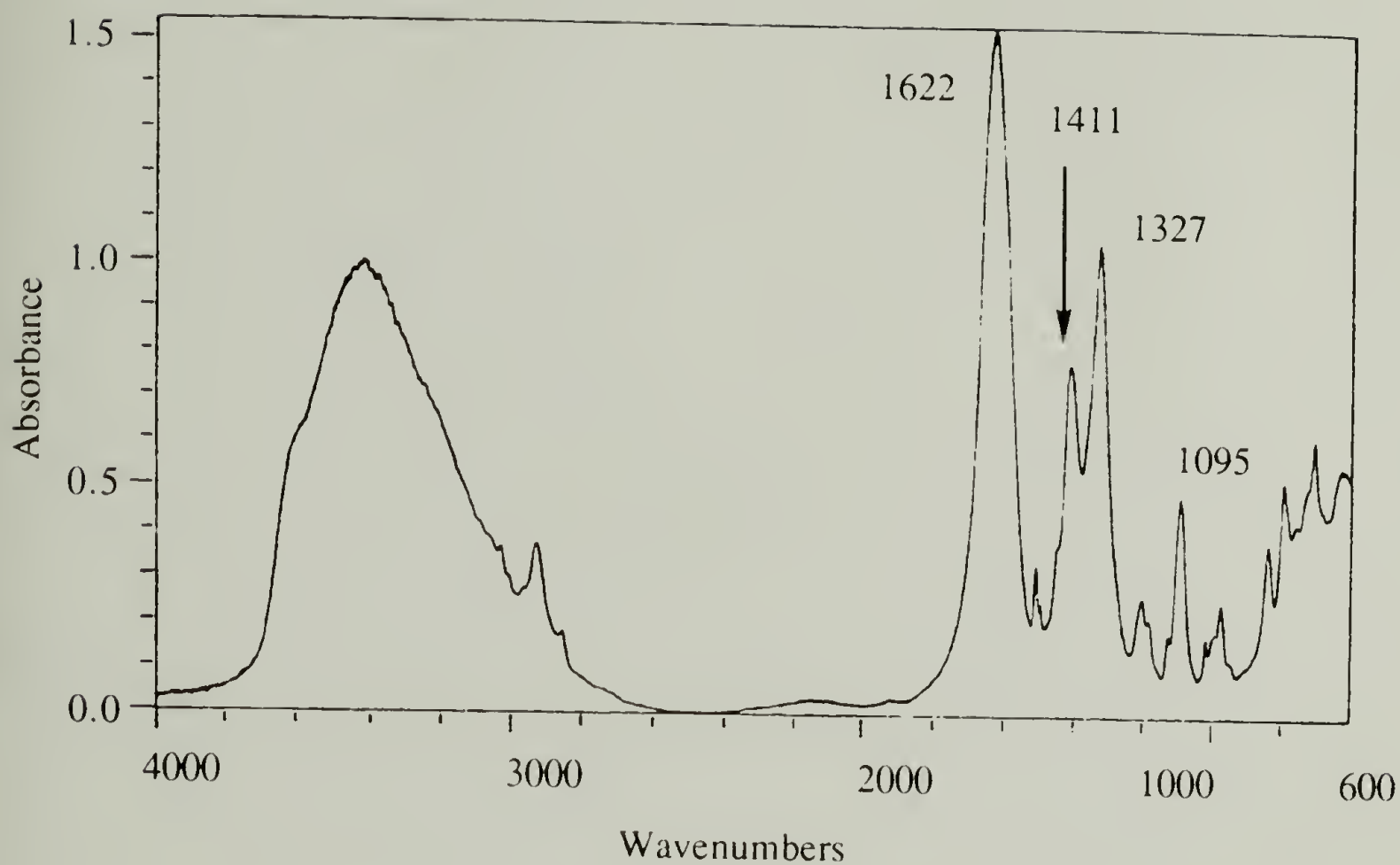
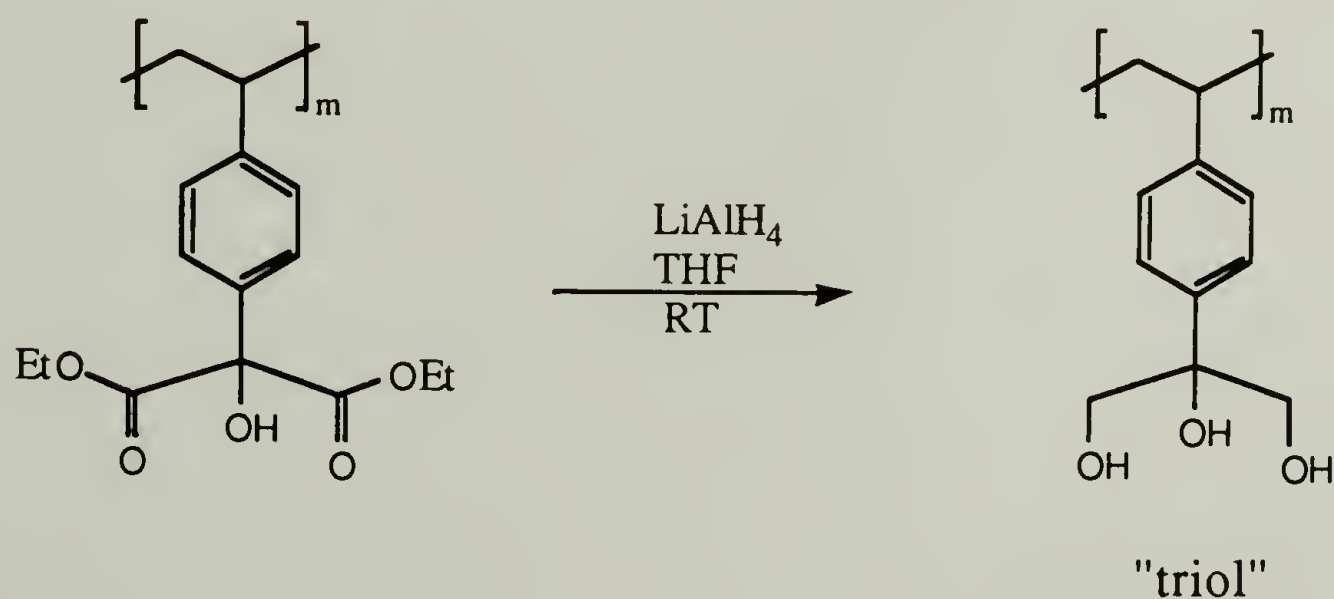


Figure 3.17 IR spectrum of a 95% SF hydrolyzed copolymer (D95/33K). The ester carbonyl stretch at 1740 cm^{-1} has disappeared and a stretch due to the acid salt is now seen at 1622 cm^{-1} . The large hydroxyl stretch is due to the alcohol and adsorbed water.

totally dissolve. Eventual dissolution was accomplished by addition of THF and methanol to the reaction mixture, and this resulted in an almost clear, blue hazy transient gel. It was thought that the need for THF may be a kinetic one (i.e. it dissolved the *tert*-butyl block enough to allow the base access to the ester groups, thus facilitating reaction and dissolution). To test this hypothesis, the polymers (in water/THF) were dialyzed against water, removing the THF. The polymers precipitated eventually, suggesting that the THF was more than just a dissolution catalyst. The dialyzed and lyophilized polymer was isolated as a nice white powder which was insoluble in water, but dissolved when THF was added. The IR spectrum of the polymer showed almost complete hydrolysis (the other polymers were totally hydrolyzed). It is possible that the extent of hydrolysis is a function of the random architecture (i.e. there may be esters buried in hydrophobic blocks too large to be accessed by the base). We also see that incorporation of water-soluble groups to only 50% of the polymer units is not enough to impart water solubility, whereas those polymers with more than 85% are water-soluble. The composition needed for water solubility is not known at this time, although it is expected to be a function of molecular weight and chain architecture. The investigation of this and related phenomena (such as cmc) are examples of future uses for these polymers. We postulate that differences observed for the hydrolysis behavior of the copolymers versus those of the homopolymer are related to both the decreased water-soluble functionalization and the increased hydrophobicity caused by the *tert*-butyl groups. It is thought that the solid polymer present in the hydrolysis mixture is actually hydrolyzed, but the high ionic strength of the NaOH solution (much higher than that of water) causes the hydrophobic groups to precipitate out of solution. It should be

noted that it may turn out to be more efficient to hydrolyze the copolymers by dissolving them in a water-miscible solvent (such as THF) and adding the polymer solution to the base in this fashion because one can greatly increase the effective interfacial surface area. To this end, addition of a phase transfer catalyst or a decrease in the base concentration may also facilitate the hydrolysis. Preparation of small percentages of ionic groups could be accomplished in an organic solvent with a phase transfer catalyst. This was accomplished to an extent, by dissolving R80/184 in THF and adding tetrabutylammonium hydroxide. Upon addition, a white precipitate formed immediately. Apparently, the hydrolysis is very rapid under these conditions. This could also be used to hydrolyze the types of polymers discussed above.

The hydroxy diethylmalonate moiety can be reduced with LiAlH_4 to obtain the 1,2,3-triol, as shown below. The IR spectrum (Figure 3.18) of the reduced 23 % SF polymer (D23/13k DM4) shows that almost all of the



Scheme 3.16 Reduction of the Sticky Foot to the Triol.

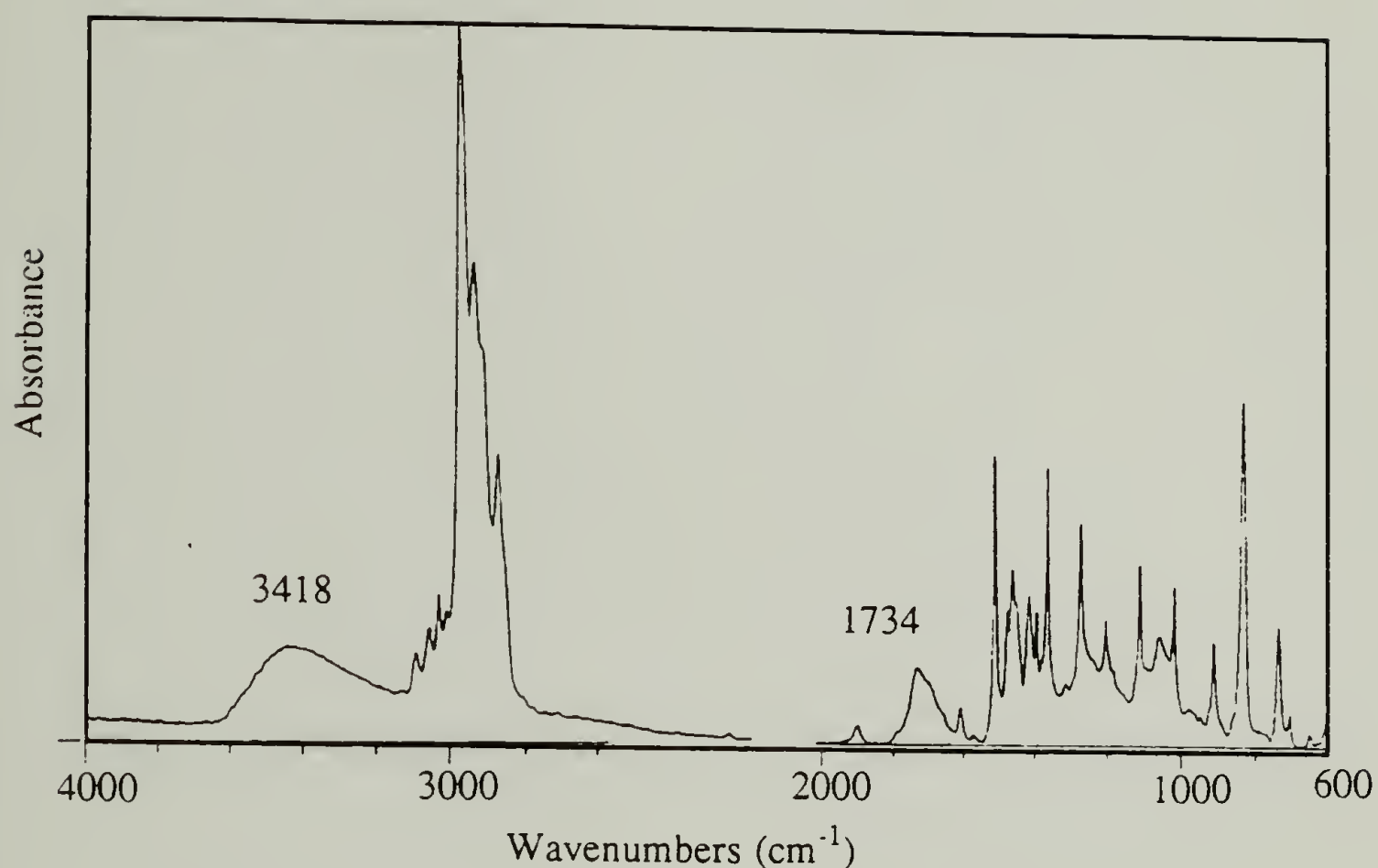


Figure 3.18 IR spectrum of 23% SF copolymer (D23/13K DM4) after reduction to the triol with LiAlH_4 . The carbonyl stretch at 1734 cm^{-1} is almost totally absent and the hydroxyl stretch at 3418 cm^{-1} is larger and broader because of the triol.

ester carbonyl stretching is eliminated and that the hydroxyl stretch has become bigger and broader (probably due to increased hydrogen bonding in the triol). The reduction was carried out with LiAlH_4 because this reagent reduces both acids and esters (the workup resulted in a small amount of acid in this sample). The polymer adsorbed to the aluminum solids present after the workup and acid (dil HCl) was needed to isolate the polymer. The use of $\text{LiB}(\text{Et})_3\text{H}$ would facilitate the workup because no solid surfaces would be available. The triol is a much stickier foot as was ascertained by TLC (THF would not elute the 23 % triol).

In conclusion, we have demonstrated that the polymer system developed in our work enables us to prepare polymer chains of desired molecular weights and with narrow molecular weight distributions. We have demonstrated control over the block architecture by the synthesis of diblock, triblock and random copolymers; the extension to other block structures is straightforward and requires no new procedures. We have demonstrated that the styrene units in these block copolymers can be selectively functionalized by reaction with DEOM to produce chains containing specific functionality. Conversion of the styrene units on the polymer can be controlled with reaction time and reagent concentration, allowing control over the extent of (random) modification. This allows us to control the overall interaction energy without significantly affecting the block size. Subsequent conversion of the hydroxy diethylmalonate to different chemical species has been discussed as a means of preparing polymers of different SF strengths. The hydrolysis reaction allows a means of preparing hydrophobically associating water-soluble polymers of controlled architecture.

Adsorption Results: Introduction

The chemistry developed in this thesis work and presented in the last section can be used to prepare SF polymers of controlled composition, architecture and molecular weight. This section involves the investigation of the adsorption characteristics of those polymers. The situation developed here is rather unique because we have the ability to tailor the polymer structure to address questions that develop during physical experiments. This has been done to some extent here, but the preliminary nature of this work and the time required to develop this system precluded any major effort in this regard. Future investigations will, however, be enhanced by the synthetic techniques developed.

Although a multitude of block architectures can be prepared, our discussion will focus on the adsorption experiments carried out with only two of these structures. We investigated the effect of chain architecture on the adsorption of diblock copolymers and triblock copolymers (where the anchoring blocks were located at the ends of the chain). Diblock copolymers will adsorb to form a polymer brush layer consisting of "tails" and triblocks will form a layer of "loops". These are two fundamentally different surface structures which should result in different layer thicknesses, amounts adsorbed and physical behavior. It will be shown that, indeed, the architecture affects the adsorption characteristics of the polymers. Secondly, we investigate the effect of the SF composition on the amount of polymer adsorbed. Theoretical predictions⁵⁰⁻⁵⁵ and experimental data⁵⁶⁻⁶⁰ pertaining to this problem have been reported by various authors. We found, as expected, that the amount adsorbed is very dependent on the chain composition. The effect of the chain architecture

was also found to be dependent on the SF composition of the polymer. These investigations were facilitated by the preparation of a series of copolymer pairs (diblock and triblock copolymers with the same molecular weight and SF composition) which allowed the effect of the chain architecture to be studied independently. Table 3.15 lists the polymers that were prepared; in particular the $M_n \sim 50K$ series is important. This series contains four diblock copolymers ($M_n \sim 50K$) with 5%, 12%, 23% and 40% SF content (Table 3.15, entries 1, 3, 18 and 20) and the corresponding triblock copolymers (Table 3.15, entries 2, 4, 19 and 21) with the same compositions. The 23% SF ($M_n = 13K$) diblock/triblock pairs were also used extensively (Table 3.15, entries 8-11 and 14-17).

Measurement of the Adsorption

There are many different ways to measure the adsorption: we can measure amount adsorbed, layer thickness, density profile, etc. The amount adsorbed has classically been measured by a depletion method where one adsorbs polymer to a high surface area solid and then separates the solid from the solution and measures the change in the concentration of the solution.⁶⁰⁻⁶² Liquid scintillation counting of adsorbed radiolabeled polymers has also been used to determine the amount of polymer on the surface.⁶³ The sensitivity of this technique allows low specific area solids to be used. These two techniques require very little reliance on data manipulation. Angle resolved XPS spectroscopy has been used to determine the amount of polymer adsorbed on flat surfaces (the absolute value of which depends on the value of the mean free path one uses etc.).⁶⁴ A number of techniques utilizing various radiations have been developed which allow the amount of polymer adsorbed to be measured in solution.

Ellipsometry has been used and this method can give the amount of polymer adsorbed as well as the solvent swelled layer thickness.^{62,65} ATR IR spectroscopy has recently been used as a simple technique to measure the amount of adsorbed polymer in situ.^{66,67} Gast and coworkers have used dynamic scanning angle reflectometry⁶⁸ and internal reflection interferometry⁶⁹ to measure the amount of PS/PVP copolymers adsorbed from cyclopentane. Surface plasmon,⁷⁰ electrokinetic⁷¹ and hydrodynamic⁷² measurements have also been used to measure the amount adsorbed. Photon correlation spectroscopy has been used to measure the hydrodynamic thickness of the adsorbed layer.⁷³ This requires that the polymer be adsorbed to colloidal spheres with a very narrow size distribution, which are usually only attainable in aqueous media. The thickness of the adsorbed layer can be measured via a surface forces apparatus^{74,75,76} where polymer is adsorbed to two plates and the plates are brought close together and the (repulsive) force is measured. The repulsive force increases when the plates come within two layer thicknesses of each other. These experiments are useful and they have helped elucidate the relationship between polymer molecular weight, graft density and layer thickness. They also give insight into such phenomena as colloid stabilization. Other researchers have used neutron reflectivity to study the segment density profile for adsorbed homopolymers and block copolymers.^{77,78} The polymers that were prepared in this work were expected to adsorb with different layer thicknesses and thus the layer thickness is very interesting to us. The equipment needed to measure this thickness was not available and thus it was left hopefully for some collaboration. Our intention was to measure the amount adsorbed as accurately and easily as possible. It was thought, rather naively, that the

easiest, most straightforward method of measurement was the depletion method. We found that this is not as straightforward as one might expect when using block copolymers because of the added stability that they can impart to colloidal systems. Our two main objectives in the work reported here were to measure the effects of chain architecture and composition on the adsorbance and to develop a standard method for the measurement of the amount adsorbed. In this vein a number of different methods were used to obtain the data reported here, all of which are based on the depletion method principle. It seems, in retrospect, that this may not have been the best choice and something like solution cell ATR IR may have been a more judicious choice.

Thin Layer Chromatography Results

Thin layer chromatography (TLC) of the polymers gave useful insight into some aspects of their adsorption behavior. The TLC experiment consists of the following procedures. An adsorbent (in this case silica) is deposited as a thin layer ($\sim 250\ \mu\text{m}$) on a glass or plastic plate. The polymer is "spotted" on the bottom of the plate by applying a small volume of solution ($\sim 10\ \text{mg/mL}$, $5\ \mu\text{g}$ total spot) to make a tight spot. The solvent is allowed to evaporate leaving just the polymer on the plate. The plate is placed in a container (which contains some solvent) so that the solvent only comes into contact with the very bottom of the plate (not the spots). Capillary action drives the solvent up the plate. The distance the solute travels up the plate (i.e. is eluted by the solvent) depends on the adsorption/desorption equilibrium. The time spent desorbed results in elution while the time spent adsorbed results in no movement. The ratio of

the distance the spot traveled to the total distance traveled by the solvent front is called the R_f (Equation 3.3) and is a measure of this equilibrium.

$$R_f = \text{distance solute travels} / \text{distance solvent travels} \quad 3.3$$

An R_f of 0.25 means that the molecule is desorbed approximately 1 quarter of the time. This adsorption/desorption equilibria depends on the solvent; strong eluting solvents interact strongly with the surface and displace the adsorbed solute molecules. Thus the stronger solvents result in higher R_f values. The relative strengths of solvents as displacers are listed as a eluotropic series. Solvents interact with silica in the following (in order of increasing interaction) way: cyclohexane, heptane, pentane, CCl_4 , ethyl benzene, toluene, benzene, CHCl_3 , diethyl ether, ethyl acetate, ethanol, water, acetone, methanol.⁷⁹ Cyclohexane interacts least with surface while methanol interacts the most. TLC behavior is a good indication of whether a polymer will adsorb from a given solvent: if $R_f=0$ the polymer will adsorb, but if R_f is not equal to zero the polymer may adsorb but not to a great extent.⁸⁰ Preliminary tests of D23/13K precursor and modified polymer (D23/13k DM1; Table 3.15) along with *para-n*-propyl(hydroxy diethylmalonato)benzene as the monomeric analog of the sticky foot (i.e. SF_1) were carried out in a number of solvents on silica (B18-51). The results are given in Table 3.16. The unmodified polymer eluted in every tried solvent except cyclohexane and CCl_4 . These are the weakest eluting solvents and it is not surprising that the styrene phenyl ring interacts more strongly with silica than either CCl_4 or cyclohexane (the phenyl ring is more polarizable). This can also be seen by the fact that the benzene,

toluene and ethyl benzene are all stronger eluting solvents than CCl₄ or cyclohexane. In the case of cyclohexane there is also a contribution due to solvency which makes the polymer stick (i.e. at room temperature cyclohexane is a poor solvent for PS). It should be noted that even though the polymer-surface interaction and toluene-surface interaction should be relatively close (but still unfavorable-see the order of the ethyl benzene, toluene and benzene in the eluotropic series), this small energy difference and the high concentration of toluene

Table 3.16 Precursor, Modified Polymer and Model Compound:
R_f Values on Silica.

<u>Solvent</u>	<u>Precursor Polymer</u>	<u>SF Polymer</u>	<u>Model Compound</u>
Cyclohexane	0.00	0.00	0.00
CCl ₄	0.00	0.00	0.00
Toluene	0.96	0.00	0.00
DCE	0.86	0.00	0.30
CH ₂ Cl ₂	0.92	0.00	0.24
Ethyl Acetate	0.92	0.90	0.65
THF	0.90	0.88	0.75

molecules compared to styrene units is enough to allow it to elute. The SF polymer, on the other hand, has an R_f of zero in every solvent except the two strongest displacers: ethyl acetate and THF (THF was not reported in the series but one can imagine that it would be a better displacer than diethyl ether). This demonstrates the SF nature of the hydroxy diethylmalonate group on silica. Note the tendency of the polymers samples to have R_f values of either 0 or close to 1 (i.e. there are no intermediate R_f values). This results from the cooperativity of the SF due their connectivity. This has been anticipated and observed experimentally by

Cohen Stuart⁸¹⁻⁸³ This cooperativity is also demonstrated by comparison of the SF polymer behavior (approximately [SF]₂₀) with that of the model compound ([SF]₁). The model compound (lone sticky foot) elutes with an R_f of 0.25-0.3 in DCE and methylene chloride, whereas the polymer does not elute at all under the same conditions ($R_f=0.0$). We can see that although the equilibrium desorbed residence times are comparable for the SF on the polymer and the SF model compound (it may be that the chain induces a somewhat different residence time because of effective concentration effects and surface availability), the small molecule moves and the polymer does not. The equilibrium constant is not large enough to ensure that all 20 SF are desorbed at the same time (the requirement for the chain to move). Thus we see that the cooperativity increases the "sticking power" of the polymer chain. This effect can also be seen in the strong displacer data where the polymers have eluted with higher R_f values than the model compound. Here the cooperativity shows up as evidence of a depletion layer where the coil is now repelled from the surface, and its residence time in solution is greater than that of the small molecule. It should be mentioned that there may be some molecular sieving effects contributing to this phenomenon as well.

The elution power of a solvent for TLC experiments can be increased by adding a stronger interacting molecule to the solvent. Small molecule chemists have used mixed solvent systems for a long time: in general a change in the solvent strength will result in a change in the R_f value (smoothly from 0 to 1) for a small molecule eluent. Cohen Stuart⁸¹⁻⁸³ et. al. have applied mixed solvent systems to the study of polymer adsorption and have termed the additive the "displacer". They report a

method for measuring the segment-surface interaction parameter, χ_s , for a given polymer. The method involves adding a displacer molecule to the solvent and measuring the concentration at which the polymer is desorbed (critical displacer concentration, ϕ_{cr}) and elutes with a R_f of approximately 1.0. Their derivation assumes that, at ϕ_{cr} the polymer is only barely adsorbed (i.e. moving on the plate); the segment concentration is only perturbed in the layer directly in contact with the surface. An energy balance then leads to a relatively simple relation between $\chi_{s^{po}}$ (polymer/solvent), $\chi_{s^{do}}$ (displacer/solvent), the critical displacer concentration (ϕ_{cr}) and the solution χ parameters. Assuming athermal conditions (all solution $\chi=0$) simplifies the expression to that given in Equation 3.4.

$$\chi_{s^{po}} - \chi_{sc} = \chi_{s^{do}} + \ln(\phi_{cr}) \quad 3.4$$

One can see from the equation that better displacers yield lower critical displacer concentrations as we would expect. Four sets of experiments (i.e. determination of ϕ_{cr} with two solvents and two displacers) allows one to calculate the corresponding four surface interaction parameters. Cohen Stuart et. al. note a very rapid transition from an R_f of 0 to full elution and attribute it to the connectivity of the chain. It is worth noting that the molecular weight of the sample does not affect the critical displacer concentration as long as the number of segments is high. Presumably after a certain chain size is reached a decreasing percentage of the segments can interact with the surface at any one time (due to geometric constraints). No molecular weight effect was seen for polymers of 100K and 500K.⁸³

We have carried out displacer studies on the SF polymers to determine whether chain structure or composition has an effect on the critical displacer concentration and thus on the effective surface interaction parameter. The displacer studies were carried out with four different solvent/displacer combinations: CCl₄/ethyl acetate, DCE/ethyl acetate, DCE/THF and DCE/isopropanol (Figures 3.19 through 3.22). In each case the SF polymer is immobile in the solvent (100% DCE or CCl₄) but upon addition of a given amount of displacer the polymer elutes. It was found that typically a given polymer spot has R_f of zero and then it smears out and becomes very streaked as the displacer concentration is increased. At this point it is very difficult to accurately determine the R_f value. With increasing displacer concentration, ϕ_d , the spot begins to tighten up again and finally (at high enough ϕ_d) it is again seen as a fairly tight spot with an R_f close to 1.0. The R_f values did not always reach 1.0; this is attributed to a number of effects including molecular sieving, solvent demixing and evaporation during elution.

Carbon tetrachloride was used as an elution solvent on silica with ethyl acetate as the displacer (Figure 3.19) and the TLC data of a total of ten polymers and the *n*-propyl(hydroxy diethymalonato)benzene model compound were investigated. Three polystyrene homopolymer samples (M_n =7.5K, 40K and 196K), homopolymer PtBS, a PtBS DEOM control reaction (PtBS88M1) and two unmodified precursor polymers (D23/13k-p and T23/12k-p) were run. Three modified polymers were also run

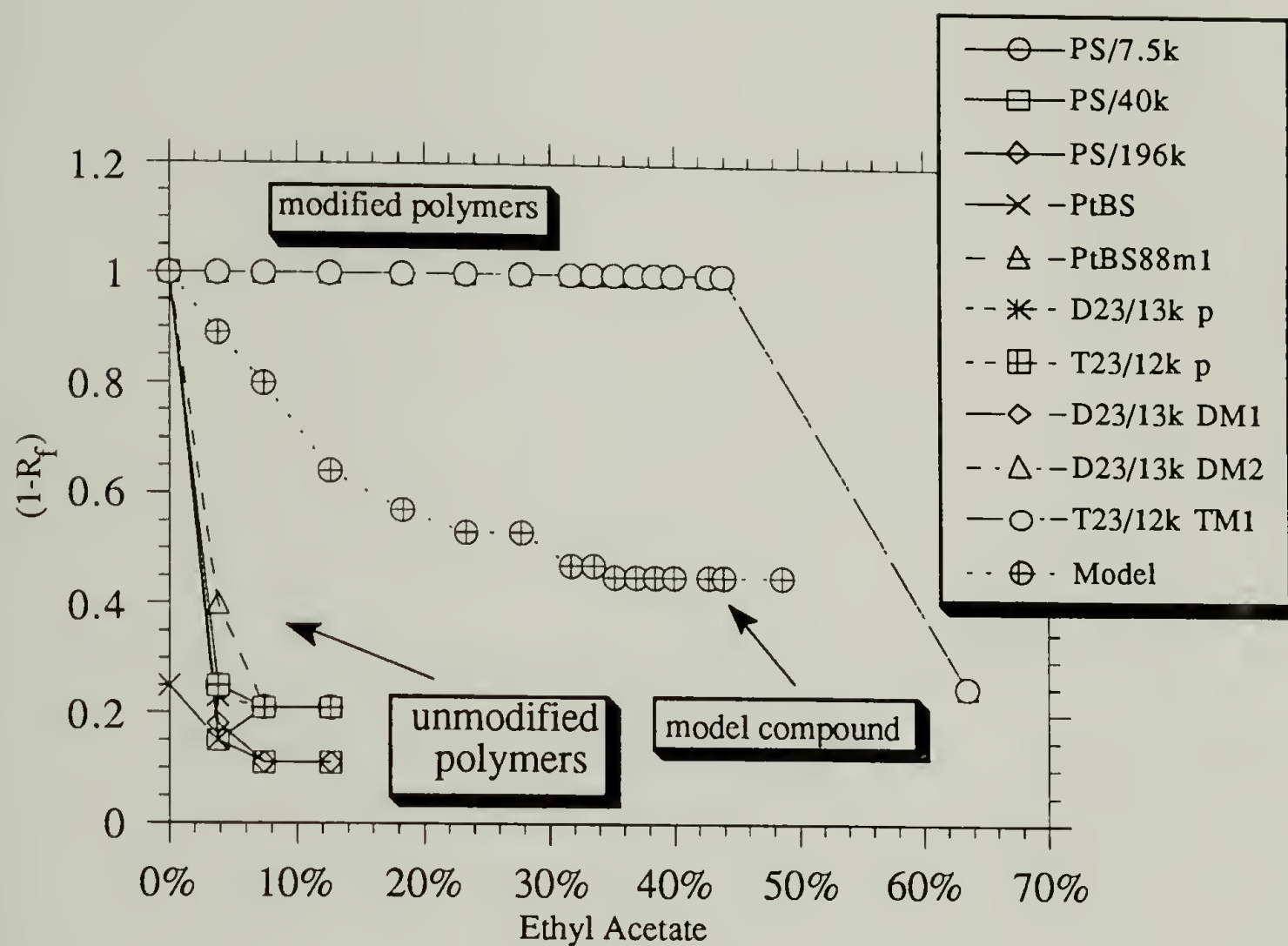


Figure 3.19 TLC displacer data for modified and precursor polymers on silica (eluent CCl_4 , displacer ethyl acetate). The modified polymes are 23% SF with $M_n = 13 \text{ K}$.

(D23/13k DM1, D23/13k DM2 and T23/13k TM1, Table 3.15). The only spot to fully move in 100% CCl₄ was the PtBS homopolymer ($R_f=0.75$); all of the other samples (including PtBS88M1)⁸⁴ had an R_f of 0. The styrene monomer units act as SF in CCl₄ (PS $R_f=0.0$) whereas the *tert*-butyl styrene units do not adsorb. The two precursor copolymers (23% styrene) are SF polymers under these conditions and were seen as very streaked and diffuse spots that were smeared through a large R_f range (in CCl₄). This is sticky foot polymer adsorption behavior; PtBS is the buoy and the styrene units are the anchors. This shows the effect of solvent quality on the behavior of the system. At a volume fraction of 0.038 ethyl acetate all of the unmodified polymers have R_f values of close to 1.0 and can be considered to be totally displaced. This shows how weak the styrene/silica interaction is. It also should be pointed out that the displacer concentration was not a function of molecular weight for the three PS samples (this agrees with the results of Cohen Stuart^{81,82} and van der Beek⁸³). Molecular sieving was also observed in these experiments: the two polystyrene samples with molecular weights of 40K and 196K have R_f values of 0.89 as compared to the other polymers ($M_n \sim 15K$) with an R_f value of approximately 0.79. The smaller polymers, it seems, have more possible pores to elute through.

Figure 3.19 shows a plot of $1-R_f$ (i.e. a value of 1.0 means the polymer did not elute) versus % displacer and one can see that all of the unmodified polymers have been displaced by about 7% ethyl acetate (EA). Increasing the displacer concentration steadily increased the R_f of the SF₁ (model sticky foot) from 0 to its plateau value of ~ 0.55 (at a volume fraction of 0.35, and after this the R_f stayed constant at least to a volume

fraction of 0.5) whereas a volume fraction of 0.63 was required to displace the modified polymers. The modified polymer spots began to streak at about 48% EA and finally tightened up with an R_f value of 0.79 at 63% ethyl acetate. One of the questions we were attempting to answer is whether the architecture of the sticky blocks on the polymer chain have an effect on the adsorption/desorption equilibria observed via these TLC experiments. We have seen that attaching a string of about 20 SF together really affects the adsorption/desorption behavior of the molecule by comparing the SF₁ to the SF polymer. The model sticky foot begins to elute at 3.8% displacer whereas the polymer does not start until somewhere between 48-62%. Elution of the polymer chain necessitates that all 20 sticky feet desorb at the same time (cooperativity between the SF on the chain). A higher displacer concentration and a higher individual desorbed fraction are required to accomplish this. It was thought that this cooperativity might be affected by sticky foot placement (i.e. the diblock would be a little stickier than the triblock because the triblock has two short blocks as opposed to one long one). With this in mind we ran 15 different TLC plates (at different solvent composition) from 49% to 63% ethyl acetate in an attempt to see differences in the diblock sticky foot versus the triblock. No significant differences were found although qualitatively it looked like the triblock may have been a little less sticky.

Displacer experiments using DCE as the eluting solvent were carried out with the following polymers: D5/50k, T5/50k, D12/50k, T12/50k, D23/13k, T23/12k, D23/50k, T23/50k, D40/50k, T40/50k, D95/33k and the single sticky foot (SF₁). Three displacers were used: ethyl acetate (Figure 3.20), THF (Figure 3.21) and isopropanol (Figure 3.22), and the

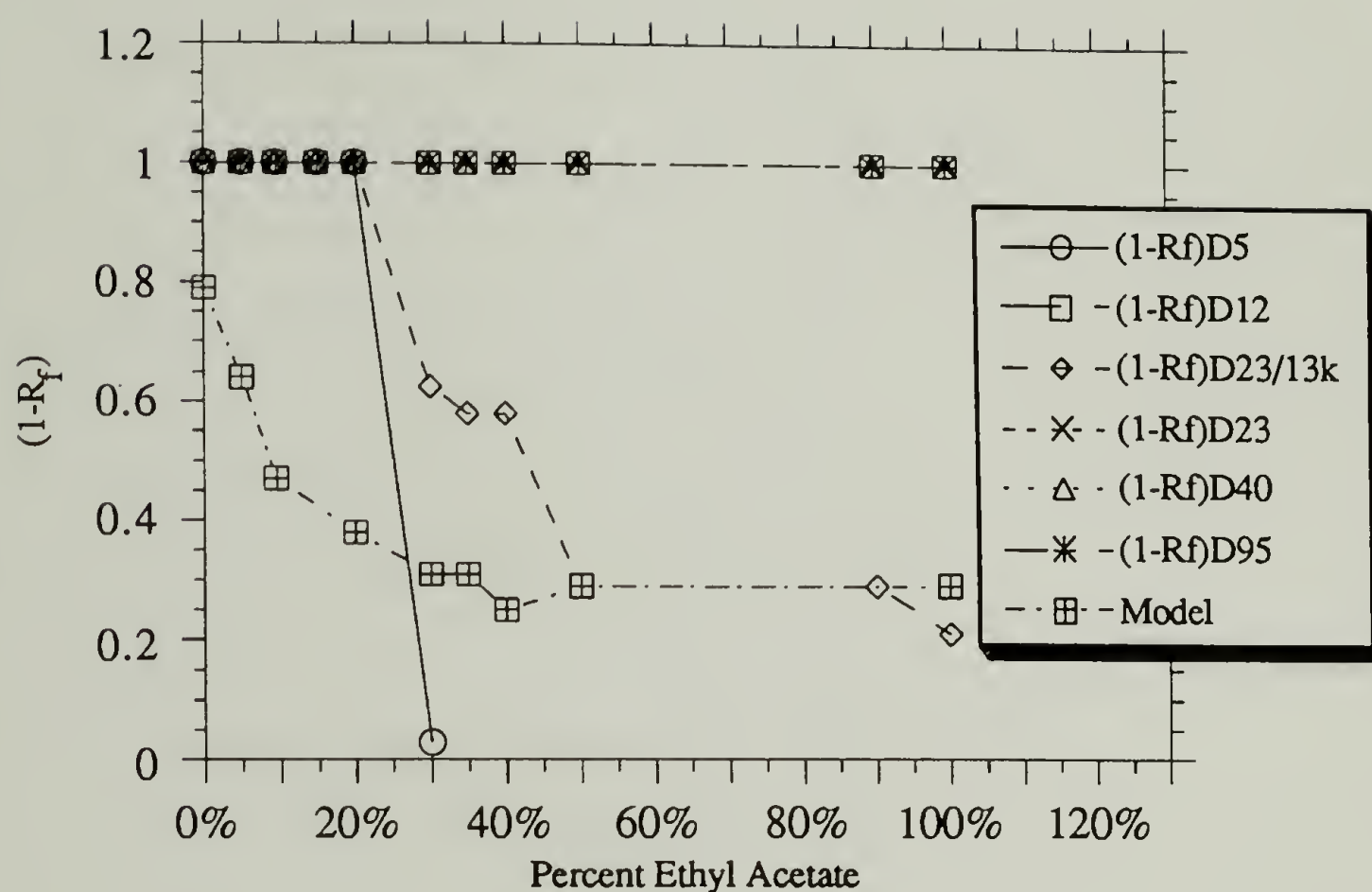


Figure 3.20 TLC displacer data for modified polymers on silica (eluent DCE, displacer ethyl acetate). D12/50k, D23/50k, D40/50k, D95/33k are not displaced at any concentration.

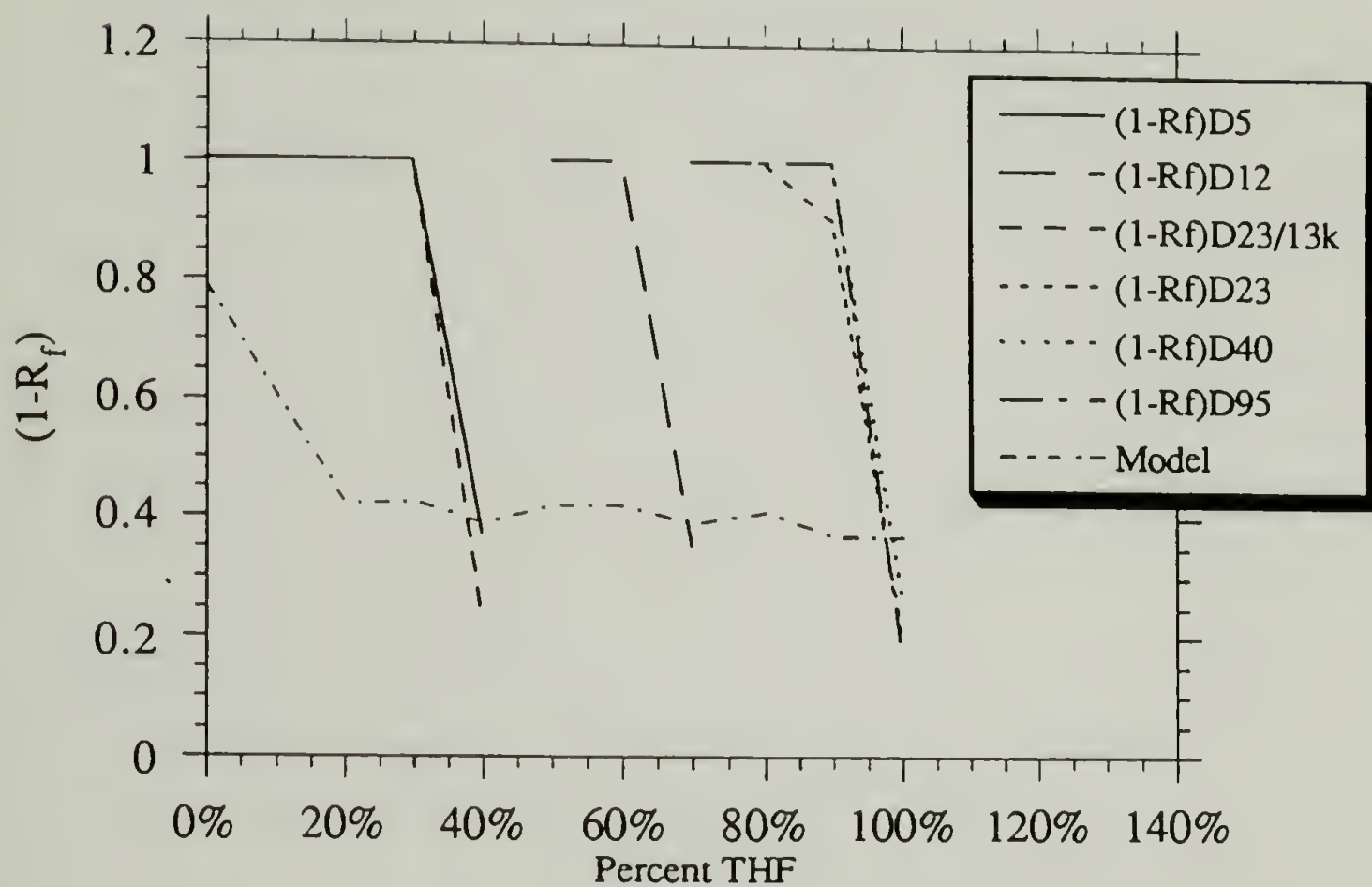


Figure 3.21 TLC displacer data for modified polymers on silica (eluent DCE, displacer THF).

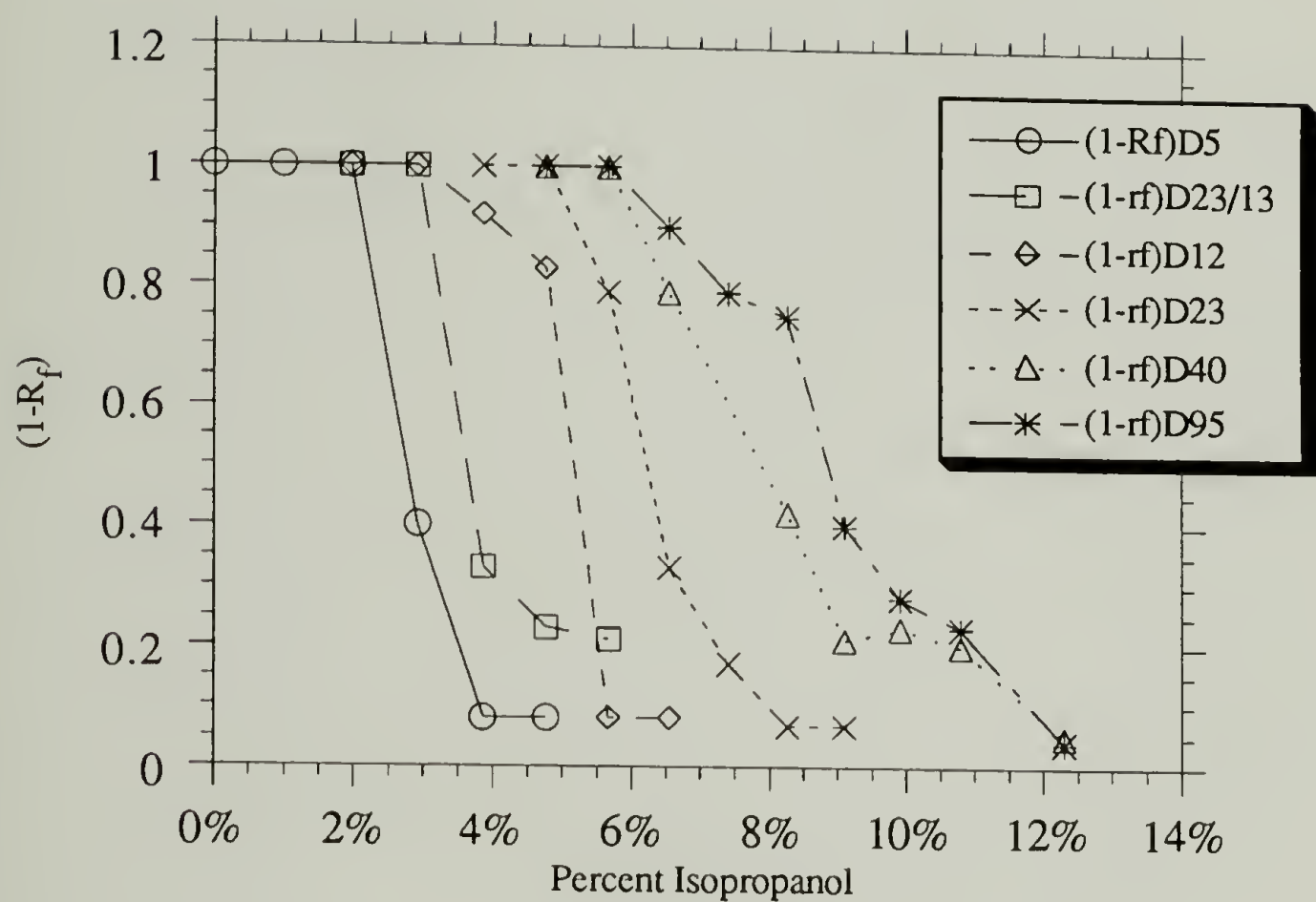


Figure 3.22 TLC displacer data for modified polymers on silica (eluent DCE, displacer IsoOH).

same general behavior was seen in these experiments as in the one previously described. The polymer initially had an $R_f=0$ and upon addition of displacer it began to streak and then eventually tightened up again at higher ϕ_d . We found that differences between the diblock and triblock behavior were not experimentally significant and thus the triblock data are not shown in the figures. The displacement by EA is shown in Figure 3.20. The model compound in this case elutes with a $R_f=0.2$ in pure DCE (DCE is a stronger displacer, note Table 3.16) and the R_f changes smoothly with displacer concentration. The D5/50k ($\sim[\text{SF}]_{15}$) is totally displaced at $\sim 25\%$ EA followed by the D23/13k ($\sim[\text{SF}]_{21}$) at $\sim 50\%$ EA. Pure ethyl acetate is not strong enough to elute any of the other polymers. Note that the 23% SF ($M_n=13\text{K}$) elutes while the 12% SF ($M_n=50\text{K}$) does not. Figure 3.21 shows the data obtained when THF was used the displacer. We observed similar model compound behavior. The D5/50k and D23/13k again eluted at the lowest displacer concentrations. We note that in this case the two ϕ_{cr} are essentially equal and at a higher value than for EA. The D12/50k elutes next at about 70% THF. The remaining three polymers all elute but require over 90% THF. The displacement by isopropanol (Figure 3.22) follows a trend of behavior similar to the other two displacers with the same order of displacement observed but at lower displacer concentrations.

The data above indicate that isopropanol was the strongest displacer requiring a composition of only 12.3% to displace the stickiest polymer (D95/33K), while the ethyl acetate was the weakest displacer with even 100% able to displace only the two weakest adsorbing polymers. This trend agrees with the elutropic data series presented previously. The data

are plotted in Figure 3.23 as the ϕ_{cr} (volume % of displacer) versus the percent SF. All of the data for the $M_n \sim 50K$ polymers fall in predictable order but the $M_n = 13K$ data are too low to fit well on the plot. This is because the determining factor for the ease of displacement was found to be the absolute number of SF on the chain and not the % SF of the chain. This can be seen in Table 3.17 where the ϕ_{cr} is shown along with the DP of the sticky block for the modified copolymers. We found in each case that more sticky feet required more displacer, but that with increasing SF content, the discrepancy grew smaller so that D40 and D23 were much closer together than the D5 and D12. We found that the percent SF on the chain was not the determining factor: in all cases the 23% SF/13K polymers were displaced more easily than the 12% 50k polymers. This suggests that the important factor is the absolute length of the sticky block, and not its percentage of the chain.

Table 3.17 Critical Displacer Concentrations (ϕ_{cr}):
Solvent (DCE).

<u>Polymer</u>	<u>DP of Sticky Block</u>	<u>ϕ_{cr} (IsoOH)</u>	<u>ϕ_{cr} (THF)</u>	<u>ϕ_{cr} (Ethyl Acetate)</u>
D5/50k	15	3.6	42	25
D23/13k	21	4.6	43	50
D12/50k	36	5.5	70	> 100%
D23/50k	69	8.3	93	> 100%
D40/50k	120	12.0	97	> 100%
D95/33k	270	12.0	97	> 100%

According to Cohen Stuart et. al., the molecular weight of a homopolymer is not a factor in the displacement of the polymers (as long

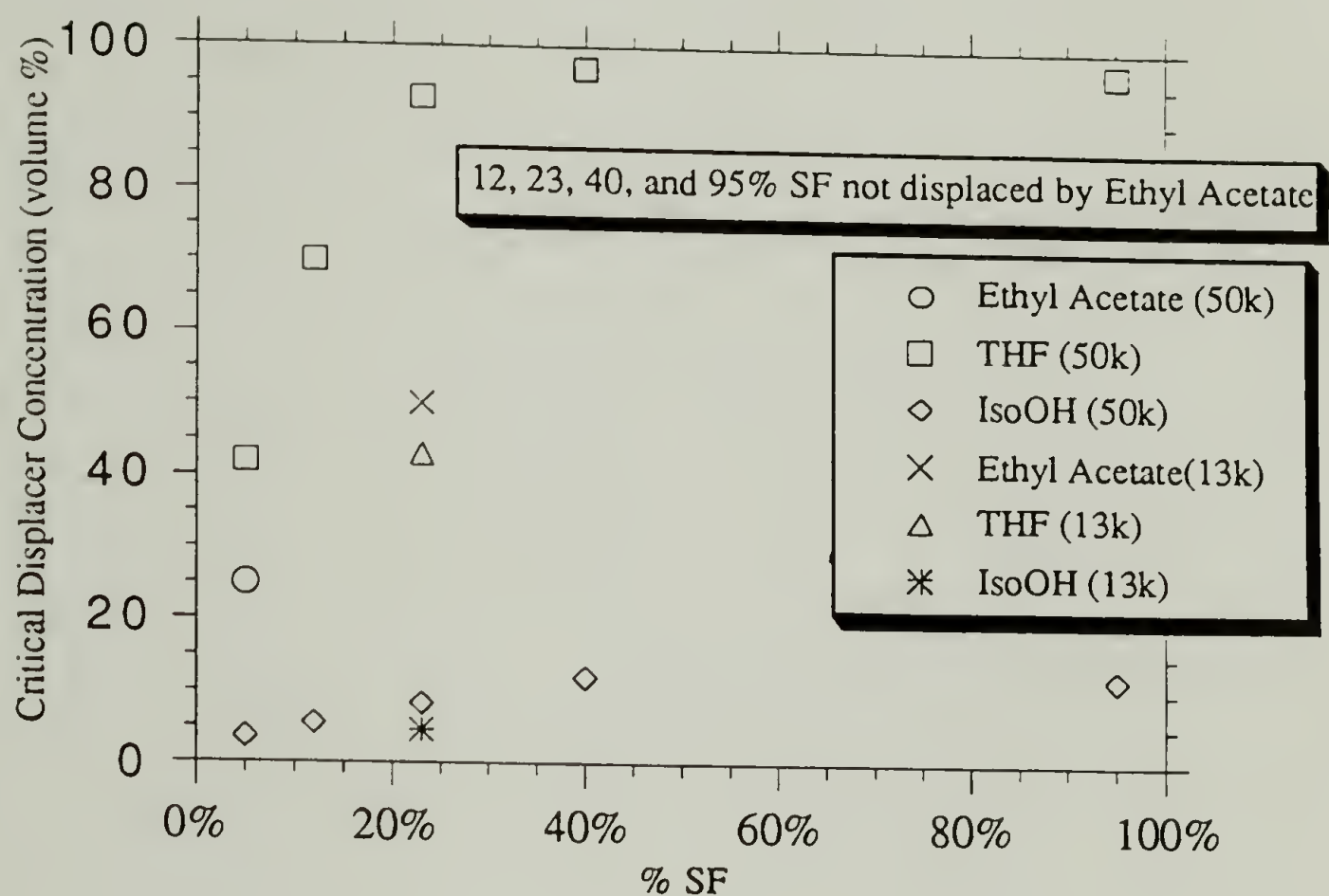


Figure 3.23 Critical displacer concentrations.

as the MW is above some minimum value). This comes about directly from their derivation and is also born out by their experiments with polystyrene on silica. What we are seeing in the data presented above is the transition from small molecule adsorption characteristics (where the length of the sticky block matters) to polymer adsorption characteristics where the critical displacer concentration is independent of molecular weight. The fact that we observed no differences between the elution behavior of the diblock and triblock copolymers but we do see a difference for the chain composition suggests that the triblock copolymer is adsorbed with both feet down forming a looped structure. If this were not the case (i.e. only one end of the triblock is adsorbed) then the T12/50k copolymer would elute with characteristics similar to the D5/50k. This cannot be attributed to a alternation between the two ends being adsorbed because we are measuring a critical displacer concentration not an R_f value and thus the kinetics are different. A final note with is that it seems then that even 7-8 of the hydroxy diethylmalonate SF in a block are enough to cause both ends to be adsorbed even under these conditions.

In conclusion, we have observed a cooperativity on going from one SF to many on a single molecule. We have also seen evidence that triblock copolymers adsorb with both blocks on the surface as evidenced by the similarity of the elution behavior. We had imagined that the cooperativity would be dependant on the number of segments between two sticky feet. For instance each SF would more greatly influence the adsorption/desorption behavior of a SF on an adjacent segment than if the SF were on opposite ends of the chain. We also have seen this cooperativity greatly influence the "stickyness" of the molecule. This cooperativity should also

be dependent on the SF strength. We postulate that the sticky block sizes were too large (for the strength of our interaction) for all the polymers tested and thus these were well on their way to the cooperativity plateau. In other words all the individual blocks were too sticky by themselves for us to measure the architecture effect. One may be able to see this effect by using even smaller block sizes and weaker surface interactions.

Polymer Adsorptions: Solvents and Surfaces

The solvent surface combination used for adsorption experiments must fulfill certain requirements. We want a system where the SF block will adsorb but the *tert*-butylstyrene block will not. The solvent should also be a good solvent for both blocks. We want the bouy block to be in good solvent conditions to observe repulsion in this layer and so it doesn't adsorb merely to get out of solution. The solvent should also be relatively good for the hydroxy diethylmalonate block so that no micelles are formed and so that the interaction energy is the sole driving force for adsorption. If a poor solvent for the SF block was used, its effect would probably change with copolymer composition. Because most of the adsorption measurements were made using UV spectroscopy to measure polymer concentration, the solvent should also be transparent to UV. The phenyl ring chromophore (which we will be looking at) has a finger print absorption spectrum from approximately 250 -275 nm. There is also a much more intense absorbance at about 230 nm. The solution properties of PtBS have been reported^{85,86} for a number of solvents. Good solvents include THF, dioxane, cyclohexane, and benzene. By comparison of this data and that for PS it is likely that solvents such as DCE, CCl₄ and chloroform are good solvents as well. The poor solvents include 3-

nonanol, 2-octanol and 1-hexanol. No published information exists the solution properties of the hydroxy diethylmalonate sticky foot polymer. As was discussed in the synthesis section, the n-propyl derivative monomeric sticky foot is miscible in CH_2Cl_2 and MeOH down to at least -60 °C while in pentane it phase separates above -20 °C. This suggests that pure hydrocarbon solvents are not good solvents for the SF block. It was found that homopolymer PS modified with DEOM was easily soluble in DCE, CDCl_3 , THF, benzene and MeOH among others. Thus along with the small molecule miscibility data given above, we conclude that these solvents are relatively good for the SF block. (No light scattering measurements and no intrinsic viscosity measurements were carried out to determine the Mark Houwink Coefficients.) From a UV spectroscopy perspective the solvents that could be used include THF, dioxane, cyclohexane and DCE.⁸⁷ THF and dioxane were considered, but it was found that they form a UV impurity when exposed to silica in adsorption experiments (probably peroxides). These impurities can both affect the measurement by changing the baseline and also by acting as displacers for the adsorption. It was also found that THF desorbed most of the polymers. Cyclohexane was not chosen because it is probably a poor solvent for the hydroxy diethylmalonate block. DCE was found to best fill all the requirements and all the adsorption data presented here were obtained using DCE as the solvent.

Adsorptions on Glass Microscope Slides

Some of the polymers were adsorbed onto glass microscope slides and this provided a flat surface which facilitated XPS and contact angle analysis (H_2O was used as the probe fluid). Modified diblock (D23/13K)

and triblock (T23/12K) copolymers and an unmodified precursor (T23/12k-p) copolymer were adsorbed onto glass microscope slides from a range of concentrations in DCE. Figure 3.24 shows representative 15° takeoff angle XPS spectra for adsorbed layers of the diblock copolymer, triblock copolymer, unmodified precursor polymer as well as a control which used pure DCE (polymer solutions of ~1.0 mg/mL). The 15° takeoff angle samples approximately the top 11 Å of the surface. Note the increasing intensity of the C_{1s} photoelectron line (and decreasing intensity of the Si_{2p} line) as one goes from a slide exposed to pure solvent to one where a diblock copolymer was adsorbed. These data are indicative of a carbon overlayer of increasing thickness. The XPS composition data are shown in Figures 3.25 through 3.30 as a function of adsorbing solution concentration (i.e. isotherms). These are high affinity type isotherms with plateaus above approximately 0.25 mg/mL. Note that the diblock copolymer data show a consistently higher percentage of carbon than the triblock data thus indicating that the polymers with diblock architecture adsorbed to a larger extent than the corresponding triblock. Note also that the oxygen content is relatively low and that the percentage of oxygen is higher at greater sampling depths (75 ° takeoff angle, 40 Å depth); this indicates that the oxygen is located below the carbon as we would expect for the malonate-induced adsorption. (This is also where the SiO₂ oxygens are located.) This angle-dependent oxygen concentration is observed for both copolymers suggesting that the triblocks adsorb with both anchors down and form loops. Also note that the precursor copolymer adsorbs to a small degree; this can be seen from the carbon layer that is thicker than that for the DCE control.

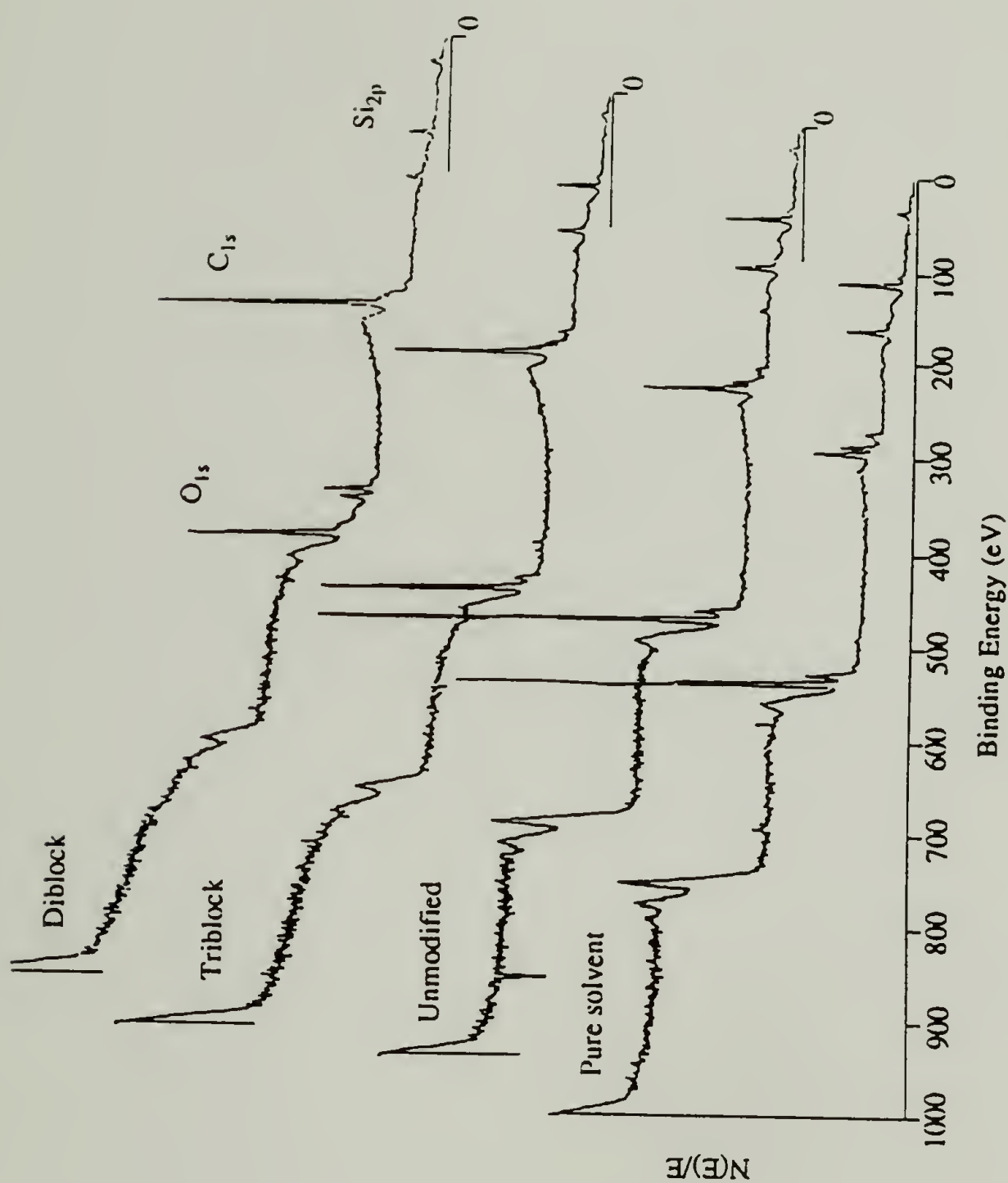


Figure 3.24 XPS spectra (15° takeoff angle) of a 23% SF diblock, 23% triblock, unmodified precursor and solvent control for the adsorption onto glass microscope slides from DCE (25°C , 24 h, approximately 1.0 mg/mL). Note the increasing amount of carbon and decreasing amount of silicon in going from the control to the diblock. The diblock has a higher percent carbon than the triblock.

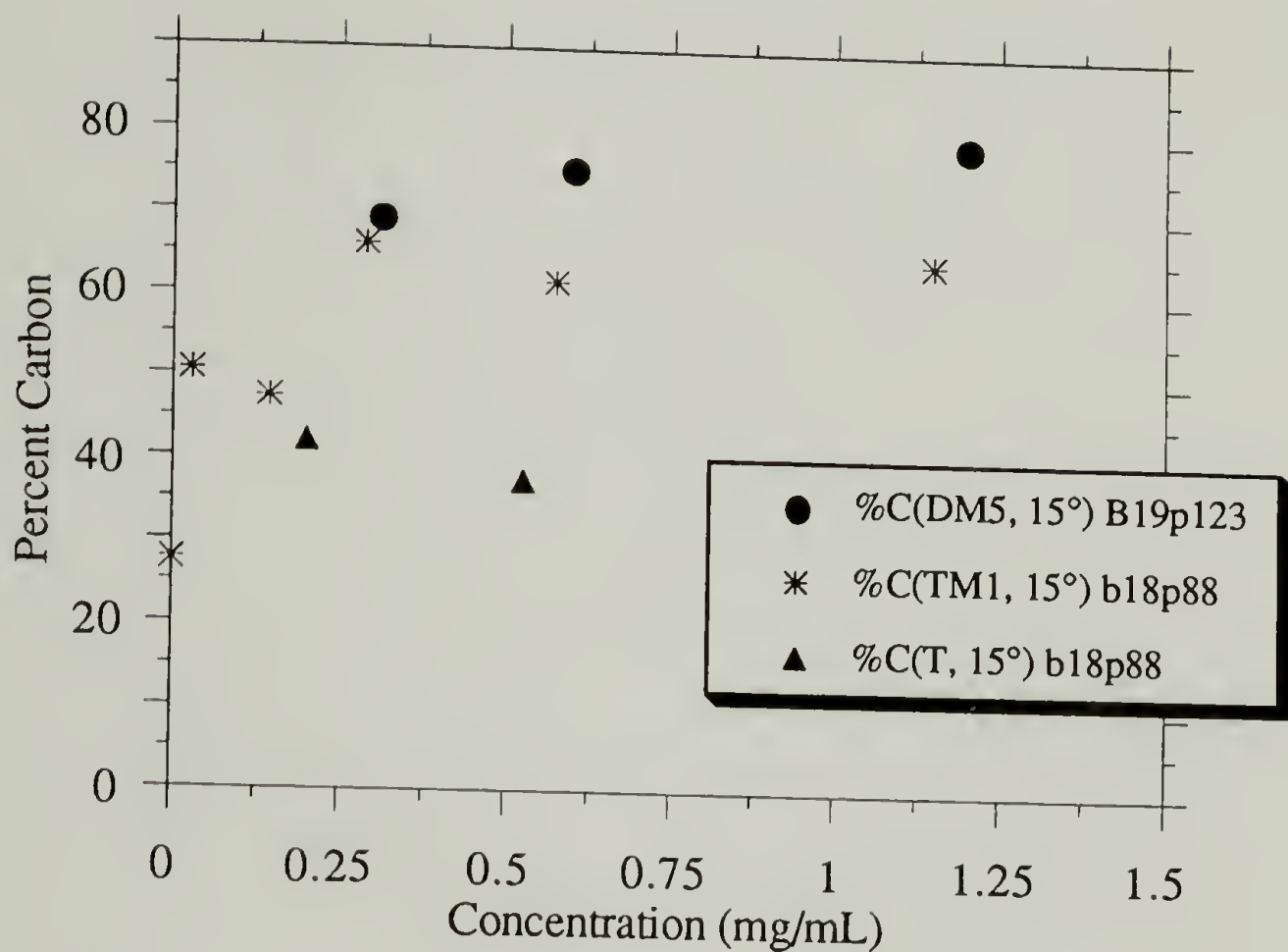


Figure 3.25 XPS atomic composition data (% carbon, 15° takeoff angle) for polymers adsorbed onto glass microscope slides from DCE (22 °C, 24 h). Data shown for 23% SF diblock (circles, D23/15K DM5), triblock (stars, T23/12K TM1) and unmodified (triangles, T23/12Kp) copolymers.

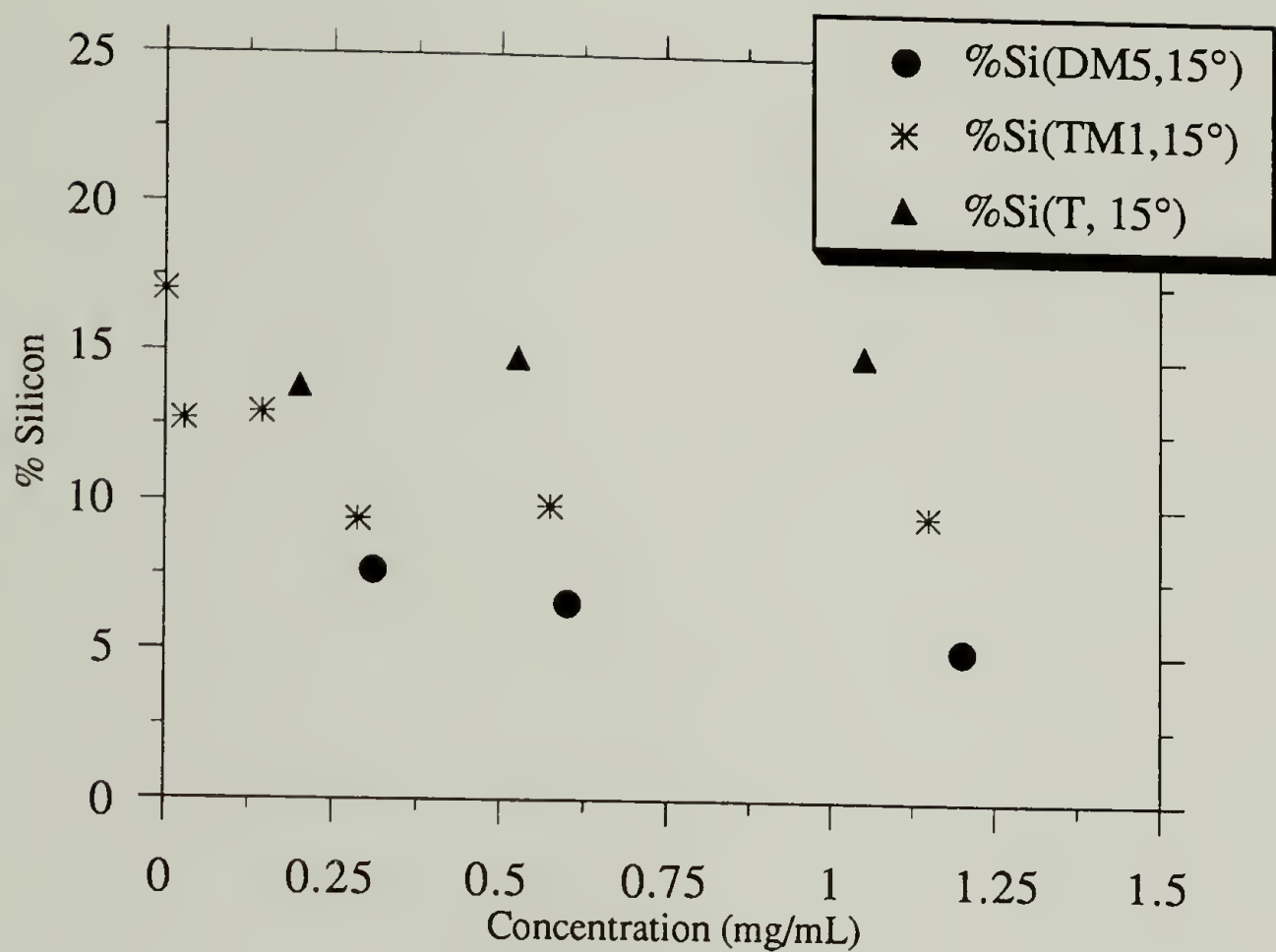


Figure 3.26 XPS atomic composition data (% silicon, 15° takeoff angle) for polymers adsorbed onto glass microscope slides from DCE (22 °C, 24 h). Data shown for 23% SF diblock (circles, D23/15K DM5), triblock (stars, T23/12K TM1) and unmodified (triangles, T23/12Kp) copolymers.

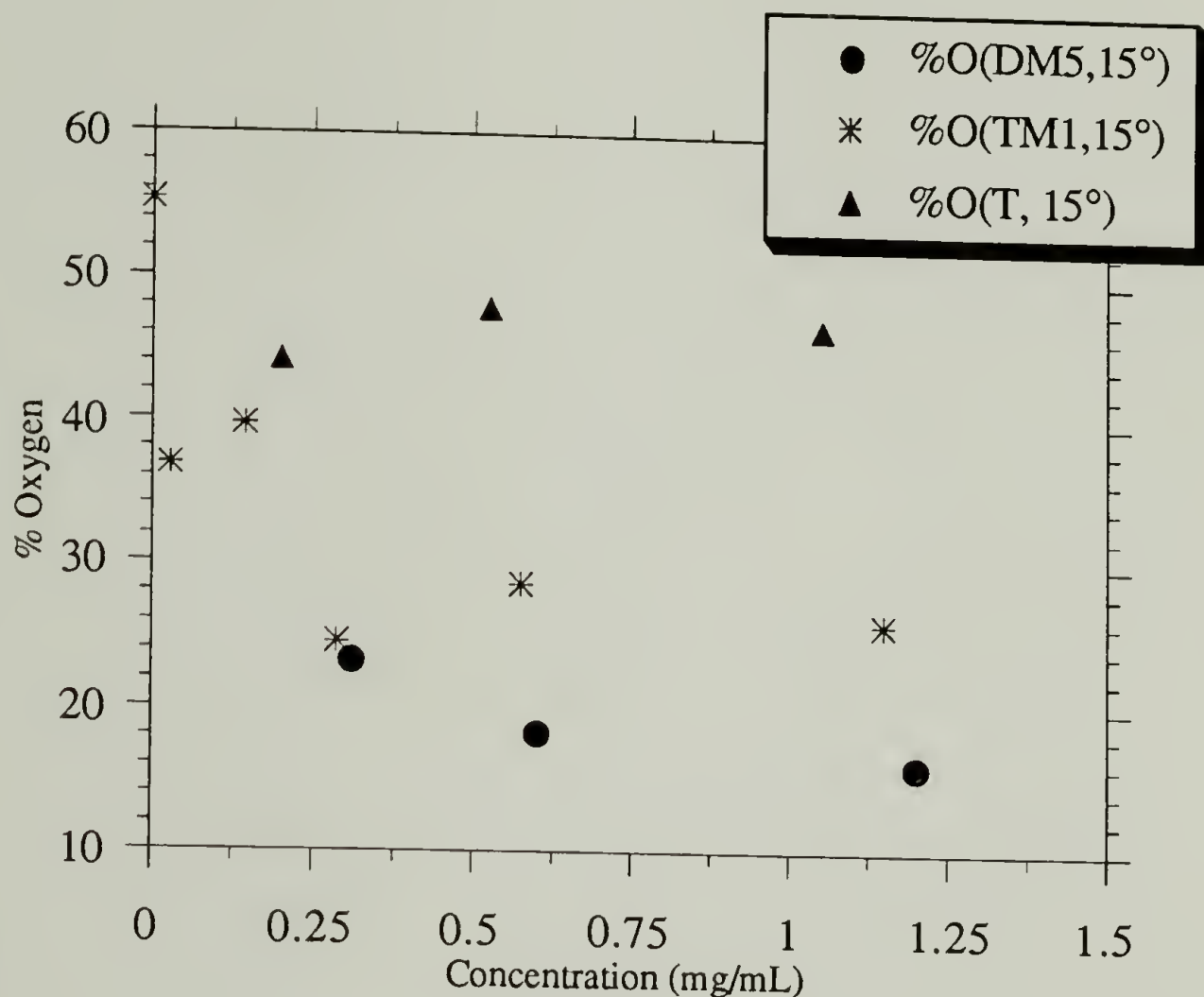


Figure 3.27 XPS atomic composition data (% oxygen, 15° takeoff angle) for polymers adsorbed onto glass microscope slides from DCE (22 °C, 24 h). Data shown for 23% SF diblock (circles, D23/15K DM5), triblock (stars, T23/12K TM1) and unmodified (triangles, T23/12Kp) copolymers.

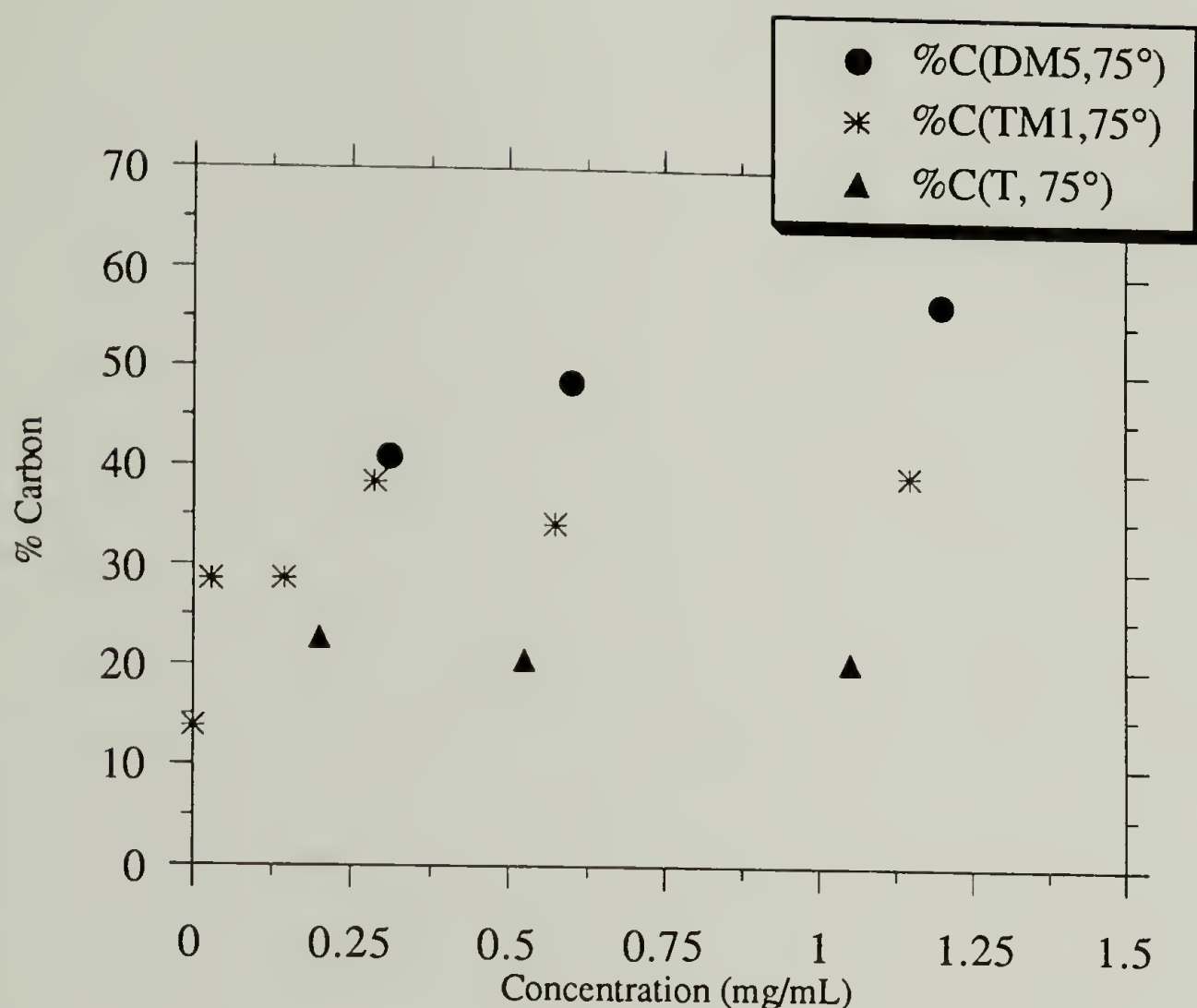


Figure 3.28 XPS atomic composition data (% carbon, 75° takeoff angle) for polymers adsorbed onto glass microscope slides from DCE (22 °C, 24 h). Data shown for 23% SF diblock (circles, D23/15K DM5), triblock (stars, T23/12K TM1) and unmodified (triangles, T23/12Kp) copolymers.

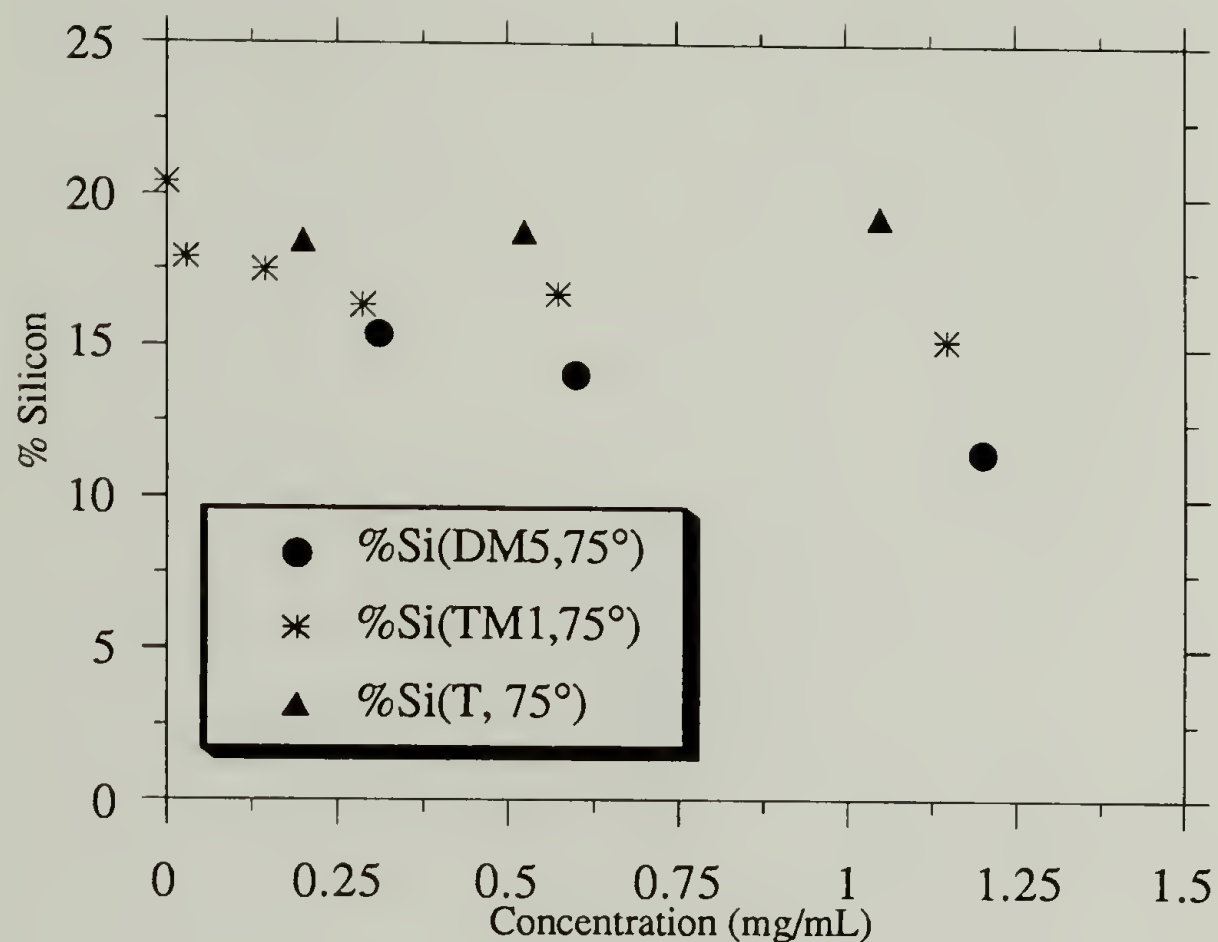


Figure 3.29 XPS atomic composition data (% silicon, 75° takeoff angle) for polymers adsorbed onto glass microscope slides from DCE (22 °C, 24 h). Data shown for 23% SF diblock (circles, D23/15K DM5), triblock (stars, T23/12K TM1) and unmodified (triangles, T23/12Kp) copolymers.

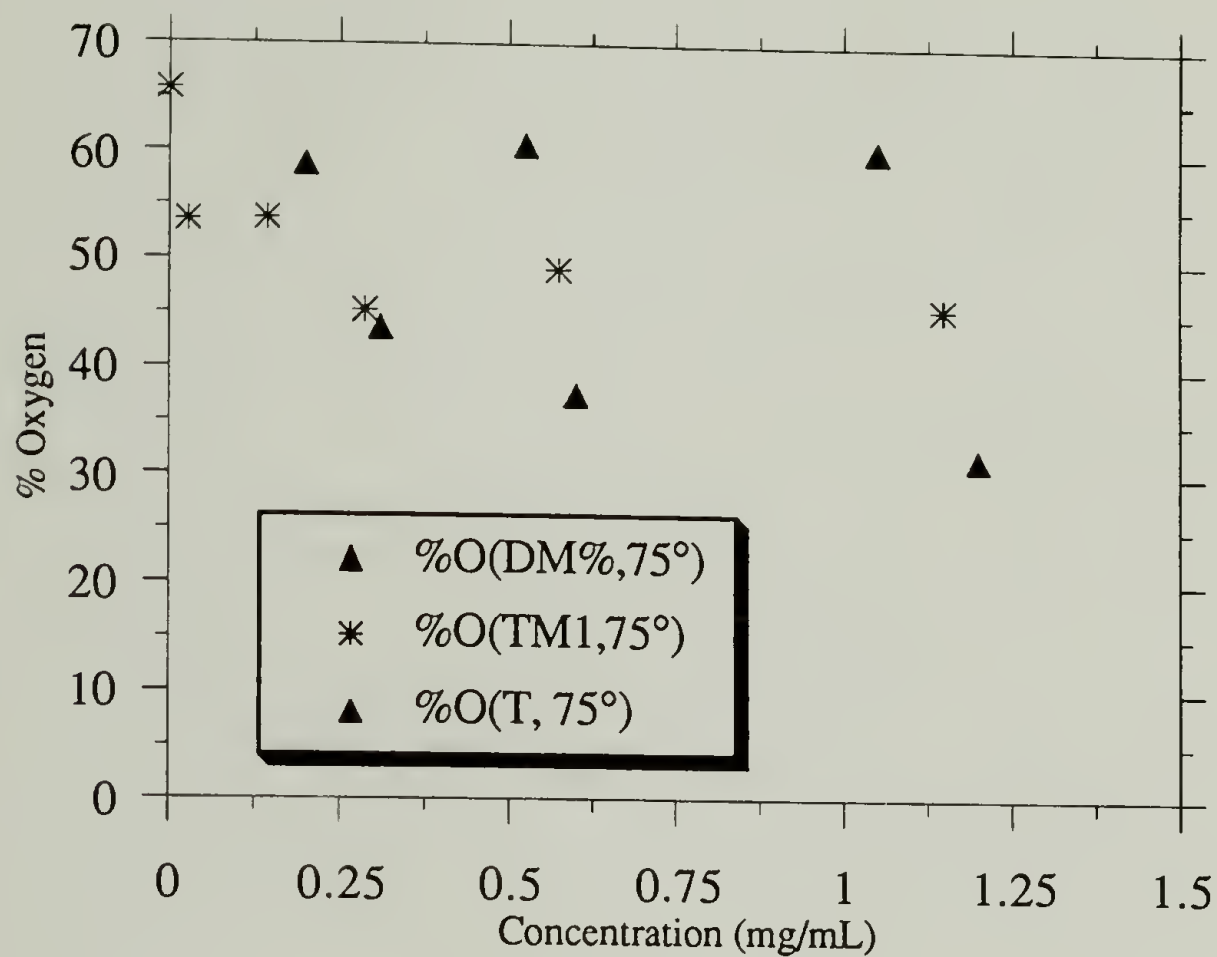


Figure 3.30 XPS atomic composition data (% oxygen, 75° takeoff angle) for polymers adsorbed onto glass microscope slides from DCE (22 °C, 24 h). Data shown for 23% SF diblock (circles, D23/15K DM5), triblock (stars, T23/12K TM1) and unmodified (triangles, T23/12Kp) copolymers.

The thickness of the adsorbed layer was estimated in two separate ways,^{88,89} and both methods utilized comparison of the relative intensities of the C_{1s}, Si_{2p} and O_{1s} peaks from the XPS data. We multiplied the atomic composition data by the electron mean free path (14 Å C_{1s}, 21 Å Si_{2p} and 6 Å O_{1s}); these values were obtained from Clark.⁹⁰ The adsorbed layer thickness was then determined by comparison to calculated [C/(C+Si)] intensities (overlayer calculations were done assuming a sharp interface and atomic concentrations of each element were taken into account) as a function takeoff angle and overlayer thickness, *t*. Table 3.18 gives the data obtained from the calculation at 15° and 75° takeoff angles. There are rather large discrepancies between the thickness determined at these two angles, but in each case the diblock coverage was consistently higher than that of the triblock. These discrepancies are due to an inaccurate assumption (inherent in the calculation) that the mean free path of an electron from a Si_{2p} orbital is 21 Å in glass as well as the carbon overlayer. If the λ is less than 21 Å in glass, the inaccuracy increases as greater depths are sampled. This causes the 75 ° takeoff data to be artificially high. An alternative method for determining the layer thickness utilizes attenuation of the Si peak and depends only on the λ_{Si} in the carbon overlayer and not that in glass. If one normalizes the Si peak intensity (for effects due to change in angle), Equation 3.5 can be used to obtain the layer thickness. The ideal way to do this is to construct a plot ($\ln\{Si(\theta_1)/Si(\theta_2)\}$ vs. $\{1/(\sin\theta_1) - 1/(\sin\theta_2)\}$) from the data obtained at several angles and then determine the thickness from the slope of that line; as it were we had data at only two angles so these were the points that was used.

$$\ln\{Si(\theta_1)/Si(\theta_2)\}=t/\lambda\{1/\sin\theta_1-1/\sin\theta_2\} \quad 3.5$$

Table 3.18 shows the normalized intensity ratio at to the Si_{2p} intensity at two 15° and 75° and the layer thickness calculated from this using Equation 3.5. We see that the same trend in the amount adsorbed is seen as was determined by the previous method. The thicknesses calculated by this method are not as different as the other method used. The determination is relatively inaccurate considering that only two angles were used, but it does show the same trend as the other data.

Table 3.18 Adsorbed Layer Thickness as Determined by XPS.

<u>Sample</u>	<u>[C/(C+Si)] (15°)</u>	<u>Thickness (15°)</u>	<u>[C/(C+Si)] (75°)</u>	<u>Thickness (75°)</u>	<u>Si(15°)/ Si(75°)</u>	<u>Thickness (Eq 3.5)</u>
Diblock	0.889 ± 0.021	~10 Å	0.729 ± 0.036	~20 Å	0.316	8.48 Å
Triblock	0.803 ± 0.017	~7 Å	0.589 ± 0.015	12-13 Å	0.366	7.41 Å
Precursor	0.642 ± 0.023	3-4 Å	0.442 ± 0.016	7-8 Å	0.418	6.49 Å
DCE	0.520	~2 Å	0.312	4-5 Å	-----	-----

Dynamic contact angle measurements were made on these surfaces prepared by the adsorption described for the XPS experiments above. The data are shown in Figures 3.31 (advancing) and 3.32 (receding) using water as the probe fluid. One can see that all three polymer samples show a high affinity isotherm shape where the advancing contact angle of the clean surface (~44°) increases to a plateau value at higher solution

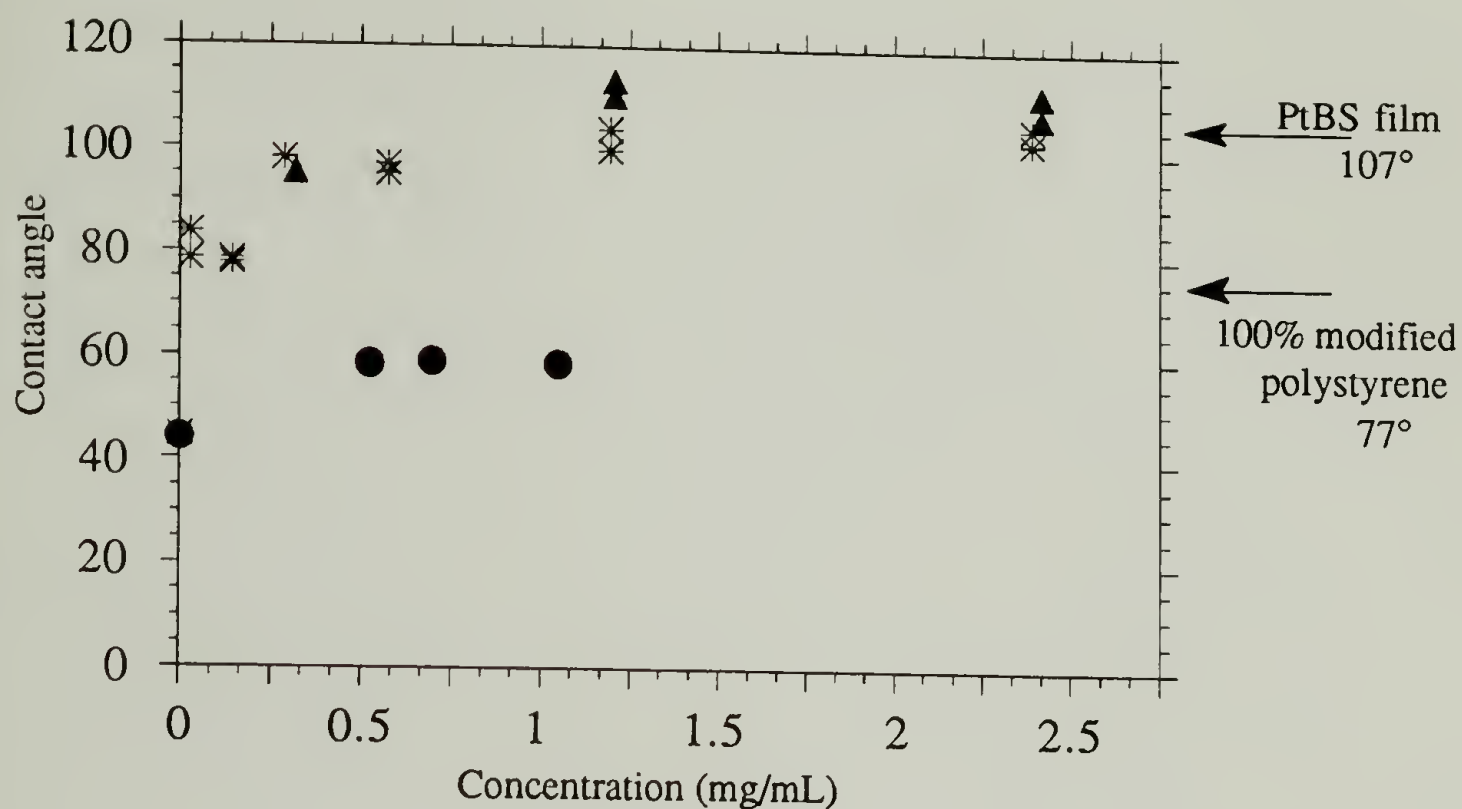


Figure 3.31 Advancing contact angle data (water is probe liquid) for polymers adsorbed onto glass microscope slides from DCE (22 °C, 24 h). Data shown for 23% SF diblock (triangles, D23/15K DM5), triblock (stars, T23/12K TM1) and unmodified (circles, T23/12Kp) copolymers.

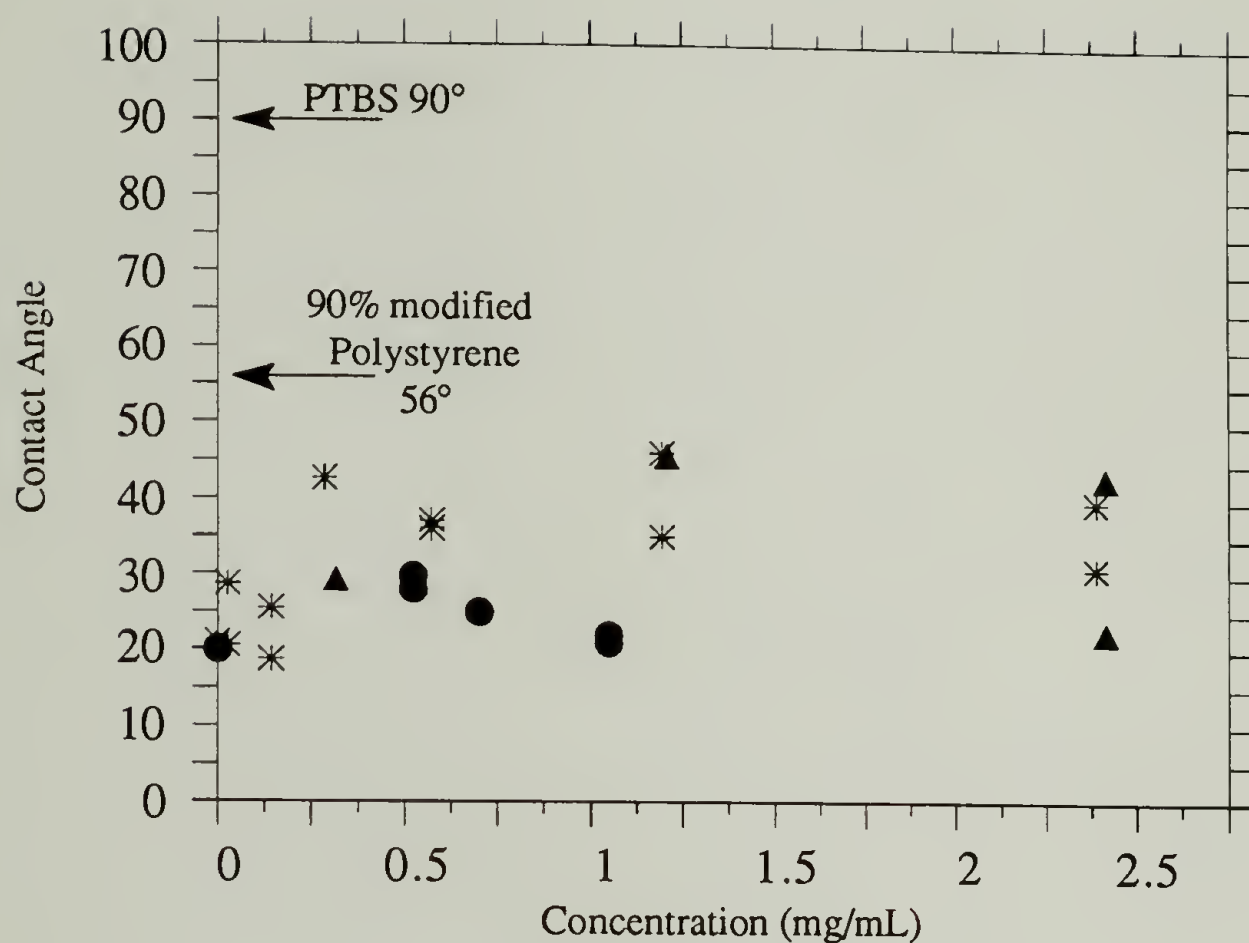


Figure 3.32 Receding contact angle data (water is probe liquid) for polymers adsorbed onto glass microscope slides from DCE (22 °C, 24 h). Data shown for 23% SF diblock (triangles, D23/15K DM5), triblock (stars, T23/12K TM1) and unmodified (circles, T23/12Kp) copolymers.

concentrations. The unmodified polymer increases to a value of $\sim 59^\circ$. Both the modified diblock and triblock polymers yield advancing contact angles ranging from 95 - 110° in the plateau region. A cast film of PtBS homopolymer gives an advancing contact angle of 107° and thus we see that the data are consistent with a air/solid interface of PtBS, as is expected for the adsorption of these types of polymers. The receding contact angle data are much more scattered as can be seen from Figure 3.32. The values are all higher than the DCE control but they do not approach that of the PtBS cast film (90°). This suggests that there some number of hydrophilic patches on the surface. It is known that even small amounts of lyophilic surface structures can greatly affect the receding contact angles.⁹⁰ A film of modified PS homopolymer ($\sim 95\%$, PSM2) was cast and the contact angles were determined to be $77^\circ/56^\circ$. This was done in an attempt to determine what contact angles to expect if the hydroxy diethylmalonate sticky foot were at the surface (i.e. the air interface). The data suggest that the more hydrophilic parts of the polymer are buried due to surface energy minimization, but we still see a very large difference between the PtBS surface and the modified polymer. The advancing angle data suggest that there are negligible SF at the air interface for both the diblock and triblock polymer films. In the case of the diblock, there is not much else that could happen. In the case of the triblock, the data suggest that the adsorption has resulted in a loop structure with both sticky blocks of each chain adsorbed to the surface. One must also note the possibility that even if some of the triblock copolymers formed tails (i.e. only one block adsorbed) this may not be seen in the contact angle measurements because the high energy sticky block may be buried (due to surface energy minimization). The

loop structure is inferred from other measurements and this lends credence to our postulate.

The XPS and contact angle data suggest some interesting experiments that could be performed using chains endcapped with a relatively small perfluorinated chain. We prepared three precursor copolymers (Table 3.1 entries 2,6 and 10) and endcapped them with ethylene oxide resulting in a hydroxy terminated polymer chain. The hydroxyl end group can be reacted with perfluorodecanoyl chloride to obtain the perfluorinated ester. This was discussed in the synthesis section of this chapter along with the feasibility of modifying the end-capped polymer to a chain with both the fluorinated endgroup and the hydroxymalonate SF. These three component polymers should show some interesting results, for example, a modified diblock with the fluorine tag on the buoy end should show enhanced fluorine content in the surface of the adsorbed layer (one may even find SF block sizes that results in a teflon-like air interface). If the fluorine tag is at the sticky end one would expect to see much less fluorine by XPS because it should be forced to the silica surface by the SF block. The third experiment would confirm the loop structure: here a fluorine ended triblock copolymer would be adsorbed and compared to the two experiments above. If the surface looks like the second one (i.e. low fluorine content), then we can say the triblock adsorbs in a loop structure. A couple of things should be mentioned here. First, failure of this experiment (i.e. higher fluorine concentration in the triblock than the diblock) would not disprove the existence of the loops (in the normal triblocks) because the fluorine may affect the energetics and cause the block not to stick. If this were the case then this would be a means of using

ABA triblock copolymers to create an array of functionality at the solvent interface. One should also note that these differences may need to be determined via angle resolved XPS and not just as "amount fluorine" because of the effect the amount of polymer adsorbed would have on the measured fluorine content.

Adsorptions on Aerosil 120

Adsorption experiments were carried out from dichloroethane onto Aerosil 120. Aerosil 120 (Degussa) is a colloidal silica that exists as aggregates of fused silica spheres,⁹² the spheres range in size from approximately 30-300 Å with an average diameter of 120 Å. The aggregates range in size, but there are two distinct populations: one with maximum dimensions of greater than 5000 Å, and the other with maximum dimensions less than 1000 Å. These aggregates are in the colloidal size range and they exist (under normal conditions) as agglomerates held together by van der Waals interactions. We used Aerosil in our experiments for a number of reasons. The chemical nature of the surface has been rather well characterized as chemically pure SiO₂⁹³ (as opposed to glass which has various other ions and elements present with the SiO₂). The adsorptions have been found to occur via interaction with the silanol functionality on the surface thus these surfaces are well understood in this regard. The specific area (120 m²/g) is very high for a "non-porous" solid and thus Aerosils are the adsorbent of choice for many of the adsorptions reported in the literature⁹⁴ (porosity adds another complication to the system). This claim of non-porosity is rather dubious considering the fused nature of the solid. Killman⁹² et. al have reported the average porosity of a Aerosil 200 aggregate to be 0.89 (porosity is defined as the

void volume/total volume). The effect of this fused structure will no doubt be a function of the size of the polymer coil (i.e. a smaller coil may have more surface available to it), and thus effects similar to those seen for porous materials should be expected. The reported specific area was determined by BET measurements with N_2 and this probably overestimates the surface area actually available to the polymer sample. This will result in measured adsorbances that are biased low (compared to the real situation). One should also note that the radius of curvature of the spheres (and probably even the linear dimension of the aggregates) are rather small when compared to the coil sizes used. This has been predicted to allow increased amounts of polymer to adsorb in polymer brushes because of relaxed packing requirements as the brush extends away from the surface (i.e. surface area increases with radius squared). Therefore we see that Aerosils are not the model substrates that they are usually thought to be. From a standpoint of understanding aspects of colloidal stabilization, polymer adsorption onto aerosil yields valuable information.

A series of four polymers, two diblock and two triblock copolymers, were used for these studies. These four polymers were prepared by modification of diblock and triblock precursor polymers (D23/13k-p and T23/12k-p, Table 3.1). Two polymers were prepared by 100% conversion of the styrene units in the precursor polymers (D23/13k DM2 and T23/12k TM1, Table 3.15). The remaining two polymers (D23/13k DM3 and T23/13k TM2, Table 3.15) were modified only to approximately 55 to 60% conversion of the styrene units, thus yielding polymers with the same geometric chain length sticky block as the 100% conversion samples, but with only half the number of sticky feet. These sticky feet are distributed

randomly over the length of the sticky block. This yields polymers with the same length sticky blocks but fewer sticky feet and thus a lower overall interaction energy. The blocks should take up approximately the same amount of room on the surface but with only about 1/2 the interaction energy. This is a way to look at the effect of the sticky block size versus surface interaction energy on the characteristics of the adsorption. To summarize, four polymers were used in the adsorption studies reported below. Each polymer had the the same overall size ($M_n \sim 13,000$), but two architectures were prepared (two diblock and two ABA triblock copolymers). One diblock and one triblock had a total of 23 mole % SF, and the second pair had 13 mole % SF.

The amount of polymer adsorbed in these experiments was determined using depletion (UV spectroscopy was used to measure the concentrations) in the following method: a known volume (V) of polymer solution (concentration= c_o) was exposed to a known weight of aerosil (w_a) for the desired length of time. The solution was separated from the aerosil by centrifugation and the concentration (c_f) of polymer remaining in solution was measured by UV spectroscopy. The amount adsorbed (Γ , mg/m²) was then determined by mass balance and the known amount of surface area (Equation 3.6). (The specific area is given as A_s .)

$$\Gamma = V(c_o - c_f) / w_a A_s \quad 3.6$$

This method is simple and usually works well, but is dependent upon efficient separation of the solid substrate from the remaining solution. Because of the colloidal nature of the silica (Aerosil), this separation was

problematic. This separation must be efficient in two regards. First, if all the solid is not removed from the solution, the measured final concentration will be high because the polymer adsorbed on the non-separated solid will also be counted in the measurement. Inefficient separation can also cause scattering effects caused by the particles, which also compromise the UV concentration determination. The other consideration is the stability of the adsorbed polymer/solution equilibrium to the separation process. The separation of the solid from the solution must be accomplished without disturbing the amount polymer adsorbed. It is of course true that if one can minimize (and know accurately) or eliminate these effects then the above method gives useful information. The experiments we ran had some problems with this separation and can be best explained through example as given below.

We found that phenomenologically the behavior of the diblock and triblock copolymers differed significantly. This was observed visually and inferred to be due to physically different phenomena. Initially the aerosil/DCE suspension was almost transparent, presumably due to the similarities of the refractive indices (of the solvent and silica). Aerosil agglomerates were observed, on closer inspection, and these were found to settle at the bottom of the tube when agitation ceased (at least a significant portion of them did). The addition of unmodified polymer (no sticky feet) caused no visual changes in the solution/suspension. When either the modified diblock or triblock copolymer was added, the polymer adsorbed and the aerosil became visible as hazy "clouds" (the concentrated adsorbed polymer layer changes the refractive index). These clouds readily settle out to the bottom of the tube forming a hazy bottom layer and a clear

upper layer. At this point the two architectures began to behave differently. The triblock system, upon stirring, did not change significantly. When agitation ceased the suspension settled out into a hazy bottom layer and crystal clear top layer. In contrast upon stirring, the diblock system resulted a "blue" hazy (light scattering type) suspension and when the stirring was stopped some large hazy structures did settle out but the top layer remained this hazy blue color. We propose that the triblock copolymers are flocculating the aerosil, resulting in a system that sediments easily (larger particles sediment faster). The diblock, on the other hand, stabilized the dispersion and made it more difficult for the silica to sediment. This observation is interesting in the sense that we see a major (and explicable) difference in the adsorption characteristics of the two architectures. The diblock copolymers are adsorbing to form a protective corona of segments around the silica particles and this keeps them from aggregating; this behavior is postulated and expected.⁹⁵ The triblock copolymers adsorb with both sticky blocks and form bridges between the particles, inducing flocculation. The phenomenological differences described above are interesting and serve to indicate that changing the chain architecture (everything else held constant) can have a major impact on the system characteristics. It should also be stressed that ultimately it is these types of behavioral differences that we desire to control (i.e. the amount adsorbed is not important in itself but rather in how it helps to determine the adsorbed layer properties) and thus even if the measured adsorbances are comparable, the differences between the architectures are still quite apparent. The possibilities of using architecture to tailor the adsorption properties is a long range goal of this work and many interesting applications will be elaborated on in the subsequent discussion.

Unfortunately the stabilization induced by the diblock copolymers also made them much more difficult to separate from the solution. This resulted in an increase in the scatter in the diblock adsorption data. As can be seen from the data provided, there is a much larger amount of scatter in the diblock data than the triblock data. Separation via sedimentation is dependent upon a difference between the "particle density" and solvent density. Another factor is the size of the particle; smaller particles are more subject to movement caused by currents and thermal fluctuations; this results in a more difficult separation. When the diblock adsorbs to the silica it disperses the agglomerates in the solution. This both decreases the particle size and also overall density difference (the thickness of the polymer corona now has to be added to the calculation and its density is less than that of the silica and therefore the overall density decreases). Both of these effects make separation via centrifugation much more difficult. Another factor that exacerbates the problem is that the solvent used (DCE) has a relatively high density (1.256 g/mL) which is higher than that of the polymer (~1 g/mL), and thus there is a crossover where the amount of polymer adsorbed is so high that the overall density of the particles is less than that of the solvent and centrifugation would cause the polymer to rise and not fall. This problem would not exist if a hydrocarbon solvent were used. As long as the density of the particle is higher than that of the solvent, in principle one can separate them either by spinning for longer times or increasing the spin rate (i.e. the force the particle experiences) which increases the sedimentation speed. The measurement is further complicated because the polymer desorbs at higher temperatures and centrifugation heats up the solution; therefore one cannot spin for extended periods of time. One should also note that the amount of

scatter in the diblock data could probably be somewhat decreased by adhering to a given separation procedure (we tried many different procedures here) but this would not necessarily give the correct value for the amount adsorbed.

The data show that the adsorption on aerosil is essentially complete in minutes and that unmodified polymer does not adsorb. Figure 3.33 shows the adsorbance versus time of a modified triblock copolymer (T23/12k TM1) and the unmodified precursor polymer. Note the very rapid adsorption ($\sim 1.05 \text{ mg/m}^2$ in less than 15 min.) with no subsequent changes over the period of 50 h. Also note that the unmodified polymer has not adsorbed to any appreciable extent. High affinity type isotherms for all four polymers are observed with the knee occurring at less than 0.5 mg/mL (Figures 3.34 through 3.37). Inspection of the isotherm data shows there is much more scatter in the diblock data than there is for the corresponding triblocks, the explanation of which has already been discussed. Figure 3.38 plots all four isotherms together and one can see that both the chain architecture and the percent sticky feet have an effect on the amount of polymer adsorbed. We found that the amount adsorbed was highest for the fully modified diblock followed by the fully modified triblock. Thus it seems that the extent of modification has a larger effect than the architecture but that both have significant effects. The diblock copolymers have a higher adsorbance than their triblock counterparts but the lower sticky foot content has a slightly larger effect. This will be discussed more fully subsequently.

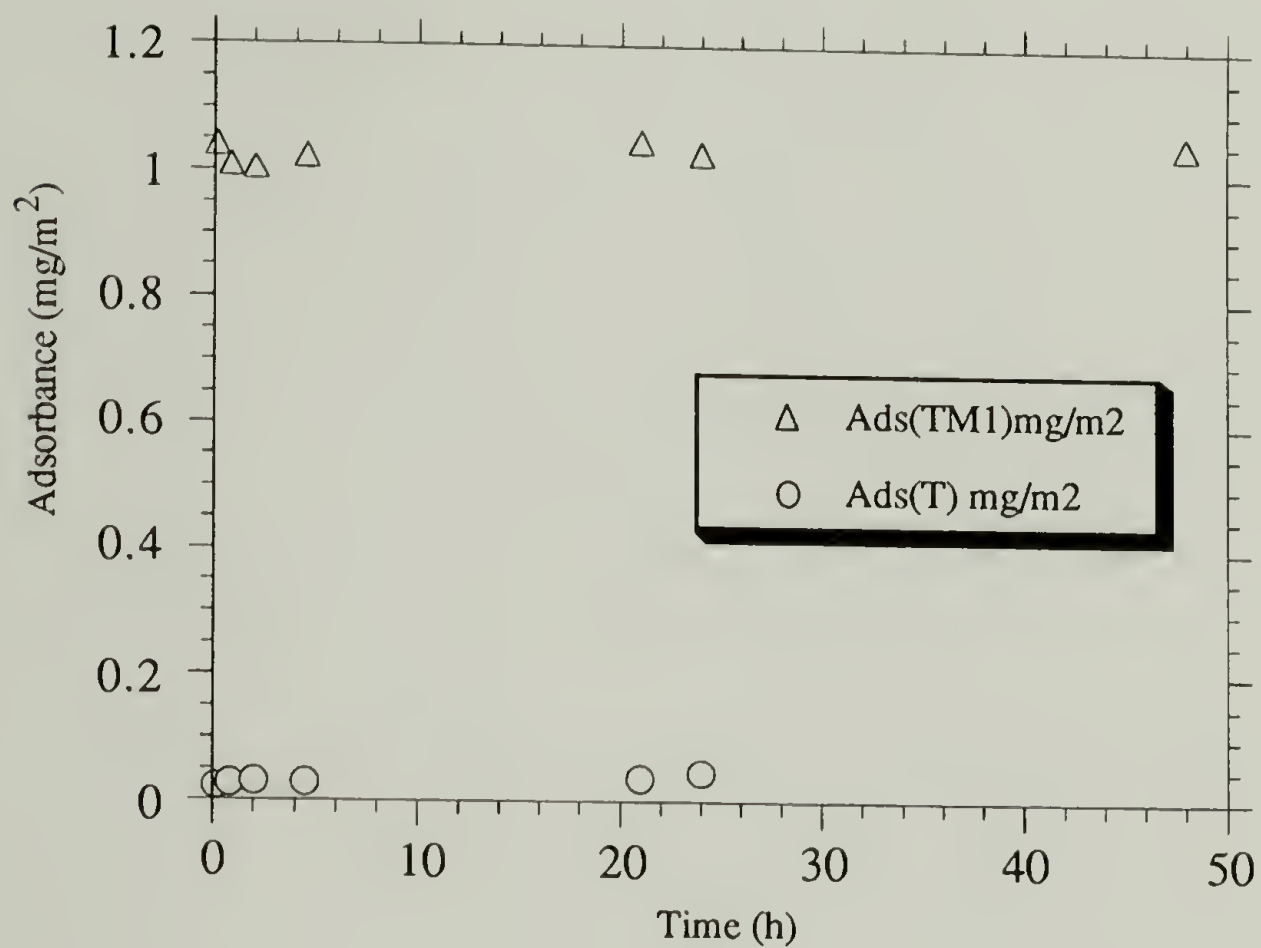


Figure 3.33 Adsorption kinetics of triblock copolymer (23% SF, 12K) modified (TM1) and unmodified (T) on Aerosil 120 (Solvent DCE, 22 °C).

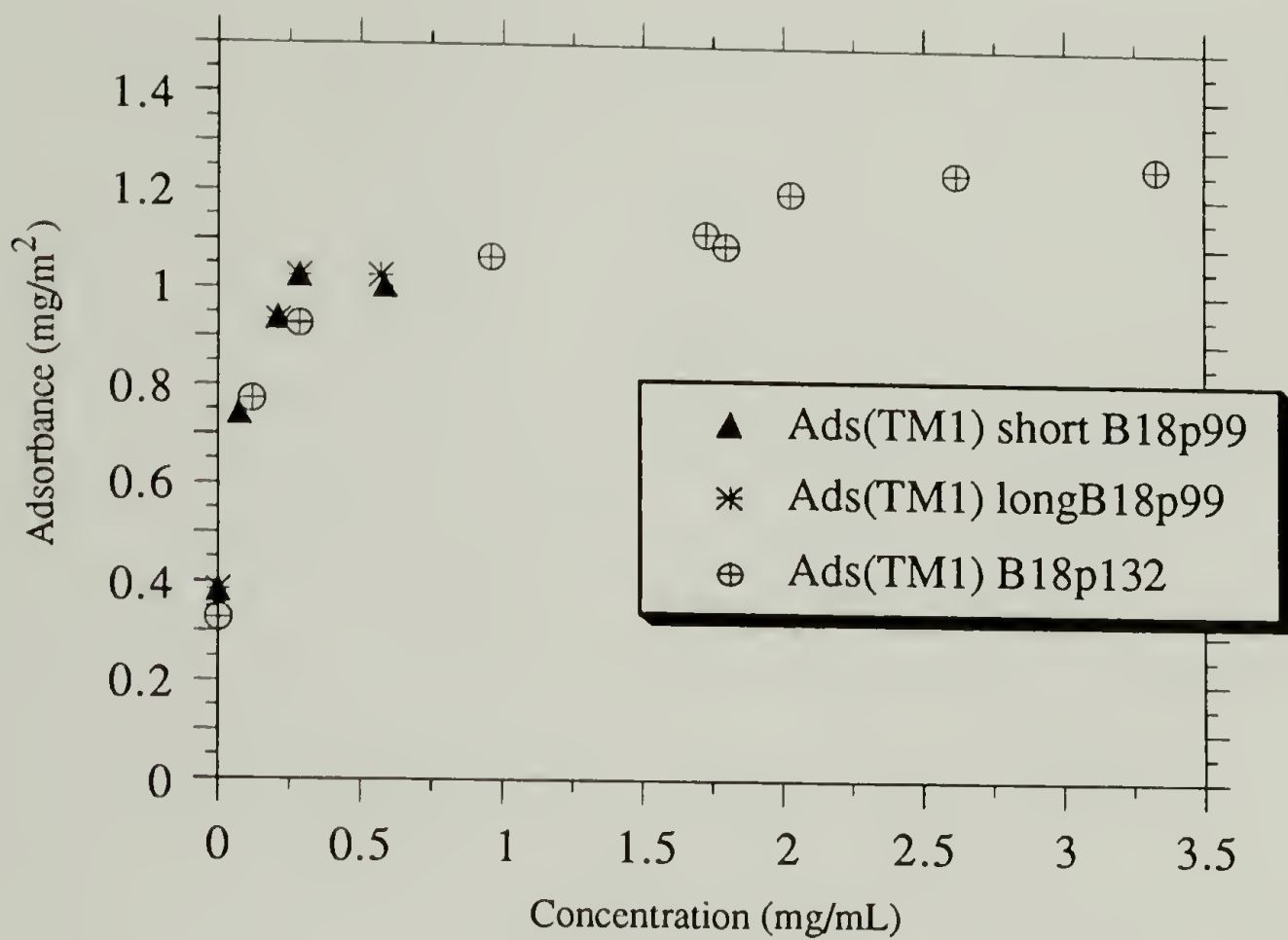


Figure 3.34 Adsorption isotherm of 23% triblock copolymer ($M_n=12K$, T23/12K TM1) on Aerosil 120 from DCE at 22 °C. Results are from three different sets of experiments.

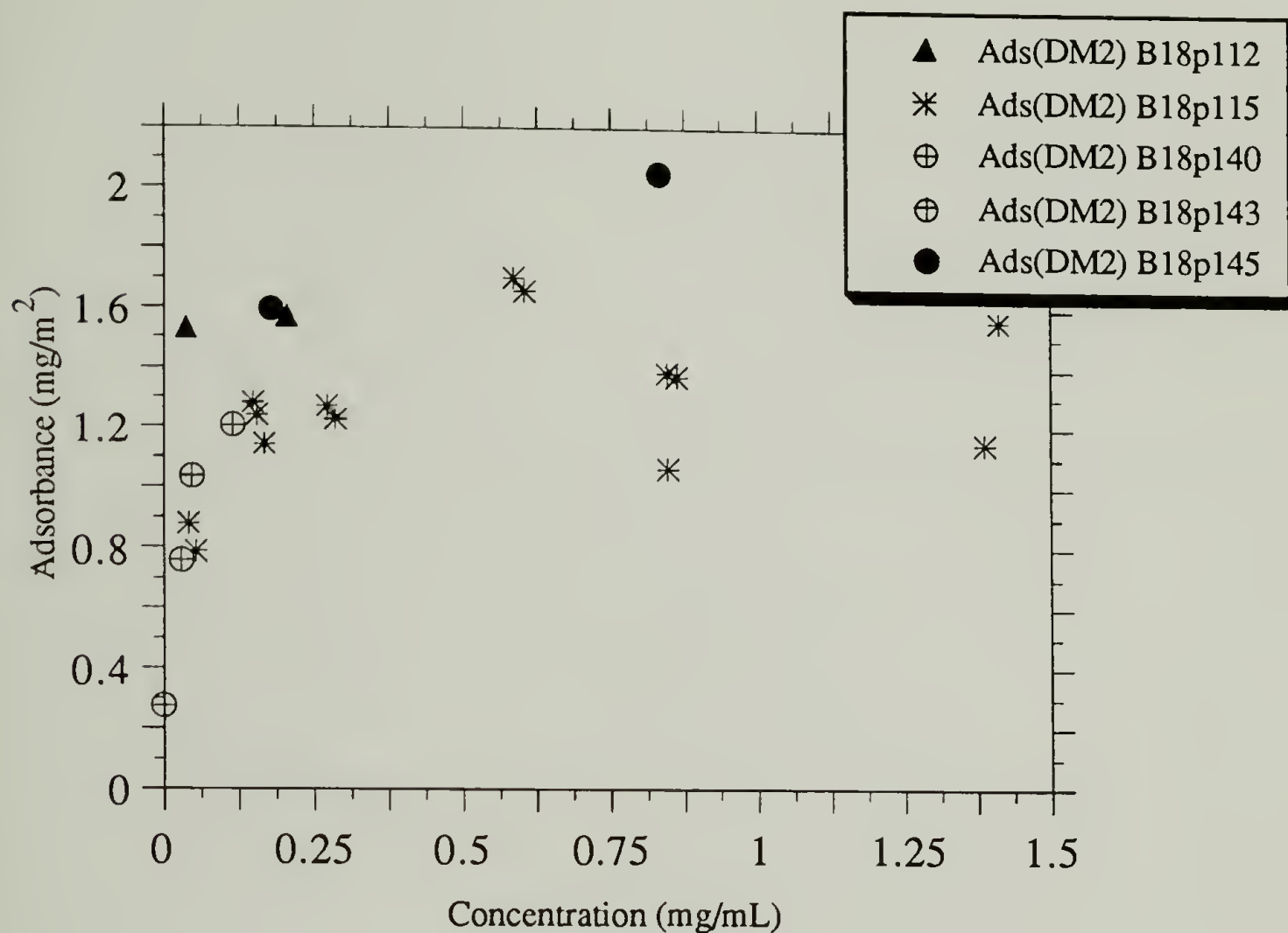


Figure 3.35 Adsorption isotherm of 23% diblock copolymer (M_n=13K, D23/13K DM2) on Aerosil 120 from DCE at 22 °C. The results are from five different sets of experiments.

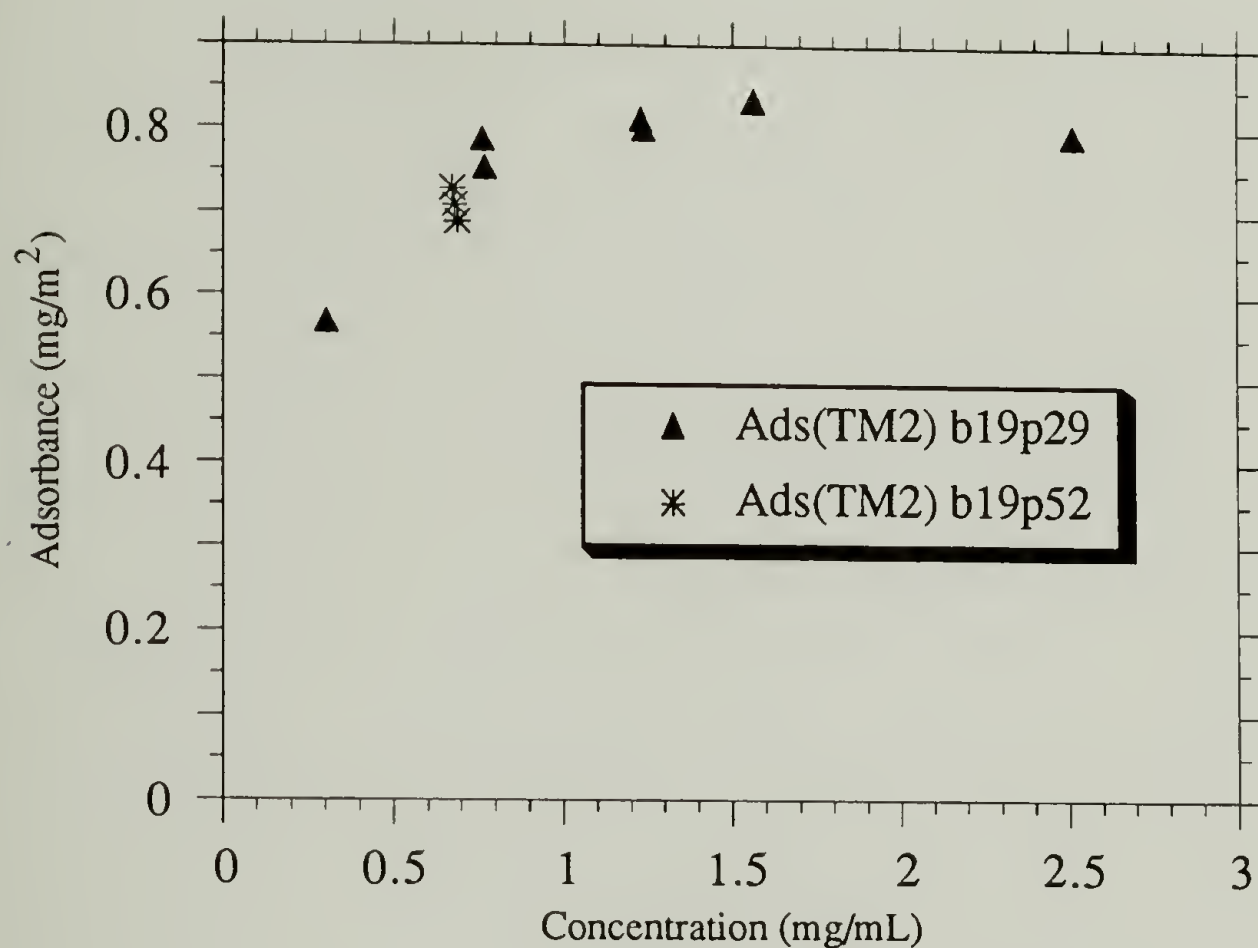


Figure 3.36 Adsorption isotherm of 23% triblock copolymer modified to 60% conversion ($M_n=12K$, T23/12K TM2) on Aerosil 120 from DCE at 22 °C. Results are from two different sets of experiments. Sticky block size is that of a 23% diblock but it is modified to only 60% which gives 14% SF.

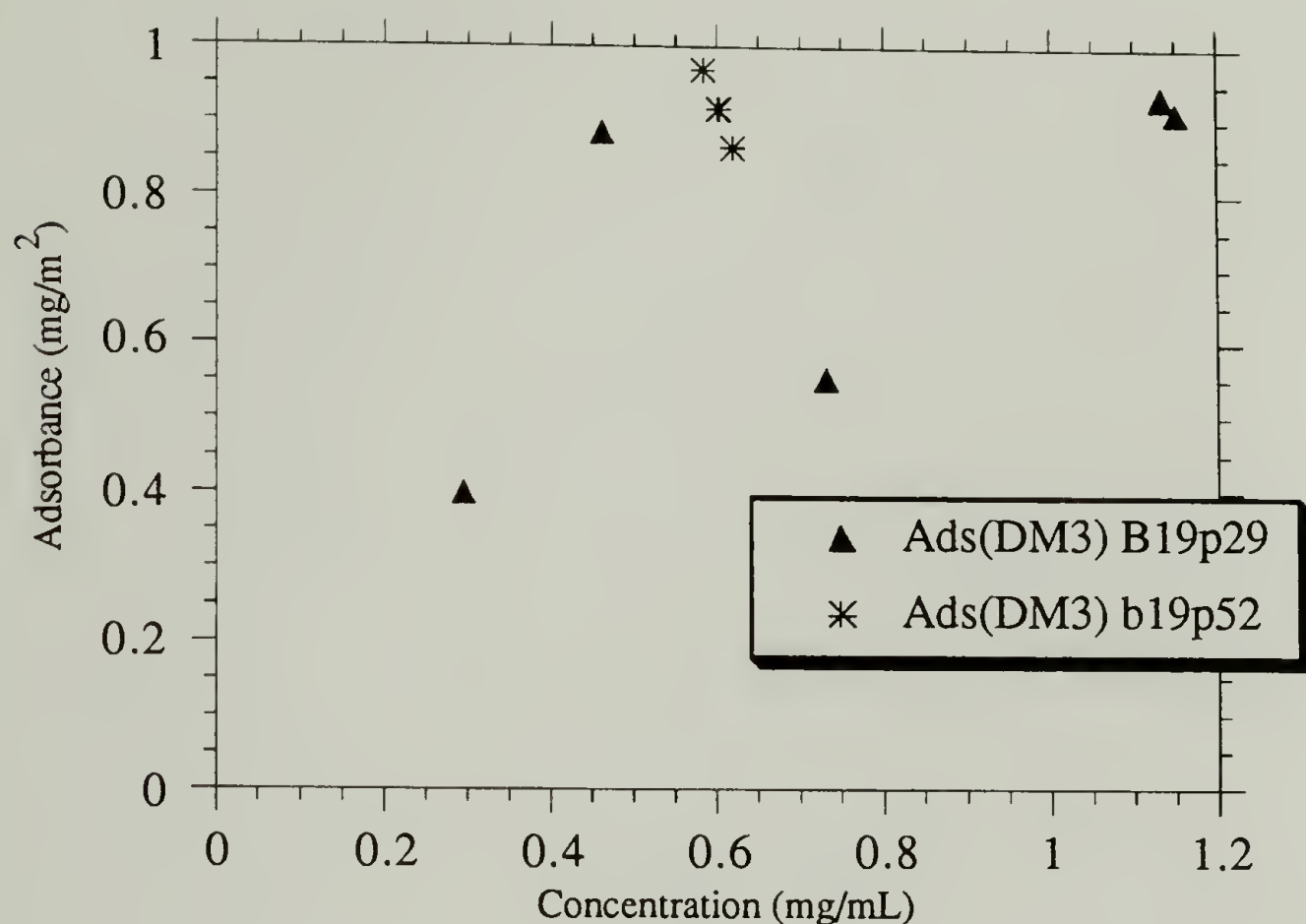


Figure 3.37 Adsorption isotherm of 23% diblock copolymer modified to 56% conversion ($M_n=12K$, T23/12K TM2) on Aerosil 120 from DCE at 22 °C. Results are from two different sets of experiments. Sticky block size is that of a 23% diblock but it is modified to only 56% which gives 13% SF.

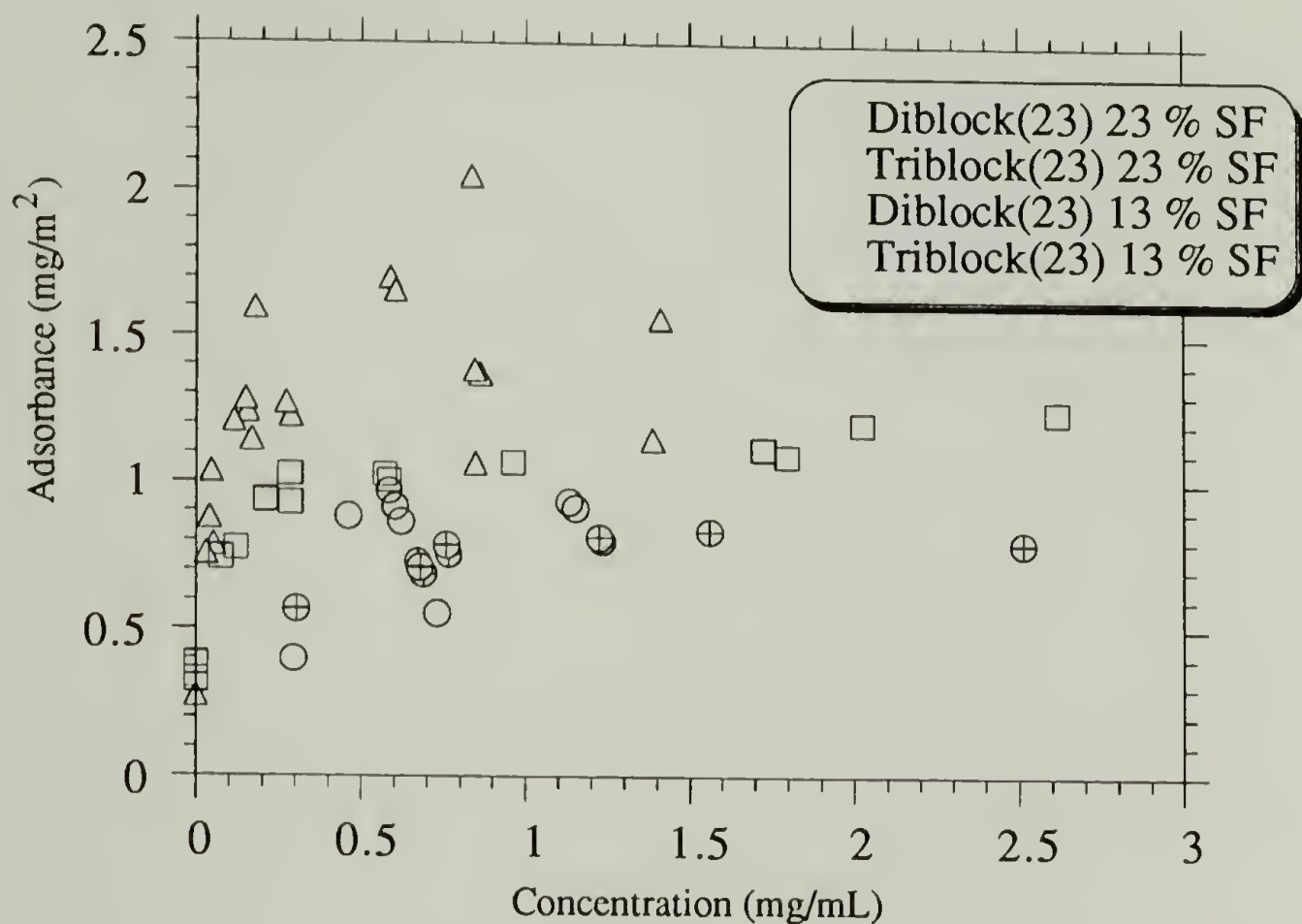


Figure 3.38 Combined adsorption isotherms for D23/13K DM2, D23/13K DM3, T23/12K TM1 and T23/12K TM2. Chain architecture, as well as percent SF, affect amount of polymer adsorbed. Note the scatter in the diblock data compared to the triblock data.

The isotherm experiments were carried out by two different methods: 1) each concentration point on the isotherm was determined from a separate solution adsorption experiment, or 2) the adsorption was carried out in the step fashion described below. A RB flask (~50 mL) with a known amount of aerosil and DCE was used. A known volume of concentrated polymer solution was added to give concentration c_1 . This was allowed to adsorb (for the required length of time) then an aliquot was taken and the adsorbance measured. This determined the first point (lowest concentration) on the isotherm, and then another known volume of polymer solution was added to give c_2 (where $c_2 > c_1$) and an aliquot taken. This was the second point on the isotherm. In this way the whole isotherm was determined. It was found that methods 1 and 2 yielded the same results. This can be seen in Figure 3.34 where the isotherm was determined using both methods. The B18p99 series was determined via the batch method whereas the B18p132 series was determined via the continuous step method. One can see that the same results are obtained in each case. On the other hand, when we tried the opposite experiment and tried to go down the isotherm (i.e. desorb by dilution) the polymer did not desorb. This can be seen in Figure 3.39 where the triangles are the data obtained via increasing concentration and the squares are the results from the attempted desorption. One can see that most of the polymer is not desorbed even after 24 h (some of the data points were determined 24 h after the dilution was carried out). We found that addition of small amounts of THF to the solution resulted in desorption of the polymer (exact quantification was not performed but it is estimated at close to 100% desorption). This experiment with THF indicates that the experimental procedure used to measure the desorption isotherm was sensitive and that if

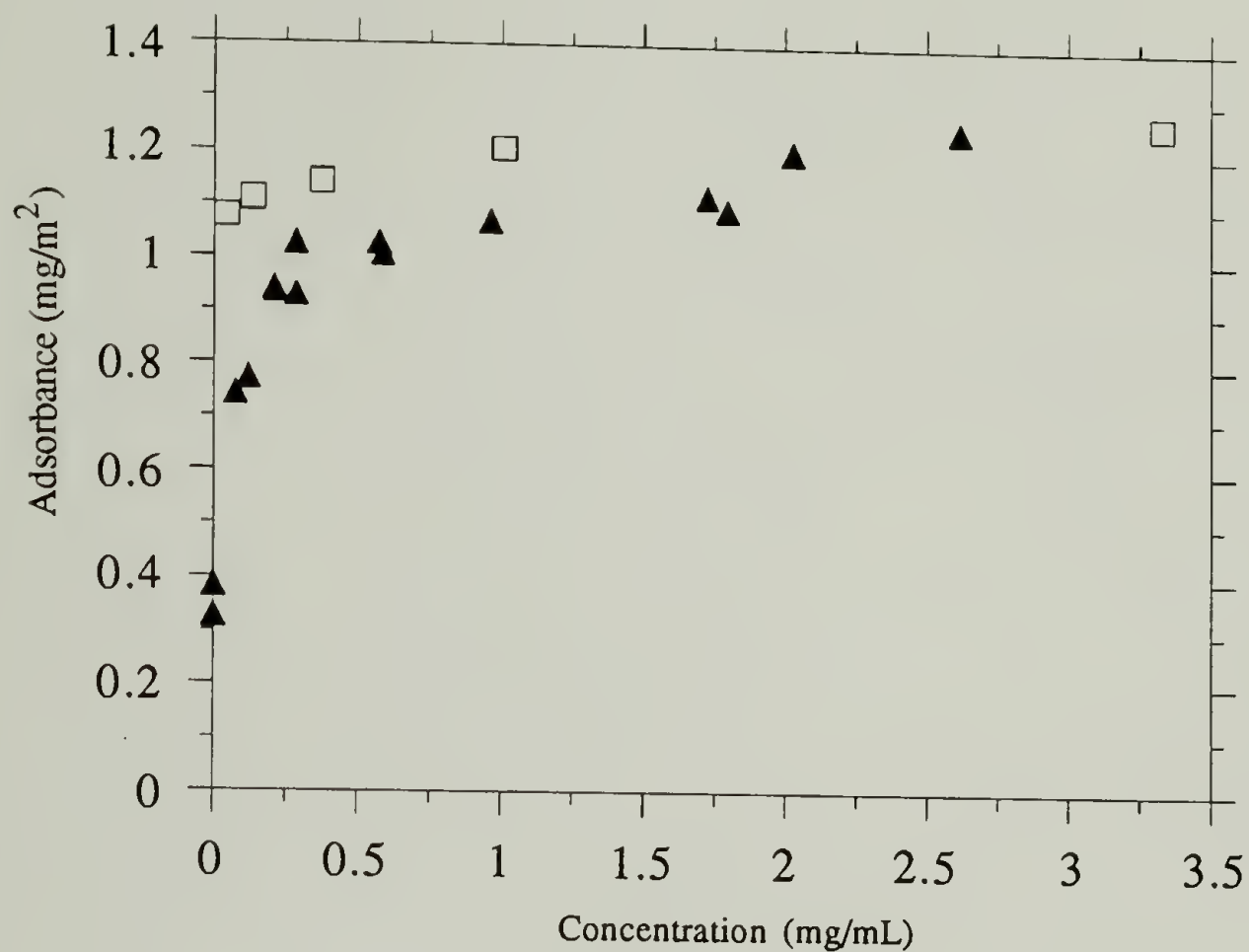


Figure 3.39 Adsorption (triangles) and desorption (squares) isotherms for 23% triblock copolymer ($M_n=12K$, T23/12K TM1) on Aerosil 120 from DCE at 22 °C. Most of the polymer is not desorbed upon dilution even after 24 h.

polymer was desorbing we would have seen it. It also tells us that the addition of just a small amount of a displacer molecule results in the desorption of the polymer; this is also in agreement with the TLC data obtained. We found that the amount of polymer adsorbed (T23/12k TM1) was a function of the temperature. Figure 3.40 shows that the adsorbance decreases with increasing temperature. This is explained by the fact that the solvent strength is increasing and causing the osmotic crowding term to increase which in turn makes some of the polymer desorb (or adsorb as the case may have it). We found that the effect of temperature was extremely facile: the solution was cooled and the adsorbance increased, and then the solution was warmed and the adsorbance decreased (this happens at most on the order of minutes). The high and low temperature data shown in Figure 3.40 are only approximate values because the separation had to be carried out at room temperature (the centrifuge tubes were insulated and spun for short periods of time, the triblock copolymer was measured thus separation was not a problem). Nonetheless the main trends are very interesting. These results indicate that the adsorbance is affected by the concentration of the polymer in solution and the solution temperature. The fact that dilution would not effect the desorption of the polymer suggests the adsorbed polymer chains are not exchanging with the chains in solution (if they were equilibrium would be easily attained). Thus, there is probably a dynamic equilibrium between the sticky feet of the adsorbed chains but not an exchange with the chains in solution. Adsorbed polymer that is placed in a more dilute solution is in a kinetically trapped nonequilibrium state because there is no means of displacing the polymer chains (the activation energy required for all the SF to desorb at once is too high). On the other hand when the solution concentration is increased the

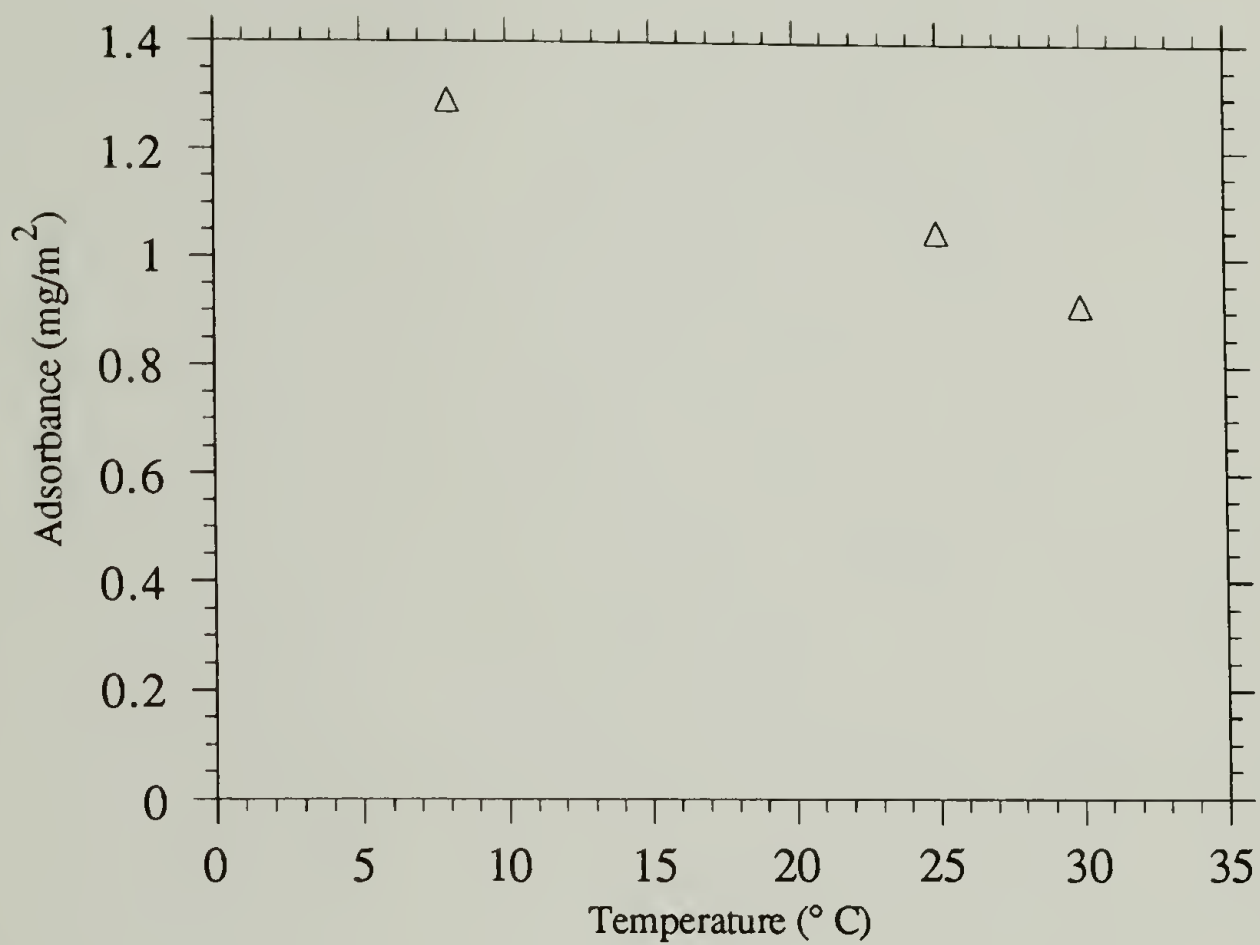


Figure 3.40 Effect of temperature on adsorbance of 23% triblock (Mn=12K, T23/12K TM1). Increasing temperature decreases adsorbance.

new equilibrium can be easily attained because the new chains can come in and displace some of the segments of chains that are already there. The effect of the displacer molecule is also easily explained in this regard; the added THF is able to displace the adsorbed sticky feet and thus cause the polymer to desorb (i.e. it has an effective pathway to desorption). The effect of temperature is rather intriguing and there are two possible scenarios. The first is that the increase in temperature causes a decrease in the interaction energy of the surface because of its exothermic nature. A alternative explanation (the one which is favored here) is that the adsorbed polymer crowding energy increases with temperature so that as the feet are in dynamic equilibrium, the chains segments pull back when the feet let go. In other words polymer chains in the adsorbed layer directly feel the effect of the temperature whereas the lower solution concentration is not felt directly by the chains. The increased temperature also gives more thermal energy to the system which may result in more rapid individual SF adsorption/desorption dynamics and thus give the polymer chain a better chance to desorb.

Batch Adsorptions on Glass Beads

Because of the separation difficulties encountered in the diblock adsorptions onto aerosil we decided to try a different substrate. The requirements (for this new substrate) were: that it be approximately silica (we used glass), non-porous, have a large enough size to allow easy separation, and that the specific area be high enough that a measurable decrease in solution volume could be seen. Glass beads with a diameter of 3-10 μm were used in these experiments. The beads were obtained from Polysciences and no size distribution information was available, so an

accurate specific area could not be calculated (BET was not performed either). The specific area should range from $0.4 \text{ m}^2/\text{g}$ to $0.12 \text{ m}^2/\text{g}$, this is calculated for 100% $3 \text{ }\mu\text{m}$ and 100% $10 \text{ }\mu\text{m}$ beads respectively (neglecting any surface roughness). This is approximately 4 orders of magnitude less than the aerosil. These beads which have a radius of curvature on the order of microns are essentially flat in the eyes of a polymer coil ($\sim 80 \text{ }\text{\AA}$). It should be noted that this is quite different than the situation with aerosil where the coils was of the same size scale as the adsorbing polymer. The adsorptions were carried out in a fashion similar to those for aerosil, but due to the much lower specific area about half of the suspension volume consisted of these beads. These adsorption experiments worked well and separation was not a problem. Figure 3.41 shows that the polymers adsorbed with high affinity type isotherms that had a knee at less 0.5 mg/mL . We see that the diblock copolymers (plateau value $\sim 1.7 \text{ mg/g}$) again are found to adsorb to a greater extent than the triblock copolymer (plateau $\sim 1.4 \text{ mg/g}$). This corresponds to an adsorbance range of 4.25 mg/m^2 - 14.2 mg/m^2 for the diblock and 3.5 mg/m^2 - 11.7 mg/m^2 for the triblock copolymer (calculated using the specific area values given above). In contrast to the results obtained on aerosil, the effect of SF conversion within the block is minimal. We ascribe this to the differences in the geometry of the two surfaces. Here we see that the flat surface does not show the effect. The aerosil exists as branches of fused spheres where each branch has approximately the same diameter size scale as the adsorbing polymer coil. We postulate that this causes a decrease in the bound fraction of the sticky block as opposed to the adsorption on a flat surface. The polymer coil has to distort more to obtain the same number of SF/surface contact points. This causes the adsorptions on aerosil to be more

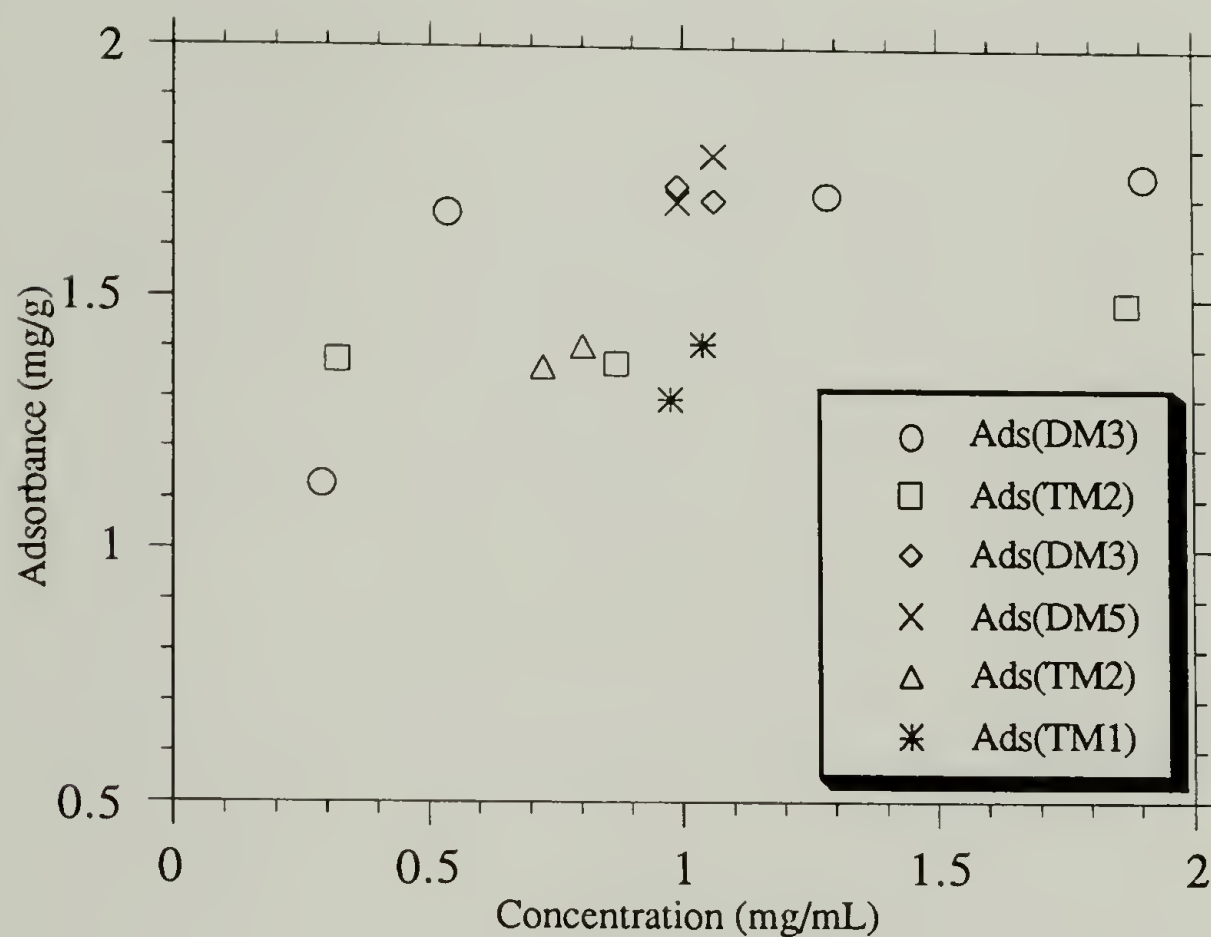


Figure 3.41 Adsorption data for 23% SF diblock and triblock copolymers from DCE onto 3-10 μm glass beads. Diblocks (D23/13K DM5 and D23/13K DM3) adsorb significantly more than triblocks (T23/12K TM1 and T23/12K TM2). The DM3 and TM2 are approximately 50% modified.

sensitive to the fraction of modification on the sticky block. The other argument is that the aerosil geometry allows the chain to adsorb with a higher higher bound fraction, thus a lowering of the functionalization (of the sticky block) would be expected to have a greater effect on the chain adsorbed to aerosil.

Column Adsorption: Measurements and Results

As discussed in the previous sections, measuring the amount of polymer adsorbed was not a trivial matter. The aerosil tended to be stabilized by the diblock copolymers and accurate determination of the amount adsorbed was compromised. We found that glass beads (3-10 μm) could be used to obtain accurate data. These small beads are expensive; if one does not recycle them, each run costs \$15. (The beads were recycled to economize.) To solve this problem the adsorbent was packed in an HPLC column and in this way it was thought that the adsorbent could be used repeatedly. Different sized columns were packed with various adsorbents and plumbed into an HPLC system, and polymer solution was pumped through at a known flowrate. To determine the amount adsorbed the detector response was measured as a function of time. Much work was done on this and the procedure evolved as it went; the final setup and procedure are described below. A somewhat similar set-up has been reported by Pfefferkorn using a continuous stirred tank apparatus and radio labeled polymers.⁹⁶

We measured the amount of polymer adsorbed to a given surface via the setup diagrammed in Figure 3.42 (column adsorption apparatus). The system used two adjustable flowrate HPLC pumps. Pump #1 was used to

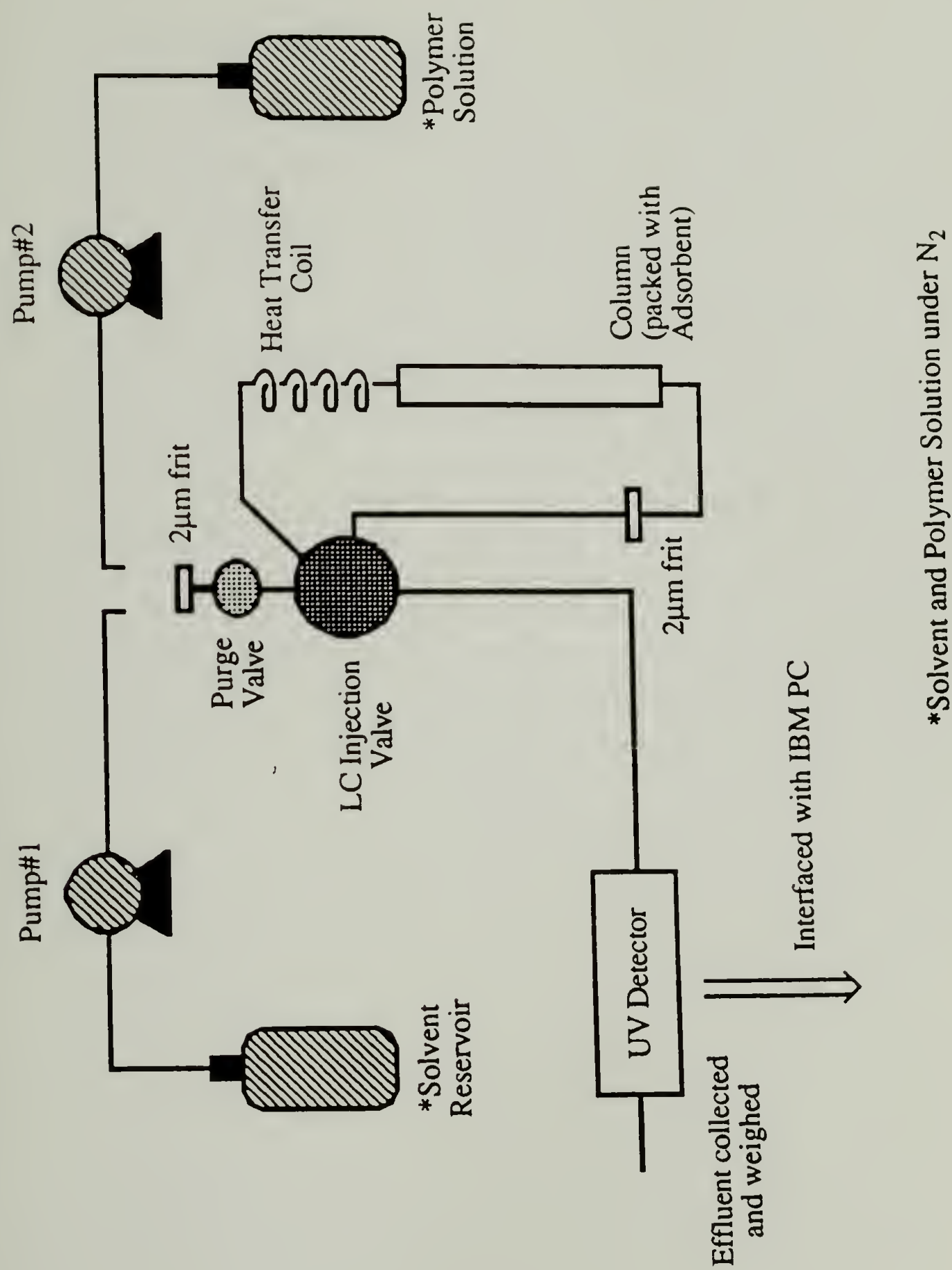


Figure 3.42 Column adsorption apparatus.

pump solvent (in most cases DCE) and pump #2 was used to pump the polymer solution. Both the solvent and the polymer solution were kept under dry N₂ during the adsorption process. The two pump systems were alternately attached to the remainder of the apparatus via connection to the 2 μ m frit. Since the connection was on the high pressure (low dead volume) side of the pumps there was very little mixing and the crossovers from solvent to polymer solution and vice versa were clean. The tubing was extended to an HPLC injector valve. An HPLC column (5.0 x 0.46 cm) was packed with adsorbent and plumbed into the sample loop ports of an HPLC injector valve. This allowed the column to be switched on- and off-line easily without leakage. The valve outlet flowed through a variable wavelength UV detector where the absorbance of the solution was measured. The detector was interfaced with an IMB PC. The effluent was collected and weighed, this weight and the time were used to determine the flowrate.

The adsorbance was measured and the detector response was plotted against time. Figure 3.43 shows a plot of the raw data obtained using the procedure described below. The column was packed with adsorbent and attached to the setup. Pump #1 was connected and pure solvent (DCE) was pumped through the column at 1 mL/min for 10 min. After the column was conditioned, it was taken off-line, the flowrate was turned down 0.25 mL/min and the DCE baseline was established (t_0 to t_1). At this point (t_1) pump #2 was attached and polymer solution of a known concentration was pumped through the system (at 0.25 mL/min). The baseline rose and became constant when all the solvent had been pushed out. This gave the polymer solution baseline as shown. The column was put in-line at t_2 , and

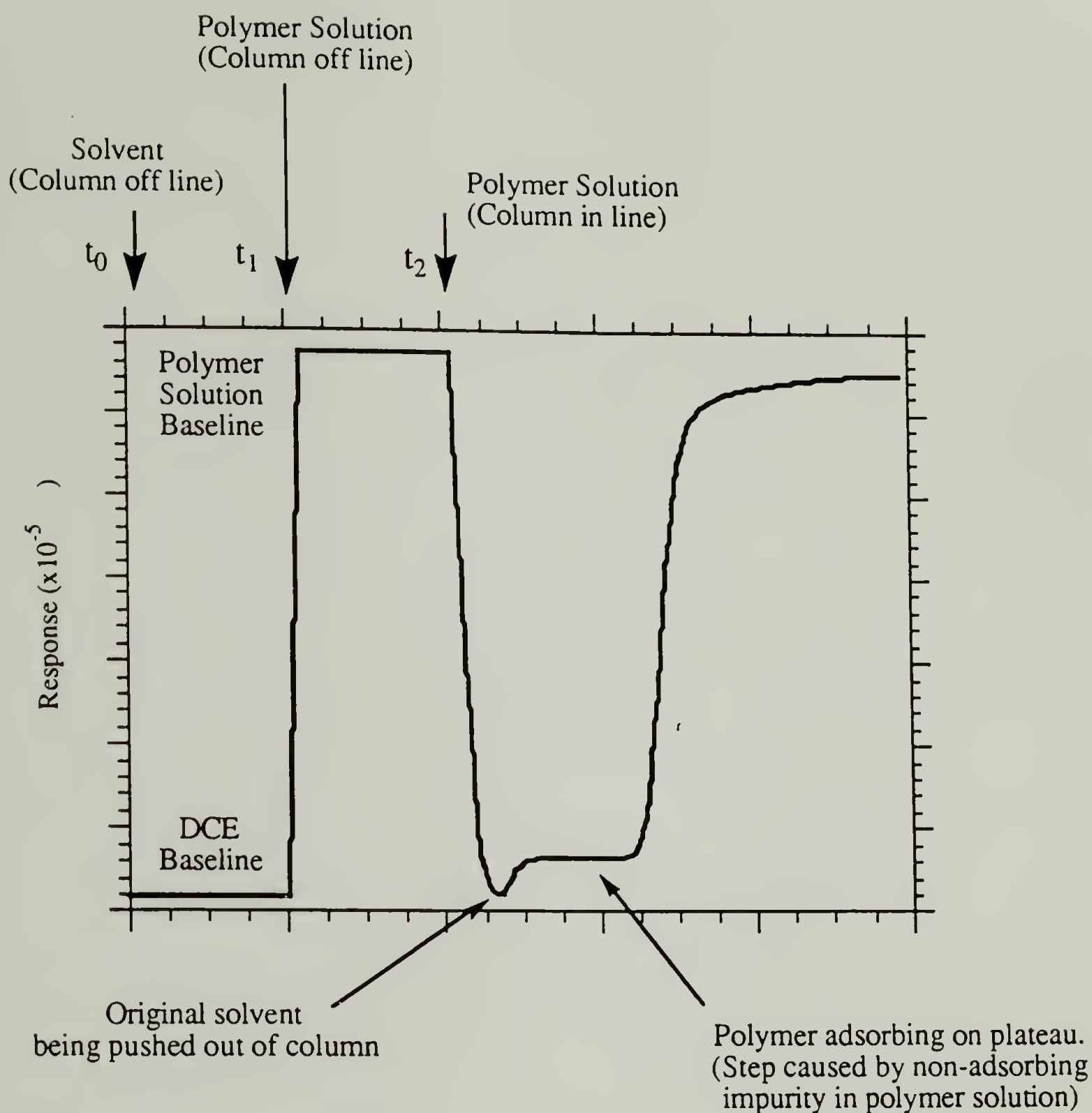
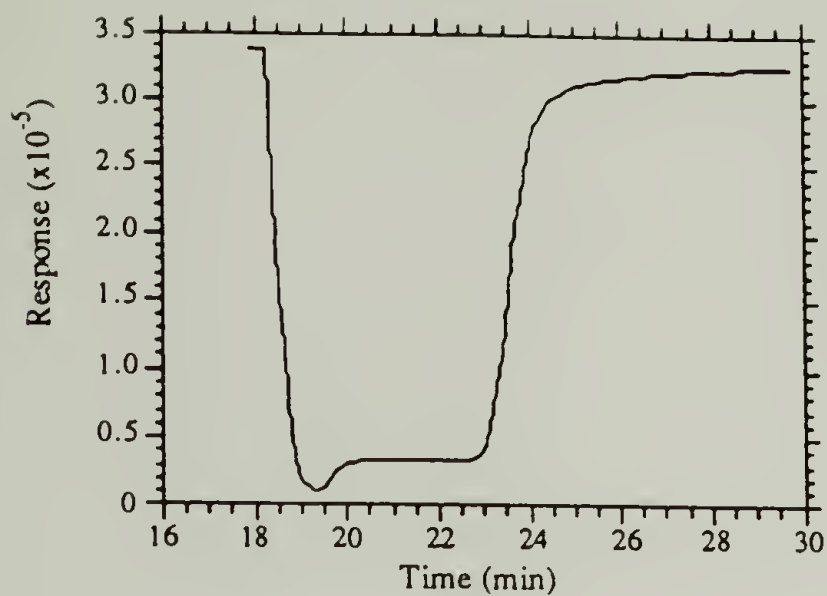


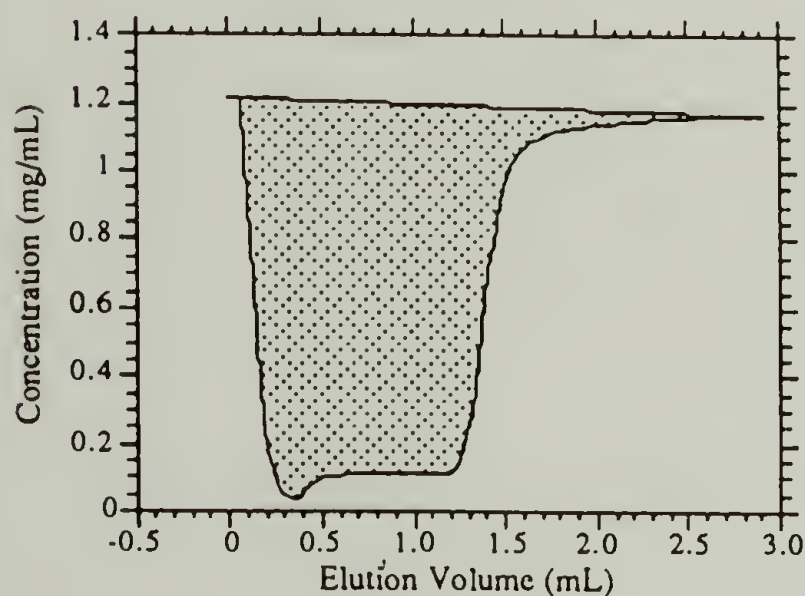
Figure 3.43 Column adsorption method explanation. Typical data for a column adsorption experiment is shown above. Initially, at t_0 , the solvent is run through and the DCE baseline obtained. The polymer solution is then put on-line (t_1) and the detector response increases to that of the polymer solution. The column is put on-line at t_2 and the response immediately drops approximately to the DCE baseline. If no polymer adsorbs, the response rises rapidly and the plot resembles a fairly symmetric inverted peak. If polymer adsorbs (as in this case), a plateau region is seen. The small rise to the plateau is caused by a small amount of non-adsorbing impurity in the polymer solution.

the absorbance dropped, initially because pure solvent was being pushed out of the column, and then because of adsorption of polymer on the column. This signal stayed near zero until the adsorbent was saturated and then rose to approach that of the initial polymer solution at the end of the run.

The amount of polymer on the column can be determined in one of two ways (see Figure 3.44). The raw data consists of detector response, R , as a function of time (Figure 3.44 (A)). The elution time can be converted to elution volume by multiplying by the flowrate. The detector response has been determined to be a linear function of the absorbance of the solution ($A=f(R)$). The absorbance can be converted to concentration via a Beer's law calibration function $c=g(f(R))$. This has been measured repeatedly and is fairly linear up to about 1.5 mg/mL (~1.5-2.0 absorbance units). At higher concentrations both 2nd and 3rd order polynomials have been used to fit the calibration curve. The response versus time can be converted into concentration versus volume as seen in the Figure 3.44 (B) (Integral method): the amount of polymer in the column (both adsorbed and in solution) is equal to the shaded area. This method, the integral method (Int), is inherently the most accurate way to determine the amount of polymer in the column. The area under the curve has been calculated (and thus the adsorption determined) using a spreadsheet program to facilitate the various conversions from the calibration (i.e. Excel). In the second method, V_{sat} , the saturation volume (volume eluted before the column was saturated) is estimated. The amount was then calculated as the product of the saturation volume and the initial polymer concentration. The saturation volume is determined by taking the derivative of the

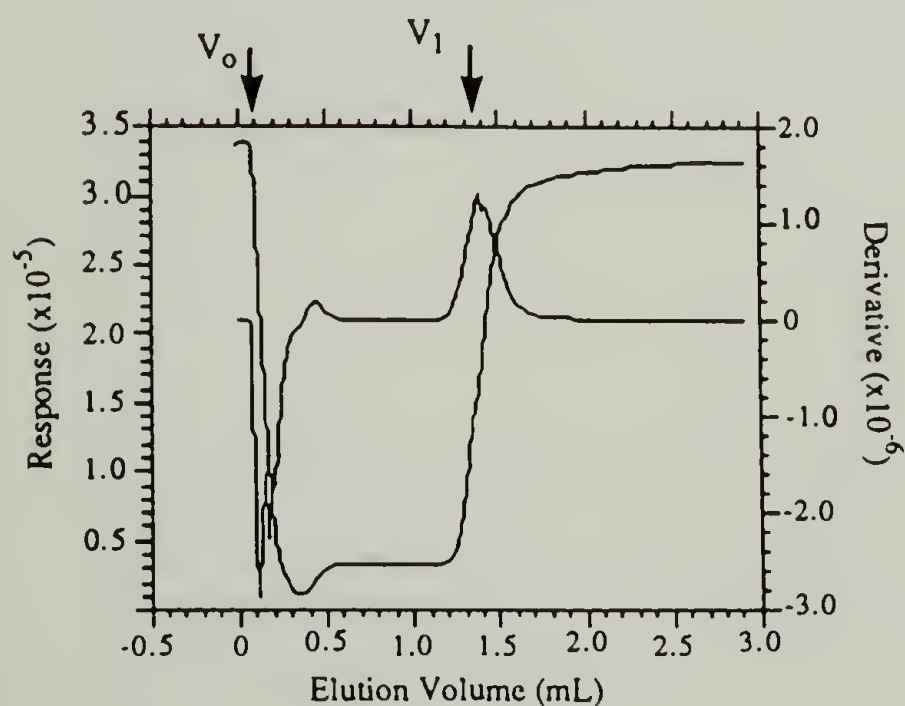


A) Raw Data is detector response versus time



B) Integral method

The shaded area equals the amount of polymer in the column (mg)



C) Vsat method

Estimate the area as
Amount = $(V_1 - V_0) \cdot C_0$

V_1 and V_0 are determined from the maximum and minimum of the derivative

Figure 3.44 Column adsorption manipulation.

response, a typical example can be seen in Figure 3.44 (C). The derivative plot shows a minimum at approximately the onset of the drop (i.e. at V_o) and a maximum approximately 1/3 to 1/2 way up the concentration rise at the end of the run (V_1). V_{sat} is taken as the difference, $V_1 - V_o$.

Determination of V_{sat} in this manner has no rigorous foundation, but it works well and is objective (i.e. can be done by the computer). The V_{sat} method was tested with the area method to insure the accuracy and the results are tabulated in Table 3.19. The agreement is fairly good and the largest discrepancy is only 8.2%.

Table 3.19 Comparison of Determination of the Amount Adsorbed:
 V_{sat} versus Integral Method.

<u>Sample</u>	<u>Conc</u> <u>(mg/mL)</u>	<u>Response</u>	<u>Ads(V_{sat})</u> <u>(mg/g)</u>	<u>Ads(Int)</u> <u>(mg/g)</u>	<u>V_{sat}-Int/V_{sat}</u>
J27-5	1.988	589,088	2.141	2.114	1.3%
J27-6	1.988	589,531	2.304	2.146	6.9%
J27-2	1.005	331,341	1.929	1.901	1.5%
J27-4	0.500	174,150	1.650	1.544	6.4%
J27-8	0.500	185,878	1.614	1.622	0.5%
J27-9	0.250	94,860	1.494	1.371	8.2%

Both methods have been tested and both have drawbacks. The integral method is inherently more accurate but depends heavily on accurate determination of the Beer's law functions for each particular polymer. Even with accurate determination, the functions become too non-linear (above approximately 2 mg/mL), thus putting an upper limit on the polymer concentrations that can be used. On the other hand, the saturated

volume, V_{sat} , method is only an estimate of the amount of polymer in the tube, but its advantage is that it requires only accurate flowrate measurements; the concentration relation is not needed and higher concentration solutions can be used. The data reported here were obtained using the saturated volume method.

Both methods determine the amount of polymer in the column which includes the adsorbed polymer and the polymer in solution. One can write this as

$$\text{Total Amount} = (V_{\text{sat}}) \times (\text{conc}) = \Gamma + (DV) \times (\text{conc}) \quad 3.7$$

where DV is the dead volume in the column. Therefore one needs to determine the dead volume to calculate the amount of polymer adsorbed (Γ). There are two ways of doing this. The total amount can be determined using a polymer that does not adsorb (PTBS for instance), and thus $\Gamma=0$. A plot of Total Amount versus concentration will give a line of slope equal to DV with an intercept of zero. The dead volume can also be determined by measuring the total amount of polymer on the column using an adsorbing polymer in the concentration range of the isotherm plateau, and then the slope will be equal to the DV with an intercept equal to the plateau adsorbance. Both methods have been used; the latter is reported here in Figure 3.45. The slopes for the two different polymers match very well and give a dead volume equal to 0.365 mL which agrees well with that calculated from the manufacture's value of 0.37 mL.

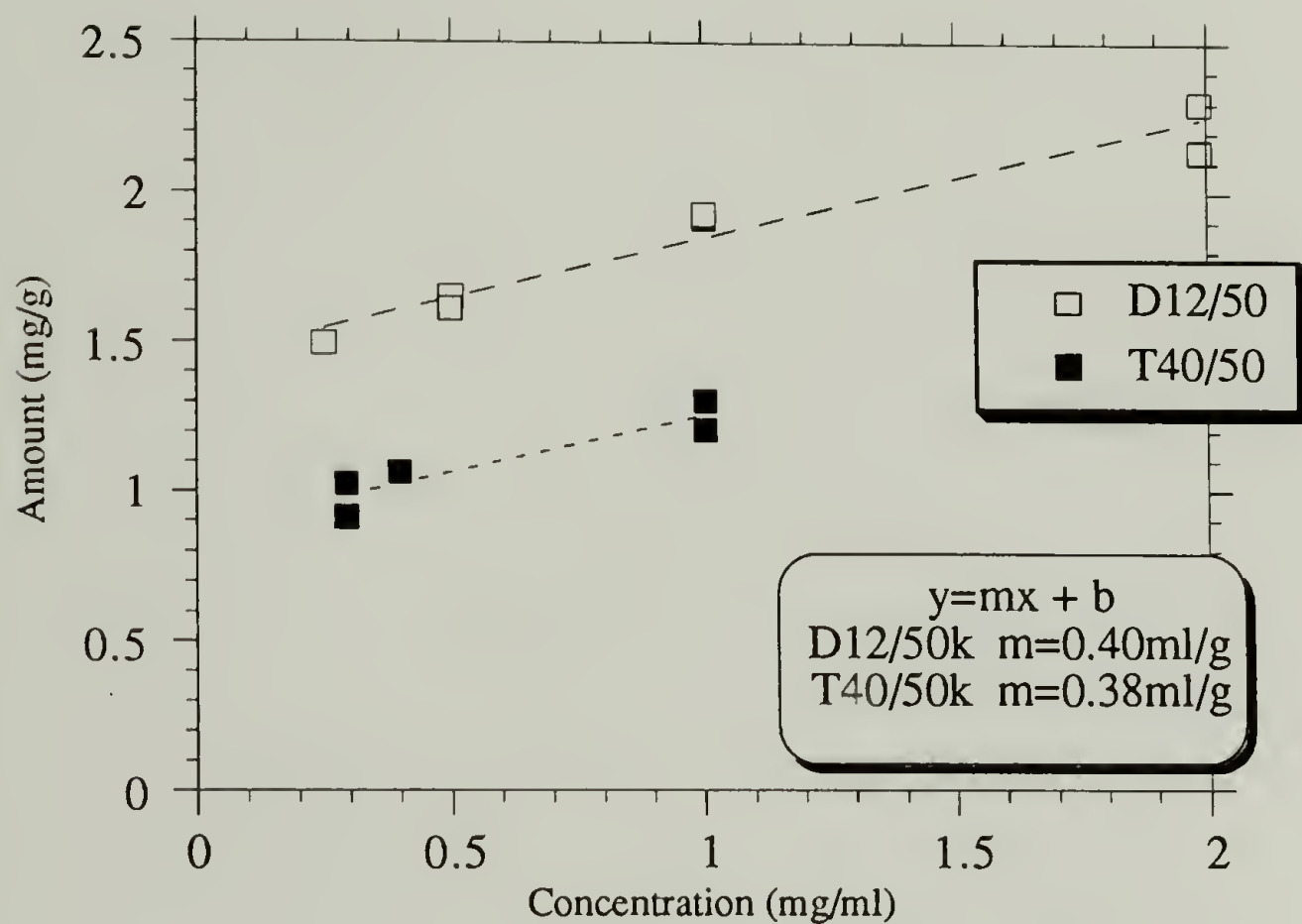


Figure 3.45 Column dead volume determination for V_{sat} method using silica gel (5 x 0.46 cm column, 0.93 g silica gel). Amount of polymer in column is plotted as a function of concentration. Slope is proportional to dead volume and intercept is plateau adsorbance. Polymers used were a 12% SF diblock (D12/50K) and a 40% SF triblock (T40/50K) both with $M_n \sim 50 \text{ K}$.

The method just described was used to measure adsorbances of eight polymers. Isotherms were determined and the temperature dependence of the adsorption was investigated. Originally we envisaged this technique to have many more applications and to be more useful than it was for this work. We planned on the following scenario: The adsorbent would be packed into the column and the column conditioned. The polymer would be adsorbed as described above and the amount adsorbed would be determined by the integral method. A displacer solvent would then be used to desorb the polymer. The desorption peak would be measured and the amount adsorbed determined from this area also. The displacer solvent would be washed out of the column with the adsorption solvent and the column would be ready for another adsorption run. In this way the expensive adsorbent would never be lost and the same amount of adsorbent would always be used. We also would measure the adsorption at different temperatures by placing the column in the appropriate temperature bath. We also planned to investigate the critical adsorption temperature by adsorbing a polymer on the column at low temperatures and then ramping the temperature up to see how and when the polymer desorbed (i.e. does it all come off at once or is it very gradual?). We also had plans to determine critical displacer concentrations via a procedure similar to that described for the temperature induced desorptions, but using a gradient HPLC procedure instead of a temperature ramp. It was found that most of the above mentioned goals could be achieved when the 23 % SF 13K polymers were used. Reproducible results were obtained using the above described procedure, DCE as the adsorption solvent and THF as the displacer. It was found, though, that the $M_n=50K$ polymers would foul the column (this was not noticed with the smaller polymers). Thus successive

adsorptions lead to a steady decrease in the amount of polymer adsorbed (this decrease was only 1-2 % usually but the direction was always toward less polymer adsorbed). The fact that the THF would not totally clean the column of the higher molecular weight samples can be understood at least reasonably from the TLC data that was presented previously where we found that these samples required substantially higher displacer concentrations before they were desorbed. We investigated using different column washes such as THF/MeOH and DCE/isopropanol but found the results less than satisfactory (the alcohols are better displacers but poorer solvents, thus they were used as mixtures with good solvents). The columns were cleaned with these solvent mixtures, but the amount of defouling was difficult to quantify. Also it was seen that the alcohol washing caused the column frits to clog, thus creating new experimental difficulties and also suggesting that new ill-understood phenomena were occurring. It was decided that there were too many variables and that the determination of the cleanliness of the column was problematic. It also seemed that the column was fouled progressively more at higher temperatures; this prohibited adsorbance measurements at elevated temperatures and also the investigation of the critical desorption temperature. It can be surmised that the combination of high temperatures and high SiO₂ surface area (or some minor impurity in the glass) catalyzed hydrolysis of the esters or reaction with the hydroxyl group. These complications necessitated that the column be repacked with new adsorbant for each run. Thus, another advantage of using this method was lost. For this reason very small columns (Upchurch guard columns 2x0.19 cm) were used and packed with the small (3-10 μ m) glass beads. These held approximately 1/13th the amount of adsorbent as the other

columns and allowed us to use the small beads economically. The results obtained using these small columns were very reproducible (the detector responses matched well) but determining the amount adsorbed from the data was a little dubious. The amounts of polymer that were adsorbed were so small that the concentrations never dropped to zero on most of the runs (usually they dropped down about half way). The plateau regions were either small or nonexistent. Determination by the integral method was greatly effected by nonlinearity in the calibration because the peaks did not go all the way down. The small saturation volumes also prohibited accurate determination by the V_{sat} method. The obvious ways to remedy these problems are by the use of slower flow rates and lower concentrations. The latter could not be used because we wanted to measure the adsorbance in the plateau region of the isotherm. The slower rates were not viable because the HPLC pump became unreliable at low flow rates (we were already using 0.25 ml/min). Thus, there were logistic problems with the adsorption measurement on these small columns. It was determined that the small columns were too small and that larger columns were needed. The larger columns required larger amounts of adsorbent and so we decided to use silica gel. We then decided to check out the reproducibility of the columns with Silica gel and found that it worked very well.

The V_{sat} method was used to measure the adsorbance of a series of eight polymers ($M_n \sim 50$ K), four diblocks and four triblocks with sticky foot (SF) contents of 5%, 12%, 23% and 40%, from dichloroethane onto silica gel. The original response versus volume data are plotted (Figures 3.46 through 3.53) for all eight polymers. One can see that there is good

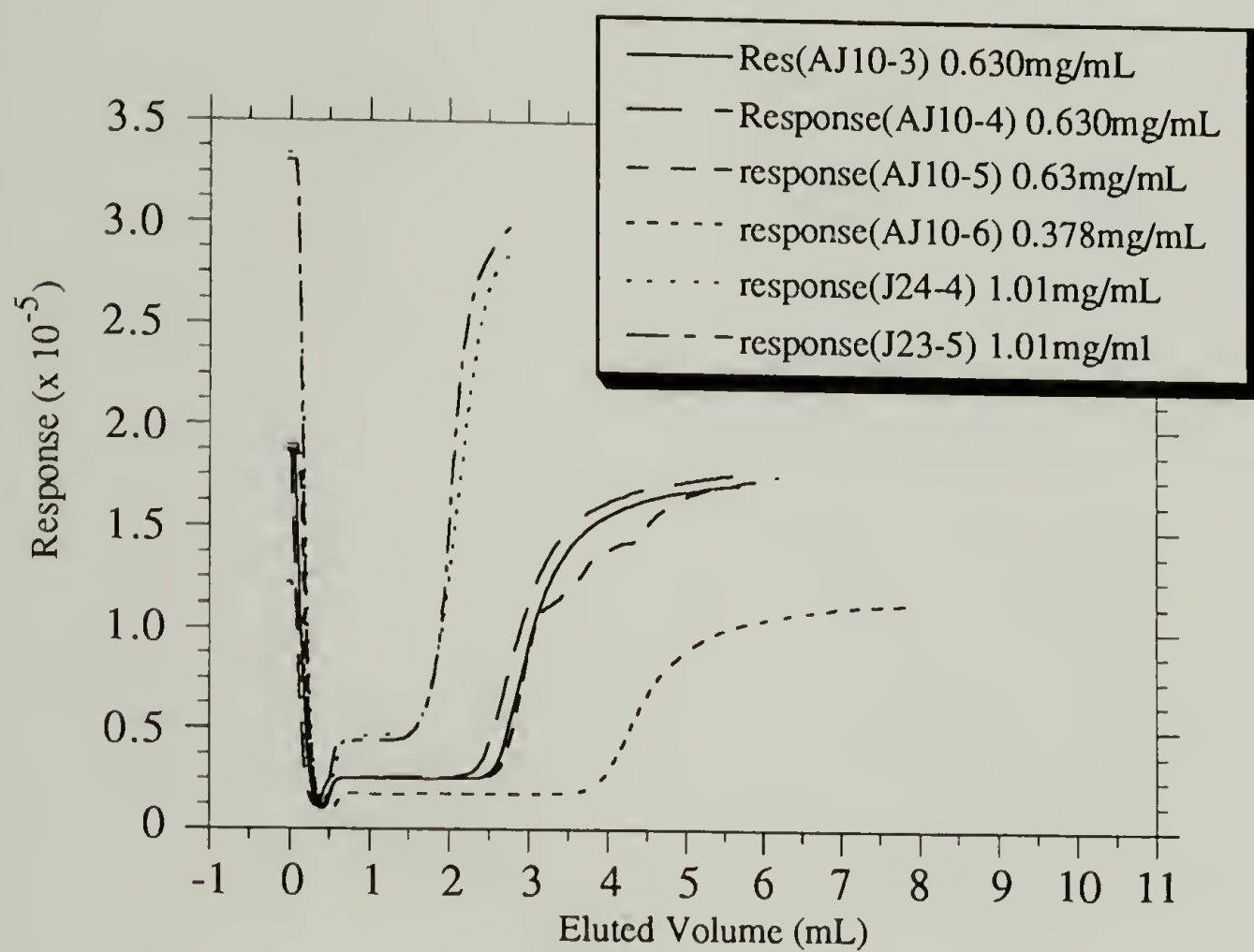


Figure 3.46 Vsat data for 5.8% SF diblock copolymer, $M_n = 51K$ (D5/50K). Polymers adsorbed from DCE onto silica gel at 22 °C.

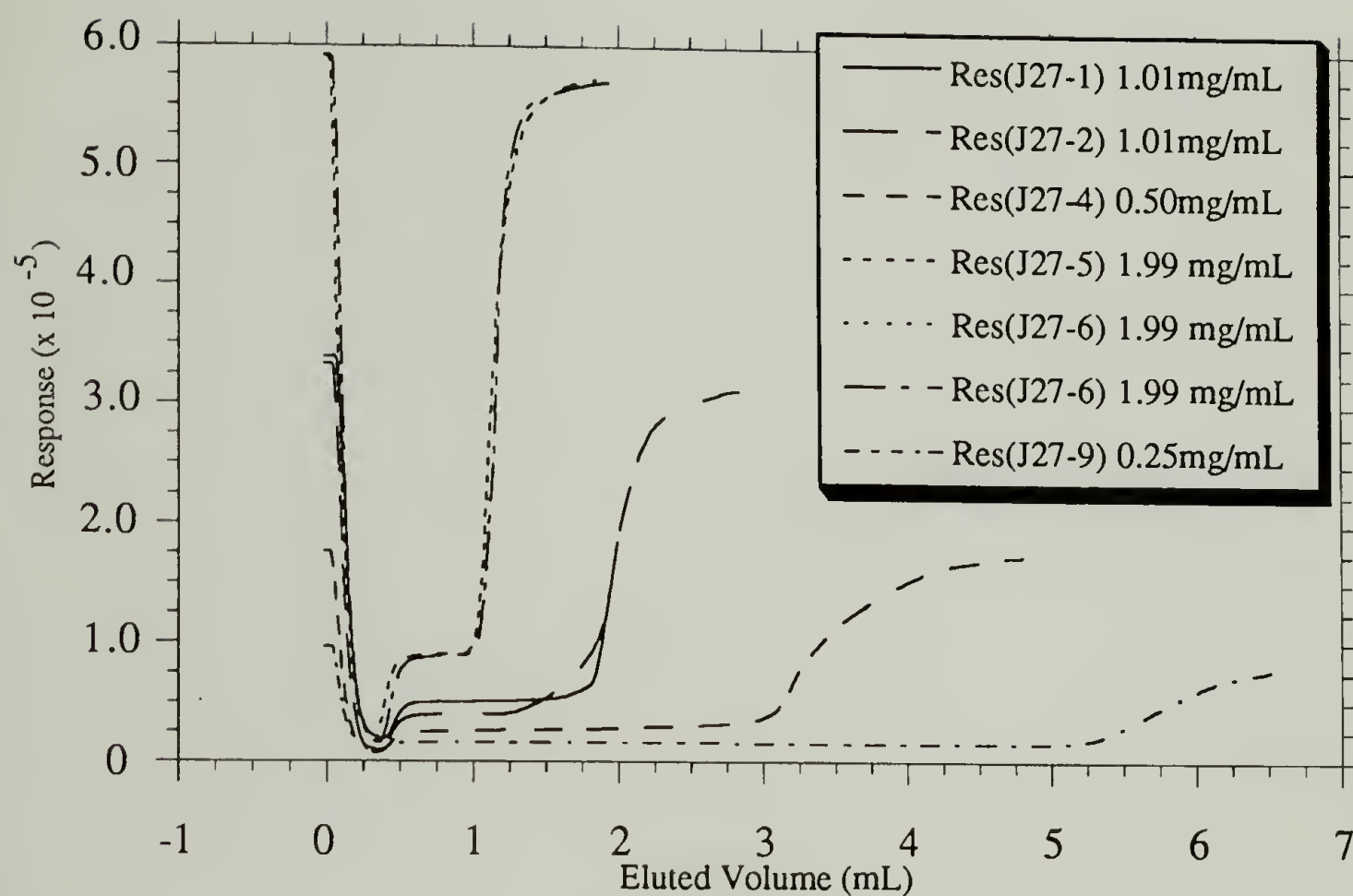


Figure 3.47 Vsat data for 13.0% SF diblock copolymer, $M_n=49K$ (D12/50K). Polymers adsorbed from DCE onto silica gel at 22 °C.

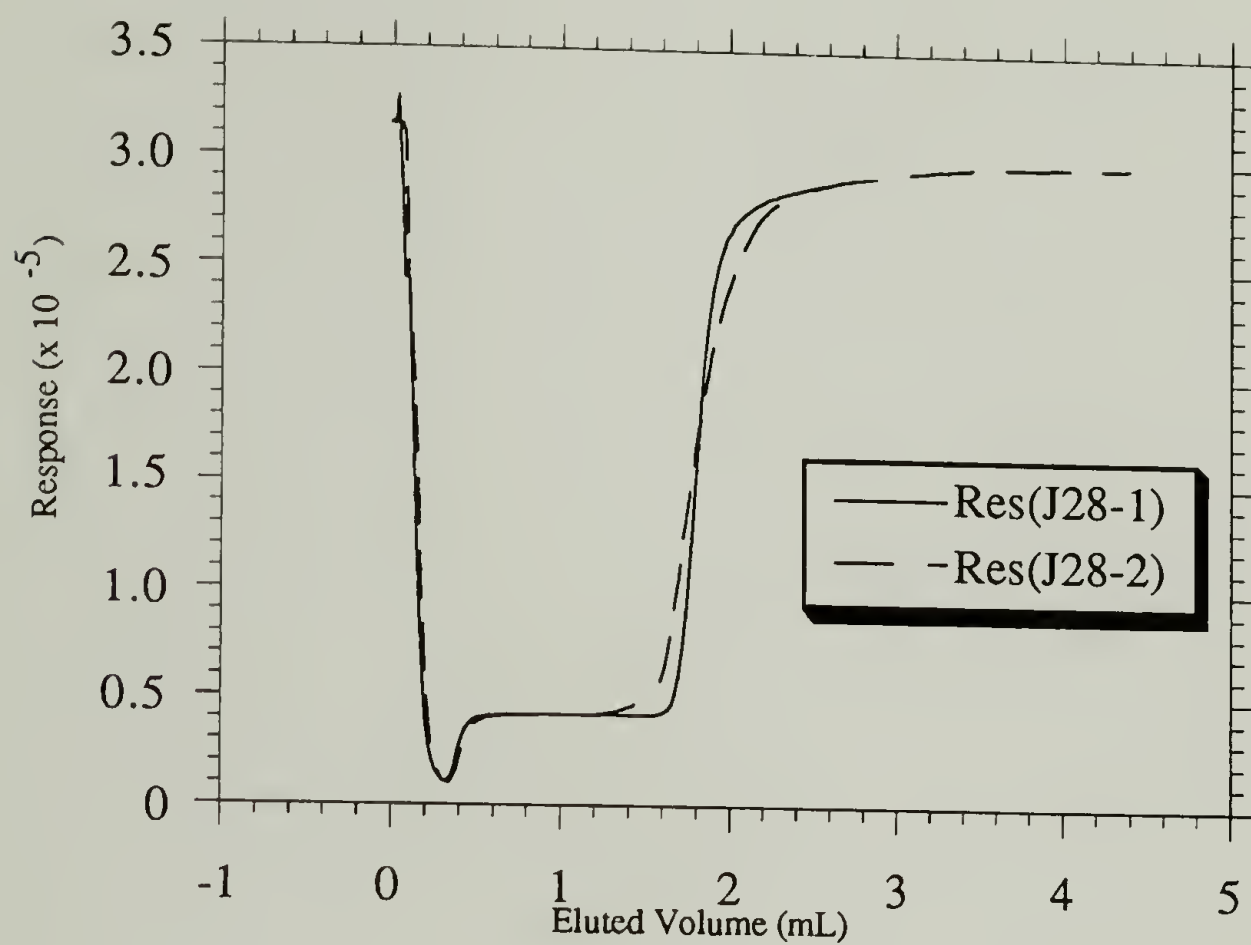


Figure 3.48 Vsat data for 23.5% SF diblock copolymer, $M_n = 46.5K$ (D23/50K). Polymers adsorbed from DCE onto silica gel at 22 °C.

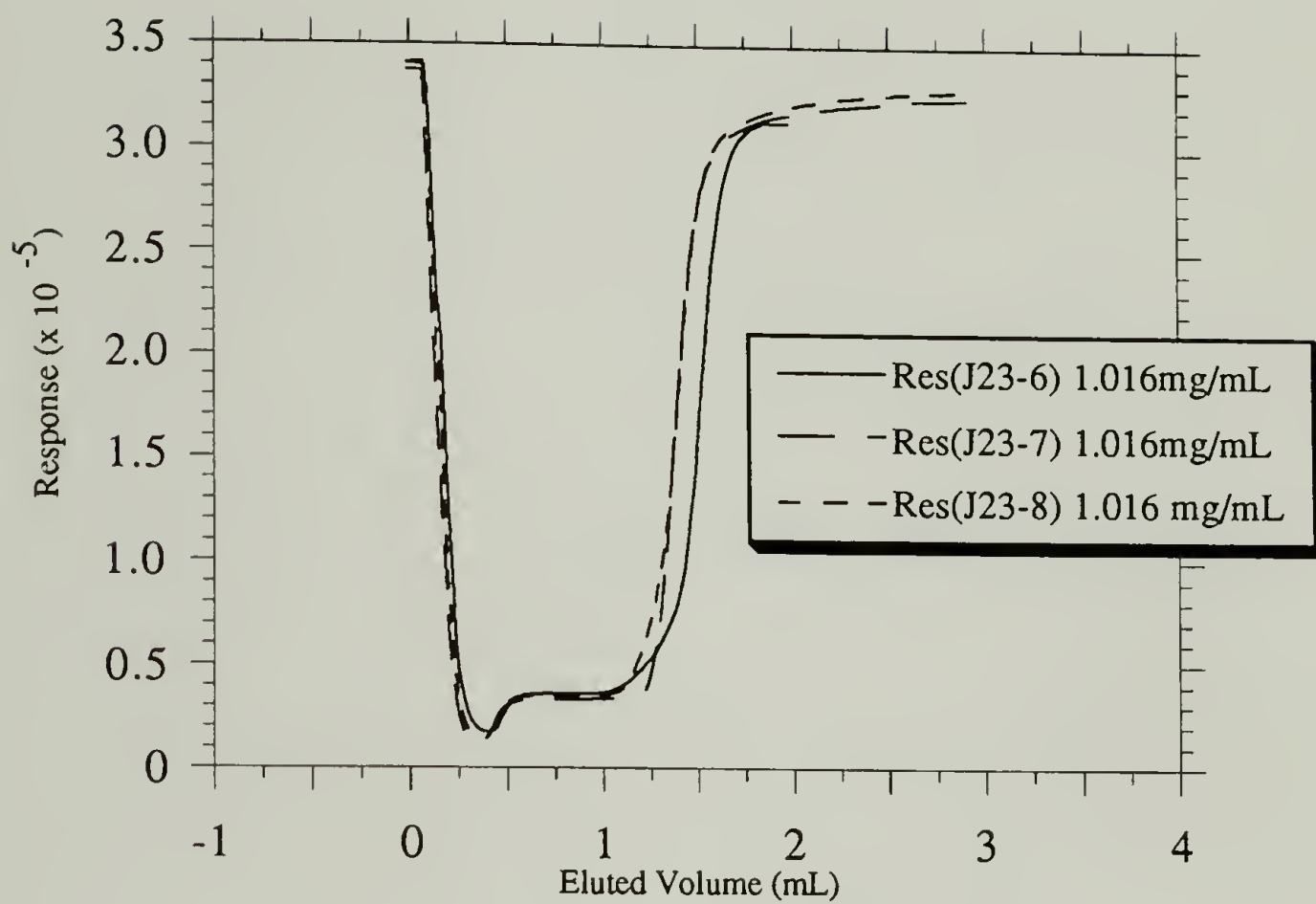


Figure 3.49 Vsat data for 38.2% SF diblock copolymer, $M_n = 52.2$ K (D40/50K). Polymers adsorbed from DCE onto silica gel at 22 °C.

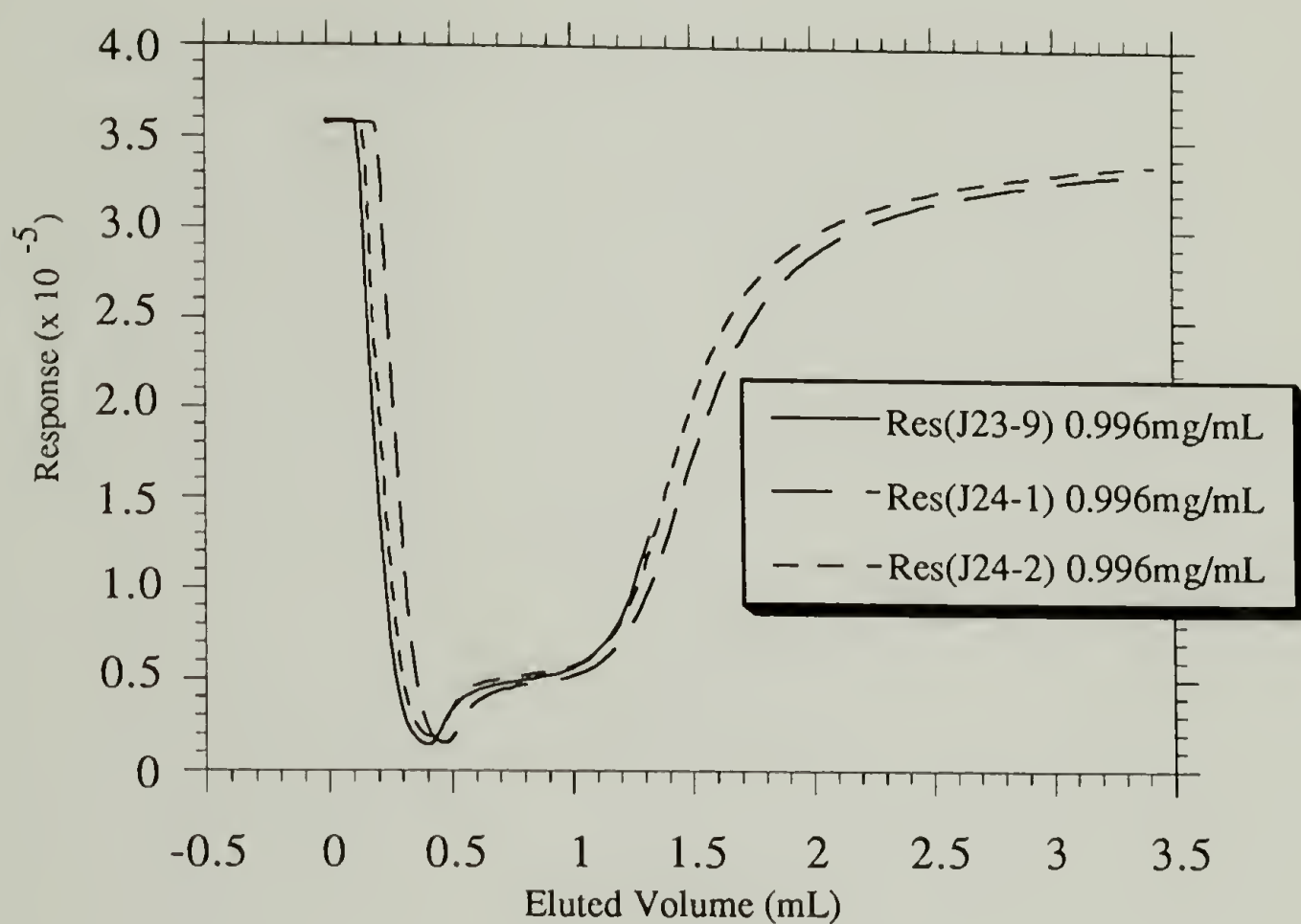


Figure 3.50 Vsat data for 6.2% SF triblock copolymer, $M_n = 46$ K (T5/50K). Polymers adsorbed from DCE onto silica gel at 22 °C.

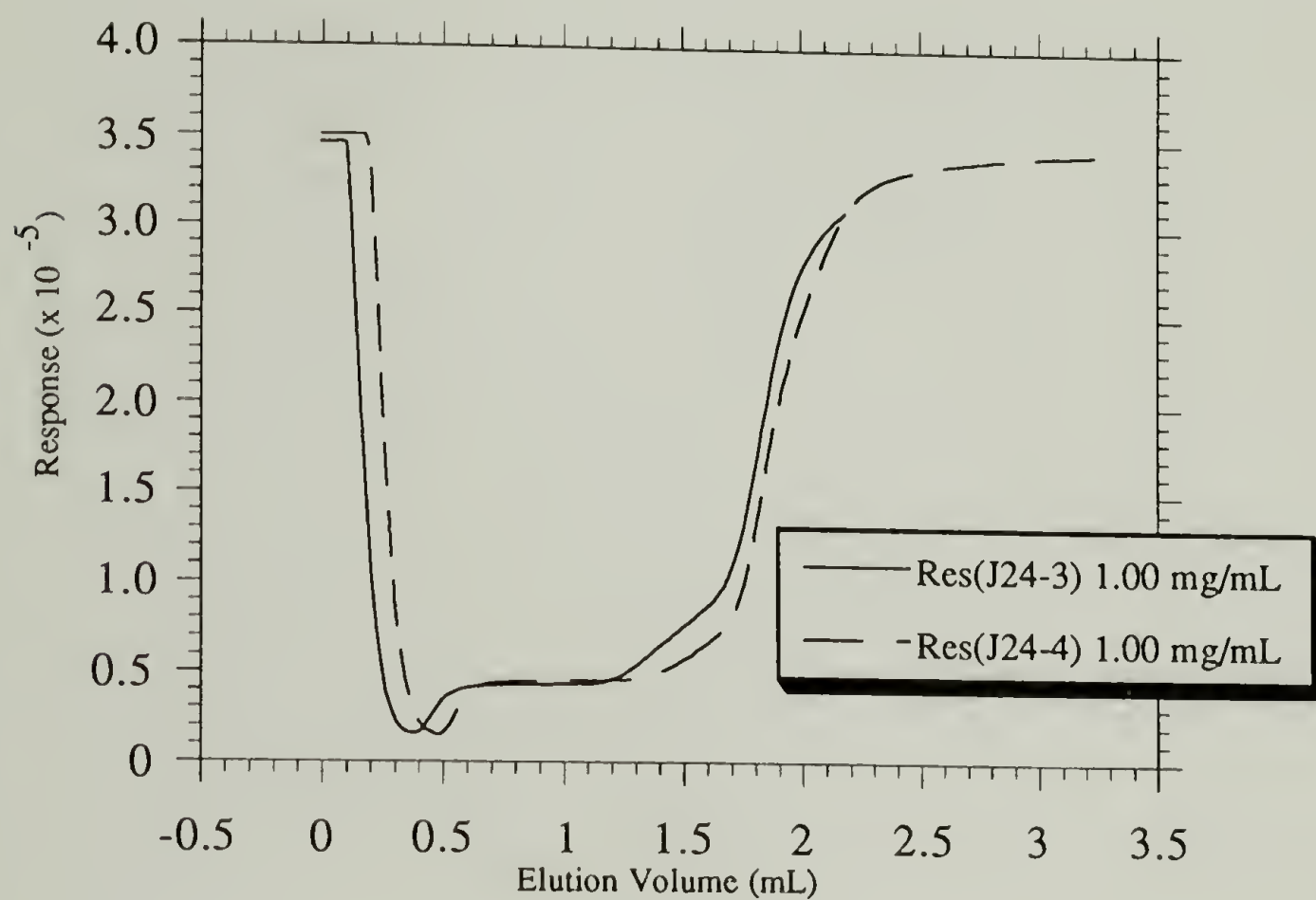


Figure 3.51 Vsat data for 13.8% SF triblock copolymer, $M_n = 50.2$ K (T12/50K). Polymers adsorbed from DCE onto silica gel at 22 °C.

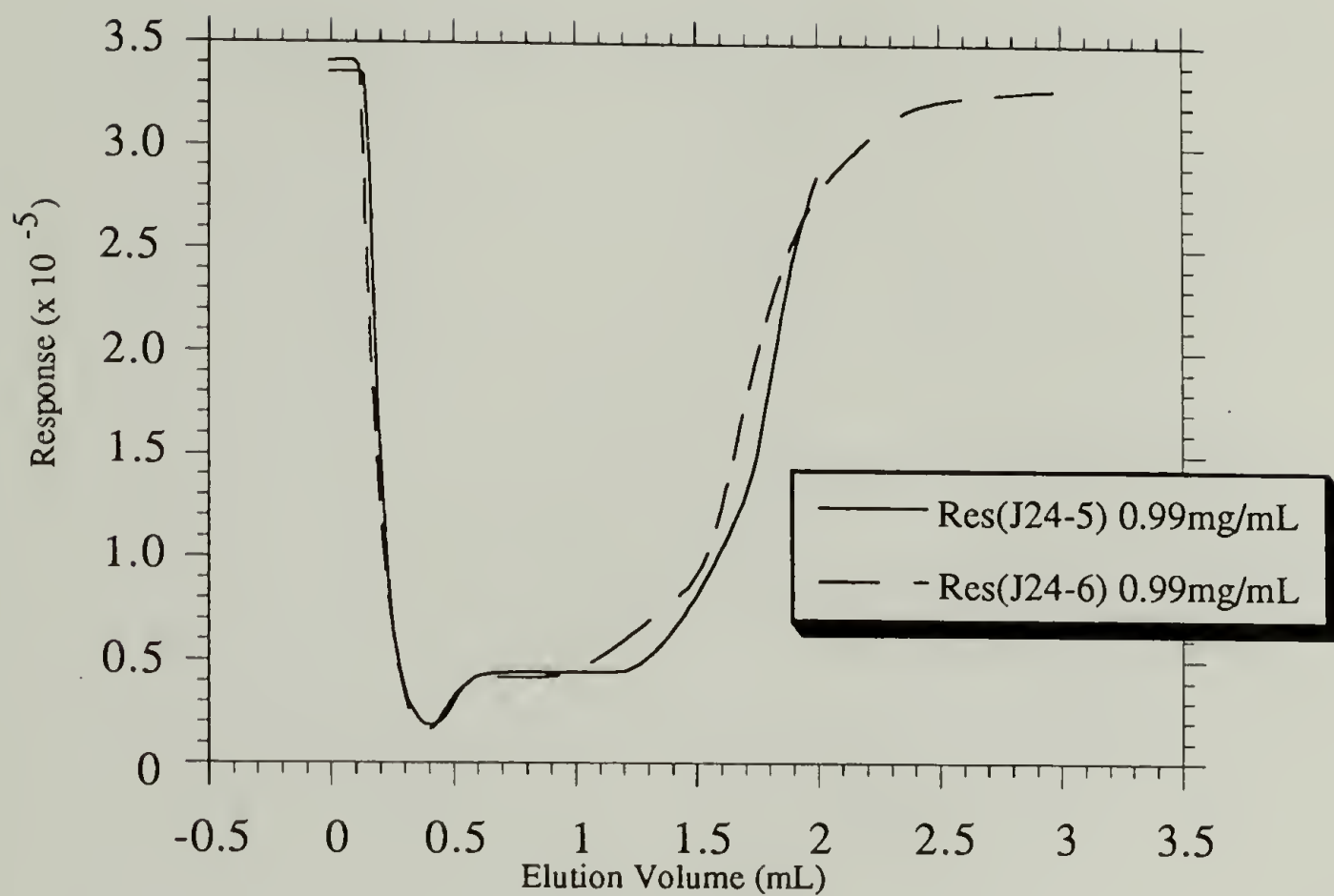


Figure 3.52 Vsat data for 24% SF triblock copolymer, $M_n = 46$ K (T23/50K). Polymers adsorbed from DCE onto silica gel at 22 °C.

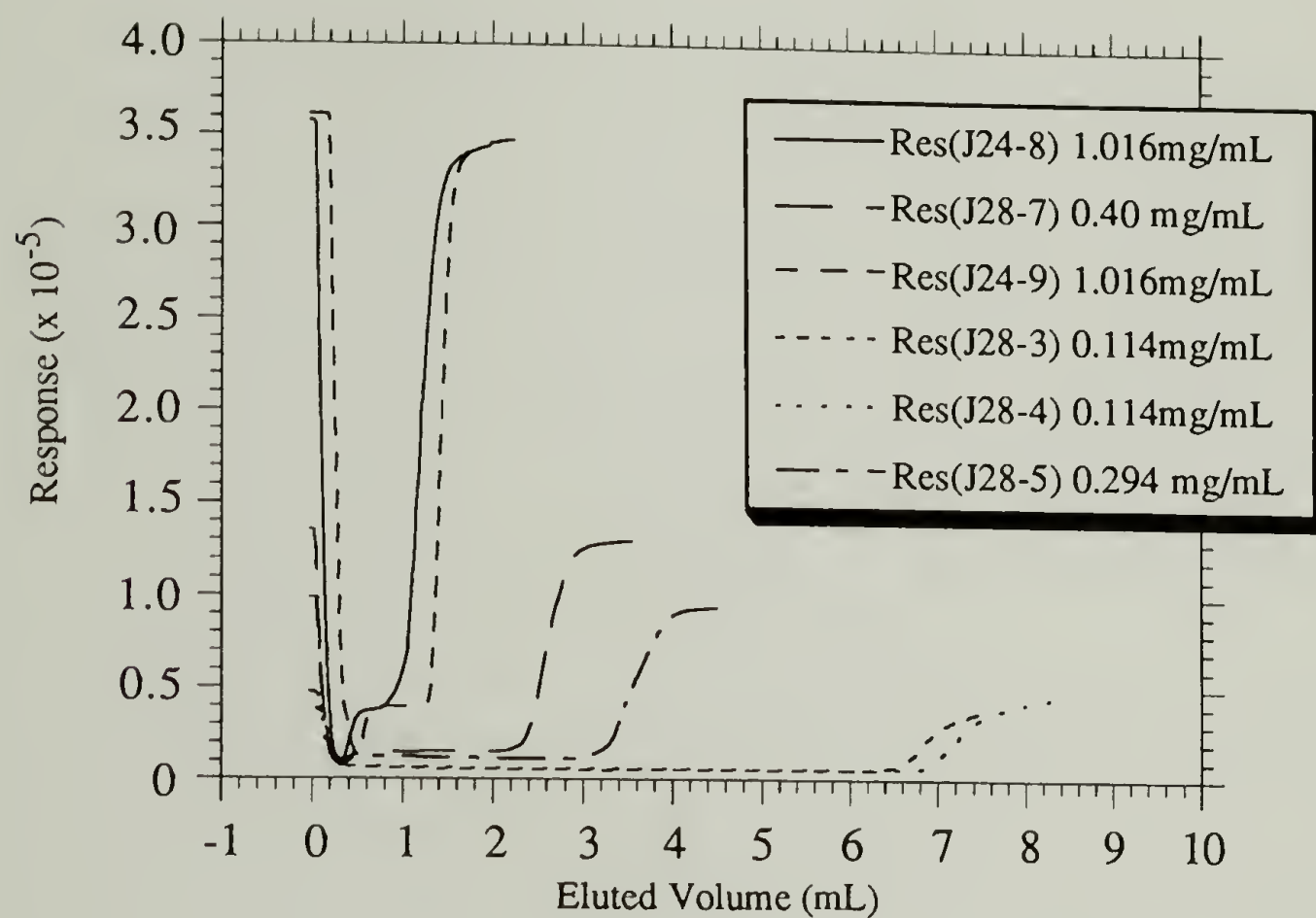


Figure 3.53 Vsat data for 41.2% SF triblock copolymer, $M_n = 58.5$ K (T40/50K). Polymers adsorbed from DCE onto silica gel at 22 °C.

reproducibility among the runs. When comparing the curves it should be noted that they do not start at the same place so the whole curve should be compared not just the front edge. Qualitatively we see what is expected, (Figures 3.46, 3.47 and 3.53) the lower concentration runs (i.e. lower initial response baseline) result in a larger elution volume before the column is saturated. This is what is expected as can be seen from Equation 3.7. Also note that there is a lower plateau (see Figure 3.43) during the time the polymer is adsorbing; the concentration of the eluent is greater than zero (it is expected to be zero if all the polymer is adsorbed). This plateau is due to impurities that accumulated in the solid polymer samples when they were stored on the vacuum line. This was the only time contamination of this sort was seen and its identity remains unknown. It was originally thought that the low plateau phenomenon was caused by channels or voids in the packed column which allowed a fraction of the column throughput to pass without exposure to the adsorbent. But the impurity was discovered as a small molecule peak during GPC runs of these polymers. The impurity was easily washed out of the solid samples with MeOH. The polymers containing a higher SF content did not have larger amounts of this impurity which suggests that SF degradation is not the source of the impurity. We also see that the impurity does not adsorb on the column (if it did we would not have noticed it) and thus assume that it did not affect the adsorption results. This impurity is thought to be part of the reason we had problems with the integral method because the amount of impurity and thus the UV calibrations did not stay constant. Close inspection of the raw data reveals that as the polymer concentration is decreased the rise to the original baseline on the front edge of the curve becomes slower. This can be attributed to the fact that higher polymer

concentrations result in faster adsorption rates.⁷⁰ The front edge analysis of a high concentration pulse through an HPLC column has also been used to measure adsorption isotherms of small molecules.⁹⁷ We observe this effect most noticeably in the adsorption data of T5/50K (Figure 3.50). Here we see that even at high concentrations the front edge rise is not as steep as with the other polymers and not much of a plateau is present. These comparisons suggest that the surface interaction energy of the T5/50 copolymer is significantly less than that of the others copolymers. It will be shown subsequently that this is indeed true and T5/50 is on the low composition side of v_{opt} .

The adsorption of these polymers onto both aerosil and glass beads was quite rapid (on the order of minutes) and we expected the same type of behavior in the adsorptions measured with this column setup. This indeed was true and was substantiated by the following experiment. An adsorption run was obtained in the normal fashion, the breakthrough was observed and the baseline was allowed to rise and level off at the original value. The column was then switched off-line (or the pump was shut off) and the column and polymer solution were left to equilibrate for the desired length of time (up to 3 hours was tested). After this time, flow through the column was continued and any adsorption (or desorption) of the polymer that occurred during the incubation period resulted in a change in the concentration of the polymer in the column and was seen as a peak in the baseline. If polymer adsorbed during the incubation then a negative peak was observed (i.e. the solution concentration decreased) and vice versa. The adsorptions were randomly checked by this method and it was found that for a normal adsorption run the area of the incubation peak was less

than a percent of the total area of the adsorption. This indicated that the adsorbances measured were steady state values. This incubation method was well-suited for the observation of small changes in the amount of polymer adsorbed. It was utilized in the measurement of the temperature dependence of the adsorption. The same procedure as above was used. A polymer was adsorbed and the baseline reestablished, then the column was taken off-line and the temperature was either raised or lowered and allowed to equilibrate for the desired length of time (the column was immersed in a bath connected to a temperature controlled circulator). When the flow was resumed the change in the amount adsorbed was observed as either a positive or negative peak. Quantitative results for this are not reported here because of other complications that were encountered in that stage of development of this process.

The adsorption data reported here were determined using the V_{sat} method that was discussed on pages 255 through 259. The raw data runs for the eight polymer samples are given in Figures 3.46 to 3.53. The saturation volume was determined as the volume between the minimum and maximum of the derivative (of the response) versus elution volume curve. A sample of this data (i.e. the derivative plots) is given in Figures 3.54 through 3.60, these figures are included to allow comparison of the raw data with the saturated volume that was used in the calculation of the reported adsorbance.

Isotherms were obtained for three polymers: D5/50k, D12/50k and T40/50k (Figures 3.61 through 3.64). These are all high affinity type isotherms with the knee coming at concentrations lower than about 0.25

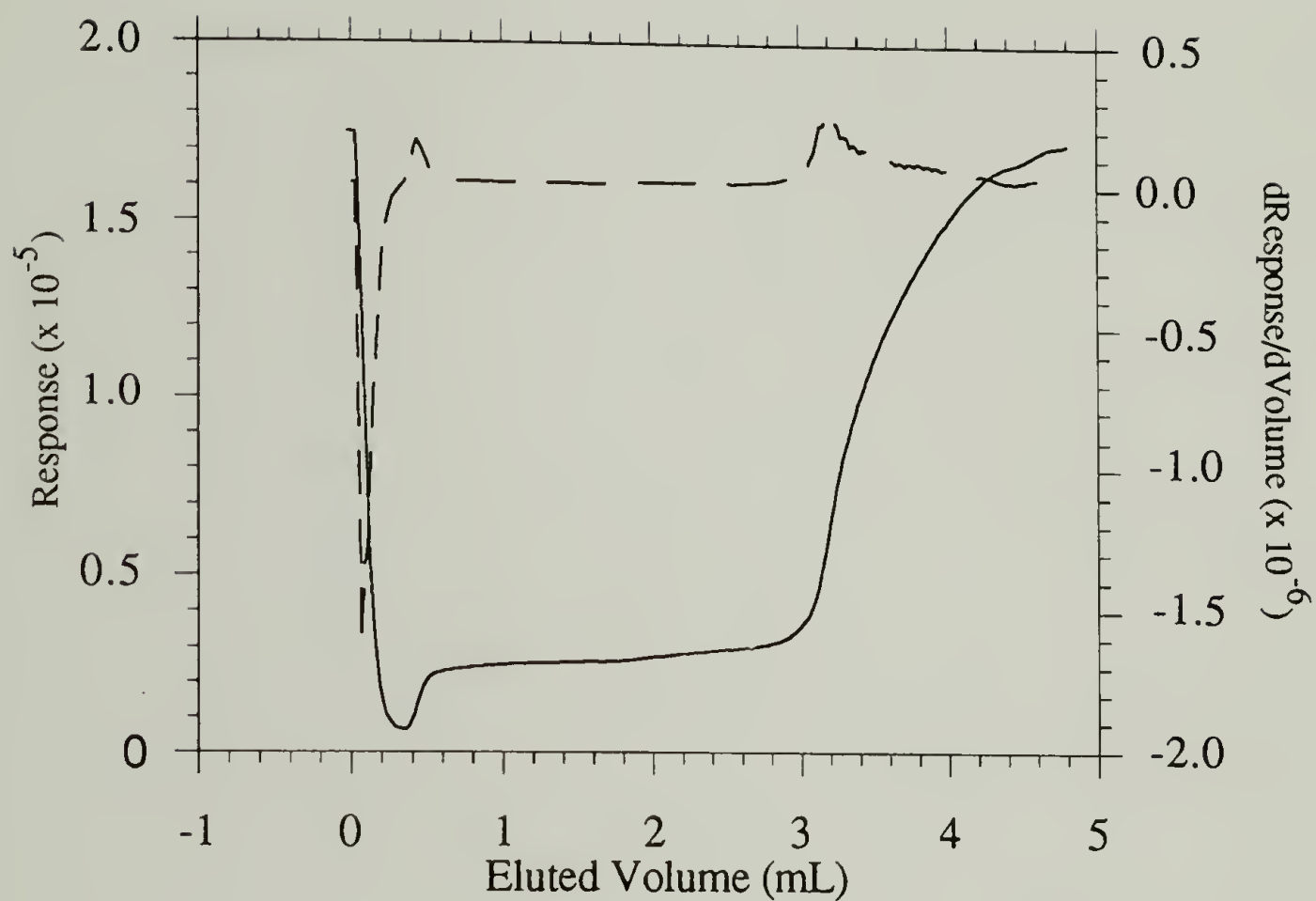


Figure 3.54 Vsat response and derivative data for D12/50K (0.5 mg/mL).
Adsorptions to silica gel from DCE at 22 °C (J27-4).

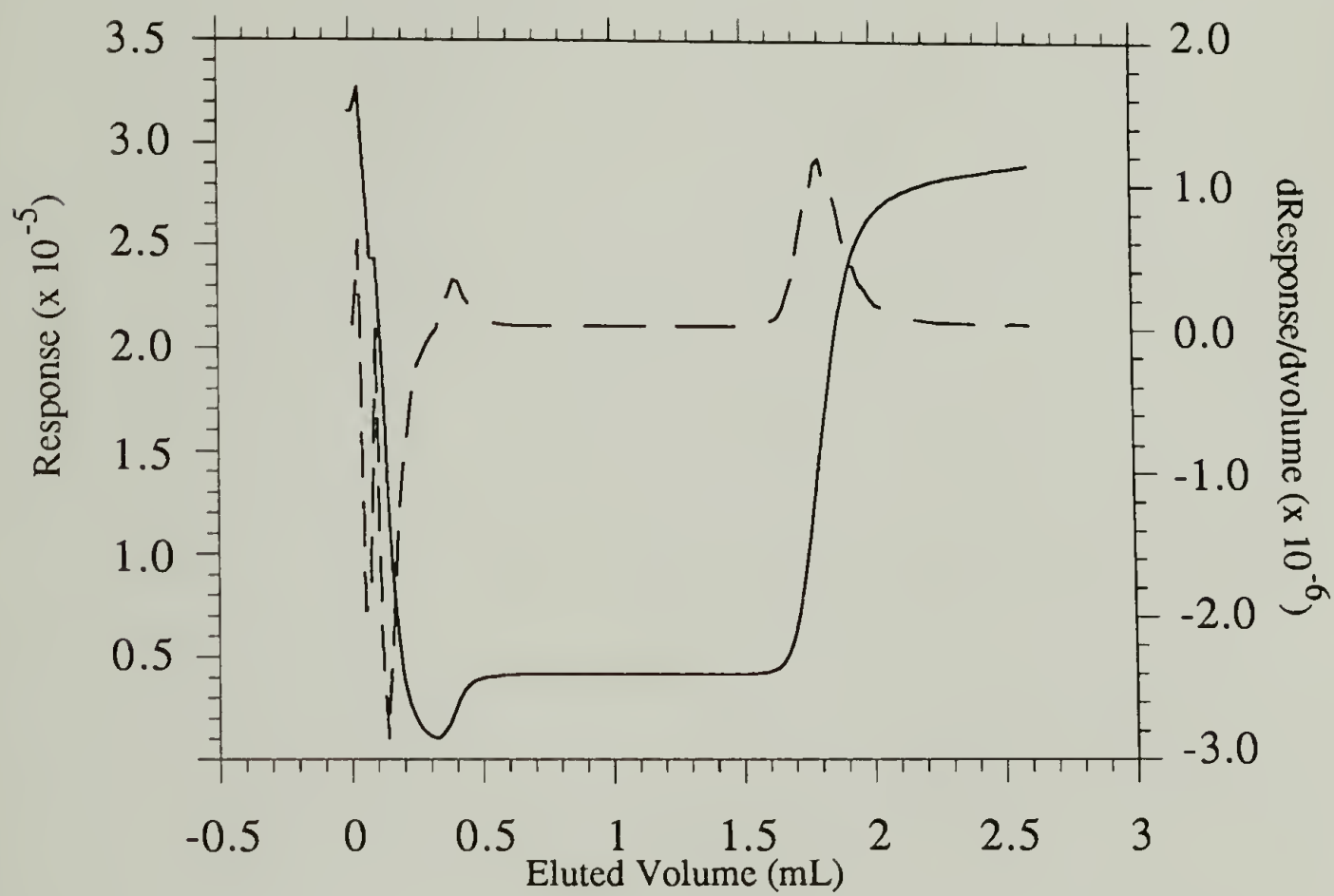


Figure 3.55 Vsat response and derivative data for D23/50K (0.98 mg/mL).
Adsorptions to silica gel from DCE at 22 °C (J28-1).

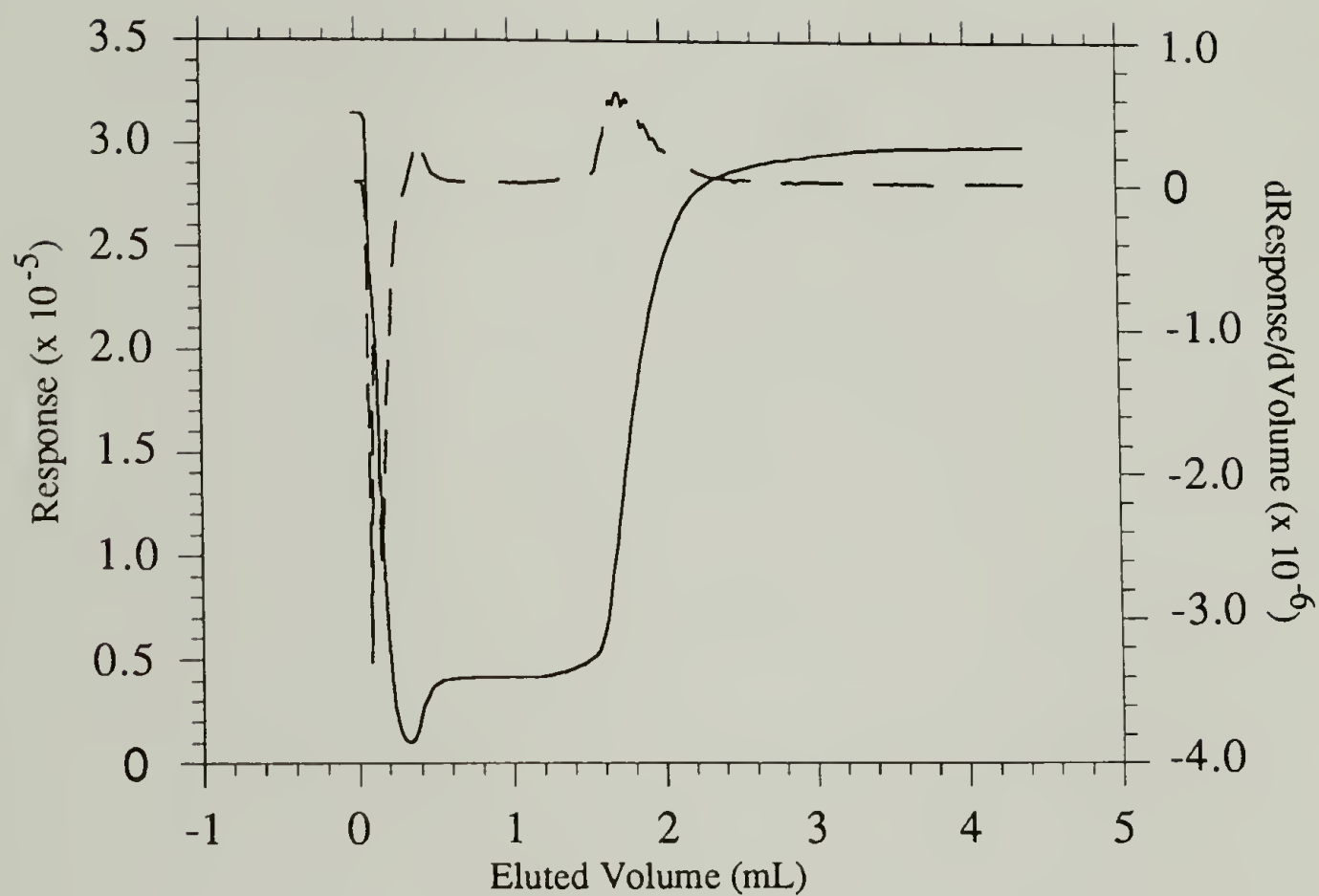


Figure 3.56 Vsat response and derivative data for D23/50K (0.98 mg/mL).
Adsorptions to silica gel from DCE at 22 °C (J28-2).

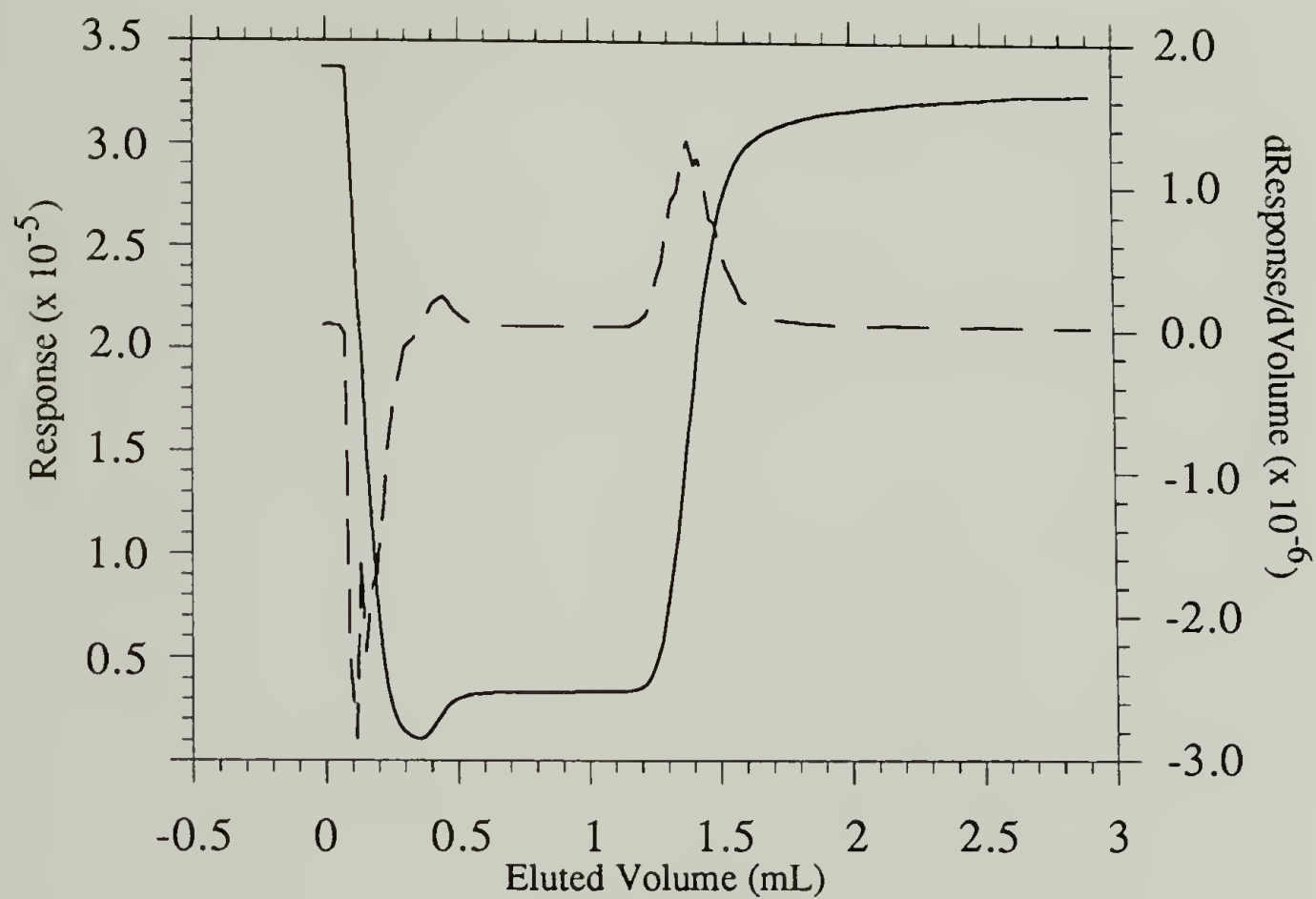


Figure 3.57 Vsat response and derivative data for D40/50K (1.02 mg/mL).
Adsorptions to silica gel from DCE at 22 °C (J23-7).

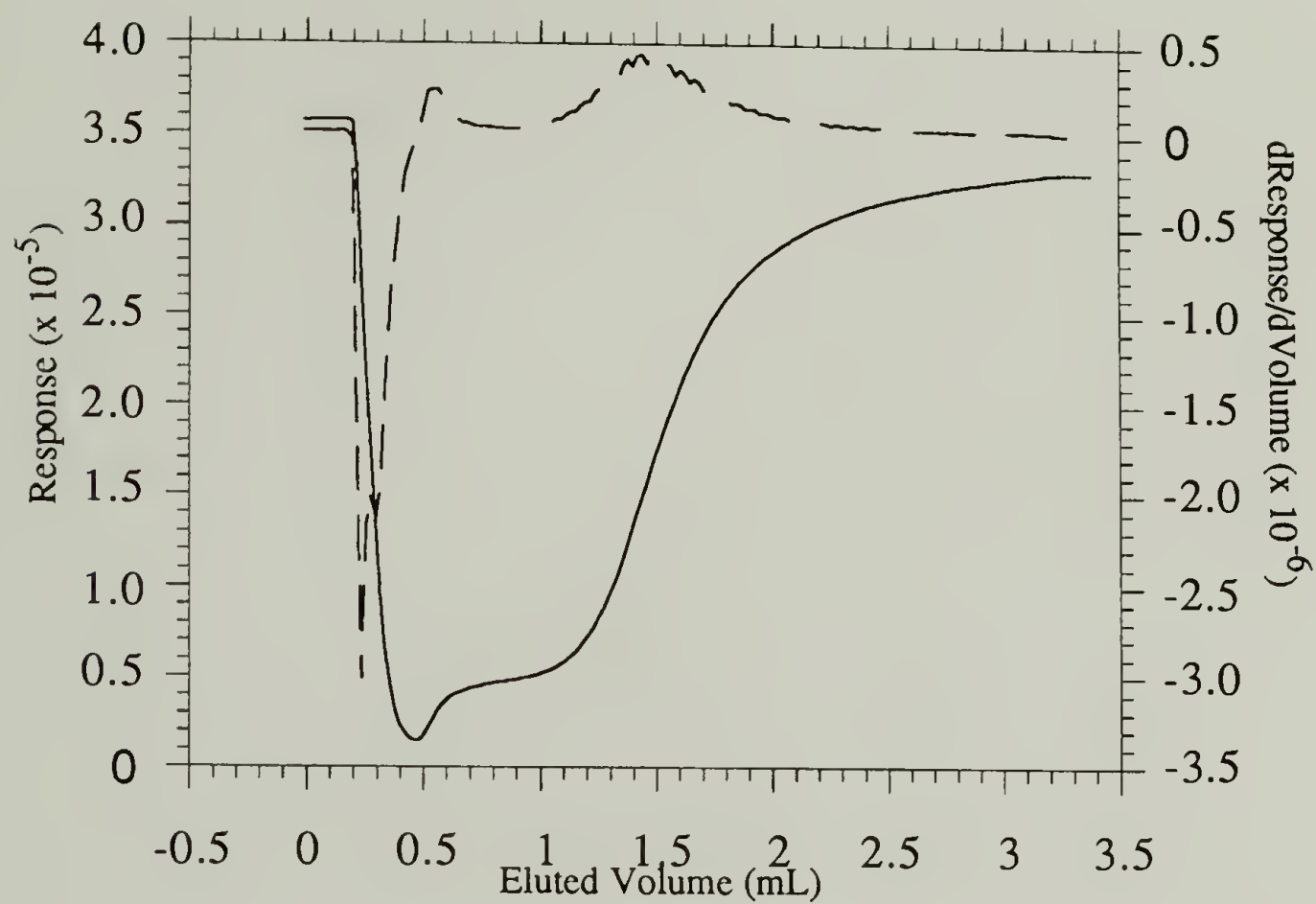


Figure 3.58 Vsat response and derivative data for T5/50K (1.00 mg/mL).
Adsorptions to silica gel from DCE at 22 °C (J24-1).

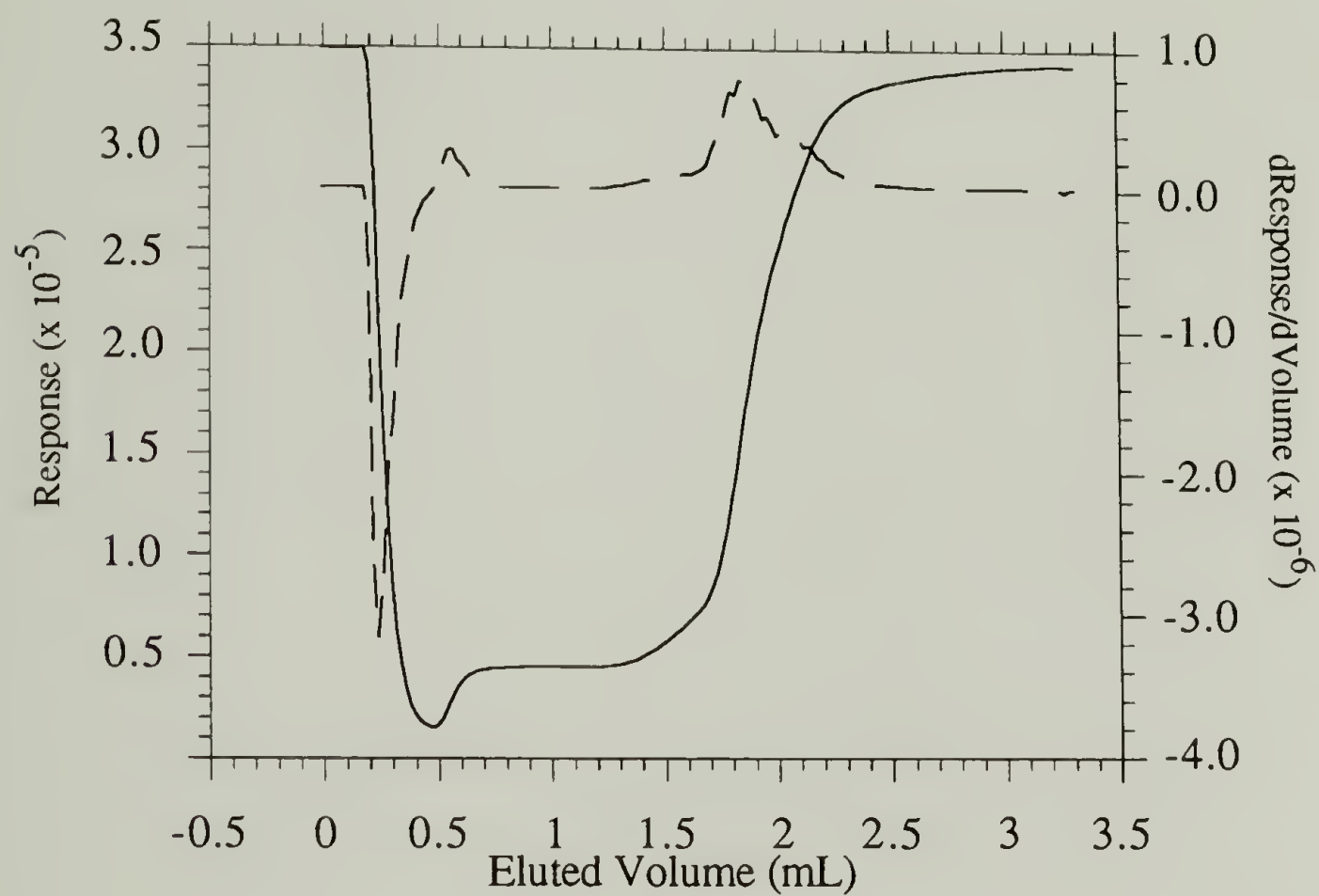


Figure 3.59 Vsat response and derivative data for T12/50K (1.00 mg/mL).
Adsorptions to silica gel from DCE at 22 °C (J24-4).

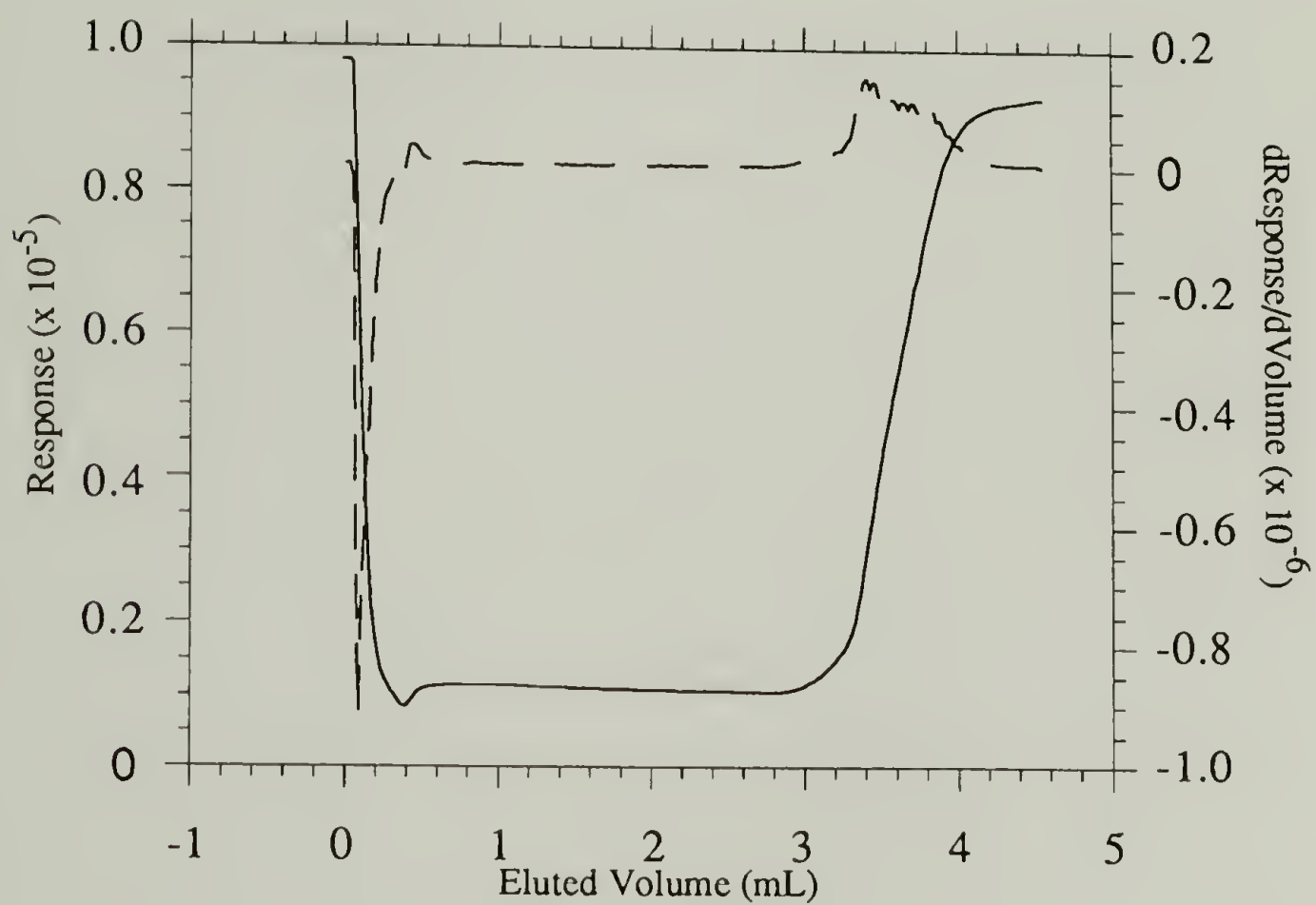


Figure 3.60 Vsat response and derivative data for T40/50K (0.29 mg/mL). Adsorptions to silica gel from DCE at 22 °C (J28-5).

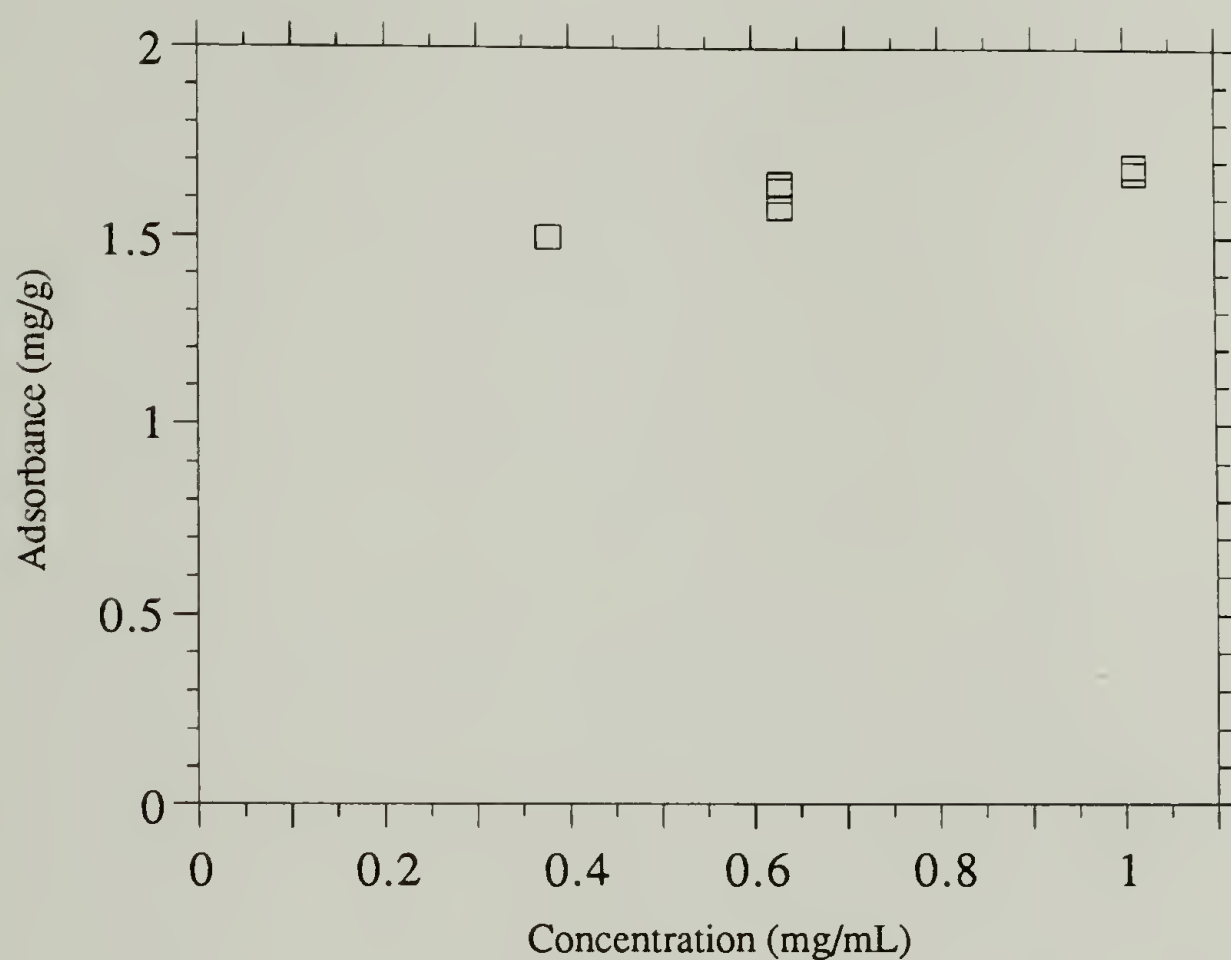


Figure 3.61 Adsorption isotherm 5.8% SF diblock copolymer, $M_n = 51$ K, (D5/50K) on silica gel determined using the Vsat method. (DCE, 22°C)

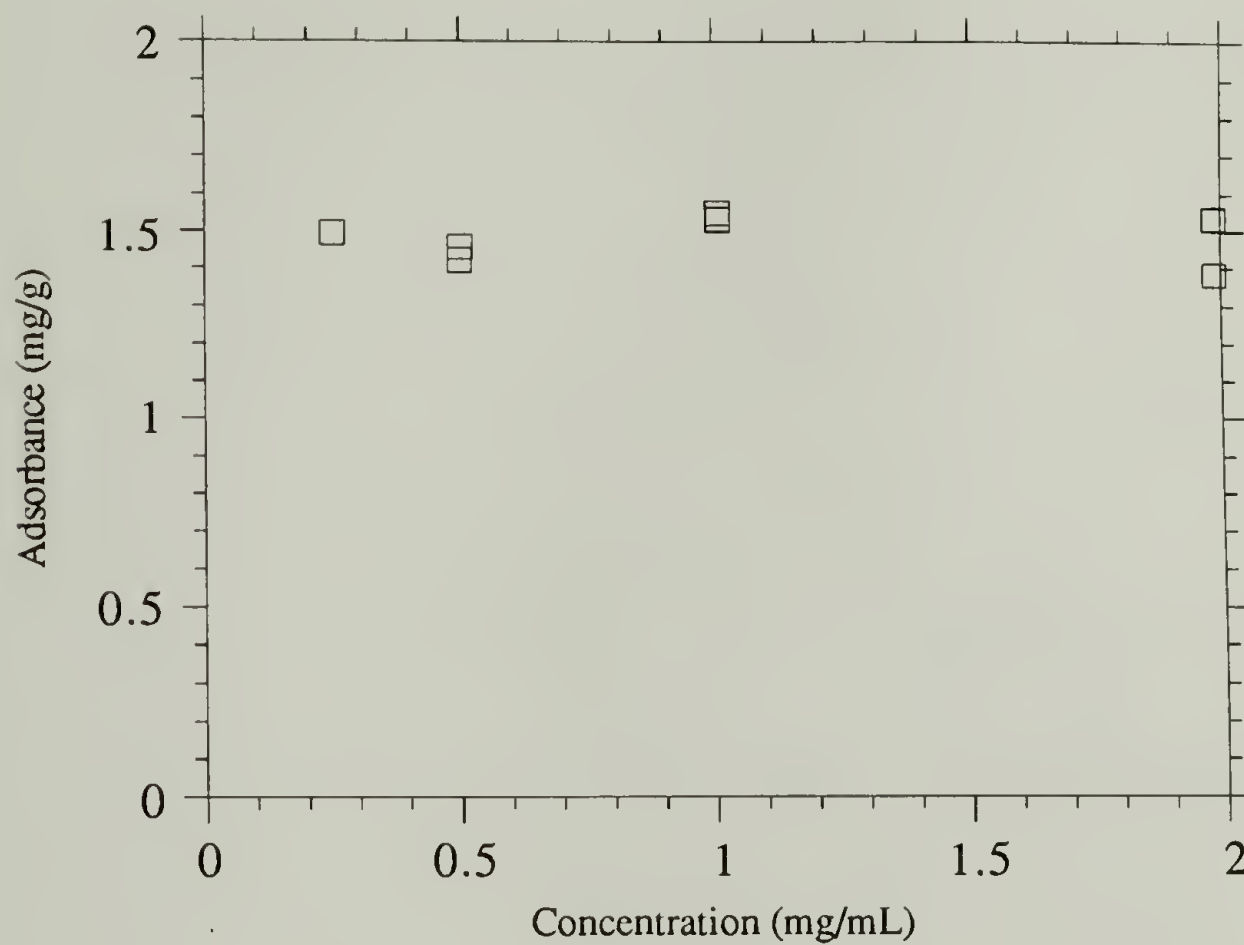


Figure 3.62 Adsorption isotherm 13.2 % SF diblock copolymer, $M_n = 49$ K, (D12/50K) on silica gel determined using Vsat method (DCE, 22°C).

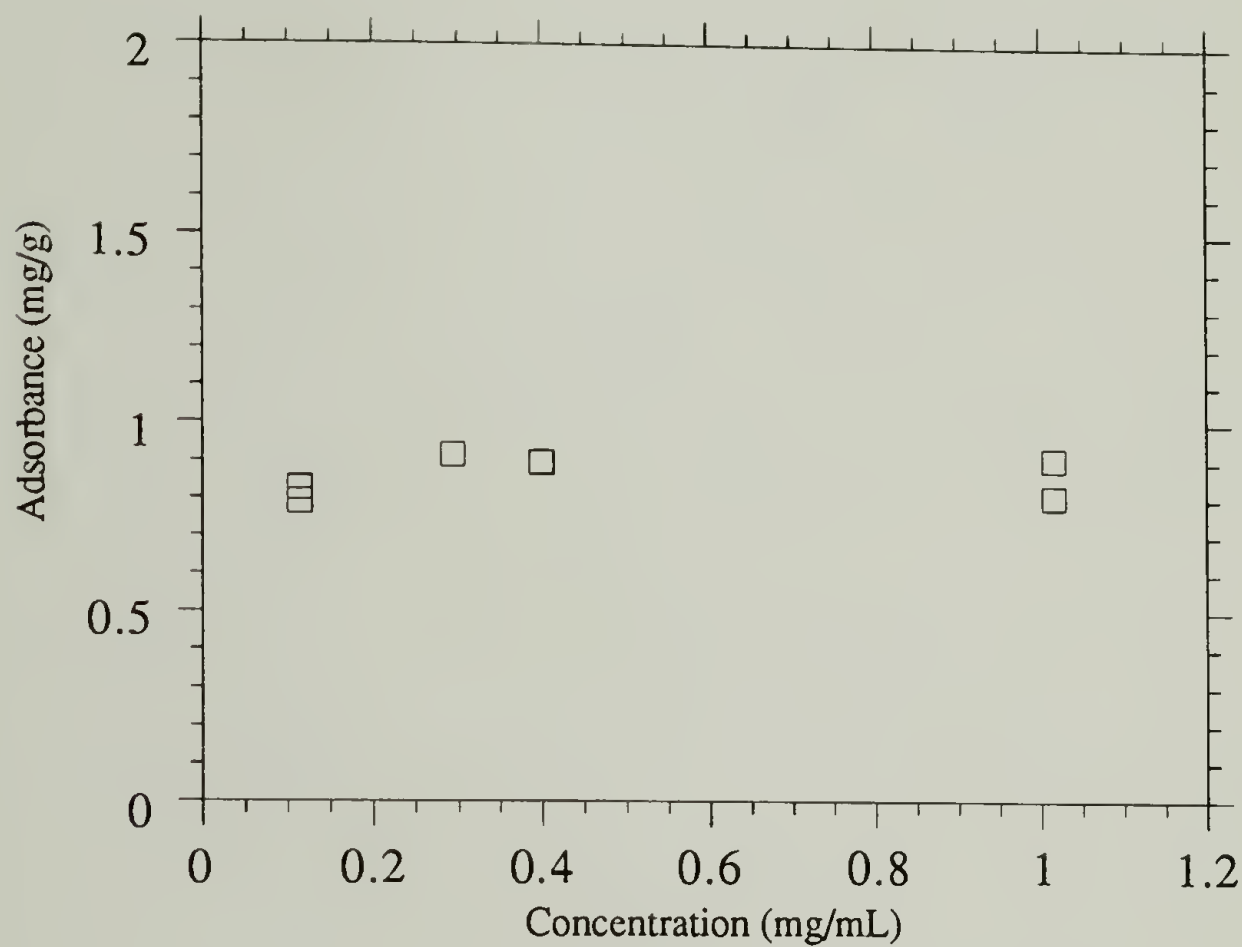


Figure 3.63 Adsorption isotherm 41.7 % SF diblock copolymer, $M_n = 58.5$ K, (T40/50K) on silica gel determined using Vsat method (DCE, 22°C).

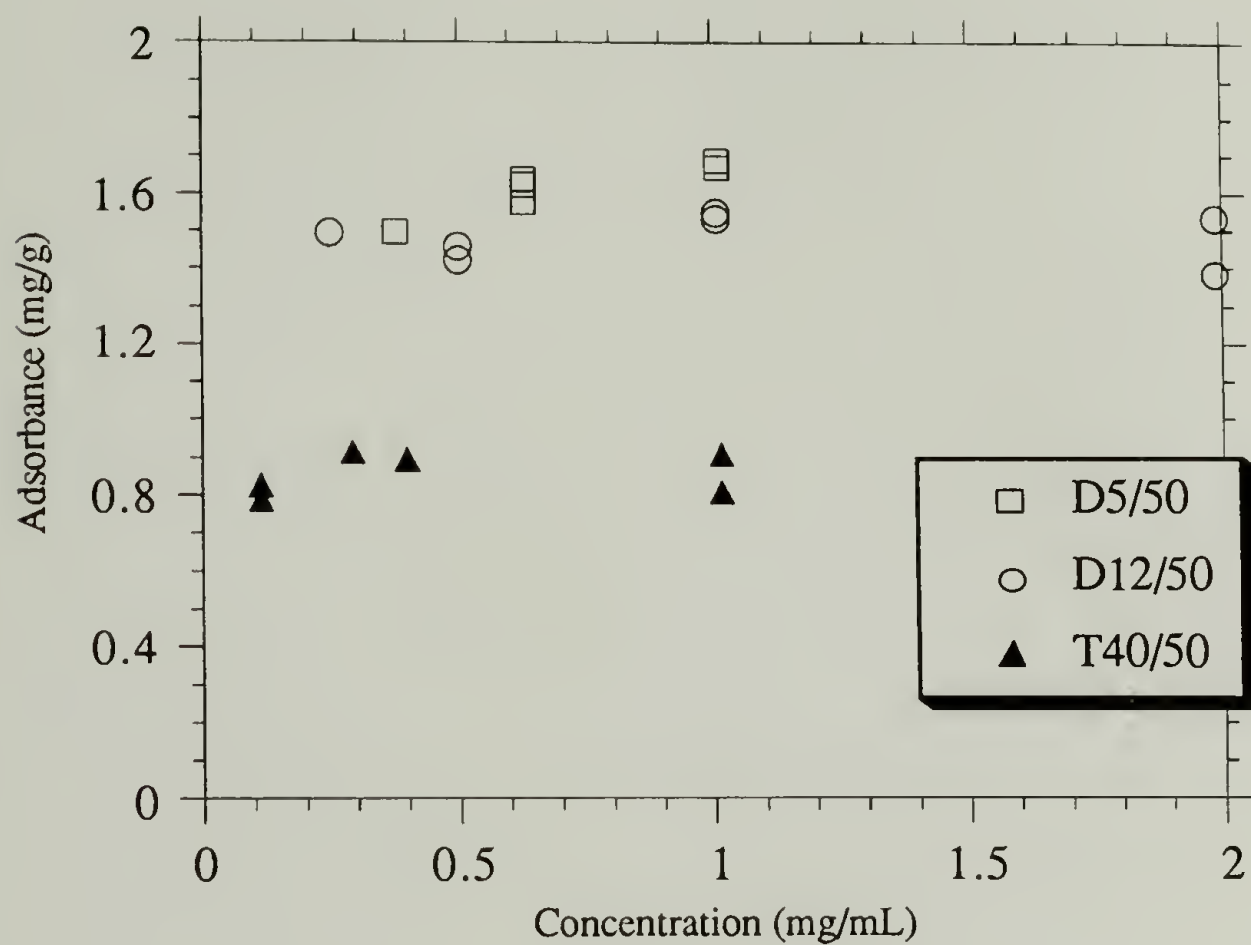


Figure 3.64 Combined adsorption isotherms for D5/50K (5.8% SF, 51K), D12/50K (13.2% SF, 49 K) and T40/50K (42% SF, 58.5K) copolymers on silica gel using Vsat method (DCE, 22 °C).

mg/mL. High affinity type isotherms were also obtained for adsorptions on aerosil and the small glass beads. The combined isotherms are shown in Figure 3.64 and one can see that, as expected the smaller SF blocks result in a larger amount adsorbed. Plateau regions above 0.25 mg/mL were obtained for both diblock and triblock copolymers and high and low SF composition. We have assumed that the other polymer samples will give similar high affinity type plateaus. Thus, the adsorbance determined at ~1.0 mg/mL was well into the plateau region of the isotherm. The adsorbance at ~1.0 mg/mL for each of the eight polymers is plotted versus sticky foot content in Figure 3.65. For each architecture the amount adsorbed initially increases with decreasing sticky foot content. This is expected and was discussed in detail in chapter I. Both the theories of Evers⁵⁰⁻⁵² and Marques/Joanny⁵³ (MJ) predict a maximum in the Γ vs v_A curve. The diblock data show no apparent maximum for the four compositions measured. The MJ theory predicts that $\beta=N_A^{1/2}$ at the crossover; this gives $v_A=0.075$ as the predicted composition at the maximum (v_A^{opt}) for these polymers ($N=300$). The 5.8% SF polymer should be just barely on the buoy/anchor side (left side) of the maximum. It is conceivable that the maximum exists at $v_A=0.075$; the data can not rule this out (although we think this is unlikely). A comparison of our data with the predictions of Evers (see Figure 1.5) shows that the shape of the curve much more resembles that of Evers than those predicted by MJ (see Figure 1.4). The rise is not as sharp as predicted by MJ and there is little curvature in our data. The predicted curvature (for MJ theory) is a result of the total anchor dominated assumption ($\sigma=1/N_A$) which has been discussed in Chapter I; this results in the $1/v_A$ dependence seen plotted in Figure 1.4(B). The low curvature can result from a decrease in the SF

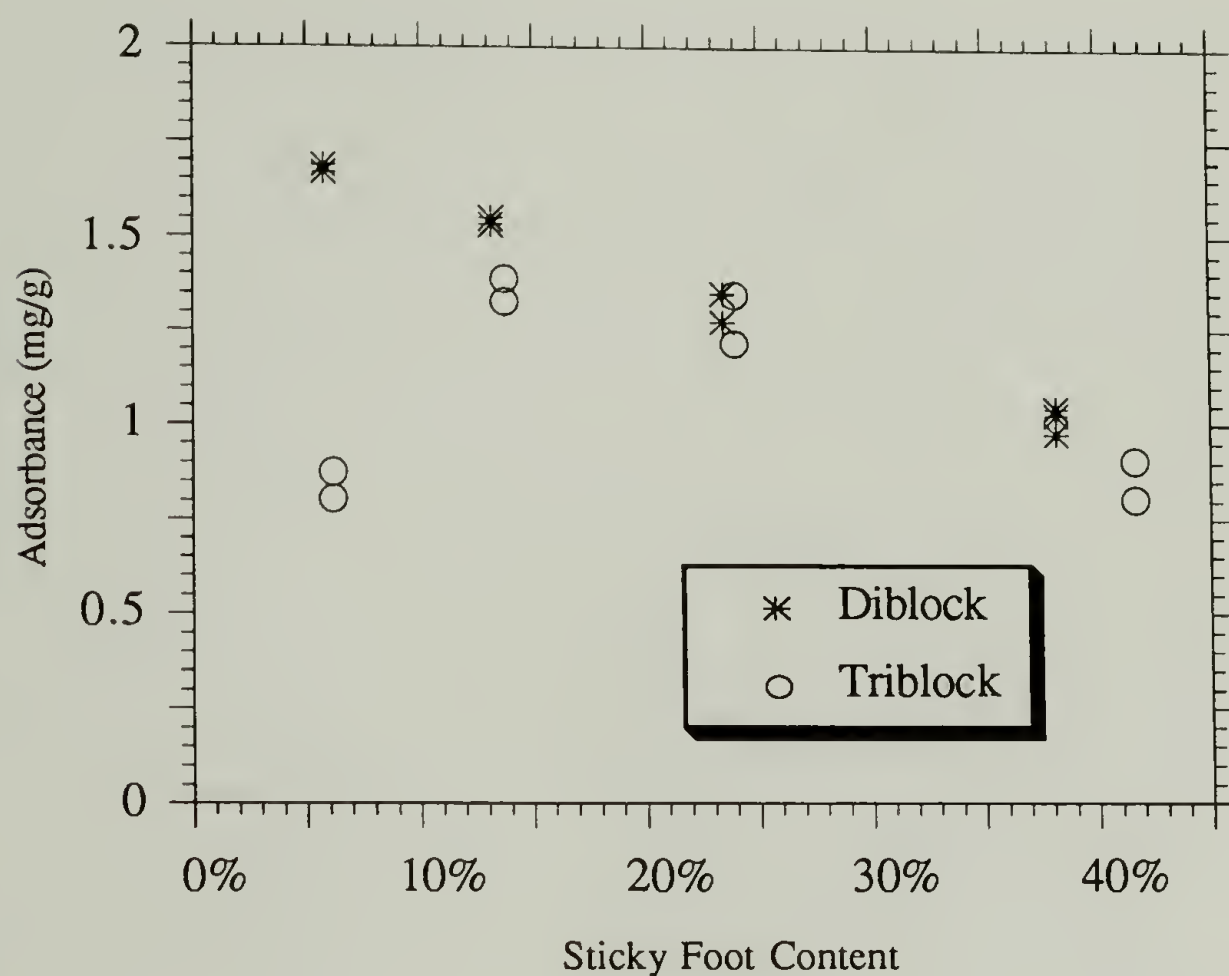


Figure 3.65 Adsorbance (@ 1.0 mg/mL, in the plateau region) vs. Sticky Foot content for diblock and triblock copolymers ($M_n \sim 50$ K). Adsorptions to silica gel via Vsat method (DCE, 22 °C).

strength as was shown by Evers in Figure 1.6. This is understood in the following way. The bound fraction of the sticky block increases with decreasing v_A ; the added crowding is compensated by the increase in the interactions with the surface (actually the bound fraction has to go up just to stay even). As the bound fraction increases the SF block flattens out and takes up more space on the surface thus the $1/N_A$ relation is not strictly obeyed. As one would imagine this effect is more pronounced at lower SF strengths because more compensation is required. When the bound fraction reaches a value close to one (Evers calculates 0.85) any further asymmetry results in less polymer being adsorbed and thus we see this as the maximum. Exact comparisons to Evers predictions can not be made because they depend on the SF strength which is not known for these polymers. It should be noted that the data presented in Figure 3.65 are not normalized i.e. the 40% SF polymers are of considerably higher molecular weight than the 5% SF because of the large difference in number of SF on these polymers (SF monomer unit 279 g/mole, *tert*-butylstyrene monomer unit 160 g/mole). The data points were normalized to account for these molecular weight differences and it was found that the slope was increased but the curvature of the curve remained relatively unchanged. Also another point is the difference in the size of the hydroxy diethylmalonate group versus *tert*-butyl group.

Our data also resemble experimental data reported for diblock systems. Figure 1.8 shows the data obtained by Wu for the adsorption of MMA/DMAEM block copolymers (from isopropanol onto silica spheres); the Γ vs v_A data are plotted for two different chain lengths. The solid curves represent the predictions of MJ theory. One can see that the fit with

MJ theory is in qualitative agreement. The curvature that they have in their data is a little stronger than seen in our data. This could result from a stronger SF than we have. Wu et al. observe a maximum in the data and found that it is at a lower SF fraction than predicted by the theory. As with our data the position of the maximum can not really be determined for this few of data points. The data reported by Guzonas and shown in Figure 1.9 for the adsorption of PEO/PS block copolymers on mica shows a good fit with the MJ predictions but again the maximum must be inferred. At any rate the data presented here show qualitative agreement with that predicted by theory and also agree with data reported for similar adsorption experiments.

The data of the triblock copolymers are very interesting. Figure 3.65 shows that there is not much difference in the amount adsorbed for the diblock and the triblock copolymers when the SF content is relatively high. At 12% SF the triblock copolymer adsorbance is slightly less than that of the diblock. The triblock shows a drastic drop in adsorbance on going from 12% to 5% SF. This suggests that the buoy repulsions have become a comparable factor contributing to the energy balance at this point. We see a definite maximum in the triblock adsorption curve and the maximum occurs at a higher v_A than for the diblock copolymer. We explain this in the following fashion. It is easy to see that a loop of the same length chain will result in a thinner layer than the corresponding tail and that this would result in a higher segment density than that predicted for the diblock copolymer in Equation 1.6. As was discussed in chapter I the osmotic crowding of the segments in the adsorbed layer is a major factor opposing the adsorption. We showed how the increased segment

density could be used to explain the shift of v_{opt} to higher values as the molecular weight of the chain decreases. We propose that the loop structure of the adsorbed triblock copolymer results in an increase in the segment density and thus has an effect similar to decreasing the chain length: the position of the maximum is shifted to the right and less polymer is adsorbed. Thus the triblock copolymers loop architecture causes the transition from a regime dominated primarily by the anchor block (anchor/buoy regime) to one in which the buoy block crowding is of comparable magnitude (buoy/anchor regime) to occur at higher SF composition. A major factor in this description is that the triblock does indeed adsorb with both sticky blocks on the surface to form the more dense loop structure. If only one block were adsorbing then the triblock should act like a diblock copolymer with $v_A/2$. In other words the data in Figure 3.65 would show that the 42% SF triblock copolymer would have a comparable adsorbance with the 23% SF diblock data and the 23 % triblock the same as the 12 % diblock and so on. We easily see that this is not the case. One may argue that the second block desorbs at the lower compositions (5% SF in this case) and that at this composition (~2.5% SF diblock) the diblock would be well to the left of v_{opt} (i.e. down the hill) and thus would correspond to the triblock measurement. If that were the case it would still mean that the triblock loop structure causes an increase in the osmotic crowding (as compared with the diblock) in the adsorbed layer and thus the main hypothesis is still intact; there is just a weaker link in the chain. It is actually very conceivable that this is what we would see for the case of assymetric triblock copolymers. We have also pointed out other evidence throughout this thesis that suggests that the triblock copolymer is adsorbed in a loop fashion. Thus we have seen that TLC data

show no differences in critical displacer concentrations between the two isomers and that XPS gave results that suggest that the triblock copolymers have both blocks down. Contact angle data also show no evidence for for the polar hydroxy diethylmalonate on the surface.

We have postulated that the buoy repulsions (i.e. osmotic pressure, entropy) become a major factor in the energy balance at compositions around v^{opt} . At higher higher SF contents than this the adsorption is pretty much anchor dominated (i.e. enthalpy) with small adjustments made by the sticky block flattening out a little so that the graft density dependence is less than $1/N_A$. We also suggest that since the sticky block architectures affect mainly the buoy crowding term (entropy) one would expect little dependence on the architecture at high v_A values where the buoy contribution is minimal. This is what is seen for the diblock and triblock data presented here (see Figure 3.65). A similar phenomenon is seen in both the Evers and MJ predictions for the effect of chain length on the adsorbance. Figures 1.4 and 1.5 show that the largest differences between the molecular weights are found at the low v_A values. We have sought to substantiate this claim in the following way. The adsorbance for two SF polymers (T5/50k and D40/50k) was measured at 0 °C. The raw data can be found in Figures 3.66 and 3.67. It was found that the D40 polymer was not affected by the temperature drop whereas the T5 polymer showed a significant (approximately 20-25%) increase in adsorbance at the lower temperature (Figure 3.68). The main contribution to the temperature dependence should be the decrease in osmotic crowding (entropy term) at the lower temperature. The significant change in adsorption behavior of the 5% SF triblock copolymer suggests that this polymer is, indeed, in the

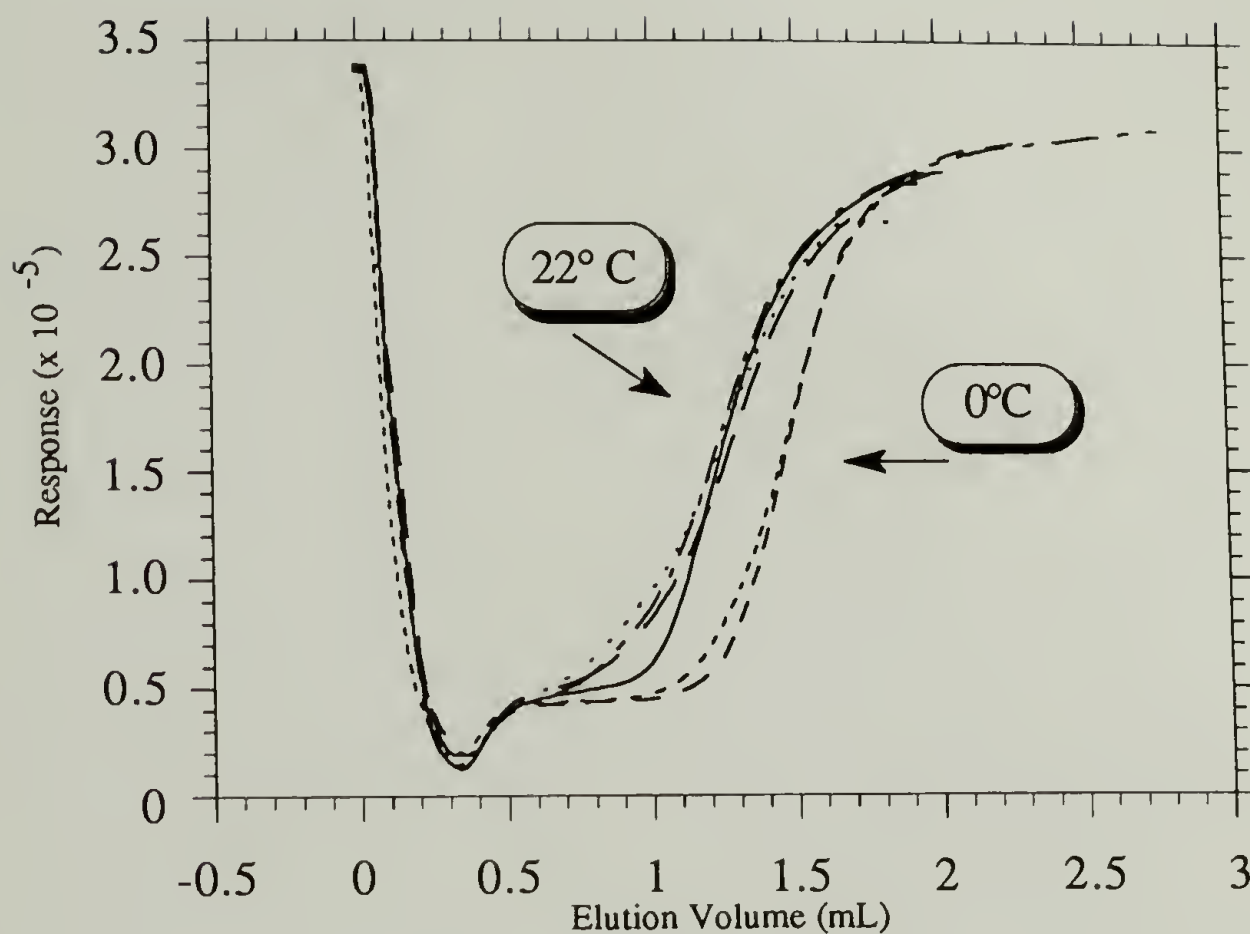


Figure 3.66 Vsat data for 6.2% SF triblock copolymer, $M_n = 46$ K (T5/50K). Polymers adsorbed from DCE onto silica gel at 22 °C and 0 °C. The lower temperature results in more polymer adsorbed.

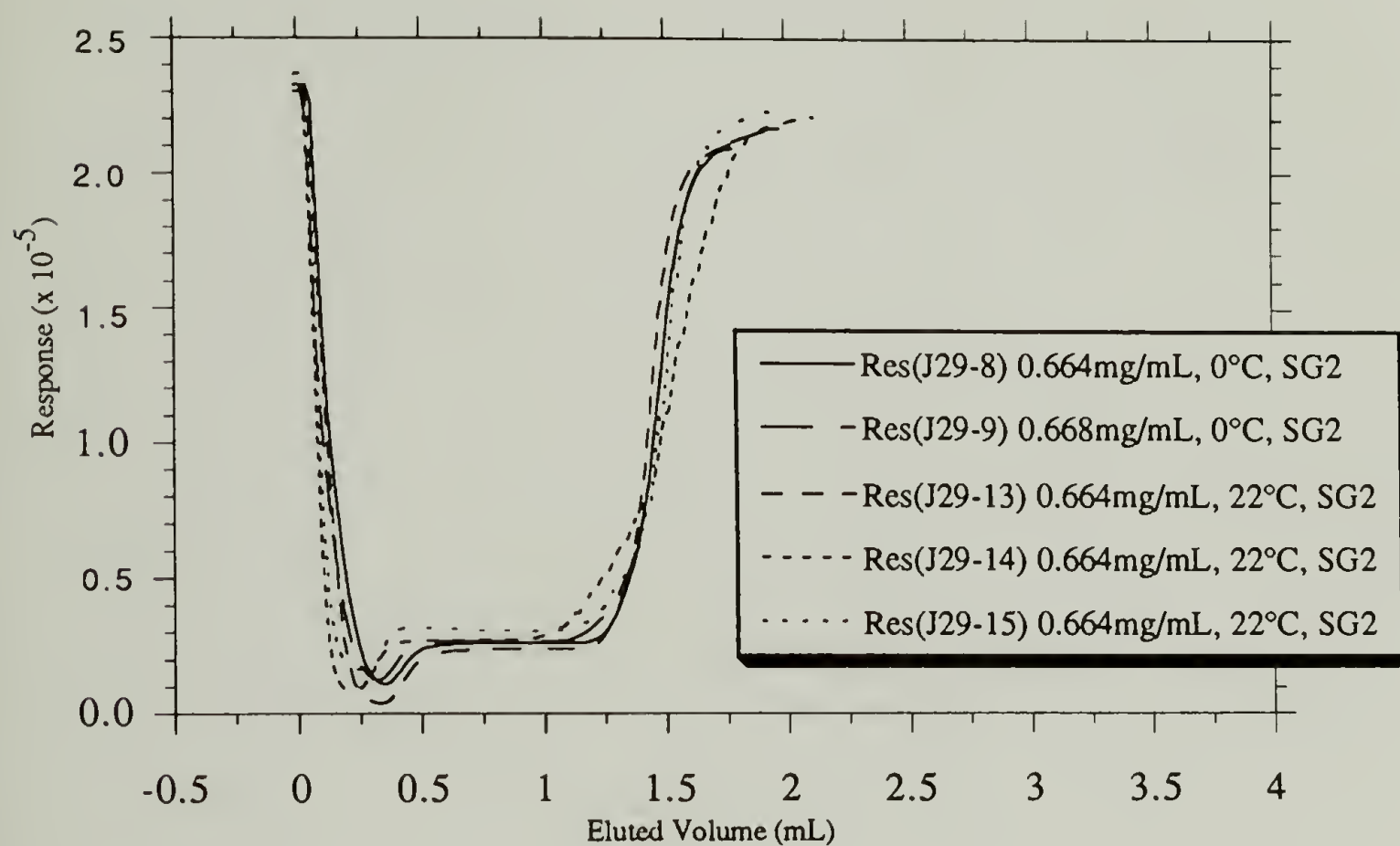


Figure 3.67 Vsat data for 38.2% SF triblock copolymer, $M_n = 52$ K (D40/50K). Polymers adsorbed from DCE onto silica gel at 22 °C and 0 °C. Adsorbance is the same at both temperatures.

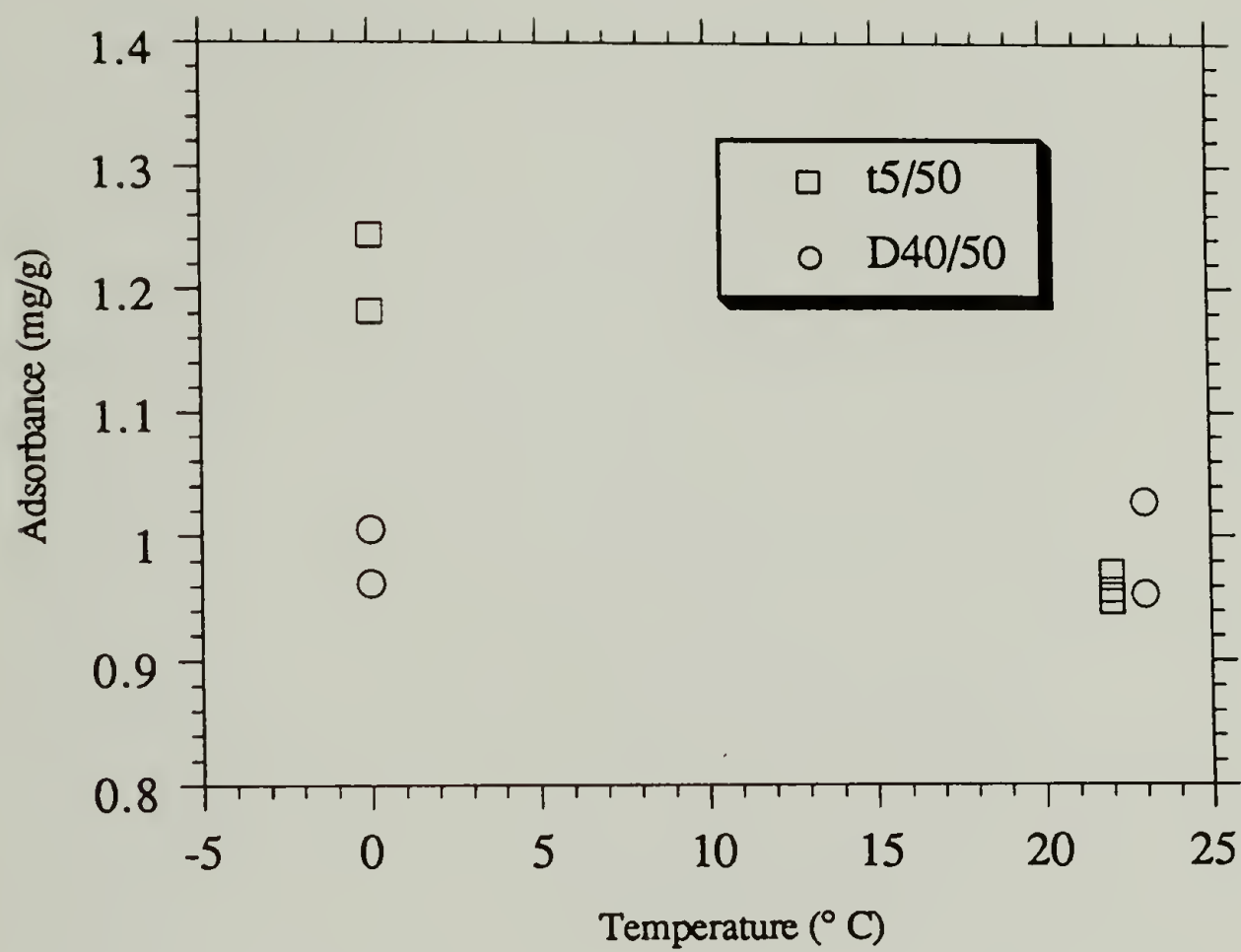


Figure 3.68 Effect of temperature on adsorbance of T5/50K and D40/50K copolymers to silica gel via Vsat method (DCE, 22 °C).

buoy/anchor regime. On the other hand the D40 shows no effect as one would imagine for an anchor dominated polymer. Thus we have shown that the buoy contribution to the adsorption energetics is significant at some compositions and is the cause for the decrease in the amount adsorbed at low v_A . We have also shown that the effect of temperature is a good way to probe for the effects of buoy repulsions in different architectures and at different compositions. In conclusion we do see a difference in the adsorption characteristics for the two different architectures.

Conclusions

We have presented data for the adsorption of SF polymers on silica gel, aerosil, glass beads and microscope slides. Quantitative comparison of the adsorbed amounts between these measurement techniques was precluded by the lack of information regarding the specific area of these solids. The various measurements were carried out in an attempt to find the best, most reproducible means of measuring the adsorbance of these polymers. This goal was not realized; the best method of measurement has not been ascertained. The use of the batch depletion method with an appropriate solid may be the most straightforward method of measurement. This may require recycling and reusing the 3-10 μm beads or adsorbing to a suitably large mesh size (small particles), small pore size silica. Other researchers have reported the use of mica powders⁹⁸ and homemade silica spheres in the sub-micron size range.⁹⁹ Solution ATR IR and angle-resolved XPS analysis are also means of measurement that are relatively straightforward. The column method used here works fairly well, but we do not know if it was worth the hassle for normal adsorption measurements. It is very likely that this method would have worked better and all of the advantages that

were originally envisioned would have been realized if another, less sticky and less reactive polymer system were used.

The data have shown that for a series of block copolymers (with $M_n \sim 50K$) adsorbed onto silica, the diblock and triblock architectures adsorbed to the same extent above $\sim 23\%$ SF. At 12% SF the triblock had an adsorbance of 1.35 mg/g whereas the diblock was somewhat higher with $\Gamma \sim 1.55 \text{ mg/g}$ ($\sim 15\%$ difference). The diblock adsorbance increased to $\Gamma \sim 1.67 \text{ mg/g}$ at 5% SF, but the triblock adsorbance dropped dramatically over this same change in composition to only $\sim 0.82 \text{ mg/g}$ at 5% SF. This is an 82% difference in the adsorbance between the two architectures. We have attributed this increasing difference (in the amount adsorbed as v_A is decreased) between the two architectures as the result of the increasing contribution of the osmotic crowding term as compared to the surface interactions in the overall energy balance. We also reported that for the smaller polymers ($M_n = 13K$) with 23% SF content, the diblock adsorbed to a greater extent than the triblock on three different surfaces. The adsorption of the triblock copolymer to Aerosil gave a plateau adsorbance of $\sim 1.05\text{-}1.2 \text{ mg/m}^2$ whereas the diblock adsorbed to a greater extent but with much more scatter in the data (for reasons already discussed); the plateau value was $\sim 1.2\text{-}1.7 \text{ mg/m}^2$. This is a difference of $\sim 35\%$. The triblock copolymers were found to flocculate the Aerosil, so we know that a substantial fraction of the polymers did not adsorb in the loop structures that we postulated in the previous discussion. We also postulate though, that flocculation, which is caused by bridging the polymer chains between the silica particles, results in an increase in segment density similar to that observed for the triblock adsorbed layer loop structure; thus we see the

architecture effects that have been discussed. Another piece of evidence indicating that the triblock copolymers adsorb to form a loop structure is indicated by the flocculation of the Aerosil particles when the triblock copolymer adsorbs. This is visual evidence that both blocks (of the triblock) can adsorb to form a very dense adsorbed polymer layer. The adsorption on glass beads gave plateau values of ~ 1.7 mg/g and 1.4 mg/g for the diblock and triblock copolymer respectively. The question of why these polymers showed a substantial difference in adsorption to these surfaces at 23% SF although adsorptions to silica (of the $M_n \sim 50K$ polymer samples) measured by the column method showed no significant differences at this composition can be explained using the predictions of Evers and MJ. These theories predict that the position of the v_A^{opt} shifts to the right as the molecular weight is decreased (see Figures 1.4 and 1.5(A)). The position predicted for this maximum, calculated from MJ theory ($\beta = N_A^{1/2}$), is 0.12-0.13 mole fraction sticky feet which is substantially higher than that for the larger chains ($v_A^{opt} = 0.075$). We also noted that the data for the $M_n \sim 50K$ series indicate a small difference between the two architectures at 12% SF (i.e. a substantially higher composition than the predicted v_A^{opt}). The differences measured for the adsorbance of the smaller chains were less than those found for the 5% SF triblock and diblock ($M_n \sim 50K$); this suggests that the measurements made were on the righthand side of v_A^{opt} . We postulate that if these same experiments were carried out with the low molecular weight polymer of the same compositions, we would see a maximum in both the diblock and triblock data and that the maximum for the triblock would occur at a higher SF content (than that for the diblock) but at a value less than 23% SF. We also postulate that adsorption of the same $M_n \sim 50K$ polymer series (described above) functionalized with a

weaker SF would result in the shifting of v_A^{opt} for both architectures. This would further substantiate the predictions of Evers and our extension of these predictions to triblock copolymer systems given in the discussion. Examination of this effect could be accomplished rather easily in one of two ways. The adsorption could be carried out from a stronger displacing solvent or from a weaker solvent spiked with a displacer. In this fashion one might be able to generate a whole series of curves resembling the predictions given by Evers and shown in Figure 1.6. This, in fact, is the most efficient method of verifying the predictions of Evers because as it was shown, the effects of molecular weight and SF strength are very similar (compare Figures 1.5(A) and 1.6(A)). Using the SF strength as the variable would generate the largest amount of data with the fewest number of polymers. We have also shown that the unmodified styrene monomer unit can act as a sticky foot in such solvents as cyclohexane and CCl_4 and therefore adsorption of the unmodified polymers from one of these solvents would be further substantiation of this effect. The subsequent modifications of the hydroxy diethylmalonate SF that were discussed in the synthesis section could also be used to obtain sticky feet of different interaction energies.

We have seen that the amount of polymer adsorbed on surface of a solid is a function of both the composition and the molecular SF architecture of that chain. The data indicate that the adsorbance measured for a diblock copolymer is greater than that for an isomeric triblock copolymer. These were obtained from measurements on four different surfaces using a different analytical techniques. We have presented evidence suggesting that the adsorbed triblock copolymers have a loop

structure when adsorbed on the surface. We have also shown that the temperature of the adsorption can be used to affect the amount of polymer adsorbed and that this effect can be used to probe the contribution of buoy repulsions in the various adsorption regimes. In the anchor dominated regime, increasing the temperature has a minimal effect on the amount of polymer adsorbed, but when the chain size, composition and architecture are such that the chain is in the buoy/anchor regime, it has a substantial effect. We postulate the lower adsorbance is a direct result of the looped nature of the adsorbed triblock interface. The adsorption of block polymers is basically a competition between a gain in energy due to SF interactions with the surface and a loss of energy due to crowding of the buoy segments in the adsorption layer. This competition results in an approximately $1/N_A$ dependence of the graft density when the anchor is relatively large and in control. It has been shown that the length of the chain can affect the amount adsorbed by affecting the transition from the anchor dominated regime through the anchor/buoy and into the buoy/anchor regime. Lower chain lengths result in higher segment density and thus the transition between the two regimes occurs at higher SF fractions. The same trend is also seen with a decrease in the sticky foot strength. We propose that the effect of the triblock copolymers architecture can also be understood by these means. The loop structure causes a higher segment density relative to the diblock and thus causes the transition between the two regimes to happen sooner. We propose that the loop structure just shift the maximums down and to the right. One can also postulate the effect of other architectures on this same basis; in general we can predict that as the number of blocks increases, the thickness of the adsorbed layer decreases and the osmotic crowding effect will become

important sooner. Evers has already shown data for inverted triblocks (i.e. BAB) that indicate that they adsorb to a lesser amount than the diblocks, presumably for these same reasons. The two tails will make a layer of a smaller thickness than that of the diblock and thus the crowding term comes into play faster. In this work we developed a synthetic procedure to prepare a great multitude of polymeric structures. With these structures we should be able to determine the contributions of each factor as a function of chain length, architecture, SF strength on the amount of polymer adsorbed and the layer thickness, etc.

The study of these sticky foot polymer systems will provide useful and practical information for the application of these types of polymers to functions such as colloidal stabilization, drag control, biocompatibility and adhesion. Colloidal stabilization is one of the main areas of application for these polymers. Understanding the adsorption curves and their dependence on such variables as SF content, SF strength, molecular weight and solvent effects should lead to more economical use of polymers for controlling colloidal stability; polymers can be designed perform these tasks more efficiently, i.e. with less material. For instance designing a polymer with a composition near the v_A^{opt} would lead to the best stabilization because this is where the amount of polymer adsorbed and the layer thickness is the greatest. One would also stay on the high SF side of the maximum because the polymer is strongly held here. On the other hand if the polymer needs to be easily desorbed then the use of the product on the left side v_A^{opt} is more desirable. One can see how a better understanding of these phenomena and the ability to prepare these types of polymers would enhance the use of polymers for such applications. Different architectures

have different applications, for instance we have seen that triblock copolymers can be used to induce flocculation. Other architectures may find other applications. The effect of random modification also has economic ramifications because more than likely the sticky foot is the most expensive component of the polymer and if less of it can be used, the product will be less expensive. This also may be useful when the solvent system is not a good solvent for the sticky foot and micellization and other complications could occur; partial modification of the sticky block may alleviate these problems. The control of drag properties and these types of things may greatly depend on the tail/loop structure of the adsorbed polymer layer. The actual segment density distribution may be important and the use of BAB type polymers with two B blocks of different sizes may be an easy means of tailoring the segment density and a bimodal type structure with control of each thickness could be achieved. In this sense one may even be able to hide functional groups inside a tail layer by attaching them to the short blocks, or if they are attached to the long block the inside tail ends should drive the longer ends (containing the functionality) to the outside. It may also even be the case that these double tiered structures will form a better layer for colloidal stabilization. One of the most interesting applications of this work is in the use of asymmetric polymer chains for specific uses the possibility of using these to dynamically change the structure of the adsorbed layer. Triblock copolymers containing three different chemical components are the ultimate structures in this regard. One block could be used to anchor the chain to the surface, one block would be inert and act as a tether and the third component would carry some wanted functionality or the ability to do a specific task. This could be a catalyst moiety or some other functional group that needs to be

attached to a surface. This optimal design has not been fully realized in the system developed here but we have come close in couple ways. One obvious way is to prepare an end functionalized block copolymer. The end group can then be used for any number of things as is or could be further reacted as in the example of the perfluoroalkyl end group that we prepared. The second way of preparing asymmetric copolymers is to prepare triblock copolymers sticky blocks of different sizes on either end. With judicious choice of block size and conditions, the structure of the adsorbed layer could be interconverted between loops and tails. This could be used as a way to flocculate and deflocculate a system at will. For example we have seen with this research that the amount of polymer adsorbed can be affected by the temperature (or displacer concentration) we have also seen that the larger the polymer block the "stickier" it is. Thus a polymer chain with one large block and one small block would adsorb in a loop structure at low temperature, but upon raising the temperature the smaller block would desorb. The newly formed tail layer should be thicker, have different solvent drag properties and also could be used to put functionality out into solution. If the polymer were flocculating a dispersion the particles should now be released. We can envision a transition to and from a molecular velcro where one could use this transition to increase adhesion or entrap molecules in a surface region for release later. We may even find that a catalyst could be hidden from contamination and brought out for future use after the danger is gone. One may find that small tight loops are better at repelling other adsorbing molecules and biological species, etc. Adhesion may also be increased by knitting of the surface by using multiblock copolymers that will form loops on the surface that will not disentangle easily.

References

1. Valint Jr., P. L.; Bock, J. *Macromolecules* **1988**, *21*, 175.
2. Valint Jr., P. L.; Bock, J. U.S. Patent 4,492,785 1985, Jan. 8.
3. Fetters, L. J.; Firer, E. M.; Dafauti, M. *Macromolecules* **1977**, *10*, 1201.
4. Chen, J.; Fetters L. J. *Polymer Bull.* **1981**, *4*, 275.
5. Morton, M.; Fetters, L. J. *Rubber Chem. & Tech.*, **1975**, *8*(3), 359.
6. Carey, F. A.; Sundberg, R. J. *Advanced Organic Chemistry Part A: Structure and Mechanisms 2nd ed.*, Plenum Press: New York, 1984, Chapter 9.
7. Carey, F. A.; Sundberg, R. J. *Advanced Organic Chemistry Part B: Reactions and Synthesis 2nd ed.*, Plenum Press: New York, 1984, Chapter 8.
8. March, J. *Advanced Organic Chemistry 3rd ed.*, John Wiley & Sons: New York, 1977, Chapter 11.
9. Streitwieser Jr., A.; Heathcock, C. H. *Introduction to Organic Chemistry 2nd ed.* Macmillan Pub.: New York, 1981, Chapter 23.
10. Norman, R. O. C.; Taylor, R. *Electrophilic Substitution in Benzenoid Compounds*, Elsevier Pub.: New York, 1965.
11. Olah, G. A. *Acc. Chem. Res.* **1970**, *4*, 240.
12. Olah, G. A.; Kobayashi, S. *J. Am. Chem. Soc.* **1971**, *93*, 6964.
13. Reference 7, p 382, and Reference 8, p 480.
14. Reference 8, p 476.
15. Reference 8, p 508.
16. Smisek, D. L. Ph.D. dissertation, Univ. of Mass., Chemical Engineering Department, 1991.
17. Kawaguchi, M.; Hayashi, K.; Takahashi, A. *Macromolecules*, **1988**, *21*, 1016.
18. Cerfontain, H. *Mechanistic Aspects of Sulfonation and Desulfonation*, Interscience: New York, 1968.

19. Reference 10, p 101, and reference 8, p 473.
20. Reference 8, p 473.
21. The SO₃ was transferred in a N₂ purged glove bag and turned the inside of the bag green in less than 1 h.
22. Turbek, A. F. *I&EC Product Research and Development* **1962**, *1*, 275.
23. Carroll, W. R.; Eisenburg, H. *J Poly. Sci.: Part A-2* **1966**, *4*, 599.
24. Vink, H. *Makromol. Chem.* **1981**, *182*, 279.
25. Personal communication with K. Antolin.
26. Manacke, G.; Wetzel, G.; Storck, W. *Die Makromol. Chemie* **1975**, *176*, 3251.
27. Manecke, G.; Beier, W. *Die Angewandte Makromolekulare Chemie* **1981**, *97*, 23.
28. Reference 8 p 475.
29. Gupta, S. K. *Synthesis* **1977**, 39.
30. Searles, S.; Nukina, S. *Chemical Reviews*, **1959**, *59*, 1077.
31. Reference 8, p 508 and references therein.
32. Reference 6, p 518 and references therein.
33. Roberts, R. M.; Khalaf, A. A. *Friedel Crafts Alkylation Chemistry* Marcel Dekker Inc.: New York, 1984.
34. Reference 33, p 676.
35. Reference 6, p 499.
36. Ghosh, S.; Pardo, S. N.; Solomon, R. G. *J. Org. Chem.* **1982**, *47*, 4692.
37. Ando, T. *Nippon Kagaku kaishi* 1935, 56, 745.
38. Riebsomer, J. L.; Baldwin, R.; Buchanan, J.; Burkett, H. *J. Am. Chem. Soc.* **1938**, *60*, 2974.
39. Riebsomer, J. L.; Stauffer, D.; Glick, F.; Lambert, F. *J. Am. Chem. Soc.* **1942**, *64*, 2080.

40. Riebsomer, J. L.; Irvine, J.; Andrews, R. *J. Am. Chem. Soc.* **1938**, *60*, 1015.
41. Riebsomer, J. L.; Irvine, J. *Organic Syntheses* **3**, 326.
42. Aldrich NMR catalog, Vol. 2 Methyl mandelate M5,410-4 among others.
43. This was determined from a survey of mandelate structures in the Aldrich NMR vol 2.
44. Reference 7, pp.199-213 and Reference 8 pp.1093-1102.
45. Reference 7, pp.193-199 and Reference 8 pp.392-393.
46. Reference 7, pp 213-217 and Reference 8 pp.389-393.
47. Reference 7, p.196.
48. Reference 7, p.217.
49. Reference 8, p.393.
50. Evers, O. A.; Scheutjens, J. M. H. M.; Fleer, G. J. *Macromolecules* **1990**, *23*(25), 5221.
51. Evers, O. A.; Scheutjens, J. M. H. M.; Fleer, G. J. *J. Chem. Soc. Faraday Trans.* **1990**, *86*(9), 1333.
52. Evers, O. A.; Scheutjens, J. M. H. M.; Fleer, G. J. *Macromolecules* **1991**, *24*(20), 5558.
53. Marques, C.; Joanny, J. F. *Macromolecules* **1989**, *22*(4), 1454.
54. Marques, C.; Joanny, J. F.; Leibler, L. *Macromolecules* **1988**, *21*(4), 1051.
55. Munch, M. R.; Gast, A. P. *Macromolecules* **1988**, *21*(5), 1360-1366, 1366.
56. Guzonas, D. A.; Boils, D.; Tripp, C. P.; Hair, M. L. *Macromolecules* **1992**, *25*(9), 2434.
57. Guzonas, D.; Hair, M. L.; Cosgrove, T. *Macromolecules* **1992**, *25*(10), 2777.
58. Guzonas, D.; Boils, D.; Hair, M. *Macromolecules* **1991**, *24*(11), 3383.

59. Parsonage, E.; Tirrell, M.; Watanabe, H.; Nuzzo, R. *Macromolecules* **1991**, 24(8), 1987.
60. Wu, D. T.; Yokayama, A.; Setterquist, R. *Polymer Journal* **1991**, 23(5), 709.
61. Kawaguchi, M.; Arai, T. *Macromolecules* **1991**, 24, 889.
62. Malmsten, M.; Linse, P.; Cosgrove, T. *Macromolecules* **1992**, 25(9), 2474.
63. Stouffer J. M.; McCarthy, T. J. *Macromolecules* **1988**, 21(5), 1204.
64. Parsonage, E.; Tirrell, M.; Watanabe, H.; Nuzzo, R. *Macromolecules* **1991**, 24(7), 1987.
65. Nagata, K; Kawaguchi M. *Macromolecules* **1990**, 23, 3957.
66. Johnson, H.; Granick, S. *Macromolecules* **1991**, 24(10), 3023.
67. van der Beek, G. P.; Cohen Stuart, M. A. *Macromolecules* **1991**, 24(12), 3553.
68. Leermakers, F. M. A.; Gast, A. P. *Macromolecules* **1991**, 24(3), 718.
69. Munch, M. R.; Gast, A. P. *J. Chem. Soc. Faraday Trans.* **1990**, 86(9), 1341.
70. Tassin, J. F.; Siemens, R. L.; Wing, T. T.; Hadziioannou, G.; Swalen, J. D.; Smith, B. A. *J. Phys. Chem.* **1989**, 93(5), 2106.
71. Cohen Stuart, M. A.; Tamai, H. *Macromolecules* **1988**, 21, 1863.
72. Webber, R. M.; Anderson J. L.; Jhon, M. S. *Macromolecules* **1990**, 23(4), 1026.
73. Cohen Stuart, M. A.; Waajen, F. H. W. H.; Cosgrove, T.; Vincent, B.; Crowley, T. L. *Macromolecules* **1984**, 17, 1825.
74. Israelachvili, J. N.; Tirrell, M.; Klein, J.; Almog, Y. *Macromolecules*, **1984**, 17(2), 204.
75. Guzonas, D.; Boils, D.; Hair, M. *Macromolecules* **1991**, 24(11), 3383.

76. Hadziioannou, G.; Patel, S.; Granick, S.; Tirrell, M. *J. Am. Chem. Soc.* **1986**, *108*(11), 2869-2876.
77. Cosgrove, T.; Heath, T. G.; Phipps, J. S.; Richardson, R. M. *Macromolecules* **1991**, *24*(1), 94-98.
78. Field, J. B.; Toprakcioglu, C.; Ball, R. C.; Stanley, H. B.; Dai, L.; Barford, W.; Penfold, J.; Smith, G.; and Hamilton, W. *Macromolecules* **1992**, *25*(1), 434.
79. Gordon, A. J.; Ford, R. A. *The Chemist's Companion: A Handbook of Practical Data, Techniques, and References*, Wiley-Interscience: New York, 1972, p375.
80. Iyengar, D. R.; McCarthy, T. J. *Macromolecules* **1990**, *23*(20), 4344-4346.
81. Cohen Stuart, M. A.; Fleer, G. J.; Scheutjens, J. M. H. M. *J. Colloid and Interface Science* **1984**, *97*(2), 515.
82. Cohen Stuart, M. A.; Fleer, G. J.; Scheutjens, J. M. H. M. *J. Colloid and Interface Science* **1984**, *97*(2), 526.
83. van der Beek, G. P.; Cohen Stuart, M. A.; Fleer, G. J.; Hofman, J. E. *Langmuir* **1989**, *5*, 1180.
84. The control reaction resulted in half the spot eluting the same as the virgin PtBS but about half the spot remaining and requiring 3.8-7% displacer (EA) before eluting. This is discussed in the synthesis section.
85. Mays, J. M.; Ferry, W. M.; Hadjichristidis, N.; Funk, W. G.; Fetters, L. J. *Polymer*, **1986**, *27*, 129.
86. Mays, J. W.; Nan, S.; Whitfield, D. *Macromolecules*, **1991**, *24*, 315.
87. Silverstein, R. M.; Bassler, C. G.; Morrill, T. C. *Spectrometric Identification of Organic Compounds 4th ed.*, John Wiley & Sons: New York, 1981, Chapter 6.
88. Andrade, J.D.; Gregonis, D.E.; Smith, L.M. In *Surface and Interfacial Aspects of Biomedical Polymers* Andrade, J.D. ed. Plenum: New York, 1986, Vol. 1, Ch. 5.
89. Muilenberg, G.E. *Handbook of X-Ray Photoelectron Spectroscopy*, Perkin-Elmer Corp., 1979.

90. Clark, D.T.; Thomas, H.R. *J. Polym. Sci., Polym. Chem. Ed.* **1977**, *15*, 2843.
91. Reference 88, Ch. 7.
92. Eisenlauer, J.; Killmann, E. *J. Colloid and Interface Sci.* **1980**, *74*, 108.
93. Degussa product literature.
94. See for example Reference 92.
95. Napper, D. *Polymeric Stabilization of Colloidal Dispersions*; Academic: London, 1983.
96. Pepperkorn, E.; Jean-Chronberg, A. C.; Varoqui, R. *Macromolecules*, **1990**, *23*, 1735.
97. Guiochon, G.; Golshan-Shirazi, S.; Jaulmes, A. *Anal. Chem.* **1988**, *60*, 1856; Golshan-Shirazi, S.; Ghodbane, S.; Guiochon, G. *Anal. Chem.* **1988**, *60*, 2630; Diack, M.; Guiochon, G. *Anal. Chem.* **1991**, *63*, 2608.
98. Thambo, G.; Miller, W. G. *Macromolecules* **1990**, *23*, 4397.
99. Stober, W.; Fink, A.; Bohn, E. *J. Colloid and Interface Sci.* **1968**, *26*, 62.

CHAPTER IV

SYNTHESIS OF STYRENE-PROPYLENE SULFIDE BLOCK COPOLYMERS AND THEIR ADSORPTION TO THE GOLD-SOLUTION INTERFACE

Introduction

The work presented in this chapter involves the study of the adsorption of styrene-propylene sulfide block copolymers to the gold-solution interface; this was a collaborative effort with D. Waldman.¹⁻³ The sulfide-gold interaction energy is high, and thus the sulfide moiety acts as a very strong sticky foot. Reports of studies with thiols and sulfides have estimated that the binding energy due to coordination of sulfur to three gold atoms is on the order of 15 - 30 kcal/mole⁴, roughly 15 - 50 times greater than the nonbonded and/or weak hydrogen bonding surface-segment interactions typical of hydrocarbons (such as a polystyrene chain). We found that the styrene-propylene sulfide copolymers would adsorb from good displacer solvents like THF. One of the prerequisites for this study was the synthesis of well defined block copolymers from these two monomers; however, this synthesis was not straightforward. The main body of this chapter discusses the development of a reliable synthesis of these block structures and also some of the more general experimental aspects of anionic block polymerizations. A summary of the adsorption results is presented at the end of the chapter.

Poly(styrene-*co*-propylene sulfide) block copolymers of varying block ratios but constant overall degree of polymerization were prepared

via anionic block polymerization. This synthetic route produced monodisperse polymers and allowed good control over the molecular weight and block sizes. These copolymers were readily soluble in common organic solvents. Adsorption studies were carried out on gold surfaces (prepared by vapor-depositing gold vapor onto glass) from both good solvent (THF) and theta solvent (cyclohexane, 35 °C) conditions.

Synthesis of Poly(styrene-*co*-propylene sulfide) Block Copolymers

The objective of the synthesis reported here was to prepare styrene-propylene sulfide block copolymers (PS-*b*-PPrS) with a high degree of monodispersity and in such a fashion as to maintain the same overall degree of polymerization while altering the molar block ratios. The synthetic method chosen was sequential living anionic polymerization; polystyryllithium blocks of the desired molecular weight were used to initiate polymerization of propylene sulfide (PrS) (Figure 4.1).

Background

The polymerizations of thiiranes were first reported in 1920⁵, and they were found to polymerize both in the presence of base (anionically) and acid (cationically). Polymerizations of ethylene sulfide, propylene sulfide, isobutylene sulfide and others were attempted, and it was found that a wide variety of compounds would initiate polymerization. Alkali metals, hydroxides, hydrides, and alkoxides, amines and other transition metal complexes were found to initiate polymerization to low molecular weight material. Boileau and Sigwalt ⁶ reported high molecular weight anionically polymerized PPrS in 1961 and started a 10-12 year period of extensive research on anionic polymerizations of thiiranes. During this

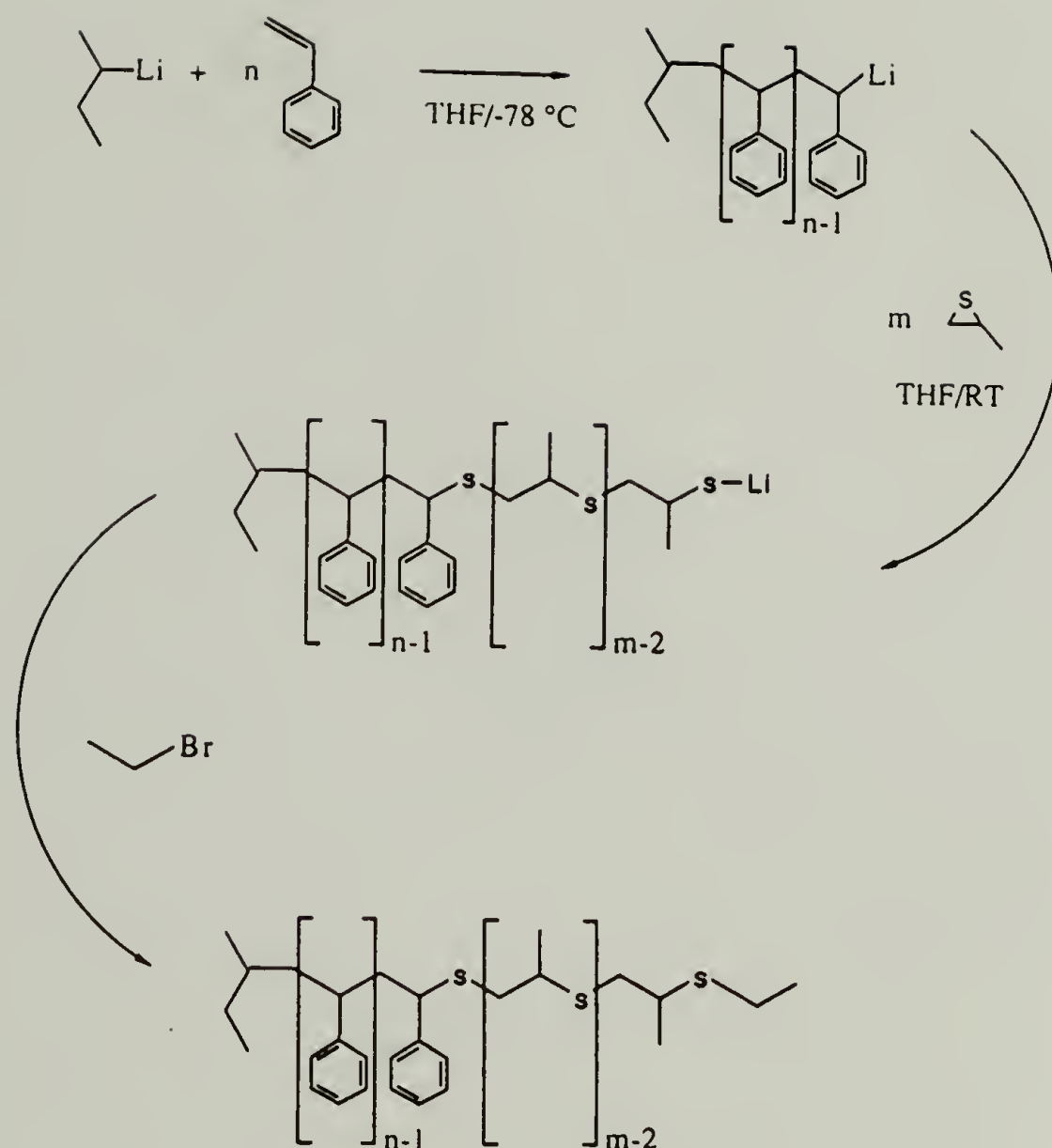


Figure 4.1 Reaction scheme for synthesis of poly(styrene-*co*-propylene sulfide) block copolymers. The synthesis involves initial polymerization of styrene followed by propylene sulfide polymerization. The polymers were endcapped with ethyl bromide.

period it was discovered that anionic polymerizations of thiiranes in polar solvents under anhydrous conditions were living in nature and gave molecular weights that were proportional to the amount of initiator used. It should be noted that the typical analysis of the molecular weight and polydispersity was performed with vapor pressure osmometry (VPO) and light scattering. GPC traces of these sulfur containing polymers are rarely seen in journal articles and thus the actual distributions in most cases are not really known (although they are assumed to be monodisperse and monomodal in shape). Anionic polymerization of thiiranes have been reviewed in the literature.^{5, 7-11}

Block copolymers of styrene (S), α -methylstyrene (α MeS) and methyl methacrylate (MMA) with ethylene sulfide (ES) and propylene sulfide (PrS) were reported by Nevin and Pearce in 1965.¹² Since that time others have also reported block copolymers with polythiiranes and a number of other polymers: polystyrene/poly(propylene sulfide),¹³ poly(α -methylstyrene)/poly(propylene sulfide),¹⁴ polybutadiene/poly(ethylene sulfide) and polyisoprene/poly(ethylene sulfide),¹⁵⁻¹⁷ poly(ethylene sulfide)/poly(propylene sulfide),¹⁸ poly(ethylene sulfide)/polyisobutylene,¹⁹ poly(vinyl pyridine)/poly(propylene sulfide)²⁰ and other variations thereof. In all cases the vinyl monomer was polymerized first and used to initiate the polymerization of the thiirane. Initiation in these cases was found to occur by a sulfur extrusion mechanism to yield the thiolate and the corresponding alkene.²¹ The reports of Nevin et. al. and Morton et. al. are the most pertinent to our work. Nevin et. al. carried reactions out under an inert atmosphere and used dried solvents (Na/naphthalene) and monomers (CaH_2). The reactions were carried out in

THF with *sec*-butyllithium initiation; styrene was polymerized at -78 °C, and PPrS at room temperature. The copolymer was precipitated in acidic methanol. The polymers were prepared with approximately 50/50 (PS/PPrS) composition and had molecular weights between 10,000 and 20,000. The authors reported that polystyrene homopolymer comprised 5% of the reaction product (as was determined from extraction studies), and that the copolymers were unstable. No GPC data were reported. Morton et. al. reported the synthesis of triblock copolymers ABA (P α MeS-co-PPrS-co-P α MeS) prepared by coupling thiol-ended diblock copolymers with phosgene. These polymers were comprised of 20-40% α -methylstyrene and had an average molecular weight around 90,000. GPC results indicated a low molecular weight peak corresponding to about 5% uncoupled product. The homopolymer PPrS was also prepared and endcapped with ethylbromide to increase its stability. Morton et. al. reported the molecular weight of this polymer from VPO but no GPC data were shown. A search of the Citation Index revealed about 40 papers that have cited the work of either Nevin or Morton; 25 to 30 of these papers were reviewed and only one (Cooper's) included GPC data.¹⁷ Cooper et. al. reported the synthesis of a triblock copolymer of styrene, isoprene and ethylene sulfide (PS/PI/PES). The GPC data (which are not very good) indicate the presence of a substantial amount of homopolymer and diblock copolymer. The triblock peak comes at a much shorter elution time and is rather broad; they identify it as an aggregate but it could easily include some of the coupled product (disulfide). The Cooper paper reveals a rather poor synthesis. The Morton paper does not show the GPC of the homopolymer and it is obvious that the GPC of the coupled product would mask the dimer in the chromatogram. These traces are of such breadth

that it is ambiguous whether any dead homopolymer was present. The point is that earlier synthesis of these materials probably had the same problems as will be described in this report, but the lack of GPC data masks this fact.

Experimental: Synthetic Aspects

THF (Aldrich) was purified a number of ways. THF distilled from Na/benzophenone dianion was used for adsorption experiments, disulfide reductions and some polymerizations (although this is not recommended). THF was also dried by distillation from CaH_2 followed by trap-to-trap distillation from *sec*-butyllithium; this was the procedure used to dry THF for polymerizations.

DMF (Aldrich) was distilled from MgSO_4 under reduced pressure.

sec-Butyllithium (Aldrich) was used as received (~1.3 M solution in hexanes) or diluted before use with dry hexane or benzene.

Benzene (Aldrich) was distilled from Na/benzophenone or CaH_2 .

Ethylbromide (Aldrich) was degassed via greater than three freeze/pump/thaw cycles.

Dithiothreitol (Aldrich) was used as received and stored in a refrigerator in a glove box.

Acetic Acid (Fisher) was used as received.

Zinc (Fisher) was used as received.

Chlorine (Merriam Graves) was used as received and dispensed from a lecture bottle via the appropriate regulator.

Styrene (Aldrich) was distilled from CaH_2 and stored in Schlenk flasks in freezer. Before polymerization styrene was further dried by distillation (trap-to-trap) from dibutylmagnesium.

Propylene Sulfide (Aldrich) was distilled from CaH_2 and stored in Schlenk flasks in a freezer. Before polymerization PrS was further dried by distillation (trap-to-trap) from dibutylmagnesium.

Polymer Synthesis. All polymerizations were carried out in basebath-cleaned glassware that was stored in a drying oven at approximately $80\text{-}100^\circ\text{C}$ for at least 12 h. All glassware was assembled hot and under N_2 purge. Teflon stopcocks were preferred to grease stopcocks, but vacuum grease was used and found preferable to teflon sleeves on ground glass joints. A 250 mL Schlenk flask fitted with a glass plug was used as the reaction vessel in most situations. This allowed more adequate stirring and greater reaction volumes than using a 50 ml Schlenk tube; pressure bottles were tried, but small pieces of the black rubber seal were found to contaminate (and affect) the polymerization. All transfers were done via cannula or gas-tight luer-tip syringe. All needles and cannula were cleaned with hexane, 1.0 M HCl, 1.0 M NaOH, H_2O , and acetone, and then purged dry and kept in the oven until right before use. Transfers were also facilitated by a portable antechamber made from 750 x 9 mm glass tubing fitted on both ends with the appropriate septa and then purged

with N₂. Prepurified N₂ was used as received at 6 to 9 psig without further drying. During the assembly and transfers, clean latex gloves were worn at all times to minimize contamination by perspiration and oils from hands. All assembled glassware (reaction vessels, distillation apparatus, trap-to-trap and storage apparatus) were further dried by purging 10 min with N₂ then a repeated pump/heat/backfill cycle. All solvents and monomers were distilled directly before use. *sec*-butyllithium (*s*BuLi) was diluted with dry hexane or heptane and stored in 15 ml Schlenk tubes with dessicant in a freezer and at 0 °C on the bench.

THF was used as the polymerization solvent and the following procedure was used to dry it. THF (distilled from CaH₂) was cooled to -78 °C in a Schlenk tube and *sec*-butyllithium was added until a green color was obtained (green color indicates that the lithium reagent is present, i.e. the solvent is dry). The green solution was stirred for 30 min and then degassed and distilled (trap-to-trap) into a new tube. The THF was then transferred to the polymerization flask and cooled to -78 °C and a very small amount of *sec*-butyllithium was added until a light green color appeared (indicating dryness). The THF was allowed to warm up to room temperature over a 30 - 45 min time span during which time the *sec*-butyllithium reacted with the THF and the solution became clear. At this point, the reaction flask and contents were ready to cool to -78 °C to begin the polymerization [B8-79-87, 94-100, 113, 114; B9-5].

The solvent in the reaction vessel was cooled to -78 °C and stirred; the stoichiometric amount of *sec*-Butyllithium was added via syringe. The appropriate amount of styrene was then added via syringe and the

characteristic orange/red color appeared. It was allowed to react for 15 - 30 min which is sufficient time for completion of styrene polymerization as determined by GC. It is important that the styrene be added to well stirred *s*BuLi and not the other way around because the polymerization in THF is so fast that one can see stirring effects in the molecular weight distributions if the initiator is added to a solution of the monomer. Aliquots of polystyrene were taken to determine the polydispersity and molecular weight of the polystyrene block. The appropriate amount of PrS was then added via syringe, at which time the color disappeared. The polymerization was allowed to warm to room temperature and proceed to 100% conversion as determined by GC. Endcapping of the block copolymers was achieved by addition of either degassed acidic methanol, or degassed, distilled ethyl bromide. The polymer was then precipitated in cold, degassed methanol, redissolved in THF, reprecipitated in methanol and dried at reduced pressure. The larger propylene sulfide blocks can result in rather poor reprecipitation of the polymer (i.e. the polymers tend to want to form emulsions).

Triphenyl Phosphine Reductions. The reduction attempts with this reagent are recorded in Table 4.1 (entries 1 and 2). 450 mg polymer was dissolved in ~20 mL THF and approximately 5 mL water and 2 drops of HCl (concentrated) were added and over time the solution turned cloudy. Triphenyl phosphine (TPP) (10 mg or 100 mg) was added and the reaction carried out at 40 °C for 3 h (or 12 h). The reaction was cooled to room temperature and ethyl bromide (EtBr) (~0.5 mL) was added and allowed to react for 2 h. The polymer was precipitated in MeOH. GPC data showed no change in the triblock to diblock ratio.

Reductions with Zinc/Acetic Acid. Attempts were made to reduce the disulfide using zinc/acetic acid; these data are found in Table 4.1 (entries 3 and 4). The polymer (240 mg) and zinc metal (54 mg) were put into a 50 mL Schlenk tube (water-jacketed to enable reflux) and purged with N₂. THF (5 mL) and acetic acid (2.5 mL) were added to dissolve the polymer. The solution was refluxed for 4 hours and some white solid formed in the tube. The tube was cooled to room temperature and the polymer was precipitated in methanol.

Reductions with Cl₂. Attempts were made to reduce the disulfide using chlorine gas; these data are found in Table 4.1 (entry 5). The polymer was dissolved in CH₂Cl₂ and Cl₂ gas was bubbled through the solution. 1-hexene was added to end-cap the resultant sulfenyl chloride and the polymer was precipitated in methanol.

Dithiothreitol Reductions. The reductions using dithiothreitol (DTT) were performed in a number of different ways, indicated in Tables 4.2 and 4.3. In all situations well degassed solvents and Schenk transfer techniques were used to exclude oxygen from the system. The method of base catalysis was varied also. In some cases, no base was added to the reaction mixture, in others a NaOH/water solution was prepared and 1-2 mL were added to the reaction flask, and at other times a "pinch" of NaH was added to the reaction solution. The final method entailed placing a pellet of NaOH in the bottom of the reaction tube and allowing it to saturate the solution (these different methods are recorded in Tables 4.2 and 4.3). In a typical reaction without base [B6-92] 600 mg of polymer was added to a 50

Table 4.1 Various Disulfide Reduction Attempts.

<u>Notebook Ref.</u>	<u>Sample</u>	<u>Results^a</u>	<u>Conditions</u>
1. B6-79	B6-77 50/50; 66K 15.5% dimer	No change	450 mg polymer 10 mg triphenylphosphine THF:H ₂ O (20 mL:5 mL) 40 °C, 3 h
2. B6-79	B6-77 50/50; 66K 15.5% dimer	No change	450 mg polymer 100 mg triphenylphosphine THF:H ₂ O (25 mL:5 mL) 40 °C, 12 h
3. B6-78	B6-77 50/50; 66K 15.5% dimer	PPrS block Cleaved	250 mg polymer zinc 15 mL acetic acid, 25 mL THF Room temperature, 2 h
4. B6-86	B6-81 50/50; 45K 11% dimer	PPrS block Cleaved	250 mg polymer 50 mg zinc 2.5 mL acetic acid, 5 mL THF reflux, 4 h
5. B6-80	B6-77 50/50; 66K 15.5% dimer	PPrS block Cleaved	250 mg polymer Cl ₂ gas CH ₂ CCl ₂ Room temperature, 1 h This reaction was run a couple of times with the same result

^a Results determined by GPC analysis.

mL Schlenk flask which was then purged with N₂; 6-8 mL of THF was added to the polymer and the mixture dissolved. DTT (2 mL of a 0.62 M (190 mg) solution in THF) was added and the reaction carried out at room temperature for 12 h. Ethylbromide (<0.05 mL) was added to end-cap the resultant thiolate ends. The endcapping reaction was allowed to proceed for the desired time (in this case 15 min). Isolation of the polymers proved to be a problem sometimes; attempts at normal precipitation procedures in methanol resulted in very fine precipitates (in some cases milky solutions were obtained) and these were difficult or impossible to filter. A couple of different methods were tested in an effort to alleviate this problem. In some cases the solvent was pulled off under reduced pressure with or without heat. This resulted in a polymeric goo which was then redissolved in minimum amount of methylene chloride or toluene and precipitated in methanol. Another method that worked on occasion was to cool the solution down to -78 °C and then precipitate in methanol. This method usually resulted in a filterable precipitate that could be collected and redissolved in a minimum amount of methylene chloride and then precipitated again.

Results and Discussion: Synthetic Aspects

Anionic living polymerizations, in general, require extreme cleanliness in all aspects of the process; any source of protons is sure to kill some fraction of the living chains (see references 22-24 for general reviews) . Because each sequential addition must leave all the living ends alive, the cleanliness requirement is even more stringent for the synthesis of block copolymers and specifically endcapped chains. Anything less than

Table 4.2 Disulfide Reductions of Block Copolymers with DTT in THF.

<u>Notebook Reference</u>	<u>% Dimer Initial</u>	<u>% Dimer Final</u>	<u>Conditions</u>
1. B6-89 B6-81 50/50; 94K	11%	5.5%	250 mg polymer (31 mg/mL) 190 mg DTT (24 mg/mL) 8 mL THF, H ₂ O, EtOH, NaOH 1 h < 0.5 mL EtBr 10 min
2. B6-92 B6-81 50/50; 94K	11%	0%	600 mg polymer (60 mg/mL) 190 mg DTT (19 mg/mL) 10 mL THF, no base 12 h < 0.5 mL EtBr, 15 min
3. B6-98 B6-82 50/50; 42K	5%	0%	350 mg polymer (50 mg/mL) 190 mg DTT (27 mg/mL) 7 mL THF, NaH 4 h < 0.5 ml EtBr, 12 h
4. B8-45 B8-44 50/50; 77K	8.3%	0%	100 mg polymer (6.7 mg/mL) 300 mg DTT (20 mg/mL) 15 mL THF, NaH 4 h < 0.5 mL EtBr, 12 h
5. B8-46 B8-44 50/50; 77K	8.3%	0%	100 mg polymer (6.7 mg/mL) 300 mg DTT (20 mg/mL) 15 mL THF, NaH 20 h < 0.5 mL EtBr, 12 h
6. B8-52 B8-51 90/10; 82K	9.1%	3%	400 mg polymer (20 mg/mL) 400 mg DTT (20 mg/mL) ~20 mL THF, NaH 12 h < 0.5 mL EtBr, 30 min
7. B8-52 B8-51 90/10; 82K	9.1%	2%	150 mg polymer (~7.5 mg/mL) 200 mg DTT (~10 mg/mL) ~20 mL THF, NaH 12 h < 0.5 mL EtBr, 30 min

continued next page

Table 4.2 continued

8. B8-52	9.1%	0%	Continued reaction of #7 with the addition of 250 mg DTT and 10 mL THF Reacted an additional 1.5 h.
B8-51 90/10; 82K			
	9.1%	0%	Same as #8 reacted an additional 1.5 h
9. B8-52			
B8-51 90/10; 82K			
10. B8-52	9.1%	0%	Same as #8 reacted an additional 3.5 h
B8-51 90/10; 82K			
11. B8-61	6.8%	4%	260 mg polymer (29 mg/mL) 450 mg DTT (50 mg/mL) 9 mL THF, H ₂ O/NaOH 2.5 h < 0.5 mL EtBr, 30 min
B8-60 90/10; 121K			
12. B8-140	8.3%	0.5%	100 mg polymer (8.3 mg/mL) 1500 mg DTT (125 mg/mL) 12 mL THF, 1 mL Pyridine 4 h < 0.5 mL EtBr, 12 h
B8-44 50/50, 78K			

Table 4.3 Disulfide Reductions of Block Copolymers with DTT in DMF.

<u>Notebook Reference</u>	<u>% Dimer Initial</u>	<u>% Dimer Final</u>	<u>Conditions</u>
1. B8-72 B8-51 90/10; 82K	9.1%	1%	250 mg polymer 250 mg DTT DMF, H ₂ O/NaOH 1 h ~1.0 mL EtBr, 20 h
	9.1%	1%	+ 250 mg DTT, 2.5 h 1.0 mL EtBr, 30 min
2. B8-101 B8-95 80/20; 101K	8.6%	5.9%	420 mg polymer (21 mg/mL) 700 mg DTT (35 mg/mL) 20 mL DMF, NaH 10 min < 0.5 mL EtBr, 10 min
	8.6%	3.5%	+ 30-60 min < 0.5 mL EtBr, 12 h
3. B8-103A B8-95 80/20; 101K	8.6%	5.3%	100 mg polymer (~6.7 mg/mL) 250 mg DTT (~16.7 mg/mL) ~10-20 mL DMF, NaH 3 h < 0.5 mL EtBr, 10 min
4. B8-103B B8-95 80/20; 101K	8.6%	5%	100 mg polymer (~6.7 mg/mL) 250 mg DTT (~16.7 mg/mL) ~10-20 mL DMF, NaOH(pellet, satd.) 1 h < 0.5 mL EtBr, 10 min
5. B8-103C B8-95 80/20; 101K	8.6%	5%	100 mg polymer (~6.7 mg/mL) 450 mg DTT (~30 mg/mL) ~10-20 mL DMF, No base 1 h < 0.5 mL EtBr, 10 min
6. B8-103D B8-95 80/20; 101K	8.6%	3.3%	100 mg polymer (~6.7 mg/mL) 250 mg DTT (~16.7 mg/mL) ~10 mL DMF, NaOH(pellet, satd.) 3 h < 0.5 mL EtBr, 10 min

continued next page

Table 4.3 continued

7. B8-103E	8.6%	3.0%	100 mg polymer (~6.7 mg/mL) 450 mg DTT (~30 mg/mL) ~10 mL DMF, NaH 1 h < 0.5 mL EtBr, 10 min
B8-95 80/20; 101K			
8. B8-105	3.1%	0%	100 mg polymer (~20 mg/mL) 500 mg DTT (~100 mg/mL) ~5 mL DMF, NaOH(pellet, satd.) 2 h 0.5 mL EtBr, 12 h
B8-95 95/5; 63K			
9. B8-106	8.6%	2.8%	100 mg polymer 500 mg DTT DMF, NaOH(pellet, satd.) 2 h < 0.5 mL EtBr, 10 min
B8-95 80/20; 101K			
10. B8-106	28.8%	19%	100 mg polymer 500 mg DTT DMF DMF, NaOH(pellet, satd.) 2 h < 0.5 mL EtBr, 10 min
B8-100 0/100; 47K			
11. B8-107	8.6%	2%	100 mg polymer 600 mg DTT DMF, NaOH(pellet, satd.) 2 h < 0.5 mL EtBr, 10 min
B8-95 80/20; 97K			
12. B8-107	7.7%	0%	120 mg polymer 700 mg DTT 10 mL DMF, NaOH(pellet, satd.) 2 h ~0.5 mL EtBr, 10 min
B8-85 90/10; 63K			
13. B8-109	7.7%	0%	100 mg polymer 1000 mg DTT DMF, NaOH(pellet, satd.) 2 h EtBr, 15 h
B8-85 90/10; 63K			

continued next page

Table 4.3 continued

14. B8-130 ^a	9.6%	4.9%	100 mg polymer (9.1 mg/mL) 1000 mg DTT (90 mg/mL) 11 mL DMF, No base 2.5 h 1 mL EtBr, 20 h
B8-87 80/20; 41K			
15. B8-130 ^a	8.6%	4.4%	100 mg polymer (9.1 mg/mL) 1000 mg DTT (9.1 mg/mL) 11 mL DMF, No base 2.5 h 1.0 mL EtBr, 20 h
B8-95 80/20; 101K			
16. B8-132 ^a	8.6%	4.3% ^b	100 mg polymer (~6.6 mg/mL) 1500 mg DTT (~100 mg/mL) ~15 mL DMF, NaOH 2 h 2 mL EtBr, 12 h
B8-87 80/20; 101K			

^a These samples were not isolated by precipitation like the others. Instead the DMF was pulled off under vacuum with heat and this resulted in discolored polymers and may be the reason for incomplete dimer cleavage.

^b 4% PSH from degradation was observed.

100% (dryness/cleanliness) will result in dead polystyrene homopolymer, which is difficult to separate from the desired copolymer. The high reactivity (especially towards water) of the propagating species requires that special attention be given to reaction vessels and polymerization temperatures. For example, polymerizations in THF require an all glass apparatus and cooling to $-78\text{ }^{\circ}\text{C}$. Special attention must also be given to the drying (purification in general) of all monomers and solvents. Typically these polymerizations are done with very small amounts of very reactive compounds (10-100 mmol per 30 mL) and one needs to obtain essentially 100% conversion because of the difficulty in purification of polymeric products. The molecular weight of the polymer to be synthesized is important because a higher molecular weight requires proportionally fewer anions which means that smaller amounts of impurity can be tolerated. Sources of (water) impurities for this reaction system include those acquired via transfer processes and those already present in the reagents and solvent. Problems caused by the first type can be effectively removed (or minimized) by scaling up the reaction (or improving one's technique). To eradicate the second source of impurities requires judicious choice of drying agents and purification methods.

A variety of problems specifically associated with synthesis of the propylene sulfide block were encountered in these experiments. Figure 4.2 shows a typical GPC chromatogram of a block copolymer synthesized early on in this project.²⁵ Three separate monodisperse peaks are present, but only the large middle peak corresponds to the desired diblock copolymer (PS-*b*-PPrS). The peak at higher elution time is the polystyrene block homopolymer (PS) which resulted from termination of a portion of the

living chain ends during the addition of the second monomer, "wet" PPrS. The peak at lower elution time corresponds to a polymer twice the size of the desired diblock. This results from coupling of the diblock copolymer (PS-*b*-PPrS-*b*-PS) after the polymerization is complete (forming a triblock copolymer). It was also found that (in the diblock copolymer) the PPrS block was not stable; it degraded with time. This was evidenced by a characteristic sulfur smell detected from vials of stored polymer and also by GPC which showed broadening of the molecular weight distribution [B6-62-67].

To restate the (initial) status of the synthesis of these copolymers, it was found that standard drying procedures were insufficient and resulted in dead homopolymer and that the thiolate/thiol end groups of the copolymers were unstable to coupling reactions and PPrS block degradation. It was determined that none of these imperfections could be tolerated in the adsorption experiments and that, since there was no good means of purification, the polymers had to be made without these impurities to begin with. The work presented in this chapter shows the accomplishment of these goals. In the following discussion, each problem and the subsequent solution will be dealt with in greater detail.

Methods for Synthesis. All polymerizations were carried out in basebath-cleaned glassware that was stored in a drying oven at approximately 80-100°C for at least 12 h. All glassware was assembled hot and under N₂ purge. Teflon stopcocks were preferred to grease stopcocks, but vacuum grease was used and found preferable to teflon sleeves on

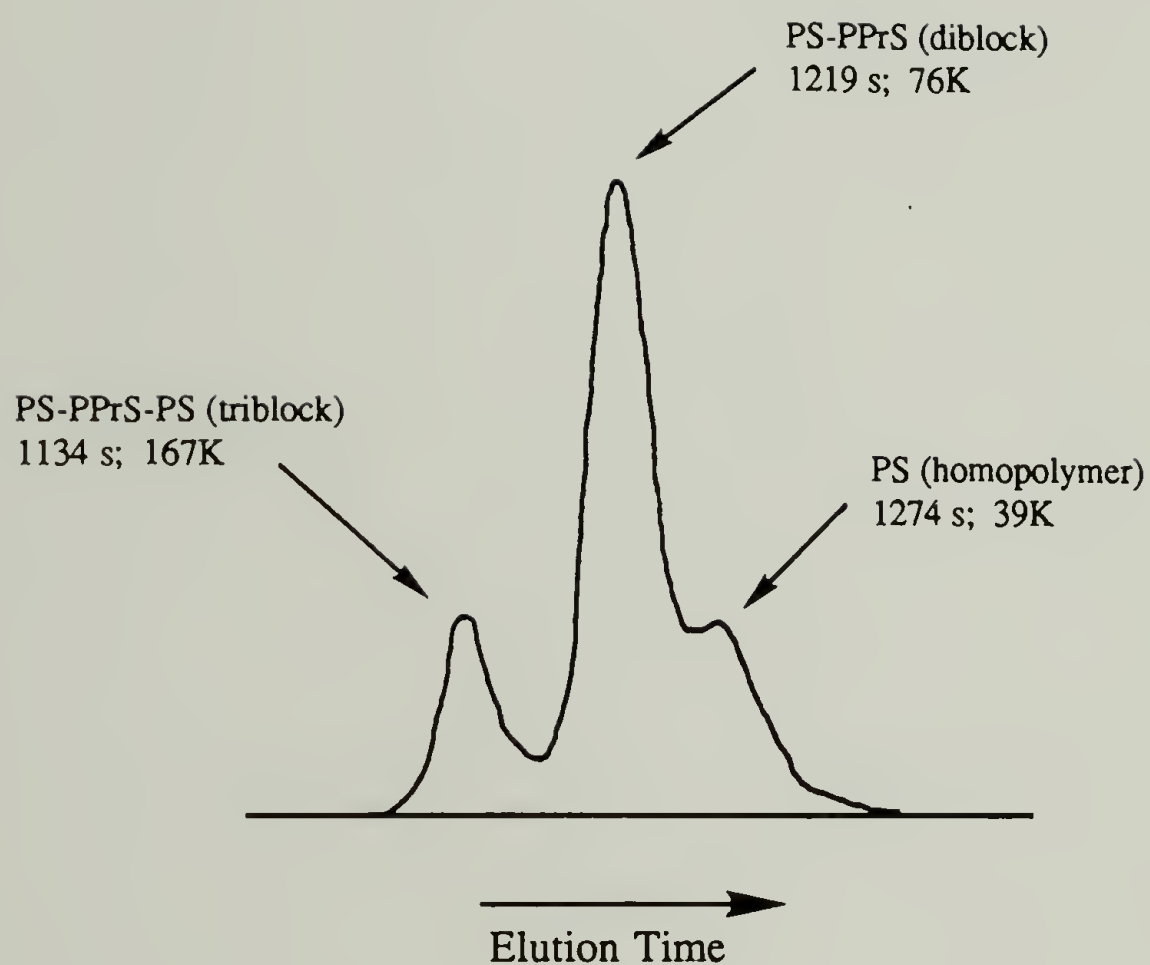


Figure 4.2 Typical GPC trace of PS/PPrS block copolymer that was synthesized at the start of this research (MeOH/H⁺ terminated; CaH₂ drying agent). The three peaks correspond to the disulfide triblock, diblock and PS homopolymer.

ground glass joints. A 250 mL Schlenk flask fitted with a glass plug was used as the reaction vessel in most situations. This allowed more adequate stirring and greater reaction volumes than using a 50 ml Schlenk tube; pressure bottles were tried but small pieces of the black rubber seal were found to contaminate (and affect) the polymerization. All transfers were done via cannula or gas-tight luer-tip syringe. All needles and cannula were cleaned with hexane, 1.0 M HCl, 1.0 M NaOH, H₂O, and acetone, and then purged dry and kept in the oven until right before use. Transfers were also facilitated by a portable antechamber made from 750 x 9 mm glass tubing fitted on both ends with the appropriate septa and then purged with N₂. Prepurified N₂ was used as received at 6 to 9 psig without further drying. During the assembly and transfers, clean latex gloves were worn at all times to minimize contamination by perspiration and oils from hands. All assembled glassware (reaction vessels, distillation apparatus, trap-to-trap and storage apparatus) were further dried by purging 10 min with N₂ then a repeated pump/heat/backfill cycle. All solvents and monomers were distilled directly before use. *sec*-Butyllithium (*s*BuLi) was diluted with dry hexane or heptane and stored in 15 ml Schlenk tubes with dessicant in a freezer and at 0 °C on the bench.

Purification of Materials for Synthesis. The purification of solvents and monomers evolved throughout this project; the correct drying procedure is paramount for successful anionic polymerizations. Below, the established drying conditions are described.

Approximately 300 ml of styrene was distilled from CaH₂ at 30 mm Hg and stored under N₂ in a storage flask in the freezer. It was further

dried with dibutylmagnesium (Bu_2Mg) just prior to use following a procedure developed from Morton.²² Approximately 1 - 4 mL of 0.5 M Bu_2Mg (Alfa) in hexane was transferred via cannula into a purged Schlenk tube (with a grease joint) and then the solvent was pulled off, leaving a white solid. Styrene (10 - 20 mL) was added (via cannula) and stirred at room temperature for 1 - 4 h, after which time the solution became bright yellow. This color indicates living polymerization of styrene and the absence of water and other impurities. This polymerization is extremely slow (occurring over days), so the dry styrene can be used at much later points in time. The tube containing the yellow solution was attached to a trap-to-trap distillation apparatus and the solution was degassed with three freeze-pump-thaw cycles and then transferred. The dry monomer was used within a hour or so. If CaH_2 were the only drying agent used, there would be a substantial amount of dead polymer resulting from each monomer addition. It should be noted that GC was used to monitor "trapped over" styrene for higher molecular weight components (dimers etc.), but none were found even in styrene that had been over Bu_2Mg for a few weeks [B8-17]. (Other vinyl monomers such as isoprene have been dried in the same way but one does not get the nice color change as an indicator.)

The Propylene Sulfide drying procedure reported in the literature for all poly(propylene sulfide) (PPrS) block copolymer syntheses is distillation from CaH_2 . However, it was found that even after repeated drying with CaH_2 , the addition of PrS to living polystyryllithium resulted in a substantial fraction of dead polystyrene (PS) observable by GPC (Figure 4.2) [B6-32,35,36,81; B8-44,48,50]. Since the dead polymer

cannot be isolated easily from the diblock copolymer, this is unacceptable. (This insufficient drying most likely has been a problem in past studies because of all the studies involving block copolymers of PrS or ES, only two could be found that reported GPC chromatograms.^{17,26} In both of these studies the procedure involved the sequential addition of the thiirane monomer and evidence of dead PS homopolymer is observed in the chromatograms.) The conclusion is that CaH_2 does not have a low enough threshold drying power to dry monomers well enough (as the final purification step) for the synthesis of block copolymers.

Attempts made to find a new drying agent were complicated by the fact that PrS readily polymerizes cationically and anionically. Attempts to dry with sodium and NaH resulted in a solid PPrS block in a matter of minutes [B8-46,47]. The addition of dibutylmagnesium to freshly distilled propylenesulfide (from CaH_2) caused the solution to turn bright orange and polymerize (at RT) in approximately one hour. PrS could be isolated by trap-to-trap distillation from this polymerization and used in block copolymer synthesis. The resulting block copolymer showed no indication of dead PS by GPC (Figure 4.3). This indicates that the Bu_2Mg is a sufficient drying agent for this synthesis. Many other polymerizations have been carried out with this procedure and they have all resulted in block copolymers free of any dead PS homopolymer [B8-46, 47, 51, 58, 60, 61, 85, 87, 95]. It should be noted that PrS distilled (trap-to-trap) from orange Bu_2Mg solution will remain clear (colorless) upon reexposure to Bu_2Mg which indicates that the Bu_2Mg removed some impurity from the PrS. If PrS is not pre-dried with CaH_2 (before treatment with Bu_2Mg) the monomer polymerizes much more violently. Subsequent addition to living

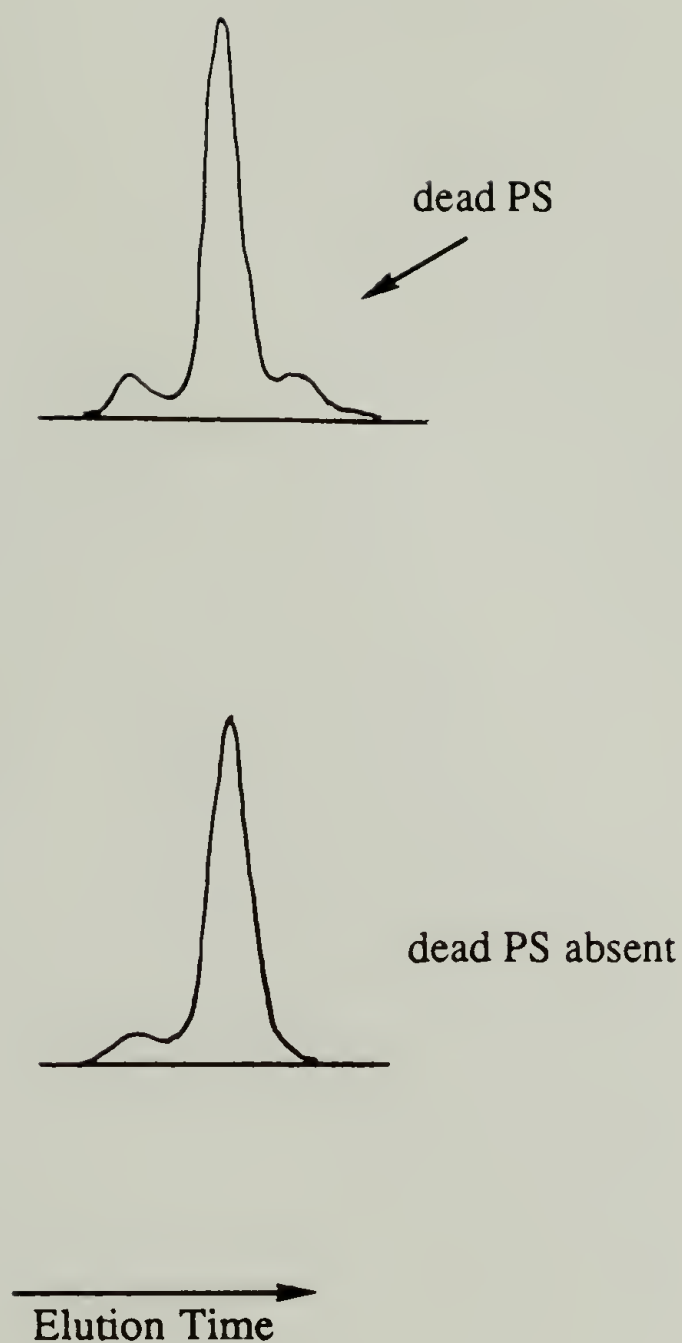


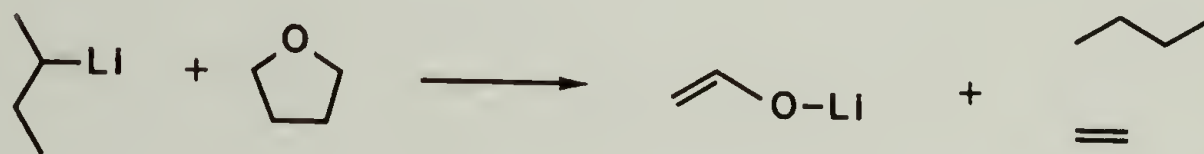
Figure 4.3 Upper GPC trace shows the presence of a “dead PS” fraction due to inefficient drying of PrS with CaH_2 . Lower GPC trace gives no indication of the PS homopolymer; this is the result of the much improved drying of PrS accomplished with Bu_2Mg (high molecular weight peaks are due to the triblock copolymer).

polystyrene yields a small amount of dead PS and readdition of Bu_2Mg to the monomer yields orange color [B8-83, 84]. It is probable that the impurity responsible for the orange color is also responsible for the dead PS.

Molecular weight determinations made by GPC for polymers from polymerizations carried out in THF dried with sodium benzophenone dianion (continuous still) were in disagreement with the molecular weight calculated from monomer and initiator concentrations. A number of these polymerizations, especially those for higher molecular weight polymers, died before completion. After many failed attempts to remedy the situation, we concluded that the problem was the gradual accumulation of some sort of impurity in the THF from the continuous still. The concentration of the contaminant seemed to vary with time and we thought that this impurity competed with styrene for the *s*-BuLi resulting in unpredictable molecular weights. The impurity may be benzophenone itself, benzaldehyde or some other byproducts. For the case of benzophenone, the detrimental side reactions include direct addition or hydride transfer. Suffice it to say this assertion has not been proven but, polymerizations have been more predictable using alternative drying techniques.

The optimum procedure for preparing the solvent for polymerization was a final drying step from *s*-BuLi followed by trap-to-trap distillation. This alternate procedure for drying THF has resulted in improved control over the molecular weight. The procedure developed indicates dryness with a color change and can be used to dry the solvent

(THF) after it has been introduced to the reaction flask. This was possible for two reasons: 1) *s*BuLi is light green in THF at -78 °C, therefore *s*BuLi added to THF at -78 °C will first dry the solvent and then a light green color will appear (indicating dryness) and 2) *s*BuLi reacts rapidly with THF at room temperature and gives products that are innocuous to the polymerization. The lithium reagent deprotonates the α carbon of THF and the products rearrange to form butane, ethylene and the lithium enolate of acetaldehyde.²⁷ This sequence is shown in Scheme 4.1.



Scheme 4.1 Reaction of *sec*-Butyllithium with THF.

Purification of THF was carried out as follows. THF (distilled from CaH_2) was cooled to -78 °C in a Schlenk tube and *s*BuLi was added until a green color was obtained. The green solution was stirred for 30 min and then degassed and distilled (trap-to-trap) into a new tube. The THF was then transferred to the polymerization flask and cooled to -78 °C and a very small amount of *s*BuLi was added until a light green color appeared (indicating dryness). The THF was allowed to warm to room temperature over a 30 - 45 min time span during which time the *s*BuLi reacted with the THF and the solution became clear. At this point, the reaction flask and contents were ready to cool to -78 °C to begin the polymerization [B8-79-

87, 94-100, 113, 114; B9-5]. In general, solvents such as benzene and cyclohexane are not as difficult to dry (they are not nearly as hygroscopic), but distillation from CaH_2 followed by distillation from polystyryllithium is recommended.

Polymerizations. The solvent in the reaction vessel was cooled to $-78\text{ }^\circ\text{C}$ and stirred; the stoichiometric amount of $s\text{BuLi}$ was added via syringe. The appropriate amount of styrene was then added via syringe and the characteristic orange/red color appeared. It was allowed to react for 15 - 30 min which is sufficient time for completion of styrene polymerization as determined by GC. It is important that the styrene be added to well stirred $s\text{BuLi}$ and not the other way around because the polymerization in THF is so fast that one can see stirring effects in the molecular weight distributions if the initiator is added to a solution of the monomer. Aliquots of polystyrene were taken to determine the polydispersity and molecular weight of the polystyrene block. The appropriate amount of PrS was then added via syringe, at which time the color disappeared. The polymerization was allowed to warm to room temperature and proceed to 100% conversion as determined by GC. Endcapping of the block copolymers was achieved by addition of either degassed acidic methanol, or degassed, distilled ethyl bromide. The polymer was then precipitated in cold, degassed methanol, redissolved in THF, reprecipitated in methanol and dried at reduced pressure. The larger propylene sulfide blocks can result in rather poor reprecipitation of the polymer (i.e. the polymers tend to want to form emulsions). This procedure and these purification steps provide a reliable way of making

poly(styrene-*b*-propylene sulfide) copolymers of the appropriate size and narrow molecular weight distribution.

Block copolymers terminated with acidic methanol to produce a thiol group at the chain end were unstable and the PPrS blocks degraded to PS homopolymer in solution and solid state. We found that the thiolate ends (before termination with MeOH/H⁺) and the thiol ends coupled to form triblock copolymers (PS-*b*-PPrS-*b*-PS) of twice the molecular weight as the desired diblock copolymer (PS-*b*-PPrS). The solution to each of these problems was transformation of the thiol to an ethyl sulfide species; a separate discussion of these two problems follows.

Poly(propylene sulfide) Chain Degradation. Degradation of ring-opened polymers by an unzipping process is not unusual if proper endcapping is not carried out to remove the kinetic pathway for depolymerization. The fact that dithianes do not polymerize suggests that poly(propylene sulfide) may be particularly susceptible to these types of reactions (Figure 4.4). PPrS degrades by some combination of pathways (a), (b), and/or (c) (Figure 4.4) under acidic conditions. Simonds²⁸ and subsequently Sigwalt⁵ reported the degradation of high MW stereoregular monodisperse PPrS by Et₃OBF₄ into various ratios of the dithiane, cyclic trimers, tetramers and pentamers as well as trithiapane and the corresponding olefin. The relative amounts of each degradation product depend on the type of thiirane polymerized and the amount of catalyst present. PPrS was found to show a preponderance of trithiapane over the dithiane. It is evident that the sulfur atoms of the thiol and the sulfide are nucleophilic enough to form sulfonium ions upon reaction with the catalyst.

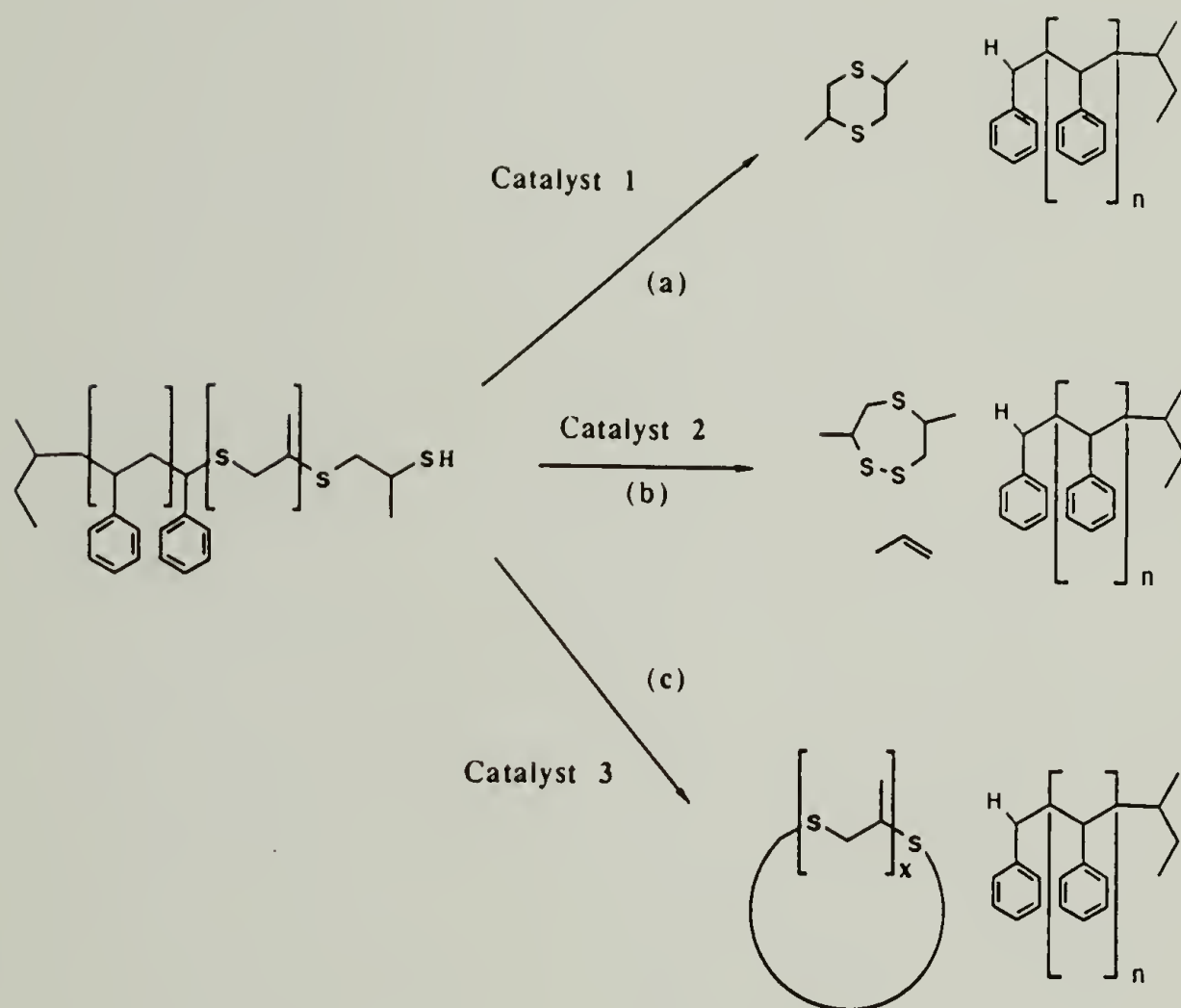


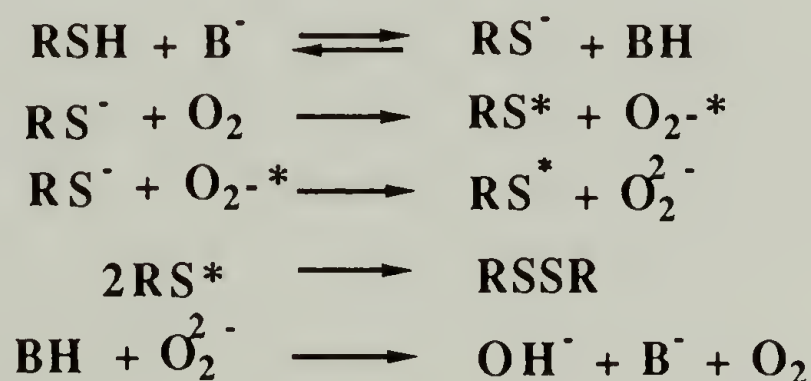
Figure 4.4 PPrS block degradation is acid catalyzed (H^+ , Et_3OBF_4); it will lead to increased polydispersity and eventually PS homopolymer. The degradation produces dithiane (a), trithiapane (b) and cyclic oligomers (c). The ratio of these products depends on the specific catalyst and the polymer.

This, in turn, makes both the sulfur of the sulfonium ion and the carbons α to it subject to nucleophilic displacement reactions by other sulfur atoms in the chain. Reaction pathways (a) & (c) result from attack on the α carbon and result in cyclic dimers, trimers and pentamers etc. If attack is on the sulfur, the seven member ring, trithiapane, and the corresponding olefin are formed. The degradation of PPrS by catalysis with Et_3OBF_4 does not require a thiol endgroup on the chain. Although no literature precedence has been found, it is conceivable that, in the absence of such a good alkylating agent, the sulfides may not be nucleophilic enough to attack and thus the degradation would be solely the responsibility of the more nucleophilic thiol end groups. It is evident, then, that transformation of the thiol endgroup to a more stable sulfide should prevent this degradation. This was carried out by reaction of the thiolate endgroup with ethyl bromide after polymerization was complete (Figure 4.1).

The degradation of the thiol-endcapped PPrS block occurred both in the solid state and in THF solution. The degradation in the solid state was evidenced by a characteristic sulfur smell present in stored polymer samples. Degradation of the PPrS block in solution was also evidenced by a broadening of the MWD. End-capping with ethyl bromide was found to stop this degradation. The MWDs of the ethyl end-capped polymers stored for over a month in both the solid state and in solution remain unchanged (Figure 4.5). Thus it has been shown that the thiol-endcapped PPrS is degradatively unstable and plausible chemistry for this degradation has been presented. It should also be noted, in this regard, that Nevin¹² reported that thiol endcapped polymers were "unstable" and Morton¹⁴ used ethyl bromide and allyl bromide to endcap the copolymers and control this

instability. These accounts are rather vague because the actual instability found in their samples was not discussed in any detail.

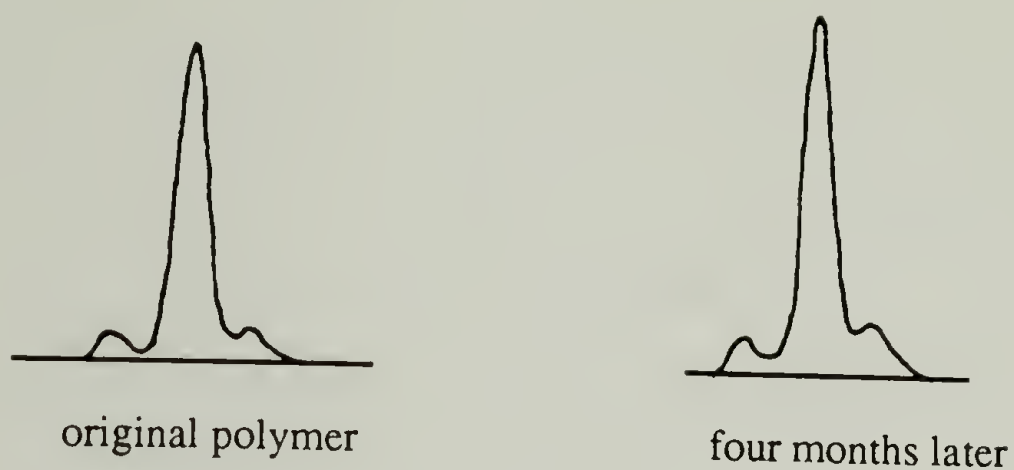
Oxidative Coupling. Oxidative coupling of sulfur-terminated polymers resulted in disulfide formation and triblock copolymers (PS-*b*-PPrS-*b*-PS) of twice the length of the diblock (PS-*b*-PPrS) were found in the samples (see Figure 4.6 (a)). Figure 4.2 shows the GPC data which illustrates this polymeric dimer peak. The oxidation of thiols to disulfides is a well known, facile reaction that can be accomplished even with mild oxidizing agents.²⁹⁻³³ The oxidation by molecular oxygen is base-catalyzed and is thought to go by the mechanism given below in Scheme 4.2.



Scheme 4.2 Disulfide Formation.

The thiol end of the polymer precipitated in acidic methanol is unstable and disulfide formation can occur when the solvent is insufficiently degassed (Figure 4.7). One can see that the diblock (middle peak) decreases in size relative to that of the dimer and the homopolymer over the period of 24 h

(a) Solid State Stability



(b) Solution Stability

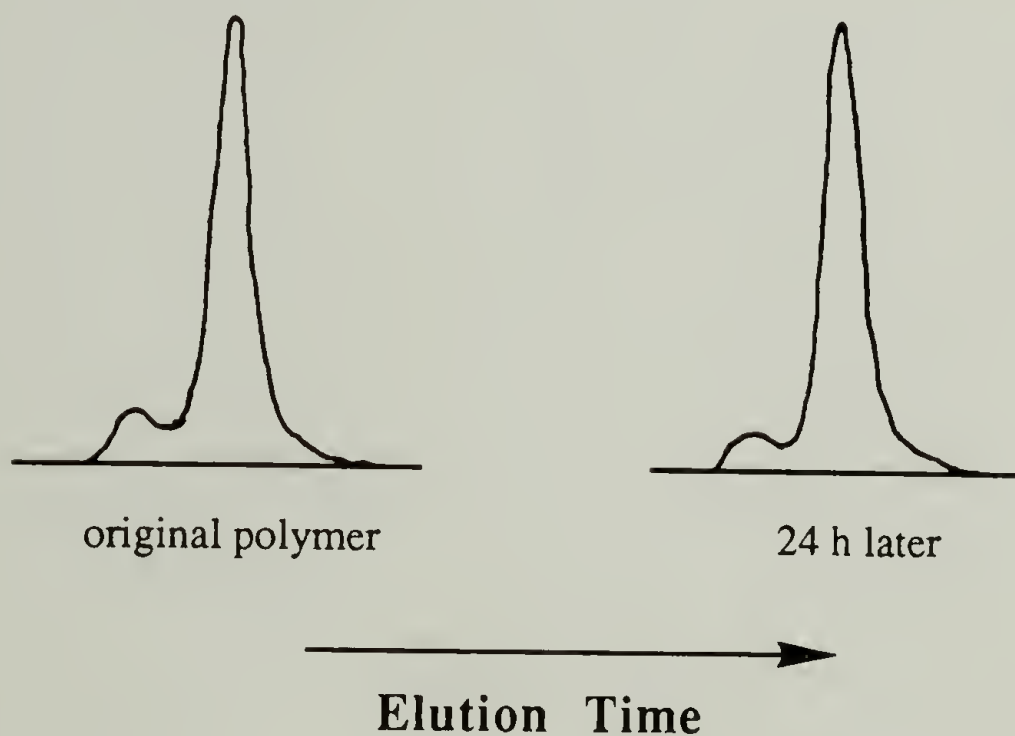


Figure 4.5 PS-*co*-PPrS block copolymers show increased stability toward degradation due to endcapping with ethyl bromide. The GPC trace of a PS₅₀-PPrS₅₀ copolymer shows no signs of degradation upon storage as a solid for four months (a). The GPC trace of PS₉₅-PPrS₅ copolymer shows no sign of degradation after storage in THF for 24 h (b).

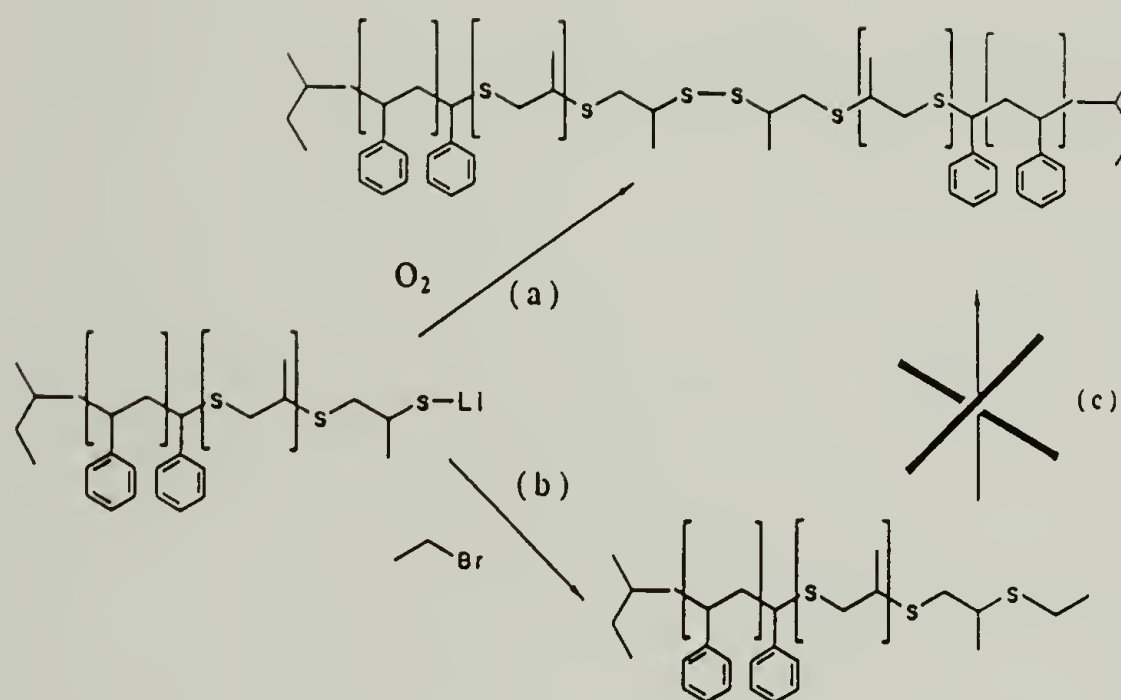


Figure 4.6 Oxidative coupling of sulfur terminated polymers results in disulfide formation (a). Reaction of the thiolate group with ethyl bromide eliminates possible disulfide formation (b and c).

and then 108 h (there may be some degradation as well). Coupling also can occur either in the reaction vessel and/or during the work up and isolation of the newly synthesized copolymer. Every copolymer prepared contained 3 - 15 weight % of this coupled product. This is to be expected because the thiolate chain end is more easily oxidized than the thiol. A combination of the thiolate anion and small amounts of adventitious oxygen caused formation of the polymeric dimer (Figure 4.6(a)). The solution to this problem was to endcap the polymer with ethylbromide and eliminate the troublesome thiol/thiolate endgroup (Figure 4.6(b,c)). The strategy was to endcap the polymers in the reaction vessel before workup and avoid the disulfide product altogether. In reality, pathway (a) competed with (b) in all cases and 100% conversion to the ethyl sulfide endcap was never achieved. Unlike the thiol-endcapped polymer which dimerized in solution (Figure 4.7), the sulfide ends were stable in solution and in the solid state. Figure 4.5 shows that there is no increase in the high molecular weight triblock peak relative to the diblock.

Reduction of Disulfides. We had determined that complete suppression of the disulfide was not possible, so attempts were made to split (reduce) the disulfides present and then to endcap them with ethyl bromide to prevent them from reforming. A variety of disulfide reductions²⁹ were attempted on the copolymer samples. The reaction conditions and results are summarized in Table 4.1. These reactions ranged from totally ineffective, as in the case of the triphenylphosphine/water ($\text{Ph}_3\text{P}/\text{H}_2\text{O}$) system which did not reduce the disulfide linkage at all (Table 4.1, entries 1 and 2), to very harsh and destructive of the PPrS block, as in the case of

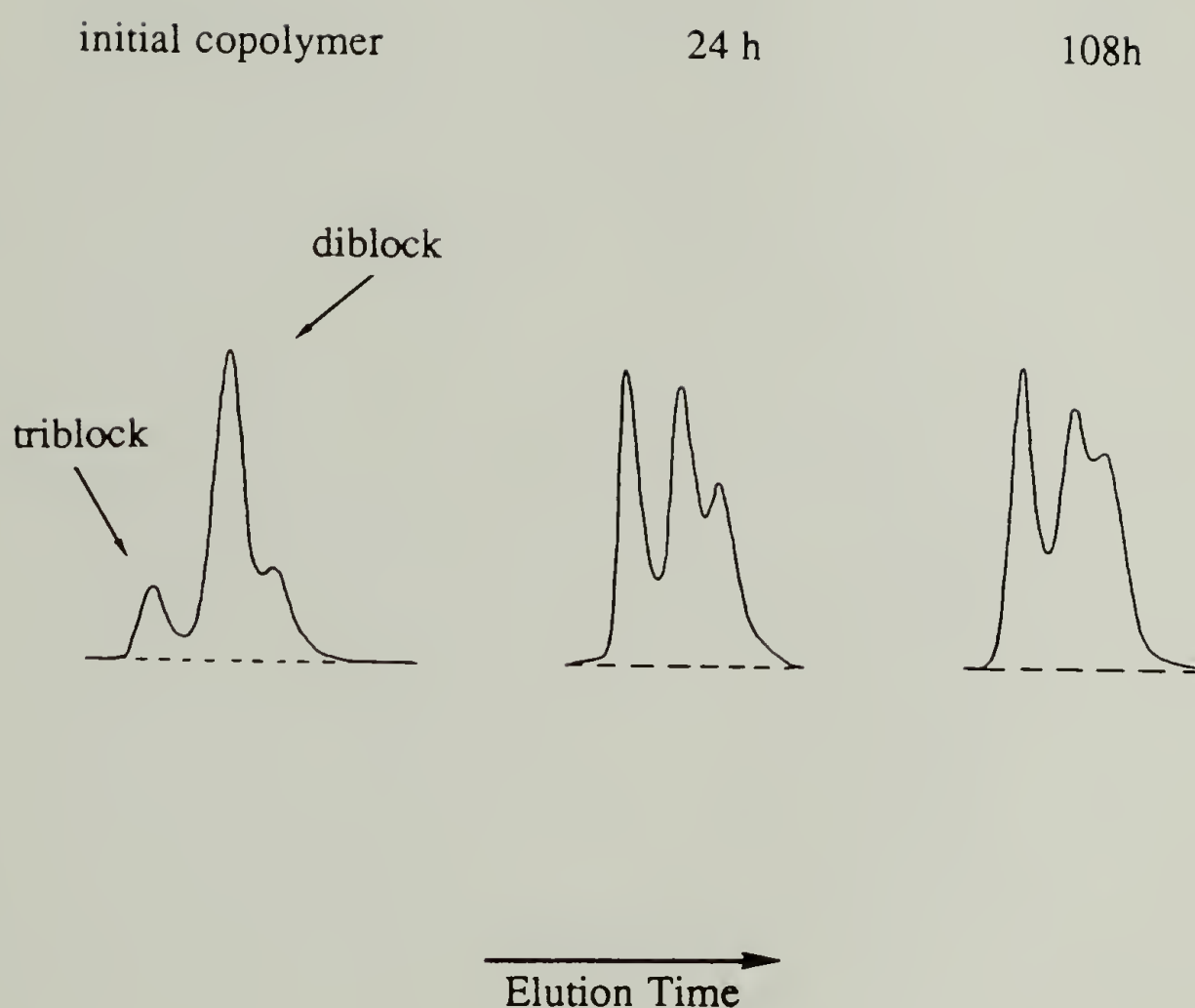


Figure 4.7 Thiol-ended polymers are unstable to disulfide formation and result in coupling to form the corresponding triblock copolymer. The GPC traces above illustrate the conversion of the diblock copolymer to the corresponding triblock copolymer over a period of 108 h in THF.

Zinc/AcOH or the Cl₂ gas systems (Table 4.1, entries 3-5). GPC data showed the emergence of a peak that corresponded to the polystyrene block and also a broad lower molecular weight fraction presumably due to the cleaved and somewhat degraded PPrS block; this was taken as evidence that the PPrS blocks were being cleaved. In several instances the PrS block was cleaved intentionally to determine the molecular weight of the PS block by GPC. In retrospect, degradation of the PPrS block under these conditions should have been expected because these polymers readily degrade in the presence of electrophiles that are subject to nucleophilic attack by the sulfides.

The reagent of choice for reducing disulfides in biological applications is dithiothreitol (DTT), otherwise known as Cleland's reagent.^{35,36} The reaction mechanism is shown in Figure 4.8; one can see that the reaction is base-catalyzed and the driving force is the formation of the six membered ring. The reagent is usually used on biological systems in aqueous or alcoholic media (at pH~8). The copolymers synthesized here are not soluble under those conditions, so the reactions were modified and carried out in either THF or DMF. Figure 4.9 shows the change in the GPC data after reaction with DTT in THF. One can see complete disappearance of the high molecular weight fraction without any adverse effects on the distribution.

Although the reaction worked well and the desired polymers were obtained, complete understanding was not achieved (i.e. the reaction did not go to completion every time). The number one objective of obtaining

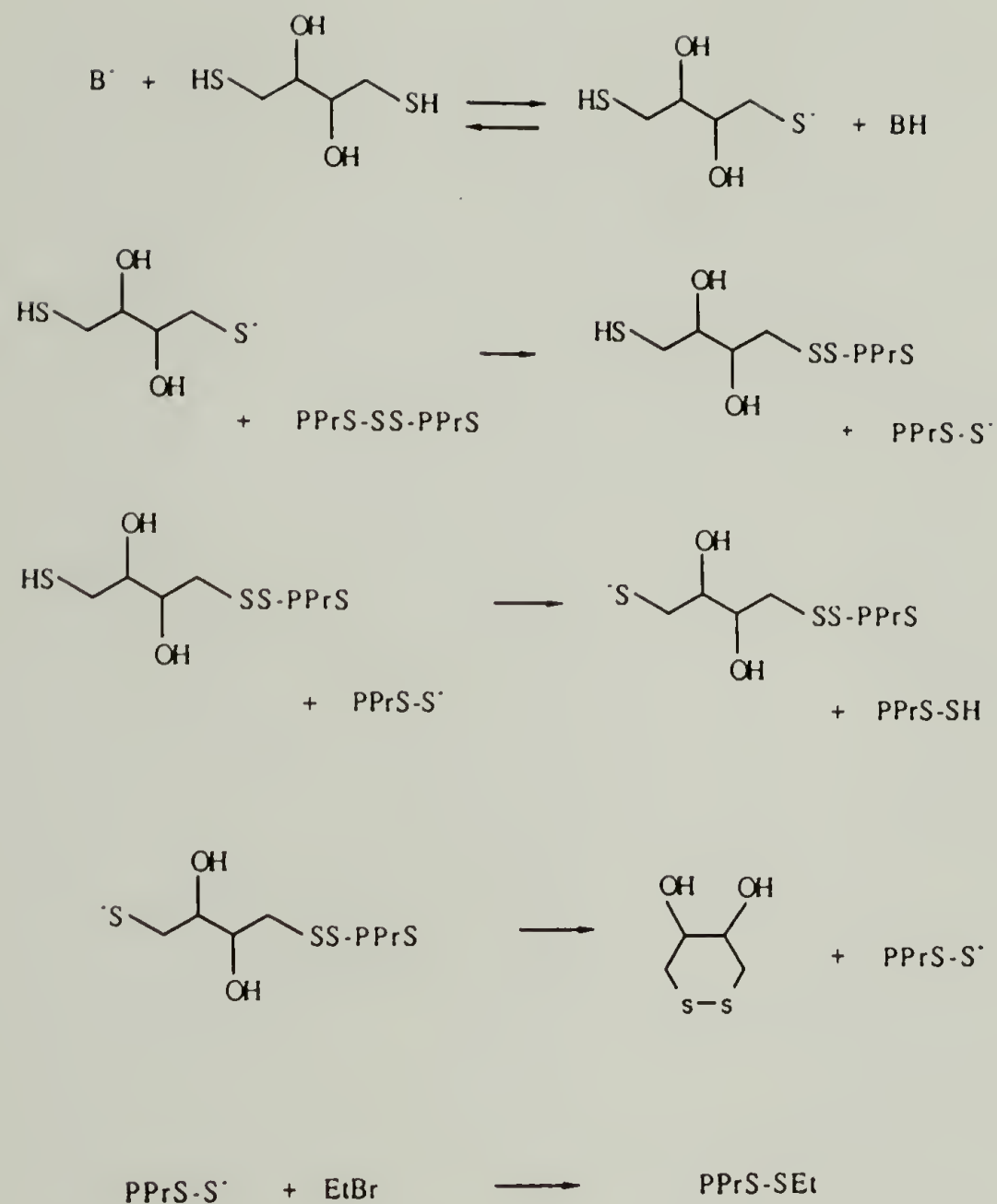


Figure 4.8 Dithiothreitol reduction of disulfide linkages in PS-*co*-PPrS block copolymers.

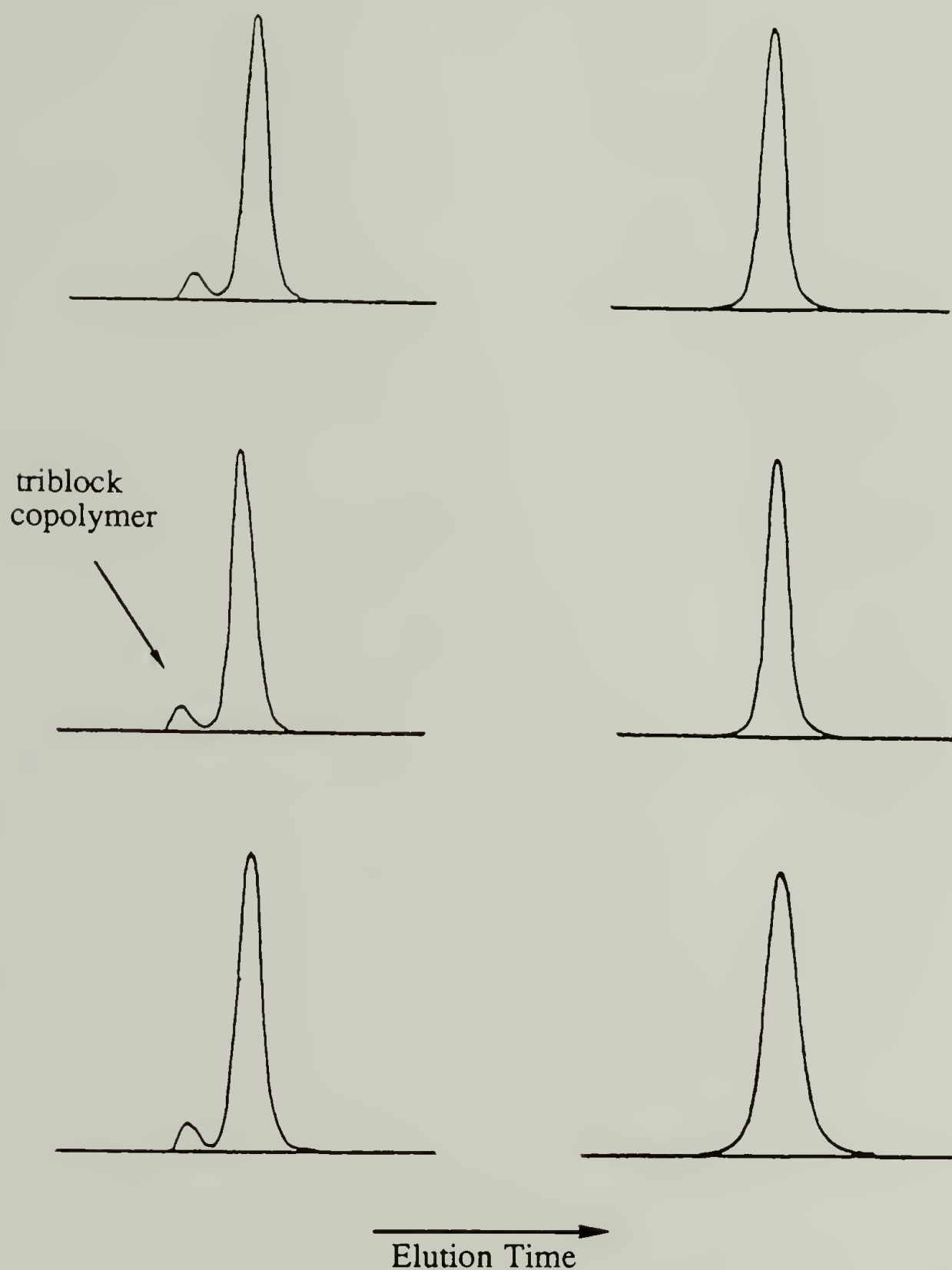


Figure 4.9 GPC traces of PS-*co*-PPrS block copolymers before (left) and after (right) reaction with DTT for PS₉₅-PPrS₅ (top), PS₉₀-PPrS₁₀ (middle) and PS₇₅-PPrS₂₅ (bottom). One can see the elimination of the triblock copolymer in each case.

the necessary copolymers for adsorption studies was achieved and some more fundamental understanding of the DTT reaction was obtained. Many reactions were carried out using DTT to split the polymeric dimer (Tables 4.2 and 4.3). The general objective was to try to understand the following situation. First the reaction conditions needed to be such that all the dimers would be cleaved in the reaction pot. The variables that were considered important are DTT:polymer ratio, reaction time, reaction solvent and method of catalysis. The ethylbromide end-capping reaction also must proceed to completion, so the ethylbromide concentration and reaction time are important here as well. If complete end-capping is not achieved then the disulfides can reform at a later time (this has been observed). A number of reactions were carried out under different conditions in an attempt to understand this chemistry. A survey of Table 4.2 shows that all of the DTT reactions that were carried out in THF resulted in a decrease in the amount of dimer in the sample, but the conversions were not always 100%. Thus we can see that out of the 12 entries, two resulted in no dimer at all and 8 had less than 1% dimer. Table 4.3 shows the results obtained when the reduction was run in DMF, and again one can see that the reaction always results in a decrease in the amount of dimer present in the sample but that 100% cleavage is not obtained in any instance. A few generalizations can be made from the data in these two tables. The most important conclusion is that the reaction can be used to obtain polymers that are 100% free of the disulfide dimer (at least sometimes). As was discussed above, greater than 0% dimer can result from either less than 100% reduction of the disulfide linkage or less than 100% end-capping followed by oxidation back to the disulfide. The first generalization is that the reaction solvent does not seem to have much of an effect as can be seen

from the fact that both of the Tables 4.2 and 4.3 have good results and bad results. In terms of the ease of reaction and isolation of the polymers, THF is the better choice. The effect of the catalyst was also very ambiguous because it can be seen that using NaH has given both high conversions (Table 4.2, entries 3, 4 and 5) and low conversions (Table 4.2, entries 6, 7; Table 4.3, entries 2, 3 and 7). The NaOH pellet (saturation) method also shows both good (Table 4.3, entries 12 and 13) and bad (Table 4.3, entries 4, 6, 8, 9, 10, 11 and 16) results; these particular odds are not good, however the two best results gave 100% reduction of the dimer. The best case for a bad choice can be made with the NaOH/water catalyzed reactions where (Table 4.2, entries 1 and 11 and Table 4.3, entry 1) the results suggest that this catalyst does not work as well. Even the case of no base catalyst yields both good and bad results (Table 4.3, entries 2, 5, 14 and 15). The information above indicates that the identity of the catalyst is not an important variable. A similar situation exists with the effect of the DTT:polymer ratio. In some cases an increase in the ratio leads to better results. Table 4.3, entries 3 and 7 show that approximately doubling the ratio of DTT:polymer decreases the amount of dimer obtained from 5.5% to 3%. On the other hand, Table 4.2, entry 2 shows that total depletion of the dimer was achieved with a DTT: polymer ratio of 1:3.15. Therefore we see that the ratio itself does not have a consistent effect. The data suggest that increasing reaction times, especially in the short time regime, does lead to better results, but one finds contradictions in this regard also. One should note that in some cases reduction may have been facilitated but complete cleavage not obtained because the amount of ethylbromide added was less than the amount of DTT. Since DTT can also be alkylated by ethyl bromide, it competes with the chain ends. If ethyl bromide is not

present in excess then full end-capping does not result and some dimer reforms. For example, one reduction (Table 4.3, entry 2) resulted in 5.9% dimer using 700 mg of DTT (4.5 mmol) and 0.5 mL of ethyl bromide (6.7 mmol). There are two thiols for every DTT molecule thus there are 9 mmol of thiols versus 6.7 mmol of ethylbromide. We were not aware of the problem at the time and naively kept adding more DTT to try and push the reaction. This was not considered important and the exact amounts of ethyl bromide added were usually not recorded. It may explain the poor results of many of the reactions reported.

In retrospect and with the knowledge of how the DEOM reaction system works (Chapter III), it seems that a very important variable (one which was not specifically investigated at the time) is the overall concentration of the solution. As was shown, this was very important in the case of the DEOM modification where it was found that if the solution was too dilute, complete conversion could not be achieved. This hypothesis, plus the fact that we used too high a ratio of DTT to ethyl bromide (in some cases), can explain many of the results that were obtained and presented in Tables 4.2 and 4.3. To test this hypothesis one needs to look at the polymer and DTT concentrations in individual cases. Because this was not perceived as important, the actual solution concentrations were not always recorded or they were recorded only approximately. Where possible the solution concentrations are recorded in the two tables. Thus one sees that the reactions that worked the best were the more concentrated ones that had a high EtBr to DTT ratio. The reason for the relatively dilute solutions is that usually a stock solution of DTT was made so that only one weighing would have to be done in the glove box, thus if one

wanted to increase the DTT:polymer ratio, the concentration in the reaction mixture was also decreased. It (now) seems likely that the reaction would work very well if carried out in the following fashion. The polymer and approximately equal weight of DTT should be placed in a Schlenk tube and purged with N_2 . The solids should be dissolved a minimum of solvent. The solvent of choice is degassed THF. The THF could be used neutral or after exposure to NaOH pellets (or NaH powder) to make the reaction slightly basic. The reduction should be allowed to proceed overnight, followed by addition of degassed ethyl bromide (substantially more than twice the moles of the DTT) and further reacted for 5 to 10 hours. The polymer should be isolated via cold precipitation (not evaporation of the solvent).

Effect of Na/Benzophenone Drying on THF. We have found that THF obtained from a continuous still using sodium/benzophenone as the drying agent has deleterious effects on anionic polymerizations. The problem seems to be one of varying degree in which a certain portion of the anions are prematurely killed. For the most part the actual notebook references and experiments needed to prove this do not exist because this was not perceived as the source of the problem for quite some time. The polymerizations were always done in THF that was refluxed at least 10-12 hours over the purple dianion before use. Because the color indicated that the solvent was free of oxygen and H_2O , we concluded that some other contaminant was killing the carbanions. This contamination was seen first hand after an attempted polymerization died [B8-48,49]. An additional THF still was set up using just Na as the drying agent. Approximately 10 mL of solvent from each source were put in separate flasks and cooled to

-78 °C. *sec*-Butyllithium (0.4 mL) was added to each of them and the THF (from the continuous Na/benzophenone still) turned green then the color discharged within a minute. The control turned green and remained that way as long as it was kept at -78 °C (2 h). This was regarded as proof of contamination of the solvent from the continuous still.

UV spectra of solvent from the continuous still were obtained on two different occasions [B6-44,45,B8-144,145]. In both cases benzene was found in the solvent as could be seen by its very characteristic finger print region around 256 nm. THF out of the bottle showed no benzene. The contaminated THF spectra actually look like a combination of benzene and a compound with a λ_{max} at a slightly lower wavelength than that of benzene. The most reasonable guess seems to be benzaldehyde. Attempts to duplicate the contaminated spectra by mixing benzene and benzaldehyde in THF met with fair success. We thought that the possible contaminants were benzophenone itself or byproducts of either photolytic or thermolytic cleavage reactions. The presence of benzene in the THF (as detected by UV) suggested some kind of degradation of the benzophenone had occurred. It is surmised that the contaminants can react with carbanions and kill the polymerization. The data do not prove the presence of the contaminant but do not disprove it either.

In conclusion the effects described above may be inherent in the Na/benzophenone system and thus use of this drying procedure under any circumstances for polymerizations is not recommended. One can also imagine that the amount of contamination, if any, is a function of the amount of benzophenone used in the still and the length of time it has been

running. In this case more judicious use of benzophenone may suffice. At any rate, one should be aware of this problem.

Reduction of PTFE Stir Bar with PS-Li. Living anionic polymerizations of styrene in THF at $-78\text{ }^{\circ}\text{C}$ should stay living indefinitely if properly sealed from the atmosphere. It was found that PS-Li in THF at $-78\text{ }^{\circ}\text{C}$ would eventually die (the color disappeared); the GPC data indicate two monodisperse peaks, one of which was twice the molecular weight of the other (the same was observed for the PrS coupling, the cause is different) [B6-24-51]. The monodispersity of the peaks suggests that either there are two simultaneous living polymerizations, one with twice the propagation rate of the other or that the polymers were coupled after the polymerization was complete. The latter of these explanations is much more reasonable and assumed to be the cause. We found that the use of glass-covered stir bars instead of PTFE-covered ones completely remedied this problem [B6-55,56]. Polymerizations with high anion concentrations were found to visibly reduce the teflon stir bars. It is postulated that the PSLi transfers an electron into the Teflon and forms polystyryl radicals which may then either disproportionate or couple. The coupled product is a polymer of approximately twice the molecular weight. An interesting application of this would be the study of whether a given type of polymer radical would couple or disproportionate. In contrast to total radical polymerization with very broad MWD, these polymers are very monodisperse and offer an easily measured polymer to uncoupled polymer ratio. I would also like to note that this reduction can also occur in benzene but it takes much longer.

This is not surprising since THF/Na/benzophenone turns PTFE stir bars black faster than benzene/Na/benzophenone. Some solvents facilitate these types of reductions better than others. In conclusion polymerizations of this type should be done with all glass apparatus. It should also be noted that any other electron acceptor can facilitate this same phenomenon.

Conclusions: Synthetic Aspects

Initially, the synthesis of polystyrene/poly(propylene sulfide) block copolymers was fraught with many problems. Figure 4.9 shows the GPC data of three block copolymers synthesized using these procedures. There is no indication of dead polystyrene homopolymer or the coupled product, and these polymers were found to be stable to both degradation and disulfide formation. These polymers should be compared to the typical result shown in Figure 4.2. This synthesis was used to prepare polymers for adsorption studies. Table 4.4 gives a list of the polymers prepared. Because reaction byproducts cannot be tolerated in adsorption experiments and purification of polymers is not a viable alternative, these polymers had to be prepared without contaminants and with the correct structures; the procedures described above fulfill this objective. Also presented in this section is the development of general anionic experimental technology for group use.

Table 4.4 PS/PPrS Block Copolymers Synthesized Using the Developed Methods.

<u>Sample</u>	<u>% PrS</u>	<u>M_n^a</u>	<u>PDI</u>	<u>Notebook Ref.</u>
1. PSSH/65k	Thiol endcap	66,789	1.15	B8-97
2. PS95/65k	5	65,494	1.02	B8-95
3. PS90/65k	10	65,052	1.03	B8-85
4. PS75/60k	25	60,126	1.1	B8-76
5. PS50/57k	50	56,754	1.07	B8-83
4. PPrS/45k ^b	100	45,238	1.02	B8-100
5. PSSH/637k	Thiol endcap	636,588	1.04	B8-114
6. PSSH/5k	Thiol endcap	5,034	1.14 ^c	B8-113
7. PS90/121k	10	121,169	1.06	B8-60
8. PS95/18k	5	18,336	1.03	B8-58
9. PS85/23k	15	23,574	1.03	B8-58
10. PS80/41k	20	41,497	1.06	B8-87
11. PS80/101k	20	101,210	1.03	B8-95

^a Molecular weights versus polystyrene standards.

^b This polymer molecular weight corresponds to the same DP as PSSH/65k.

^c PDI is high because dimer peak is not resolved from the main peak.

Adsorption of Poly(styrene-co-propylene sulfide) Block Copolymers

As has been stated already this work was a collaborative effort with D. A. Waldman. Both of us contributed in each area but for the most part I was responsible for the synthetic aspects whereas he was responsible for the adsorptions. The adsorption was studied by contact angle, XPS and Polarization Modulated Grazing External Reflection IR which was developed to measure orientation in these adsorbed layers. A summary of the results is given below.

Experimental

Materials for Adsorption Experiments. Fisherbrand glass microscope slides (25 x 50 mm) were rinsed (in succession) with acetone, distilled deionized water and methanol, washed with $\text{H}_2\text{SO}_4/\text{H}_2\text{O}_2$ and dried with a stream of nitrogen and then at reduced pressure. Gold wire (Alfa-0.5 mm) was 99.998 % pure. Evaporated gold film substrates were prepared using a modified Balzers MED 010 vapor deposition apparatus. Gold was evaporated from resistively heated tungsten baskets at a base pressure of 1×10^{-6} mm. Film thickness was controlled to a minimum of 1800 Å by monitoring the deposition process with a quartz crystal thickness monitor. After deposition, the chamber was backfilled with prepurified nitrogen and the substrates were immediately placed in Schlenk tubes and transferred to the nitrogen-purged external reflection assembly.

Materials Handling. All solutions were prepared and reactions were carried out using standard Schlenk technique. Transfers of solvents and reagents were performed using cannula and syringes.

Methods of Analysis. X-ray photoelectron spectra (XPS) were recorded using a Perkin Elmer-Physical Electronics 5100 spectrometer with Mg K α or Al K α excitation (400 W or 300 W, respectively). Spectra were analyzed at two takeoff angles, 15° and 75°, from the plane of the sample surface. Contact angle measurements were made with a Ramé-Hart telescopic goniometer using a Gilmont syringe with a 24-gauge flat-tipped needle. Doubly distilled water was used as the probe fluid. Dynamic advancing and receding angles were measured while adding or withdrawing water to or from the drop. The values reported are averages of five measurements made at random points on the adsorbed film. UV-vis spectra were recorded using a Perkin-Elmer Lambda 3A spectrophotometer. Transmission infrared measurements of extruded films and KBr pellets of adsorbate polymers, were obtained on a Bruker IFS 113v FTIR spectrometer with a MCT detector. Gas chromatography (GC) was performed with a Hewlett-Packard 5790 A gas chromatograph at 80 - 160 °C. Molecular weight determinations were made by gel permeation chromatography (GPC) using Polymer Laboratories PL gel columns (10⁴, 10³ and 10² Å), a Rainin Rabbit pump, a Knauer 98 refractive index detector and toluene as the mobile phase. GPC data accumulation and analyses were performed using Interactive Microware GPC software, an Apple IIe computer, and calibration with polystyrene standards.

Adsorption Experiments. Adsorption experiments were carried out to steady state conditions on glass-supported gold substrates. Solution concentrations ranged from 0.5 - 2 mg per mL THF or cyclohexane (distilled as described above). Adsorptions were carried out in THF at room temperature and in cyclohexane at 45 °C and 35 °C (theta

temperature for polystyrene). After steady state conditions were achieved, the polymer solution was removed and fresh (wash) solvent was introduced via cannula. The substrate was exposed to the fresh solvent for roughly 10 min at or above the adsorption temperature. This wash solvent was removed and analyzed with UV-vis spectroscopy for the presence of polystyrene (in the hopes of determining whether any physisorbed polymer was present on the gold substrate). Following the washing procedure, the substrate was dried under a stream of prepurified nitrogen and then at reduced pressure until a base pressure of 25 mTorr was attained.

Polarization Modulation External Reflection Spectroscopy (PMGRS).

External reflectance infrared spectra were obtained with polarization modulation by incorporation of the necessary optical and electronic components.³ All files were transferred to an IBM 9000 computer where subsequent analysis was performed.

Results and Discussion

Polymers prepared for adsorption studied using the methods discussed in the synthesis section are given below. There four copolymers with from 50 to 5 mole % PPrS and a DP_n of approximately 640. The molecular weights (as determined versus polystyrene standards) and the PDIs are given along with the degree of polymerization of each block. The homopolymers used are also shown. The methods developed in the last section were used to prepare these polymers and the GPC data can be seen in Figure 4.9 for 25%, 10% and 5% PrS copolymers. One can see that they are monodisperse samples with no coupled product or PS

Table 4.5 PS/PPrS Polymers Prepared for Adsorption Studies.

<u>Sample</u>	<u>Mn</u>	<u>DP_n(PS)</u>	<u>DP_n(PPrS)</u>	<u>PDI</u>
1. PPrS ₁₀₀ ^a	~45,000	0	608	~1.15
2. PS ₅₀ -PPrS ₅₀	58,200	326	326	1.07
3. PS ₇₅ -PPrS ₂₅	60,126	467	156	1.1
4. PS ₉₀ -PPrS ₁₀	65,052	579	64	1.03
5. PS ₉₅ -PPrS ₅	65,494	607	32	1.02
6. PS ₁₀₀	80,020	769	0	1.07

^a There is a substantial amount of coupled product in this polymer.

homopolymer contamination. Adsorptions of these polymers were performed at the gold-solution interface. The gold surfaces were prepared by evaporation of gold onto glass microscope slides. The polymers were adsorbed from 0.5 to 2.0 mg/mL solutions in cyclohexane (at 35.5 °C and 45 °C) and THF at room temperature. The adsorptions were carried out for 24 hours; this time was taken as steady state conditions.¹³ The adsorptions were done under dry N₂ atmosphere using Schlenk transfer techniques. The amount of polymer adsorbed (as determined by XPS) was independent of the solvent used. Thus it would seem that the polymers are in the anchor dominated regime even at 5% sticky block. This is an indication of a very strong sticky foot. It should also be noted that the polystyrene homopolymer did not adsorb (to any appreciable amount) under these conditions.

Dynamic contact angle data was recorded using water as the probe liquid and the results are given table in Table 4.6 for the three lowest PPrS block sizes. The original gold surface (exposed to the air) gives a contact angle of 65°/15°, this is due to low surface energy adventitious

Table 4.6 Contact Angle Data for PS/PPrS Polymers Adsorbed on Gold
(Water is the Probe Fluid).

<u>Sample</u>	<u>θ_a/θ_r</u>
Gold Surface (Ambient Carbon)	65°/15°
PS ₇₅ -PPrS ₂₅	86°/58°
PS ₉₀ -PPrS ₁₀	84°/63°
PS ₉₅ -PPrS ₅	86°/58°

hydrocarbon adsorbing from the air onto the high energy gold surface. When the gold surface is exposed to a solution of any of the copolymers the contact angles increase to a values of approximately 85°/60°. The contact angles of a cast polystyrene film are 91°/68° thus the surfaces match fairly well. This indicates that all three copolymers have similar air-surface interfacial energetics, which is what we expect (i.e. all surfaces are essentially polystyrene).

Evidence of the adsorbed copolymers also seen by IR via Polarization Modulated Grazing External Reflectance IR (PMGR IR). This technique was developed by D. A. Waldman and more discussion can be found in reference 3. These measurements were also used to determine the orientation of the adsorbed polymer molecules in the dry film. We use it here as evidence for the adsorbed polymer layer. The characteristic absorbance patterns of polystyrene in the CH stretching region are shown in Figure 4.10. The transmission spectrum is also shown for comparison. This demonstrates the adsorbance of the polymer to the gold surface.

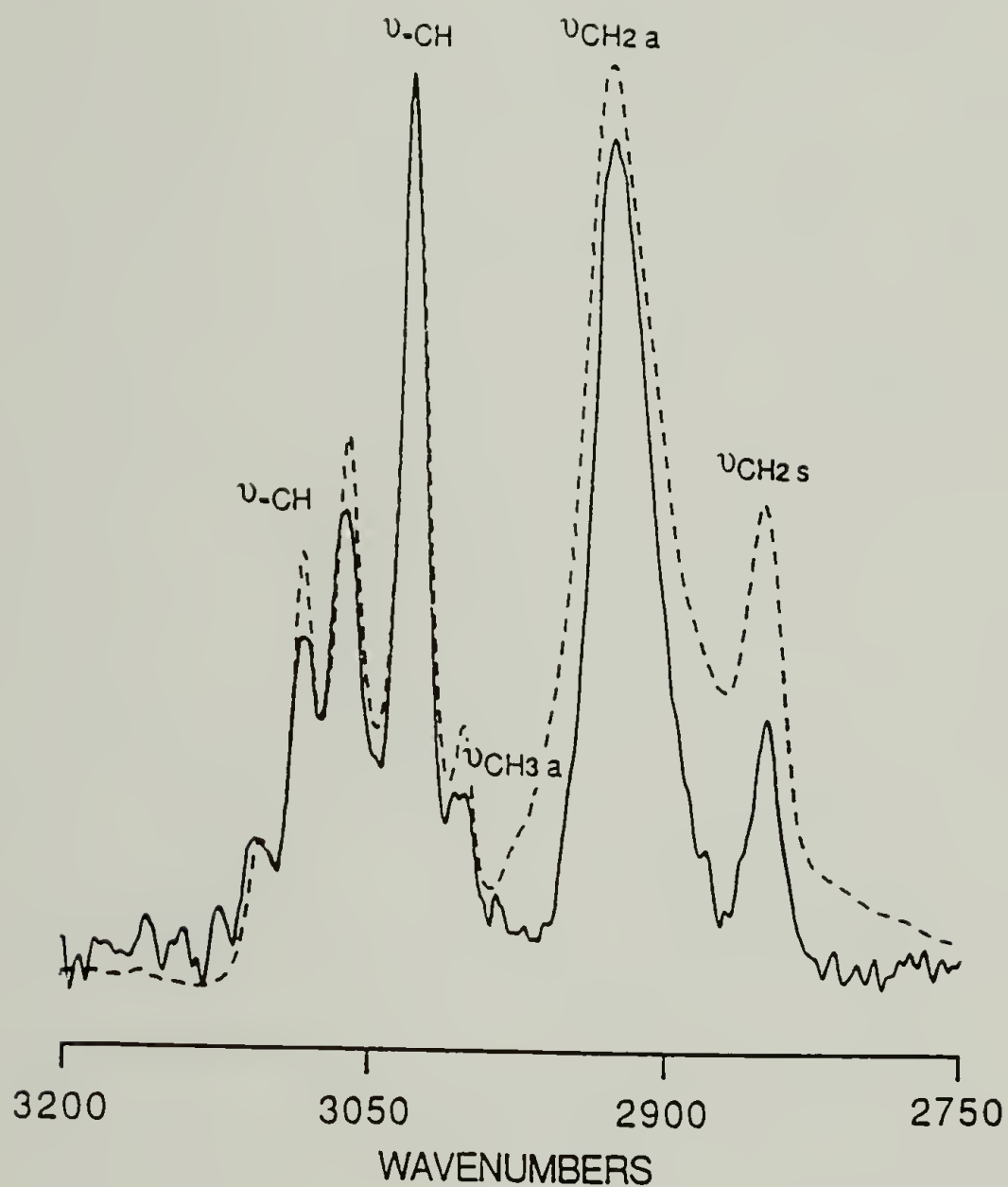


Figure 4.10 The IR spectrum of the adsorbed copolymer (PS₉₅-PPrS₅) in the C-H stretching region obtained via PMGR IR (solid line). The transmission spectrum of the polymer is given also (dashed line) for comparison.

X-ray Photoelectron Spectroscopy (XPS) was used to analyze the adsorbed polymer films. Figure 4.11 shows the survey spectrum of the PS₇₅-PPrS₂₅ and the PS₉₀-PPrS₁₀ copolymers (15° takeoff angle). The main peaks seen are the Au_{4f} doublet at 84 and 87.6 eV and the C_{1s} at approximately 285 eV. The carbon present is evidence of a carbon layer on top of the gold. Note that the C_{1s} line is larger for the 5% PPrS polymer suggesting that more polymer has adsorbed in this case. Quantitative determination of the amount adsorbed was done and the results will be presented subsequently. Small peaks at around 164 and 229 eV are due to electrons from the sulfur 2p and 2s orbitals respectively, these give evidence for the presence of the PPrS block on surface. The inset shows the C_{1s} region of the 5% PPrS polymer. The π to π^* shake up can be seen at approximately 6.7 eV higher binding energy than the main peak.³⁷ This shake up is due to a π to π^* transition with the simultaneous ejection of an electron; the energy balance requires it to have a higher binding energy. These shake up peaks are characteristic of aromatic compounds, and in particular the polystyrene shake up is known to appear at plus 6.7 eV as we see here. Thus we have evidence for polystyrene on the surface. Angle resolved XPS measurements were used to determine the total amount of polymer adsorbed to the surface for each polymer (except the 50/50 one). The adsorbed film thickness was determined by measurement of the attenuation of the Au_{4f} photoelectron peak. The absolute intensity of the gold line was measured before and after adsorption at several different takeoff angles (15°, 30°, 50° and 75°) and the intensity was found to be reproducible to within 3% for each takeoff angle. The mean free path of a electron ejected from the Au_{4f} orbital is (kinetic energy equal to 1170 eV, using a Mg anode) was taken to be 22 Å.³⁸ The calculated film thickness

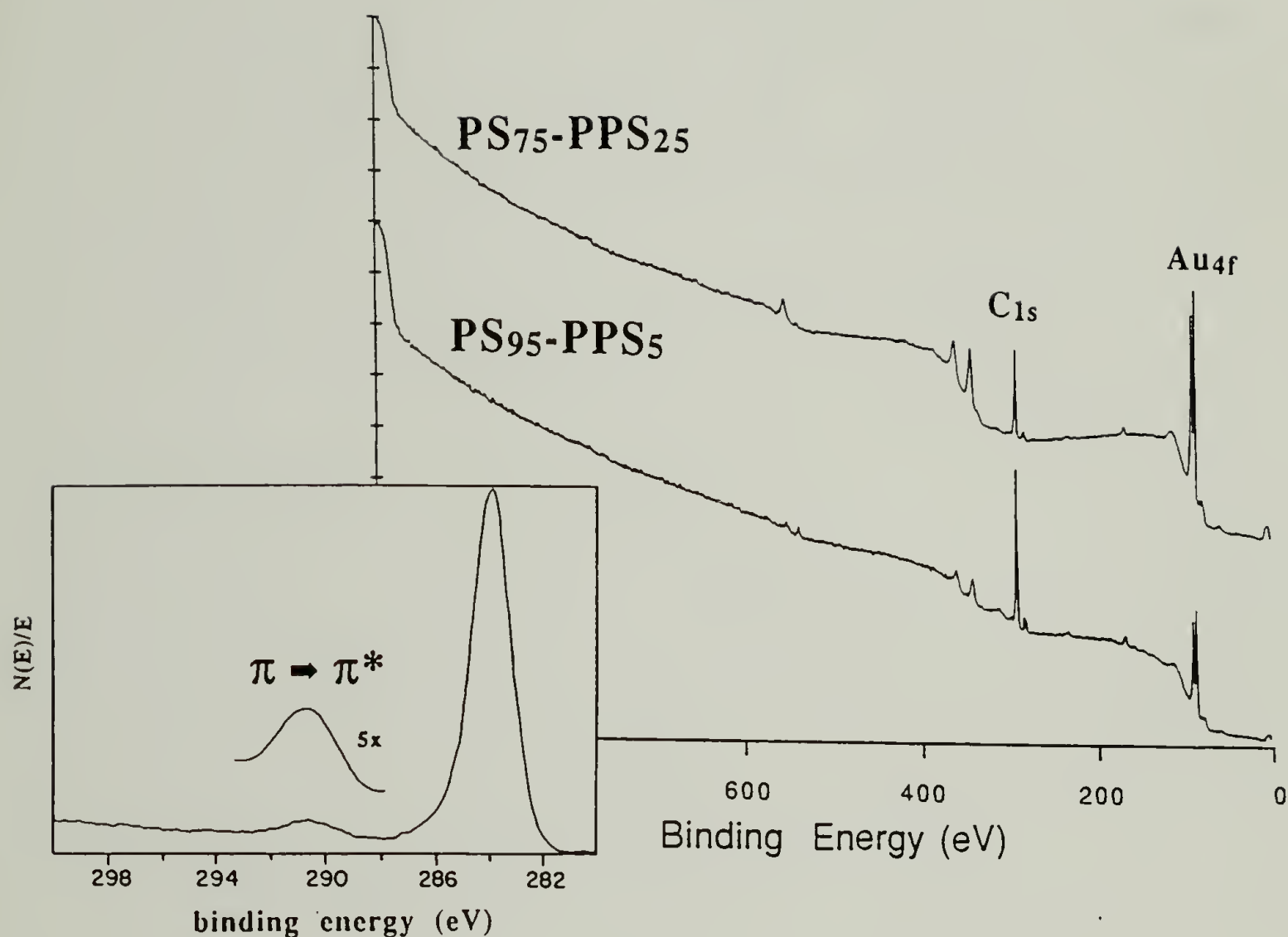


Figure 4.11 XPS survey spectra (15° takeoff) of the PS₇₅-PPrS₂₅ and PS₉₅-PPrS₅ copolymers adsorbed to gold. The hydrocarbon overlayer is indicated by the presence of the C_{1s} line. The PS₉₅-PPrS₅ copolymer shows a greater amount adsorbed. Small peaks at 164 eV and 229 eV correspond to the sulfur 2p and 2s orbitals, respectively. The inset shows the C_{1s} region of the spectrum blown up, note the presence of the π to π^* shake up peak.

for each polymer is given in Table 4.7. Also given are the adsorbance (calculated assuming an adsorbed layer thickness equal to 1.0 g/cm^3) and the graft density (calculated using a monomer length scale of $a=5.5 \text{ \AA}$).

Table 4.7 Adsorbance and Graft Density of PS-PPrS Copolymers.

<u>Sample</u>	<u>Thickness (\AA)</u>	<u>Adsorbance (mg/m^2)</u>	<u>Graft Density</u>
PS ₇₅ -PPrS ₂₅	27 ± 2	2.7	0.0221
PS ₉₀ -PPrS ₁₀	30 ± 2	3.0	0.0840
PS ₉₅ -PPrS ₅	34 ± 2	3.4	0.0946
PS ₀ -PPrS ₁₀₀	1-5	0.1-0.5	0.0010

Note that the amount adsorbed for all the copolymers is much higher than the PPrS homopolymer thus suggesting that the homopolymer is laying relatively flat on the surface. The amount adsorbed increases with decreasing PrS content in the three copolymer samples as is expected (see Chapters I and III for detailed discussion) This increase in the amount adsorbed is a direct effect of the increase in graft density because of the smaller anchor block. The graft densities are shown and one sees that they increase as expected. According to the MJ theory ³⁹(discussed in Chapter I) the amount adsorbed should increase as $1/x$ where x is size of the PPrS block. The data reported here qualitatively follow the predicted trend of increasing amounts adsorbed with decreasing size of the sticky block, but quantitatively the data do not match the predicted function. We find a $1/x^z$ dependence where $z \sim 0.14$, as opposed to the first power that is predicted. The data better fit the predictions of Evers ⁴⁰ as far the shape of the curve is concerned, the Evers calculations do not predict nearly as sharp a rise as

MJ theory does. This discrepancy is somewhat surprising because it would be expected that very strong sticky feet would come the closest to the MJ theory. The other data that we have obtained suggest a very strong interaction. The minimal effect of the adsorption solvent suggests that the buoy is not contributing much to the energy balance even at 5% SF thus the sticky block is very strong. The sticky foot strength is confirmed by the fact that the much stronger displacer solvent THF is not effective in this fashion either. Thus it is expected that the stronger sticky interactions should result in behavior that more resembles MJ predictions, but this is not what is seen.

In conclusion we have identified a number of problems that affect the anionic synthesis of styrene/propylene sulfide block copolymers. These include the inefficient drying procedure used for the PrS and the coupling reaction caused by disulfide formation. These problems were addressed and solutions obtained. Thus in this chapter we have shown the development of a synthetic procedure to prepare block copolymers of styrene and propylene sulfide without contamination of either the polystyrene homopolymer or the triblock copolymer resulting from the disulfide linkage. The resulting copolymers are also much more resistant to disulfide formation as well as degradation. A number of (polymeric) disulfide reductions were attempted and DTT proved to be the best means for accomplishing this. Evidence was also seen for an abnormally high (for small molecules) dependence of the conversion on overall solution concentration. This same phenomenon was seen in DEOM modifications (Chapter II) and it is postulated that the low concentrations effectively partition the reagent out of the coil interior thus decrease the ability to

react. Extremely high concentrations of the reagent are then needed to drive the reagent into the coil volume or increases in the polymer concentration will lead to the decrease of non-coil space and thus entry of the reagent into the coil. It was also shown that these copolymers adsorb to gold surfaces via the sulfide gold interaction and that the graft density and amount of polymer adsorbed increase as the PrS content of the polymer decreases.

References

1. Waldman, D. A.; Kolb, B. U.; McCarthy, T. J.; Hsu, S. L. *Proc. of A.C.S. Div. of Polym. Mat.*, **1988**, 59, 362.
2. Waldman, D. A.; Kolb, B. U.; McCarthy, T. J.; Hsu, S. L. *Langmuir*, in press.
3. Waldman, D. A. Ph.D. Dissertation, Polymer Science and Engineering Department, Univ. of Mass., 1990.
4. Nuzzo, R. G.; Fusco, F. A.; Allara, D. L. *Journal of American Chemical Society*, **1987**, 109, 2358.
5. Sigwalt, P.; Spassky, N. in *Ring Opening Polymerization Vol.2* ed. K.J. Ivin, T. Saegusa, Elsevier Press: New York 1984, Chapter 9.
6. Boileau, S.; Sigwalt, P. *Compt. Rend.* **1961**, 252, 882.
7. Dreyfuss, P.J. *Macromol. Sci.-Chem.* **1973**, A7(7), 1361.
8. Dreyfuss, P. *Chemtech.* **1973**, 6, 356.
9. Gobran, R.H. *Ency. of Polymer Sci. & Tech* **1972**, 10, 325.
10. Lautensschlaeger, F.J. *Macromol. Sci.-Chem.* **1972**, A6(6), 1089.
11. Yamashita, Y. *Adv. Poly. Sci.* **1978**, 28, 1.
12. Nevin, R.S.; Pearce, E.M. *Polymer Letters* **1965**, 3, 487.
13. Stouffer, J.M.; McCarthy, T. J. *Macromolecules*. **1988**, 21, 1204.
14. Morton, M.; Kammereck, R. F.; Fetters, L. J. *Macromolecules* **1971**, 4, 11.
15. Morton, M.; Mikesell, S. L. *J. Macromol. Sci.- Chem.* **1973**, A7(7), 1391.
16. Hale, P. T.; Pope, G. A. *Eur. Polym. J.* **1975**, 11, 677.
17. Cooper, W.; Hale, P. T.; Walker, J. S. *Polymer* **1974**, 15, 175.
18. MacKillop, D. A. *Journal of Polymer Sci. B* **1970**, 8, 199.
19. Roggero, A.; Zotteri, L.; Pronz, A.; Gandini, A.; Mazzei, A. *Eur. Polym. J.* **1976**, 12, 837.
20. Gourdenne, A. *Polymer Preprints (Am. Chem. Soc., Div. Polym. Chem.)* **1971**, 12(2), 129.

21. Morton, M.; Kammereck, R. F. *J. Am. Chem. Soc.* **1970**, *92*, 10.
22. Morton, M.; Fetters, L. J. *Rubber Chem. & Tech.*, **1975**, *8*(3), 359.
23. Morton, M.; Fetters, L. J. in *Stereo Rubbers* ed. W. M. Saltman, Wiley: New York, 1977, 215.
24. Young, R. N.; Quirk, R. P.; Fetters, L. J. *Adv. in Polym. Sci.* **1984**, *56*, 1
25. This polymer was synthesized before the special procedures developed for this thesis work were known. In other words it is an illustration of a "before" case and the polymers synthesized using the new procedures are the after case. The polymer was prepared in THF and PrS was dried with CaH₂; the polymer was terminated via addition of acidic methanol to produce the thiol end group.
26. MacKillop, D. A. *Journal of Polymer Sci. B* **1970**, *8*, 199.
27. Bates, R. B. Kroposki, L. M. Potter, D. E. *J. Org. Chem.*, **1972**, *37*, 560.
28. Simonds, R. P. Goethals, E. J. *Makromol. Chem.* **1978**, *179*, 1689.
29. March, J. *Advanced Organic Chemistry 2nd ed.*, John Wiley & Sons: New York, 1977, 1092.
30. Streitwieser Jr., A.; Heathcock, C. H. *Introduction to Organic Chemistry 2nd ed.*, Macmillan Pub.: New York, 1981, 810.
31. Tarbell, D. S. in *Organic Sulfur Compounds Vol. 1*, ed. N. Kharasch Plenum Press: London, 1961, Chapter 10.
32. Ohno, A. Oae, S. in *Organic Chemistry of Sulfur*, ed. Oae, S. Plenum Press: New York, 1977, Chapter 4.
33. Houk, J.; Whitesides, G. M. *J. Am. Chem. Soc.* **1987**, *109*, 6825.
34. Overman, L. E.; Smoot, J.; Overman, J. D. *Synthesis* **1974**, *1*, 59
35. Cleland, W. W. *Biochemistry* **1964**, *3*(4), 480
36. *Aldrichimica Acta* **1971**, *4*(3), 33.
37. Muilenberg, G. E. *Handbook of X-Ray Photoelectron Spectroscopy*, Perkin-Elmer Corp., 1979.
38. Clark, D. T. *Advances in Polymer Science* **1977**, *24*, 125.

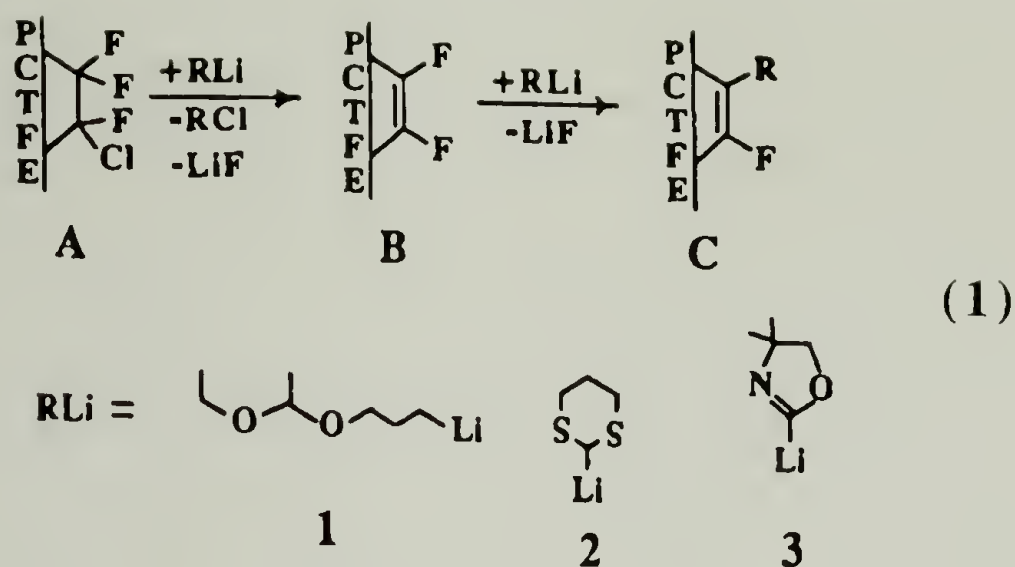
39. Marques, C.; Joanny, J. F. *Macromolecules* **1989**, 22(4), 1454.
40. Evers, O. A.; Scheutjens, J. M. H. M.; Fleer, G. J. *Macromolecules* **1990**, 23(25), 5221.
41. Evers, O. A.; Scheutjens, J. M. H. M.; Fleer, G. J. *J. Chem. Soc. Faraday Trans.* **1990**, 86(9), 1333.
42. Evers, O. A.; Scheutjens, J. M. H. M.; Fleer, G. J. *Macromolecules* **1991**, 24(20), 5558.

CHAPTER V

REACTIONS OF POLYSTYRYL ANIONS WITH POLY(CHLOROTRIFLUOROETHYLENE) AT THE FILM-SOLUTION INTERFACE

Introduction

Polymer molecules can be attached to a surface by chemical (grafting) reactions or through adsorption. The grafting of chains can be accomplished by either "grafting to" or "grafting from" an interface. The more common "grafting from" method involves the generation of a radical species at (or near) a solid surface in the presence of (or prior to exposure to) radically-polymerizable monomers.¹⁻⁹ One drawback of this grafting approach is that the structure of these interfaces is difficult to control and characterize. The molecular weight, molecular weight distribution, attachment site density, crosslink density, branch density and overall structure (i.e. covalent bond density, diffuseness) of the interface typically are not known. Given this major disadvantage, we have attempted to form an interface via the "grafting to" mechanism by reaction of an end-functionalized sticky foot polymer with a fluoropolymer film. In our work, monodisperse, anionically-polymerized polystyrene of known molecular weight is attached to the surface of poly(chlorotrifluoroethylene) (PCTFE) film by means of a surface modification reaction that has been well characterized for small molecules by previous coworkers.^{10,11} It has been found that alkylolithium reagents will react with PCTFE surfaces to incorporate alkyl groups; the reaction is amenable to producing modified layers with well-defined, controllable structures^{10,11} (equation 1).



Protected functional group-containing lithium reagents have been reacted and subsequently deprotected to incorporate thin layers of organic functional groups to the PCTFE surface. Several aspects of these reactions impact on the work described here. Lithium reagents **1-3** have been used to introduce alcohol, aldehyde and carboxylic acid groups to PCTFE, respectively, and the product surfaces are mixtures of structures **B** and **C**. For example, quantitative X-ray photoelectron spectroscopy (XPS) data for reaction with reagent **1** indicate a surface comprised of 80% **C** and 20% **B**.^{12,13} In general, the depth of reaction (thickness of resulting modified layer) depends on (at least) the following four factors: the structure of the lithium reagent, reaction temperature, reaction solvent and reaction time (for non-surface-selective modifications). Manipulation of these variables with the lithium reagents described above results in modified layers approximately 10 to 1500 Å deep.¹⁰⁻¹³ Lithium reagent **1** does not react with PCTFE surface-selectively in heptane/THF at any temperature, although the reaction depth can be varied from ~50 to 1500 Å by changing the reaction time and temperature. In heptane/THF mixtures, the lithium reagents **2** and **3** react surface-selectively and transform the outermost 10 -

60 Å of the film completely within the first five minutes of reaction and little subsequent modification follows. The thickness of the modified layer can be controlled by reaction temperature. The depth of reaction of PCTFE with reagent **2** depends strongly on solvent composition, proceeding more deeply with higher THF content, although reaction with reagent **3** is only weakly solvent dependent. These results suggest that the extent to which the solvent interacts with the product (modified surface layer) is the major controlling factor in determining the thickness of the modified layer because (with the appropriate solvent/lithium reagent combination) the modified layer can become a barrier to further reaction.

The research described here extends the PCTFE/alkyllithium chemistry to macromolecular lithium reagents in an effort to produce well-characterized graft polymer surfaces. The "grafting to" method has inherent advantages over the more common "grafting from" approach because of the (possible) control over graft polymer molecular weight and polydispersity. Data from reactions with small molecule alkyllithium reagents indicate that the thickness of the modified layer can be controlled through choice of solvent and reaction temperature. Our objectives consist of replacing the small molecule lithium reagents in eq. 1 with polymeric lithium reagents to form polymer-solid interfaces of controlled structure. This work has been in collaboration with P. A. Patton.¹⁴⁻¹⁶ The main strategies for this are shown in Figure 5.1.

The figure below indicates the structure of the polymer-solid (film) interface resulting from different experimental conditions. Path A results in a sharp interface, the thickness of which can be controlled by the (graft)

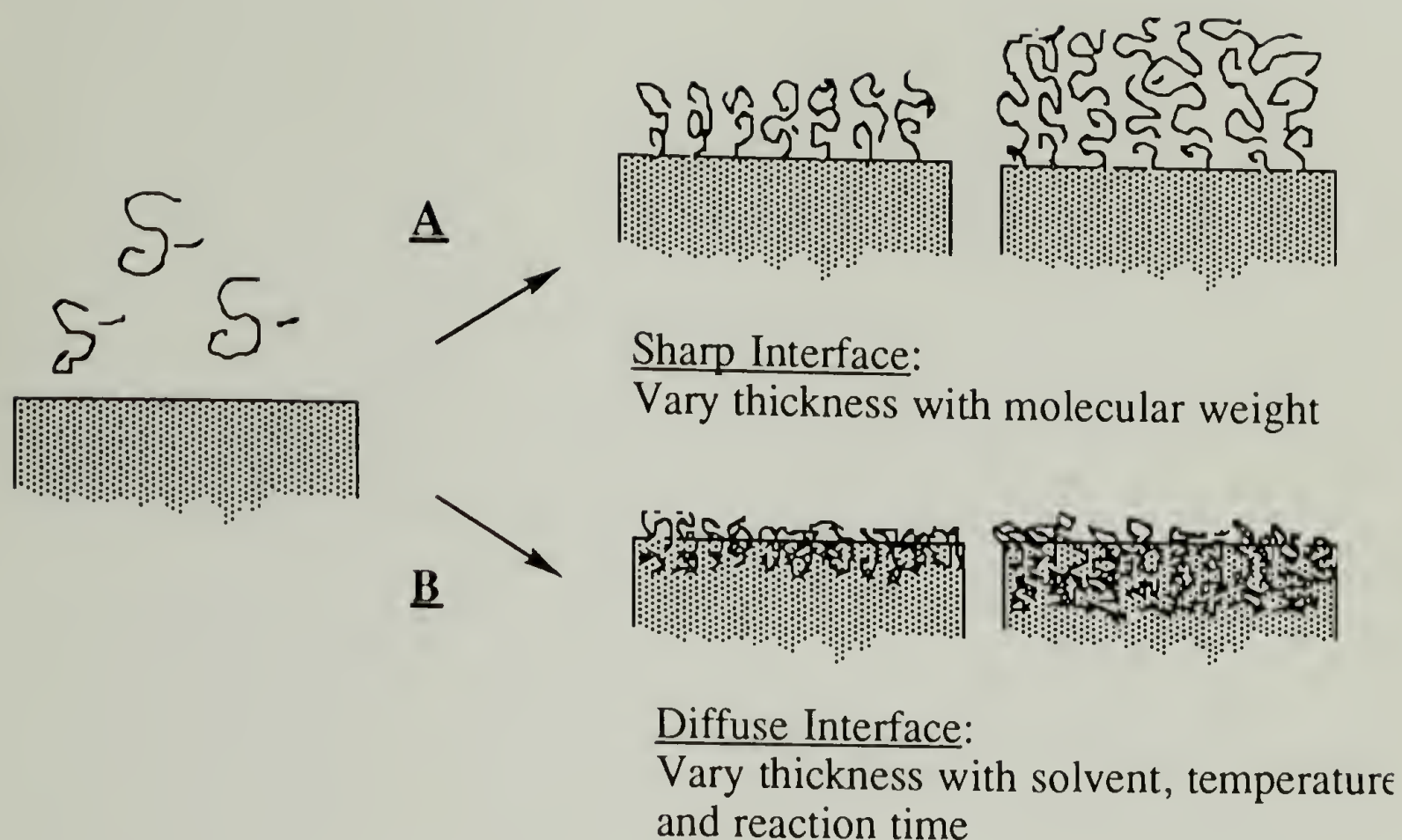


Figure 5.1 Illustration of the range of interface structures possible for reaction of polystyrene chains with the surface of PCTFE film.

polymer molecular weight. In this case, the thickness of the modified layer would be a function of the dimension of a single coil in solution. The second alternative, path B, utilizes reaction solvent, temperature and time to control the depth of reaction; in this case, polymer molecular weight should be of only secondary importance.

To our knowledge, there are no reports of grafting polystyryl anions to synthetic polymer surfaces, although, a range of surfaces including wood,¹⁷ glass,¹⁸ carbon black,¹⁹ and salt crystals²⁰ have been modified by this method. Polystyryl anions have also been grafted to halogen- or carbonyl- containing synthetic polymers in solution.²¹⁻²⁵

Experimental

Materials. PCTFE film (5-mil Aclar 33C) was obtained from Allied. Film samples (1 x 2 cm) were extracted with refluxing methylene chloride (30 min) and dried (0.05 mm) to constant mass ($\pm 1 \mu\text{g}$, achieved with two gravimetric analyses 24 h apart). Film samples were stored in Schlenk tubes under N_2 or attached to a vacuum manifold. Styrene (Aldrich) was dried with calcium hydride and distilled (from calcium hydride) immediately prior to use. Butadiene (Matheson) was dried with calcium hydride at -23°C , distilled (trap-to-trap), dissolved in THF or benzene (0.1 - 0.35 M butadiene), and stored in Schlenk tubes in the freezer. Ethylene sulfide (Aldrich) was dried over and distilled from calcium hydride. THF was distilled from sodium benzophenone dianion; benzene was distilled from sodium benzophenone dianion or calcium hydride; hexane and toluene were distilled from calcium hydride. *sec*-Butyllithium (Aldrich) was used as received and titrated periodically with 4-biphenylmethanol. 12-Crown-4 (Aldrich) was used as received and stored in a dessicator.

Materials Handling. All solvents and distilled reagents were either used immediately or stored under nitrogen for short periods of time in Schlenk flasks. All transfers of reagents and solvents were done by cannula or syringe.

Methods. All distillations and reactions were carried out under nitrogen unless otherwise indicated. Experiments were carried out on commercially available PCTFE film samples that had been extracted with

CH_2Cl_2 and dried to constant mass. X-ray photoelectron spectra (XPS) were recorded using a Perkin Elmer-Physical Electronics 5100 spectrometer with $\text{Mg K}\alpha$ or $\text{Al K}\alpha$ excitation (400 W or 300 W, respectively). Spectra were analyzed at two takeoff angles, 15° and 75° , from the plane of the sample surface. Contact angle measurements were made with a Ramé-Hart telescopic goniometer using a Gilmont syringe with a 24-gauge flat-tipped needle. Doubly distilled water was used as the probe fluid. Dynamic advancing and receding angles were measured while adding or withdrawing water to or from the drop. The values reported are averages of six measurements made at random points on the surface. Attenuated total reflectance infrared (ATR IR) spectra were recorded with an IBM 38 FTIR spectrometer using a germanium internal reflection element (45°). UV-vis spectra were recorded using a Perkin-Elmer Lambda 3A spectrophotometer; transmission spectra were obtained using a film-holding attachment. Gravimetric analyses were performed in air using a Cahn 29 electrobalance stabilized with a polonium source. Gas chromatography (GC) was performed with a Hewlett-Packard 5790A gas chromatograph at $80 - 160^\circ\text{C}$. Molecular weight determinations were made by gel permeation chromatography (GPC) using Polymer Laboratories PL gel columns (10^4 , 10^3 and 10^2 Å), a Rainin Rabbit pump, a Knauer 98 refractive index detector and toluene as the mobile phase. GPC data accumulation and analyses were performed using Interactive Microware GPC software, an Apple IIe computer, and calibration with polystyrene standards.

Reactions with PCTFE Films. PCTFE films were reacted with one of three polymeric anions (PSLi, PSBLi and PSSLi); the experimental procedures for each are described below.

Reactions of PSLi with PCTFE. PCTFE film was allowed to react in benzene or THF solutions containing varied concentrations of PSLi (of various molecular weights). The polystyryl anion was synthesized by the following procedure: styrene (1.0 - 2.0 mL) and THF or benzene (25 - 75 mL) were introduced to a dry, nitrogen-purged Schlenk tube and equilibrated to the temperature used for polymerization (-78 °C for THF and 4 °C to room temperature for benzene). The appropriate amount (for the desired molecular weight) of *sec*-butyllithium was added; the presence of the polystyryl anion (and thus initiation) was observed when the initially clear solution turned orange. The intensity of the color depends on the anion concentration, and thus one can qualitatively monitor the amount of living polymer chains in the solution. The polymerizations were allowed to proceed to completion (as determined by GC). The living polystyryl anions were used for subsequent reactions 30 min to 8 h after initiation. The reactions with the film were carried out in the following manner. A tared PCTFE film (or films) sample was placed in a Schlenk tube that was then purged with nitrogen for 15 min and equilibrated to the desired reaction temperature. Polystyryl anion solution (which had been equilibrated to the reaction temperature) (~20 mL) was added to the reaction vessel. Reactions were sometimes carried out at elevated temperatures by heating the polymer solution after transfer to the reaction vessel. Film samples were allowed to react for the desired amount of time and the reactions were stopped by removal of the reaction solution (via

cannula). The film sample was washed with reaction solvent (3 x 20 mL), water (3 x 20 mL) and hexane (2 x 20 mL), and then dried (0.05 mm) to constant mass. The reactions were carried out with polymers of a range of molecular weights using various anion concentrations, reaction times and reaction temperatures. Table 5.1 gives a list of these reactions, the conditions used and the notebook references (the contact angles are also included). One should note that a few complications were encountered in the procedures described above. Polystyryl anions are quite susceptible to adventitious impurities (i.e. adsorbed moisture on glass surfaces, etc.). Because the anion concentrations are relatively low, a significant fraction of the anions can be killed (protonated) inadvertently, and this changes the concentration of reactants to which the surfaces are actually exposed. At very low concentrations, all of the anions may be terminated, and the actual reaction time is much shorter (than we think). Because of viscosity effects, higher molecular weight polymers have to be prepared at lower concentrations, and for this reason, a larger percentage of the chains in these polymerizations are susceptible to (premature) termination by fairly small amounts of impurities. In some cases, we found that all of the anions were killed prematurely. This premature termination is exacerbated by elevated temperatures. Disappearance of the orange color is the best indication of termination of the living polymers in the system.

Reactions of PSBLi with PCTFE. PCTFE film was allowed to react with PSBLi under a variety of conditions. The PSLi anion was synthesized by the procedure given above. The living PSLi polymers were endcapped with butadiene to give PSBLi. This was accomplished by titrating with a butadiene solution (either in THF or benzene) to disperse the bright orange

Table 5.1 Reactions of PSLi with PCTFE film.

<u>Notebook Ref.</u>	<u>Temperature</u> (°C)/ <u>Time</u> ^a	<u>DP_n</u> ^b	<u>Anion</u> <u>Concentration</u> ^c	θ_a/θ_r (water)
<u>THF</u>				
1. B4-115	-78/ 3 h	754	0.001 M	96/65
2. B5-46	RT/ 17 h	50	0.035 M	97/15 rough
<u>Benzene</u>				
3. B4-34A	RT/ 1 day	100	0.001 M	N/A ^d
4. B4-34B	RT/ 1 day	100	0.001 M	N/A
5. B4-100	RT/ 10 min	1000	low	104/58
6. B5-104A'	RT/ 10 min	60	0.024 M	95/74
7. B5-104B'	RT/ 1 h	60	0.024 M	95/70
8. B5-104C'	RT/ 3.5 h	60	0.024 M	N/A
9. B5-147-1	RT/ 36 h	39	0.027 M	98/71
10. B5-147-2	RT/ 3 h	39	0.027 M	95/69
11. B5-147-3	RT/ 1 h	39	0.027 M	99/70
12. B6-106A	80 ^b / 35-40 min	250	0.002 M	105/53
13. B6-106B	80 ^b / 35-40 min	250	0.002 M	105/10
14. B6-120A	RT/ 2 h	~50	~0.01 M	93/64
15. B6-120B	RT/ 24 h	~50	~0.01 M	92/67

^a At reaction temperatures higher than room temperature the stability of the anion is not known. In fact in many cases of long reactions at high temperatures the anions were all dead and the reaction had stopped before it was worked up (i.e. the reaction times are less than those recorded)

^b The DP_ns are calculated from original stoichiometries because GPCs were not recorded.

^c The anions are very reactive and will react with adventitious protons from all sources inside the reaction flask. This decreases the actual concentration of anions present. In the extreme cases of very low anion concentration this can lead to total premature anion termination, thus the actual reaction time is less than that recorded.

^d N/A= Not available

living polystyryl anion color. The reactions with the film were carried out in the following manner. A tared PCTFE film (or films) sample was placed in a Schlenk tube that was then purged with nitrogen for 15 min and equilibrated to the desired reaction temperature. PSBLi solution (which had been equilibrated to the reaction temperature) (~20 mL) was added to the reaction vessel. The film was allowed to react for the desired amount of time. The reactions were stopped via removal of the reaction solution (in some cases the anions were killed first by addition of a small amount of ethanol). The film sample was washed with reaction solvent (3 x 20 mL), water (3 x 20 mL) and hexane (2 x 20 mL), and then dried (0.05 mm) to constant mass. The reactions were carried out with polymers of a range of molecular weights using various anion concentrations, reaction times and reaction temperatures. Table 5.2 gives a list of these reactions, the conditions used and the notebook references (the contact angles are also included). The same complications of inadvertent killing of the anions were encountered with PSBLi as with PSLi. The butadiene endcap is different from the PSLi in two senses: 1) The anion is a little more stable at elevated temperatures, and 2) The anion is not colored, and therefore the loss of anions cannot be visually monitored.

Reactions of PSSLi with PCTFE. PCTFE film was reacted with PSSLi of various molecular weights and at varied concentrations in benzene, THF and THF/hexane solutions. The PSLi anion was synthesized by the procedure given above. The living PSLi polymers were endcapped with ethylene sulfide to give PSSLi. This was accomplished by titrating with an ethylene sulfide solution (either in THF or benzene) to disperse the bright orange living polystyryl anion color. Reactions with the films were

Table 5.2 Reactions of PSBLi with PCTFE film.

<u>Notebook Ref.</u>	<u>Temperature °C/</u> <u>Time^a</u>	<u>DP_n^b</u>	<u>Anion</u> <u>Concentration^c</u>	<u>θ_a/θ_r (water)</u>
<u>THF</u>				
1. B5-45	RT/ 17.5 h	50	0.032 M	60-90/62
2. B5-50	-20/ 18 h	50	0.032 M	93/68
3. B5-52	RT/ 18.5 h	50	0.032 M	60-90/42
4. B5-54	66/ 19 h	50	0.032 M	94/66
5. B5-116-1	-78/ 1 h	500	0.004 M	N/A ^d
<u>Benzene</u>				
6. B5-65	80/ 14h	50	0.024 M	97/69
7. B5-69	80/ 3 h	50	0.024 M	92/73
8. B5-98a	80/ 3 h	350	0.005 M	N/A
9. B5-98c	80/ 40 min	350	0.005 M	N/A
10. B5-98d	80/ 90 min	350	0.005 M	N/A
11. B5-101-1	RT/ 1 h	50	0.0038 M	N/A
12. B5-101-2	80/ 12 h	50	0.0038 M	N/A
13. B5-101-3	50/ 12 h	50	0.0038 M	N/A
14. B5-101-4	80/ 12 h	50	0.0038 M	N/A
15. B5-104A	80/ 4.5 h	60	0.024 M	99/59
16. B5-104B	80/ 3 h	60	0.024 M	95/69
17. B5-104C	RT/ 3.5	60	0.024 M	94/69
18. B5-104D	RT/ 1 h	60	0.024 M	94/68
19. B5-107	80/ 35 min	350	0.0018 M	103/60
20. B5-111-1	80/ 2h	50	0.024 M	94/67
21. B5-111-2	80/ 6h	50	0.024 M	97/68
22. B5-113-3	80/ 6h	5	0.024 M	99/69
23. B5-113-4	80/ 2h	5	0.024 M	99/68
24. B6-120	80/ 24h	~50	~0.01 M	96/56
25. B6-120D	80/ 1h	~50	~0.01 M	95/45

^a At reaction temperature higher than room temperature the stability of the anion is not known. In fact in many cases of long reactions at high temperatures the anions were all dead and the reaction had stopped before it was worked up (i.e. the reaction times are less than those recorded)

^b The DP_n are calculated from original stoichiometries because GPCs were not recorded.

^c The anions are very reactive and will react with adventitious protons from all sources inside the reaction flask. This decreases the actual concentration of anions present. In the extreme cases of very low anion concentration this can lead to total premature anion termination, thus the actual reaction time is less than that recorded.

^d N/A= Not available.

carried out in the following manner. A tared PCTFE film (or films) sample was placed in a Schlenk tube that was then purged with nitrogen for 15 min and equilibrated to the desired reaction temperature. Polymer anion solution (which had been equilibrated to the reaction temperature) (~20 mL) was added to the reaction vessel. The film was allowed to react for the desired amount of time and the reactions were stopped with removal of the reaction solution (via cannula). The film sample was washed with reaction solvent (3 x 20 mL), water (3 x 20 mL) and hexane (2 x 20 mL), and then dried (0.05 mm) to constant mass. The reactions were carried out with polymers of a range of molecular weights using various anion concentrations, reaction times and reaction temperatures. Table 5.3 gives a list of these reactions, the conditions used and the notebook references (the contact angles are also included). One should note that the thiolate end-capped polymers are not as susceptible to protonation by adventitious proton sources as are the PSLi and PSBLi carbanions. However, they are easily oxidized to the disulfide by molecular oxygen and other weak oxidants (see Chapter 2).

A different method was used in some reactions (Table 5.3, entries 13, 14, 15, 35, 40 and 41). PSSH polymer (i.e. a previously made and isolated polymer) was dissolved in the appropriate reaction solvent, and either NaH or CaH₂ were added to deprotonate and form the thiolate anion. The solutions were then transferred via cannula onto the films and the reactions were carried out in the fashion described above.

The reactions listed in Tables 5.1, 5.2 and 5.3 are covered in the following notebooks: B3, B4, B5 and B6. There are other projects

Table 5.3 Reactions of PSSLi with PCTFE.

<u>Notebook Ref.</u>	<u>Temperature °C/ Time</u>	<u>DP_n</u>	<u>Anion Concentration</u>	<u>θ_a/θ_r (water)</u>
<u>THF</u>				
1. B3-51B	-20/ 36 h	18a	0.004 M	94/53
2. B3-52	-20/ 36 h	00b	0.004 M	95/53
3. B3-70	-78/ 3 h	100	0.014 M	94/56
4. B3-71	-20/ 3 h	100	0.014 M	N/A ^c
5. B3-88A	RT/ 10 min	50	0.04 M	N/A
6. B3-88D	RT/ 37 min	50	0.04 M	N/A
7. B3-88C	RT/ 10 min	50	0.004 M	N/A
8. B3-88B	RT/ 37 min	50	0.004 M	N/A
9. B3-140A	RT/ 1.5 day	50a	0.05 M	N/A
10. B3-140B	RT/ 1.5 day	50a	0.05 M	N/A
11. B3-140C	RT/ 4 day	50a	0.05 M	135/0
12. B3-140D	RT/ 4 day	50a	0.05 M	133/15
13. B4-86 ^d	RT/ 5 h	2100	0.00013 M	99/60
14. B4-88 ^e	RT/ 4 h	694	0.00028 M	97/63
15. B4-90 ^d	RT/ 5 h	2100	0.00013 M	93/35
16. B4-112	RT/ 3 h	754	0.001 M	95/72
17. B5-27	RT/ 8 h	120	0.007 M	93/68
18. B5-85	68/ 3 h	68	0.02 M	128/26
19. B5-87	68/ 10 min	68	0.02 M	N/A
<u>THF/Hexane</u>				
20. B4-127	RT/ 90 h (4:1)	500a	N/A	90/50
21. B5-18	RT/ 8 h (4:1)	120	0.007 M	93/71
22. B5-15	RT/ NA (1:1)	120	0.007 M	101/66
23. B4-124	RT/ 90 h (3:2)	500a	N/A	90/73
24. B5-21	RT/ 8 h (3:2)	120	0.007 M	94/70
25. B4-121	RT/ 90 h (2:3)	500a	N/A	100/60
26. B4-118	RT/ 90 h (1:4)	500a	N/A	96/47
27. B5-24	RT/ 8 h (1:4)	120	0.007 M	94/71
<u>Benzene</u>				
28. B3-87A	RT/ 17 min	50	0.04 M	99/63
29. B3-87B	RT/ 30 min	50	0.04 M	98/63
30. B3-87C	RT/ 27 min	50	0.004 M	98/59
31. B3-87D	RT/ 3 hr	50	0.004 M	95/60
32. B3-139B	RT/ 4 day	22a	0.005 M	96/61 sticks
33. B3-139C	RT/ 1.5 day	57a	0.005 M	92/50 sticks
34. B3-139D	RT/ 4 day	57a	0.005 M	94/58 sticks
35. B4-27 ^e	RT/ 2 day	44	0.0002 M	93/68
36. B4-34C	RT/ 1 day	100	0.001 M	N/A

continued next page

Table 5.3 continued

37.	B4-34D	RT/ 1 day	1000	0.001 M	N/A
38.	B4-34F	RT/ 5 day	1000	0.001 M	N/A
39.	B4-45	benzene control			N/A
40.	B4-47A ^e	RT/ 2 h	107	0.0054 M	N/A
41.	B4-47B ^e	RT/ 2 day	107	0.0054 M	N/A
42.	B4-54A	RT/ 12 h	2222	~0.0004 M	N/A
43.	B4-54C	RT/ 24 h	2222	~0.0004 M	N/A
44.	B4-54D	RT/ 72 h	2222	~0.0004 M	N/A
45.	B4-62	benzene control			
46.	B4-64A	RT/ 48 h	750	N/A	N/A
47.	B4-64C	RT/ 14 days	750	N/A	97/68
48.	B4-97	RT/ 16 h	high	low	104/64
49.	B4-103	60/ 12 h	1000	low	105/58
50.	B4-106	benzene control			105/68
51.	B5-67	80/ 14 h	48	0.024 M	100/46
52.	B5-71	80 3 h	48	0.024 M	105/45

^a The DPs are calculated from original stoichiometries because GPCs were not recorded.

^b No polystyrene was used; ethylene sulfide reacted directly with *sec*-butyllithium.

^c N/A= not available

^d Calcium (Ca⁺) replaces lithium (Li⁺) as counter ion. These anions were made by deprotonation of PSSH with CaH₂.

^e Sodium (Na⁺) replaces lithium (Li⁺) as counter ion. These anions were made by deprotonation of PSSH with NaH.

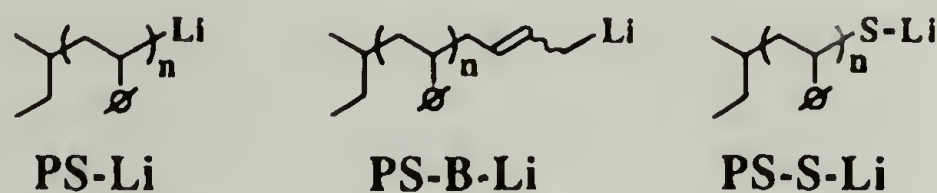
covered to various extents in these notebooks, as well. For the most part B3 is the start of the project and contains data for the sulfur end-capped polymers. The reactions with tosylated PCTFE surfaces are included in notebook 3. Notebooks B4 and B5 contain information about all of the different combinations of solvents and endgroups. B6 contains a small amount of data at the beginning, and on pages 100-130. The notebook references refer to the actual procedure, and thus contain the reaction conditions. Note that the full compliment of analytical tools (UV, gravimetrics, XPS, ATR-IR and contact angle) was not used in every case. The spectral data may be found in a number of different places. The first place to look is on the referenced notebook page and the pages directly following (although in some cases the actual data may be a significant distance away, so consult the table of contents). In a large number of instances, the spectroscopic data were not put directly in the notebook, but these can be found in various spectra catalogs (PSSLi/XPS, PSSLi/ATR, PSLi/PSBLi/XPS, PSLi/PSBLi/ATR).

Solvent Swelling of PCTFE Film. PCTFE film samples were tared, soaked in solvent for 1 h, removed, and dried under a stream of nitrogen for 5 min, and then reweighed. Results were determined as a percent mass gain. These experiments were performed in triplicate.

Results

Each of the results that follows pertains to a reaction of PCTFE film with one of three polystyryl anions: polystyryllithium (PSLi) (Table 5.1), butadiene-endcapped polystyryllithium (PSBLi) (Table 5.2), sulfur-

endcapped polystyryllithium (PSSLi) (Table 5.3). Each is prepared by anionic polymerization of styrene using *sec*-butyllithium as the initiator



in THF or benzene. PSBLi and PSSLi²⁶ were prepared by titrating the colored living PSLi with butadiene and ethylene sulfide, respectively. Reactions were carried out on PCTFE film samples in 50 mL Schlenk tubes fitted with a large O-ring joint and a teflon stopcock. The effects of reaction solvent (THF, benzene, heptane and mixtures of these), reaction temperature, reaction time and anion concentration on the structure of the modified film were investigated. It should be noted that due to the highly reactive nature of the lithium carbanions and the relatively high molecular weight molecules (and thus very low anion concentrations) the study of the variables described above was problematic. We found that often a substantial percentage of the anions present in a given reaction were terminated prematurely. The fraction could reach 100% and totally stop the reaction (this effect was exacerbated by the elevated temperatures used in some cases). We found that anion concentrations above approximately 0.01 M were stable with time.

Because of the low surface:bulk mass ratio, normal analytical techniques are usually not sensitive enough to monitor changes in a thin surface layer, such as those reported here, and special surface-sensitive

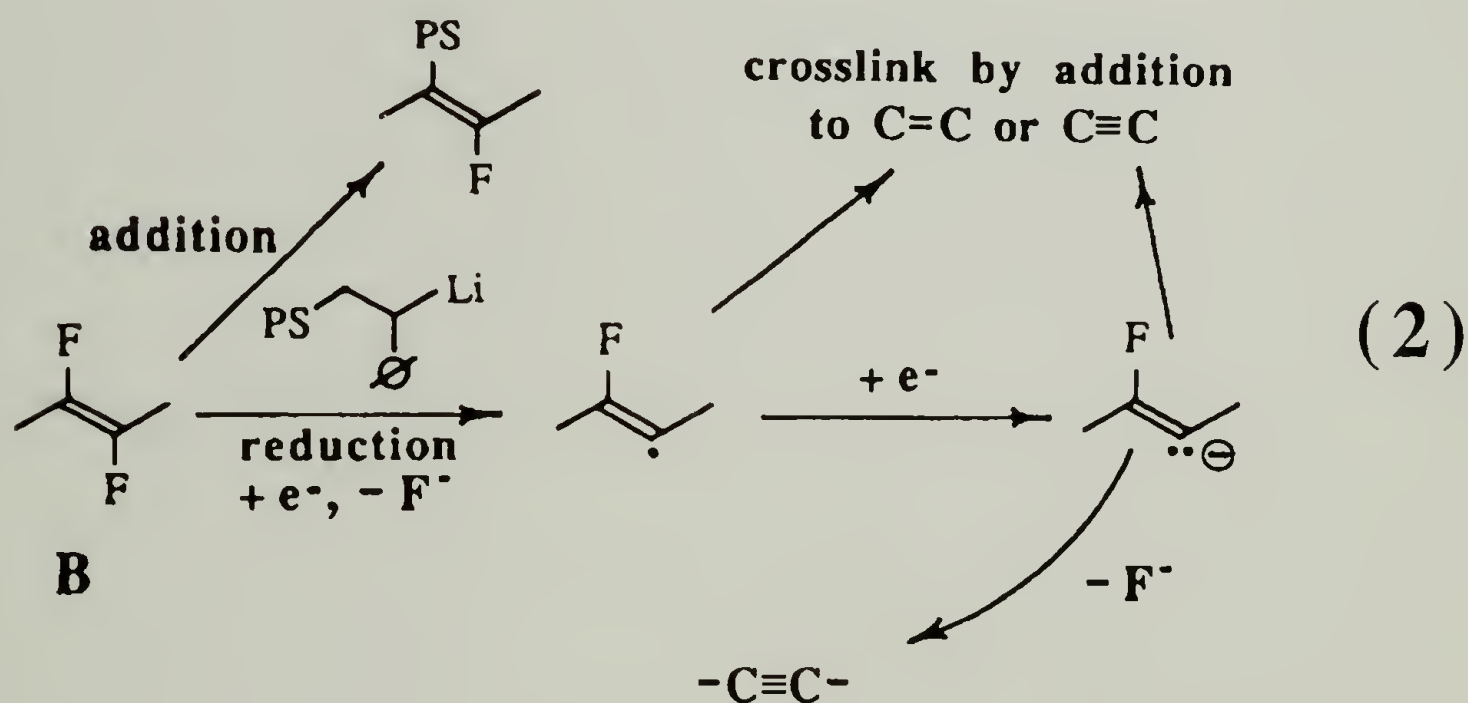
techniques are required. Each technique samples the surface at different depths, and thus more than one method must be used to build a picture of the surface. The most surface sensitive technique used involves measurement of water contact angles with the surface. This method is sensitive to only the top one or two atomic layers. PCTFE has advancing and receding water contact angles of $\theta_A/\theta_R = 104^\circ/80^\circ$, while a polystyrene film has values of $91^\circ/68^\circ$. In this work, an advancing contact angle in the 90s is regarded as evidence that polymer (i.e. polystyrene) has been grafted to the surface, although the amount is unknown. XPS probes the surface at somewhat greater depths. Our calculations indicate that a takeoff angle of 15° (with respect to the plane of the sample surface) corresponds to a carbon sampling depth of approximately 10 \AA , and a 75° takeoff angle corresponds to 40 \AA . XPS data are not sensitive to (grafted) polymer layers beyond the 40 \AA thickness. The least surface sensitive technique used in our laboratory is attenuated total reflectance infrared spectroscopy (ATR IR). The sampling depth of this technique depends on the material of the crystal used and the angle of the reflected laser beam. For work reported here, we used a 45° germanium crystal which samples an average effective thickness of 750 \AA (at 3200 cm^{-1}) to 2250 \AA (at 1000 cm^{-1}), and thus this is quite a jump in scales (of probed depths). One finds that thin layers of material that can be analyzed easily by the first two techniques described above may not even be detected by ATR IR.

Two bulk-sampling techniques were also used for analysis, and in each case, the sensitivity was enhanced by using thinner films.

Transmission UV spectroscopy (UV-vis) was used to determine relative rates of addition and reduction reactions. Gravimetric analysis involves

weighing the film before and after modification (using a balance sensitive to tenths of micrograms). The thickness of a layer can be calculated from the weight change, an assumed layer density and the surface area of the film.

Reactions of PCTFE with PSLi. The reaction of PSLi with PCTFE film is solvent-dependent; reduction of the difluoroolefin competes with addition when THF is used as the solvent (eq. 2). In THF at room temperature, PSLi ($n = 50$,²⁷ 0.02 M) reacts rapidly with PCTFE film to yield dark colored film samples that continue to darken to pitch black with further reaction. Decreasing the concentration of PSLi to 0.004 M or the



reaction temperature to -78°C slows the reaction, but the same color changes (as well as all other measured changes) occur, although the rate is diminished. This observation is in sharp contrast to reactions of PCTFE

with all other lithium reagents that have been investigated by our group: no visible color change is observed when PCTFE films are reacted with reagents **1-3**, methyllithium or phenyllithium under essentially the same conditions. Figure 5.2 shows a plot of the absorbance at 310 nm vs. reaction time for PCTFE film samples treated with PSLi ($n = 50$, 0.004 M) at room temperature. These data establish that the reduction reaction is not surface-selective and proceeds with little retardation into the bulk of the film. The UV-vis spectrum is broad with no fine structure and tails through the visible region, indicating an extended conjugated π -system. The absorbance at 310 nm indicates the extent of reactions other than polystyrene addition.²⁸⁻³⁰ Gravimetric analysis indicates a gradual and steady mass loss with reaction time. In one case, an extensively reacted sample lost ~33% of its initial mass. Quantitative determinations of extents of reactions cannot be made with these gravimetric data due to competing mass losses (caused by reductive dehalogenation and perhaps graft copolymer dissolution) and mass gains (due to addition of polystyrene). However, in conjunction with spectroscopic information, these data qualitatively indicate extensive dehalogenation and very deep reactions. For a representative modified film sample (Table 5.1, entry 2) XPS atomic composition data indicate that fluorine is absent (<1% atomic concentration) from the outer 40 Å. Water contact angle data ($\theta_A/\theta_R = 97^\circ/15^\circ$) exhibit large hysteresis, indicating a rough surface. Figure 5.3 shows an ATR IR³¹ spectrum of a PCTFE film sample that had been reacted with PSLi ($n = 50$; 0.035 M) (Table 5.1, entry 2) in THF at room temperature for 17 h. The spectrum indicates the presence of a small amount of polystyrene evidenced by aromatic C-H stretching at 3100 - 3000 cm^{-1} , and also reveals more aliphatic C-H (at 3000-2850 cm^{-1}) than is

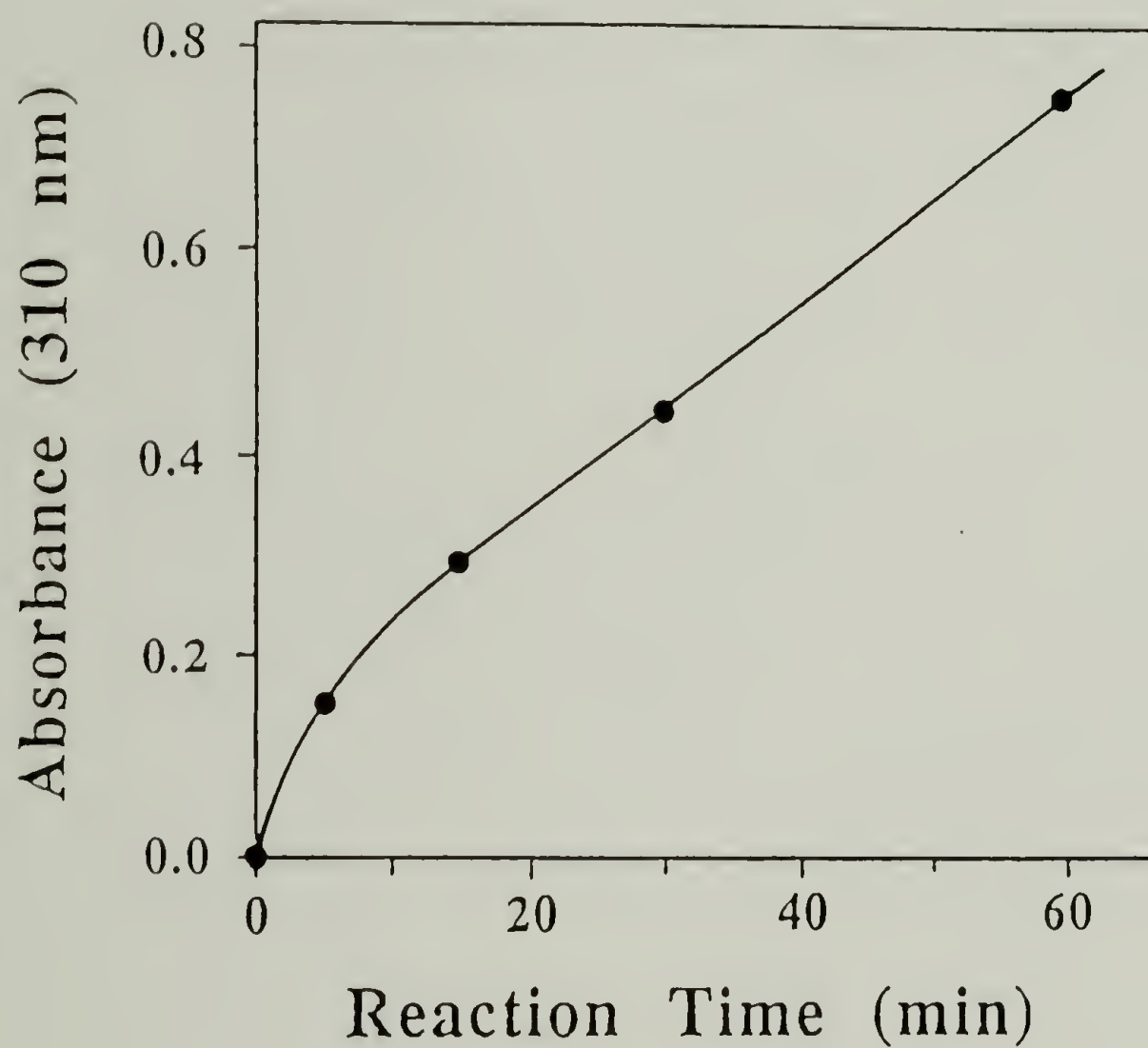


Figure 5.2 Plot of absorbance (310 nm) vs. reaction time for the reaction of PCFTE film with PSLi ($n = 50$; 0.004 M) in THF at room temperature.

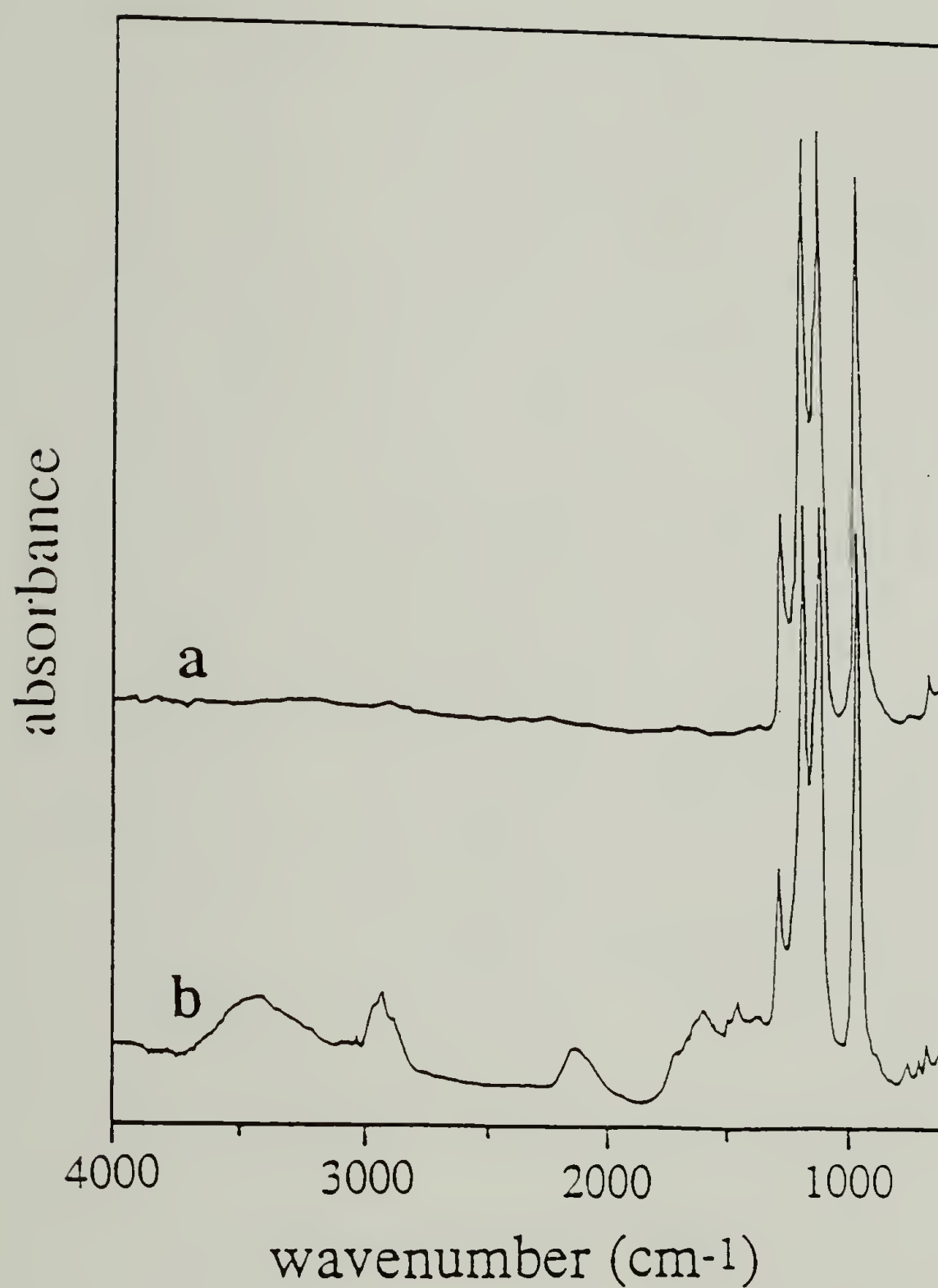


Figure 5.3 ATR IR spectra of (a) virgin PCTFE film and (b) PCTFE film which had been reacted with PSLi ($n = 50$; 0.035 M) in THF at room temperature for 17 h.

expected from polystyrene, conjugated C-C triple bonds at 2200 - 2000 cm^{-1} , conjugated C-C double bonds at 1650 - 1500 cm^{-1} , hydroxyl groups at 3420 cm^{-1} , and carbonyls at 1710 cm^{-1} . The hydroxyl and carbonyl groups can be ascribed to reactions occurring in aqueous workup. The carbon-carbon double and triple bonds indicate an extensively reduced carbonaceous product, similar in terms of structural features, to benzoin dianion-reduced poly(tetrafluoroethylene) (PTFE)³² and sodium naphthalide-reduced poly(tetrafluoroethylene-*co*-hexafluoropropylene) (FEP).³³

The anomalous reactivity of PSLi with PCTFE in THF can be explained as reduction of the PCTFE polymer competing with the addition of polystyrene chains to the difluoroolefin intermediate (**B** in eq. 1) via essentially the same mechanism proposed for reduction of PTFE.³² This mechanism leads to a crosslinked structure containing carbon-carbon double and triple bonds; eq. 2 shows an abbreviated mechanism. It is plausible that the steric requirements for addition of the secondary benzylic polymeric lithium reagent allow reduction to compete effectively.

When benzene is used as the solvent for the reaction of PCTFE film with PSLi no visible color change occurs upon reaction. Water contact angles for all reacted samples are listed in Table 5.1. Virgin PCTFE exhibits contact angles of $\theta_A/\theta_R = 104^\circ/80^\circ$ while polystyrene films cast on glass give contact angles of $91^\circ/68^\circ$. The decrease in contact angles is indicative of at least a small amount of PS addition. A survey of the data in Table 5.1 indicates that at least a monolayer of polymer is grafted to the surface under most of the conditions, and the average contact angle value is

95.3(\pm 2.5)/69(\pm 3). Higher contact angles (entries 5, 12 and 130) are observed for samples which were reacted at very low concentrations and/or elevated temperatures, indicating no addition of PS. The lack of addition is most likely due to a lack of anions (live species) in the reaction mixture. Figure 5.4 shows plots of absorbance³⁴ (at 310 nm and 230 nm) vs. reaction time for PCTFE samples reacted with PSLi ($n = 39$, 0.027 M) in benzene at room temperature (Table 5.1, entries 9-11). Very little increase in absorbance was observed at 310 nm, indicating the absence of any reduction side reactions. The absorbance at 230 nm has reached a plateau within an hour, indicating a surface-selective, auto-inhibiting reaction that stops completely within an hour (resolved aromatic fine structure, between 250 and 270 nm, was not observed). ATR IR spectra of samples reacted for 1, 3 and 36 h (Table 5.1, entries 9-11) were indistinguishable and show no indication of the reductive dehalogenation that was observed in the reactions carried out in THF. Figure 5.5 shows a representative ATR IR spectrum (Table 5.1, entry 11). Features expected for polystyrene (3061, 3027, 2924, 1601, 1493, 1452, 760, 701 cm^{-1}) and PCTFE (1286, 1192, 1122, 964, cm^{-1}) are present as well as a broad absorbance (3600 - 3200 cm^{-1}) indicating the presence of hydroxyl groups.³⁵ The inset shows the C-H stretching region; the relative sizes and shapes of the peaks compare well with polystyrene. XPS of all reacted samples were also indistinguishable; a representative spectrum along with a spectrum of PCTFE is shown in Figure 5.6. Upon reaction, the F_{1s} (692 eV), Cl_{2s} (274 eV), and Cl_{2p} (204 eV) photoelectron lines dramatically decrease in intensity. A small amount of oxygen is introduced (534 eV), and the C_{1s} line increases in intensity and shifts from 297 to 287 eV. The small peak at 293 eV in the reacted sample spectrum (b inset) is a π to π^* shake up

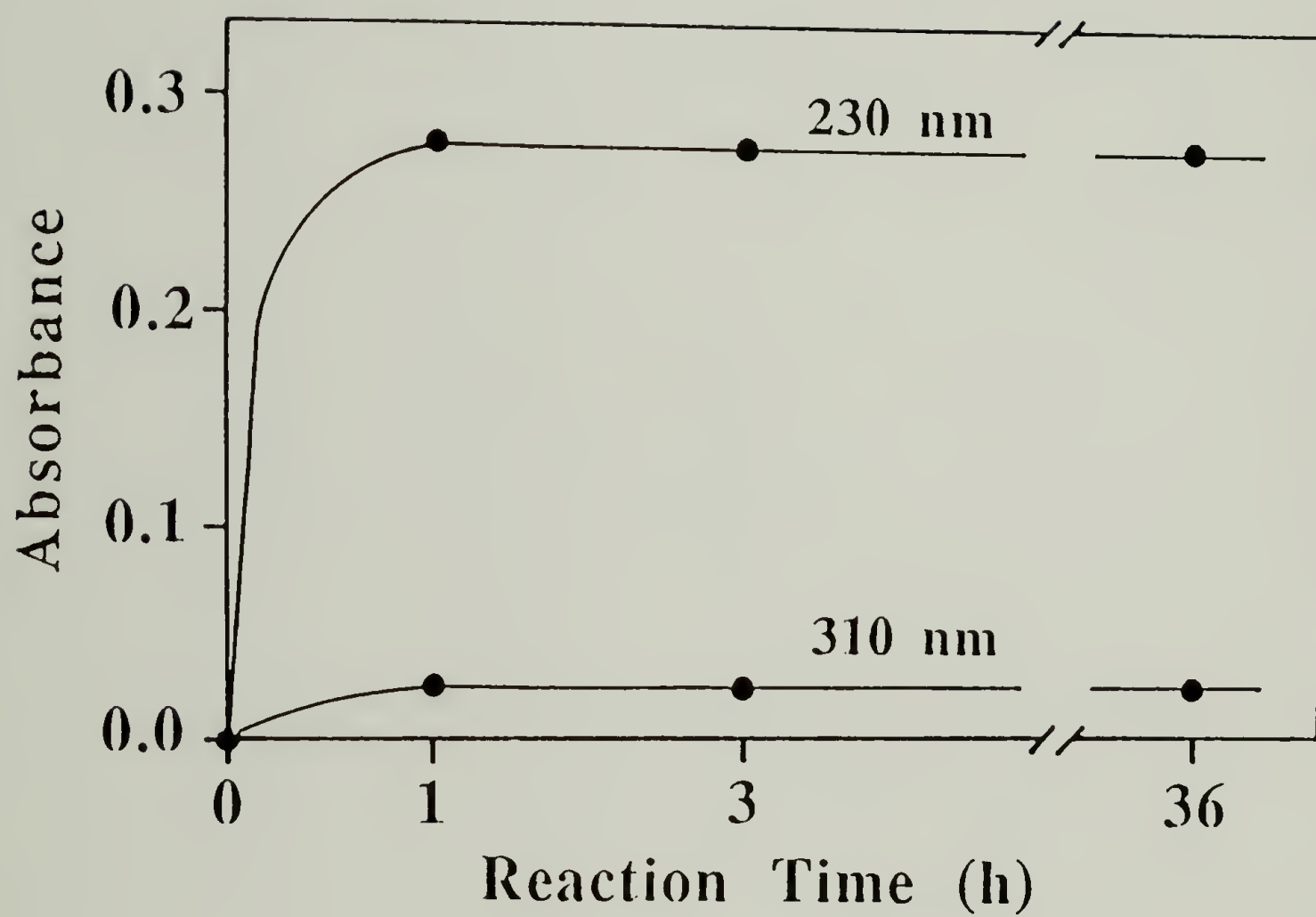


Figure 5.4 Plots of absorbance (310 nm and 230 nm) vs. reaction time for the reaction of PSLi ($n = 39$; 0.027 M) in benzene at room temperature.

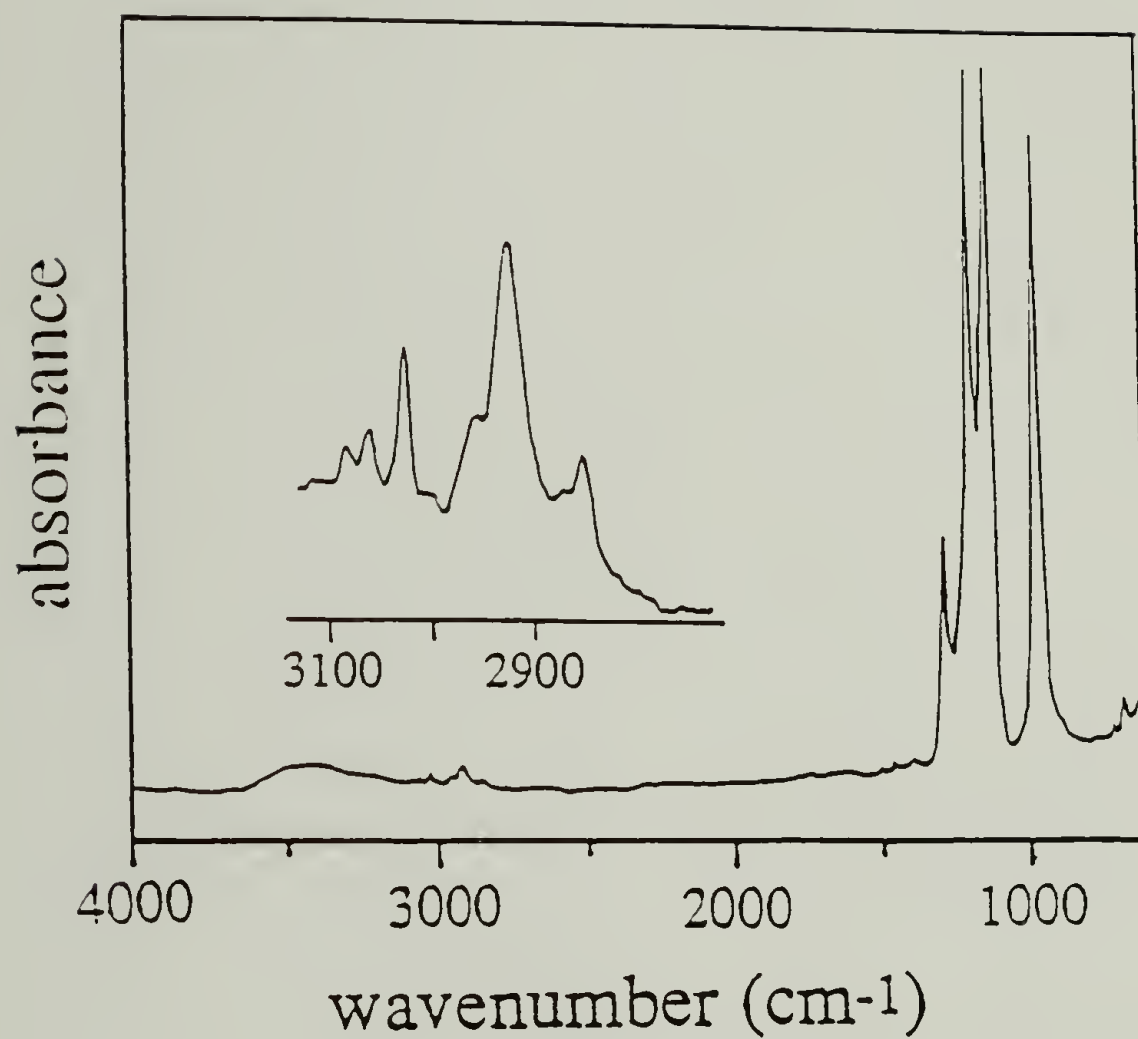


Figure 5.5 ATR IR spectrum of PCTFE film that had been reacted with PSLi ($n = 39$; 0.027) in benzene at room temperature for 1 h.

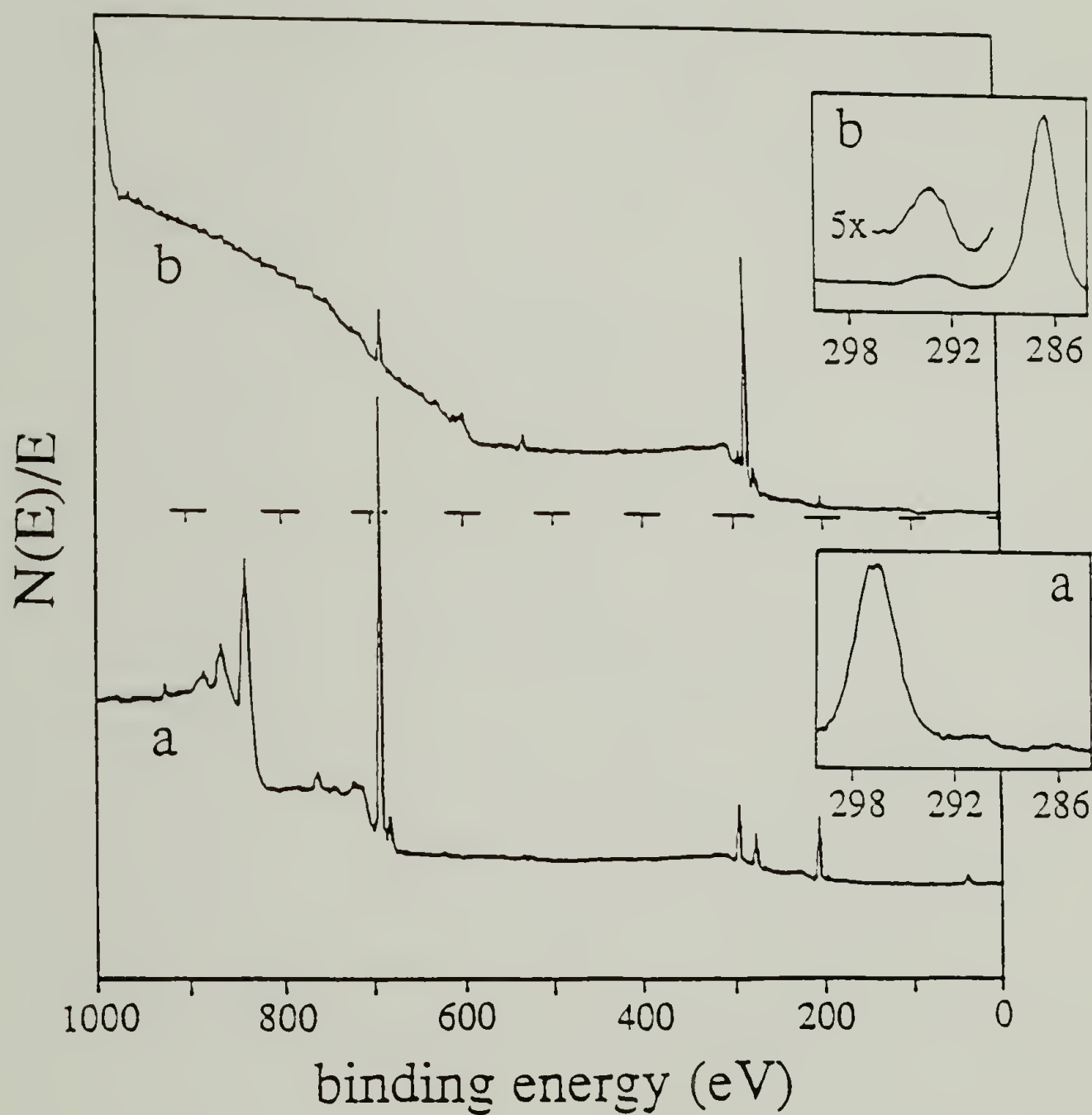


Figure 5.6 XPS spectrum of (a) PCTFE film and (b) PCTFE film which had been reacted with PSLi ($n = 39$; 0.027 M) in benzene at room temperature.

satellite due to the aromatic carbons in polystyrene. These spectra were recorded at a 75° takeoff angle and indicate the atomic composition of the outer ~40 Å of the surface. Table 5.4 gives the atomic compositions for the B5-147 series (Table 5.1, entries 9-11) and the benzene control (PCTFE film treated with benzene alone).

Table 5.4 XPS Atomic Composition Data for PSLi Reacted with PCTFE in Benzene at Room Temperature.

	<u>1 hour</u>		<u>3 hours</u>		<u>36 hours</u>		<u>Benzene Control</u>	
	<u>15° TO</u>	<u>75° TO</u>	<u>15° TO</u>	<u>75° TO</u>	<u>15° TO</u>	<u>75° TO</u>	<u>15° TO</u>	<u>75° TO</u>
C	95.6	89.1	94.0	90.1	89.4	90.7	33.0	36.6
F	1.9	5.0	3.1	4.6	1.7	4.0	46.1	46.9
Cl	0.9	4.5	0.9	3.9	0.7	3.0	13.2	15.2
O	1.3	1.3	2.1	1.1	5.3	1.5	4.3	1.2
Si	0.2	0.2	0.0	0.0	2.9	0.8	0.9	0.2

The C:F ratio (at 75° takeoff angle) is approximately 20:1, implying that this region is predominantly polystyrene (PCTFE C:F ratio is 0.78). The C:F ratio measured at a takeoff angle of 15° is 44:1. The difference between these two ratios demonstrates a composition gradient across the outer 40 Å with increasing fluorine concentration (decreasing polystyrene concentration) at greater depths. The data suggest the formation of a sharp interface, the structure of which is a thin modified layer beneath an overlayer comprised predominantly of polystyrene; the total thickness of the two layers is ~40 Å.

Reactions of PCTFE with PSBLi. As was shown in the last section, the competitive nature of the reduction (eq. 2) can be controlled by choice of solvent (benzene vs. THF); we have found that the structure of the lithium reagent also affects this competition. PSLi was endcapped with butadiene to form a primary allylic carbanion that has less steric hindrance (relative to the secondary benzylic carbanion) and the same experiments were carried out. The reaction of PSBLi with PCTFE film in THF gives no visible color change and no indication of extensive reductive dehalogenation is observed by UV-vis or ATR IR. The UV data (310 nm) shown in Figure 5.7 show no increase in absorbance after an initial burst; this behavior is typical of the auto-inhibiting character of lithium reagents **2** and **3**. UV-vis, ATR IR, and XPS were consistent with a thin film of polystyrene being incorporated in a surface-selective fashion. Water contact angle values are approximately $\theta_A/\theta_R = 97^\circ/70^\circ$.

Gravimetric analysis, however, demonstrates that the reaction is not surface-selective. Figure 5.8 shows the change in mass upon reaction of PCTFE samples treated with PSBLi ($n = 50$, 0.004 M) at room temperature for various extents of time. Film samples that were allowed to react for less than 20 minutes increased in mass, but at longer reaction times, mass loss was observed. For example, a sample that was allowed to react for 96 h lost 67% of its initial mass. The dissolution of the product (polystyrene-grafted PCTFE) in THF is not unreasonable and should have been anticipated. THF is a good solvent for polystyrene and although it is a nonsolvent for PCTFE, PCTFE grafted with enough polystyrene may be soluble. Isolation of this graft copolymer from the reaction mixture (which contains a huge excess of PSBLi) would be difficult (or impossible),

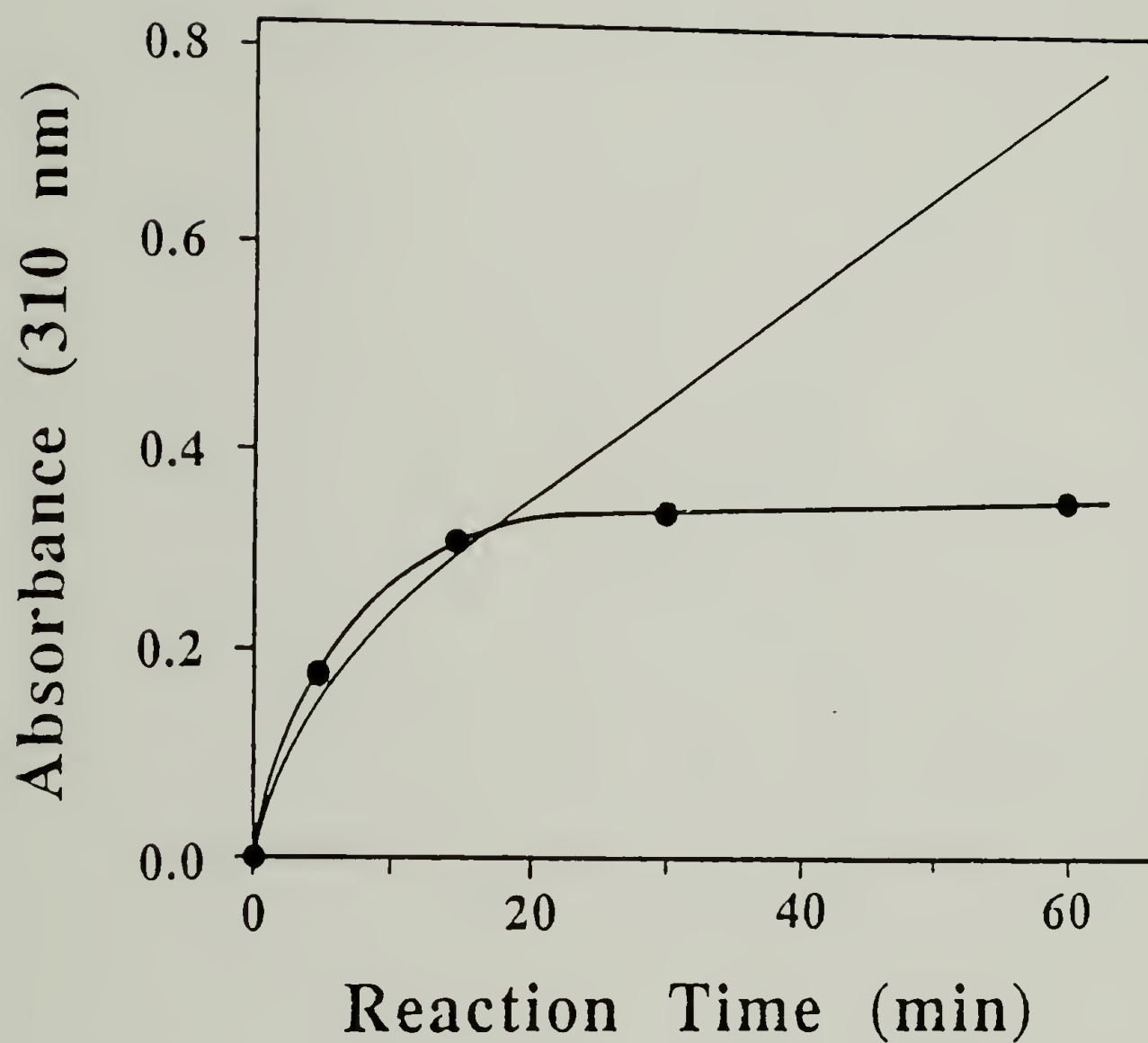


Figure 5.7 Plot of absorbance (310 nm) vs. reaction time for the reaction of PCTFE film with PSBLi ($n = 50$; 0.004 M) in THF at room temperature. The plot without data points is for PSLi, reproduced from Figure 5.2.

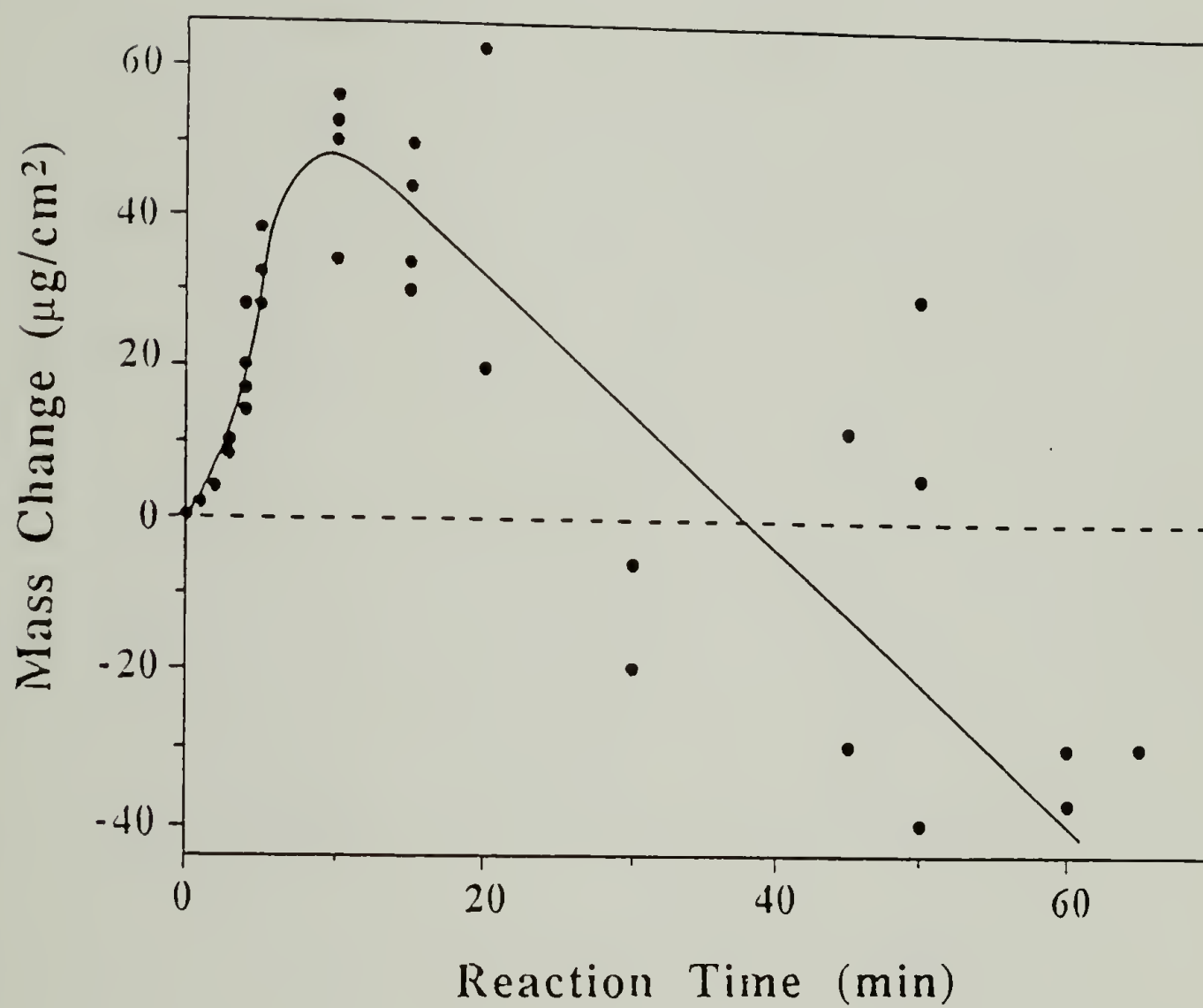


Figure 5.8 Changes in mass vs. reaction time for PCTFE film samples reacted with PSBLi ($n = 50$; 0.004 M) in THF at room temperature.

so to accomplish this, the reaction was carried out in a theta solvent for polystyrene (and a nonsolvent for PCTFE, as well) and the graft copolymer was obtained by extracting the isolated film with THF. A PCTFE film sample was allowed to react with PSBLi ($n = 50$, 0.005 M) in hexane/THF (67:33) at room temperature for 48 h. The film sample was then extracted with the same solvent mixture to remove any unreacted PSBLi, followed by extraction with THF. XPS analysis of a film cast from the THF extract indicates the presence of fluorine (>2% atomic concentration)³⁶ and GPC analysis shows this material to elute with a retention volume characteristic of polystyrene with a molecular weight of 390,000 ($n = 3750$) and a much broader molecular weight distribution. These analyses are consistent with the formation of a THF-soluble graft copolymer, the presence of which suggests that graft copolymer dissolution is responsible for the mass losses described above.

The effects of reaction temperature, PSBLi concentration, and PSBLi molecular weight were investigated in some detail, but none of these variables dramatically affected the reaction course. Temperature and concentration did not change the final product structure, only the rate at which it was obtained. Changing the PSBLi concentration over two orders of magnitude ($n = 50$, 0.0004 - 0.04 M) demonstrated that the reaction is roughly first-order in PSBLi, but the same maximum weight gains were observed at each concentration and mass losses were observed at long reaction times in all cases. Reactions were carried out at room temperature, -23 °C, -63 °C and -78 °C ($n = 50$, 0.004 M). Lower temperatures are expected to decrease the mobility of chains in the PCTFE surface and therefore limit PCTFE-THF interactions which would

ultimately reduce reaction depths and mass gains.¹¹ Lower temperatures also could decrease graft copolymer solubility and increase modified layer thicknesses and mass gains. Our experimental results indicate that lower temperatures decrease the rate of mass gain initially and at longer times decrease the rate of mass loss. The data show that a film sample reacted for 90 h at -78 °C had lost 14 $\mu\text{g}/\text{cm}^2$, which corresponds to a sample reacted at room temperature for 30 min. The maximum mass gain for a sample reacted at -78 °C was 41 $\mu\text{g}/\text{cm}^2$, which occurred after 21 h of reaction; this value is similar to the maximum obtained for reaction at room temperature. Varying the molecular weight of PSBLi over three orders of magnitude ($n = 5, 50, 500, 5000^{37}$) did not grossly affect the rate of mass change or the ultimate mass gain. These results suggest that solubilization of PCTFE requires a limiting weight percent of polystyrene grafted to it and that graft copolymer swelling and dissolution control the reaction rate.

The reaction solvent plays a more important role in determining the product structure than the variables discussed above. Figure 5.9 shows plots of the mass change vs. reaction time for PCTFE film samples reacted with PSBLi ($n = 50, 0.004 \text{ M}$) at room temperature in various solvents and solvent mixtures. Each plot demonstrates a marked difference in reaction course from the reaction in THF. In hexane/THF (67:33) (S), the reaction proceeds rapidly for a short initial period (less than 2 min) and then slows dramatically, but the reaction continues (mass increases) for at least 18 hours. In THF/benzene (75:25) (I) the reaction begins at high rate and gradually slows over the first hour of reaction. After 18 h, gravimetric data indicate that some product graft copolymer has dissolved. Reactions

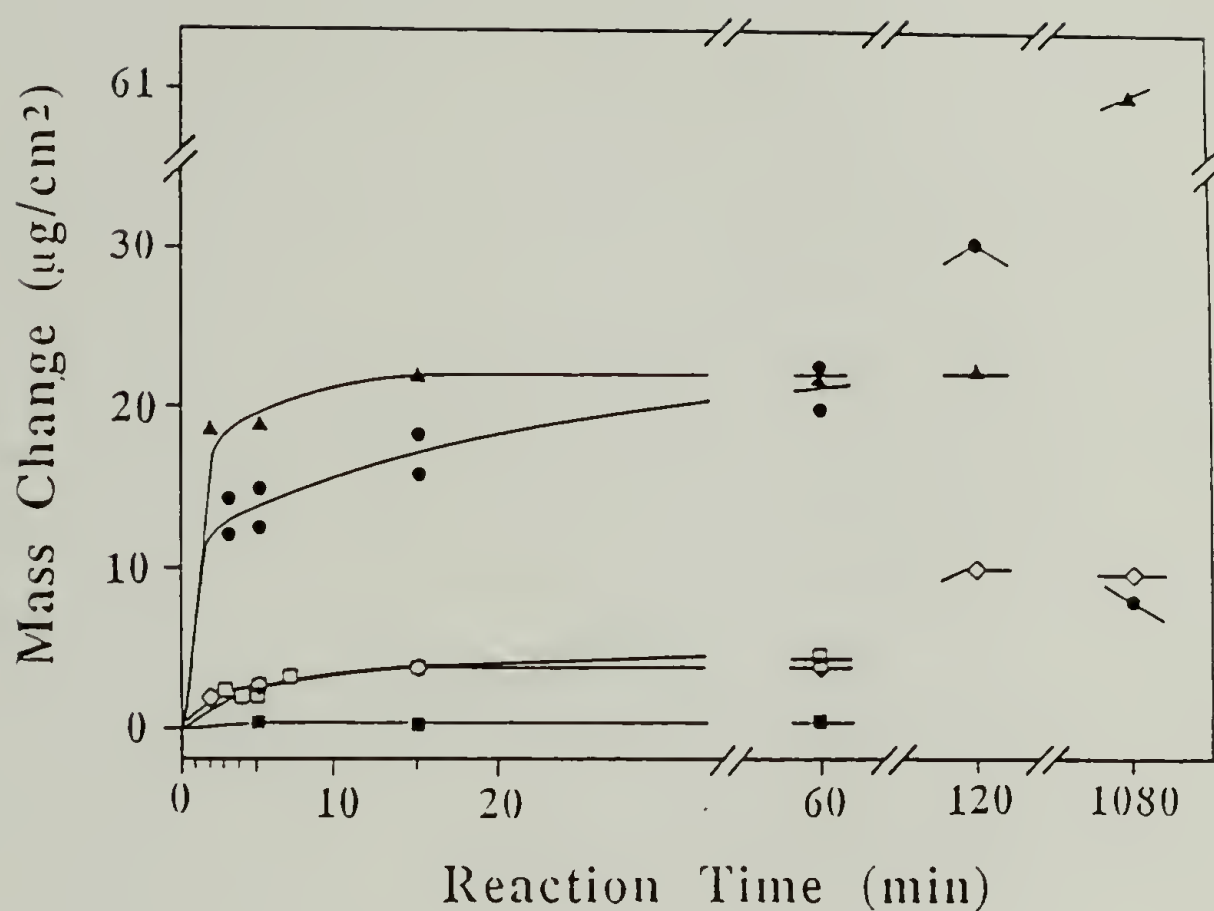


Figure 5.9 Change in mass vs. reaction time for PCTFE film samples reacted with PSBLi ($n = 50$; 0.004 M) at room temperature in hexane/THF (67:33) (▲), THF/benzene (75:25) (●), THF/benzene (50:50) (□), benzene (◇), and benzene/hexane (35:65) (■).

in benzene (G) and THF/benzene (50:50) (O) show small initial mass gains over the first 15 min of reaction and little subsequent change. Reactions in benzene/hexane (35:65) (n) were very slow.

The products of the reactions of PCTFE with PSBLi in benzene were studied in some detail (Table 5.2, entries 6-25): Film samples that were allowed to react at room temperature for 1 h showed changes in water contact angles ($\theta_A/\theta_R = 94^\circ/68^\circ$), an increase in the C:F ratio indicated by XPS, but only small changes by ATR IR. Most of the low concentration samples showed little reaction. The reaction temperature was increased to that of refluxing benzene (80 °C) in an attempt to incorporate more (enough to be visible by ATR IR) polystyrene on the surface and PCTFE samples were allowed to react with PSBLi ($n = 50$, 0.024 M) for 3, 4.5 and 14 h (Table 5.2, entries 6, 7, 15 and 16).³⁸ The product film samples showed appreciable (but indistinguishable) amounts of polystyrene by ATR IR. Figure 5.10 shows the ATR IR spectrum of a sample allowed to react for 3 h. The absorbances at 3061, 3027, 2924, 1601, 1493, 1452, 760, and 701 cm^{-1} are those expected for polystyrene. This spectrum indicates a clean addition reaction and little or no competitive reduction (Figure 5.3, eq. 2). XPS spectra of reacted samples are likewise indistinguishable and indicate complete reaction in the outer 40 Å of the film sample and that most of this region is polystyrene (Table 5.5). Figure 5.11 shows a survey spectrum, indicating a C:F ratio 60:1 and a high resolution spectrum of the C_{1s} region exhibiting the π to π^* shake-up satellite of polystyrene.

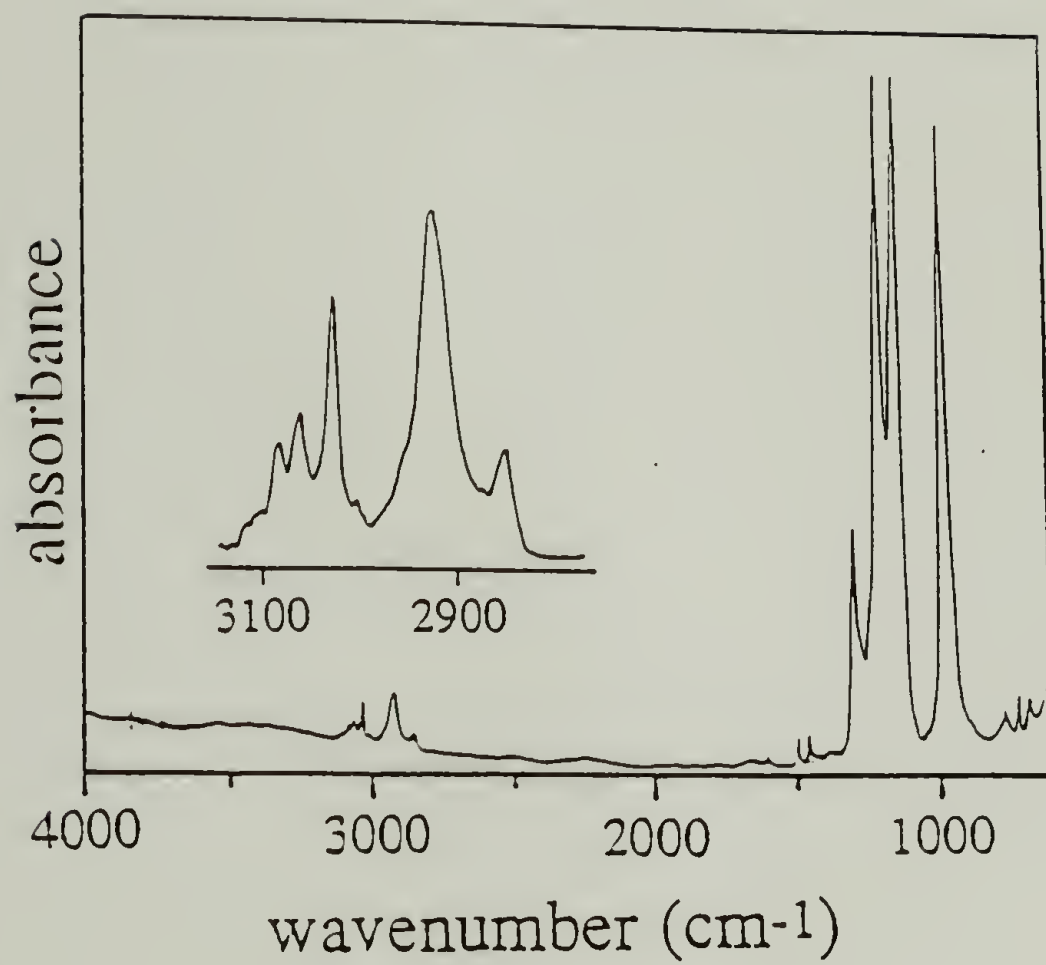


Figure 5.10 ATR IR spectrum of PCTFE film that had been reacted with PSBLi ($n = 50$; 0.024 M) in refluxing benzene for 3 h.

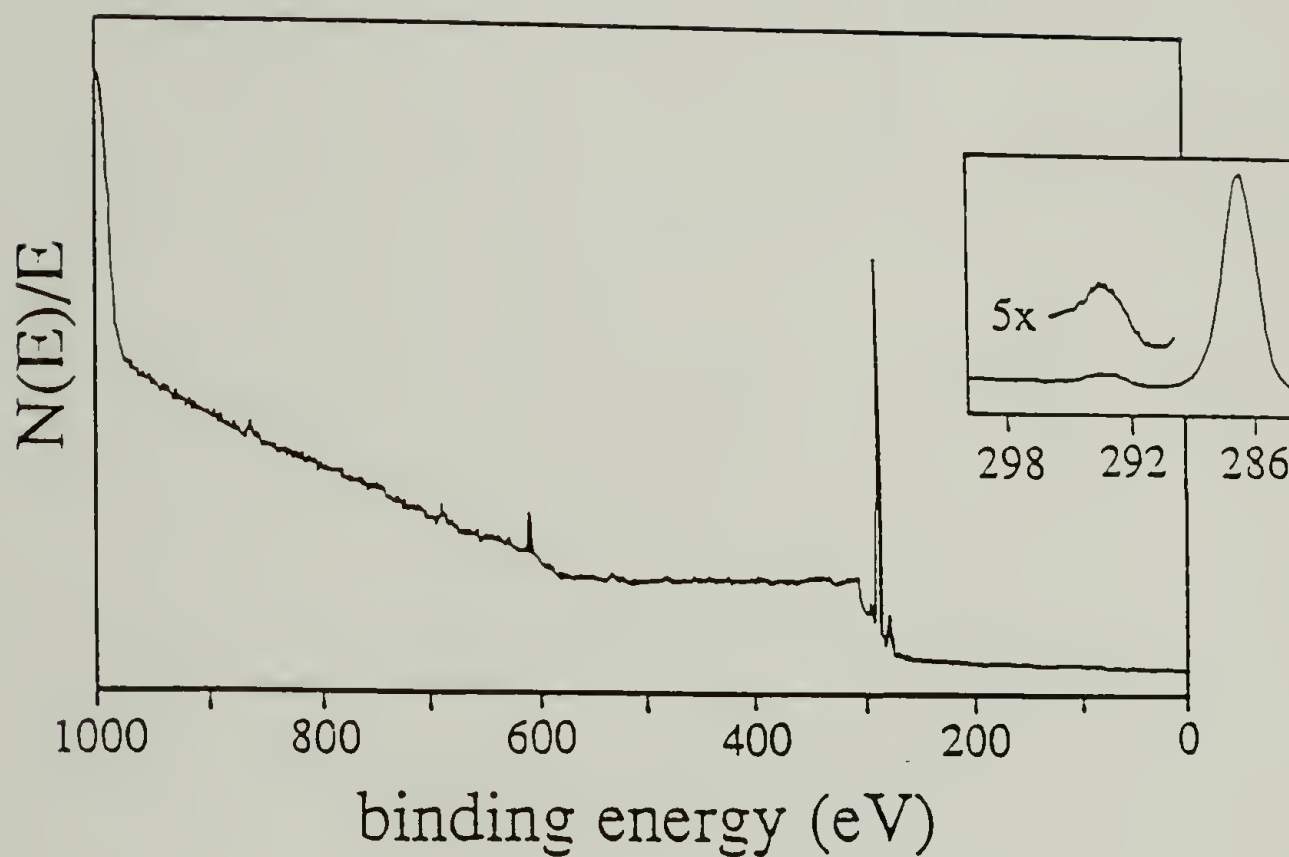


Figure 5.11 XPS spectrum of PCTFE film that had been reacted with PSBLi ($n = 50$; 0.024 M) in refluxing benzene for 14 h.

These reaction conditions were used to test whether the amount of polystyrene incorporated (i.e. the thickness of the polystyrene film) could be controlled by the PSBLi chain length. PCTFE film samples were

Table 5.5 XPS Atomic Composition Data (75 ° takeoff angle) for the Reaction of PSBLi with PCTFE in Benzene at 80 °C.

<u>Sample</u>	<u>Carbon</u>	<u>Fluorine</u>	<u>Chlorine</u>	<u>Oxygen</u>	<u>Silicon</u>
B5-65 14 hours	97.3	1.5	0.4	0.3	0.4
B5-69 3 hours	94.3	3.3	0.7	1.4	0.0

reacted with PSBLi ($n = 50$; 0.024 M) and PSBLi ($n = 5$, 0.024 M) in refluxing benzene in parallel experiments (Table 5.2, entries 20 - 23). Reaction sets were run for 2 and 6 h, and the XPS and ATR IR spectra of each set were indistinguishable. However, a pronounced difference was observed between the XPS and ATR IR spectra for $n = 5$ and $n = 50$ reactions. Figure 5.12 indicates that the longer chain PSBLi reacts to incorporate a thicker polystyrene layer.

Reactions of PCTFE with PSSLi. The initial graft reactions carried out in this work involved reaction of PSSLi with surface-tosylated PCTFE films. The idea was that the thiolate was a good nucleophile and would add to the tosylate carbon. This indeed was the case and both polymeric and small molecule thiolates were reacted in this fashion (B3-23, 36, 51a). We found that the control film (virgin PCTFE, B3-52b) was affected by the

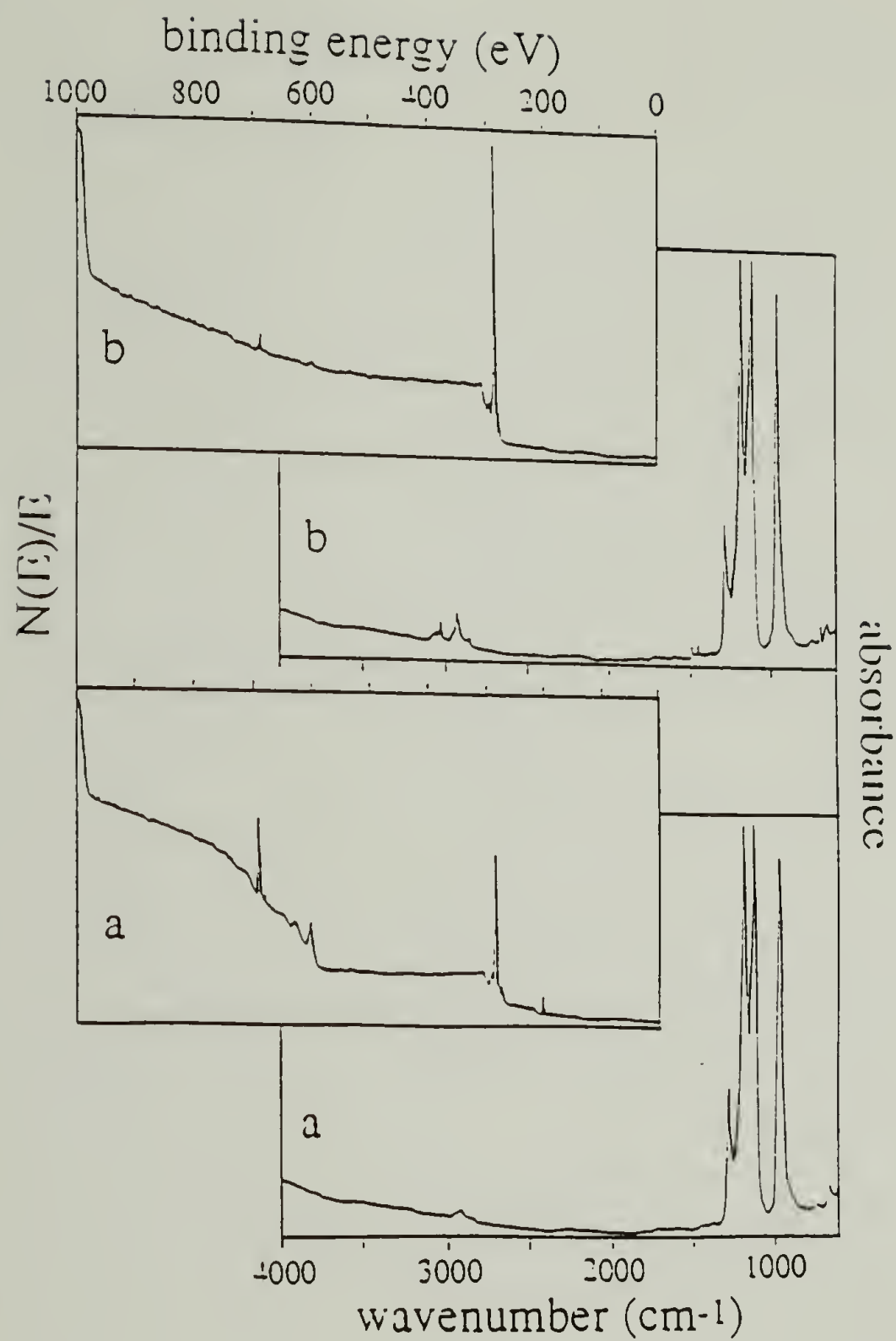


Figure 5.12 XPS and ATR IR spectra of PCTFE film samples that had been reacted with PSBLi (0.024 M) in refluxing benzene for 2 h: (a) PSBLi, $n = 5$; (b) PSBLi, $n = 50$.

reaction conditions, as well; reactions B3-51a and b were almost identical. This led to the graft reactions on unmodified PCTFE that comprise the bulk of this work. Reactions of PCTFE with thiolates have been reported,^{39,40} and a mechanism for this reaction has been proposed.³⁹ In this work PCTFE was reacted with PSSLi in both benzene and THF under a wide range of conditions.

PCTFE film samples were allowed to react with PSSLi ($n = 50-80$) in THF solution at concentrations varying from 0.004 M to 0.05 M at $-78\text{ }^{\circ}\text{C}$, $-20\text{ }^{\circ}\text{C}$, room temperature and refluxing THF ($67\text{ }^{\circ}\text{C}$) for various periods of time (Table 5.3, entries 1 - 19). ATR IR and XPS data indicate that polystyrene is incorporated in the product surface under all conditions. By these analyses, temperature and concentration appear to affect only the reaction kinetics and not the product structure. Reaction is faster at higher temperatures and higher concentrations. The product film samples varied in color, depending on the extent of reaction, over a spectrum ranging from clear to "tinted" (brown) to metallic copper-colored. Film samples that were lightly modified exhibited water contact angles of $\theta_A/\theta_R = 95^{\circ}/70^{\circ}$. More extensively modified samples showed pronounced contact angle hysteresis, indicating roughened surfaces: a sample reacted for 3 h at room temperature exhibited $\theta_A/\theta_R = 129^{\circ}/25^{\circ}$. Gravimetric analysis was performed on samples reacted in THF at room temperature for 48 h ($n = 80$; 0.05 M). The film samples gained an average mass of $100\text{ }\mu\text{g}/\text{cm}^2$ upon reaction. This is in sharp contrast to the reaction of PCTFE with PSBLi in THF which, under these conditions, exhibits mass loss and product dissolution. Figure 5.13 shows representative ATR IR spectra of PCTFE films that had been reacted with PSSLi under different conditions.

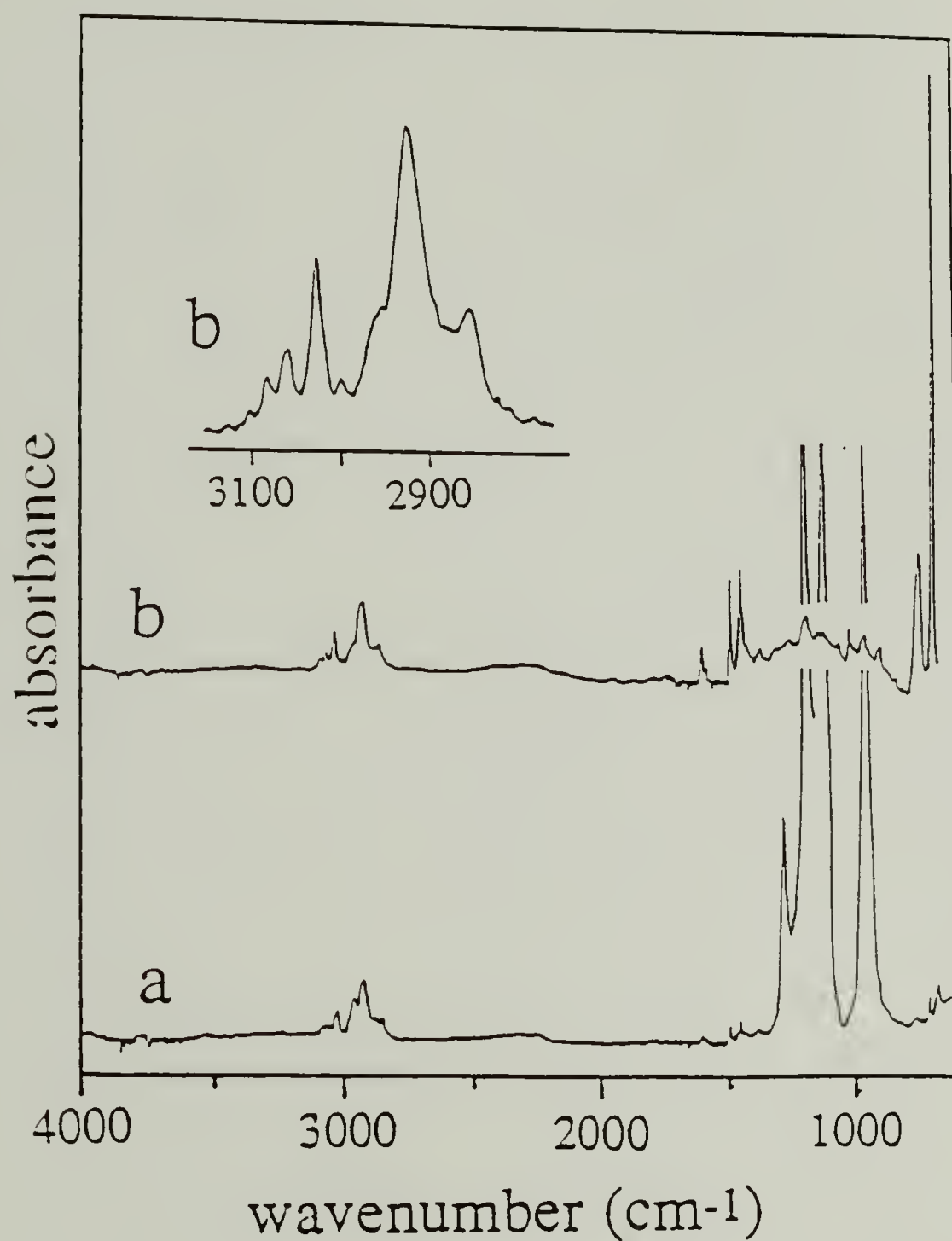


Figure 5.13 ATR IR spectra of PCTFE film samples that had been reacted with PSSLi ($n \sim 50$) in THF with the following conditions: (a) room temperature, 0.04 M, 37 min; (b) refluxing THF, 0.02 M, 3 h.

Both spectra show the expected absorbances due to polystyrene. It is noteworthy that the sample prepared in refluxing THF (Figure 5.13(b)) shows that there is little PCTFE in the ATR sampling region (outer ~ 3000 Å); this indicates that the product graft copolymer is not appreciably soluble in refluxing THF which is consistent with the gravimetric data.

Reactions of PCTFE with PSSLi using benzene as the solvent were carried out with conditions varying from 10 min to 60 h, room temperature to reflux temperature and 0.004-0.04 M PSSLi (Table 5.3, entries 28-52). No appreciable reaction was observed under any conditions, although some small changes were observed by XPS and contact angles. The changes seen by XPS (sporadically) could be ascribed to no more than sample contamination but the contact angles did drop to roughly the same values observed with other types of modification reactions. This suggests that there may be a very thin layer of polystyrene on the surface.

Discussion and Conclusions

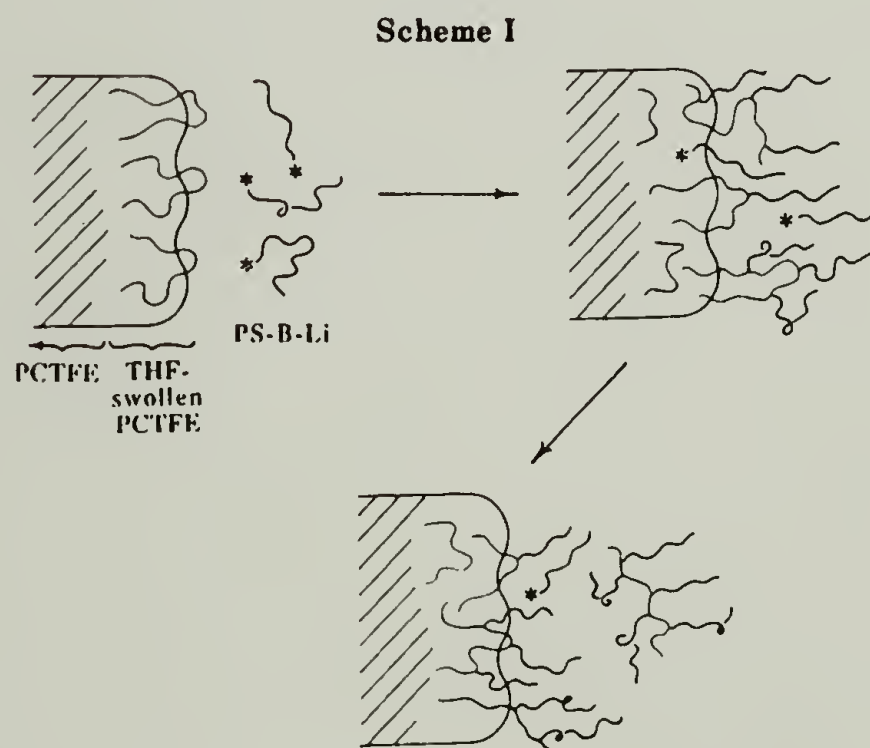
We have carried out numerous reactions of polystyryl anions (with different end-functional groups) with PCTFE films and have found that the reaction course and the structure of the modified layer depend on the identity of the end-functional group. For this reason, reactions with each polystyryl anion will be discussed separately.

Polystyryllithium (PSLi) reacts with PCTFE in THF primarily as a reducing agent (eq. 2) to form a complex carbonaceous product containing conjugated carbon-carbon double and triple bonds (Figure 5.3). A small

amount of polystyrene is incorporated as well. The modification is not surface-selective and proceeds deeply into the bulk of the film (Figure 5.2). The initial PCTFE-THF interface is rather diffuse (THF swells PCTFE), and a large number of reactive sites on PCTFE are solvated. We propose that many of these sites can react with PSLi by one electron transfer reduction steps which do not require close (bond length) encounter, but comparatively few sites can react via addition of PSLi. The carbonaceous product is most certainly less swollen by THF (and PSLi), but its formation does not inhibit reduction. We propose that the reaction continues because the product conducts electrons from solution down to virgin PCTFE. We envision a complex interfacial process occurring in which an outer layer of swollen PCTFE reacts either by reduction or addition of PS-Li (eq. 2) and a sublayer that cannot be accessed by PSLi reacts by reduction only.

When benzene is used as the solvent for reaction of PSLi with PCTFE, the deep reduction observed with THF as a solvent does not occur as evidenced by the absence the corresponding absorbances in the IR spectrum (Figure 5.5). A surface-selective addition reaction occurs that is complete within 1 hour, and no further changes result after longer reaction times. Swelling studies showed that benzene forms a much sharper interface with PCTFE than does THF, and we propose that all PCTFE reaction sites are accessible to addition by PSLi and addition competes favorably with reduction, precluding the formation of a carbonaceous layer. An additional factor could be that the relative rates of addition and reduction are different in THF- and benzene-swollen PCTFE.⁴¹

PCTFE film reacts with butadiene-terminated polystyryllithium (PSBLi) in THF to yield surface-modified PCTFE derived from only the addition reaction sequence described in equation 1. There was no evidence of the reduction that was observed with PSLi in THF. The reactivity differences between PSLi and PSBLi can be explained by their steric differences. Addition of the primary allylic lithium alkyl to the difluoroolefin is more facile. Gravimetric analyses of the product film samples of this reaction indicate that this reaction is not surface-selective and that graft copolymer product dissolves in the reaction medium. The graphic depiction below represents the progression of events in this reaction. The diffuse PCTFE-THF interface becomes more diffuse as



polystyrene is grafted (the solvent interacts to a greater extent with the product). This increases the mobility of PCTFE chains and exposes more

reaction sites. When a sufficient weight percent of polystyrene is grafted to a PCTFE chain, it becomes soluble in the reaction medium. The PCTFE film is progressively etched leaving a surface of graft copolymer.

Reactions of PCTFE with PSBLi in several different solvent systems were studied (Figure 5.9), and several points warrant discussion. In most solvents the mass gain was rapid in the first several minutes of reaction and subsequently slower. The relative magnitude of these initial weight gains correlates well with the affinity of PCTFE for the solvent. Increasing the reaction temperature to refluxing benzene causes more extensive reaction and incorporates a sufficient amount of polystyrene to be visible in the infrared spectrum (none was visible in the room temperature reaction products). The experiments described in Figure 5.12 indicate that some control of the amount of polystyrene incorporated under these conditions can be exercised by adjusting the molecular weight of PSBLi.

Reactions of PCTFE with PS-S-Li were carried out under a variety of conditions using benzene and THF as solvents. No reactions were observed under any conditions using benzene. The PCTFE-benzene interface may be too sharp to allow the reactive end of the PS-S-Li to come into intimate contact with the a reactive PCTFE site. It could also be that lithium thiolates are not reactive enough in benzene, for instance lithium thiolates are not able to polymerize thiiranes in benzene.⁴² The reactions occurred under all conditions at the comparatively diffuse PCTFE-THF interface, and the product graft copolymer interacted with the solution enough to allow very deep modification. Unlike the reaction with PSBLi, the graft copolymer is not soluble and very thick modified layers result on

the film surface. Figure 5.13(b) shows an extensively modified sample with a graft copolymer layer $>3000 \text{ \AA}$ thick. The sharply contrasting solubilities of the graft copolymers prepared with PSSLi and PSBLi is surprising and indicates that some crosslinking must occur during the reaction of PCTFE with the lithium thiolate. The insolubility of the grafted product, the extensive depth of reaction and the unique color resulting in the film suggest that the reaction of PCTFE with polystyryllithium thiolate is not as simple as that described in eq 1: no further investigation into the nature of this reaction was made.

The grafting reaction studied here is a very complex process with many variables. Possibly a more easily controlled system would have been the reaction of hydroxyl end-capped polystyrenes with modified PCTFE (of known surface structure), such as various acid chloride, ester or tosylate surfaces. In this case the polymer chain is not nearly as susceptible to loss of reactivity by adventitious impurities. In addition, the same polymer can be used for many experiments with the tedium of anionic synthesis endured only once. The effect of reversibility and reactivity could be studied by using different types of reactive surfaces. The effect of graft density could be studied in this manner. Another possibility is the use of thiol-endcapped polymers in benzene where it has been observed that addition to PCTFE does not occur (this system, however, has many more potential pitfalls than the other). The use of these types of systems would separate the surface modification reaction from the graft reaction and make analysis inherently simpler. The reactive dissolution may be stymied by crosslinking in the initial modification, or if it does happen it could be viewed as a "cleaning off" of the modified layer, in essence just leaving a

very thin polymer layer if any. The graft polymerizations performed here were practical in the sense that the means to form the grafted surfaces are one-step processes.

In conclusion, the goal of this research (the synthesis of PCTFE-PS interfaces of controlled structure) was met to some extent. We have studied a complex system and have identified a number of variables that may be useful in controlling interfacial properties, including polymer chain length, reaction solvent, polymer concentration, identity of the nucleophile and temperature. The structure of the interface can be considered to have two main variables, namely, the actual amount of polystyrene attached to the surface and the diffuseness of the interface. One could covalently attach polystyrene films of a prescribed thickness to PCTFE (and produce a very sharp interface--essentially 2-D) by either controlling the extent of reaction with a polymer of a given length or controlling the polymer length with a given extent of reaction. Chemical control of this sort may facilitate control over adhesive properties. Many popular theories attribute adhesion to polymer entanglements. The importance of such entanglements (to adhesion) could be determined by controlling both the film thickness and polymer chain length. The research developed in this project also sheds light on routes to other types of interfaces, such as ones with thick interfacial regions. Properties gradually change from those of one polymer to the other across this region. This type of interface has many variables and is difficult to characterize, and would not lend itself to model theoretical studies. However, in practice, this type of interface may offer a rational method to control adhesion between two surfaces. The experiments carried out in this research suggest that a continuum between

both types of interfaces can be prepared and that the most important structure-determining variable is the solvent that is used. This modification chemistry was considerably more complicated than originally anticipated and although it was shown that the structure of the polymer/polymer interface can, in practice, be controlled, the complexity of the modification reactions and the difficulty in characterizing the product interfaces prohibited the optimum achievement of our original goal.

References

1. Cohn, D.; Hoffman, A. S.; Ratner, B. D. *J. Appl. Polym. Sci.* **1987**, *33*, 1.
2. Yamakowa, S.; Yamamoto, F.; Kato, Y. *Macromolecules* **1976**, *9*, 754.
3. Rao, M. H.; Rao, K. N.; Lokhande, H. T.; Teli, M. D. *J. Appl. Polym. Sci.* **1987**, *33*, 2345.
4. Suzuki, M.; Kishida, A.; Iwata, H.; Ikada, Y. *Macromolecules* **1986**, *19*, 1804.
5. Lai, J. Y.; Chang, T. C.; Wu, Z. J.; Hsieh, T. S.; *J. Appl. Polym. Sci.* **1986**, *32*, 4709.
6. Omichi, H.; Chundury, D.; Stannett, V. T. *J. Appl. Polym. Sci.* **1986**, *32*, 4827.
7. Misra, B. N.; Sood, D. S.; Mehta, I. K. *J. Polym. Sci., Polym. Chem. Ed.* **1985**, *23*, 1749.
8. Yamakawa, S. *Macromolecules* **1979**, *12*, 1222.
9. Feng, X. D.; Sun, Y. H.; Qin, K. Y. *Macromolecules* **1985**, *18*, 2105.
10. Dias, A. J.; McCarthy, T. J. *Macromolecules* **1985**, *18*, 1826.
11. Dias, A. J.; McCarthy, T. J. *Macromolecules* **1987**, *20*, 2068.
12. Lee, K-W.; McCarthy, T. J. *Macromolecules* **1987**, *20*, 1437.
13. Lee, K-W.; McCarthy, T. J. *Macromolecules* **1988**, *21*, 2318.
14. Kolb, B. U.; Patton, P. A.; McCarthy, T. J. *Macromolecules* **1990**, *23*, 366.
15. Kolb, B. U.; Patton, P. A.; McCarthy, T. J. *Polym. Prepr. (Am. Chem. Soc., Div. Polym. Chem.)* **1987**, *28*(2), 248.
16. Patton, P. A. Ph.D. Dissertation, Polymer Science and Engineering Dept., Univ. of Mass., 1987.
17. Narayan, R.; Krauss, M.; Tsao, G. T. *Polym. Mater. Sci. (Am. Chem. Soc., Div. Polym. Mater.)* **1985**, *52*, 112.
18. Fery, N.; Hoene, R.; Haman, K. *Angew. Chem., Int. Ed. Eng* **1972**, *11*, 337.

19. Donnet, J. B.; Riess, G.; Majowski, G. *Eur. Polym. J.* **1971**, *7*, 1065.
20. Yanova, L. P.; Kuznetsov, V. A.; Taubman, A. B. *Kolloid-Z.* **1975**, *37*, 614.
21. Takaki, M.; Asami, R.; Kuwata, Y. *Macromolecules* **1979**, *12*, 378.
22. Takaki, M.; Asami, R.; Inukai, H.; Inenaga, T. *Macromolecules* **1979**, *12*, 383.
23. Lechermeier, G.; Revillion, A.; Pillot, C. *J. Macromol. Sci., Chem.* **1978**, *A-12*, 285.
24. Cameron, G. G.; Qureshi, M. Y. *Makromol. Chem. Rapid Commun.* **1981**, *2*, 287.
25. Ceausecu, E.; Bordeianu, R.; Buzdugen, E.; Cerchez, I.; Ghioca, P.; Stancu, R. *J. Macromol. Sci., Chem.* **1985**, *A-22*, 803.
26. Morton, M.; Kammerick, P. F. *J. Am. Chem. Soc.* **1970**, *92*, 3217.
27. Values given for *n* are approximate and are based on the degree of polymerization predicted from styrene:*sec*-butyllithium ratios. Actual values (determined by GPC) are very close.
28. Garcia-Rubio, L. H. *Macromolecules* **1987**, *20*, 3070.
29. Partridge, R. H. *J. Chem. Phys.* **1967**, *47*, 4223.
30. Klopffer, W. *Eur. Polym. J.* **1975**, *11*, 203.
31. All ATR-IR spectra shown here have been mathematically corrected by ATR correcting for the wavelength dependence of absorbance. This unfairly enhances the absorbance of a thin layer on the surface. The spectra are shown this way to better show the qualitative features; the quantitative aspects are less reliable.
32. Costello, C. A.; McCarthy T. J. *Macromolecules* **1987**, *20*, 2819.
33. Bening, R. C.; McCarthy T. J. *Polym. Prepr. (Am. Chem. Soc., Div. Polym. Chem.)* **1988**, *29(2)*, 336.
34. These absorbance values are vs. air (not PCTFE reference films) and cannot be used as absolute determinations of PS layer thickness. They give useful information concerning the kinetics of the reaction.
35. The hydroxyl stretching is most likely due to moisture trapped between the sample and the crystal when loading, not -OH functionality on the surface.

36. No quantitative information can be derived from this analysis because it indicates only that the sample is not entirely polystyrene. The structure of the cast (from THF) film likely may be perturbed to concentrate polystyrene at the surface. No chlorine was observed, but unreacted PCTFE units may be present beneath the XPS sampling depth of the film. Also it should be pointed out that chlorine should be present in less than one third the concentration of fluorine and may be lower in concentration than the detection limit.
37. The concentration of PSBLi ($n = 5000$) was 0.001 M for these experiments. The concentration was reduced to lower the solution viscosity.
38. The reactions times stated are the length of time that the films were exposed to a given polymer solution. The PSBLi is not indefinitely stable at elevated temperatures and therefore the living polymer could have been dead before the reaction was actually stopped; thus the actual reaction time would be shorter than reported.
39. Taylor, R. T.; Pelter, M. W. *J. Polym. Sci., Polym., Lett. Ed.* **1987**, 25, 215.
40. Taylor, R. T.; Pelter, M. W. *J. Polym. Sci., Polym. Chem. Ed.* **1988**, 26, 2651.
41. Teflon stir bars are much more easily reduced by sodium benzophenone in THF than in benzene. Personal experience.
42. Propylene sulfide does not polymerize anionically in benzene. Personal experience.

BIBLIOGRAPHY

- Aida, T.; Maekawa, Y.; Asano, S.; Inoue, S. *Macromolecules* **1988**, *21*, 1195.
- Aldrichimica Acta* **1971**, *4*(3), 33.
- Alexander, S. *J. Phys. (Paris)* **1977**, *38*, 983.
- Allmér, K.; Hult, A.; Rånby, B. *J. Polym. Sci. Polym. Chem.* **1989**, *27*, 1641.
- Almog, Y.; Klein, J. *Macromolecules* **1985**, *106*(1), 33-44.
- Ando, T. *Nippon Kagaku kaishi* **1935**, *56*, 745.
- Andrade, J. D.; Gregonis, D. E.; Smith, L. M. In *Surface and Interfacial Aspects of Biomedical Polymers*; Andrade, J. D. ed. Plenum: New York, 1986, Vol. 1, Ch. 2, 5, 7.
- Andrade, J. D. *Polymer Surface Dynamics*, Plenum, New York, 1988.
- Andrade, J. D. *Surf. Interf. Anal.* **1986**, *8*, 253.
- Ansarifar, A.; Luckham, P. F. *Polymer* **1988**, *29*, 329.
- Auroy, P.; Auvray, L.; Leger, L. *Macromolecules* **1991**, *24*(18), 5158.
- Baker, J. A.; Berg, J. C. *Langmuir* **1988**, *4*(4), 1055.
- Balazs, A. C.; Huang K.; Lantman, C. W. *Macromolecules* **1990**, *23*(21), 4641.
- Balazs, A. C.; Gempe, M.; Lantman, C. W.; *Macromolecules* **1991**, *24*(1), 168.
- Balazs, A. C.; Lewandowski, S. *Macromolecules* **1990**, *23*(3), 839.
- Barker, D. J.; Brewis, D. M.; Dahm, R. H. *Polymer* **1978**, *19*, 856.
- Barron, M. J.; Howard, G.J. *J. Polymer Sci.: Chem. Ed.* **1974**, *12*, 1269.
- Batich, C.D.; Wendt, R.C. In *Photon, Electron, and Ion Probes of Polymer Structure and Properties*, Dwight, D.W.; Fabishi, T.J.; Thomas, H.R., eds. ACS Symp. Ser., 1981, *162*, Ch. 15.
- Bates, R. B. Kroposki, L. M. Potter, D. E. *J. Org. Chem.*, **1972**, *37*, 560
- Bee, T. G.; McCarthy, T. J. *Macromolecules* **1992**, *25*, 2093.

- Bening, R. C.; McCarthy, T. J. *Macromolecules* **1990**, *23*, 2648.
- Bergbreiter, D. E.; Hu, H. -P.; Hein, M. D. *Macromolecules* **1989** *22*, 654.
- Bergbreiter, D. E.; Chen, Z.; Hu, H. -P. *Macromolecules* **1984**, *17*, 2111.
- Billmeyer, F. W. *Textbook of Polymer Science*, 3rd ed. Wiley Interscience, New York, 1984, p. 153, 176.
- Blaakmeer, J.; Bohmer, M. R.; Cohen Stuart, M. A.; Fler, G. J. *Macromolecules* **1990**, *23*, 2301.
- Blum, F. D.; Sihna, B. R.; Schwab, F. C. *Macromolecules*, **1990**, *23*(15), 3592.
- Bohmer, M. R.; Evers, O. A.; Scheutjens, J. M. H. M. *Macromolecules*, **1990**, *23*, 2288.
- Boileau, S.; Sigwalt, P. *Compt. Rend.* **1961**, *252*, 882.
- Bonafini, J. Master of Science Thesis, Univ. of Mass., 1985.
- Brennan, J. V.; McCarthy, T. J. *Polym. Prepr. (Am. Chem. Soc., Div. Polym. Chem.)* **1988**, *29*(2), 338.
- Brennan, J. V.; McCarthy, T. J. *Polym. Prepr. (Am. Chem. Soc., Div. Polym. Chem.)* **1989**, *30*(2), 152.
- Brewis, D. M.; Briggs, D. *Polymer* **1981**, *22*, 7.
- Brown, H. R.; Char K.; Deline, V. R. *Macromolecules* **1990**, *23*(13), 3383-3385.
- Cameron, G. G.; Qureshi, M. Y. *Makromol. Chem. Rapid Commun.* **1981**, *2*, 287.
- Campbell, T. W.; Lyman, D. J. *J. Polym. Sci.* **1961**, *55*, 169.
- Cannizzo, L. F.; Grubbs, R. H. *Macromolecules* **1987**, *20*, 1488.
- Cannizzo, L. F.; Grubbs, R. H. *Macromolecules* **1988**, *21*, 1961
- Carey, F. A.; Sundberg, R. J. *Advanced Organic Chemistry Part A: Structure and Mechanisms 2nd ed.*, Plenum Press: New York, 1984, Chapter 9.
- Carey, F. A.; Sundberg, R. J. *Advanced Organic Chemistry Part B: Reactions and Synthesis*, Plenum Press: New York, 1983.

- Carroll, W. R.; Eisenburg, H. *J Poly. Sci.: Part A-2* **1966**, 4, 599.
- Ceausecu, E.; Bordeianu, R.; Buzdugen, E.; Cerchez, I.; Ghioca, P.; Stancu, R. *J. Macromol. Sci., Chem.* **1985**, A-22, 803.
- Cerfontain, H. *Mechanistic Aspects of Sulfonation and Desulfonation*, Interscience: New York, 1968.
- Chakrabarti, A.; Toral, R. *Macromolecules* **1990**, 23(7), 2016.
- Char K.; Frank, C. W.; Gast A. P. *Langmuir* **1989**, 5(6), 1335.
- Chen, J.; Fetters L. J. *Polymer Bull.* **1981**, 4, 275.
- Chung, T. C. *Macromolecules* **1988**, 21(7), 1902.
- Clark, D. T. *Advances in Polymer Science* **1977**, 24, 125.
- Clark, D. T.; Feast, W. J. *Polymer Surfaces*, Wiley-Interscience: New York, 1978.
- Clark, D. T.; Feast, E. J.; Musgrave, W. K. R.; Ritchie, I. *J. Polm. Sci. Polym. Chem.* **1975**, 13, 857.
- Clark, D. T.; Peeling, J.; O'Malley, J. M. *J. Polym. Sci., Polym. Chem.* **1976**, 14, 543.
- Clark, D. T.; Thomas, H. R. *J. Polym. Sci., Polym. Chem. Ed.* **1977**, 15, 2843.
- Cleland, W. W. *Biochemistry* **1964**, 3(4), 480
- Cohen Stuart, M. A.; Tamai, H. *Macromolecules* **1988**, 21, 1863.
- Cohen Stuart, M. A., Fleer, G. J., Scheutjens, J. M. H. M. *J. Coll. & Interface Sci.* **1984**, 97(2), 515.
- Cohen Stuart, M. A., Fleer, G. J., Scheutjens, J. M. H. M. *J. Coll. & Interface Sci.* **1984**, 97(2), 526.
- Cohen Stuart, M. A.; Cosgrove, T.; Vincent, B. *Advances in Coll. & Interface Sci.*, **1986**, 24, 143.
- Cohen Stuart, M. A.; Waajen, F. H. W. H.; Cosgrove, T.; Vincent, B.; Crowley, T. L. *Macromolecules* **1984**, 17, 1825.
- Cohn, D.; Hoffman, A. S.; Ratner, B. D. *J. Appl. Polym. Sci.* **1987**, 33, 1.
- Cooper, W.; Hale, P. T.; Walker, J. S. *Polymer* **1974**, 15, 175.

- Coopes, I. H.; Gifkins, K. J. *Macromol. Sci.-Chem.* **1982**, A17, 217.
- Corbin, G. A.; Cohen, R. E.; Baddour, R.F. *Macromolecules* **1985**, 18, 98.
- Cosgrove, T.; Finch, N. A.; Webster, J. R. P. *Macromolecules* **1990**, 23(13), 3353.
- Cosgrove, T.; Heath, T. G.; van Lent, B.; Scheutjens, J. M. H. M. *Macromolecules* **1987**, 20, 1692.
- Cosgrove, T. *J. Chem. Soc. Faraday Trans.* **1990**, 86(9), 1323.
- Cosgrove, T.; Heath, T. G.; Phipps, J. S.; Richardson, R. M. *Macromolecules* **1991**, 24(1), 94.
- Costello, C. A.; McCarthy, T. J. *Macromolecules* **1987**, 20, 2819.
- Costello, C. A.; McCarthy, T. J. *Macromolecules* **1984**, 17, 2940.
- Cross, E. M.; McCarthy, T. J. *Polym. Prepr. (Am. Chem. Soc., Div. Polym. Chem.)* **1989**, 30(1), 422.
- Cross, E. M.; McCarthy, T. J. *Macromolecules* **1990**, 23, 3921.
- Dan, N.; Tirrell, M. *Macromolecules* **1992**, 25(11), 2890.
- deGennes, P. G. *Adv. Coll. & Int. Sci.*, **1987**, 27, 189.
- deGennes, P. G. *Macromolecules* **1980**, 13, 1069.
- deGennes, P. G. *Macromolecules* **1982**, 15, 492.
- de Gennes, P.G. *Scaling Concepts in Polymer Physics*, Cornell University Press: New York, 1979.
- Diack, M.; Guiochon, G. *Anal. Chem.* **1991**, 63, 2608.
- Dias, A. J.; McCarthy, T. J. *Macromolecules* **1984**, 17, 2529.
- Dias, A. J.; McCarthy, T. J. *Macromolecules* **1985**, 18, 1826.
- Dias, A. J.; McCarthy, T. J. *Macromolecules* **1987**, 20, 2068.
- DiMarzio, E. A. *J. Chem. Phys.* **1965**, 42, 2101.
- DiMarzio, E. A.; McCrackin, F. L. *J. Chem. Phys.* **1965**, 43, 539.
- Donnet, J. B.; Riess, G.; Majowski, G. *Eur. Polym. J.* **1971**, 7, 1065.

- Dorinson, A.; Ludema, K. C. *Mechanisms and Chemistry in Lubrication*; Elsevier: Amsterdam, 1985.
- Dreyfuss, P. J. *Macromol. Sci.-Chem.* **1973**, A7(7), 1361.
- Dreyfuss, P. J. *Chemtech.* **1973**, 6, 356.
- Eisenlauer, J.; Killmann, E. *J. Colloid and Interface Sci.* **1980**, 74, 108.
- Endo, M.; Aida, T.; Inoue, S. *Macromolecules* **1987**, 20, 2982.
- Everhart, D. S.; Reilley, C. N. *Anal. Chem.* **1981**, 53, 665.
- Evers, O. A.; Scheutjens, J. M. H. M.; Fleer, G. J. *Macromolecules* **1990**, 23(25), 5221.
- Evers, O. A.; Scheutjens, J. M. H. M.; Fleer, G. J. *Chem. Soc. Faraday Trans.* **1990**, 86(9), 1333.
- Evers, O. A.; Scheutjens, J. M. H. M.; Fleer, G. J. *Macromolecules* **1991**, 24(20), 5558.
- Fayt, R.; Forte, R.; Jacobs, C.; Jerome, R.; Ouhadi, T.; Teyssie, Ph.; Varshney, S. K. *Macromolecules* **1987**, 20, 4997.
- Feng, X. D.; Sun, Y. H.; Qin, K. Y. *Macromolecules* **1985**, 18, 2105.
- Fery, N.; Hoene, R.; Haman, K. *Angew. Chem., Int. Ed. Eng* **1972**, 11, 337.
- Fetters, L. J.; Firer, E. M.; Dafauti, M. *Macromolecules* **1977**, 10, 1201.
- Field, J. B.; Toprakcioglu, C.; Ball, R. C.; Stanley, H. B.; Dai, L.; Barford, W.; Penfold, J.; Smith, G.; and Hamilton, W. *Macromolecules* **1992**, 25(1), 434.
- Fontana, J. B. In *The Chemistry of Biological Surfaces* ed. Hair, M. Marcel Dekker: New York 1971.
- Franchina, N. L.; McCarthy, T. J. *Macromolecules* **1991**, 24, 3045.
- Franchina, N. L.; McCarthy, T. J. In *Chemically Modified Surfaces*, Mottola, H. A.; Steinmetz, J. R. eds., Elsevier Science Publishers: New York, 1991, 173.
- Franchina, N. L. Ph.D. Dissertation, Polymer Science and Engineering Department, Univ. of Mass., 1992.
- Fredrickson, G. H. *Macromolecules* **1987**, 20, 2535.

- Frish, H. L.; Simha, R. *J. Chem. Phys.* **1956**, *24*, 652.
- Frish, H. L.; Simha, R. *J. Chem. Phys.* **1957**, *27*, 702.
- Gagnon, D. R.; McCarthy, T. J. *J. Appl. Polym. Sci.* **1984**, *29*, 4335.
- Garcia-Rubio, L. H. *Macromolecules* **1987**, *20*, 3070.
- Gibson, H. W.; Bailey, F.C. *Macromolecules* **1980**, *13*, 34.
- Ghosh, S.; Pardo, S. N.; Solomon, R. G. *J. Org. Chem.* **1982**, *47*, 4692.
- Gobran, R.H. *Ency. of Polym. Sci. & Tech.* **1972**, *10*, 325.
- Golshan-Shirazi, S.; Ghodbane, S.; Guiochon, G. *Anal. Chem.* **1988**, *60*, 2630.
- Gordon, A. J.; Ford, R. A. *The Chemist's Companion: A Handbook of Practical Data, Techniques, and References*, Wiley-Interscience: New York, 1972, p. 375.
- Gourdenne, A. *Polymer Preprints (Am. Chem. Soc., Div. Polym. Chem.)* **1971**, *12*(2), 129.
- Graessley, W. W. In *Advances in Polymer Science*; Springer-Verlag, New York, **1982**, p. 67.
- Guiochon, G.; Golshan-Shirazi, S.; Jaulmes, A. *Anal. Chem.* **1988**, *60*, 1856.
- Gupta, S. K. *Synthesis* **1977**, 39.
- Guzonas, D. A.; Boils, D.; Tripp, C. P.; Hair, M. L. *Macromolecules* **1992**, *25*(9), 2434.
- Guzonas, D.; Hair, M. L.; Cosgrove, T. *Macromolecules* **1992**, *25*, 2777.
- Guzonas, D.; Boils, D.; Hair, M. *Macromolecules* **1991**, *24*, 3383.
- Hadziioannou, G.; Patel, S.; Granick, S.; Tirrell, M. *J. Am. Chem. Soc.* **1986**, *108*, 2869.
- Hair, M. L.; Guzonas, D.; Boils, D. *Macromolecules* **1991**, *24*, 341.
- Hair, M. Ed., *The Chemistry of Biosurfaces*, Vol 1 & 2, Marcel Dekker, New York, 1971.
- Hale, P. T.; Pope, G. A. *Eur. Polym. J.* **1975**, *11*, 677.

- Harrick, N. J. *Internal Reflection Spectroscopy*, Harrick Scientific Corporation: Ossining, New York, 1979.
- Hautekeer, J.; Varshney, S. K.; Fayt, R.; Jacobs, C.; Jerome, R.; Teyssie, Ph. *Macromolecules* **1990**, 23, 3893.
- Herd, J. M.; Hopkins, A. J.; Howard, G. J. *J. Polymer Sci.: Part C*, **1971**, 34, 211.
- Hirao, A.; Nakahama, S. *Macromolecules* **1987**, 20, 2968.
- Hirao, A.; Ishino, Y.; Nakahama, S. *Macromolecules* **1988**, 21, 561.
- Hoeve, C. A. J.; DiMarzio, E. A.; Peyser, P. *J. Chem. Phys.* **1965**, 42, 2558.
- Hoeve, C. A. J. *J. Polym. Sci. C*. **1970**, 30, 361.
- Hoeve, C. A. J. *J. Polym. Sci. C*. **1971**, 34, 1.
- Hopkins, A.; Howard, G. J.; *J. Polymer Sci.: Part A-2*, **1971**, 9, 841.
- Houk, J.; Whitesides, G. M. *J. Am. Chem. Soc.* **1987**, 109, 6825.
- Howard, G. J.; McGrath, M. J. *J. Polymer Sci.* **1977**, 15, 1721.
- Howard, G. J.; McGrath, M. J. *J. Polymer Sci.: Part A-2*, **1977**, 15, 1705.
- Hsieh, Y.-L.; Timm, D. A.; Wu, M. *J. Appl. Polym. Sci.* **1989**, 38, 1719.
- Huh, C.; Mason, S. G. *J. Coll. and Interf. Sci.* **1977**, 60, 11.
- Huguenard, C.; Varoqui, R.; Pfefferkorn, E. *Macromolecules* **1991**, 24, 2226
- Ingersent, K.; Klein, J.; Pincus, P. *Macromolecules* **1990**, 23, 548.
- Ishizone, T.; Kato, R.; Ishino, Y.; Hirao, A.; Nakahama, S. *Macromolecules* **1991**, 24, 1449
- Israelachvili, J. N.; Tirrell, M.; Klein, J.; Almog, Y. *Macromolecules*, **1984**, 17, 204.
- Iyengar, D.R.; McCarthy, T.J. *Macromolecules* **1990**, 23, 4344.
- Iyengar, D. Ph.D. Dissertation, Polymer Science and Engineering Department, Univ. of Mass., 1992.
- Jacobs, C.; Varshney, S. K.; Hautekeer, J.; Fayt, R.; Jerome, R.; Teyssie, Ph. *Macromolecules* **1990**, 23, 4024

- Jarvis, N. L.; Fox, R. B.; Zisman, W. A. *Adv. Chem. Ser.* **1964**, *43*, 317.
- Johner, A.; Joanny, J. F. *Macromolecules* **1990**, *23*, 5299.
- Johnson, R. E.; Dettre, R. H. *J. Phys. Chem.* **1964**, *68*, 1744.
- Johnson, H.; Granick, S. *Macromolecules* **1991**, *24*, 3023.
- Kawaguchi, M.; Arai, T. *Macromolecules* **1991**, *24*, 889.
- Kawaguchi, M.; Funayama, A.; Yamauchi, S.; Takahashi, A.; Kato, T. *J. Coll. & Interface Sci.* **1988**, *121*, 130.
- Kawaguchi, M.; Aoki, M.; Takahashi, A. *Macromolecules* **1983**, *16*, 635.
- Kawaguchi, M.; Inoue, A.; Takahashi, A. *Polymer Journal* **1983**, *15*, 537.
- Kawaguchi, M.; Itoh, K.; Yamagiwa, S.; Takahashi, A. *Macromolecules* **1989**, *22*, 2204.
- Kawaguchi, M.; Funayama, A.; Yamauchi, S.; Takahashi, A.; Kato, T. *J. Colloid and Interface Sci.* **1988**, *121*, 130.
- Kawaguchi, M.; Takahashi, A. *Macromolecules* **1983**, *16*, 1465.
- Kawaguchi, M.; Kawarabayashi, M.; Nagata, N.; Kato, T.; Yoshioka, A.; Takahashi, A. *Macromolecules* **1988**, *21*, 1059.
- Kawaguchi, M.; Hayashi, K.; Takahashi, A. *Macromolecules*, **1988**, *21*, 1016.
- Kendall, E. W.; McCarthy, T. J. *Polym. Prepr. (Am. Chem. Soc., Div. Polym. Chem.)* **1992**, *33*(2), 158.
- Killmann, E.; Fulka, C.; Reiner, M. *J. Chem. Soc. Faraday Trans.* **1990**, *86*(9), 1389.
- Kim, M. W.; Fetters, L. J.; Chen, W.; Shen, Y. *Macromolecules* **1991**, *24*(14), 4216.
- Kim, M. W.; Peiffer, D. G.; Hsiung, H.; Rasing, Th.; Shen, Y. R. *Macromolecules* **1991**, *24*, 319.
- Klein, J.; Kamiyama, Y.; Yoshizawa, H.; Israelachvili, J.; Fetters, L. J.; Pincus, P. *Macromolecules* **1992**, *25*, 2062.
- Klein, J.; Luckham, P. F. *Macromolecules* **1984**, *17*, 1041.
- Klopffer, W. *Eur. Polym. J.* **1975**, *11*, 203.

- Kolb, B. U.; Patton, P. A.; McCarthy, T. J. *Macromolecules*, **1990**, *23*, 366.
- Kolb, B. U.; Patton, P. A.; McCarthy, T. J. *Polym. Prepr. (Am. Chem. Soc., Div. Polym. Chem.)*, **1987**, *28*, 248.
- Kogoma, M.; Kasai, H.; Takahashi, K.; Moriwaki, T.; Okazaki, S. *J. Phys. D: Appl. Phys.* **1987**, *20*, 147.
- Kuroki, M.; Nashimoto, S.; Aida, T.; Inoue, S. *Macromolecules* **1988**, 3115.
- Lai, J. Y.; Chang, T. C.; Wu, Z. J.; Hsieh, T. S.; *J. Appl. Polym. Sci.* **1986**, *32*, 4709.
- Lautensschlaeger, F. J. *Macromol. Sci.-Chem.* **1972**, *A6*, 1089.
- Lechermeier, G.; Revillion, A.; Pillot, C. *J. Macromol. Sci., Chem.* **1978**, *A-12*, 285.
- Lee, K.-W.; McCarthy, T. J. *Polym. Prepr. (Am. Chem. Soc., Div. Polym. Chem.)* **1987**, *28*, 250.
- Lee, K.-W.; McCarthy, T. J. *Macromolecules* **1988**, *21*, 309.
- Lee, K.-W.; McCarthy, T. J. *Macromolecules* **1988**, *21*, 2318.
- Lee, K.-W.; McCarthy, T. J. *Macromolecules* **1988**, *21*, 3353.
- Leermakers, F. M. A.; Gast, A. P. *Macromolecules* **1991**, *24*, 718.
- Leidheiser, H., Jr. In *Corrosion Mechanisms*; Mansfield, F., Ed.; Marcel Dekker: New York, 1987.
- Luckham, P. F.; Klein J. J. *Colloid and Interface Sci.* **1987**, *117*, 149.
- MacKillop, D. A. *Journal of Polymer Sci. B* **1970**, *8*, 199.
- Malmsten, M.; Linse, P.; Cosgrove, T. *Macromolecules* **1992**, *25*, 2474.
- Manacke, G.; Wetzel, G.; Storck, W. *Die Makromol. Chemie* **1975**, *176*, 3251.
- Manecke, G.; Beier, W. *Die Angewandte Makromolekulare Chemie* **1981**, *97*, 23.
- March, J. *Advanced Organic Chemistry*, 3rd ed. Wiley-Interscience: New York, 1985.

- Marques, C.; Joanny, J. F.; Leibler, L. *Macromolecules* **1988**, *21*, 1051.
- Marques, C.; Joanny, J. F. *Macromolecules* **1989**, *22*(4), 1454.
- Marques, C. M.; Joanny, J. F. *Macromolecules* **1990**, *23*(1), 268.
- Marra, J.; Hair, M. L. *Colloids and Surfaces* **1988-89**, *34*, 215.
- Matsuda, T.; Litt, M.H. *J. Polym. Sci. Polym. Chem.* **1974**, *12*, 489.
- Mays, J. M.; Ferry, W. M.; Hadjichristidis, N.; Funk, W. G.; Fetters, L. J. *Polymer*, **1986**, *27*, 129.
- Mays, J. W.; Nan, S.; Whitfield, D. *Macromolecules*, **1991**, *24*, 315.
- Milner, S. T.; Witten, T. A.; Cates, M. E. *Macromolecules* **1988**, *21*, 2610.
- Milner, S. T. *J. Chem. Soc.; Faraday Trans.* **1990**, *86*(9), 1349.
- Misra, B. N.; Sood, D. S.; Mehta, I. K. *J. Polym. Sci., Polym. Chem. Ed.* **1985**, *23*, 1749.
- Mittal, K. L. Ed. *Adhesion Aspects of Polymer Coatings*; Plenum: New York, 1983.
- Morra, M.; Occhiello, E.; Garbassi, F. *Langmuir*, **1989**, *5*, 872.
- Morton, M.; Fetters, L. J. *Rubber Chem. & Tech.*, **1975**, *8*(3), 359.
- Morton, M.; Fetters, L. J. in *Stereo Rubbers* ed. W. M. Saltman, Wiley: New York, 1977, 215.
- Morton, M. *Anionic Polymerization: Principles and Practice*, Academic Press: New York, 1983.
- Morton, M.; Kammereck, R. F. *J. Am. Chem. Soc.* **1970**, *92*, 10.
- Morton, M.; Kammereck, R. F.; Fetters, L. J. *Macromolecules* **1971**, *4*, 11.
- Morton, M.; Mikesell, S. L. *J. Macromol. Sci.- Chem.* **1973**, *A7*(7), 1391.
- Motomura, K.; Matuura, R. *J. Chem. Phys.* **1969**, *50*, 1281.
- Motomura, K.; Sekita, K.; Matuura, R. *Bull. Chem. Soc. Jpn.* **1971**, *44*, 1243.

- Motomura, K.; Moroi, Y.; Matuura, R. *Bull. Chem. Soc. Jpn.* **1971**, *44*, 1248.
- Motschmann, H.; Stamm, M.; Toprakcioglu *Macromolecules* **1991**, *24*, 3681
- Muilenberg, G. E. *Handbook of X-Ray Photoelectron Spectroscopy*, Perkin-Elmer Corp., 1979.
- Munch, M. R.; Gast, A. P. *J. Chem. Soc. Faraday Trans.* **1990**, *86*(9), 1341.
- Munch, M. R.; Gast, A. P. *Macromolecules*, **1990**, *23*, 2313.
- Munch, M. R.; Gast, A. P. *Macromolecules* **1988**, *21*, 1360 & 1366.
- Murat, M.; Grest, G. S. *Macromolecules* **1989**, *22*, 4054.
- Nambu, K. *J. Appl. Polym. Sci.* **1960**, *4*, 69.
- Nagata, K.; Kawaguchi M. *Macromolecules* **1990**, *23*, 3957.
- Napper, D. *Polymeric Stabilization of Colloidal Dispersions*; Academic: London, 1983.
- Narayan, R.; Krauss, M.; Tsao, G. T. *Polym. Mater. Sci. (Am. Chem. Soc., Div. Polym. Mater.)* **1985**, *52*, 112.
- Nevin, R. S.; Pearce, E. M. *Polymer Letters* **1965**, *3*, 487.
- Norman, R. O. C.; Taylor, R. *Electrophilic Substitution in Benzenoid Compounds*, Elsevier Pub.: New York, 1965.
- Nuzzo, R. G.; Fusco, F. A.; Allara, D. L. *Journal of American Chemical Society*, **1987**, *109*, 2358.
- Odian, G. G. *Principles of Polymerization 2nd Ed.*, Plenum Press: New York, 1970, Chapter 5.
- Ohno, A. Oae, S. in *Organic Chemistry of Sulfur*, ed. Oae, S. Plenum Press: New York, 1977, Chapter 4.
- Olah, G. A. *Acc. Chem. Res.* **1970**, *4*, 240.
- Olah, G. A.; Kobayashi, S. *J. Am. Chem. Soc.* **1971**, *93*, 6964.
- Omichi, H.; Chundury, D.; Stannett, V. T. *J. Appl. Polym. Sci.* **1986**, *32*, 4827.
- Oster G.; Oster, G. K.; Moroson, H. *J. Polym. Sci.* **1959**, *34*, 671.

- Overman, L. E.; Smoot, J.; Overman, J. D. *Synthesis* **1974**, *1*, 59
- Parsonage, E.; Tirrell, M.; Watanabe, H.; Nuzzo, R. *Macromolecules* **1991**, *24*, 1987.
- Partridge, R. H. *J. Chem. Phys.* **1967**, *47*, 4223.
- Patton, P. A. Ph.D. Dissertation, Department of Polymer Sci. and Engineering, Univ. of Mass., 1987.
- Pepperkorn, E.; Jean-Chronberg, A. C.; Varoqui, R. *Macromolecules*, **1990**, *23*, 1735.
- Phillips, R. W.; Dettre, R. H. *J. Coll. and Interf. Sci.* **1976**, *56*, 251.
- Ploehn, H. J.; Russel, W. B. *Macromolecules* **1988**, *21*, 1075; **1989**, *22*, 266.
- Plueddemann, E. P. *Silane Coupling Agents*; Plenum: New York, 1982.
- Rao, M. H.; Rao, K. N.; Lokhande, H. T.; Teli, M. D. *J. Appl. Polym. Sci.* **1987**, *33*, 2345.
- Rasmussen, J. R.; Stredonsky, E. R.; Whitesides, G. M. *J. Am. Chem. Soc.* **1977**, *99*, 4736.
- Rasmussen, J. R.; Bergbreiter, D. E.; Whitesides, G. M. *J. Am. Chem. Soc.* **1977**, *99*, 4746.
- Reardon, J. P.; Zisman, W. A. *Macromolecules* **1974**, *7*, 920.
- Reilley, C. N.; Everhart, D. S.; Ho, F. F. L. In *Applied Electron Spectroscopy for Chemical Analysis*; Windawi, H., Ho, F. F. L., eds.; John Wiley & Sons: New York, 1982, Chapter 6.
- Rempp, P.; Franta, E.; Herz, J. E. *Adv. in Polymer Science* Vol. 86, Springer-Verlag: Berlin Heidelberg, 1984, 145.
- Riebsomer, J. L.; Baldwin, R.; Buchanan, J.; Burkett, H. *J. Am. Chem. Soc.* **1938**, *60*, 2974.
- Riebsomer, J. L.; Stauffer, D.; Glick, F.; Lambert, F. *J. Am. Chem. Soc.* **1942**, *64*, 2080.
- Riebsomer, J. L.; Irvine, J.; Andrews, R. *J. Am. Chem. Soc.* **1938**, *60*, 1015.
- Riebsomer, J. L.; Irvine, J. *Organic Syntheses* **3**, 326.

- Risse, W.; Grubbs, R. H. *Polym. Prepr. (Am. Chem. Soc., Div. Polym. Chem.)* **1983**, 30(1), 193.
- Roberts, R. M.; Khalaf, A. A. *Friedel Crafts Alkylation Chemistry* Marcel Dekker Inc.: New York, 1984.
- Roe, R. J.J. *Chem Phys.* **1965**, 43, 1591.
- Roe, R. J.J. *Chem Phys.* **1966**, 44, 4264.
- Roe, R. J. J. *Chem. Phys.* **1974**, 60, 4192.
- Roggero, A.; Zotteri, L.; Pronz, A.; Gandini, A.; Mazzei, A. *Eur. Polym. J.* **1976**, 12, 837.
- Rubin, R. J. J. *Chem. Phys.* **1965**, 43, 2392.
- Rubin, R. J. J. *Res. Natl. Bur. Stand., Sect. B* **1966**, 70, 237.
- Ruckenstein, E.; Gourisankar, S. V. *J. Coll. and Interf. Sci.* **1985**, 107, 488.
- Ruckenstein, E.; Gourisankar, S. V. *J. Coll. and Interf. Sci.* **1986**, 109, 557.
- Satija, S. K.; Majkrzak, C. F.; Russel, T. P.; Sinha, S. K.; Sirota, E. B.; Hughes, G. J. *Macromolecules* **1990**, 23, 3860.
- Sawamoto, M.; Kanaoka, S.; Omura, T.; Higashimura, T. *Polym. Prepr. (Am. Chem. Soc., Div. Polym. Chem.)* **1992**, 32(1), 148.
- Scheutjens, J. M. H. M.; Fleer, G. J. *J. Phys. Chem.* **1979**, 83, 1619.
- Scheutjens, J. M. H. M.; Fleer, G. J. *J. Phys. Chem.* **1980**, 84, 178.
- Scheutjens, J. M. H. M.; Fleer, G. J. *Macromolecules* **1985**, 18, 1882.
- Scholtens, B. J. R.; Bijsterbosch, B. H. *J. Coll. and Interf. Sci.* **1980**, 77, 162.
- Schonhorn, H. *Macromolecules* **1968**, 1, 145.
- Searles, S.; Nukina, S. *Chemical Reviews*, **1959**, 59, 1077.
- Shim, D.; Marques, C.; Cates, M. *Macromolecules* **1991**, 24, 5309.
- Shimasaki, K.; Aida, T.; Inoue, S. *Macromolecules* **1987**, 20, 3076.
- Shoichet, M. S.; McCarthy, T. J. *Macromolecules* **1991**, 24, 982.

- Sigwalt, P.; Spassky, N. In *Ring Opening Polymerization Vol.2* ed. K.J. Ivin, T. Saegusa, Elsevier Press: New York 1984, Chapter 9.
- Silberberg, A. *J. Phys. Chem.* **1962**, 66, 1872, 1884.
- Silberberg, A. *J. Chem. Phys.* **1967**, 46, 1105.
- Silberberg, A. *J. Chem. Phys.* **1968**, 48, 2835.
- Silverstein, R. M.; Bassler, C. G.; Morrill, T. C. *Spectrometric Identification of Organic Compounds 4th ed.*, John Wiley & Sons: New York, 1981, Chapter 6.
- Simha, R.; Frish, H. L.; Frish F. R. *J Phys. Chem.* **1953**, 57, 584.
- Simonds, R. P. Goethals, E. J. *Makromol. Chem.* **1978**, 179, 1689.
- Smisek, D. L. Ph.D. Dissertation, Univ. of Mass., Chemical Engineering Department, 1991.
- Stober, W.; Fink, A.; Bohn, E. *J. Colloid and Interface Sci.* **1968**, 26, 62.
- Stouffer J. M.; McCarthy, T. J. *Macromolecules* **1988**, 21, 1204.
- Streitwieser Jr., A.; Heathcock, C. H. *Introduction to Organic Chemistry 2nd ed.* Macmillan Pub.: New York, 1981, Chapter 23.
- Suzuki, M.; Kishida, A.; Iwata, H.; Ikada, Y. *Macromolecules* **1986**, 19, 1804.
- Swalen, J. D.; Allara, D. L.; Andrade, J. D.; Chandross, E. A.; Garoff, S.; Israelachvili, J.; McCarthy, T. J.; Murray, R.; Pease, R. F.; Rabolt, J. F.; Wynne, K. J.; Yu, H. *Langmuir* **1987**, 3, 932.
- Takahashi, A.; Kawaguchi, M. *Advances in Polymer Science* Vol.46, Springer-Verlag Berlin Heidelberg, 1982.
- Takaki, M.; Asami, R.; Kuwata, Y. *Macromolecules* **1979**, 12, 378.
- Takaki, M.; Asami, R.; Inukai, H.; Inenaga, T. *Macromolecules* **1979**, 12, 383.
- Taki, T.; Hirao, A.; Nakahama, S. *Macromolecules* **1991**, 24, 1455.
- Tarbell, D. S. in *Organic Sulfur Compounds Vol. 1*, ed. N. Kharasch Plenum Press: London, 1961, Chapter 10.
- Tassin, J. F.; Siemens, R. L.; Wing, T. T.; Hadziioannou, G.; Swalen, J. D.; Smith, B. A. *J. Phys. Chem.* **1989**, 93(5), 2106.

- Taunton, H. J.; Toprakcioglu, C.; Fetters, L. J.; Klein, J. *Macromolecules* **1990**, 23, 571.
- Taunton, H. J.; Toprakcioglu, C.; Klein, J. *Macromolecules* **1988**, 21, 3336.
- Taylor, R. T.; Pelter, M. W. *J. Polym. Sci., Polym., Lett. Ed.* **1987**, 25, 215.
- Taylor, R. T.; Pelter, M. W. *J. Polym. Sci., Polym. Chem. Ed.* **1988**, 26, 2651.
- ten Brinke, G.; Hadziioannou G. *Macromolecules* **1987**, 20, 489.
- Thambo, G.; Miller, W. G. *Macromolecules* **1990**, 23, 4397.
- Triolo, P.M.; Andrade, J.D. *J. Biomed. Mater. Res.* **1983**, 17, 129.
- Tripp, C. P.; Hair, M. L. *Langmuir*, **1991**, 7, 923.
- Trott, G.F. *J. Appl. Polym. Sci.* **1974**, 18, 1411.
- Turbek, A. F. *I&EC Product Research and Development* **1962**, 1, 275.
- Uchida, E.; Uyama, Y.; Ikada, Y. *J. Polym. Sci. Polym. Chem.* **1989**, 27, 527.
- Urban, M. W.; Salazar-Rojas, E. M. *Macromolecules* **1988**, 21, 372.
- Valint Jr., P. L.; Boch, J. *Macromolecules*, **1988**, 21, 175.
- Valint Jr., P. L.; Boch, J. U.S. Patent 4,492,785 1985.
- van der Beek, G. P.; Cohen Stuart, M. A.; Fler, G. J.; Hofman J. E. *Macromolecules* **1991**, 24, 6600.
- van der Beek, G. P.; Cohen Stuart, M. A.; Fler, G. J.; Hofman, J. E. *Langmuir* **1989**, 5, 1180.
- van der Beek, G. P.; Cohen Stuart, M. A. *Macromolecules* **1991**, 24, 3553.
- van der Linden, C. C.; Leermakers, F. *Macromolecules* **1992**, 25, 3449.
- van Lent, B.; Scheutjens, J. M. H. *J. Macromolecules* **1989**, 22, 1931.
- Varma, D. S.; Nedungadi, C. *J. Appl. Polym. Sci.* **1976**, 20, 681.
- Varshney, S. K.; Jacobs, C.; Hautekeer, J.; Bayard, P.; Jerome, R.; Fayt, R.; Teyssie, Ph. *Macromolecules* **1991**, 24, 4997.

- Varshney, S. K.; Hautekeer, J.; Fayt, R.; Jerome, R.; Teyssie, Ph. *Macromolecules* **1990**, *23*, 2618.
- Varshney, S. K.; Jacobs, C.; Hautekeer, J.; Bayard, P.; Jerome, R.; Fayt, R.; Teyssie, Ph. *Macromolecules* **1991**, *24*, 4997.
- Vink, H. *Makromol. Chem.* **1981**, *182*, 279.
- Waldman, D. A.; Kolb, B. U.; McCarthy, T. J.; Hsu, S. L. *Langmuir* **1991**, in press.
- Waldman, D. A.; Kolb, B. U.; McCarthy, T. J.; Hsu, S. L. *Proc. of A.C.S. Div. of Polym. Mat.* **1988**, *59*, 326.
- Waldman D. A. Ph.D. Dissertation, Polymer Science Department, Univ. of Mass., 1988.
- Ward, W. J; McCarthy, T. J. in *Encyclopedia of Polymer Science and Engineering*, 2nd ed.; Mark, H. F.; Bikales, N. M.; Overberger, C. G.; Menges, G.; Kroschwitz, J. I., eds.; John Wiley and Sons: New York, 1989; suppl. vol., p. 674.
- Webber, R. M.; Anderson J. L.; Jhon, M. S. *Macromolecules* **1990**, *23*, 1026.
- Webster, O. W.; Hertler, W. R.; Sogah, D. Y.; Fornham W. B.; RajanBabu, T. V. *J. Am. Chem. Soc.* **1983**, *105*, 5706.
- Webster, O. W.; Hertler, W. R.; Sogah, D. Y.; Fornham W. B.; RajanBabu, T. V. *Polym. Prepr. (Am. Chem. Soc., Div. Polym. Chem.)* **1983**, *24*(2), 52, 54.
- Whitmore, M. D.; Noolandi, J. *Macromolecules* **1990**, *23*, 3321.
- Wijmans, C. M.; Scheutjens, J. M. H. M., Zhulina, E. B. *Macromolecules* **1992**, *25*(10), 2657.
- Wu. D. T.; Yokayama, A.; Setterquist, R. *Polymer Journal* **1991**, *23*(5), 709-714.
- Yamagiwa, S.; Kawaguchi, M.; K, Kato, Takahashi, A. *Macromolecules* **1989**, *22*, 2199.
- Yamakawa, S. *Macromolecules* **1979**, *12*, 1222.
- Yamakowa, S.; Yamamoto, F.; Kato, Y. *Macromolecules* **1976**, *9*, 754.
- Yamashita, Y. *Adv. Poly. Sci.* **1978**, *28*, 1.

- Yang, J.; Wegner, G. *Macromolecules* **1992**, 25, 1791.
- Yanova, L. P.; Kuznetsov, V. A.; Taubman, A. B. *Kolloid-Z.* **1975**, 37, 614.
- Yasuda, H.; Sharma, A. K.; Yasuda, T. *J. Polym. Sci., Polym. Phys. Ed.* **1981**, 19, 1285.
- Yasuda, T.; Okuno, T.; Yoshida, K.; Yasuda, H. *J. Polym. Sci., Polym. Phys.* **1988**, 26, 1781.
- Young, R. N.; Quirk, R. P.; Fetters, L. J. *Advances in Polymer Science* Vol. 56, Springer-Verlag: Berlin Heidelberg, 1984.
- Yu, H. S.; Choi, W. J.; Lim, K. T.; Choi, S. K. *Macromolecules* **1988**, 21, 2893.
- Zisman, W. A. *Adv. Chem. Ser.* **1964**, 43, 1.

